

# 第40回記念 フラーレン・ ナノチューブ 総合シンポジウム

The 40<sup>th</sup>  
Commemorative  
Fullerenes-Nanotubes  
General Symposium

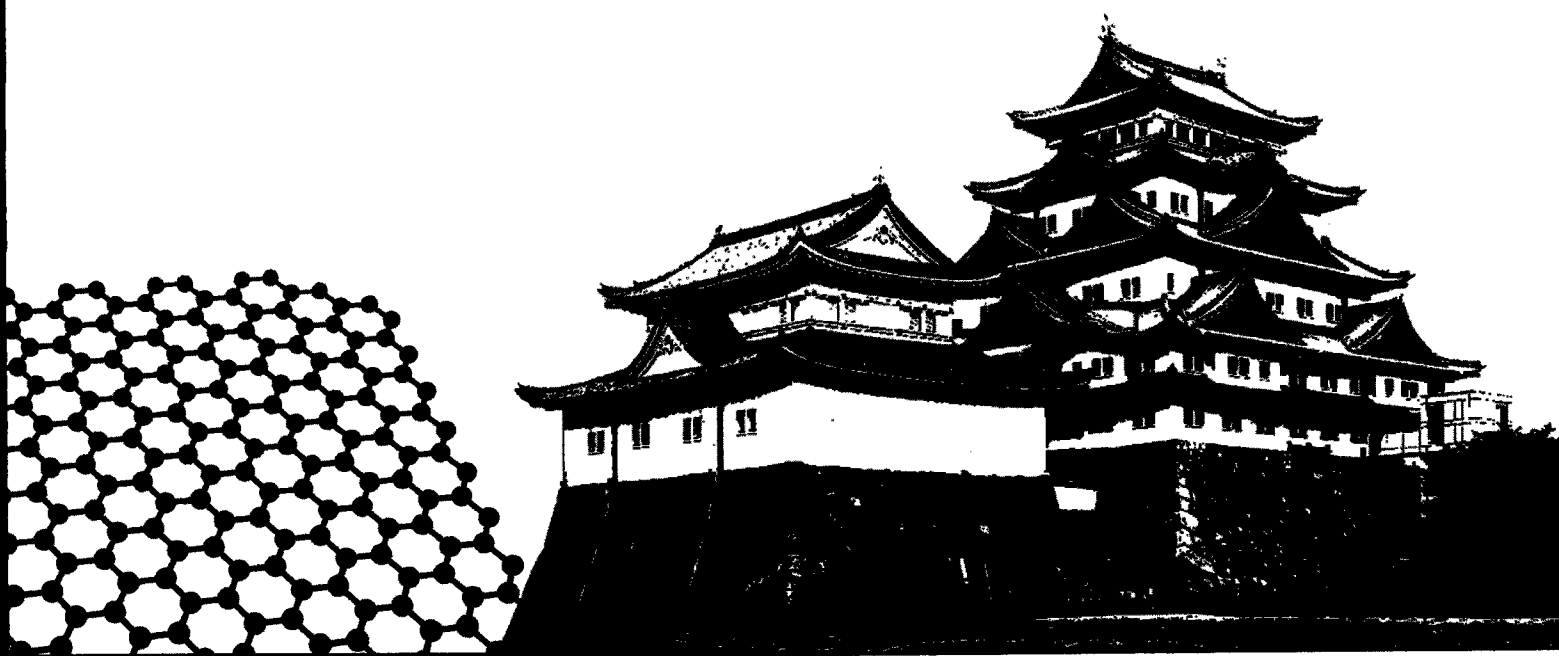
## 講演要旨集 Abstracts

2011年3月8日[火]-10日[木]

March . 8(Tue)-10(Thu), 2011

名城大学 天白キャンパス 共通講義棟北館

Meijo University Tenpaku Campus Lecture Hall (North), Nagoya, Aichi



【共催】日本化学会  
The Chemical Society of Japan

【協賛】日本物理学会 応用物理学会 高分子学会 電気化学会  
The Physical Society of Japan, The Japan Society of Applied Physics,  
The Society of Polymer Science Japan, The Electrochemical Society of Japan

【主催】フラーレン・ナノチューブ学会  
The Fullerene and Nanotubes Research Society

**F-NTRS**®

銘 柄		分子構造	純度(HPLC面積%、代表値) 内容他	最低数量 (g)
<b>nanom purple</b> フラーレンC60	ST		99	10
	TL		99.5	2
	SU		99.5/昇華精製品	2
	SUH		99.9/昇華精製品	1
<b>nanom orange</b> フラーレンC70	ST		97	1
	SU		98/昇華精製品	0.5
<b>nanom mix</b> 混合フラーレン	ST		C60,C70,その他高次 フラーレンの混合物 ※微粒化品(ST-F)もあります	50
<b>nanom spectra</b> [60]PCBM (phenyl C61-butyric acid methyl ester)	E100		99	1
	E100H		99.5	1
	E102		99.9	0.5
<b>nanom spectra E400</b> bis[60]PCBM (bis-phenyl C61-butyric acid methyl ester)			98/異性体トータル ※位置異性体の混合物	1
<b>nanom spectra E200</b> [60]PCBNB (phenyl C61-butyric acid n-butyl ester)			99	1
<b>nanom spectra E210</b> [60]PCBIB (phenyl C61-butyric acid l-butyl ester)			99	1
<b>nanom spectra E123</b> [60,70]PCBM			[60]PCBM、[70]PCBMの混合物	1
<b>nanom spectra</b> [70]PCBM (phenyl C71-butyric acid methyl ester)	E110	 主成分	99/異性体トータル ※位置異性体の混合物	0.5
	E112		99.5/異性体トータル ※位置異性体の混合物	0.5
<b>nanom spectra D100</b> 水酸化フラーレン			C <sub>60</sub> OH <sub>n</sub> n=10を主成分とする混合物	1
<b>nanom spectra A100</b> 水素化フラーレン			C <sub>60</sub> H <sub>n</sub> n=30を主成分とする混合物	1
<b>nanom spectra G100</b>			PRATO体。有機溶媒に可溶。	1

銘柄、取扱数量等は予告無く変更する場合がございます。予めご了承下さい。

2011年2月1日現在

当社製品は、下記2社から購入いただけます。詳細は直接お問い合わせください。

・関東化学株式会社 試薬事業本部

〒103-0022 東京都中央区日本橋室町2-2-1 TEL:03-6214-1090 FAX:03-3214-1047

http://www.kanto.co.jp E-mail:reag-info@gms.kanto.co.jp

・第一実業株式会社 新事業推進室【担当: 鎰広(カギヒロ)】 E-mail:masaru.kagihiro@djk.co.jp

〒102-0084 東京都千代田区二番町11-19 TEL:03-5214-8579 FAX:03-5214-8502

<本資料に関するお問い合わせ先>

フロンティアカーボン株式会社 営業販売センター【担当: 梶原】

〒806-0004 福岡県北九州市八幡西区黒崎城石1-1

TEL:093-643-4400 FAX:093-643-4401 http://www.f-carbon.com

※弊社へのお問い合わせはHPよりお願いいたします。

Abstract  
The 40<sup>th</sup> Commemorative Fullerene-Nanotubes  
General Symposium

第40回記念フラーレン・ナノチューブ  
総合シンポジウム

講演要旨集

The Fullerenes and Nanotubes Research Society

The Chemical Society of Japan

The Japan Society of Applied Physics

The Physical Society of Japan

The Electrochemical Society of Japan

The Society of Polymer Science, Japan

主催：フラーレン・ナノチューブ学会

共催：日本化学会

協賛：日本物理学会・応用物理学会・電気化学会・高分子学会

Date: March 8<sup>nd</sup>(Tue)–10<sup>th</sup>(Thu), 2010

Place: Meijo University

1-501 Shiogamaguchi, Tempaku-ku, Nagoya 468-8502

TEL: 052-832-1151

Presentation: Special Lecture (25 min presentation, 5min discussion)  
General Lecture (10 min presentation, 5min discussion)  
Poster Preview (1 min presentation, no discussion)

日時：平成23年3月8日(火)～10日(木)

場所：名城大学

〒468-8502 愛知県名古屋市天白区塩釜口 1-501

TEL: 052-832-1151

発表時間：基調講演	(発表 40分・質疑応答 5分)
特別講演	(発表 25分・質疑応答 5分)
一般講演	(発表 10分・質疑応答 5分)
ポスタープレビュー	(発表 1分・質疑応答 なし)

展示団体御芳名(アイウエオ順、敬称略)

IOP英国物理学会出版局  
アイクストロン(株)  
    (株)あすみ技研  
    コスモ・バイオ(株)  
(株)イメージミッション木鏡社  
    (株)サーモ理工  
    (株)島津製作所  
(株)セントラル科学貿易  
    ナカライテスク(株)  
    日本電子(株)  
    日立工機(株)  
(株)ニューメタルスエンドケミカルスコーポレーション  
    (株)堀場製作所  
(株)名城ナノカーボン  
    和光純薬工業(株)

広告掲載団体御芳名(アイウエオ順、敬称略)

イクストロン(株)  
    (株)ATR  
    (株)岡村製作所  
    (株)カーク  
    コスモ・バイオ(株)  
(株)シーエムシー出版  
シグマ アルドリッチ ジャパン(株)  
    (株)島津製作所  
(株)セントラル科学貿易  
    東洋炭素(株)  
    ナカライテスク(株)  
    日本電子(株)  
(株)ニューメタルスエンドケミカルスコーポレーション  
    (有)菱田商店  
    フロンティアカーボン(株)  
    (株)マシナックス  
    (株)ユニソク  
    理科研(株)



## Contents

Time Table	.....	i
Chairperson	.....	iii
Program	Japanese .....	iv
	English .....	xviii
Abstracts	Special lecture .....	1
	General lecture .....	7
	Poster preview .....	49
Author Index	.....	211

## 目次

早見表	.....	i
座長一覧	.....	iii
プログラム	和文 .....	iv
	英文 .....	xviii
講演予稿	特別講演 .....	1
	一般講演 .....	7
	ポスター発表 .....	49
発表索引	.....	211

# プログラム早見表

各項目敬称略

	3月8日(火)	3月9日(水)	3月10日(木)	
9:00	基調講演(飯島 澄男) 9:00~9:45	特別講演(弓削 亮太) 9:00~9:30	基調講演(Young Hee Lee) 9:00~9:45	9:00
9:45	一般講演3件 (ナノチューブの物性と応用) 9:45~10:30	一般講演4件 (ナノチューブの生成と精製) 9:30~10:30	一般講演3件 (ハイブリットカーボン) 9:45~10:30	9:45
10:30	休憩 10:30~10:45			10:30
10:45	一般講演4件 (ナノチューブの物性と応用) 10:45~11:45	一般講演4件 (グラフェン) 10:45~11:45	一般講演4件 (グラフェン) 10:45~11:45	10:45
11:45	昼食 11:45~13:00			11:45
13:00	一般講演5件 (ナノチューブの物性と応用) 13:00~14:15	授賞式 13:00~13:45	特別講演(長谷川 雅考) 13:00~13:30	13:00
14:15	休憩 14:15~14:30	特別講演(平本 昌宏) 13:45~14:15	一般講演3件 (ナノチューブの生成と精製) 13:30~14:15	14:15
14:30	特別講演(Amanda S. Barnard) 14:30~15:00	一般講演4件 (フラーレン) 14:15~15:15	ポスタープレビュー 1分×53件 14:15~15:10	14:30
15:10	一般講演4件 (ハイブリットカーボン) 15:00~16:00	休憩 15:15~15:30	ポスターセッション 15:10~16:30	15:10
16:00	ポスタープレビュー 1分×54件 16:00~17:00	一般講演3件 (フラーレン) 15:30~16:15		16:00
17:00	ポスターセッション 17:00~18:20	ポスタープレビュー 1分×54件 16:15~17:10		16:30
18:20		ポスターセッション 17:10~18:30		

3月8日(火)  
チュートリアル 103講義室  
15:00~16:30  
講師 榎 敏明先生  
東京工業大学大学院理工学  
研究科 教授

18:45~懇親会

基調講演 発表40分 質疑5分  
特別講演 発表25分 質疑5分  
一般講演 発表10分 質疑5分  
ポスタープレビュー  
発表1分 質疑なし

## TIME TABLE

	Tue. Mar. 8	Wed. Mar. 9	Thu. Mar. 10	
9:00	Plenary Lecture (S.Iijima) 9:00~9:45	Special Lecture (R.Yuge) 9:00~9:30	Plenary Lecture (Y.H.Lee) 9:00~9:45	9:00
9:45	General Lecture[3] (Properties and Applications of Nanotubes) 9:45~10:30	General Lecture[4] (Formation and Purification of Nanotubes) 9:30~10:30	General Lecture[3] (Hybrid Carbon) 9:45~10:30	9:45
10:30	Break 10:30~10:45			10:30
10:45	General Lecture[4] (Properties and Applications of Nanotubes) 10:45~11:45	General Lecture[4] (Graphene) 10:45~11:45	General Lecture[4] (Graphene) 10:45~11:45	10:45
11:45	Lunch 11:45~13:00			11:45
13:00	General Lecture[5] (Properties and Applications of Nanotubes) 13:00~14:15	Awards Ceremony 13:00~13:45	Special Lecture (M.Hasegawa) 13:00~13:30	13:00
14:15	Break 14:15~14:30	Special Lecture (M.Hiramoto) 13:45~14:15	General Lecture[3] (Formation and Purification of Nanotubes) 13:30~14:15	13:30
14:30	Special Lecture (A.S.Barnard) 14:30~15:00	General Lecture[4] (Fullerenes) 14:15~15:15	Poster Preview 1min × [53] 14:15~15:10	14:15
16:00	General Lecture[4] (Hybrid Carbon) 15:00~16:00	Break 15:15~15:30	Poster Session 15:10~16:30	15:10
16:30	Poster Preview 1min × [54] 16:00~17:00	General Lecture[3] (Fullerenes) 15:30~16:15		16:30
17:00	Poster Session 17:00~18:20	Poster Preview 1min × [54] 16:15~17:10		17:00
18:20		Poster Session 17:10~18:30		18:20

**18:45~ Banquet**

<b>Tue. Mar. 8</b> <b>Tutorial Room103</b> <b>15:00~16:30</b> <b>Prof. Toshiaki Enoki</b>
--

Plenary Lecture: 40min Presentation, 5min Discussion  
 Special Lectures: 25min Presentation, 5min Discussion  
 General Lectures: 10min Presentation, 5min Discussion  
 Poster Previews: 1min Presentation, No Discussion

## 座長一覧

3月8日(火)

(敬称略)

	時 間	座 長
基 調 講 演(飯島)	9:00 ~ 9:45	齋藤 晋
一 般 講 演	9:45 ~ 10:30	大野 雄高
一 般 講 演	10:45 ~ 11:45	片浦 弘道
一 般 講 演	13:00 ~ 14:15	菅井 俊樹
特 別 講 演(Barnard)	14:30 ~ 15:00	大澤 映二
一 般 講 演	15:00 ~ 16:00	小塩 明
ポスタープレビュー	16:00 ~ 17:00	沖本 治哉
ポスターセッション	17:00 ~ 18:20	宮田 耕充

3月9日(水)

	時 間	座 長
特 別 講 演(弓削)	9:00 ~ 9:30	宮本 良之
一 般 講 演	9:30 ~ 10:30	藤ヶ谷 剛彦
一 般 講 演	10:45 ~ 11:45	近藤 大雄
特 別 講 演(平本)	13:45 ~ 14:15	篠原 久典
一 般 講 演	14:15 ~ 15:15	加藤 立久
一 般 講 演	15:30 ~ 16:15	宮崎 隆文
ポスタープレビュー	16:15 ~ 17:10	北浦 良
ポスターセッション	17:10 ~ 18:30	田中 丈士

3月10日(木)

	時 間	座 長
基 調 講 演(Lee)	9:00 ~ 9:45	齋藤 理一郎
一 般 講 演	9:45 ~ 10:30	若林 知成
一 般 講 演	10:45 ~ 11:45	岡田 晋
特 別 講 演(長谷川)	13:00 ~ 13:30	吾郷 浩樹
一 般 講 演	13:30 ~ 14:15	齋藤 毅
ポスタープレビュー	14:15 ~ 15:10	千足 昇平
ポスターセッション	15:10 ~ 16:30	岸 直希

3月8日(火)

基調講演 発表40分・質疑応答5分  
特別講演 発表25分・質疑応答5分  
一般講演 発表10分・質疑応答5分  
ポスタープレビュー 発表1分・質疑応答なし

**基調講演 (9:00-9:45)**

- 1S-1 ナノカーボン材料の構造評価と産業応用 1  
○飯島澄男

**一般講演 (9:45-10:30)**

**ナノチューブの物性と応用**

- 1-1 Raman分光法によるSWCNT表面の界面活性剤の検出 7  
西出大亮、藤井俊治郎、田中丈士、○片浦弘道
- 1-2 溶液中に分散された単層カーボンナノチューブのラマン散乱分光による評価 8  
○鈴木信三、栗津勝元、池田泰朗、畑野雄哉、中西碧、水澤崇志、小野晶、岡崎俊也、阿知波洋次
- 1-3 二層カーボンナノチューブから抜き出した微小径単層カーボンナノチューブの励起子間相互作用 9  
○小山剛史、宮田耕充、篠原久典、岸田英夫、中村新男

☆☆☆☆☆☆ 休憩 (10:30-10:45) ☆☆☆☆☆☆

**一般講演 (10:45-11:45)**

**ナノチューブの物性と応用**

- 1-4 金属・半導体分離単層カーボンナノチューブ薄膜の連続的キャリア密度制御 10  
○下谷秀和、津田諭、袁洪涛、蓬田陽平、守屋理恵子、竹延大志、柳和宏、岩佐義宏
- 1-5 気相過・転写法により作製したカーボンナノチューブ薄膜トランジスタの移動度とオン/オフ比 11  
○孫 東明、ティメルマンズ マリナ、Ying Tian、ナシブリン アルバート、岸本 茂、水谷 孝、カウピネン エスコ、大野 雄高
- 1-6 長さ分離された半導体単層カーボンナノチューブを用いた高移動度トランジスタ 12  
○塩沢一成、宮田耕充、浅田有紀、大野雄高、北浦良、水谷孝、篠原久典
- 1-7 非常に柔軟なAll-SWNT電界効果トランジスタ 13  
○相川 慎也、エリック エイナルソン、千足 昇平、塩見 淳一郎、西川 英一、丸山 茂夫

☆☆☆☆☆☆ 昼食 (11:45-13:00) ☆☆☆☆☆☆

**一般講演 (13:00-14:15)**

**ナノチューブの応用**

- 1-8 Infrared Solar Cell Based on C<sub>60</sub> Encapsulated Semiconducting Single-Walled Carbon Nanotubes 14  
○李 永峰、兒玉宗一郎、金子 俊郎、島山 力三
- 1-9 ポリベンゾイミダゾール被覆カーボンナノチューブの炭素化による非金属燃料電池カソード触媒の作製 15  
○内海剛志、藤ヶ谷剛彦、中嶋直敏
- 1-10 極微量の合成原料で決まる単層カーボンナノチューブの分散性と導電性ポリマーコンポジットへの応用 16  
○野々口斐之、二葉ドン、阿多誠介、湯村守雄、島賢治
- 1-11 カーボンナノチューブの-190℃から970℃の温度範囲で安定なクリープおよびクリープ回復 17  
○徐 鳴、二葉ドン、湯村 守雄、島 賢治
- 1-12 光応答カーボンナノチューブ細胞培養基板の開発 18  
○佐田貴生、藤ヶ谷剛彦、中嶋直敏

☆☆☆☆☆☆ 休憩 (14:15-14:30) ☆☆☆☆☆☆

3月8日(火)

特別講演 (14:30-15:00)

- 1S-2 The Advantages and Applications of Nanocarbon Phase Transformations 2  
○Amanda S. Barnard

一般講演 (15:00-16:00)

ハイブリッドカーボン

- 1-13 多段イオントラップ気相移動度測定装置の開発 19  
篠崎祐志、澤西慶彦、○菅井俊樹
- 1-14 ナノ分子構造体に埋め込まれた直線型ポリイン分子の電子状態 20  
○若林知成、才川真央、手柴雅臣、和田資子
- 1-15 ナノカーボンの細胞内取り込みにおけるサイズ依存性 21  
○張民芳、周シン、田原喜夫、飯島澄男、湯田坂雅子
- 1-16 高温において炭素原子と相互作用する白金クラスターの高分解能電子顕微鏡観察 22  
○小林慶太、末永和知

ポスタープレビュー (16:00-17:00)

ポスターセッション (17:00-18:20)

ナノチューブの生成と精製

- 1P-1 アルコールガスソース法によるZnO(000-1)基板上カーボンナノチューブ成長 49  
○筒井智之、五百川隆康、丸山隆浩、成塚重弥
- 1P-2 QM/MD Simulations of Carbon Nanotube Cap Nucleation Using Acetylene Feedstock and an Fe<sub>38</sub> Catalyst Nanoparticle 50  
○Ying Wang, HuJun Qian, Alister J. Page, Keiji Morokuma, Stephan Irle
- 1P-3 Raman散乱を用いたSWCNTの純度評価:界面活性剤の効果 51  
○田賀美樹、西出大亮、藤井俊治郎、田中丈士、片浦弘道
- 1P-4 高真空アルコールガスソース法によるPt触媒を用いたSWNTの低圧力成長 52  
○水谷芳裕、丸山隆浩、成塚重弥、飯島澄男
- 1P-5 表面分解法で4H-SiCと6H-SiCから成長したカーボンナノチューブのラマン分光法での比較 53  
○石黒祐樹、榊原悟史、伊藤宏晃、丸山隆浩、成塚重弥
- 1P-6 湿式微粒化装置によるCNTの新分散法 54  
○高島正、村井有美、宮城邦雄、宇高勝之、加藤伸一郎、宮崎祐介
- 1P-7 単層カーボンナノチューブの分子組立型合成 55  
○宮田耕充、鈴木麻里絵、Jinying Zhang、藤原美帆、北浦良、片浦弘道、篠原久典
- 1P-8 触媒蒸気供給基板式CVD法によって合成したカーボンナノコイル純度のSn触媒濃度の影響 56  
○石井裕一、瀧本幸太郎、須田善行、田上英人、滝川浩史、植仁志、清水一樹、梅田良人
- 1P-9 サイズ排除クロマトグラフィーによる単層CNTの長さ分離 57  
○浅野 敏、田中丈史、片浦弘道
- 1P-10 カーボンナノチューブ室温合成における電気化学プロセスの制御 58  
アハマドシャウキイ、田邊昌大、○保田諭、村越敬
- 1P-11 Selective synthesis of (6, 5) carbon nanotubes from C<sub>60</sub> precursor 59  
○張錦英、宮田耕充、北浦良、篠原久典
- 1P-12 触媒CVD法を用いてSn/Fe/MgOから多層カーボンナノコイルの合成 60  
○リムシュリン、瀧本幸太郎、須田善行、田上英人、滝川浩史、植仁志、清水一樹、梅田良人
- 1P-13 様々な炭素源ガスによるフラーレンC<sub>60</sub>を核としたカーボンナノチューブの成長 61  
高木大輔、前田文彦、○根岸良太、阿形省吾、小林慶裕、本間芳和

## 3月8日(火)

1P-14	DFTB/MD法を用いた単層カーボンナノチューブ閉端・開端シミュレーション ○原 裕訓、Stephan Irle	62
1P-15	[n]シクロパラフェニレンを用いた単層カーボン・ナノチューブへの変換:SCC-DFTBによるDiels Alder 反応およびラマンスペクトル ○梅田亮太、西村好史、イレステファン	63
1P-16	長尺かつ高純度半導体単層カーボンナノチューブの抽出 ○塩沢一成、宮田耕充、北浦良、篠原久典	64
<b>ナノチューブの応用</b>		
1P-17	ナノカーボン-ポリマー複合体の電極特性 ○坂下智啓、岡村光起、川崎晋司	65
1P-18	低閾値かつ高導電率を有するカーボンナノチューブ/ポリイソプレン複合材料の電気、力学特性 ○長岡朋弥、酒井歩、内田勝美、土屋好司、伊藤眞義、古川猛夫、矢島博文	66
1P-19	誘電泳動を用いたカーボンナノチューブ培養担体への細胞集積 ○松岡真琴、赤坂司、橋本剛、戸塚靖則、亘理文夫	67
1P-20	カーボンナノチューブFET特性におけるデバイスプロセスの影響 ○田中幹人、伊藤陽一、張奉鎔、林靖彦、岸直希、曾我哲夫、神保孝志	68
1P-21	分子内包単層カーボンナノチューブ透明導電膜の作製と評価 ○岸直希、三輪郁馬、岡崎俊也、斎藤毅、水谷年寿、土屋裕彰、曾我哲夫、神保孝志	69
1P-22	アガロースゲルクロマトグラフィーにより分離した配向半導体単層カーボンナノチューブを用いた 薄膜トランジスタ ○藤井俊治郎、田中丈士、片浦弘道	70
1P-23	シンプルな方法によるカーボンナノチューブと分子との相互作用分析 ○ユジョンテ、藤ヶ谷剛彦、中嶋直敏	71
1P-24	カーボンナノチューブの分散制御 ○内山直行、中嶋直敏	72
1P-25	高伝導性葉脈状SWNT網目 ○小橋和文、阿多誠介、山田健郎、二葉ドン、湯村守雄、畠賢治	73
1P-26	イオンゲルを用いた単層カーボンナノチューブ薄膜トランジスタ ○ウエンディー、蓬田陽平、下谷秀和、柳和宏、岩佐義宏、竹延大志	74
1P-27	DNA/カーボンナノチューブ複合体と生体親和性ポリカチオンの複合化 ○藤ヶ谷剛彦、山本悠喜、狩野有宏、丸山厚、中嶋直敏	75
1P-28	インクジェット法によるカーボンナノチューブ薄膜へのキャリアドーピング ○松崎怜樹、柳和宏、竹延大志	76
<b>ナノチューブの物性</b>		
1P-29	Chirality dependence of coherent phonon amplitudes in single wall carbon nanotubes ○Ahmad-Ridwan Tresna Nugraha、佐藤 健太郎、齋藤 理一郎	77
1P-30	ジケトン生成を利用したナノチューブ開裂に関する密度汎関数法計算 ○湯村尚史、金光俊幸	78
1P-31	SWCNT分散過程におけるG <sup>+</sup> /G <sup>-</sup> 比変化 ○西山聡子、田中丈士、片浦弘道	79
1P-32	ホウ素、窒素含有原料から成長したSWNTのラマン分光 ○鈴木哲、日比野浩樹	80

## グラフェン

1P-33	ラマン強度とシフトのグラフェンの層構造依存性 ○佐藤健太郎、Jin Sung Park、齋藤理一郎	81
1P-34	グラフェンのX線吸収スペクトルにおける偏光依存性 ○モハマッド タレック チョウデュリ、齋藤理一郎	82
1P-35	ペリペンタセンの合成と分光学的な分析 ○石井陽祐、坂下智啓、加藤秀典、高鳥正重、川崎晋司	83
1P-36	Chemical and Electrical Characterization of Graphene Formed by Gallium Flux Liquid Phase Epitaxy ○リーマイケル、日浦英文、アナスタシア ツィルニナ、塚越一仁	84
1P-37	大気圧アルコールCVDを用いた単層グラフェンの合成 ○深谷彰二、岸直希、杉田遼、曾我哲夫、神保孝志	85
1P-38	異なるスタッキングにおける単層、二層、三層グラフェンの量子静電容量 ○江口貴啓、佐藤健太郎、齋藤理一郎	86
1P-39	真空中加熱によるカーボンナノウォールの高品質化 ○鈴木誠也、吉村雅満	87
1P-40	Electronic-structure control of thin film of graphite: Interlayer spacing and thickness dependency ○Nguyen Thanh Cuong, Minoru Otani, Susumu Okada	88
1P-41	C <sub>2</sub> 分子によるグラフェン上欠損の修復QM/MDシミュレーション ○沖田吉孝、原裕訓、Lili Liu、Stephan Irlle	89

## ハイブリッドカーボン

1P-42	起毛したカーボンナノツイストにPtをコーティングした電界放出素子 ○杉岡由基、須田善行、田上英人、滝川浩史、植仁志、清水一樹、梅田良人	90
1P-43	ナノカーボンのためのLipid-PEG分散剤の分散効果の評価 メイヤング、和田百代、張民芳、コスタス コスタレロス、飯島澄男、増田光俊、○湯田坂雅子	91
1P-44	イオントラップ気相移動度を用いた荷電微粒子の長時間構造観測 ○澤西慶彦、篠崎祐志、菅井俊樹	92
1P-45	アークブラック担持RuO <sub>2</sub> を用いたスーパーキャパシタの作製およびその比容量 ○佐藤寿之、池田峻、須田善行、田上英人、滝川浩史、桶真一郎、植仁志、大川隆、青柳伸宜、清水一樹	93

## 若手奨励賞候補者

1P-46	液液界面近傍におけるフラーレンの電子受容特性 ○林亜実、奥垣智彦、高橋英志、前田耕治、田路和幸	94
1P-47	高結晶性二層カーボンナノチューブの簡便で効率的な合成 ○中村俊也、宮田耕充、林宏恩、北浦良、篠原久典	95
1P-48	電氣的性質による二層カーボンナノチューブの分離 ○藤原美帆、宮田耕充、鈴木麻里恵、北浦良、篠原久典	96
1P-49	ヘキサゲン中におけるポリリン-ヨウ素錯体の電子スペクトル ○和田資子、若林知成	97
1P-50	周期ナノホールを持つグラフェンシートの電子輸送特性におけるジグザグ端の重要性 ○實宝秀幸、大淵真理、金田千穂子	98
1P-51	単層カーボンナノチューブにおけるスピンに関連した新奇光学現象 ○小鍋哲、岡田晋	99



## 3月8日(火)

- 1P-52 ヨウ化銀ナノワイヤー内包カーボンナノチューブの合成と評価 100  
○伊東真一、北浦良、山田鉄兵、北川宏、金東榮、野田優、吉川浩史、阿波賀邦夫、篠原久典
- 1P-53 固体表面の原子構造を用いたグラフェンの加工制御 101  
○塚本貴広、萩野俊郎
- 1P-54 スカンジウムカーバイド内包フラーレンの構造と電子的特性 102  
○溝呂木直美、赤阪健、永瀬茂

3月9日(水)

特別講演 発表25分・質疑応答5分  
一般講演 発表10分・質疑応答5分  
ポスタープレビュー 発表1分・質疑応答なし

特別講演 (9:00-9:30)

- 2S-3 カーボンナノチューブ・カーボンナノホーンの平面型照明応用 3  
○弓削亮太

一般講演 (9:30-10:30)

ナノチューブの生成と精製

- 2-1 電界印加による層形成分離法の反復による金属・半導体性単層カーボンナノチューブの純度向上 23  
○井原和紀、斎藤毅、二瓶史行
- 2-2 ピレン分子ピンセットを用いた単層カーボンナノチューブの直径分離 24  
○小松直樹、A. F. M. Mustafizur Rahman、Feng Wang、松田一成、木村隆英
- 2-3 単層カーボンナノチューブの長さ分布に対する超音波分散の影響 25  
○大森 滋和、斎藤 毅、浅田 有紀、湯村守雄、飯島澄男
- 2-4 QM/MD Simulation of SWNT Nucleation on Transition-Metal Carbide Nanoparticles 26  
○Stephan Irlle、Alister J Page、Honami Yamane、Y. Ohta、Keiji Morokuma

☆☆☆☆☆☆ 休憩 (10:30-10:45) ☆☆☆☆☆☆

一般講演 (10:45-11:45)

グラフェン

- 2-5 グラフェンの積層構造に依存したRamanモード 27  
○齋藤理一郎、佐藤健太郎、C. Cong、Y. Ting、M. S. Dresselhaus
- 2-6 HfO<sub>2</sub>表面に吸着したグラフェンのエネルギー論と電子構造 28  
○神谷克政、梅澤直人、岡田晋
- 2-7 CVDによる樟脳からの大面積グラフェンと有機太陽電池への応用 29  
○ゴラップ・カリタ、松島 真央、脇田紘一、梅野正義
- 2-8 グラフェン薄膜における磁気抵抗ゆらぎの解析 30  
○A. Mahjoub、本岡正太郎、阿部拓斗、青木伸之、D. K.Ferry、J. P. Bird、落合勇一

☆☆☆☆☆☆ 昼食 (11:45-13:00) ☆☆☆☆☆☆

授賞式 (13:00-13:45)

特別講演 (13:45-14:15)

- 2S-4 有機薄膜太陽電池の基礎と最近の進展 4  
○平本昌宏

一般講演 (14:15-15:15)

フラーレン

- 2-9 フラーレンピーポッドーポリ(3-ヘキシルチオフェン)複合体 31  
○梅山有和、手塚記庸、俣野善博、今堀博
- 2-10 亜鉛(II)ポルフィリン-金属内包フラーレン連結分子の合成と光物性:内包クラスターの影響 32  
○馮業、Shankara Gayathri Radhakrishnan、溝呂木直美、Zdenek Slanina、二川秀史、土屋敬広、赤阪健、永瀬茂、Nazario Mart&iacut;n、Dirk M. Guldi
- 2-11 内包C<sub>78</sub>フラーレンの電子構造と内包クラスター構造 33  
○宮崎隆文、青木雄祐、大北壮祐、八木創、日野照純

## 3月9日(水)

- 2-12 光渦照射を用いたC<sub>60</sub>薄膜の光重合 34  
○青木伸之、土井達也、魏小均、小山恭平、宮本克彦、尾松孝茂、バード P. ジョナサン、落合勇一

### ☆☆☆☆☆☆ 休憩 (15:15-15:30) ☆☆☆☆☆☆

#### 一般講演 (15:30-16:15)

##### フラーレン

- 2-13 塩素化フラーレンC<sub>60</sub>Cl<sub>6</sub>を経由した水酸化フラーレンC<sub>60</sub>(OH)<sub>6</sub>の合成およびそのESI-MSスペクトル 35  
○上野裕、菅井俊樹、森山広思
- 2-14 マルチアリアル化[60]フラーレン誘導体の熱的および酸化的安定性 36  
○小久保研、柏原宮人、矢野智美、田中克知、伊熊直彦、大島巧
- 2-15 LLIP法で合成したC<sub>60</sub>ナノウィスカーのポリマー化におけるUV照射の影響 37  
○王 英輝、宮澤薫一

#### ポスタープレビュー (16:15-17:10)

#### ポスターセッション (17:00-18:30)

#### ナノチューブの応用

- 2P-1 Synthesis and Applications of Carbon Nanotube Sponge Macrostructures 103  
Xuchun Gui, Tianzhun Wu, ○Rong Xiang, Zikang Tang
- 2P-2 カーボンナノチューブコートディッシュ上での細胞種による細胞増殖への影響 104  
○赤坂司、松岡真琴、横山敦郎、橋本剛、亘理文夫
- 2P-3 Synthesis and characterization of highly conducting Carbon nanotube-Copper composite 105  
○Chandramouli Subramaniam, Takeo Yamada, Don. N. Futaba, Kenji Hata
- 2P-4 レーザー照射によってCoMoCATカーボンナノチューブから形成されたトランス-ポリアセチレン 106  
袴塚麻里、○渡邊文章、橘勝
- 2P-5 多層カーボンナノチューブファイバーおよびシートの作製 107  
○井上翼、島村佳伸、岡田守弘、三村秀典、内藤公喜
- 2P-6 高伝導率かつ透明な単層カーボンナノチューブ自立薄膜の作製 108  
○劉慶豊、藤ヶ谷剛彦、中嶋直敏
- 2P-7 カーボンナノチューブ/ポリベンゾオキサゾール複合体フィルムの開発 109  
○福丸貴弘、藤ヶ谷剛彦、中嶋直敏
- 2P-8 単層カーボンナノチューブ内包高分子複合ゲルカプセルの作製と評価 110  
○堤優介、藤ヶ谷剛彦、中嶋直敏
- 2P-9 表面修飾を利用した単層カーボンナノチューブ薄膜の微細パターンニング 111  
○野房勇希、蓬田陽平、柳和弘、竹延大志
- 2P-10 配向CNT-waferを用いた歪みセンサーのさらなる展開 112  
○山田健郎、山本由貴、早水裕平、蓬田美樹、イザディナジャファバディアリ、二葉ドン、湯村守雄、  
嶋賢治
- 2P-11 原子スケールの金属/ナノチューブ/金属接合に関するシミュレーション 113  
○草部浩一、斉藤北斗

#### ナノチューブの生成と精製

- 2P-12 ミリメートル長単層カーボンナノチューブの成長停止 114  
○長谷川馨、野田優

## 3月9日(水)

2P-13	樟脳を用いたステンレス基板上への高配向カーボンナノチューブの熱CVD法合成 ○瀬田悠、山際清史、小泉幸平、綾戸勇輔、桑野潤	115
2P-14	アルコールCVD法によるzigzagチューブの選択的合成 ○嘉陽安理、阿知波洋次、岡崎俊也	116
2P-15	先端放電型マイクロプラズマCVDにおける二酸化炭素とメタンを用いたCNTs合成 ○落合拓海、大原一慶、飯塚正知、川原田洋	117
2P-16	SWNT内における金属ナノワイヤー形成と触媒CVD法によるSWNT成長の分子動力学シミュレーション 松尾哲平、○野口拓哉、千足昇平、塩見淳一郎、丸山茂夫	118
2P-17	Ir触媒を用いたレーザー蒸発法による単層カーボンナノチューブの選択的合成 ○児玉拓也、井上亮人、児玉健、橋本健朗、阿知波洋次、岡崎俊也	119
2P-18	結晶性Coナノ粒子のエピタキシャル成長とナノチューブ触媒への応用 ○小川友以、吾郷浩樹、辻正治	120
2P-19	単層カーボンナノチューブのカイラリティ選択的可溶化を示すフルオレンポリマーの分子設計・合成 ○赤崎浩二郎、小澤寛晃、藤ヶ谷剛彦、中嶋直敏	121
2P-20	Separation of Single-Wall Carbon Nanotubes using Four Kinds of Gel Column Chromatography ○黄陽、劉華平、馮叶、田中丈士、藤井俊治郎、片浦弘道	122
2P-21	炭素源および成長温度が水平配向単層カーボンナノチューブの直径に与える影響 ○綾垣喬史、吾郷浩樹、辻正治	123
2P-22	クラスターをテンプレートとした化学気相成長法によるカーボンナノチューブの合成 ○中山拓哉、北浦良、角山寛規、宮田耕充、孫隕、佃達哉、篠原久典	124
2P-23	Interaction-dependent Chirality Separation of Single-Wall Carbon Nanotubes by Multicolumn Gel Chromatography ○劉華平、西出大亮、田中丈士、片浦弘道	125
2P-24	OPOレーザーによる金属単層カーボンナノチューブの選択分離におけるレーザー波長・強度効果 ○熊沢陽、田島勇、土屋好司、内田勝美、石井忠浩、矢島博文	126
2P-25	スーパーグロース:高結晶性単層カーボンナノチューブの高効率成長 ○木村寛恵、二葉ドン、湯村守雄、畠賢治	127
<b>ナノ炭素粒子</b>		
2P-26	ケイ素またはホウ素を含むグラファイトのレーザー蒸発により成長したグラファイト性多面体の精製 およびキャラクタリゼーション ○野口絵理子、野崎伊織、千種甫、田野上誉、小塩明、小海文夫	128
2P-27	ヒドロキシル修飾されたナノダイヤモンドの構造と振動スペクトル ○臼井孝介、西本佳央、Alister J. Page, Henryk A. Witek, Stephan Irle	129
2P-28	カーボンナノコイルにより構成されたDMFC電極の空隙の観測 ○甲斐田翔太、須田善行、田上英人、滝川浩史、桶真一郎、植仁志、大川隆、青柳伸宜、清水一樹	130
2P-29	Vibrational and NMR properties of Polyyynes and Microscopic studies of Polyyynes@SWNT ○Md. Mahbulul Haque, Lichang Yin, Ahmad R. T. Nugraha, Riichiro Saito, Tomonari Wakabayash, Yohei Sato, Masami Terauchi	131
2P-30	ポリグリセロールで被覆された水溶性ナノダイヤモンドのクロマトグラフィーによるサイズ分離 ○小松直樹、Li Zhao、瀧本竜哉、伊藤雅章、北川直子、木村隆英	132
2P-31	1MeV 電子照射によるダイヤモンドナノ粒子の構造変化 ○安坂幸師、寺田朋広、荒井重男、田中信夫、大澤映二、齋藤弥八	133

## 3月9日(水)

2P-32	鉄を含まない炭素粉末より作製した泡状ナノ炭素の超常磁性的挙動 ○神野誠、浅野洋仁、水野貴裕、飯島澄男、坂東俊治	134
2P-33	サブマリン式基板加熱法によるカーボンナノウォールの合成 ○横井裕之、石原史大、磯田竜成、武末健太郎	135
2P-34	LaC <sub>2</sub> ナノ結晶内包多層カーボンナノカプセルを含むサンプルにおけるTG-DTA曲線形状の サンプル質量依存性 ○山本和典、赤阪健	136
<b>グラフェン</b>		
2P-35	BNドープグラファイト薄膜のCVD成長 ○鈴木哲、日比野浩樹	137
2P-36	NICS値によるナノグラフェンの芳香族性に関する理論的研究 ○津村佳弘、笛野博之、田中一義	138
2P-37	エタノールおよびDMEからのグラフェンCVD合成比較 ○侯博、陳嘯、Erik Einarsson、千足昇平、丸山茂夫	139
2P-38	金属フリー・多層グラフェンの基板上への直接形成 ○高野宗一郎、野田優	140
2P-39	コルゲートしたグラフェンのエネルギー論と電子状態 ○岡田 晋	141
2P-40	金属上のグラフェンの電子状態の空間的変調 ○高木祥光、岡田晋	142
2P-41	アルコールCVD法で作製された二層グラフェンのラマン分光による研究 岡野真、松永隆祐、○松田一成、増淵寛、町田友樹、金光義彦	143
2P-42	アンチドット格子におけるエッジ状態に起因した強磁性 ○宮崎 涼、多田 健吾、上川正太、春山純志、松井 孝、福山寛	144
2P-43	室温マイルドプラズマトリートメントによるグラフェンエッジの選択修飾 ○加藤俊顕、ジアオリーイン、ワングシンラン、ワングハイリャン、リシャオリン、ザングリ、畠山力三、 ダイホンジエ	145
2P-44	穴のあいたグラフェンの電子構造とバンドギャップ制御 ○櫻井誠大、斎藤晋	146
2P-45	Density-Functional Tight-Binding Studies of Hexagonal Graphene Flakes ○Lili Liu、Francisco J. Martin-Martinez、Santiago Melchor、Jose A. Dobado、Thomas Heine、 Stephan Irle	147
<b>若手奨励賞候補者</b>		
2P-46	サブ秒パルス加熱によるガラス上でのCNTエミッタの形態および位置選択成長 ○関口康太郎、白鳥洋介、野田優	148
2P-47	フラーレン及びプラズマイオン挙動制御による窒素原子内包フラーレンの高効 ○趙順天、金子 俊郎、畠山 力三	149
2P-48	電子銃利用プラズマイオン照射法を用いたニッケル内包フラーレンの合成 ○馬越達也、石田裕康、金子俊郎、畠山力三	150
2P-49	金属型・半導体型含有量を制御した単層カーボンナノチューブネットワークにおける電気伝導機構 ○鶴戸口浩樹、柳和宏、大島勇吾、竹延大志、片浦弘道、石田敬雄、松田和之、真庭豊	151
2P-50	世界最短のピーポッド:フラーレンのCPP包摂錯体 ○中西勇介、宮田耕光、大町遥、松浦沙奈枝、瀬川泰知、伊丹健一郎、北浦良、篠原久典	152

### 3月9日(水)

2P-51 異なる環境における単層カーボンナノチューブのフェムト秒コヒーレントフォノン分光 ○牧野孝太郎、田所宏基、平野篤、白木賢太郎、前田優、長谷宗明	153
2P-52 SiC(0001)表面上グラフェンの結晶学的特徴 ○乗松航、楠美智子	154
2P-53 単層カーボンナノチューブの還元的化学修飾における置換基効果 ○千葉友莉子、加藤敬明、奥井裕美、赤松範久、山田道夫、前田優、長谷川正、永瀬茂	155
2P-54 様々な鉄化合物からなるSWNTフォレスト成長触媒の一般的な調整方法の開発 ○桜井俊介、西野秀和、二葉ドン、保田諭、山田健郎、Alan Maigne、中村栄一、湯村元雄、畠賢治	156

3月10日(木)

基調講演 発表40分・質疑応答5分  
特別講演 発表25分・質疑応答5分  
一般講演 発表10分・質疑応答5分  
ポスタープレビュー 発表1分・質疑応答なし

**特別講演 (9:00-9:45)**

- 3S-5 Carrier Control of Carbon Nanotube Transistor 5  
○Young Hee Lee

**一般講演 (9:45-10:30)**

**ハイブリッドカーボン**

- 3-1 単層カーボンナノチューブ内のコロネン1次元構造体 38  
○岡崎俊也、飯泉陽子、大窪清吾、片浦弘道、劉崢、末永和知、田原善夫、湯田坂雅子、岡田晋、飯島澄男
- 3-2 金属硫化物ナノワイヤー内包カーボンナノチューブの成長 39  
○小塩明、山崎貴之、山本誠、小海文夫
- 3-3 BNナノチューブに内包された $K_xC_{60}$ の第一原理計算 40  
○是常隆、斎藤晋、Jesse Noffsinger、Marvin L. Cohen

☆☆☆☆☆☆ 休憩 (10:30-10:45) ☆☆☆☆☆☆

**一般講演 (10:45-11:45)**

**グラフェン**

- 3-4 サファイア上で結晶化した金属触媒上での単層グラフェンのエピタキシャルCVD成長 41  
○吾郷浩樹、伊藤由人、胡宝山、カルロ・オロフェオ、辻正治、水田典章、池田賢一、水野清義
- 3-5 CVD法による数層及び多層グラフェンの低温成長 42  
○近藤大雄、八木克典、林賢二郎、佐藤信太郎、横山直樹
- 3-6 縮環芳香族化合物を用いるグラフェン物質の表面合成 43  
○中江隆博、櫛田芳裕、溝淵真吾、大西竜二、佐藤久子、坂口浩司
- 3-7 液体金属フラックス法による絶縁体上グラフェンの形成 44  
○日浦英文、M. L. リー、A. V. チュルニナ、塚越一仁

☆☆☆☆☆☆ 昼食 (11:45-13:00) ☆☆☆☆☆☆

**特別講演 (13:00-13:30)**

- 3S-6 マイクロ波プラズマCVDによるグラフェンの低温合成 6  
○長谷川雅考

**一般講演 (13:30-14:15)**

**ナノチューブの生成と精製**

- 3-8 シリコン貫通電極形成のためのCNT高速成長 45  
○大原一慶、落合拓海、飯塚正知、川原田洋
- 3-9 水晶基板上での水平配向単層カーボンナノチューブ高密度合成 46  
○井ノ上泰輝、長谷川 大祐、千足昇平、丸山茂夫
- 3-10 選択的(6,5)カーボンナノチューブの成長と機構 47  
○阿知波洋次、井上亮人、児玉健、橋本健朗、岡崎俊也

3月10日(木)

ポスタープレビュー (14:15-15:10)

ポスターセッション (15:10-16:30)

### ナノチューブの物性

- 3P-1 ナノ光ファイバー上に成長させたカーボンナノチューブの共鳴レイリー散乱分光 157  
長能卓哉、平井宏昌、岡田圭介、○毛利真一郎、室清文
- 3P-2 金属型単層カーボンナノチューブから作製した二層カーボンナノチューブの光電子分光 158  
○鷲谷智、米森啓太、柿原隆介、羽瀨隆文、平山大裕、林博和、姜健、岩澤英明、島田賢也、  
生天目博文、谷口雅樹、石井廣義、門脇広明、松田和之、柳和宏、真庭豊
- 3P-3 多糖類とSWNTとの相互作用に関する計算化学的究明 159  
○篠宮弘行、伊藤哲、土屋好司、矢島博文
- 3P-4 X線回折法による単層、2層、数層カーボンナノチューブのマクロ的層数分析 160  
○二葉ドン、山田 健郎、小橋 和文、湯村 守雄、嶋賢治
- 3P-5 単層カーボンナノチューブの電子状態への環境効果 161  
○平分康彦、田中泰彦、新留康郎、中嶋直敏
- 3P-6 らせん対称性を用いた第一原理計算によるカーボンナノチューブの系統的研究 162  
○加藤幸一郎、是常隆、斎藤晋
- 3P-7 窒素ドーパカーボンナノチューブの構造的多様性と電子特性制御 163  
○藤本義隆、斎藤晋
- 3P-8 有限長アームチュア炭素ナノチューブのケクレ構造とHOMO-LUMOギャップ 164  
○溝口 則幸
- 3P-9 水素吸着カーボンナノチューブにおける電気伝導の第一原理計算 165  
○川崎智代、石井史之、澤田啓介、斎藤峯雄
- 3P-10 遠赤外線領域における単層カーボンナノチューブの光学的応答 166  
○鄭 淳吉、岡崎俊也
- 3P-11 ホウ素ドーパカーボンナノチューブ一本の圧力下での電気輸送特性 167  
○渡邊徹、富岡史明、石井聡、津田俊輔、山口尚秀、高野義彦

### ナノチューブの生成と精製

- 3P-12 DNAを用いた半導体カーボンナノチューブの再分散およびその長さ分離 168  
○浅田有紀、井原和紀、大森滋和、二瓶史行、斎藤毅
- 3P-13 微小金属針先端におけるカーボンナノチューブ成長制御 169  
○金山久倫、嶋中康太、佐藤英樹
- 3P-14  $Al_2O_3$ 膜厚のMWCNTフォレストと屋根状グラファイトへの効果 170  
○厚味広樹、瀧本幸太郎、須田善行、田上秀人、滝川浩史、植仁志、清水一樹、梅田良人
- 3P-15 ゲルを用いた金属型/半導体型カーボンナノチューブの分離におけるpHとNaCl濃度の影響 171  
○ト部泰子、田中丈士、片浦弘道
- 3P-16 縦型高温パルスアーク放電装置の開発 172  
○安部優一、菅井俊樹
- 3P-17 直径1.4nm近傍の単層カーボンナノチューブ試料における直径選択分離法の開発 173  
○鈴木拓也、柳和宏、尾崎裕之、片浦弘道、真庭豊

### フラーレン

- 3P-18 X-ray Structure of a Divalent Metallofullerene  $Yb@C_{80}$  174  
○Xing Lu, Naomi Mizorogi, Zdenek Slanina, Takeshi Akasaka, Shigeru Nagase



## 3月10日(木)

3P-19	$M_2C_2@C_{82}$ (M=Sc, Ti, Fe) 金属内包フラーレンの電子 ○西本佳央、ステファンイレ	175
3P-20	Li@C <sub>60</sub> の電子状態 ○小笠原直子、八木創、善木将嗣、財満壮晋、宮崎隆文、才田守彦、木下冬子、日野照純	176
3P-21	DFTを用いたSc <sub>3</sub> C <sub>2</sub> @C <sub>80</sub> の最安定構造と電子構造の計算 ○大北壮祐、財満壮晋、八木創、宮崎隆文、沖本治哉、泉乃里子、中西勇介、篠原久典、日野照純	177
3P-22	γ-シクロデキストリンに包摂されたN@C <sub>60</sub> 水溶液のESR測定 ○加藤立久、柴田大樹、若林知成	178
3P-23	高周波スパッタ装置を用いたフラーレンへの原子インプランテーション ○若林知成、佐藤康介、木野村尚也、熊本渚	179
3P-24	Structures and Relative Stability of Gd <sub>2</sub> @C <sub>98</sub> W. Y. Gao, ○X. Zhao	180
3P-25	ハイブリッドプラズマを用いた金属内包フラーレンの連続多量合成 ○小牧久、中西勇介、篠原久典	181
3P-26	UV照射ポリマー化によるフラーレンナノウィスカーの新たな電子状態の出現 ○土井達也、小山恭平、青木伸之、落合勇一	182
3P-27	Optical, Electric and Magnetic Properties of Thin Polymerized Fullerene C <sub>60</sub> Films Deposited via Electron-Beam Dispersion ○ラザナウ イハル、三重野哲、カザチェンコ ビクトル	183
3P-28	水酸化フラーレンナノ結晶の作製と評価 馬場啓輔、○緒方啓典	184
3P-29	フラーレンナノウィスカー結晶の粉末X線回折による構造評価 ○緒方啓典、大波英幸	185
3P-30	QM/MD Simulations of Dynamic Fullerene Self-Assembly in Carbon Vapor With Inert Carrier Gas ○Hu-Jun Qian, Ying Wang, Keiji Morokuma, Stephan Irle	186
3P-31	高強度フェムト秒レーザーを用いた溶液内反応によるC <sub>70</sub> からのnon-IPRフラーレンの合成 ○兒玉健、佐藤祐旭、城丸春夫、Joseph H. Sanderson、藤野竜也、和田資子、若林知成、阿知波洋次	187
3P-32	固体NMRを用いて明らかになったポルフィリン-フラーレン複合体中の超分子構造 ○林宏暢、梅山有和、俣野善博、梶弘典、今堀博	188
3P-33	モルホリノシクロアルケンとC <sub>60</sub> フラーレンの熱[2+2]環付加 ○三木江翼、浅原時泰、長尾和明、伊熊直彦、小久保研、大島巧	189
3P-34	C <sub>60</sub> ナノウィスカーの成長制御 ○赤坂夢、宮澤薫一	190

### 内包ナノチューブ

3P-35	Fe内包カーボンナノチューブの磁気特性におけるPt添加の効果 ○松井悠祐、金子哲也、長田篤、佐藤英樹、藤原裕司、畑浩一	191
3P-36	有限長SWCNTに内包された水の構造:SWCNTエッジ効果 ○客野遥、松田和之、八尋瞳、伊波悠、福岡智子、宮田耕充、柳和宏、真庭豊、高井和之、榎敏明、片浦弘道、斎藤毅、湯村守雄、飯島澄男	192
3P-37	ゼオライト鑄型カーボンに吸着した水の挙動 ○松田和之、福岡智子、佐藤康史、客野遥、柳和宏、真庭豊、西原洋知、京谷隆	193
3P-38	Growth of Inner Nanotubes from Confined Ionic Liquid inside a Tip-closed SWNT ○Shimou Chen, Hong En Lim, Yasumitsu Miyata, Ryo Kitaura, Takeshi Saito, and Hisanori Shinohara	194

## 3月10日(木)

3P-39	アルコールCVD法による金属化合物内包ならびに“ティー型”カーボンナノチューブの成長 ○古山祐介、山崎貴之、小塩明、小海文夫	195
3P-40	直径の大きな単層カーボンナノチューブと剛直ポリマーとの間の相互作用によって誘起された 光学的励起状態 ○丹下将克、岡崎俊也、飯島澄男	196
3P-41	$\alpha$ -シクロデキストリン結晶中に包接されたポリインおよびシアノポリイン ○オ川真央、若林知成	197
3P-42	水素末端ポリインを内包した単層カーボンナノチューブの光学吸収スペクトル ○手柴雅臣、和田資子、吉田善紀、若林知成	198
3P-43	サイズ選別したポリインおよび銀イオンからなる1次元配位高分子の合成 ○富岡万貴子、若林知成、末永勇作	199
<b>ナノホーン</b>		
3P-44	グラフェン質ナノ物質のTGA構造解析における弱酸化効果 中村真紀、弓削亮太、飯島澄男、○湯田坂雅子	200
3P-45	ナノホーンとアミノ酸の相互作用 ○シン ツォウ、張 民芳、飯島澄男、湯田坂雅子	201
<b>若手奨励賞候補者</b>		
3P-46	その場ラマン分光電気化学法による電位印加時の単層カーボンナノチューブの電子構造評価 ○坂本伸悟、富永昌人	202
3P-47	金属原子ワイヤー内包カーボンナノチューブの合成と物性評価 ○崔 大憲、北浦 良、中西 良、宮田 耕充、篠原 久典	203
3P-48	原子内包カーボンナノチューブ薄膜トランジスタの作製と電気伝導特性 ○小山内陽祐、加藤俊顕、島山力三	204
3P-49	濃度勾配を用いたゲルクロマトグラフィーによるSWCNTの分離 ○禰 竜治、岡田貴子、有江隆之、秋田成司	205
3P-50	エレクトロクロミックなカーボン電極: 金属型単層カーボンナノチューブの色制御 ○守屋理恵子、柳和宏、竹延大志、内藤泰久、片浦弘道、松田和之、真庭豊	206
3P-51	再生医工学のためのキトサン/カーボンマイクロコイル複合膜の生体適合性評価 ○高橋克宗、土屋好司、矢島博文	207
3P-52	蛍光ゲル温度センサを用いた水中での単一カーボンナノチューブの熱伝導率評価 ○富田恭平、丸山央峰、新井史人	208
3P-53	燃料電池特性への多層カーボンナノチューブの構造依存性 ○喜多村慎也、橋新剛、玉置純、小島一男	209

**Tuesday, March 8th**

**Plenary Lectures: 40 min (Presentation) + 5 min (Discussion)**  
**Special Lectures: 25 min (Presentation) + 5 min (Discussion)**  
**General Lectures: 10 min (Presentation) + 5 min (Discussion)**  
**Poster Previews: 1 min (Presentation), No Discussion**

**Plenary Lecture (9:00-9:45)**

- 1S-1 Science and Industrial Applications of Nano-carbon Materials 1  
○Sumio Iijima

**General Lecture (9:45-10:30)**

**Properties and Applications of Nanotubes**

- 1-1 Probing surfactant molecules on SWCNTs by Raman spectroscopy 7  
Daisuke Nishide, Shunjiro Fujii, Takeshi Tanaka, ○Hiromichi Kataura
- 1-2 Evaluation of single-walled carbon nanotubes dispersed in surfactant solution by using Raman spectroscopy 8  
○Shinzo Suzuki, Masayuki Awazu, Yasuro Ikeda, Yuuya Hatano, Midori Nakanishi, Takashi Mizusawa, Akira Ono, Toshiya Okazaki, Yohji Achiba
- 1-3 Exciton-Exciton Interactions in Thin SWNTs Extracted from DWNTs 9  
○Takeshi Koyama, Yasumitsu Miyata, Hisanori Shinohara, Hideo Kishida, Arao Nakamura

☆☆☆☆☆☆ **Coffee Break (10:30-10:45)** ☆☆☆☆☆☆

**General Lecture (10:45-11:45)**

**Properties and Applications of Nanotubes**

- 1-4 Continuous Carrier Tuning in Metallic and Semiconducting SWNT Film 10  
○Hidekazu Shimotani, Satoshi Tsuda, Hongtao Yuan, Yohei Yomogida, Rieko Moriya, Taishi Takenobu, Kazuhiro Yanagi, Yoshihiro Iwasa
- 1-5 Carrier mobility and on/off ratio of carbon nanotube thin-film transistors fabricated by gas-phase filtration and transfer process 11  
○Dong-Ming Sun, Marina Y. Timmermans, Ying Tian, Albert G. Nasibulin, Shigeru Kishimoto, Takashi Mizutani, Esko I. Kauppinen and Yutaka Ohno
- 1-6 High mobility thin-film transistors using length-sorted semiconducting single-wall carbon nanotubes 12  
○Kazunari Shiozawa, Yasumitsu Miyata, Yuki Asada, Yutaka Ohno, Ryo Kitaura, Takashi Mizutani and Hisanori Shinohara
- 1-7 Highly Flexible All-SWNT Field-Effect Transistors 13  
○Shinya Aikawa, Erik Einarsson, Shohei Chiashi, Junichiro Shiomi, Eiichi Nishikawa, Shigeo Maruyama

☆☆☆☆☆☆ **Lunch Time (11:45-13:00)** ☆☆☆☆☆☆

**General Lecture (13:00-14:15)**

**Properties and Applications of Nanotubes**

- 1-8 Infrared Solar Cell Based on C<sub>60</sub> Encapsulated Semiconducting Single-Walled Carbon Nanotubes 14  
○Yongfeng Li, Soichiro Kodama, Toshiro Kaneko, and Rikizo Hatakeyama
- 1-9 Metal-free Fuel Cell Cathode Catalyst Prepared by Carbonization of Polybenzimidazole-wrapped Carbon Nanotubes 15  
○Takeshi Uchinoumi, Tsuyohiko Fujigaya, Naotoshi Nakashima
- 1-10 Improved Dispersibility of Single-walled Carbon Nanotubes (SWNTs) Using Subtle Growth Ambient and Its Enhancement of Conductivity in SWNT/Polymer Composites 16  
○Yoshiyuki Nonoguchi, Don N. Futaba, Seisuke Ata, Motoo Yumura, Kenji Hata
- 1-11 Carbon Nanotubes with Temperature-Invariant Creep and Creep-Recovery from -150°C to 970°C 17  
○Ming Xu, Don N. Futaba, Motoo Yumura, Kenji Hata

## Tuesday, March 8th

- 1-12 Applications of optical responsive carbon nanotubes cell cultured substrate 18  
○Takao Sada, Tsuyohiko Fujigaya, Naotoshi Nakashima

### ☆☆☆☆☆☆ Coffee Break (14:15-14:30) ☆☆☆☆☆☆

#### Special Lecture (14:30-15:00)

- 1S-2 The Advantages and Applications of Nanocarbon Phase Transformations 2  
○Amanda S. Barnard

#### General Lecture (15:00-16:00)

##### Hybrid Carbon

- 1-13 Development of Multi-stage Ion Trap Mobility System 19  
Masashi Shinozaki, Yoshihiko Sawanishi, ○Toshiki Sugai
- 1-14 Electronic States of Linear Polyene Molecules Embedded in Nano-Structured Molecular Assemblies 20  
○Tomonari Wakabayashi, Mao Saikawa, Masashi Teshiba, Yoriko Wada
- 1-15 Size-Dependent Cellular Uptake of Carbon Nanoparticles 21  
○Minfang Zhang, Xin Zhou, Yoshio Tahara, Sumio Iijima, Masako Yudasaka
- 1-16 HRTEM observation of the platinum clusters interacting with carbon atoms at elevated temperatures 22  
○Keita Kobayashi, Kazu Suenaga

#### Poster Preview (16:00-17:00)

#### Poster Session (17:00-18:20)

##### Formation and Purification of Nanotubes

- 1P-1 Carbon Nanotube Growth on ZnO(000-1) Substrates using Alcohol Gas Source Method 49  
○Tomoyuki Tsutsui, Takayasu Iokawa, Takahiro Maruyama, Shigeya Naritsuka
- 1P-2 QM/MD Simulations of Carbon Nanotube Cap Nucleation Using Acetylene Feedstock 50  
and an Fe<sub>38</sub> Catalyst Nanoparticle  
○Ying Wang, HuJun Qian, Alister J. Page, Keiji Morokuma, Stephan Irlle
- 1P-3 PERIPUTOS: Purity Evaluation of SWCNTs Using Raman Spectroscopy, Effect of Surfactants 51  
○Miki Taga, Daisuke Nishide, Shunjiro Fujii, Takeshi Tanaka, and Hiromichi Kataura
- 1P-4 Low Pressure Growth of SWNT using Pt catalyst by Alcohol Gas Source Method in High Vacuum 52  
○Yoshihiro Mizutani, Takahiro Maruyama, Shigeya Naritsuka, Sumio Iijima
- 1P-5 Comparison of Carbon Nanotube Growth from 4H-SiC and 6H-SiC by 53  
Surface Decomposition using Raman Spectroscopy  
○Yuki Ishiguro, Satoshi Sakakibara, Hiroaki Ito, Takahiro Maruyama, Shigeya Naritsuka
- 1P-6 Novel atomization and dispersion method of CNT using wet-type super atomizer "Nanovater". 54  
○Tadashi Takashima, Yumi Murai, Kunio Miyashiro, Katsuyuki Utaka, Shin-ichiro Kato,  
Yusuke Miyazaki
- 1P-7 Molecular-assembled synthesis of single-wall carbon nanotubes 55  
○Yasumitsu Miyata, Marie Suzuki, Jinying Zhang, Miho Fujihara, Ryo Kitaura, Hiromichi Kataura,  
Hisanori Shinohara
- 1P-8 Effect of Sn catalyst concentration on purity synthesis of carbon nanocoil by substrate CVD 56  
with catalytic vapor supply  
○Yuichi Ishii, Kotaro Takimoto, Yoshiyuki Suda, Hideto Tanoue, Hirofumi Takikawa, Hitoshi Ue,  
Kazuki Shimizu, Yoshito Umeda
- 1P-9 Length Sorting of Single-Wall Carbon Nanotubes using Size Exclusion Gel Chromatography 57  
○Satoshi Asano, Takeshi Tanaka, Hiromichi Kataura

## Tuesday, March 8th

1P-10	Control on the Electrochemical Process at Carbon Nanotube Synthesis at Room Temperature Ahmed Shawky, Masahiro Tanabe, ○Satoshi Yasuda and Kei Murakoshi	58
1P-11	Selective synthesis of (6, 5) carbon nanotubes from C <sub>60</sub> precursor ○Jinying Zhang, Yasumitsu Miyata, Ryo Kitaura, and Hisanori Shinohara	59
1P-12	Synthesis of Multi-Walled Carbon Nanocoils over Sn/Fe/MgO Catalyst by Catalytic CVD ○Lim Siew Ling, Kotaro Takimoto, Yoshiyuki Suda, Hideto Tanoue, Hirofumi Takikawa, Hitoshi Ue, Kazuki Shimizu, Yoshida Umeda	60
1P-13	Carbon nanotube growth from C <sub>60</sub> -fullerene nuclei with various source gases Daisuke Takagi, Fumihiko Maeda, ○Ryota Negishi, Shogo Agata, Yoshihiro Kobayashi, Yoshikazu Homma	61
1P-14	Single-walled carbon nanotubes closing and opening: a density-functional tight-binding molecular dynamics study ○Hironori Hara, Stephan Irle	62
1P-15	Transition from [n]Cycloparaphenylenes to SWCNTs: SCC-DFTB Studies of Diels Alder Reactions and Raman Spectra ○Ryota Umeda, Yoshifumi Nishimura, Stephan Irle	63
1P-16	Extraction of high purity and micrometer-long semiconducting single-wall carbon nanotubes ○Kazunari Shiozawa, Yasumitsu Miyata, Ryo Kitaura, Hisanori Shinohara	64
<b>Applications of Nanotubes</b>		
1P-17	Electrode Properties of Nanocarbon-Polymer Composites ○Tomohiro Sakashita, Kouki Okamura, Shinzi Kawasaki	65
1P-18	Electrical and Mechanical Properties of Carbon Nanotube/Polyisoprene Composites with Low Percolation Threshold and High Conductivity ○Tomoya Nagaoka, Ayumu Sakai, Katsumi Uchida, Koji Tsuchiya, Masayosi Ito,	66
1P-19	Cell aggregation to a carbon nanotube scaffold with dielectrophoresis ○Makoto Matsuoka, Tsukasa Akasaka, Takeshi Hashimoto, Yasunori Totsuka, Fumio Watari	67
1P-20	Influence of Device Processing on Electrical Properties of Carbon Nanotube Field Effect Transistors ○Mikito Tanaka, Yoichi Ito, Bongyong Jang, Yasuhiko Hayashi, Naoki Kishi, Tetsuo Soga, Takashi Jimbo	68
1P-21	Transparent Conductive Thin Films of Single-Wall Carbon Nanotubes Encapsulating Organic Molecules ○Naoki Kishi, Ikuma Miwa, Toshiya Okazaki, Takeshi Saito, Toshihisa Mizutani, Hiroaki Tsuchiya, Tetsuo Soga, Takashi Jimbo	69
1P-22	Thin-film transistors using aligned semiconducting single-wall carbon nanotubes separated by agarose gel chromatography ○Shunjiro Fujii, Takeshi Tanaka, Hiromichi Kataura	70
1P-23	The simple method for analyzing the interaction between carbon nanotube and molecules ○JongTae Yoo, Tsuyohiko Fujigaya, Naotoshi Nakashima	71
1P-24	Controllable Dispersity of Carbon Nanotubes ○Naoyuki Uchiyama, Naotoshi Nakashima	72
1P-25	Highly Conductive Vein-Like SWNT Network ○Kazufumi Kobashi, Seisuke Ata, Takeo Yamada, Don N. Futaba, Motoo Yumura, Kenji Hata	73
1P-26	Ion-Gel Gating of Single-Walled Carbon Nanotube Films ○Di Wen, Yohei Yomogida, Hidekazu Shimotani, Kazuhiro Yanagi, Yoshihiro Iwasa, Taishi Takenobu	74
1P-27	Hybridization of DNA/carbon nanotube hybrid with biocompatible polycation ○Tsuyohiko Fujigaya, Yuki Yamamoto, Arihiro Kano, Atsushi Maruyama, Naotoshi Nakashima	75

## Tuesday, March 8th

- 1P-28 Inkjet carrier doping to single-walled carbon nanotube film 76  
○Satoki Matsuzaki, Kazuhiro Yanagi, Taishi Takenobu

### Properties of Nanotubes

- 1P-29 Chirality dependence of coherent phonon amplitudes in single wall carbon nanotubes 77  
○Ahmad-Ridwan Tresna Nugraha, Kentaro Sato, Riichiro Saito
- 1P-30 Density Functional Theory Calculations of the Cleavage of CC Bonds of Nanotubes by Diketone Formation 78  
○Takashi Yumura, Toshiyuki Kanemitsu
- 1P-31  $G^+$ / $G^-$  behavior of SWCNTs under the dispersion process 79  
○Satoko Nishiyama, Takeshi Tanaka, Hiromichi Kataura
- 1P-32 Raman spectroscopy of SWNTs grown from boron- and nitrogen-containing feedstocks 80  
○Satoru Suzuki, Hiroki Hibino

### Graphene

- 1P-33 Dependence of Raman intensity and shift on different layer stacking of graphene 81  
○Kentaro Sato, Jin Sung Park, Riichiro Saito
- 1P-34 Polarization dependence of x-ray absorption spectra of Graphene 82  
○Md. Tareque Chowdhury, Riichiro Saito
- 1P-35 Synthesis and Spectroscopical Characterization of Peripentacene 83  
○Yosuke Ishii, Tomohiro Sakashita, Hidenori Kato, Masashige Takatori, Shinji Kawasaki
- 1P-36 Chemical and Electrical Characterization of Graphene Formed by Gallium Flux Liquid Phase Epitaxy 84  
○Michael V. Lee, Hidefumi Hiura, Anastasia V. Tyurnina, and Kazuhito Tsukagoshi
- 1P-37 Synthesis of Single-Layer Graphenes by Atmospheric Alcohol-Chemical Vapor Deposition 85  
○Akiji Fukaya, Naoki Kishi, Ryo Sugita, Tetsuo Soga, Takashi Jimbo
- 1P-38 Quantum capacitance of mono- bi- and tri-layer graphene with different stacking orders 86  
○Takahiro Eguchi, Kentaro Sato and Riichiro Saito
- 1P-39 Structural Changes of Carbon Nanowalls by Heat Treatment in Vacuum 87  
○Seiya Suzuki, Masamichi Yoshimura
- 1P-40 Electronic-structure control of thin film of graphite: Interlayer spacing and thickness dependency 88  
○Nguyen Thanh Cuong, Minoru Otani, Susumu Okada
- 1P-41 QM/MD Simulation of Graphene Hole Repair by  $C_2$  molecules 89  
○Yoshitaka Okita, Hironori Hara, Lili Liu, Stephan Irle

### Hybrid Carbon

- 1P-42 Field Emitter Using Upright Carbon Nanotwists with sputtered Pt coat 90  
○Yuki Sugioka, Yoshiyuki Suda, Hideto Tanoue, Hirofumi Takikawa, Hitoshi Ue, Kazuki Shimizu, Yoshito Umeda
- 1P-43 Evaluation of Dispersant Effectiveness of Lipid-PEG For Nano-Carbons Using Carbon Nanohorns 91  
Mei Yang, Momoyo Wada, Minfang Zhang, Kostas Kostarelos, Sumio Iijima, Mitsutoshi Masuda,  
○Masako Yudasaka
- 1P-44 Long-term Structural Observation of Charged Particles by Ion Trap Mobility System 92  
○Yoshihiko Sawanishi, Masashi Shinozaki, Toshiki Sugai
- 1P-45 Preparation of supercapacitor using  $RuO_x$ -supported-Arc-Black and its specific capacitance 93  
○Toshiyuki Sato, Takashi Ikeda, Yoshiyuki Suda, Hideto Tanoue, Hirofumi Takikawa, Shinichiro Oke, Hitoshi Hue, Takashi Okawa, Nobuyoshi Aoyagi, Kazuki Shimizu

### Candidates for the Young Scientist Poster Award

- 1P-46 Electron-accepting properties of fullerenes at the liquid/liquid interface 94  
○Tsumumi Hayashi, Tomohiko Okugaki, Hideyuki Takahashi, Kohji Maeda, Kazuyuki Tohji

## Tuesday, March 8th

1P-47	Facile and efficient synthesis of high-crystallinity double-wall carbon nanotubes ○Toshiya Nakamura, Yasumitsu Miyata, Hong En Lim, Ryo Kitaura, Hisanori Shinohara	95
1P-48	Sorting of double-wall carbon nanotubes by electronic structure ○Miho Fujihara, Yasumitsu Miyata, Marie Suzuki, Ryo Kitaura, Hisanori Shinohara	96
1P-49	Electronic Spectra of Polyynes-Iodine Complexes in Hexane ○Yoriko Wada, Tomonari Wakabayashi	97
1P-50	Significance of zigzag edges in electron transport properties of graphene sheets with periodic nanoholes ○Hideyuki Jippo, Mari Ohfuchi, Chioko Kaneta	98
1P-51	Spin-Related Novel Optical Phenomena in Single-Walled Carbon Nanotubes ○Satoru Konabe, Susumu Okada	99
1P-52	Synthesis and characterization of AgI nanowires encapsulated in carbon nanotubes ○Shin-ichi Ito, Ryo Kitaura, Teppei Yamada, Hiroshi Kitagawa, Dong Yong Kim, Suguru Noda, Hirofumi Yoshikawa, Kunio Awaga, Hisanori Shinohara	100
1P-53	Control of graphene etching by atomic structure of solid surfaces ○Takahiro Tsukamoto, Toshio Ogino	101
1P-54	Structures and Electronic Properties of Scandium Carbide Endohedral Metallofullerenes ○Naomi Mizorogi, Takeshi Akasaka, Shigeru Nagase	102

Wednesday, March 9th

**Special Lectures: 25 min (Presentation) + 5 min (Discussion)**  
**General Lectures: 10 min (Presentation) + 5 min (Discussion)**  
**Poster Previews: 1 min (Presentation), No Discussion**

**Special Lecture (9:00-9:30)**

- 2S-3 Application of Flat-Panel Field Emission Lamp using Carbon Nanotube-Carbon Nanohorn Cathodes 3  
○Ryota Yuge

**General Lecture (9:30-10:30)**

**Formation and Purification of Nanotubes**

- 2-1 Cyclic purification of semiconducting and metallic carbon nanotubes using separation by Electric-field inducing Layer Formation 23  
○Kazuki Ihara, Takeshi Saito, Fumiyuki Nihey
- 2-2 Diameter-Based Separation of Single-Walled Carbon Nanotubes through Selective Extraction with Dipyrene Nanotweezers 24  
○Naoki Komatsu, A. F. M. Mustafizur Rahman, Feng Wang, Kazunari Matsuda, Takahide Kimura
- 2-3 Effect of Sonication on the Length Distribution of Single Wall Carbon Nanotubes 25  
○Shigekazu Ohmori, Takeshi Saito, Yuki Asada, Motoo Yumura, Sumio Iijima
- 2-4 QM/MD Simulation of SWNT Nucleation on Transition-Metal Carbide Nanoparticles 26  
○Stephan Irlé, Alister J Page, Honami Yamane, Y. Ohta, Keiji Morokuma

☆☆☆☆☆☆ **Coffee Break (10:30-10:45)** ☆☆☆☆☆☆

**General Lecture (10:45-11:45)**

**Graphene**

- 2-5 Stacking-order sensitive Raman modes of graphene 27  
○R. Saito, K. Sato, C. Cong, Y. Ting, M. S. Dresselhaus
- 2-6 Energetics and Electronic Structures of Graphene Adsorbed on HfO<sub>2</sub> Surfaces 28  
○Katsumasa Kamiya, Naoto Umezawa, Susumu Okada
- 2-7 Large area graphene from camphor for organic solar cells application 29  
○Golap Kalita, Masahiro Matsushima, Koichi Wakita and Masayoshi Umeno
- 2-8 Analysis of Magneto Resistance Fluctuation in graphene thin film 30  
○A. Mahjoub, Shotarou Motooka, Tkuto Abe, Nobuyuki Aoki, D. K.Ferry, J. P. Bird, Yuuichi Ochiai

☆☆☆☆☆☆ **Lunch Time (11:45-13:00)** ☆☆☆☆☆☆

**Awards Ceremony (13:00-13:45)**

**Special Lecture (13:45-14:15)**

- 2S-4 Fundamentals and Recent Progress of Organic Thin-film Solar Cells 4  
○Masahiro Hiramoto

**General Lecture (14:15-15:15)**

**Fullerenes**

- 2-9 Fullerene Peapod-Poly(3-hexylthiophene) Hybrids 31  
○Tomokazu Umeyama, Noriyasu Tezuka, Yoshihiro Matano, Hiroshi Imahori
- 2-10 Synthesis and Photophysical Properties of Metallofullerenes — Zinc Porphyrin Conjugates: Impact of Endohedral Clusters 32  
○Lai Feng, Shankara Gayathri Radhakrishnan, Naomi Mizorogi, Zdenek Slanina, Hidefumi Nikawa, Takahiro Tsuchiya, Takeshi Akasaka, Shigeru Nagase, Nazario Martı́n, Dirk M. Guldi



## Wednesday, March 9th

- 2-11 Electronic structure and entrapped cluster structure of  $C_{78}$  endohedral fullerenes 33  
○Takafumi Miyazaki, Yusuke Aoki, Sousuke Ookita, Hajime Yagi and Shojun Hino
- 2-12 Photo-polymerization of  $C_{60}$  thin film using optical vortex irradiation 34  
○Nobuyuki Aoki, Tatsuya Doi, Xiaojun Wei, Kyouhei Koyama, Katsuhiko Miyamoto, Takashige Omatsu, Jonathan P. Bird and Yuichi Ochiai

☆☆☆☆☆☆ Coffee Break (15:15-15:30) ☆☆☆☆☆☆

### General Lecture(15:30-16:15)

#### Fullerenes

- 2-13 Synthesis of Polyhydroxylated Fullerene  $C_{60}(OH)_6$  via Chlorofullerene  $C_{60}Cl_6$  and its Characterization using ESI-MS Spectroscopy 35  
○Hiroshi Ueno, Toshiki Sugai, Hiroshi Moriyama
- 2-14 Thermal and oxidative stabilities of multi-arylated [60]fullerene derivatives 36  
○Ken Kokubo, Miyato Kashiara, Yano Tomomi, Katsutomo Tanaka, Naohiko Ikuma, Takumi Oshima
- 2-15 Influence of UV Irradiation on Polymerization of LLIP-Prepared  $C_{60}$  Nanowhiskers 37  
○Ying-Hui Wang, Kun'ichi Miyazawa

### Poster Preview(16:15-17:10)

### Poster Session(17:10-18:30)

#### Applications of Nanotube

- 2P-1 Synthesis and Applications of Carbon Nanotube Sponge Macrostructures 103  
Xuchun Gui, Tianzhun Wu, ○Rong Xiang, Zikang Tang
- 2P-2 Cell proliferation on Carbon Nanotubes Coated Dishes in Different Cell Lines 104  
○Tsukasa Akasaka, Makoto Matsuoka, Atsuro Yokoyama, Takeshi Hashimoto
- 2P-3 Synthesis and characterization of highly conducting Carbon nanotube-Copper composite 105  
○Chandramouli Subramaniam, Takeo Yamada, Don. N. Futaba, Kenji Hata
- 2P-4 Formation of trans-polyacetylene from CoMoCAT carbon nanotubes by laser irradiation 106  
Mari Hakamatsuka, ○Fumiaki Watanabe, Masaru Tachibana
- 2P-5 Spinning multiwalled carbon nanotube fibers and sheets 107  
○Yoku Inoue, Yoshinobu Shimamura, Morihiko Okada, Hidenori Mimura, Kimiyoshi Naito
- 2P-6 Fabrication of Free-Standing Ultrathin Single-Walled Carbon Nanotube Films with Highly Conductivity and transparency 108  
○Qingfeng Liu, Tsuyohiko Fujigaya, Naotoshi Nakashima
- 2P-7 Development of Carbon Nanotube/Polybenzoxazole Composite Films 109  
○Takahiro Fukumaru, Tsuyohiko Fujigaya, Naotoshi Nakashima
- 2P-8 Preparation and evaluation of polymer gel capsules containing SWNTs 110  
○Yusuke Tsutsumi, Tsuyohiko Fujigaya, Naotoshi Nakashima
- 2P-9 Fine patterning of single-walled carbon nanotube thin-film by surface modification 111  
○Yuki Nobusa, Yohei Yomogida, Kazuhiro Yanagi, Taishi Takenobu
- 2P-10 Further development of Aligned Carbon Nanotube Wafer based Strain Sensors 112  
○Takeo Yamada, Yuki Yamamoto, Yuhei Hayamizu, Yoshiki Yomogida, Ali Izadi-Najafabadi, Don N. Futaba, Motoo Yumura, Kenji Hata
- 2P-11 A simulation of an atomic-scale metal/nanotube/metal junction 113  
○Koichi Kusakabe, Hokuto Saito

## Wednesday, March 9th

### Formation and Purification of Nanotubes

- 2P-12 Growth Termination of Millimeter-Tall Single-Walled Carbon Nanotubes 114  
○Kei Hasegawa, Suguru Noda
- 2P-13 Synthesis of Highly Aligned Carbon Nanotubes on Stainless steel substrates by a Thermal CVD Method with Camphor 115  
○Hisashi Seta, Kiyofumi Yamagiwa, Kohei Koizumi, Yusuke Ayato, Jn Kuwano
- 2P-14 The enhancement of zigzag and near zigzag tubes in the production of single wall carbon nanotube by alcohol CVD 116  
○Yasumichi Kayo, Yohji Achiba, Toshiya Okazaki
- 2P-15 Synthesis of CNTs by Antenna-edge Microwave Plasma CVD from Carbon dioxide and Methane Gas 117  
○Takumi Ochiai, Kazuyosho Oohara, Iizuka Masatomo, Hiroshi Kawarada
- 2P-16 Molecular Dynamics Simulations of Metal Nanowire Formation within a SWNT and the SWNT Growth Process by Catalytic CVD 118  
Tepei Matsuo, ○Takuya Noguchi, Shohei Chiashi, Junichiro Shiomi, Shigeo Maruyama
- 2P-17 Selective growth of SWNTs on Ir catalyst combined with a laser vaporization method 119  
○Takuya Kodama, Akihito Inoue, Takeshi Kodama, Kenrou Hashimoto, Yohji Achiba, Toshiya Okazaki
- 2P-18 Epitaxial growth of faceted Co nanoparticles and their application to carbon nanotube growth 120  
○Yui Ogawa, Hiroki Ago, Masaharu Tsuji
- 2P-19 New approach for chirality recognition of single-walled carbon nanotubes using fluorene-based copolymers 121  
○Kojiro Akazaki, Hiroaki Ozawa, Tsuyohiko Fujigaya, Naotoshi Nakashima
- 2P-20 Separation of Single-Wall Carbon Nanotubes using Four Kinds of Gel Column Chromatography 122  
○Yang Huang, Huaping Liu, Ye Feng, Takeshi Tanaka, Shunjiro Fujii, Hiromichi Kataura
- 2P-21 Effects of carbon source and growth temperature on diameter of horizontally-aligned single-walled carbon nanotubes on sapphire 123  
○Takafumi Ayagaki, Hiroki Ago, Masaharu Tsuji
- 2P-22 Chemical vapor deposition growth of carbon nanotubes using cluster templates 124  
○Takuya Nakayama, Ryo Kitaura, Hironori Tsunoyama, Yasumitsu Miyata, Sun Yun, Tatsuya Tsukuda, Hisanori Shinohara
- 2P-23 Interaction-dependent Chirality Separation of Single-Wall Carbon Nanotubes by Multicolumn Gel Chromatography 125  
○Huaping Liu, Daisuke Nishide, Takeshi Tanaka, Hiromichi Kataura
- 2P-24 Effects of Laser Wavelength and Power on the Selective Separation for Metal Single-walled Carbon Nanotubes with OPO Laser Irradiation 126  
○Akira Kumazawa, Isamu Tajima, Katsumi Uchida, Koji Tsuchiya, Tadahiro Ishii, Hirofumi Yajima
- 2P-25 Super-growth: Combining High Yield with High Crystallinity 127  
○Hiroe Kimura, Don N. Futaba, Motoo Yumura, Kenji Hata

### Carbon Nanoparticles

- 2P-26 Purification and Characterization of Graphitic Polyhedra Grown by Laser Vaporization of Graphite Containing Silicon or Boron 128  
○Eriko Noguchi, Iori Nozaki, Hajime Chigusa, Homare Tanogami, Akira Koshio, Fumio Kokai
- 2P-27 The molecular structure and vibrational spectroscopy of hydroxylated nanodiamonds. 129  
○Kousuke Usui, Yoshio Nishimoto, Alister J. Page, Henryk A. Witek, Stephan Irle
- 2P-28 Observation of void in DMFC electrode composed with carbon nanocoil 130  
○Shota Kaida, Yoshiyuki Suda, Hideto Tanoue, Hirohumi Takikawa, Shin-ichiro Oke, Hitoshi Ue, Takashi Okawa, Nobuyoshi Aoyagi, Kazuki Shimizu

## Wednesday, March 9th

- 2P-29 Vibrational and NMR properties of Polyynes and Microscopic studies of Polyynes@SWNT 131  
○Md. Mahbubul Haque, Lichang Yin, Ahmad R. T. Nugraha, Riichiro Saito, Tomonari Wakabayash, Yohei Sato, Masami Terauchi
- 2P-30 Chromatographic Separation of Highly Soluble Nanodiamond Prepared by Polyglycerol Grafting 132  
○Naoki Komatsu, Li Zhao, Tatsuya Takimoto, Masaaki Ito, Naoko Kitagawa, Takahide Kimura
- 2P-31 1 MeV electron irradiation-induced structural changes of nanometer-sized diamond particles 133  
○Koji Asaka, Tomohiro Terada, Shigeo Arai, Nobuo Tanaka, Eiji Osawa, Yahach Saito
- 2P-32 Superparamagnetic behavior of carbon nanofoam produced from iron free carbon powder 134  
○Makoto Jinno, Hirohito Asano, Takahiro Mizuno, Sumio Iijima, Shunji Bandow
- 2P-33 Synthesis of Carbon Nanowalls by a Submarine-style Substrate Heating Method 135  
○Hiroyuki Yokoi, Fumihito Ishihara, Tatsunori Isoda, Kentaro Takesue
- 2P-34 Evolution of the DTA-TG curves as a function of sample mass containing LaC<sub>2</sub> nano-crystallites encaged in multi-shell carbon nanocapsules 136  
○Kazunor Yamamoto, Takeshi Akasaka

### Graphene

- 2P-35 Chemical vapor deposition of BN-doped graphite thin films 137  
○Satoru Suzuki, Hiroki Hibino
- 2P-36 Theoretical Study of Aromaticity by Nucleus-Independent Chemical Shifts in Nanographenes 138  
○Yoshihiro Tsumura, Hiroyuki Fueno, Kazuyoshi Tanaka
- 2P-37 Comparison study on CVD synthesis of graphene using ethanol and dimethyl ether 139  
○Bo Hou, Xiao Chen, Erik Einarsson, Shohei Chiashi, Shigeo Maruyama
- 2P-38 Direct Fabrication of Metal-Free Multilayer Graphene on Substrates 140  
○Soichiro Takano, Suguru Noda
- 2P-39 Energetics and Electronic Structure of Corrugated Graphene 141  
○Susumu Okada
- 2P-40 Spatial Modulation of Electronic Structure of Graphene on Metal Surfaces 142  
○Yoshiteru Takagi, Susumu Okada
- 2P-41 Raman Spectroscopic Study in a Bilayer Graphene Synthesized by Alcohol Chemical Vapor Deposition Method 143  
Makoto Okano, Ryusuke Matsunaga, ○Kazunari Matsuda, Satoshi Masubuchi, Tomoki Machida, Yoshihiko Kanemitsu
- 2P-42 All-carbon ferromagnetism derived from edge states in antidot-lattice graphenes 144  
○Ryo Miyazaki, Kengo Tada, Syota. Kamikawa, Junji. Haruyama, Takashi Matsui, Hiroshi Fukuyama
- 2P-43 Selective Edge Functionalization of Graphene by Room-Temperature Mild Plasma Treatment 145  
○Toshiaki Kato, Liying Jiao, Xinran Wang, Hailiang Wang, Xiaolin Li, Li Zhang, Rikizo Hatakeyama, and Hongjie Dai
- 2P-44 Electronic structure and band gap control of graphene with holes 146  
○Masahiro Sakurai, Susumu Saito
- 2P-45 Density-Functional Tight-Binding Studies of Hexagonal Graphene Flakes 147  
○Lili Liu, Francisco J. Martin-Martinez, Santiago Melchor, Jose A. Dobado, Thomas Heine, Stephan Irle

### Candidates for the Young Scientist Poster Award

- 2P-46 Morphology- and Position-Selective Growth of CNT Emitters on Glasses by Subsecond Heating Pulses 148  
○Kotaro Sekiguchi, Yosuke Shiratori, Suguru Noda

## Wednesday, March 9th

- 2P-47 Highly-Efficient Synthesis of Nitrogen Atom Endohedral Fullerene by Controlling Fullerene and Plasma Ion Behaviors 149  
○Soon Cheon Cho, Toshiro Kaneko, and Rikizo Hatakeyama
- 2P-48 Synthesis of Nickel Atom Endohedral Fullerene Using Plasma Ion Irradiation Method with Electron Beam Gun 150  
○Tatsuya Umakoshi, Hiroyasu Ishida, Toshiro Kaneko, Rikizo
- 2P-49 Transport Mechanisms in Single-Wall Carbon Nanotube Networks formed by Controlled Content-ratio of Metallic and Semiconducting Types 151  
○Hiroki Udoguchi, Kazuhiro Yanagi, Yugo Oshima, Taishi Takenobu, Hiromichi Kataura, Takao Ishida, Kazuyuki Matsuda, Yutaka Maniwa
- 2P-50 The shortest nano-peapods : Complexation of fullerenes with cycloparaphenylenes 152  
○Yusuke Nakanishi, Yasumitsu Miyata, Haruka Omachi, Sanae Matsuura, Yasutomo Segawa, Kenichiro Itami, Ryo Kitaura and Hisanori Shinohara
- 2P-51 Femtosecond Coherent Phonon Spectroscopy of Carbon Nanotubes in Different Environments 153  
○Kotaro Makino, Hiroki Tadokoro, Atsushi Hirano, Kentaro Shiraki, Yutaka Maeda, Muneaki Hase
- 2P-52 Crystallographic features of graphene on SiC (0001) 154  
○Wataru Norimatsu, Michiko Kusunoki
- 2P-53 Substituent Effects on the Reductive Functionalization of SWNTs 155  
○Yuriko Chiba, Takaaki Kato, Yumi Okui, Norihisa Akamatsu, Michio Yamada, Yutaka Maeda, Tadashi Hasegawa, Takeshi Akasaka, Shigeru Nagase
- 2P-54 Generalized Preparation Method of the Catalyst for Single-Walled Carbon Nanotube Forest Growth from Various Iron Compounds 156  
○Shunsuke Sakurai, Hidekazu Nishino, Don N Futaba, Satoshi Yasuda, Takeo Yamada, Alan Maigne, Eiichi Nakamura, Motoo Yumura, and Kenji Hata

Thursday, March 10th

**Plenary Lectures: 40 min (Presentation) + 5 min (Discussion)**

**Special Lectures: 25 min (Presentation) + 5 min (Discussion)**

**General Lectures: 10 min (Presentation) + 5 min (Discussion)**

**Poster Previews: 1 min (Presentation), No Discussion**

**Plenary Lecture (9:00-9:45)**

- 3S-5 Carrier Control of Carbon Nanotube Transistor 5  
○Young Hee Lee

**General Lecture (9:45-10:30)**

**Hybrid Carbon**

- 3-1 Coaxially Stacked Coronene Column inside Single-Walled Carbon Nanotube 38  
○Toshiya Okazaki, Yoko Iizumi, Shingo Okubo, Hiromichi Kataura, Zhen Liu, Kazu Suenaga, Yoshio Tahara, Masako Yudasaka, Susumu Okada, Sumio Iijima
- 3-2 Growth of Carbon Nanotubes Filled with Metal Sulfide Nanowires 39  
○Akira Koshio, Takayuki Yamasaki, Makoto Yamamoto, Fumio Kokai
- 3-3 First-principles study of  $K_xC_{60}$  encapsulated in boron-nitride nanotubes 40  
○Takashi Koretsune, Susumu Saito, Jesse Noffsinger, Marvin L. Cohen

☆☆☆☆☆☆ Coffee Break (10:30-10:45) ☆☆☆☆☆☆

**General Lecture (10:45-11:45)**

**Graphene**

- 3-4 Epitaxial CVD growth of single-layer graphene over metal films crystallized on sapphire 41  
○Hiroki Ago, Yoshito Ito, Baoshan Hu, Carlo Orofeo, Masaharu Tsuji, Noriaki Mizuta, Ken-ichi Ikeda, Seigi Mizuno
- 3-5 Low-temperature synthesis of few-layer and multi-layer graphene by chemical vapor deposition 42  
○Daiyu Kondo, Katsunori Yagi, Kenjiro Hayashi, Shintaro Sato, Naoki Yokoyama
- 3-6 Surface Synthesis of Graphene Materials using Polyaromatic Hydrocarbon Derivatives 43  
○Takahiro Nakae, Yoshihiro Kushida, Shingo Mizobuchi, Ryuji Ohnishi, Hisako Sato, Hiroshi Sakaguchi
- 3-7 Formation of Graphene on Insulator by Liquid Metal Flux Method 44  
○Hidefumi Hiura, Michael V. Lee, Anastasia V. Tyurnina, Kazuhito Tsukagoshi

☆☆☆☆☆☆ Lunch Time (11:45-13:00) ☆☆☆☆☆☆

**Special Lecture (13:00-13:30)**

- 3S-6 Low-temperature synthesis of graphene using microwave plasma CVD 6  
○Masataka Hasegawa

**General Lecture (13:30-14:15)**

**Formation and Purification of Nanotubes**

- 3-8 High rate growth of carbon nanotubes in tens of micrometer deep through silicon vias 45  
○Kazuyoshi Oohara, Takumi Ochiai, Masatomo Iiduka, Hiroshi Kawarada
- 3-9 High-Density Growth of Horizontally Aligned Single Walled Carbon Nanotubes on Crystal Quartz Substrates 46  
○Taiki Inoue, Daisuke Hasegawa, Shohei Chiashi, Shigeo Maruyama
- 3-10 Highly selective growth of (6,5) tube-Why (6,5) nanotube is so special in the growth of carbon nanotubes- 47  
○Yohji Achia, Akihito Inoue, Takeshi Kodama, Kenro Hashimoto, Toshiya Okazaki

**Poster Preview (14:15-15:10)**

**Poster Session (15:10-16:30)**

## Properties of Nanotubes

3P-1	Resonance Rayleigh scattering spectroscopy of CNTs grown on the optical tapered nano fiber Takuya Nagano, Hiromasa Hirai, Keisuke Okada, ○Shinichiro Mouri, Kiyofumi Muro	157
3P-2	Photoemission spectroscopy of double-walled carbon nanotubes based on host metallic SWCNTs ○S. Sagitani, K.Yonemori, R.Kakihara, H.Takahumi, D.Hirayama, H.Hayashi, J.Jiang, H.Iwasawa, K.Shimada,H.Namatame, M.Taguchi, H Ishii, H.Kadowaki,K.Matsuda,K. Yanagi, Y.Maniwa	158
3P-3	Computational Chemistry Study of the Interaction between Single-walled Carbon Nanotubes and Polysaccharides ○Hiroyuki Shinomiya, Akira Itoh, Koji Tsuchiya, Hirofumi Yajima	159
3P-4	Macroscopic Wall Number Analysis of Single-walled, Double-walled, and few-walled Carbon Nanotubes by X-ray Diffraction ○Don N. Futaba, Takeo Yamada, Kazufumi Kobashi, Motoo Yumura, Kenji Hata	160
3P-5	Dielectric Environment Effect on the Electronic States of (n,m) Single-Walled Carbon Nanotubes ○Yasuhiko Hirana, Yasuhiko Tanaka, Yasuro Niidome, Naotoshi Nakashima	161
3P-6	Systematic First-Principles Study of Single-Walled Carbon Nanotubes with Helical-Symmetry Operation ○Koichiro Kato,Takashi Koretsune, Susumu Saito	162
3P-7	Structural Stability and Electronic Manipulation of Nitrogen-doped Carbon Nanotube ○Yoshitaka Fujimoto, Susumu Saito	163
3P-8	Kekule Structures and HOMO-LUMO Gaps of Armchair Carbon Nanotubes with Finite Length ○Noriyuki Mizoguchi	164
3P-9	Transport property of hydrogen adsorbed carbon nanotube : first-principles density functional study ○Tomoyo Kawasaki, Fumiyuki Ishii, Keisuke Sawada, Mineo Saito	165
3P-10	Optical response of single-walled carbon nanotubes in far-infrared region ○Soon-Kil Joung, Toshiya Okazaki	166
3P-11	Transport properties of individual boron-doped carbon nanotube under pressure ○Tohru Watanabe, Shirou Tomioka, Satoshi Ishii, Shunsuke Tsuda, Takahide Yamaguchi, Yoshihiko Takano	167

## Formation and Purification of Nanotubes

3P-12	Redispersing Semiconducting Single Wall Carbon Nanotubes by DNA and Their Size Exclusion Chromatography ○Yuki Asada, Kazuki Ihara, Shigekazu Ohmori, Fumiyuki Ohmori, Takeshi Saito	168
3P-13	Growth control of carbon nanotubes on a metal tip apex ○Hisanori Kanayama, Kota shimanaka, Hideki Sato	169
3P-14	Effect of Al <sub>2</sub> O <sub>3</sub> Film Thickness on Growth of MWCNT Forest with Graphite Roof ○Hiroki Atsumi, Kotaro Takimoto, Yoshiyuki Suda, Hideto Tanoue, Hirofumi Takikawa, Hitosi Ue, Kazuki Shimizu, Yoshito Umeda	170
3P-15	Effect of pH and NaCl Concentration on Metal/Semiconductor Separation of Carbon Nanotubes using Gel ○Yasuko Urabe, Takeshi Tanaka, Hiromichi Kataura	171
3P-16	Development of large scale vertically aligned high-temperature pulsed-arc discharge ○Yuuichi Abe, Toshiki Sugai	172
3P-17	Diameter Selection techniques for Single-Wall Carbon Nanotubes With Around 1.4 nm Diameters ○Takuya Suzuki, Kazuhiro Yanagi, Hiroyuki Ozaki, Hiromichi Kataura, Yutaka Maniwa	173

## Fullerenes

3P-18	X-ray Structure of a Divalent Metallofullerene Yb@C <sub>80</sub> ○Xing Lu, Naomi Mizorogi, Zdeneck Slanina, Takeshi Akasaka, Shigeru Nagase	174
-------	---	-----

## Thursday, March 10th

3P-19	Electronic Properties of $M_2(C_2)@C_{82}$ (M=Sc, Ti, Fe) Endohedral Metallofullerenes ○Yoshio Nishimoto, Stephan Irle	175
3P-20	Electronic property of $Li@C_{60}$ ○Naoko Ogasawara, Hajime Yagi, Masashi Zenki, Takeyuki Zaima, Takafumi Miyazaki, Morihiko Saida, Fuyuko Yamashita, Shojun Hino	176
3P-21	Most stable structure and electronic structure of endohedral fullerenes $Sc_3C_2@C_{80}$ by density functional theory calculations ○Sosuke Okita, Takeyuki Zaima, Hajime Yagi, Takafumi Miyazaki, Haruya Okimoto, Noriko Izumi, Yusuke Nakanishi, Hisanori Shinohara, Shojun Hino	177
3P-22	ESR measurement of $N@C_{60}$ encapsulated by $\gamma$ -cyclodextrin ○Tatsuhisa Kato, Hiroki Shibata, Tomonari Wakabayashi	178
3P-23	Implantation of Atoms into Fullerenes using High-Frequency Sputtering Apparatus ○Tomonari Wakabayashi, Kosuke Sato, Naoya Kinomura, Nagisa Kumamoto	179
3P-24	Structures and Relative Stability of $Gd_2@C_{98}$ W. Y. Gao, ○X. Zhao	180
3P-25	A large-scale consecutive synthesis of metallofullerenes ○Hisashi Komaki, Yusuke Nakanishi and Hisanori Shinohara	181
3P-26	An Appearance of the New Electronic State in Fullerene Nano-Whisker due to UV Polymerization ○Tatsuya Doi, Kyouhei Koyama, Nobuyuki Aoki, Yuichi Ochiai	182
3P-27	Optical, Electric and Magnetic Properties of Thin Polymerized Fullerene $C_{60}$ Films Deposited via Electron-Beam Dispersion ○Ihar Razanau, Tetsu Mieno, Viktor Kazachenko	183
3P-28	Fabrication and Characterization of $C_{60}(OH)_x$ Nanocrystals by a Reprecipitation Method Keisuke Baba, ○Hironori Ogata	184
3P-29	Structural characterization of fullerene-nanowhiskers by powder x-ray diffraction ○Hironori Ogata, Hideyuki Ohnami	185
3P-30	QM/MD Simulations of Dynamic Fullerene Self-Assembly in Carbon Vapor With Inert Carrier Gas ○Hu-Jun Qian, Ying Wang, Keiji Morokuma, Stephan Irle	186
3P-31	Synthesis of non-IPR fullerenes from $C_{70}$ in Liquid Phase by Irradiation of Intense Femtosecond Laser Pulses ○Takeshi Kodama, Yuki Sato, Haruo Shiromaru, Joseph H. Sanderson, Tatsuya Fujino, Yoriko Wada, Tomonari Wakabayashi, Yohji Achiba	187
3P-32	Supramolecular Elementary Units in Porphyrin-Fullerene Composites Revealed by Solid-State NMR ○Hironobu Hayashi, Tomokazu Umeyama, Yoshihiro Matano, Hironori Kaji, Hiroshi Imahori	188
3P-33	The thermal [2+2] cycloaddition of morpholinocycloalkenes with [60]fullerene ○Tsubasa Mikie, Haruyasu Asahara, Kazuaki Nagao, Naohiko Ikuma, Ken Kokubo, Takumi Oshima	189
3P-34	Growth control of $C_{60}$ fullerene nanowhiskers ○Yumeno Akasaka, Kun'ichi Miyazawa	190
<b>Endohedral Nanotubes</b>		
3P-35	Effect of addition of Pt on Magnetic properties of iron-filled carbon nanotubes ○Yusuke Matsui, Tetsuya Kaneko, Atsushi Nagata, Hideki Sato, Yuji Fujiwara, Koichi Hata	191
3P-36	Water Structure inside Finite Length Single-Walled Carbon Nanotubes: SWCNT-Edge Effect ○Haruka Kyakuno, Kazuyuki Matsuda, Hitomi Yahiro, Yu Inami, Tomoko Fukuoka, Yasumitsu Miyata, Kazuhiro Yanagi, Yutaka Maniwa, Kazuyuki Takai, Toshiaki Enoki, Hiromichi Kataura, Takeshi Saito, Motoo Yumura, and Sumio Iijima	192

## Thursday, March 10th

- 3P-37 Dynamics of water confined in zeolite templated carbon 193  
○Kazuyuki Matsuda, Tomoko Fukuoka, Yasufumi Sato, Haruka Kyakuno, Kazuhiro Yanagi, Yutaka Maniwa, Hiroto Nishihara, Takashi Kyotani
- 3P-38 Growth of Inner Nanotubes from Confined Ionic Liquid inside a Tip-closed SWNT 194  
○Shimou Chen, Hong En Lim, Yasumitsu Miyata, Ryo Kitaura, Takeshi Saito, and Hisanori Shinohara
- 3P-39 Growth of Carbon Nanotubes Filled with Metal Compounds and “Tee-like” Carbon Nanotubes by Alcohol CVD 195  
○Yusuke Furuyama, Takayuki Yamasaki, Akira Koshio, Fumio Kokai
- 3P-40 Optical excited state induced by the interaction between rigid polymers and single-wall carbon nanotubes with large diameters 196  
○Masayoshi Tange, Toshiya Okazaki, and Sumio Iijima
- 3P-41 Polyynes and Cyanopolyynes Included in  $\alpha$ -Cyclodextrin Crystals 197  
○M. Saikawa, T. Wakabayashi
- 3P-42 Optical Absorption Spectra of Single Wall Carbon Nanotubes Containing Hydrogen-End-Capped Polyynes Inside 198  
○M. Teshiba, Y. Wada, Y. Yoshida, and T. Wakabayashi
- 3P-43 Synthesis of One-Dimensional Coordination Polymer of Size-Selected Polyynes and Silver Ions 199  
○M. Tomioka, T. Wakabayashi and Y. Suenaga
- Nanohorns**
- 3P-44 Weak Pre-Oxidation of Graphene-Based Nanomaterials for Enhanced Structure Distinction by Thermogravimetric Analysis 200  
Maki Nakamura, Ryota Yuge, Sumio Iijima, ○Masako Yudasaka
- 3P-45 Interaction between carbon nanohorns and amino acids 201  
○Xin Zhou, Minfang Zhang, Sumio Iijima, Masako Yudasaka
- Candidates for the Young Scientist Poster Award**
- 3P-46 *In-situ* Raman Spectroelectrochemical Investigation of Potential Dependent Electronic Structure of Single-Walled Carbon Nanotubes 202  
○Shingo Sakamoto, Masato Tominaga
- 3P-47 Synthesis of metal-nanowire@SWNTs and their physical properties 203  
○Daeheon Choi, Ryo Kitaura, Ryo Nakanishi, Yasumitsu Miyata, and Hisanori Shinohara
- 3P-48 Fabrication and Electrical Transport Properties of Atom Encapsulated Single-Walled Carbon Nanotubes Thin Film Transistors 204  
○Yosuke Osanai, Toshiaki Kato, Rikizo Hatakeyama
- 3P-49 Separation of SWCNTs by gel chromatography using gradient of surfactant concentration 205  
○Ryuji Inori, Takako Okada, Takayuki Arie, and Seiji Akita
- 3P-50 Electrochromic Carbon Electrodes: Controllable Visible Color Changes 206  
○Rieko Moriya, Kazuhiro Yanagi, Taishi Takenobu, Yasuhisa Naitoh, Hiromichi Kataura, Kazuyuki Matsuda, Yutaka Maniwa
- 3P-51 Biocompatibility of Chitosan/Carbon Materials Composite Membranes for Tissue Engineering 207  
○Katsumune Takahashi, Koji Tsuchiya, Hirofumi Yajima
- 3P-52 Evaluation of Thermal Conductivity of Single Carbon Nanotube Using Fluorescent Gel Temperature Sensor in Liquid 208  
○Kyohei Tomita, Hisataka Maruyama, Fumihito Arai
- 3P-53 Structural dependence of Multi-Walled Carbon Nanotubes on fuel cell performance 209  
○Shinya Kitamura, Takeshi Hashishin, Jun Tamaki, Kazuo Kojima



**基調講演**  
**Plenary Lecture**

**特別講演**  
**Special Lecture**

**1S - 1 ~ 1S - 2**

**2S - 3 ~ 2S - 4**

**3S - 5 ~ 3S - 6**

## Science and Industrial Applications of Nano-carbon Materials

Sumio Iijima

*Faculty of Science and Technology, Meijo University,  
1-501, Shiogamaguchi, Tenpaku, Nagoya, Aichi 468-8502, Japan  
National Institute of Advanced Industrial Science and Technology/Nanotube Research Center,  
Nagoya University*

The state of the art of synthesis of various nano-carbon materials that we have studied so far will be reviewed. One of challenge in the formation of SWCNT is to control its diameter and chirality, for which we have tried to grow SWCNTs by a conventional CVD method using metal catalyst of “uni-sized” metal clusters that are prepared by a mass-separator. Carbon nanohorn (CNH) aggregates are useful for nano-carbon materials where only large surface area and high dispersion are needed for medical applications, potable super-capacitor, polymer or metal composites etc. The usual size of CNH aggregates is about 80 nm in diameter but for some applications we need its smaller size, for example, less than 30nm for a bio-medical application. For this purpose we have developed a method to control a CNH aggregate size by optimizing vaporization conditions of CO<sub>2</sub> laser ablation of a carbon graphite rod. Some industrial applications will be introduced.

Formation of a large size graphene sheet by thermal CVD method using a copper substrate foil has been reported recently [1]. The method requires a high temperature CVD reactor (near 1000°C), so that it cannot be used in a conventional Si device process and therefore an alternative low temperature synthesis of graphene is needed. For this purpose we utilized a new surface-wave micro-wave CVD method which has been developed originally for the nano-diamond film growth at low temperature down to room temperature [2]. We shall demonstrate the growth of an A4-size graphene sheet grown at 300°C.

In the last half part of the presentation will be concerned with structural characterization of nano-carbon materials using atom-resolution electron microscopes as well as other characterization methods of Raman, photoluminescence and optical absorption spectroscopy, etc. The advantage of high resolution electron microscopy (HRTEM) over other techniques is to be able to characterize local atomic structures such as lattice defects and edge structures of nano materials which cannot be studied in conventional techniques. Another emphasis of HRTEM will be on dynamic observation of a reaction process which is not available for other high resolution probe microscope techniques such as STM. We thank for a recent progress of HRTEM technology such as aberration correction and EELS, which has made possible elemental analysis, distinction of valency and more on individual atom basis. Some latest examples of above mentioned observations will be demonstrated [3-12].

- (1) S. Bae, et al. *Nature Nanotech.*, (2010).
- (2) M. Hasegawa et al., *PRB*, (2010).
- (3) K. Suenaga, et al. *Nature Nanotech.* **2**, 358 (2007)
- (4) Z. Liu, et al., *Nature Nanotech.*, **2**, 422 (2007).
- (5) Y. Sato, et al., *Nano Lett.*, **7**, 3704 (2007).
- (6) C. H. Jin, et al., *Nature Nanotech.* **3**, 17 (2008).
- (7) C. H. Jin, et al., *PRL*, **101**, 176102(1)-(4) (2008).
- (8) M. Koshino, et al., *Nature Chemistry* (2010).
- (9) Z. Liu, et al., *PRL*, **102**, 015501 (1)-(4) (2009).
- (10) C. H. Jin, et al., *PRL*, **102**, 195505 (1)-(4) (2009).
- (11) C. H. Jin, et al., *PRL*, **102**, 205501 (1)-(4) (2009).
- (12) K. Suenaga et al., *Nature*, **468**, 1088 (2010).

Corresponding Author: Sumio Iijima  
Tel & Fax: +81-52-834-4001 E-mail: [ijimas@meijo-u.ac.jp](mailto:ijimas@meijo-u.ac.jp)

## The Advantages and Applications of Nanocarbon Phase Transformations

○Amanda S. Barnard<sup>1</sup>

<sup>1</sup>*CSIRO Materials Science & Engineering, Clayton, Victoria 3186, Australia*

The family of carbon nanomaterials is a rich and exciting area of research, that spans materials science, engineering, physics and chemistry, [1]; and most recently, is having an impact in biology and medicine [2]. Although a wide range of applications are emerging, the basic science of nanocarbon is still receiving considerable attention, due to advanced methods allowing fabrication of carbon nanomaterials with different dimensionalities, and the existence (and co-existence) of more than one allotrope. The low dimensional  $sp^2$ -bonded structures have  $sp^3$ -bonded siblings, and like all siblings they share a complicated relationship. Just as fullerenes and nanotubes have unique properties (ideal for specific applications), diamond nanorods and diamond nanoparticles (nanodiamonds) are also unique, and have slowly carved out a complementary niche in the field of carbon-based nanotechnology. However, spontaneous, inefficient (reversible and irreversible) phase transformations prevail at small sizes, and most diamond nanomaterials are decorated with a full or partial fullerene or nanotubular sheath [3]. For some applications this can be a hindrance, but one may argue that the most interesting and exciting properties are revealed when these materials are combined. As we will see in this presentation, we often find that the combination is greater than the sum of the two, and entirely new properties can emerge [4]. If we embrace the advantages of nanocarbon phase transformations, and learn to control this new structural degree of freedom, even more opportunities will undoubtedly materialize.

[1] E. Ōsawa, *Chemistry of Single-Nano Diamond Particles*, in *Chemistry of Nanocarbons*, ed. F. Wudl, S. Nagase and K. Akasaka, John Wiley & Sons, Oxford, UK, (2010).

[2] *Nanodiamonds: Applications in Biology and Nanoscale Medicine*, ed. D. Ho, Springer Science + Business Media, Inc., Norwell, MA, USA (2010).

[3] A.S. Barnard, *Diamond Relat. Mater.* **15**, 285 (2006).

[4] A. S. Barnard, *J. Mater. Chem.*, **18**, 4038 (2008).

Corresponding Author: Amanda S. Barnard

TEL: +61-3-9545-7840, FAX: +61-3-9545-2059, E-mail: [amanda.barnard@csiro.au](mailto:amanda.barnard@csiro.au)

## Application of Flat-Panel Field Emission Lamp using Carbon Nanotube-Carbon nanohorn Cathodes

○Ryota Yuge

*Green Innovation Research Laboratories, NEC Corporation, 34 Miyukigaoka, Tsukuba  
305-8501, Japan*

Carbon nanotubes (CNTs) have been reported as one of the best cold cathode emitter for field emission display (FED) and field emission lamp (FEL) applications owing to their large aspect ratio, high mechanical strength, good electrical conductivity, and possibility of large-area application via thick film processing.<sup>1-2</sup> In the fabrication of the CNT cathodes for FEDs and FELs, CNTs are deposited on the substrate by direct growth,<sup>3</sup> electrophoresis,<sup>4</sup> or printing.<sup>5</sup>

For the FELs, a simple, scalable, and low-cost method of printing is especially appropriate. Here, we introduce recent progress in flat-panel FEL using CNTs and carbon nanohorns (CNHs). For the manufacture of highly efficient FE devices, we synthesized single-wall carbon nanotubes (SWNTs) on catalyst-supported single-wall carbon nanohorns (SWNHs) by chemical vapor deposition.<sup>6</sup> In the obtained SWNT-SWNH hybrids (NTNHs), the SWNTs diameters were 1–1.7 nm and the bundle diameters became almost uniform, *i.e.*, less than 10 nm, since the SWNTs were separated by SWNH aggregates. As a result, FELs using NTNH hybrids achieved highly bright and homogeneously bright emission as a result of having both the promising FE properties of SWNTs and the high-dispersion properties of SWNHs. We also confirmed that a stable long-term operating period for the lamp became possible by optimizing the CNT cathode preparation process.

Uniform lighting emission from a phosphor on the anode is essential for improving flat-panel FELs using CNTs. By developing triode-type CNT-FELs, our research groups have succeeded in decreasing the non-uniformity of lighting emission to half that of the diode-type CNT-FEL.

### References:

- [1] A. G. Rinzler et al. *Science*, **296**, 1550 (1995).
- [2] J. M. Bonard et al. *Appl. Phys. Lett.*, **78**, 2775 (2001).
- [3] T. Hirakoka et al. *J. Am. Chem. Soc.*, **128**, 13338 (2006).
- [4] B. Gao et al. *Adv. Mater.*, **13**, 1770 (2001).
- [5] J. Li et al. *Appl. Surf. Sci.*, **220**, 96 (2003).
- [6] R. Yuge et al. *ACS Nano* in press.

**Corresponding Author: Ryota Yuge**

**TEL:** +81-29-850-1566, **FAX:** +81-29-856-6137, **E-mail:** r-yuge@bk.jp.nec.com

## Fundamentals and Recent Progress of Organic Thin-film Solar Cells

Masahiro Hiramoto

*Institute for Molecular Science, Myodaiji, Okazaki 444-8787, Japan*

e-mail address: hiramoto@ims.ac.jp

Organic EL television was commercialized last year. Next target of organic electronics is organic solar cell. The present lecture includes fundamental science and history of organic solar cells, concept of organic p-i-n cells [1], nanostructure design of codeposited i-interlayer [2], ultra-high purification of organic semiconductors [3], and future prospects of organic solar cells.

High-purified organic semiconductors can be obtained by forming large single crystals (Fig. 1). p-i-n cells incorporating seven-nine (7N) C<sub>60</sub> showed the world record conversion efficiency of 5.3% (Fig. 2). Essence of high efficiency is the utilization of entire visible light of solar spectrum without decreasing fill factor by the black-colored cell incorporating very thick (1 μm) C<sub>60</sub>:H<sub>2</sub>Pc i-interlayer.

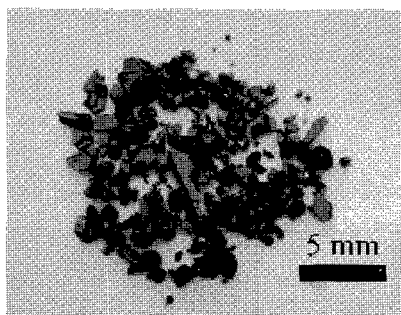


Fig. 1 Single crystals of seven-nine (99.99999, 7N) C<sub>60</sub>.

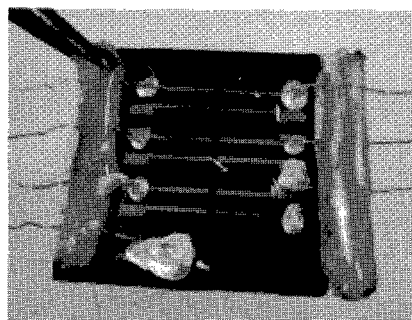


Fig. 3 p-i-n cell having 1 μm-thick C<sub>60</sub>:H<sub>2</sub>Pc codeposited i-interlayer, which showed efficiency of 5.3%.

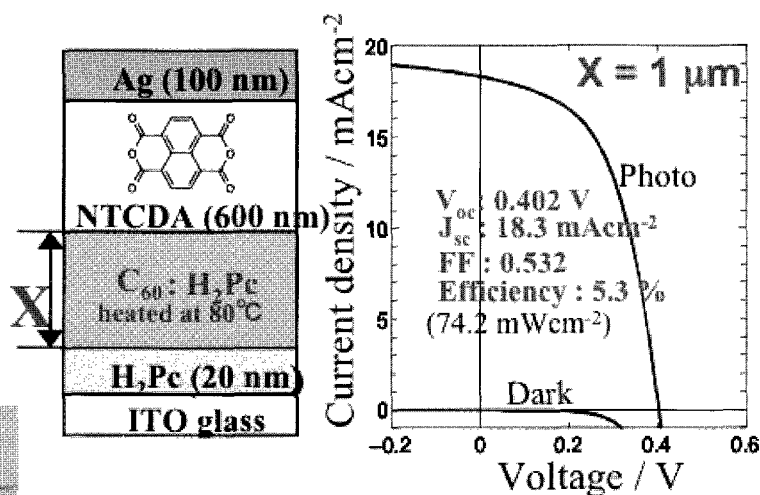


Fig. 2 p-i-n cell structure and current-voltage characteristics of p-i-n cell incorporating 7N-C<sub>60</sub>.

- [1] M. Hiramoto, H. Fujiwara, M. Yokoyama, *J. Appl. Phys.*, **72**, 3781 (1992).  
 [2] K. Suemori, T. Miyata, M. Yokoyama, M. Hiramoto, *Appl. Phys. Lett.*, **86**, 063509 (2005).  
 [3] M. Hiramoto, Proceedings of SPIE Vol. 7052, Organic photovoltaics IX, San Diego, CA, 12-14 Aug. (2008).

## Carrier Control of Carbon Nanotube Transistor

Young Hee Lee

*<sup>1</sup>Department of Physics, Department of Energy Science, Center for Nanotubes and Nanostructured Composites, Sungkyunkwan Advanced Institute of nanotechnology, Sungkyunkwan University, Suwon 440-746, Korea*

Nanocarbons such as fullerenes, carbon nanotubes, carbon nanofibers, graphite oxides, and graphenes have been the key words in 21th century and has led nanoscience and nanotechnology. Due to the various allotropes of carbons, unexpected scientific new findings and their related applications have been extensively investigated. In this talk, I will focus key issues in CNT-based transistors: metal-CNT contact, chemical doping, doping-dependent conductivity, and trap charge doping, and ambipolarity. Pure carbon nanotubes have been known to exhibit ambipolarity. This is very different from the conventional semiconductors that are controlled by an intentional doping with extrinsic materials. The ambipolarity has been a serious drawback in adopting carbon nanotubes for CMOS technology. Carbon nanotubes show p-type behavior in ambient conditions. The difficulty arises from the absence of stable n-type dopants in ambient conditions. A series of chemical approaches have been done in our group to search for n-type dopants. NADH and viologen molecules have demonstrated successfully to show n-type behavior by donating electrons to nanotubes and furthermore show high stability in ambient conditions.[1-7] Trap-charge doping without chemical doping was also discussed.[8] In addition to these approaches, we will also demonstrate a way of utilizing ambipolarity of nanotubes without such intentional dopings that ambipolarity is in fact advantageous in fabricating CMOS inverter and logic circuits.[9] These doping ideas have been further used for CVD-grown graphene.[10-11]

[1] K. Kim et al., J. Am. Chem. Soc. 130, 12757-12761 (08).

[2] S. M. Yoon et al., J. Am. Chem. Soc. 130, 2610-2616 (08).

[3] H. J. Shin et al., J. Am. Chem. Soc. 130, 2062-2066 (08).

[4] S. M. Kim et al. ACS NANO, online (2010)

[5] S. M. Kim et al., J. Am. Chem. Soc. 131, 327-331 (09).

[6] B. R. Kang et al., Adv. Func. Mat. 19, 2553-2559 (09).

[7] K. K. Kim et al., New J. Chem. 34, 2183 (2010).

[8] W. J. Yu et al. Adv. Mat. 21, 4821 (2009).

[9] W. J. Yu et al., Nanolett. 9, 1401-1405 (09).

[10] S. J. chae et al., Adv. Mat. 21, 2328 (09).

[11]. F. Gunes et al. ACS NANO 4, 4595 (2010).

[12] H. J. Shin et al., J. Am. Chem. Soc. 132, 15603 (2010).

Lee Young Hee: leeyoung@skku.edu

## Low-temperature graphene synthesis by using microwave plasma CVD

AIST Nanotube Research Center, Masataka Hasegawa, Jaeho Kim, Masato Ishihara, Yoshinori Koga,

Kazuo Tsugawa, and Sumio Iijima

E-mail: hasegawa.masataka@aist.go.jp

Because of its high electrical conductivity as well as chemical and physical stability graphene-based films are expected to be utilized for transparent conductive films for next-generation electrical and optoelectronic devices and various other applications. Recently the synthesis methods of graphene by using thermal chemical vapor deposition (CVD) have been developed, in which large area graphene are synthesized on Ni<sup>(1)</sup> or Cu<sup>(2)</sup> substrates. In this thermal CVD, high temperature of 1000degC for the decomposition of CH<sub>4</sub> and the duration of the order of hour are required. For the realization of graphene industries the fast synthesis methods at lower temperature are desirable.

In this study we have developed a low-temperature and rapid synthesis method of graphene on A4 size-Cu foils by using microwave (2.45GHz) plasma assisted CVD sustained by surface waves. The reaction gas is the mixture of CH<sub>4</sub>, H<sub>2</sub> and Ar, the pressure is less than 10Pa, the substrate temperature during the deposition is about 400degC, and the duration of CVD is around 60seconds. After the deposition the Cu foil is etched away using FeCl<sub>3</sub> aqueous solution, and the graphene films are transferred to glass plates. The typical sheet resistance is 1-2 kΩ/□, and the optical transmittance is about 80%at 550nm. Figure 1 shows the typical Raman spectrum (excitation wavelength 638nm) of the graphene. In addition we have fabricated a capacitive type touch panel. Figure 2 shows a picture of the demonstrated touch panel which works properly by the finger touch.

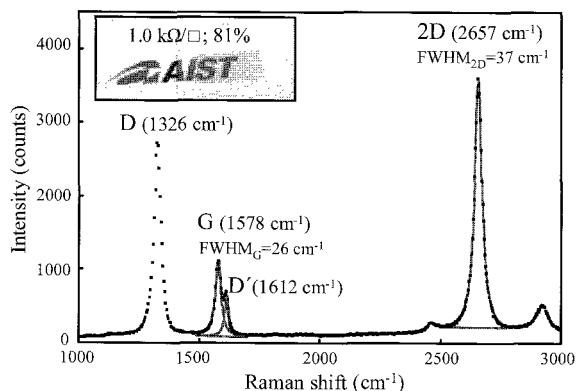


Fig.1 Typical Raman spectrum of graphene synthesized by microwave plasma CVD (Excitation wavelength 638nm).

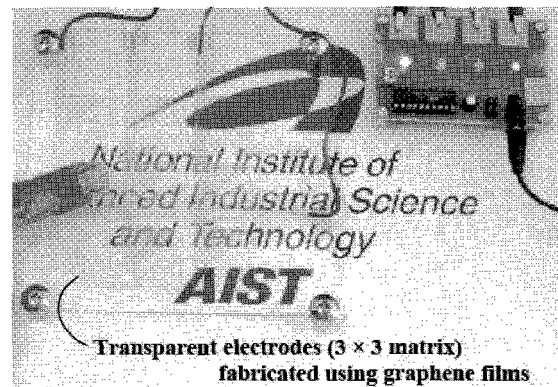


Fig.2 Fabricated capacitive type-touch panel using graphene.

(1) Q. Yu, J. Lian, S. Siriponglert, H. Li, Y. P. Chen, S.-S. Pei, Appl.Phys.Lett.93(2008)113103.

(2) X. Li, W. Cai, J. An, S. Kim, J. Nah, D. Yang, R. Piner, A. Velamakanni, I. Jung, E. Tutuc, S. K. Banerjee, L. Colombo, R. S. Ruoff, Science 324(2009)1312.

一般講演  
General Lecture

1-1 ~ 1-16

2-1 ~ 2-15

3-1 ~ 3-10



## Probing surfactant molecules on SWCNTs by Raman spectroscopy

Daisuke Nishide<sup>1,2</sup>, Shunjiro Fujii<sup>1,2</sup>, Takeshi Tanaka<sup>1</sup>, ◯Hiromichi Kataura<sup>1,2</sup>

<sup>1</sup> *Nanosystem Research Institute, National Institute of Advanced Industrial Science and Technology (AIST), Tsukuba, Ibaraki 305-8562, Japan*

<sup>2</sup> *Japan Science and Technology Agency, CREST, Kawaguchi, Saitama 330-0012, Japan*

Raman spectroscopy of single-wall carbon nanotubes (SWCNTs) dispersed in water using five kinds of surfactant was investigated. It was revealed that G-band Raman spectral feature was strongly changed depending on the kind of surfactant, which means that Raman spectra of SWCNTs can be used for probing the surfactant molecules adsorbed on SWCNTs. By changing the relative concentrations of two surfactants in the solution, Raman spectral modulation detected a surfactant exchange process on the SWCNT surface. It was found that Raman spectral changes were not reversible, meaning that the surfactant exchange on the SWCNTs was irreversible reaction probably due to the different affinities. Interestingly, this irreversible surfactant exchange process was also confirmed by the different results on the metal semiconductor separation by density gradient ultracentrifugation for the different pretreatments. We claim that the only monolayer of surfactant molecules can be detected by the Raman measurement. This new probe of surfactant is very useful to analyze the mechanism of metal-semiconductor separation of SWCNTs where the surfactant plays very important roles.

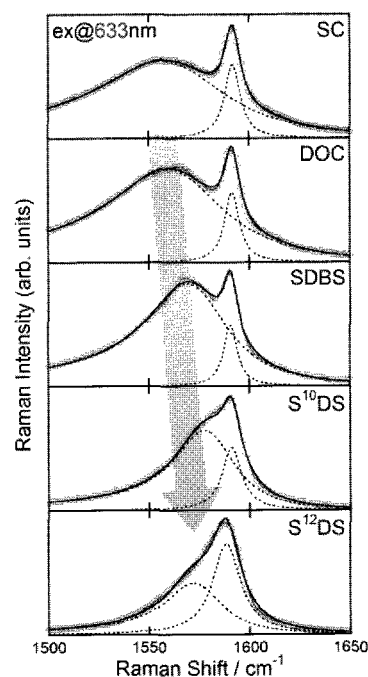


**Figure 1.** G-band Raman spectra of SWCNTs dispersed in 5 kinds of surfactant water solution.

Corresponding Author: Hiromichi Kataura

Tel:+81-29-861-2551, Fax: +81-29-861-2786

E-mail: h-kataura@aist.go.jp

## Evaluation of single-walled carbon nanotubes dispersed in surfactant solution by using Raman spectroscopy

○Shinzo Suzuki<sup>1</sup>, Masayuki Awazu<sup>1</sup>, Yasuro Ikeda<sup>1</sup>, Yuuya Hatano<sup>1</sup>, Midori Nakanishi<sup>1</sup>,  
Takashi Mizusawa<sup>1</sup>, Akira Ono<sup>2</sup>, Toshiya Okazaki<sup>3</sup>, and Yohji Achiba<sup>4</sup>

<sup>1</sup>*Department of Physics, Kyoto Sangyo University, Kyoto 603-8555, Japan*

<sup>2</sup>*Department of Engineering, Kanagawa University, Yokohama 221-8686, Japan*

<sup>3</sup>*Nanotube Research Center, AIST, Tsukuba 305-8565, Japan*

<sup>4</sup>*Department of Chemistry, Tokyo Metropolitan University, Tokyo 192-0397, Japan*

### Abstract:

Raman spectroscopy is a powerful technique and has been extensively used for the evaluation of diameter/chirality distribution of single-walled carbon nanotubes (SWNTs). One of the characteristic features of Raman spectroscopy is that, it gives information about not only for semi-conductive nanotubes, but also for metallic ones [1]. On the other hand, recent progress in dispersion technique of SWNTs in DNA solution, indicates that, SWNTs can be well extracted from the soot prepared even in He atmosphere by making use of arc-burning technique [2]. Since the uniformity of SWNTs in solution is considered to be much better than that in as-grown soot or film, it is worth while investigating Raman spectroscopy of SWNTs dispersed in solution phase furthermore.

In this presentation, single-walled carbon nanotubes (SWNTs) were prepared by making use of arc-burning [2,3] and laser-oven technique, respectively, and those SWNTs were further dispersed by single-stranded DNA (ss-DNA) solution. Those dispersed SWNTs were then used as sample solution for Raman spectroscopy.

Fig.1 shows an example of Raman spectra of SWNTs (excitation wavelength: 532 nm) made with laser-oven (LV) technique in nitrogen atmosphere with different oven temperature. The figure clearly shows that the relative G-band intensity by semi-conductive SWNTs increases extensively, as the oven temperature increases. This behavior can be explained by considering about the diameter distribution of SWNTs prepared in each case.

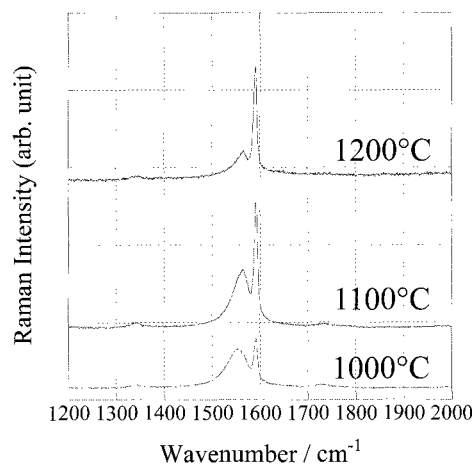


Fig.1

### References:

- [1] C. Fantini, A. Jorio, M. Souza, M.S. Strano, M.S. Dresselhaus, and M. A. Pimenta, *Phys. Rev. Lett.*, **93**, 147406(2004).
- [2] S. Suzuki, T. Mizusawa, T. Okazaki, and Y. Achiba, *Eur. Phys. J. D*, **52**, 83-86 (2009).
- [3] S. Suzuki, K. Hara, T. Fujita, T. Mizusawa, T. Okazaki, and Y. Achiba, *J. Nanosci. Nanotech.*, **10**, 4060-4063(2010).

**Corresponding Author:** Shinzo Suzuki

**TEL:** +81-75-705-1631, **FAX:** +81-75-705-1640, **E-mail:** suzukish@cc.kyoto-su.ac.jp

## Exciton-Exciton Interactions in Thin SWNTs Extracted from DWNTs

○Takeshi Koyama,<sup>1</sup> Yasumitsu Miyata,<sup>2</sup> Hisanori Shinohara,<sup>2</sup> Hideo Kishida,<sup>1</sup>  
and Arao Nakamura<sup>1</sup>

<sup>1</sup>*Department of Applied Physics, Nagoya University, Nagoya 464-8603, Japan*

<sup>2</sup>*Department of Chemistry, Nagoya University, Nagoya 464-8602, Japan*

Optical properties in single-walled carbon nanotubes (SWNTs) are governed by one-dimensional exciton effects, and studying exciton dynamics is of great importance to understand both transient and steady-state responses. In the high excitation density regime, a nonlinear relaxation process of excitons, i.e., bimolecular Auger recombination, takes place. Due to the exciton collision one exciton annihilates and the other exciton is excited into a higher state. Hence, a key parameter is the initial number density of excitons per tube generated by an optical pulse. In this work, we investigate exciton dynamics in the high excitation density regime in SWNTs with the (6,4) chirality by means of non-degenerate pump-probe spectroscopy, and reveal a pump-fluence dependence of the initial exciton number. We also estimate an exciton size by taking into account a phase-space filling effect on the change of absorption coefficient.

(6,4) SWNTs used in this work were prepared by an extraction method based on sonication and further density gradient ultracentrifugation of double-walled carbon nanotubes (DWNTs) [1]. The SWNTs were micelle-encapsulated by sodium cholate in water. Pump-probe measurements were carried out by using two optical parametric amplifiers (OPAs) pumped by a regenerative amplifier (1 kHz, 800nm, 120 fs), which was seeded by a Ti:sapphire laser (80 MHz, 800 nm, 80 fs). Pump and probe photon energies were 2.1 and 1.4 eV, respectively, which are resonant with the  $E_{22}$  and  $E_{11}$  band of (6,4) tube. Polarizations of the pump and probe pulses are parallel to each other.

Figure 1 shows the transmittance change ( $\Delta T/T$ ) at  $E_{11}$  band in (6,4) SWNTs at the pump fluences of 0.024, 0.12, 0.95, and  $4.8 \times 10^{15}$  photons/cm<sup>2</sup>. As the pump-fluence increases, the sharp rising at time origin and its steep decay till  $\sim 1$  ps are pronounced. This behavior is explained by the bimolecular Auger recombination of excitons: As the number of excitons generated by a pump pulse increases, the collision rate of them increases and the signal decay becomes fast. By fitting the experimental results to the analytical expression of the bimolecular Auger recombination model [2], the initial exciton number per tube is determined to be 2, 8, 19, and 38 for the corresponding pump fluence. Assuming the typical tube length of  $\sim 760$  nm determined by AFM observations, the exciton size is estimated to be  $\sim 1.7(\pm 0.7)$  nm.

[1] Y. Miyata *et al.*, ACS Nano **4**, 5807 (2010).

[2] A. V. Barzykin and M. Tachiya, Phys. Rev. B **72**, 075425 (2005).

**Corresponding Author:** Takeshi Koyama

**E-mail:** koyama@nuap.nagoya-u.ac.jp

**Tel:** 052-789-4452, **Fax:** 052-789-5316

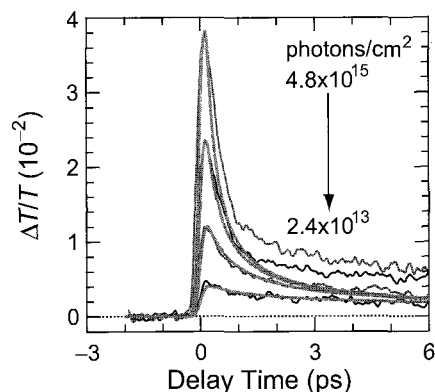


Fig. 1. Time evolution of differential transmittance ( $\Delta T/T$ ) at  $E_{11}$  band in (6,4) SWNTs. Thin and thick lines represent the experimental and fitting results.

## Continuous Carrier Tuning in Metallic and Semiconducting SWNT Film

○Hidekazu Shimotani<sup>1</sup>, Satoshi Tsuda<sup>2</sup>, Hongtao Yuan<sup>1</sup>, Yohei Yomogida<sup>2</sup>, Rieko Moriya<sup>3</sup>,  
Taishi Takenobu<sup>4</sup>, Kazuhiro Yanagi<sup>3</sup>, Yoshihiro Iwasa<sup>1</sup>

<sup>1</sup>Quantum-Phase Electronics Center, The University of Tokyo, and JST-CREST, Tokyo 113-8656, Japan. <sup>2</sup>Department of Physics, Tohoku University, Sendai 980-8578, Japan. <sup>3</sup>Department of Physics, Tokyo Metropolitan University, Tokyo 192-0397. <sup>4</sup>Department of Applied Physics, Waseda University, and JST-PRESTO, Tokyo 169-8555, Japan

Recent success in isolating SWNTs of narrow chirality distributions enabled making pure metallic (m-) and semiconducting (s-) SWNT films. Their unique feature is the existence of sharp peaks in the density of states at van Hove singularities (vHs's). Hence, it is expected that their conduction properties change dramatically when the Fermi level ( $E_F$ ) is at a vHs. Chemical doping or field-effect transistor is unsuitable for the purpose because of the lack of precise and reversible  $E_F$  controllability, and the narrow controllable  $E_F$  range, respectively. The problems are solved by our electric double layer transistor (EDLT, Fig.1) technique, where the gate voltage ( $V_G$ ) is applied through an electrolyte. We have realized superconducting transition in SrTiO<sub>3</sub> [1] and ZrNCl [2] with EDLT. Therefore, this work was done to investigate conduction properties of s- and m-SWNT films with EDLT.

The conductance, optical absorption spectra, and temperature dependence of the resistance of s- and m-SWNT films were measured at various  $V_G$ . The conductance of the s-SWNT film showed stepwise change against  $V_G$  (Fig.2). The absorbance spectra (Fig.3) indicate the steps correspond to reaching of the  $E_F$  to a vHs. The  $E_F$  shift across a vHs was also observed in the m-SWNT films. The conductance of the m-SWNT film sharply increased at the point and its temperature dependence changed from that of variable range hopping to a metallic behavior. These results demonstrate that the conduction properties strongly depend on the  $E_F$ , reflecting one dimensionality of SWNTs.

[1] K. Ueno *et al.*, *Nat. Mater.* **7**, 855 (2008).

[2] J. T. Ye *et al.*, *Nat. Mater.* **9**, 125 (2010).

Corresponding Author: Hidekazu Shimotani

E-mail: shimotani@ap.t.u-tokyo.ac.jp

Tel & Fax: +81-3-5841-6871 / +81-3-5841-6822

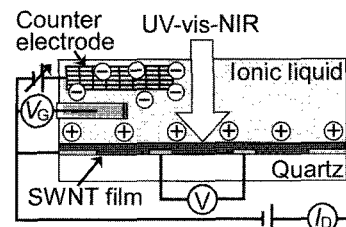


Fig.1. Illustration of electric double layer transistor. The gate voltage ( $V_G$ ) was measured with a  $\text{Ag}/\text{Ag}^+$  reference electrode. The conductance ( $I_D/V$ ) was measured by 4-probe method. Ionic liquid: *N,N*-Diethyl-*N*-methyl-*N*-(2-methoxyethyl)ammonium.

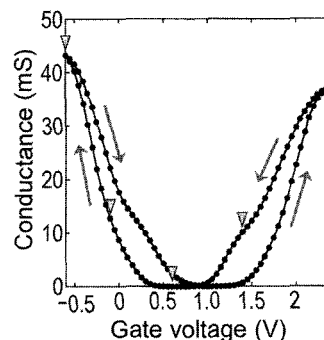


Fig.2. The conductance of a semiconducting SWNT film plotted against the gate voltage. Triangles indicate voltages, at which absorption spectra in Fig.3 were measured.

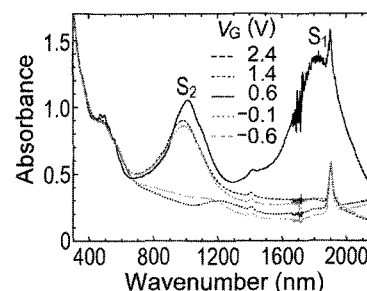


Fig.3. Absorption spectra of the semiconducting SWNT film at various gate voltages ( $V_G$ ).  $S_1$  and  $S_2$  denote the transition between the first subbands and the second subbands, respectively.

## Carrier mobility and on/off ratio of carbon nanotube thin-film transistors fabricated by gas-phase filtration and transfer process

○Dong-Ming Sun<sup>1</sup>, Marina Y. Timmermans<sup>2</sup>, Ying Tian<sup>2</sup>, Albert G. Nasibulin<sup>2</sup>, Shigeru Kishimoto<sup>1</sup>, Takashi Mizutani<sup>1</sup>, Esko I. Kauppinen<sup>2</sup> and Yutaka Ohno<sup>1</sup>

<sup>1</sup>Department of Quantum Engineering, Nagoya University, Nagoya 464-8603, Japan

<sup>2</sup>Department of Applied Physics and Center for New Materials, Aalto University, Finland

Carbon nanotube (CNT) thin-film transistors (TFTs) are expected to allow the fabrication of high-performance, flexible, and transparent devices with relatively simple techniques. Previously, we have presented a gas-phase filtration and transfer process to fabricate CNT TFTs, demonstrated high-performance CNT TFTs with a mobility of  $35 \text{ cm}^2\text{V}^{-1}\text{s}^{-1}$  and an on/off ratio of  $6 \times 10^6$ , and flexible logic integrated circuits, including a 21-stage ring oscillator and master-slave delay flip flops, representing the first nanotube-based sequential logic [1]. Here, we present the detailed characterization of the high-performance CNT TFTs.

There are two models to estimate gate capacitance used for the carrier mobility evaluation: the parallel plate model and the rigorous model taking into account the realistic electrostatic coupling between sparse nanotubes and the gate electrode [2] (Figure 1). By the parallel plate model, the mobility of the TFT is evaluated to be  $35 \text{ cm}^2\text{V}^{-1}\text{s}^{-1}$ . On the other hand, the mobility is evaluated to be  $634 \text{ cm}^2\text{V}^{-1}\text{s}^{-1}$  by the rigorous model. We will discuss which method is appropriate for the performance evaluation of CNT TFTs.

In the case of CNT TFTs, it is often reported that the on/off ratio degrades with increasing  $V_{\text{DS}}$  [2]. However, Figure 2 shows the transfer characteristics of a typical CNT TFT at various  $V_{\text{DS}}$  ranging from  $-0.5$  to  $-5$  V; the on/off ratio decreased slightly with increasing  $V_{\text{DS}}$ , but remains as high as  $1 \times 10^6$  at  $V_{\text{DS}} = -5$  V. In contrast, the on/off ratios decreased significantly for the TFTs with larger-diameter CNTs. The on/off degradation can be attributed to electrons tunneling through the narrow bandgap at the high drain field.

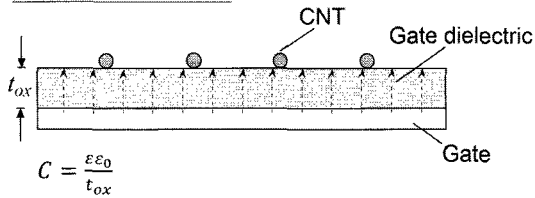
[1] D.-M. Sun *et al.*, *Nature Nanotech.* (2011) in press.

[2] Q. Cao *et al.*, *Appl. Phys. Lett.* **90**, 023516 (2007).

Corresponding Author: Yutaka Ohno. This work is supported by NEDO Grant '08.

TEL: +81-52-789-5387, FAX: +81-52-789-5387, E-mail: yohno@nuee.nagoya-u.ac.jp

### a. parallel plate model:



### b. rigorous model:

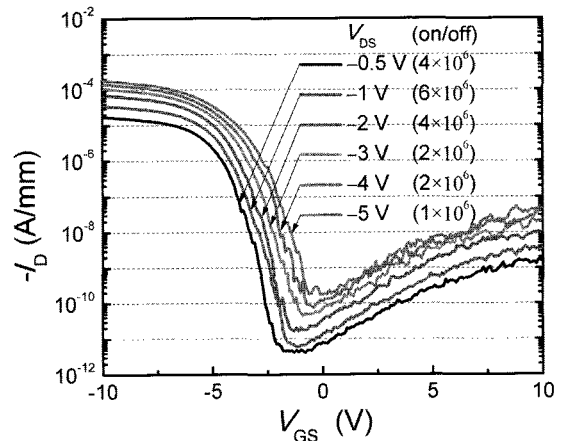
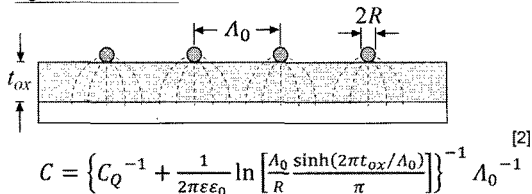


Fig. 1. Schematics of electric force lines in (a) parallel plate and (b) rigorous model.

Fig. 2.  $I_D$ - $V_{\text{GS}}$  characteristics at  $V_{\text{DS}}$  from  $-0.5$  to  $-5$  V.

## High mobility thin-film transistors using length-sorted semiconducting single-wall carbon nanotubes

○Kazunari Shiozawa<sup>1</sup>, Yasumitsu Miyata<sup>1</sup>, Yuki Asada<sup>1</sup>,  
Yutaka Ohno<sup>2</sup>, Ryo Kitaura<sup>1</sup>, Takashi Mizutani<sup>2</sup> and Hisanori Shinohara<sup>1</sup>

<sup>1</sup> Department of Chemistry & Institute for Advanced Research,  
Nagoya University, Nagoya 464-8602, Japan

<sup>2</sup> Department of Quantum Engineering, Nagoya University, Nagoya 464-8603, Japan

Single-wall carbon nanotubes (SWCNTs) are a promising material for a channel of thin film transistors (TFTs) because of their high carrier mobility, flexibility, and solution processability. Recently, the performance of liquid-processed SWCNT-TFTs has been improved as the purification methods of semiconducting SWCNTs (s-SWCNTs) are developed. For instance, Rouhi *et al.* reported the TFTs using 99% s-SWCNTs (which were purified by density gradient ultracentrifugation) showed an on/off ratio of  $10^4$  and a mobility of  $40 \text{ cm}^2\text{V}^{-1}\text{s}^{-1}$ [<sup>1</sup>]. However, this mobility is still lower than that of TFTs fabricated by as-grown SWCNTs [<sup>2</sup>]. This suggests that it is essential to consider not only the purity but also the other factors such as nanotube length for further improvements of TFT performance.

In this study, we have fabricated TFTs using length-sorted, high-purity semiconducting SWCNTs. To obtain these samples, we have developed a separation/purification method based on gel filtration that have been reported by Moshhammer *et al.*[<sup>3</sup>] and Tanaka *et al.*[<sup>4</sup>]. Our method includes a recycling filtration process of SWCNTs with an eluate containing competing mixtures of surfactants. This process allows us to extract micrometer-long and highly pure s-SWCNTs. We fabricated the TFTs using the aligned networks of separated SWCNTs. Figure 1 shows the  $I_D$ - $V_{DS}$  characteristics of the TFT fabricated. The device has an on/off ratio  $\sim 10^6$ , a mobility of  $\sim 170 \text{ cm}^2\text{V}^{-1}\text{s}^{-1}$ , and a normalized maximum transconductance of  $0.78 \text{ Sm}^{-1}$ . This corresponds to the highest performance compared with the SWCNT-TFTs that have been reported so far[<sup>2</sup>]. The present result represents an important milestone toward post silicon high-performance electronics.

### Reference

- [1] N. Rouhi et al., *Adv. Mater.*, **23**, 94 (2010)
- [2] Q. Cao et al., *Nature*, **454**, 495 (2008)
- [3] K. Moshhammer et al., *Nano Res.*, **2**, 599 (2009)
- [4] Tanaka et al., *Appl. Phys. Express*, **2**, 125002 (2009)

Corresponding Author: Hisanori Shinohara

E-mail: noris@nagoya-u.jp

Tel&Fax: 052-789-2482 & 052-747-6442

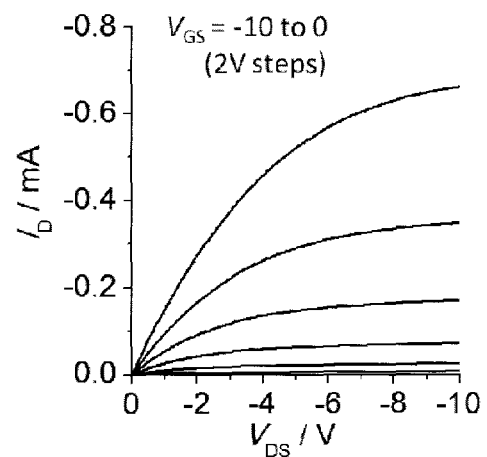


**Figure 1**  $I_D$ - $V_{DS}$  characteristics of TFT using high purity and micrometer-long s-SWCNT (channel width :  $200 \mu\text{m}$ , channel length :  $40 \mu\text{m}$ )

## Highly Flexible All-SWNT Field-Effect Transistors

○Shinya Aikawa<sup>1,2</sup>, Erik Einarsson<sup>1</sup>, Shohei Chiashi<sup>1</sup>, Junichiro Shiomi<sup>1</sup>, Eiichi Nishikawa<sup>2</sup> and Shigeo Maruyama<sup>1</sup>

<sup>1</sup>Department of Mechanical Engineering, The University of Tokyo, 7-3-1 Hongo, Bunkyo-ku, Tokyo 113-8656, Japan

<sup>2</sup>Department of Electrical Engineering, Tokyo University of Science, 1-3 Kagurazaka, Shinjuku-ku, Tokyo 162-8601, Japan

With the recent development of novel electronic devices there is a desire for flexible, transparent, high-performance field-effect transistors (FETs). A single-walled carbon nanotube (SWNT) is expected to be a strong candidate for realizing such next-generation devices due to their mechanical robustness and excellent electrical properties.

Based on our unique patterned-growth technique using a self-assembled monolayer (SAM) [1], we have reported that high-performance all-SWNT FETs can be easily fabricated [2]. Such all-SWNT devices can work on a flexible substrate without degrading their electrical properties [3], and may realize metal-free electronics. Here, flexible and transparent all-SWNT FETs were fabricated by a transfer printing method.

Figure 1 shows a schematic diagram of the flexible FET and SEM image of the all-SWNT FET before transfer. Poly(vinyl alcohol) (PVA) was spin coated onto the patterned SWNTs and then dried. An SWNT film attached to the plastic substrate acted as the global gate electrode. The transfer characteristics before transfer (on Si substrate) and after transfer (in PVA film) are shown in Figure 2. The resulting all-SWNT FET was highly flexible, and could be crumpled without degradation of the properties.

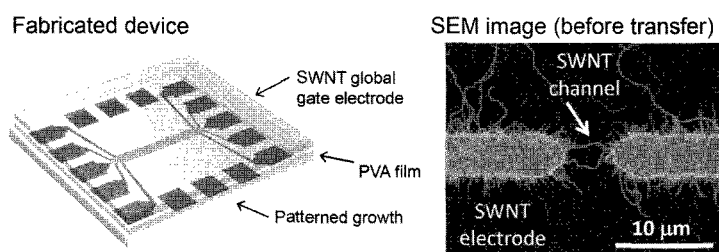


**Fig. 1** Schematic diagram of the flexible all-SWNT device and SEM image of the channel region before transfer.

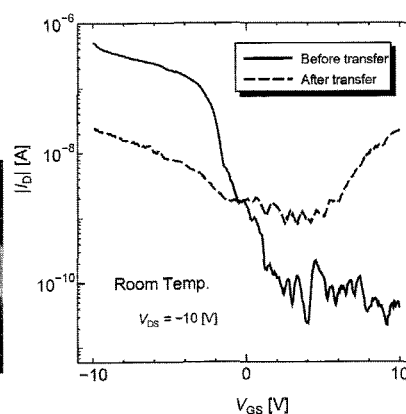


**Fig. 2** Transfer characteristics before and after transfer.

[1] R. Xiang et al. *J. Am. Chem. Soc.* **131**, 10344 (2009).

[2] S. Aikawa et al. *The 39th Fullerene Nanotubes General Symposium*, p.53 (2010).

[3] Q. Cao et al., *Appl. Phys. Lett.* **88**, 113511 (2006).

**Corresponding Author:** Shigeo Maruyama

TEL: +81-3-5841-6421, FAX: +81-3-5800-6983, E-mail: maruyama@photon.t.u-tokyo.ac.jp

## Infrared Solar Cell Based on C<sub>60</sub> Encapsulated Semiconducting Single-Walled Carbon Nanotubes

○Y. F. Li, S. Kodama, T. Kaneko, and R. Hatakeyama

*Department of Electronic Engineering, Tohoku University, Sendai 980-8579, Japan*

Semiconducting single-walled carbon nanotubes (S-SWNTs) are quasi one-dimensional materials exhibiting interesting optical properties, which makes them promising candidates for fabrication of solar cells. More importantly, the near-infrared band gap transition of S-SWNTs makes them suitable to harvest the infrared solar spectrum.<sup>1</sup>

In this work, we have systematically investigated the possibility of making infrared solar cells, as schematically shown in Fig. 1(a), based on *n*-silicon and S-SWNTs including pristine S-SWNTs and C<sub>60</sub> encapsulated semiconducting SWNTs (C<sub>60</sub>@S-SWNTs) which serve as energy conversion material. Our results have demonstrated that S-SWNTs can be used to convert infrared light (800-1550 nm) into electrical energy under the configuration of solar cells, as shown in Fig. 1(b) where the *I-V* characteristic is measured under 1200 nm light illumination. Interestingly, the performance of solar cells based on S-SWNTs is much better than that observed in solar cells fabricated by SWNTs containing both metallic and semiconducting SWNTs, and the solar cells based on C<sub>60</sub>@S-SWNTs are found to show a better power conversion efficiency than pristine S-SWNTs due to the charge transfer effect between SWNTs and C<sub>60</sub> fullerene.<sup>1</sup> In addition, it is found that when the light energy is higher than two times of the first van Hove transition energy of S-SWNTs ( $E_{11}$ ), the efficiency suddenly increases, suggesting the possibility for the occurrence of multiple exciton generation in the C<sub>60</sub>@S-SWNTs based solar cell.

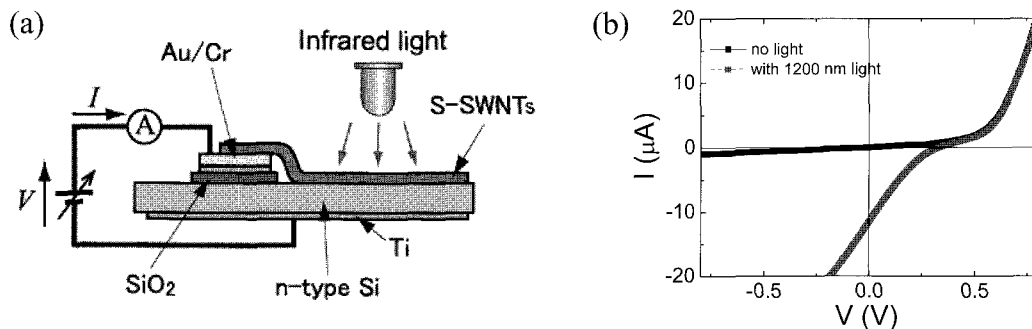


Fig.1: (a) Schematic illumination of solar cell based on S-SWNTs. (b) *I-V* characteristic of solar cell based on C<sub>60</sub>@S-SWNTs measured under 1200 nm light illumination.

[1] R. Hatakeyama, Y.F. Li, T. Y. Kato, and T. Kaneko, *Appl. Phys. Lett.* **97**, 013104 (2010).

Corresponding Author: Yongfeng Li  
 E-mail: yfli@plasma.ecei.tohoku.ac.jp  
 FAX: +81-22-263-9225



## Metal-free Fuel Cell Cathode Catalyst Prepared by Carbonization of Polybenzimidazole-wrapped Carbon Nanotubes

○Tsuyohiko Fujigaya<sup>1</sup>, Takeshi Uchinoumi<sup>1</sup> and Naotoshi Nakashima<sup>1,2</sup>

<sup>1</sup> Department of Applied Chemistry, Graduate School of Engineering,

Kyushu University, 744, Motoooka Nishi-ku Fukuoka, Japan

<sup>2</sup> JST-CREST, 5 Sanbancho, Chiyoda-ku, Tokyo 102-0075, Japan

**Abstract:** Polymer electrolyte fuel cell systems using non-precious metal as a catalyst are the strong request from industry side. One of the promising approaches for the non-precious metal cathode catalyst is the nitrogen-containing graphite structure proposed by Ozaki et al., which were prepared from the metal complex of the nitrogen-containing polymers<sup>1)</sup>. We recently reported the pyridine-containing polybenzimidazole (PyPBI: **Fig. 1**) adsorbed to MWNTs through  $\pi$ - $\pi$  interaction and formed PyPBI-wrapped MWNT (MWNT/PyPBI)<sup>2)</sup>. Based on the finding, we fabricated the cobalt(II) or iron(II) complex of the MWNT/PyPBI (MWNT/PyPBI/Co and MWNT/PyPBI/Fe) and the composites were pyrolyzed at 600 °C for 1.5 h, followed by the washing with concentrated HCl in order to remove the cobalt species. Fig. 2 shows the linear sweep voltammograms of the composites (line: pyrolyzed MWNT/PyPBI/Co, dashed line: pyrolyzed MWNT/PyPBI/Fe), which were measured by rotating electrode voltammetry (1600 rpm) in 0.5 M H<sub>2</sub>SO<sub>4</sub>. We observed similar current on both catalysts for oxygen reaction (Fig. 2, lower). On the other hand, in Fig.2 (upper), lower current was observed for pyrolyzed MWNT/PyPBI/Fe, indicating pyrolyzed MWNT/PyPBI/Fe exhibited better catalytic activity for one step oxygen reduction than pyrolyzed MWNT/PyPBI/Co.

### References:

- 1) J. Ozaki, S. Tanifuji, N. Kimura, A. Furuichi, A. Oya, *Carbon* **2006**, *44*, 1324.
- 2) T. Fujigaya, M. Okamoto, N. Nakashima, *Carbon* **2009**, *47*, 3227.

**Corresponding Author:** Naotoshi Nakashima

**E-mail:** [nakashima-tcm@mail.cstm.kyushu-u.ac.jp](mailto:nakashima-tcm@mail.cstm.kyushu-u.ac.jp)

**Tel&Fax:** +81-92-802-2840

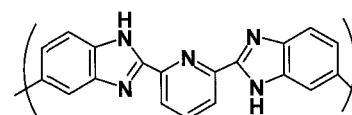


Fig. 1 Chemical structure of PyPBI

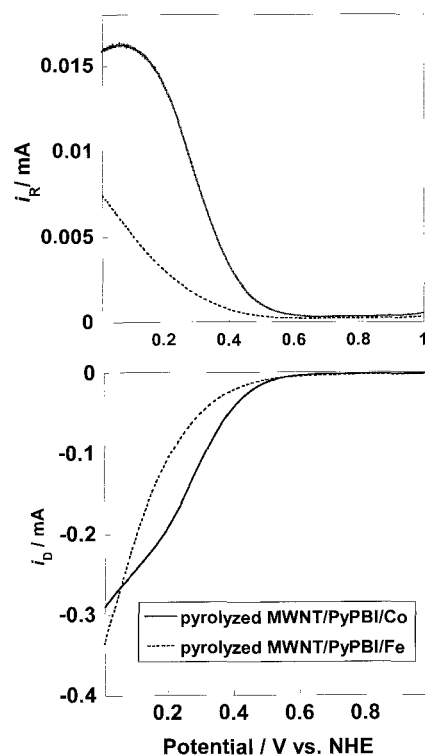


Fig. 2 Oxygen reduction voltammograms for the pyrolyzed composites. (Upper) ring current, (bottom) disk current

## Improved Dispersibility of Single-walled Carbon Nanotubes (SWNTs) Using Subtle Growth Ambient and Its Enhancement of Conductivity in SWNT/Polymer Composites

○Yoshiyuki Nonoguchi<sup>1</sup>, Don N. Futaba<sup>1,2</sup>, Seisuke Ata<sup>1,2</sup>, Motoo Yumura<sup>1,2</sup>,  
and Kenji Hata<sup>1,2</sup>

<sup>1</sup>*Nanotube Research Center, National Institute of Advanced Industrial Science and Technology, Tsukuba 305-8565, Japan*

<sup>2</sup>*Technology Research Association for Single Wall Carbon Nanotubes (TASC), Tsukuba 305-8565, Japan*

Dispersing single-walled carbon nanotubes (SWNTs) in solvents is a key step for producing uniform SWNT composites, and extracting their intrinsic properties. Here we demonstrate that dispersibility of SWNTs is dramatically improved by subtle growth ambient, and the improved dispersibility affects conductivity in the SWNT/polymer composite.

SWNTs were synthesized using a “Super-growth” method which is based on chemical vapor deposition with small amount of molecular oxygen including water and acetone. SWNTs in dimethylformamide (DMF) were then subjected to a water-cooled sonication bath for five hours. DMF dispersion of acetone-grown SWNTs was homogenous and stable, although a part of SWNTs were readily aggregated and precipitated in dispersion of water-grown SWNTs (Figure 1). Quantitative laser diffraction data revealed that an averaged diameter and its homogeneity were improved by five times for acetone-grown SWNTs, compared to water-grown SWNTs.

We then applied these dispersions to making conducting SWNT/polymer composites. In the composites, SWNTs would serve as conducting channels. For 0.2wt% SWNT, a composite made from acetone-grown SWNTs showed 0.36 S/cm of conductivity, roughly two times larger than that of a water-grown SWNT composite.

Corresponding Author: Kenji Hata

E-mail: kenji-hata@aist.go.jp Tel&Fax: 029-861-4654/029-861-4851

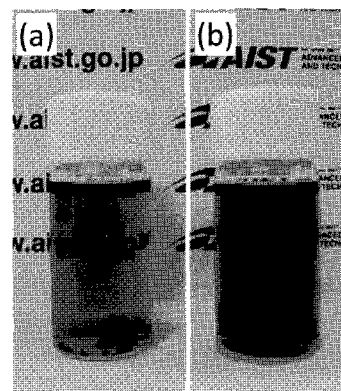


Figure 1. DMF dispersions of (a) water-grown and (b) acetone-grown SWNTs.

## Carbon Nanotubes with Temperature-Invariant Creep and Creep-Recovery from -150°C to 970°C

\* Ming Xu<sup>1</sup>, Don N. Futaba<sup>1</sup>, Motoo Yumura<sup>1</sup>, Kenji Hata<sup>1,2</sup>

<sup>1</sup> Technology Research Association for Single Wall Carbon Nanotubes (TASC), Tsukuba, 305-8565, Japan & Nanotube Research Center, National Institute of Advanced Industrial Science and Technology (AIST), Tsukuba, 305-8565, Japan

<sup>2</sup> Japan Science and Technology Agency (JST), Kawaguchi, 332-0012, Japan

Creep and creep recovery are important properties of viscoelastic materials. Creep is the time-dependent increase in deformation (strain) of a viscoelastic material subjected to a constant stress, and creep recovery is the time dependent elastic recovery from deformation. Creep and creep recovery (together referred to as creep recovery) are phenomena that can be found everywhere. For example, when we sit onto a cushion (applying a stress), the cushion gradually deforms to conform to our body (creep), and after we stand thereby releasing the stress, the cushion gradually recovers its shape (creep recovery). As exemplified, creep recovery is not an instantaneous process and occurs progressively over time. This aspect of creep recovery enables the gradual distribution of stress, and is thus very useful to prevent fracturing caused by stress concentration. Since conventional viscoelastic materials are composed of polymers, their operational temperature range of creep recovery is limited. Specifically, the operational range of the most temperature stable rubber, silicone rubber, is -55-300°C.

Here, we present the creep recovery from the nonaligned, entangled CNT material demonstrated at extreme temperatures (-150-970°C) where conventional viscoelastic materials fails (Fig.1). Quantitatively, the creep recovery properties such as deformability (how much the material can be deformed), percent recovery (the ability to return from deformation), and compliance (how easily a material deforms) were measured by shear-mode static loading-unloading. The CNT material showed the similar level of creep recovery properties (35% strain deformability,  $\sim 1.3\text{E-}6 \text{ Pa}^{-1}$  compliance with  $\sim 70\%$  percent recovery) with silicone rubber, yet kept stable behaviors from -150°C to 600°C. Furthermore, it showed the superior thermal resistance to both continuous exposure across low and high temperatures and long term exposure to stress at high temperatures. Based on our modeling, we interpret that the contacts between the long, traversing CNTs are the origin of the creep and creep recovery.

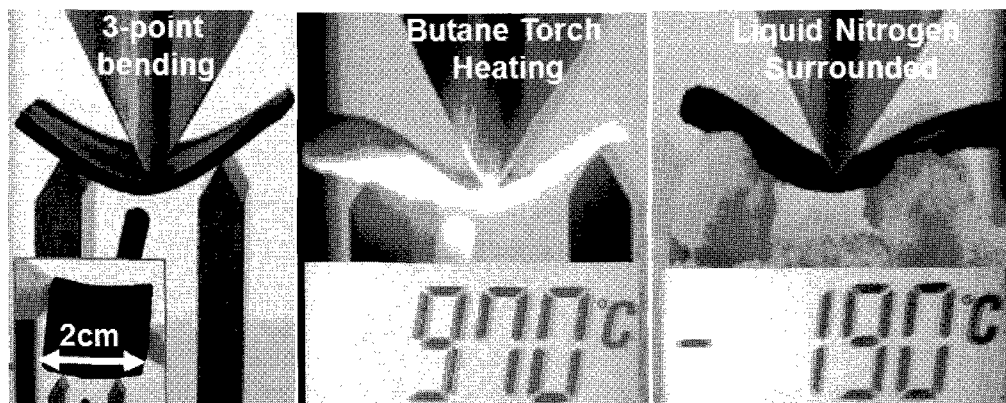


Fig. 1 The CNT materials show elasticity and compliance across -190-970°C by three-bending test.

[1] M. Xu, D. N. Futaba, T. Yamada, M. Yumura, K. Hata., *Science* **330**, 1364 (2010).

\*Corresponding Author: Kenji Hata, Don N. Futaba

TEL & Fax: (029) 861-5080 ext 46763, E-mail: [kenji-hata@aist.go.jp](mailto:kenji-hata@aist.go.jp), [d-futaba@aist.go.jp](mailto:d-futaba@aist.go.jp)

## Applications of optical responsive carbon nanotubes cell cultured substrate

○Takao Sada<sup>1</sup>, Tsuyohiko Fujigaya<sup>1</sup>, Naotoshi Nakashima<sup>1,2</sup>

<sup>1</sup>*Department of Applied Chemistry, Graduate School of Engineering, Kyushu University,  
744 Motoooka, Fukuoka 819-0395, Japan*

<sup>2</sup>*JST-CREST, 5 Sanbancho, Chiyoda-ku, Tokyo, 102-0075, Japan*

Single-walled carbon nanotubes (SWNTs) are nanomaterials that possess remarkable electrical, mechanical, and thermal properties and have been explored for biological applications [1]. One of the applications of SWNTs in biology is the cell culture substrate, where the unique one-dimensional high aspect structure and hydrophobic nature of SWNTs gave better substrate to culture the cells [2]. In addition, SWNTs have unique near-IR (NIR) responsive properties such as strong photoabsorption, photothermal conversion and photoacoustic generation. In this report, we describe development and application of photo responsive SWNT substrate for the cell collection and the cell patterning. These techniques is of interest especially for basic study of cells, stem cell research, organ culture, or tissue engineering.

SWNT-coated cell culture substrate was fabricated using the spray coating method. Near-IR laser pulse (1064 nm) was irradiated to the cells and, of interest, we found the quick desorption of the cells around irradiated area (Fig. 1), whereas the control dish without SWNT-coating does not lead any change in cells morphology. The results indicate the removal of the cells was obviously due to the effect of the

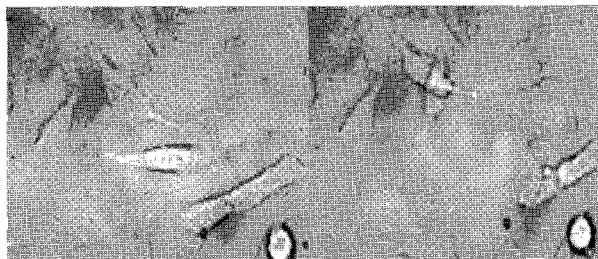


Fig.1 Microscopic images of SWNT-coated dish before NIR laser irradiation (left) and after irradiation (right).

SWNT-coating respond to the NIR laser irradiation. We assumed that the mechanism of the cell removal is the photoacoustic effect of SWNTs and the collapse of SWNTs substrate. By reducing the water layer above the cell, irradiated cells were successfully catapulted from the medium and captured at the top lid of the dish. We estimated the viability of the cells by means of fluorescent stain. The captured cells showed the red fluorescent, which clearly indicate the removed cells are dead. For the cell patterning, nonadhesive polymer functionalized with phospholipid was patterned the photo responsive SWNT substrate using polydimethylsiloxane stamp. We found the cells adhered on the non-patterning area. When the patterning area was irradiated by the NIR laser, the new cell adhesion area was formed in this irradiated area. It showed the nonadhesive polymer was detached from the SWNTs due to the heat generated by the photothermal effect of SWNTs.

[1] Z. Liu, S. Tabakman, K. Welsher, and H. Dai, *Nano Res.* **2009**, *2*, 85.

[2] N. Aoki, T. Akasaka, F. Watari and A. Yokoyama, *Dent. Mater. J.* **2007**, *26*, 178.

Corresponding Author: Naotoshi Nakashima

E-mail: [nakashima-tcm@mail.cstm.kyushu-u.ac.jp](mailto:nakashima-tcm@mail.cstm.kyushu-u.ac.jp)

Tel&Fax: +81-92-802-2840

## Development of Multi-stage Ion Trap Mobility System

Masashi Shinozaki, Yoshihiko Sawanishi, and Toshiki Sugai

*Department of Chemistry, Toho University, Miyama 2-2-1 Funabashi, 274-8510, Japan*

Ion mobility measurements have been utilized to analyze structures of nanocarbon materials[1]. We have been developing an ion trap mobility system to enable long-term measurements and to enhance sensitivity[2]. However the trap system has low mobility resolution since the length of the particle movement is limited to several millimeters by the size of the trap. The system has also low sample injection and ejection efficiency so that it is difficult to connect other measurement systems such as mass spectrometers. Here we present the development of the multi-stage ion trap mobility system with the total trap length of 500 mm and an ion funnel[3] to enhance the mobility resolution and injection and ejection efficiency.

Figure 1 shows a schematic and an image of the system which consists of the ion funnel located at the top and the following stacked linear ion trap. The charged particles produced from NaCl water solution are converged by the ion funnel and are injected into the trap. RF electric fields with some DC gradients are applied to the linear trap electrodes to focus the particles and to analyze their mobility. The length of the trap is 500 mm which can realize much higher resolution than that of the previous system. The performance and the structural analyses will be discussed in the presentation.

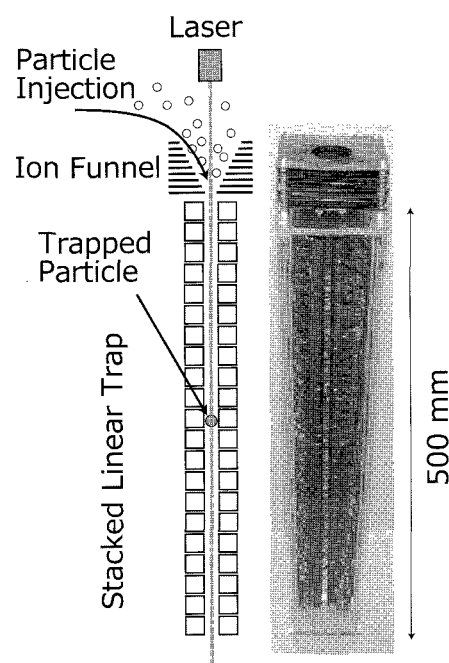


Fig. 1 Schematic and image of multi-stage ion trap mobility system.

[1] T. Sugai *et al.*, *J. Am. Chem. Soc.* **123**, 6427 (2001).

[2] M.Sawanishi and T.Sugai, The 38th symposium abstract p.37 (2010).

[3] A.V.Tolmachev *et al.*, *Int. J. Mass Spec.* **203**, 31 (2000).

TEL: +81-47-472-4406, FAX: +81-47-472-4406, E-mail: sugai@chem.sci.toho-u.ac.jp

## Electronic States of Linear Polyene Molecules Embedded in Nano-Structured Molecular Assemblies

T. Wakabayashi, M. Saikawa, M. Teshiba, and Y. Wada

*Department of Chemistry, Kinki University, Higashi-Osaka 577-8502, Japan*

The HOMO-LUMO transition of the electron in the polyene molecule has a character of  $\pi$ - $\pi$ . The single-electron excitation between the doubly degenerated orbitals gives rise to distinct three excited states of  $\Sigma^+$ ,  $\Sigma^-$ , and  $\Delta$ . The electric-dipole transition from the ground state is *fully allowed* for the former one, namely  $\Sigma^+$ , while not allowed (being *forbidden*) for the latter two. Under isotropic conditions such as in solutions, vibronic bands in the *forbidden* transition of the molecule are orders of magnitude weaker than those in the *allowed* transition. On the other hand, under anisotropic conditions in crystalline forms, the intrinsically *forbidden* transition of the molecule can be intensified due to symmetry lowering in the crystal field. We examined such systems as solid forms in which polyene molecules were stabilized inside the cavity of  $\alpha$ -cyclodextrin ( $\alpha$ -CD), single wall carbon nanotubes (SWNTs), and the cluster of iodine molecules ( $I_6$ ). Spectral changes for polyenes in the nano-structured molecular assemblies are presented and discussed along the symmetry considerations. The resonance excitation curve observed for the Raman signal of  $C_{10}H_2$  in SWNT is discussed in comparison with the absorption spectra in the relevant excitation energies.

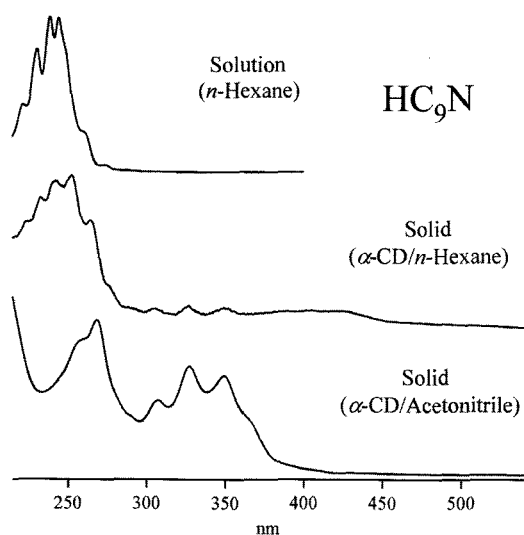


**Fig. 1.** UV/VIS absorption spectra for  $HC_9N$  in solution and crystalline solids of  $\alpha$ -CD.

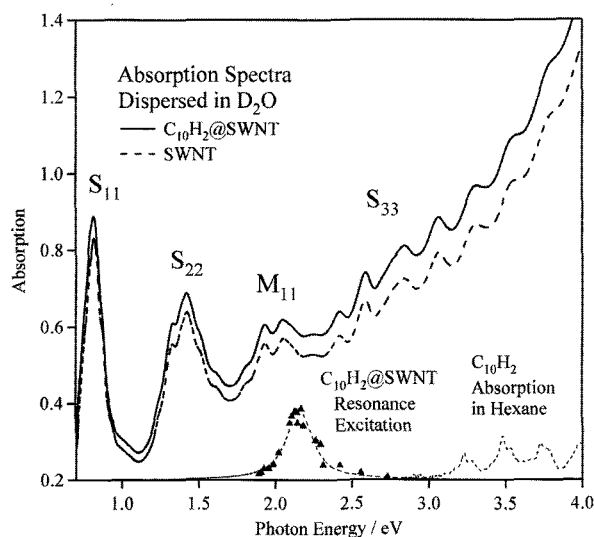


**Fig. 2.** Absorption spectra for SWNT with and without polyene  $C_{10}H_2$  measured for those dispersed with sodium cholate in  $D_2O$ .

Correspondence to Tomonari Wakabayashi

E-mail: wakaba@chem.kindai.ac.jp

Tel. 06-6730-5880 (ex. 4101)

## Size-Dependent Cellular Uptake of Carbon Nanoparticles

M. Zhang<sup>1</sup>, X. Zhou<sup>1</sup>, Y. Tahara<sup>1</sup>, S. Iijima<sup>1,2</sup>, M. Yudasaka<sup>1</sup>

<sup>1</sup>AIST, Tsukuba, <sup>2</sup>Meijo University

Nanocarbons such as nanotubes, nanohorns and graphene ribbons have been considered as useful carriers for delivering drugs to cancer and other diseased sites. The nanocarbons have various sizes (lengths and diameters) and assemblies, which is believed to influence interactions of nanocarbons with cells and the drug delivery efficiency. Due to the lack of well-defined structures of nanocarbons with uniform sizes, it has been difficult to study the cellular uptake of nanocarbons depending on the nanocarbon sizes. We have recently succeeded in preparing small- and uniform-sized aggregates of single wall carbon nanohorns (CNHs) [1]. Using these small-sized CNH aggregates, we have evidenced for the first time that the cellular uptake of nanocarbons was size-dependent.

We used two-sized CNHs for this study: one was normal CNH aggregates (about 100 nm,) and the other was the small-sized CNH aggregates (30-50 nm, S-CNHs). S-CNHs were produced from 100-nm CNH aggregates by an oxidation exfoliation method. S-CNTs exhibited high hydrophilic properties, large pore volumes, and high potential for chemical or biological functionalization. The normal-sized CNH aggregates (100 nm) were treated with light assisted oxidation [2] to make them hydrophilic as similar to S-CNHs.

Using the black color of nanocarbons (without fluorescent labels), the cellular uptake of S-CNHs and CNHs were easily observed with confocal microscopy and quantified by optical absorption measurements. The results showed that the uptake-quantities of S-CNHs by HeLa and macrophage (Raw 267.4) cells were much lower than those of large-sized CNHs. Furthermore, S-CNTs with noncovalent functionalization with DSPE-PEG completely avoided the phagocytosis by macrophage cells while the general sized CNHs did not.

The results suggest that S-CNHs are optimum for the drug delivery application as they are resistive to the macrophages phagocytosis due to the small sizes, which can be even more intensified by the PEG coating of S-CNHs.

### References:

- [1] M. Zhang, T. Yamaguchi, S. Iijima, M. Yudasaka, *J. Phys. Chem. C* 113 (2009) 11184
- [2] M. Zhang, M. Yudasaka, K. Ajima, J. Miyawaki, S. Iijima, *ACS Nano*, 1(2007), 265-272.

**Corresponding Author: M. Zhang, M. Yudasaka**

**E-mail:** [m-zhang@aist.go.jp](mailto:m-zhang@aist.go.jp); [m-yudasaka@aist.go.jp](mailto:m-yudasaka@aist.go.jp)

**Tel&FAX:** 029-861-6290

## HRTEM observation of the platinum clusters interacting with carbon atoms at elevated temperatures

○Keita Kobayashi, Kazu Suenaga

*Research Center for Advanced Carbon Materials, National Institute of Advanced Industrial Science and Technology (AIST), Tsukuba 305-8565, Japan*

Platinum is widely used as a catalyst in many fields of industrial chemistry, such as a catalytic-hydrogenation of organic molecules [1]. In addition, since platinum can form solid solution with carbon up to ~3 at.% at ~1,980 K [2], it has also been known as a useful metal for catalytic-graphitization [3]. Actually, although the catalytic-activity of platinum for graphitization is considered to be less effective than the iron-group metals, platinum has been used as the catalyst of synthesis of carbon nanocapsules [4] and carbon nanotubes (CNTs) [4, 5]. Therefore, catalytic-activity of platinum has attracted significant research interests. Particularly, considerable efforts have been devoted to fabricate and characterize the platinum catalytic nanoparticles because of their unique and outstanding activity. However, the detailed size dependency of platinum cluster on catalytic-activity has not been clarified yet.

In this study, we have observed behaviors of platinum clusters on a surface of CNTs at several temperatures by a high-resolution transmission electron microscope (HRTEM) in order to estimate the “magic number” of platinum atoms for a most efficient catalytic behavior for graphitization. We try to figure out how the platinum clusters interact with carbon atoms by in-situ observation at elevated temperatures within column of HRTEM. In addition, we will discuss the cluster size dependency of the catalytic-graphitization based on the HRTEM observations.

### References

- [1] P. N. Rylander, *Catalytic hydrogenation over platinum metals*, Academic press, New York (1967).
- [2] T. B. Massalski et al., *Binary alloy phase diagrams 2<sup>nd</sup> edition*, vol. 1, ASM international, Material Park (1990).
- [3] L. J. Collier et al., *Trans. Faraday Soc.*, **30**, 581 (1934).
- [4] Y. Saito et al., *J. Appl. Phys.*, **80**, 3062 (1996).
- [5] D. Takagi et al., *Nano Lett.*, **6**, 2642 (2006).

**Corresponding Author:** Keita Kobayashi, **E-mail:** kobayashi-z@aist.go.jp



## Cyclic purification of semiconducting and metallic carbon nanotubes using separation by Electric-field inducing Layer Formation

○Kazuki Ihara<sup>1,2</sup>, Takeshi Saito<sup>1,3</sup>, Fumiyuki Nihey<sup>1,2</sup>

<sup>1</sup>Technology Association for Single Wall Carbon Nanotube (TASC), Tsukuba, 305-8565, Japan.

<sup>2</sup>Green Innovation Res. Labs., NEC Corp., Tsukuba, 305-8501, Japan.

<sup>3</sup>National Institute of Advance Industrial Science and Technology (AIST)<sup>3</sup>, Tsukuba, 305-8565, Japan.

Extraction of purely semiconducting (s-) single walled carbon nanotubes (SWCNTs) removing metallic (m-) ones is essential for the electronic application of SWCNTs such as carbon nanotube thin film transistors (CNT-TFTs). Separation methods of s- and m-SWCNTs providing highly pure and ion-free s-SWCNTs are required to improve the electronic device performance. Recently, we had proposed a separation method by "Electric-field inducing Layer Formation (ELF)" as an ion-free separation method with high purity of s-SWCNTs. Here, we report a cyclic ELF separation aiming at the improvement in the purity of separated SWCNTs.

SWCNTs were dispersed into D<sub>2</sub>O with 1 wt% of polyoxyethylene stearyl ether (Brij 700, Aldrich) by sonication and ultracentrifugation. After the dispersing process, the concentrations of SWCNTs and Brij 700 in the solution were adjusted by adding Brij 700-D<sub>2</sub>O solution. The adjusted solution was introduced into a vertical cell with a pair of electrodes, which was used for applying electric field to the solution by a DC power supply. For the separation, a constant voltage of 30 V was applied between the lower (anode) and upper (cathode) electrodes for more than 24 hours. Then, two colored layers were separately formed, and they were fractionated. After the fractionation, ELF method was repeatedly applied to the both of fractionated samples twice. Raman spectra by 633-nm laser excitation of pristine, 1-time and 3-times of separation sample are shown in fig. 1 and 2, for m- and s-SWCNTs, respectively. Purities of 1-time and 3-times separated s- (m-) SWCNTs are calculated as 92 (55) % and 97 (84) % from these spectra. These results suggest that cyclic ELF separations effectively improve the purity of separated SWCNTs.

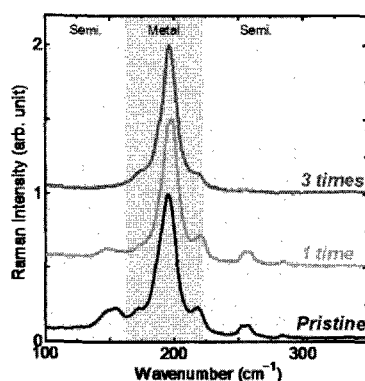


Fig. 1 Characterization of the effect of cyclic separations by Raman spectra in *m*-SWCNTs

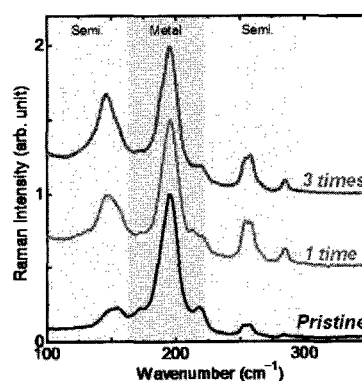


Fig. 2 Characterization of the effect of cyclic separations by Raman spectra in *s*-SWCNTs

**References:**[1] K. Ihara, *et al.*, NT10: 11<sup>th</sup> International Conference on the Science and Application of Nanotubes, Montreal, Canada (2010) pp. 54.

**Corresponding Author:** Kazuki Ihara

**E-mail:** ihara@tasc-nt.or.jp, **Tel:**+81-29-861-6357, **Fax:** +81-29-858-6330

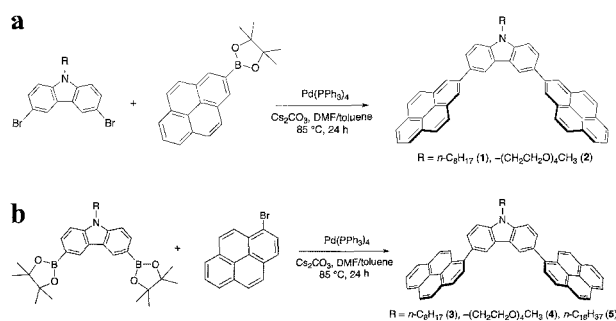
## Diameter-Based Separation of Single-Walled Carbon Nanotubes through Selective Extraction with Dipyrene Nanotweezers

○Naoki Komatsu<sup>1</sup>, A. F. M. Mustafizur Rahman<sup>1</sup>, Feng Wang<sup>1</sup>, Kazunari Matsuda<sup>2</sup>, Takahide Kimura<sup>1</sup>

<sup>1</sup>Department of Chemistry, Shiga University of Medical Science, Seta, Otsu 520-2192, Japan

<sup>2</sup>Institute of Advanced Energy, Kyoto University, Uji, Kyoto 611-0011, Japan

We have been developing host-guest methodology for separation of single-walled carbon nanotubes (SWNTs) according to the handedness and diameter with gable-type chiral diporphyrins, designated as porphyrin nanotweezers, consisting of two porphyrins and rigid spacer in between [1]. As an extension of our strategy, novel nanotweezers having two pyrenes instead of porphyrins have been designed, because pyrene is known to have high affinity toward SWNT surface [2]. The pyrene nanotweezers presented here consist of two 1- or 2-pyrenes and 3,6-carbazolylenes with various *N*-substituents. They were synthesized through Suzuki coupling reactions between 1- or 2-substituted pyrene with 3,6-disubstituted carbazoles as shown in Scheme 1. For the extraction of SWNTs, the 1- and 2-pyrene nanotweezers show the marked contrast; 1-pyrene nanotweezers **3** – **5** selectively extracted SWNTs with diameters ranging from 0.84 nm to 0.97 nm, while 2-pyrene nanotweezers **1** – **2** were not able to extract SWNTs at all. The marked difference in the extraction ability may be ascribed to the difference in the solubility and the stability of the complexes. As compared with the porphyrin nanotweezers previously reported by us [1], the pyrene nanotweezers have advantage in practical separation for diameter of SWNTs because of their facile synthesis.



**Scheme 1.** Synthesis of 2-pyrene nanotweezers **1** – **2** (a) and 1-pyrene nanotweezers **3** – **5** (b) via Suzuki-Miyaura coupling reactions.

**Reference:** [1] F. Wang, K. Matsuda, A. F. M. M. Rahman, X. Peng, T. Kimura, N. Komatsu, *J. Am. Chem. Soc.*, **132**, 10876 (2010); X. Peng, F. Wang, A. F. M. M. Rahman, A. Bauri, N. Komatsu, *Chem. Lett.*, **39**, 1022 (2010); N. Komatsu, F. Wang, *Materials*, **3**, 3818 (2010); X. Peng, F. Wang, T. Kimura, N. Komatsu, A. Osuka, *J. Phys. Chem. C.*, **113**, 9108 (2009); X. Peng, N. Komatsu, T. Kimura, A. Osuka, *ACS Nano*, **2**, 2045 (2008); X. Peng, N. Komatsu, T. Kimura, A. Osuka, *J. Am. Chem. Soc.*, **129**, 15947 (2007); X. Peng, N. Komatsu, T. Shimawaki, S. Aonuma, T. Kimura, A. Osuka, *Nature Nanotechnology*, **2**, 361 (2007).

[2] A. F. M. M. Rahman, F. Wang, K. Matsuda, T. Kimura, N. Komatsu, submitted.

**Corresponding Author:** Naoki Komatsu, **E-mail:** nkomatsu@belle.shiga-med.ac.jp

**Tel:** +81-77-548-2102, **Fax:** +81-77-548-2405

## Effect of Sonication on the Length Distribution of Single Wall Carbon Nanotubes

○Shigekazu Ohmori<sup>1</sup>, Takeshi Saito<sup>1</sup>, Yuki Asada<sup>1</sup>, Motoo Yumura<sup>1</sup>, Sumio Iijima<sup>1</sup>

<sup>1</sup>*Nanotube Research Center, National Institute of Advanced Industrial Science and Technology (AIST), Japan*

Single wall carbon nanotubes (SWCNTs) were frequently dispersed into suspension by sonication with the help of various dispersing reagents (detergents), not only for fundamental but also for applied research. Although it has been considered that the dispersing process using sonication might cut or shorten SWCNTs, to date its detailed cutting effect, such as dependences on detergents, sonication power, and so on, has not been fully clarified yet. In this work, we have investigated the differences in length distribution of SWCNTs between their sonication processes using various detergents.

Four detergents, sodium dodecyl sulfate (SDS), sodium dodecylbenzene sulfate (SDBS), sodium cholate (SC), and ethylene glycol (100) stearyl ether (Brij 700) have been intentionally selected to explore the effect of cutting SWCNTs during their dispersing. The length of SWCNTs in each sample, deposited on the aminopropyltriethoxysilane (APTES) functionalized silicon substrate, were statistically characterized by the analysis of topographic images taken by atomic force microscope (AFM). Diameter dependence on the length distribution after the dispersing process were also investigated.

As a result of dispersing SWCNTs by bath sonication at 70 W, although the length distributions of SWCNTs, especially in SDS dispersing, highly depended on the dispersing process, roughly SC and Brij 700 dispersing results show shorter length distributions compared with SDBS. In particular, the diameter dependence in length distribution showed clear contrast between SC and Brij 700 dispersing: Whereas the length distributions of SC dispersing showed relatively regular dependence on the SWCNTs diameter, less or almost no dependence on the diameter was observed in Brij 700 dispersing. Furthermore, when SWCNTs were dispersed by using Brij 700 with the horn-type sonication homogenizer at 300 W for 10 hours, all measured SWCNTs were even shorter and in the range less than 600 nm with the average length of 119 nm. These results suggest that Brij 700 possesses the considerably strong ability that effectively cuts SWCNTs at their dispersing process.

This work has been supported by NEDO project.

Corresponding Author: Takeshi Saito

TEL: +81-29-861-4863, FAX: +81-29-861-4413, E-mail: [takeshi-saito@aist.go.jp](mailto:takeshi-saito@aist.go.jp)

## QM/MD Simulation of SWNT Nucleation on Transition-Metal Carbide Nanoparticles

○Stephan Irlé,<sup>1</sup> Alister J Page,<sup>2</sup> Honami Yamane,<sup>2</sup> Y. Ohta,<sup>2</sup> and Keiji Morokuma<sup>2</sup>

<sup>1</sup>*Institute for Advanced Research and Department of Chemistry, Nagoya University, Nagoya 464-8602, Japan*

<sup>2</sup>*Fukui Institute for Fundamental Chemistry, Kyoto University, Kyoto, 606-8103, Japan*

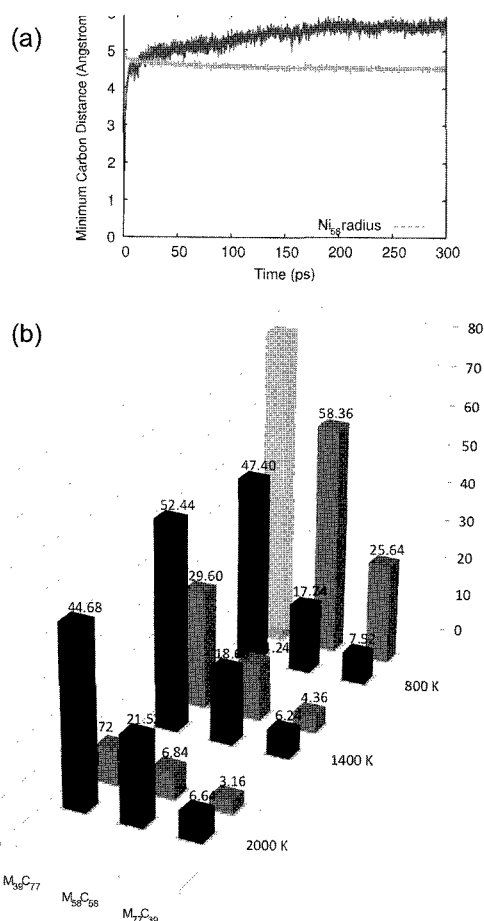


**Figure 1.** (a) Minimal distance (red) between all carbon atoms and Ni<sub>58</sub> center of mass during SWNT nucleation from Ni<sub>58</sub>C<sub>58</sub> nanoparticle. “Average carbon precipitation time” is defined as the first time at which this distance is greater than the Ni<sub>58</sub> radius. (b) Average carbon precipitation times (ps) from Ni<sub>x</sub>C<sub>y</sub> and Fe<sub>x</sub>C<sub>y</sub> nanoparticles at 800, 1400 and 2000 K. Grey and brown columns represent data for Ni<sub>x</sub>C<sub>y</sub> and Fe<sub>x</sub>C<sub>y</sub>, respectively. Transparent columns indicate an average carbon precipitation time > 300 ps. All data averaged over 10 trajectories.

The mechanism and kinetics of single-walled carbon nanotube (SWNT) nucleation from Fe- and Ni-carbide nanoparticle precursors have been investigated using quantum chemical molecular dynamics (QM/MD) methods [1]. It was observed that SWNT nucleation occurred via three distinct stages, viz. the precipitation of the carbon from the metalcarbide, the formation of a “surface/subsurface” carbide intermediate species, and finally the formation of a nascent *sp*<sup>2</sup>-hybridized carbon structure supported by the metal catalyst. The kinetics of SWNT nucleation exhibited distinct dependences on carbon concentration and temperature (see Fig. 1). In particular, SWNT nucleation from Ni<sub>x</sub>C<sub>y</sub> nanoparticles proceeded more favorably compared to nucleation from Fe<sub>x</sub>C<sub>y</sub> nanoparticles. The stability of the surface/subsurface carbide was also influenced by the phase of the nanoparticle itself. The observations agree well with experimentally available data for SWNT growth on iron and nickel catalyst particles.

### References

[1] A. J. Page *et al.* J. Am. Chem. Soc. **132**, 15699 (2010).

**Corresponding Authors:** Stephan Irlé and Keiji Morokuma

**TEL:**+81-52-747-6397,**FAX:**+81-52-788-6151

**E-mail:** [sirle@iar.nagoya-u.a.jp](mailto:sirle@iar.nagoya-u.a.jp),

[keiji.morokuma@emory.edu](mailto:keiji.morokuma@emory.edu)

**Stacking-order sensitive Raman modes of graphene**○R. Saito<sup>1</sup>, K. Sato<sup>1</sup>, C. Cong<sup>2</sup>, Y. Ting<sup>2</sup>, M. S. Dresselhaus<sup>3</sup><sup>1</sup>*Department of Physics, Tohoku University, Aoba, Sendai 980-8578, Japan*<sup>2</sup>*Division of Physics and Applied Physics, Nanyang Tech. University, Singapore*<sup>3</sup>*Massachusetts Institute of Technology, Cambridge, USA*

Bilayer and multi-layer graphene are considered to be a candidate for semiconducting devices with an energy gap by applying the electric field. However, when we make a bilayer graphene, for example, the stacking order of the two layers does not always have so-called ABAB Bernal stacking order but some commensurate or incommensurate stacking orders which modify the electronic structure significantly. In nature, there is ABC rhombohedral stacking order of graphite, too. Thus characterization of the stacking order is now investigated by many methods. Here we propose that some combinational Raman spectra are useful for characterizing the stacking order such as overtone of oTO (M band), the combination mode of iTA+LO, whose frequency appear around 1700-1900cm<sup>-1</sup> [1]. Especially, in the case of single layer graphene or folded bilayer graphene, overtone of oTO is completely suppressed because of the symmetry requirement. For the combinational modes, layer dependence of the frequencies as a function of laser excitation energy provides a much clearer explanation than the analysis by the conventional characterization of G' (2D) Raman bands. Combining with the calculated double resonance Raman spectra, we will discuss how we can understand the stacking order of graphene systems from the Raman spectra.

[1] C. Cong, Y. Ting, R. Saito, M. S. Dresselhaus, unpublished.

Corresponding Author: Riichiro Saito

TEL: +81-22-795-7754 FAX: +81-22-795-6447,

E-mail: [rsaito@flex.phys.tohoku.ac.jp](mailto:rsaito@flex.phys.tohoku.ac.jp)

Web: <http://flex.phys.tohoku.ac.jp/>

## Energetics and Electronic Structures of Graphene Adsorbed on HfO<sub>2</sub> Surfaces

○Katsumasa Kamiya<sup>1,2</sup>, Naoto Umezawa<sup>3</sup>, and Susumu Okada<sup>1,2</sup>

<sup>1</sup>*Graduate School of Pure and Applied Sciences, University of Tsukuba, 1-1-1 Tennodai, Tsukuba, Ibaraki 305-8571, Japan*

<sup>2</sup>*Japan Science and Technology Agency, CREST, 5 Sanbancho, Chiyoda-ku, Tokyo 102-0075, Japan*

<sup>3</sup>*Photocatalytic Materials Center, National Institute for Materials Science, 1-2-1 Sengen, Tsukuba, Ibaraki 305-0047, Japan*

Graphene has the great potential to advance both the low-dimensional sciences and the nano-scale electronic engineering. Recently, the integration of the graphene with a scalable gate dielectric, such as high permittivity (high- $k$ ) materials, has been the subject of the research with the goal of the realization of graphene-based electronic devices. For the fabrication of the graphene on insulating substrates, an understanding of its interactions with the substrates is critical, since they could directly affect the intrinsic electronic properties of the graphene. However, its underlying characteristics of the interaction are still far from being explained. Thus, we here study the energetics, geometry, and electronic structure of graphene adsorbed on (111) surfaces of cubic hafnia (HfO<sub>2</sub>) using first-principles calculations in the framework of density functional theory. To simulate a hybrid structure of graphene and HfO<sub>2</sub>, we considered an oxygen-terminated (111) surface of a cubic phase of HfO<sub>2</sub> possessing a triangular lattice of O atoms at the topmost layer. The surfaces were simulated using a repeated-slab model that includes five HfO<sub>2</sub> layers, graphene, and a 7 Å -vacuum region.

We found that the graphene is bound to the HfO<sub>2</sub> surfaces via interactions with an interlayer spacing of 3.05 Å. The calculated binding energy is about 110 meV per C atom. The electronic structure of the HfO<sub>2</sub>-adsorbed graphene originates primarily from that of the graphene near the Fermi level. However, a detailed analysis of the electronic structure shows that the linear bands at the Fermi level are slightly split, because of the interaction between the graphene and the HfO<sub>2</sub> substrate. The physical origin of this splitting is the hybridization between the  $\pi$  states of the graphene and the O 2 $p$  state with Hf  $d$  character.

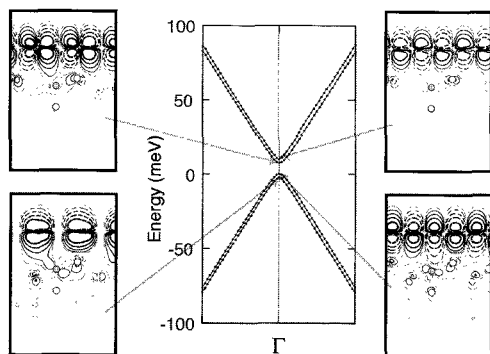


Fig.1. Contour maps of the electron states near the Fermi level at the  $\Gamma$  point in graphene adsorbed on HfO<sub>2</sub>. Each contour denotes twice (or half) the values of the adjacent contour lines from  $\pm 0.128 (e/\text{\AA}^3)^{1/2}$ . The solid and dotted lines show the positive and negative values, respectively. The two O atoms and one Hf atom that define a cross section are shown by white and gray circles, respectively.

**Corresponding Author:** Katsumasa Kamiya

**E-mail:** kkamiya@comas.frsc.tsukuba.ac.jp

**Tel:** +81-29-853-5922

## Large area CVD graphene from camphor for organic solar cells application

°Golap Kalita, Masahiro Matsushima, Koichi Wakita and Masayoshi Umeno

*Department of Electronics and Information Engineering, Chubu University, 1200  
Matsumoto-cho, Kasugai-shi 487-8501, Japan*

We present synthesis of large area graphene sheets by control pyrolysis of solid botanical derivative camphor ( $C_{10}H_{16}O$ ). At the very beginning of CVD based graphene, we demonstrated possible fabrication process of few layer graphene by thermal CVD from camphor. Few layer graphene sheets with minimum 3 layers or much higher number of layers were obtained by pyrolysing on Ni surface. Voltage aberration corrected high resolution TEM studies were done to observe the packing structure of the few layer graphene by directly imaging the atomic structure. Large area monolayer or bi-layer graphene were also synthesized from camphor on Cu foils. We have demonstrated graphene film synthesized from camphor can be transferred to arbitrary substrate for fabrication of transparent electrode.

Solution processed organic solar cells were fabricated on graphene based transparent electrode. A P3HT:PCBM solar cell fabricated on graphene shows very good dark current characteristic having minimum leakage current. Under illumination of light device performance is comparable with standard ITO based P3HT:PCBM solar cells. Details studies on organic solar cells fabrication in few layers graphene based transparent electrode will be discussed. The technique to fabricate few layer of graphene as transparent electrode from camphor is both viable and scalable for potential large area solar cells and other optoelectronic applications.

### References:

1. P. R. Somani, M. Umeno et al., Chem. Phys. Letts. **430**, 56 (2006).
2. G. Kalita, K. Wakita and M. Umeno et al., Mater. Lett. **64**, 2180 (2010).
3. G. Kalita, K. Wakita and M. Umeno et al., J. Mater. Chem. **20**, 9713 (2010).

Corresponding author: Tel/Fax: +81 568 51 9056 E-mail: [golapkalita@yahoo.co.in](mailto:golapkalita@yahoo.co.in)

## **Analysis of Magneto Resistance Fluctuations in Graphene Thin Films**

S. Motooka<sup>A</sup>, A. Mahjoub<sup>A</sup>, T. Abe<sup>A</sup>, N. Aoki<sup>A</sup>, D. K. Ferry<sup>B</sup>, J. P. Bird<sup>C</sup>, & Y. Ochiai<sup>A</sup>

<sup>A</sup> Graduate School of Advanced Integration Science, Chiba University.

<sup>B</sup> Arizona state university.

<sup>C</sup> University of Buffalo.

In our recent years a chain of experimental studies on graphene electrical conductivity were carried out. Physical phenomena due to Weak localization states<sup>1</sup>, universal conductance fluctuation<sup>1,2</sup> has provided us with clear expansion up to the observations under quantum interference basics understanding. As part of our research group background, Universal Fluctuation Conductance (UCF) for magneto- transport properties of graphene has been observed at low-temperature.

Hence by, our summery to the Japanese physics Society meeting two years ago<sup>3</sup> came to, the detailed observations of conductance fluctuations where external magnetic field was swept to observe the Fourier power spectrum analysis of Universal Fluctuation Conductance that clearly showed the periodicity (quasi-periodicity). The Universal conductivity had shown strong non-periodic behavior that varied with fluctuations hence the irrelevance to the presence Universal Fluctuation Conductance has been observed.

Experimental study research of electrical conduction in open semiconductor quantum dot research<sup>4</sup> has been reported. And in recent years, theoretical study<sup>5</sup> was accompanied alongside indicating such pseudo periodicity in graphene UFC observation is true. These experimental and theoretical facts shown in graphene materials strongly suggest the conductance fluctuation periodicity in electrical conduction mechanism.

Pursuing furthermore, the observed UCF at low temperature magneto-resistance of a relatively larger grapheme sample had gave us the lead. The analysis in bigger graphene samples area had implied that effect of impurities which also referred to as metallic-effect in graphene surface are even thought to be more susceptible than that of a small graphene samples area. As a result, the large graphene sample has not shown any quasi periodic fluctuation in our observations. Here by the final conclusion was generalized in the two graphene samples for the Universal Conductance Fluctuation observations.

### References:

- (1) R. V. Gorbachev, et al., Phys. Rev. Lett. 98, 176805 (2007).
- (2) N. E. Staley, et al., Phys. Rev. B 77, 155429 (2008).
- (3) Y. Ujiie, et al., J. Phys.: Condens. Matter 21 382202 (2009).
- (4) J. P. Bird, et al., Chaos, Solitons, & Fractals 8, 1299 (1997).
- (5) Huang L, et al., Phys. Rev. Lett. 103, 054101 (2009).



**Fullerene Peapod– Poly(3-hexylthiophene) Hybrids**

○Tomokazu Umeyama<sup>1,2</sup>, Noriyasu Tezuka<sup>1</sup>, Yoshihiro Matano<sup>1</sup>,  
and Hiroshi Imahori<sup>1,3</sup>

<sup>1</sup>*Graduate School of Engineering, Kyoto University, Kyoto 615-8510, Japan*

<sup>2</sup>*PRESTO, Japan Science and Technology Agency, Kawaguchi 332-0012, Japan*

<sup>3</sup>*Institute for Integrated Cell-Material Sciences, Kyoto University,  
Kyoto 615-8510, Japan*

Novel nanohybrids of single-walled carbon nanotubes (SWNTs) encapsulating C<sub>60</sub> or C<sub>70</sub> with poly(3-hexylthiophene) (P3HT) have been prepared and their photophysics and photoelectrochemical properties are studied in detail for the first time. Strong  $\pi$ - $\pi$  interaction between the SWNT sidewalls and P3HT afforded successful dissolution of the so-called fullerene peapods into an organic solvent, as in the case of empty SWNTs. Fluorescence emission of P3HT in the SWNT–P3HT hybrids was completely quenched by the SWNTs regardless of the fullerenes insertion. Transient absorption and fluorescence lifetime measurements revealed the excited state dynamics of the nanohybrids, where exciplex formation from the short-lived P3HT singlet excited state ( $\sim 0.2$  ps) with the fullerene peapods and subsequent relaxation to the ground state within  $\sim 1$  ps occurred dominantly. Significant difference in the photodynamics upon encapsulation of C<sub>60</sub> or C<sub>70</sub> was not detected, implying little participation of the fullerenes in the excited state event and thus the inability of the encapsulated fullerenes to generate the charge-separated state between the fullerene peapods and P3HT. Photoelectrochemical devices based on the peapod–P3HT nanohybrids showed almost the same incident photon-to-current efficiencies as those for the empty SWNT–P3HT-based device, which is in good agreement with the results of the time-resolved spectroscopies.

[1] N. Tezuka, T. Umeyama, Y. Matano, T. Shishido, K. Yoshida, T. Ogawa, S. Isoda, K. Stranius, V. Chukharev, N. V. Tkachenko, H. Lemmetyinen and H. Imahori, *Energy Environ. Sci.*, in press (DOI: 10.1039/C0EE00482K).

Corresponding Author: Tomokazu Umeyama

TEL: +81-75-383-2568, FAX: +81-75-383-2571, E-mail: umeyama@scl.kyoto-u.ac.j

## Synthesis and Photophysical Properties of Metallofullerenes — Zinc

## Porphyrin Conjugates: Impact of Endohedral Clusters

Lai Feng,<sup>†</sup> Shankara Gayathri Radhakrishnan,<sup>‡</sup> Naomi Mizorogi,<sup>†</sup> Zdenek Slanina,<sup>†</sup> Hidefumi Nikawa,<sup>†</sup> Takahiro Tsuchiya,<sup>†</sup> Takeshi Akasaka,<sup>\*,†</sup> Shigeru Nagase<sup>\*,§</sup>, Nazario Martín,<sup>#</sup> Dirk M. Guldi,<sup>\*,‡</sup>

<sup>†</sup>Center for Tsukuba Advanced Research Alliance, University of Tsukuba, Tsukuba 305-8577, Japan,

<sup>‡</sup>Department of Chemistry and Pharmacy & Interdisciplinary Center for Molecular Materials, Friedrich-Alexander-Universität Erlangen-Nürnberg, 91058 Erlangen, Germany, <sup>§</sup>Department of Theoretical and Computational Molecular Science, Institute for Molecular Science, Okazaki 444-8585, Japan, <sup>#</sup>Departamento de Química Orgánica, Facultad de Química, Universidad Complutense, 28040 Madrid, Spain and IMDEA-Nanoscience, Campus de Cantoblanco, 28049 Madrid, Spain

Novel covalent metallofullerenes (i.e., Ce<sub>2</sub>@I<sub>h</sub>-C<sub>80</sub>, La<sub>2</sub>@I<sub>h</sub>-C<sub>80</sub>, Sc<sub>3</sub>N@I<sub>h</sub>-C<sub>80</sub>) — Zinc 5,10,15,20-tetraphenylporphyrin (ZnP) dyads (**1-3**) were prepared via [1+2] cycloaddition reactions of a diazo precursor. Their structures were characterized with the help of reference compounds (**4-6**). Combined studies of crystallography and NMR suggest a common (6,6)-open addition pattern for all the dyads and reference compounds. On the other hand, subtly different conformations, that is, a restricted and a comparatively more flexible one, emerge for **1**, **2** and **3**, respectively. In line with this difference are the electrochemical and spectral studies, which imply appreciably stronger I<sub>h</sub>-C<sub>80</sub> / ZnP interactions in **1** and **2** when compared to those in **3**. Density functional calculations reveal significant attractions between the two entities of these conjugates, as well as their separately localized HOMOs and LUMOs. The geometrical conformations and LUMO distributions of **2** and **3**, at our applied computational level, are slightly varied with their different endohedral clusters. The clusters also exert different impact on the excited state reactivity of the conjugates. For example, **1** and **2** undergo, upon photoexcitation, a fast charge separation process and yield a radical ion pair, whose nature, namely (M<sub>2</sub>@C<sub>80</sub>)<sup>-</sup>-(ZnP)<sup>+</sup> versus (M<sub>2</sub>@C<sub>80</sub>)<sup>++</sup>-(ZnP)<sup>-</sup> (M= Ce, La), varies with solvent polarity. **3**, on the other hand, affords the same (Sc<sub>3</sub>N@C<sub>80</sub>)<sup>-</sup>-(ZnP)<sup>+</sup> radical ion pair regardless of the solvent.

## Electronic structure and entrapped cluster structure of $C_{78}$ endohedral fullerenes

○Takafumi Miyazaki, Yusuke Aoki, Sousuke Ookita, Hajime Yagi and Shojun Hino  
*Graduate School of Science and Engineering, Ehime University*

Ultraviolet photoelectron spectroscopy has been revealing the valence band electronic structure of fullerenes and endohedral fullerenes, and now it has been verified to be a powerful tool to investigate the electronic structure of endohedral fullerenes as well as the geometry of entrapped clusters with an aid of theoretical calculation. We present the ultraviolet photoelectron spectra (UPS) of  $Sc_3N@C_{78}$ ,  $La_2@C_{78}$  and  $Ti_2C_2@C_{78}$ , all of them have  $D_{3h}$  (No. 5) symmetry, and the results of DFT calculation.

Figure 1 shows the upper valence band UPS of  $Sc_3N@C_{78}$ ,  $Ti_2C_2@C_{78}$  and  $La_2@C_{78}$  obtained with  $h\nu = 30$  eV incident photon energy. Their UPS are completely different from those of other endohedral fullerenes reported until now. In the UPS of other fullerenes, a large structure is observed at about 5.5 eV and a few structures appear at lower binding energy side. However, the corresponding peak of  $Sc_3N@C_{78}$ ,  $Ti_2C_2@C_{78}$  and  $La_2@C_{78}$  shifted toward higher binding energy side by 0.3 eV and at lower binding energy side several complicated structures can be observed in the UPS of  $La_2@C_{78}$  and  $Ti_2C_2@C_{78}$ .

The results of DFT calculation (B3LYP) and simulation spectra obtained by broadening of the Eigen-values with Gaussian functions are also shown in Figure 1. The abscissa of the simulation spectra is shifted so that the peak positions of each spectrum appear at the same region. The simulation spectra reproduced the UPS so well that the DFT calculation is good enough to elucidate the geometry of entrapped species. The geometries of entrapped clusters of these endohedral fullerenes are a Ti-C-C-Ti linear shape for  $Ti_2C_2@C_{78}$  and a nitrogen atom centered planar triangle shape for  $Sc_3N@C_{78}$ .

It should be noted that their spectral onset energy is the same 0.7 eV although the amounts of transferred electrons from the entrapped clusters to the cage differ in these endohedral fullerenes. This suggests that the difference in the amounts of transferred electrons does not reflect the onset energy (corresponding band gap of the materials).

Corresponding Authors: T. Miyazaki, E-mail: [miyazaki@eng.ehime-u.ac.jp](mailto:miyazaki@eng.ehime-u.ac.jp), phone: 089-927-9930; S. Hino, E-mail: [hino@eng.ehime-u.ac.jp](mailto:hino@eng.ehime-u.ac.jp), phone: 089-927-9924.

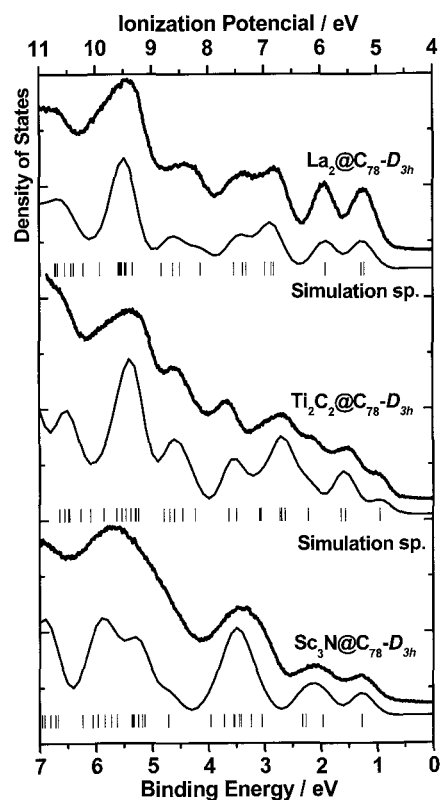


Fig. 1. The UPS of  $Sc_3N@C_{78}$ ,  $Ti_2C_2@C_{78}$  and  $La_2@C_{78}$  and their simulation spectra.

## Photo-Polymerization of C<sub>60</sub> Thin Film using Optical Vortex Irradiation

○Nobuyuki Aoki<sup>1</sup>, Tatsuya Doi<sup>1</sup>, Xiaojun Wei<sup>1</sup>, Kyouhei Koyama<sup>1</sup>, Katsuhiko Miyamoto<sup>1</sup>, Takashige Omatsu<sup>1</sup>, Jonathan P. Bird<sup>2</sup> and Yuichi Ochiai<sup>1</sup>

<sup>1</sup> *Graduate School of Advanced Integration Science, Chiba University,  
1-33 Yayoi, Inage, Chiba, 263-8522, Japan*

<sup>2</sup> *Department of Electrical Engineering, University at Buffalo, The State University of  
New York, Buffalo, NY 14260-1920, USA*

A state of the art photo-polymerization method of a C<sub>60</sub> thin film has been studied using an optical vortex irradiation [1]. Since the beam has a herical wavefront and a rotation of angular momentum, a confinement force due to the photo pressure toward the center of the beam. Therefore, a highly-packed and uniform photo-polymerization can be expected in a C<sub>60</sub> thin film compared with conventional laser beam. Moreover, a circular polymerization might be realized forming concentric-multiple-ring structures.

Photo-polymerization is one of the promising solutions for electrical device application of C<sub>60</sub> molecules, where inter-molecular covalent bonds could protect an intercalation of oxygen atoms. Some kinds of beam irradiations have been performed so far. However, a shrink of inter-molecule distance causes a serious problem such an introduction of cracks into the thin film [2]. The film is divided into a lot of domains of a size of several  $\mu\text{m}^2$ . Consequently, a mobility of the film decreases a few orders of magnitude after the irradiation, although a good transport characteristic can be expected for within each domain.

In our trial of irradiation of a focused optical vortex (532 nm) on a C<sub>60</sub> thin film, circular patterns have successfully resolved after the irradiations for a few minutes. The irradiated region does not have solubility into a toluene and the  $A_g(2)$  peak of Raman spectrum shows polymerization of the C<sub>60</sub> molecules. Moreover, no crack has been observed by SEM observation. These results suggest that a highly-packed and uniform photo-polymerization have been realized by optical vortex irradiation. The transport properties will also be discussed in the presentation.

[1] T. Omatsu *et al.*, *Optics Express*, **18**, 17967 (2010).

[2] Y. Chiba *et al.*, *J. Phys: Conf. Ser.*, **159**, 012017 (2009).

Corresponding Author: Nobuyuki Aoki

TEL: +81-43-290-3430, FAX: +81-43-290-3427, E-mail: n-aoki@faculty.chiba-u.jp

## Synthesis of Polyhydroxylated Fullerene $C_{60}(OH)_6$ via Chlorofullerene $C_{60}Cl_6$ and its Characterization using ESI-MS Spectroscopy

○Hiroshi Ueno, Toshiki Sugai and Hiroshi Moriyama

*Department of Chemistry, Toho University, Funabashi, 274-8510 Japan*

Polyhydroxylated fullerenes, known as fullerenols, have attracted much attention because they have useful properties and various potential applications. However, it is still an open question as to how many, and where, hydroxyl groups are added to the surface of fullerenes. Because the fullerenols reported so far have been a mixture of fullerenols with a different number of hydroxyl groups, along with their many isomers, only an average number of hydroxyl groups per fullerene cage has been determined using the elemental analysis. In this work, we synthesized a fullereneol consisting of a single isomer via chlorofullerene, and have characterized its structure by ESI-MS and  $^{13}C$  NMR spectroscopy.

At the present stage of our work, we have synthesized fullereneol,  $C_{60}(OH)_6$ , and the number of hydroxyl groups has been determined from the negative ESI-MS spectrum. The reaction of  $C_{60}Cl_6$  with water proceeded almost completely, and formed  $C_{60}(OH)_6$  when  $Ag^+TPFPB^-$  was added to the system as a reagent. We supposed that the  $Ag^+$  ions weakened C–Cl bond strength because of the strong interaction between  $Ag^+$  ions and Cl atoms. Therefore, weak nucleophiles, such as water, can react with  $C_{60}Cl_6$  to form fullereneol. We are identifying appropriate procedures to achieve complete substitution of the Cl moieties.

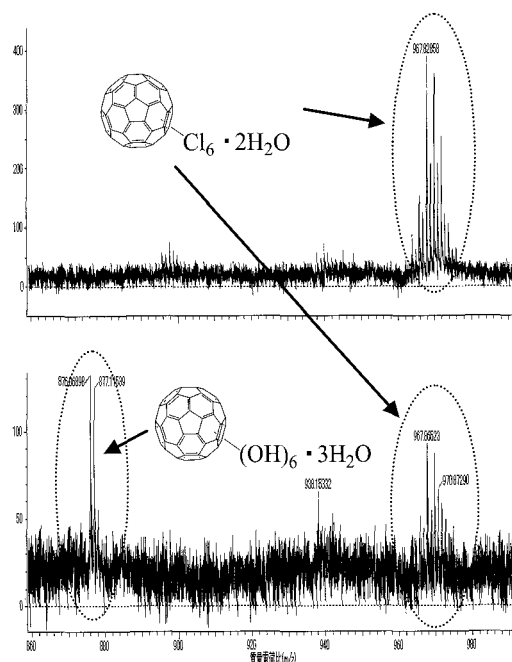


**Fig 1.** Negative ESI-MS spectra of  $C_{60}Cl_6 \cdot 2H_2O$  (top) and  $C_{60}(OH)_6 \cdot 3H_2O$  (bottom).

[1] Birkett, P. R.; Avent, A. G.; Darwish, A. D.; Kroto, H. W.; Taylor, R.; Walton, D. R. M. *J. Chem. Soc., Chem. Commun.* **1993**, 15, 1230-1232.

[2] Kuprat, M.; Lehmann, M.; Schulz, A.; Villinger, A. *Organometallics* **2010**, 29, 1421-1427.

Corresponding Author : Hiroshi Moriyama

TEL: +81-47-472-1211, FAX: +81-47-476-9449, E-mail: moriyama@chem.sci.toho-u.ac.jp

## Thermal and oxidative stabilities of multi-arylated [60]fullerene derivatives

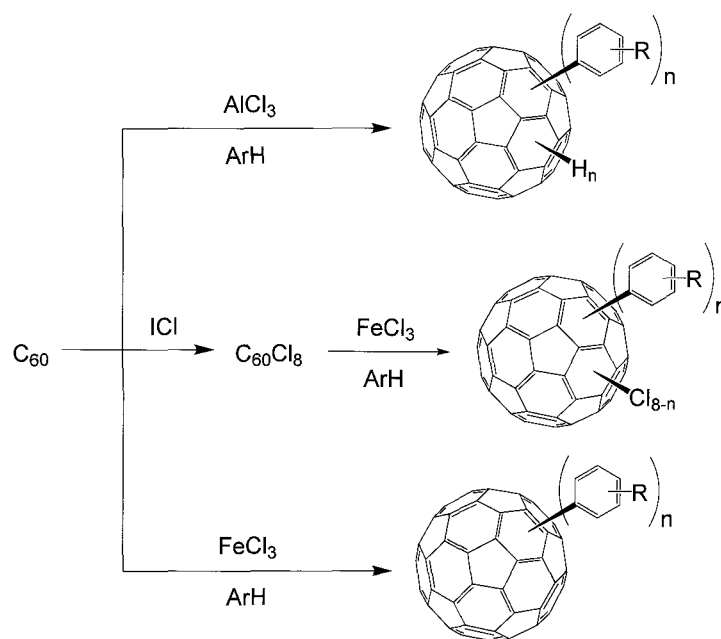
○Ken Kokubo<sup>1</sup>, Miyato Kashihara<sup>1</sup>, Yano Tomomi<sup>2</sup>, Katsutomo Tanaka<sup>2</sup>,  
Naohiko Ikuma<sup>1</sup>, and Takumi Oshima<sup>1</sup>

<sup>1</sup>*Division of Applied Chemistry, Graduate School of Engineering, Osaka University,  
2-1 Yamadaoka, Suita, Osaka 565-0871, Japan*

<sup>2</sup>*Mitsubishi Chemical Corporation, 1-1 Shiroishi, Kurosaki, Yahatanishi-ku,  
Kitakyusyu 806-0004, Japan*

High thermal and oxidative stabilities, as well as high etching durability, are the crucial requirements for resist materials. A soluble carbon material, fullerene, has the high potential for dry etching durability and thus for higher resolution of semiconductor devices as compared to the current resist materials. However, pristine fullerene exhibits low solubility to the current common resist solvent in wet process, *e.g.*, propylene glycol methyl ether acetate (PGMEA). Thus, it is desired to synthesize the highly PGMEA-soluble fullerene derivatives without hetero atoms to retain the high carbon content by a facile synthetic method.

In this study, we synthesized multi-*hydro*arylated and multi-arylated [60]fullerene derivatives by three different methods, 1) hydroarylation of C<sub>60</sub> mediated by AlCl<sub>3</sub>, 2) arylation of polychlorinated fullerene C<sub>60</sub>Cl<sub>8</sub> mediated by FeCl<sub>3</sub>, and 3) direct multi-arylation of C<sub>60</sub> mediated by FeCl<sub>3</sub> in various aromatic solvents. The products were found to exhibit the high PGMEA-solubility (>20 wt%) depending on the type and the number of aryl groups introduced. Moreover, the thermogravimetric analysis both under air and under N<sub>2</sub> revealed that the thermal and oxidative stabilities of one of them exceeded over 300 °C.



Corresponding Author: Ken Kokubo

TEL: +81-6-6879-4592, FAX: +81-6-6879-4593, E-mail: kokubo@chem.eng.osaka-u.ac.jp

## Influence of UV Irradiation on Polymerization of LLIP-Prepared C<sub>60</sub> Nanowhiskers

○Ying-Hui Wang and Kun'ichi Miyazawa

*Fullerene Engineering Group, Exploratory Nanotechnology Research Laboratory  
National Institute for Materials Science  
1-1 Namiki, Tsukuba, Ibaraki, 305-0044, Japan*

Solid C<sub>60</sub> has been known to be polymerized under irradiation of ultraviolet (UV) light and the molecules link together in a covalently bonded structure [1]. However, there has little study on the polymerization status of C<sub>60</sub> nanowhiskers (C<sub>60</sub>NWs) formed by the liquid-liquid interfacial precipitation method (LLIP method) [2]. In this presentation, we report the influence of UV irradiation on the polymerization of C<sub>60</sub>NWs synthesized by the LLIP method. Raman scattering spectra of C<sub>60</sub>NWs under specified UV region and irradiation time were measured according to the absorption spectra of C<sub>60</sub> thin films prepared on LiF (100) and NaCl (100) substrates [3]. The spectrum shown in Figure 1 (b) exhibits that the LLIP-prepared C<sub>60</sub>NWs are polymerized under a 263 nm UV irradiation with a power density of  $8 \times 10^{-3}$  mW/mm<sup>2</sup> for 12 h. We will interpret the detailed status of the polymerized condition in this research.

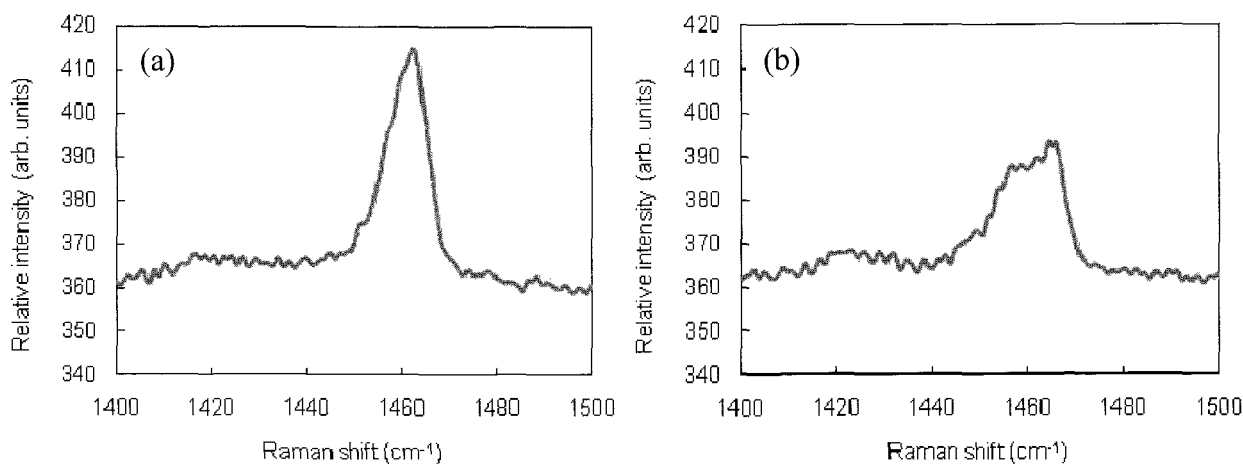


Fig. 1. The Raman spectra near the Ag(2) pentagonal pinch mode of the LLIP-prepared C<sub>60</sub>NWs under a 263 nm UV irradiation with a power density of  $8 \times 10^{-3}$  mW/mm<sup>2</sup>: (a) before irradiation and (b) after irradiation for 12 h.

[1] A. M. Rao, P. Zhou, K. A. Wang, G. T. Hager, J. M. Holden, Y. Wang, W. T. Lee, X. X. Bi, P. C. Eklund, D. S. Cornett, M. A. Duncan, I. J. Amster, *Science*, **259**, 955 (1993).

[2] K. Miyazawa, *Journal of Nanoscience and Nanotechnology*, **9**, 41(2009).

[3] Y. Achiba, T. Nakagawa, Y. Matsui, S. Suzuki, H. Shiromaru, K. Yamauchi, K. Nishiyama, M. Kainosho, H. Hoshi, Y. Maruyama and T. Mitani, *Chemistry Letters*, 1233 (1991).

Corresponding Author: Kun'ichi Miyazawa

TEL& FAX: +81-29-860-4528, E-mail: [MIYAZAWA.Kunichi@nims.go.jp](mailto:MIYAZAWA.Kunichi@nims.go.jp)

## Coaxially Stacked Coronene Column inside Single-Walled Carbon Nanotube

○Toshiya Okazaki<sup>1,2,3</sup>, Yoko Iizumi<sup>3,1</sup>, Shingo Okubo<sup>1,†</sup>, Hiromichi Kataura<sup>4</sup>, Zhen Liu<sup>1</sup>, Kazu Suenaga<sup>1</sup>, Yoshio Tahara<sup>1</sup>, Masako Yudasaka<sup>1</sup>, Susumu Okada<sup>5</sup> and Sumio Iijima<sup>1</sup>

<sup>1</sup>*Nanotube Research Center, AIST, Tsukuba 305-8565, Japan*

<sup>2</sup>*PRESTO, JST, 4-1-8 Honcho, Kawaguchi 332-0012, Japan*

<sup>3</sup>*Department of Chemistry, University of Tsukuba, Tsukuba 305-8571, Japan*

<sup>4</sup>*Nanosystem Research Institute, AIST, Tsukuba 305-8565, Japan*

<sup>5</sup>*Institute of Physics, Center for Computational Science, University of Tsukuba, Tsukuba 305-8571, Japan*

<sup>†</sup>*Current address: K. K. AIR LIQUIDE LABORATORIES, Tsukuba 300-4247, Japan*

One of the most interesting features of molecular materials is the fact that their physical properties change with the molecular arrangement as well as the properties of the molecule itself. Self-organization is an efficient pathway through which organic molecules assemble to form well-ordered nanometre-scale objects that are hardly synthesized by conventional chemical reactions. In these systems, two or more molecules are held together and assembled by means of intermolecular (noncovalent) bonding such as ion-dipole or dipole-dipole interactions, hydrogen bonding, hydrophobic interactions, or  $\pi$ - $\pi$  stacking.

Single-walled carbon nanotubes (SWCNTs) can offer a suitable interior space for accommodating molecules. The nanostructures produced by incorporating such molecules into SWCNTs are expected to exhibit several superior features. For example, because the diameter of SWCNTs can be adjusted to the size of the molecules, well-ordered molecular arrangements beyond a micro-metre long can be easily produced. The synthesized molecular arrangements are also expected to be strong and flexible against mechanical strain because the nanotube templates sustain the structure. Furthermore, the synthesized nanostructures are isolated from active molecules by the tube wall, which leads to the superior durability of the encapsulated molecules.

Here we demonstrate such an 1D SWCNT-templated nanostructure using planner  $\pi$ -conjugated molecules, coronenes. Encapsulated coronenes form nano-scale columns in a way that differs from 3D solid coronenes, resulting in electronic and optical properties peculiar to the 1D structure. The unique physical properties of the produced coronene columns and their biological application for molecular imaging probes will be discussed in detail.

**Corresponding Author:** Toshiya Okazaki, **E-mail:** toshi.okazaki@aist.go.jp, **Fax:** 029-861-6241



## Growth of Carbon Nanotubes Filled with Metal Sulfide Nanowires

○Akira Koshio, Takayuki Yamasaki, Makoto Yamamoto, and Fumio Kokai

*Division of Chemistry for Materials, Graduate School of Engineering, Mie University, 1577 Kurimamachiya-cho, Tsu, Mie 514-8507, Japan*

The hybridization of metal/metal compound nanowires and carbon nanotubes (CNTs) has been tried as one of the ideas for improving the quality, such as stability and crystallinity, of metal/metal compound nanowires. Many researches on various metal/metal compound-filled CNTs have been reported to date. However, it is difficult to achieve long one-dimensional growth by one-step synthesis. We have succeeded in the one-step syntheses of copper sulfide-filled CNTs (CuS@CNTs) and nickel sulfide-filled CNTs (NiS@CNTs) by two types of vaporization methods using ethanol and carbon disulfide (CS<sub>2</sub>), alcohol arc discharge and alcohol chemical vapor deposition (CVD), respectively. In this study, we investigated their effective formation conditions and structures.

CuS@CNTs were produced by conventional carbon arc discharge with ethanol vapor introduced into the arc plasma. Graphite rods were used for electrodes. A hole was drilled in the center of a graphite anode and filled with copper powder. The electrodes were set vertically in a vacuum chamber. The ethanol vapor was introduced into the chamber by bubbling argon through ethanol containing CS<sub>2</sub> of 10% heated at 50 °C. NiS@CNTs were formed by alcohol CVD method. Ethanol solutions of NiCl<sub>2</sub> were sprayed on a Si plate maintained at 400 °C followed by heating at 640 °C for 30 min. in an Ar atmosphere. The CVD growth was carried out at 900-1000 °C for 30 min. at a vapor pressure of ethanol containing a small amount of CS<sub>2</sub> in a vacuum.

The filling rate of CuS@CNTs was extremely high and few hollow CNTs were in the as-grown sample (Fig. 1(a)). The CuS@CNTs were classified into two types, thin (diameters of 20-50 nm) (Fig. 1(b)) and thick (diameters of 100-500 nm) (Fig. 1(c)), depending on the arc current. We assume that the additional carbon and hydrogen sources from the ethanol vapor lead to suitable density of carbon and hydrogen species in the arc plasma compared to that of the previous methods. The filling rate of NiS@CNTs was about 80%, and had diameters of about 100 nm and lengths of about 3 μm. Moreover, the NiS@CNTs grew vertically on the substrate. In this study we investigated growth conditions and mechanism of metal-compound filled nanotubes via the alcohol CVD process. We will present the detail of the structure of the two metal sulfide nanowire-filled CNTs in the presentation.

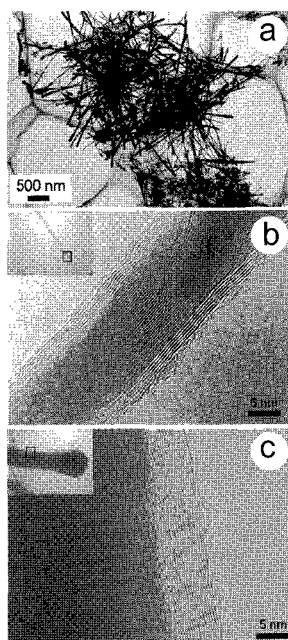


Fig. 1 (a) A typical TEM image of CuS@CNTs. High-magnification TEM images of (b) thin and (c) thick CuS@CNT.

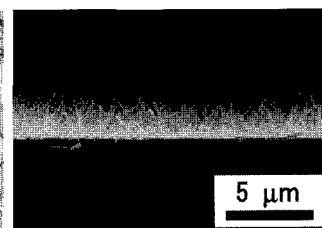


Fig. 2 A cross-sectional SEM image of NiS@CNTs grown on a substrate.

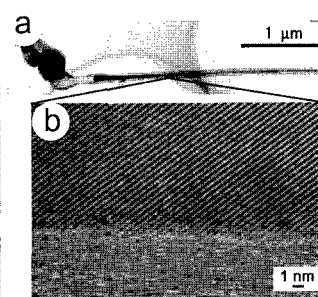


Fig. 3 (a) A TEM image of a NiS@CNT and (b) the high-magnification TEM image.

## First-principles study of $K_xC_{60}$ encapsulated in boron-nitride nanotubes

○Takashi Koretsune<sup>1</sup>, Susumu Saito<sup>1</sup>, Jesse Noffsinger<sup>2</sup> and Marvin L. Cohen<sup>2</sup>

1. *Department of Physics, Tokyo Institute of Technology, Meguro-ku, Tokyo, Japan*

2. *Department of Physics, University of California, Berkeley, California 94720, USA*

The important difference between boron-nitride nanotubes and carbon nanotubes is that boron-nitride nanotubes have large band gap independent of chirality and diameter whereas carbon nanotubes can be semiconducting or metallic. Thus, considering these nanoscale tubular materials as a host material to encapsulate atoms and/or molecules, boron-nitride nanotubes are more suitable nanotubes to investigate the encapsulated one-dimensional materials. Here, in order to examine the characteristics of one-dimensional alkali-doped fullerene compounds, we study the electronic structure of potassium-doped  $C_{60}$  encapsulated in the (10,10) boron-nitride nanotube shown in Fig. 1 using first-principles methods based on the density functional theory. We demonstrate that the material is one-dimensional metal where conducting electrons are only in the  $C_{60}$  chain. The Fermi-level density of states varies depending on the doping level and can be large in some cases, which indicates the possibility of various phase transitions including superconductivity as in the case of fcc  $K_3C_{60}$ . Interestingly, the Fermi-level density of states shows peculiar pressure dependence because of one-dimensional geometry. We also compute the electron-phonon couplings and discuss the difference from the three-dimensional fcc  $K_3C_{60}$ .

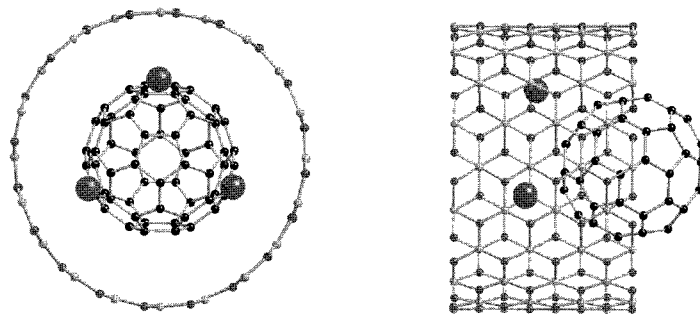


Fig. 1 Geometry of optimized  $K_3C_{60}$  encapsulated in the (10,10) boron-nitride nanotube.

Corresponding Author: Takashi Koretsune

E-mail : koretune@stat.phys.titech.ac.jp

## Epitaxial CVD growth of single-layer graphene over metal films crystallized on sapphire

○Hiroki Ago,<sup>\*a,b,c</sup> Yoshito Ito,<sup>b</sup> Baoshan Hu,<sup>a</sup> Carlo M. Orofeo,<sup>b</sup> Masaharu Tsuji,<sup>a,b</sup>  
Noriaki Mizuta,<sup>b</sup> Ken-ichi Ikeda,<sup>b</sup> and Seigi Mizuno<sup>b</sup>

<sup>a</sup> Institute for Materials Chemistry and Engineering, Kyushu University, Fukuoka 816-8580

<sup>b</sup> Graduate School of Engineering Sciences, Kyushu University, Fukuoka 816-8580

<sup>c</sup> PRESTO-JST

Graphene is emerging as a new building block of future nanoelectronics and microelectro-mechanical systems. Recently, catalytic CVD growth has attracted considerable interest as an effective means to produce large-area graphene films [1-3]. However, because most of the CVD growth has been done over polycrystalline metal films/foils, as-grown graphene has relatively small domain size and its orientation is not controlled. We studied the growth of graphene films over crystalline metal films deposited on single crystalline substrates and found the formation of square and triangular-shaped graphene sheets inside pits appeared on the crystalline metal film [4]. However, the graphene sheets were mainly few-layer and did not cover the whole area of the metal film.

Here, we performed atmospheric CVD over crystalline Co and Cu films deposited on c-plane sapphire substrates (Fig. 1) [5,6]. With the highly crystalline metal catalyst films, the preferential formation of uniform single-layer graphene is realized not only for Cu but also for Co. Moreover, as shown in Fig. 2, we observed the epitaxial relationship between single-layer graphene and Co (or Cu) lattices when synthesized at 1000 °C. The single-layer graphene showed the field-effect mobility of  $>1000 \text{ cm}^2/\text{Vs}$ . We also demonstrate that other carbon sources, like amorphous carbon, can be converted to single-layer graphene by simply annealing over the crystalline metal films [7,8]. Our work expands a possibility of synthesizing single-layer graphene over various metal catalysts. Moreover, our CVD growth gives a graphene film with predefined orientation, and thus can be applied to graphene engineering, such as cutting along a specific crystallographic direction, for future electronics applications.

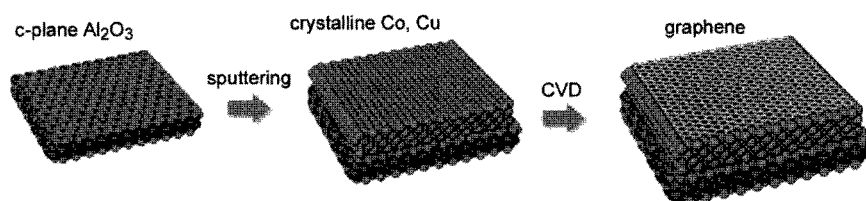


**Figure 1.** Schematics of the epitaxial CVD growth of graphene over crystalline metal films deposited on sapphire c-plane.

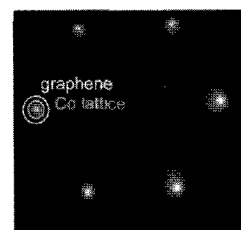


**Figure 2.** LEED pattern of graphene and Co lattices

### References:

- [1] A. Reina *et al.*, *Nano Lett.*, **9**, 30 (2009). [2] X. Li *et al.*, *Science*, **324**, 1312 (2009). [3] S. Bae *et al.*, *Nat. Nanotech.*, **5**, 574 (2010). [4] H. Ago *et al.*, *Small*, **6**, 1226 (2010). [5] H. Ago *et al.*, *ACS Nano*, **4**, 1414 (2010). [6] B. Hu *et al.*, submitted. [7] C. M. Orofeo *et al.*, *Nano Res.*, in press. [8] B. Hu *et al.*, submitted.

**Corresponding Author:** Hiroki Ago (Tel&Fax: +81-92-583-7817, E-mail: ago@cm.kyushu-u.ac.jp)

## Low-temperature synthesis of few-layer and multi-layer graphene by chemical vapor deposition

○Daiyu Kondo<sup>1,2</sup>, Katsunori Yagi<sup>2</sup>, Kenjiro Hayashi<sup>1,2</sup>, Shintaro Sato<sup>1,2</sup>,  
and Naoki Yokoyama<sup>1,2</sup>

<sup>1</sup>*Fujitsu Laboratories Ltd., 10-1 Morinosato-Wakamiya, Atsugi 243-0197, Japan*

<sup>2</sup>*Green Nanoelectronics Collaborative Research Center (GNC), AIST, 16-1 Onogawa, Tsukuba, Ibaraki 305-8569, Japan*

Graphene has been attracting much attention as a candidate for a novel material utilized in future electronics due to its excellent physical properties since a success in isolation from graphite [1]. For such applications, low-temperature synthesis of graphene on a desired substrate is important in order to prevent from thermal damages to devices during the synthesis process. However, there have not been many reports regarding low-temperature synthesis of graphene. In this study, we demonstrate synthesis of few-layer and multi-layer graphene at temperatures lower than 650°C by using thermal chemical vapor deposition (CVD), and fabricate graphene field-effect transistors (FETs) directly on a substrate without using graphene-transfer processes [2].

Graphene was synthesized by thermal CVD method with a mixture of acetylene and argon as the carbon source. As a catalyst, iron (Fe) films with thicknesses of 20-500 nm were sputtered on a SiO<sub>2</sub>/Si substrate. The CVD was performed at 500-650°C. Analyzing the results, we have found that the thickness of multi-layer graphene depends on the catalyst thickness and the synthesis conditions including substrate temperature, partial pressure of acetylene and growth time. By optimizing the synthesis conditions, we have obtained few-layer graphene at temperatures between 590 and 650°C. Figure 1 shows a cross-sectional TEM image of few-layer graphene grown at 590°C. Furthermore, we have fabricated graphene FETs all over the substrate without transferring to another substrate. In the presentation, electrical properties dependent on the growth temperature will be also described.

This research is partly supported by the Japan Society for the Promotion of Science (JSPS) through its “Funding Program for World-Leading Innovative R&D on Science and Technology (FIRST Program).

[1] K.S. Novoselov *et al.*, *Science* 306 (2004) 666.

[2] D. Kondo *et al.*, *Appl. Phys. Express* 3 (2010) 025102.

**Corresponding Author: Daiyu Kondo**

**E-mail: [kondo.daiyu@jp.fujitsu.com](mailto:kondo.daiyu@jp.fujitsu.com)**

**Tel&Fax: +81-46-250-8234&+81-46-250-8844**

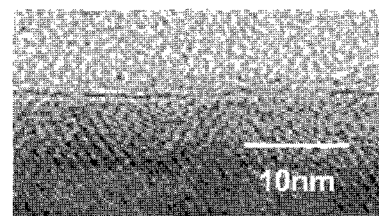


Figure 1 TEM image of few-layer graphene grown at a temperature of 590°C

## Surface Synthesis of Graphene Materials using Polyaromatic Hydrocarbon Derivatives.

○Takahiro Nakae,<sup>1</sup> Yukihiro Kushida,<sup>2</sup> Shingo Mizobuchi,<sup>1</sup> Ryuji Ohnishi,<sup>1</sup> Hisako Sato<sup>1</sup> and Hiroshi Sakaguchi<sup>2</sup>

*1 Department of Chemistry, Graduate School of Science and Engineering, Ehime University, Matsuyama 790-8577, Japan*

*2 Institute of Advanced Energy, Kyoto University, Kyoto 611-0011, Japan*

Graphene ribbon is a promising material for Organic semiconductor with high mobility. Build-up surface synthesis of graphene ribbon is required for precise control of the structure and evaluation of electronic properties, because of its performance depends on its carbon structure.

Metal surface is an eligible template for self-assembled molecules due to its strong interactions between surface and molecules. We previously demonstrated a single-molecular processing technique using electrochemistry, termed 'electrochemical epitaxial polymerization'.<sup>[1,2]</sup> This technique is based on sequential electropolymerization of the monomer by applying voltage pulses to a monomer–electrolyte solution. Using this technique, we can control length, direction, and density of conjugated polymer wires, and produced single conjugated-polymer wires as long as 200 nm in uniaxial propagation on iodine-modified Au(111) electrode. Towards two-dimensional conjugated polymers,<sup>[3]</sup> we examined to produce conjugated graphene material on metal surface from small polyaromatic organic molecules by applying external stimuli. Thus obtained materials were evaluated by Raman spectra.

[1] H. Sakaguchi, H. Matsumura, H. Gong *Nat. Mater.* 3, 551 (2004).

[2] H. Sakaguchi, H. Matsumura, H. Gong, A. M. Abouelwafa *Science* 310, 1002 (2005).

[3] D. G. Perepichka, F. Rosei *Science* 323, 216 (2009).

Corresponding Author: Hiroshi Sakaguchi

Tel&Fax: +81-774-38-3505 E-mail:sakaguchi@iae.kyoto-u.ac.jp

## Formation of Graphene on Insulator by Liquid Metal Flux Method

○ Hidefumi Hiura,<sup>1,2</sup> Michael V. Lee,<sup>2,3</sup> Anastasia V. Tyurnina,<sup>2</sup> and Kazuhito Tsukagoshi<sup>2,3</sup>

<sup>1</sup>Green Innovation Research Laboratories, NEC Corporation, 34 Miyukigaoka, Tsukuba 305-8501, JAPAN.

<sup>2</sup>International Center for Materials Nanoarchitectonics (MANA), National Institute for Materials Science (NIMS), 1-1 Namiki, Tsukuba 305-0044, JAPAN.

<sup>3</sup>CREST, Japan Science and Technology Agency, Kawaguchi 332-0012, JAPAN.

**Abstract:** Much interest has been focused on graphene since the electric field effect in single-layer graphene was discovered in 2004 [1]. So far, graphene preparation has been achieved by three principal methods, exfoliation [1], CVD [2], and thermal decomposition of silicon carbide (SiC) [3]. Each of the methods has its distinctive drawbacks to hinder industrial use. Thus, we aspire to develop a new manufacturing process free of these challenges that will enable commercialization of graphene.

Here we report an unconventional approach to synthesize graphene, namely by liquid metal flux method. Our innovation was originally triggered by the report of Fujita *et al.*, in which they show the graphitization at an interface between amorphous carbon and liquid gallium [4]. As is shown in Fig. 1, the method is based on a two-step process; the dissolution of carbon from a carbon source into a flux by heating up to  $\sim 1000$  °C, and the segregation of carbon from the flux onto a substrate by cooling. Raman spectroscopy revealed that graphene can be formed directly on various substrates (Fig. 2). In the best case, the ratio of the intensity of the D-band to that of the G-band (D/G ratio) was less than 0.1, suggesting that the quality of graphene was acceptable for devices. We anticipate that the LPE method has the following merits. First, it will be scalable to produce large-area graphene. Second, it requires a heating temperature that is lower than that for thermal decomposition and nearly equal to that required for CVD growth of graphene. Third and most remarkably, graphene can be formed directly on a substrate, thus realizing “graphene on insulator” substrates.

**Acknowledgment:** The authors would like to thank Prof. Jun-ichi Fujita for valuable discussions. This work is partly supported by the Japan Science and Technology Agency.

### References:

- [1] K. S. Novoselov *et al.* *Science* **306**, 666 (2004). [2] X. Li *et al.* *Science* **324**, 1312 (2009). [3] C. Berger *et al.* *Science* **312**, 1191 (2006). [4] J. Fujita *et al.* *J. Vac. Sci. Technol. B* **27**(6) 3036 (2009).

**Corresponding Author:** Hidefumi Hiura

**E-mail:** h-hiura@bq.jp.nec.com (or HIURA.Hidefumi@nims.go.jp)

**Tel&Fax:** ; +81-29-860-4872 / +81-29-860-4702

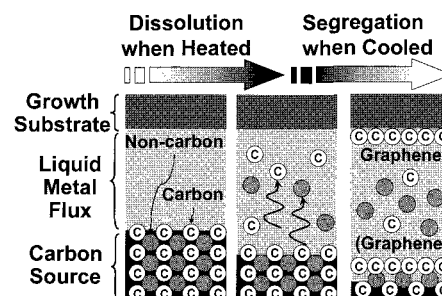


Fig.1. A principle of graphene formation by liquid metal flux method.

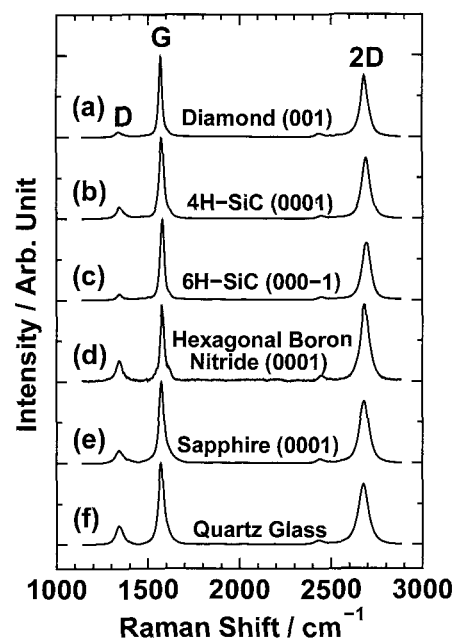


Fig.2. Raman spectra of graphene formed on various substrates by liquid metal flux method

## High rate growth of carbon nanotubes in tens of micrometer deep through silicon vias

K. Oohara, T. Ochiai, M. Iiduka, H. Kawarada

Waseda university, school of Sci & Eng, 3-4-1, Ohkubo, Shinjuku-ku, Tokyo, 169-8555, Japan

[Kaz-oohara@akane.waseda.jp](mailto:Kaz-oohara@akane.waseda.jp)

### 1. Introduction

Stacking chips in a three-dimensional (3D) manner is expected in downscaling of electronics. One key enabling technology for 3D chip stacking is the formation of through silicon vias (TSVs). The most popular method of making interconnects in TSVs is by plating of metals, such as copper. But, it takes a long time to fill the via by metal plating. We have developed mm-long single wall CNT (SWCNT) technology [1], where CNTs of tens of micrometer length grow faster than plating of metals. In this study, our CNT vias technology [2] is applied to tens of micrometer deep vias.

### 2. Experimental

40-65 $\mu\text{m}$  diameter, and 33 $\mu\text{m}$  depth vias are fabricated, and deposited catalyst layer by magnetron sputtering system, bottom Al 5nm, Fe 1.0nm, top Al 0.5nm. Then CNTs were synthesized by remote plasma CVD.  $\text{CH}_4$  flow 5 sccm, and  $\text{H}_2$  flow 45 sccm, growth temperature is 650 $^\circ\text{C}$ , input microwave power was 120W corresponding to 30W/cm $^3$  in power density, growth pressure is 60 Torr.

### 3. Result and Discussion

Figure 1 shows SEM image of CNTs grown from Si via (via height is 33 $\mu\text{m}$ , via diameter is 65 $\mu\text{m}$ ). CNTs were grown up to via height in one minute. The relation between via diameter and growth rate is shown in Figure 2. Figure 2 said CNTs kept high growth rate ( $\approx 30\mu\text{m} / \text{min}$ ) notwithstanding decrease of via diameter. Figure 3 shows Raman spectrum that CNTs grown on non pattern area and CNTs grown from via. Laser wavelength is 633nm, and both CNTs grown on non pattern area and CNTs grown from via are measured upper side. RBM peak is confirmed at 250 $\text{cm}^{-1}$ , this peak shows existence of single walled CNTs.

### 4. Conclusion

CNTs can be synthesized from the bottom of vias. Via diameter does not affect the CNT growth mode. The CNT growth rate is about 20 times higher than the rate of copper plating and applicable for TSV technology.

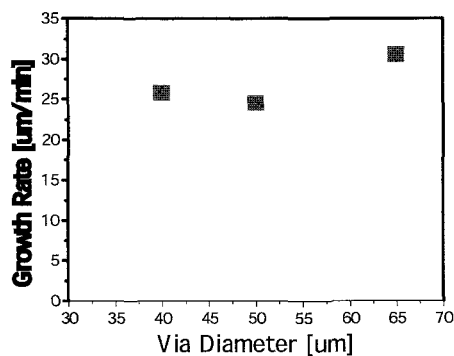


Fig.2 Growth rate of SWCNTs

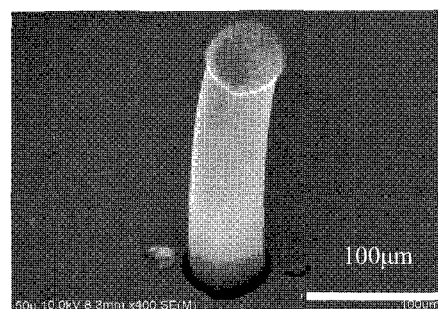


Fig.1 SEM image of CNTs grown from Si vias  
(Via diameter is 65 $\mu\text{m}$ )

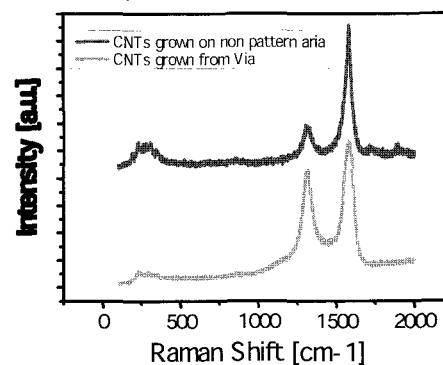


Fig.3 Raman spectrum

(laser wavelength is 633nm)

### References

- [1] GF.Zhong, T.Iwasaki, H.Kawarada, Phys.Chem.B 111, 1907(2007)
- [2] D. Yokoyama, H. Kawarada, et al., Appl. Phys. Lett. 91, 263101(2007)

\* [kaz-oohara@akane.waseda.jp](mailto:kaz-oohara@akane.waseda.jp)

## High-Density Growth of Horizontally Aligned Single Walled Carbon Nanotubes on Crystal Quartz Substrates

○Taiki Inoue, Daisuke Hasegawa, Shohei Chiashi and Shigeo Maruyama

*Department of Mechanical Engineering, The University of Tokyo, Tokyo 113-8656, Japan*

Toward device applications of single walled carbon nanotubes (SWCNTs), the alignment control is of great importance. Horizontally aligned SWCNTs have been grown on crystal quartz substrates [1] and applied to fabrication of field-effect transistors (FETs) [2], but in order to increase the drive current and transconductance of FETs enhancement of the SWCNT density is desired. High-density growth has been studied [3], but optimum CVD conditions have not yet been determined.

On R-cut crystal quartz substrates [4], we performed a parametric study of CVD growth of horizontally aligned SWCNTs. Stripe patterns of Fe ( $\sim 0.2\text{nm}$ ) were deposited as catalyst by thermal evaporation, and synthesis was by the alcohol CVD method using ethanol as the carbon source. SEM images of horizontally aligned SWCNTs grown at  $800\text{ }^\circ\text{C}$  and various ethanol partial pressures are shown in Fig. 1. In the case of vertically aligned SWCNT growth, a higher decomposition rate and higher partial pressure of ethanol is known to be effective for rapid and high-yield growth [5,6]. On the contrary, high-density growth of horizontally aligned SWCNTs was achieved by lower decomposition rate and lower partial pressure of ethanol. Rapid growth of horizontally aligned SWCNTs is considered to result in bundling at the onset, preventing continuous and high-density SWCNT growth.

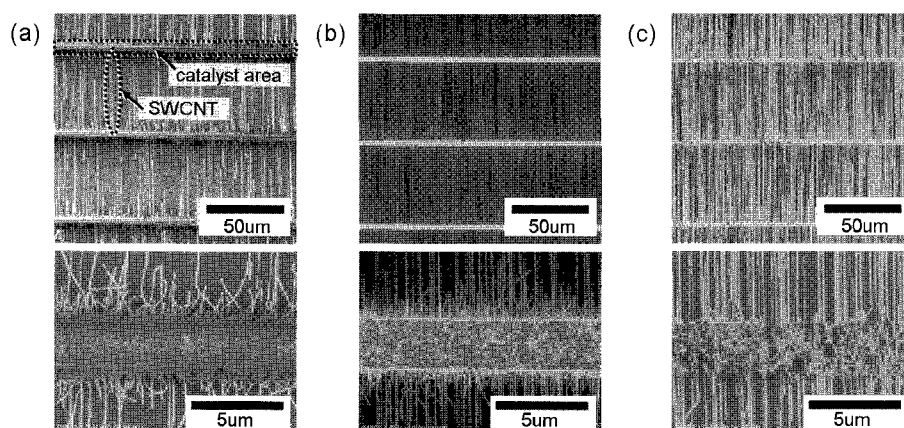


Fig. 1 SEM images of horizontally aligned SWCNTs grown at ethanol partial pressures of (a) 1300 Pa, (b) 300 Pa, and (c) 60 Pa. In the case of (c), ethanol was supplied by bubbling, with Ar/H<sub>2</sub> as the carrier gas.

[1] C. Kocabas, S. H. Hur, A. Gaur, M. A. Meitl, M. Shim, J. A. Rogers, *Small*, **1**, (2005) 1110. [2] S. J. Kang, C. Kocabas, T. Ozel, M. Shim, N. Pimparkar, M. A. Alam, S. V. Rotkin, J. A. Rogers, *Nat. Nanotechnol.*, **2**, (2007) 230. [3] S. W. Hong, T. Banks, J. A. Rogers, *Adv. Mater.*, **22**, (2010) 1826. [4] H. Okabe, S. Chiashi, T. Inoue, J. Shiomi, S. Maruyama, to be submitted. [5] E. Einarsson, Y. Murakami, M. Kadowaki, S. Maruyama, *Carbon*, **46**, (2008) 923. [6] R. Xiang, E. Einarsson, J. Okawa, T. Thurakitserree, Y. Murakami, J. Shiomi, Y. Ohno, S. Maruyama, *J. Nanosci. Nanotechnol.*, **10**, (2010) 3901.

Corresponding Author: Shigeo Maruyama

E-mail: maruyama@photon.t.u-tokyo.ac.jp

TEL: +81-3-5841-6421, FAX: +81-3-5800-6983



## Highly selective growth of (6,5) carbon nanotube - Why (6,5) nanotube is so special in the growth of carbon nanotubes-

○ Yohji Achiba<sup>1)</sup>, Akihito Inoue<sup>1)</sup>, Takshi Kodama<sup>1)</sup>, Kenrou Hashimoto<sup>1)</sup> and  
Toshiya Okazaki<sup>2)</sup>

1) *Department of Chemistry, Tokyo Metropolitan University, Minami Osawa 1-1, Hachioji, Tokyo 192-0367, Japan*

2) *Advanced Industrial Science and Technology, Tsukuba, 305-8565, Ibaragi, Japan*

Controlling size and chirality distributions in the production of single wall carbon nanotubes (SWNTs) is undoubtedly one of the most important issues in the potential applications of the SWNTs to nano-material technology. So far, many experimental attempts have been carried out on the selective production of specific (n,m) tubes by various kinds of the SWNT production methods. Among these attempts, so called “CoMoCAT” and “Co-MCM-41” are typical successful examples in which the (6,5) tube formation has been demonstrated to be of fairly prominence. In these experiments, the selection of the (6,5) tube seems to be realized by combination of CO disproportionation reaction and Co metal catalyst. The prominent growth of (6,5) nanotube in CVD experiments was also found in our recent alcohol CVD experiments for which carbon supply was taken place by simple decomposition of ethanol instead of CO disproportionation reaction, contrary to the suggestion mentioned above.

On the other hand, the laser vaporization method combined with RhPd catalyst under some specific condition gives another good example for the highly selective SWNT growth of a single chirality, in which over 80% selective growth of (6,5) species has clearly been shown, suggesting the presence of some special reasons for the favorable growth of (6,5) tube. It should be interesting to note here that in the course of our laser vaporization experiments, there have been no evidence for the formation of the (5,5) nanotubes under similar condition optimized for the growth of the (6,5) carbon nanotube, although both (5,5) and (6,5) tubes possess similar chiral angle.

In the present paper, on the basis of both experimental and computational calculation evidences, we will discuss the growth process of a single wall carbon nanotube, placing a special emphasis on the properties of the reaction site of the growing-up carbon nanotubes.

Corresponding Author Yohji Achiba

E-mail [achiba-yohji@tmu.ac.jp](mailto:achiba-yohji@tmu.ac.jp) Tel&Fax: +81-52-789-2482, +81-52-789-1169

**ポスター発表**  
**Poster Preview**

**1P-1 ~ 1P-54**

**2P-1 ~ 2P-54**

**3P-1 ~ 3P-53**

## Carbon Nanotube Growth on ZnO(000-1) Substrates using Alcohol Gas Source Method

○Tomoyuki Tsutsui, Takayasu Iokawa, \*Takahiro Maruyama, Shigeya Naritsuka

*Department of Materials Science & Engineering, Meijo University  
1-501 Shiogamaguchi, Tempaku, Nagoya 468-8502, Japan*

Carbon nanotubes (CNTs) have been anticipated for application to various electronic devices. In order to achieve this goal, it is necessary to grow CNTs on semiconductor single crystal substrates. However, few have been reported on CNT growth on those surfaces, except for growth on insulating oxide surfaces such as SiO<sub>2</sub> and Al<sub>2</sub>O<sub>3</sub>. In this study, we attempted CNT growth on ZnO single crystal substrate using an alcohol gas source method [1]. ZnO is one of wide band gap semiconductors and has been expected for a variety of electronic applications. Therefore, CNT growth on ZnO is expected to be an important technique for fabrication of CNT devices.

ZnO(000-1) (O-face) substrates were used for CNT growth. After either Co or Pt catalyst was deposited on them, CNT growth was carried out using alcohol gas source method. Catalyst thickness was varied between 0.01 and 0.1 nm. The growth temperature and the ethanol pressure were varied between 400 and 700 °C, and  $1 \times 10^{-4}$  and  $1 \times 10^{-1}$  Pa, respectively. The grown CNTs were characterized by SEM, Raman spectroscopy and XPS.

Fig.1(a) shows an SEM image of CNTs grown at 700 °C and  $1 \times 10^{-1}$  Pa using Co catalyst. Dense CNTs were grown, but a lot of grooves arose on the ZnO surface after the growth. By decreasing both growth temperature and ethanol pressure, these grooves could be suppressed. Fig. 1(b) shows an SEM image of CNTs grown at 400 °C and  $1 \times 10^{-4}$  Pa, indicating that CNTs grew on a flat ZnO(000-1) surface. For the purpose of increasing the CNT yield, we also carried out CNT growth using Pt catalyst. Fig. 1(c) shows an SEM image of CNTs grown at 500 °C and  $1 \times 10^{-4}$  Pa using Pt catalyst. Compared with Co catalyst, the CNT density was drastically enhanced, keeping the ZnO surface flat.

A part of this study was supported by the Japan Society for the Promotion of Science (JSPS), a Grant-in-Aid for Scientific Research (C) 21510119. This work was partly performed in Nanotechnology Support Project in Central Japan (Institute for Molecular Science).

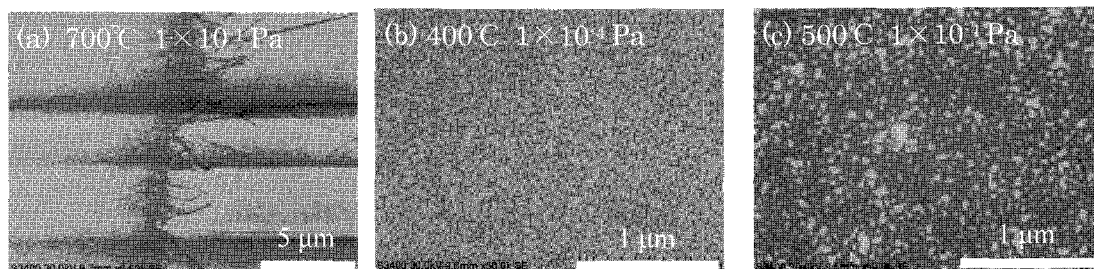


Fig.1 SEM images of CNTs grown on ZnO substrates

### References

[1] T. Maruyama et al. J. Nanosci. Nanotechnol. 10 (2010) 4095.

Corresponding Author: Takahiro Maruyama

TEL: +81-52-838-2386, FAX: +81-52-832-1172 E-mail: takamaru@meijo-u.ac.jp

## QM/MD Simulations of Carbon Nanotube Cap Nucleation Using Acetylene Feedstock and an Fe<sub>38</sub> Catalyst Nanoparticle

○Ying Wang,<sup>1</sup> HuJun Qian,<sup>1</sup> Alister J. Page,<sup>2</sup> Keiji Morokuma<sup>2</sup> and Stephan Irle<sup>1</sup>

<sup>1</sup>Institute for Advanced Research and Department of Chemistry, Nagoya University, Nagoya 464-8602, Japan

<sup>2</sup>Fukui Institute for Fundamental Chemistry, Kyoto University, Kyoto, 606-8103, Japan

The growth of carbon nanotubes by catalytic chemical vapor deposition (CVD) is of great interest for many applications, although the growth mechanism is still unclear. Since Fe substrate is known to be highly effective for the CNT growth in the CCVD process, and C<sub>2</sub>H<sub>2</sub> is an excellent carbon source for high yield, we performed quantum chemical molecular dynamics (QM/MD) simulations to investigate the self-assembly process of carbon nanotubes from acetylene molecules on an Fe<sub>38</sub> particle.

We found H of C<sub>2</sub>H<sub>2</sub> transfers to the iron particle or other C<sub>2</sub>H<sub>2</sub> units, followed by oligomerization of C<sub>2</sub>H<sub>x</sub> units to longer chains.

Since oligomerization proceeds at a faster rate than hydrogen abstraction, the developing carbon structures C<sub>x</sub>H<sub>y</sub> remain hydrogenated with y < x. Compared to simulations with carbon-only source (C<sub>2</sub> or atomic carbon), the presence of hydrogen atoms prohibits ring-condensation and prevents fast sp<sup>2</sup> carbon network growth. Moreover, we find that hexagons are similarly likely to be formed compared to pentagons, which differs from the carbon-only simulations. In order to simulate the effect of the slower H removal processes, we shot C<sub>2</sub>H<sub>2</sub> and at the same time removed H atoms randomly from the cluster on the metal particle. In our ~500 ps QM/MD simulations, we found that at a low H:C

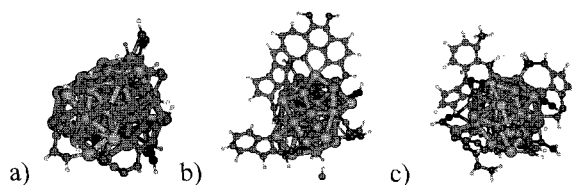


**Figure 1.** Last snapshots a) “standing wall” structures; b) “cap” structures; c) “fragments”

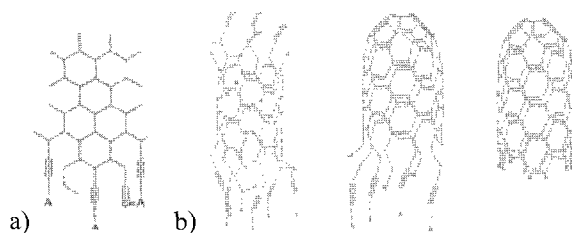


**Figure 2.** Proposed mechanism by Eres *et al.* (J. Phys. Chem. C 2009, 113, 15484): a) graphene fragment formation; b) coalescence and capped CNT formation.

ratio, cap formation occurs as shown in Figure 1a, followed by base growth. If the H:C ratio is higher, ‘standing wall’ structures were formed, as shown in Figure 1b. We assume this kind of graphene-like sheet may coalesce to form the open tube, similar to the mechanism proposed by Eres *et al.*, as shown in Figure 2. We demonstrate that, contrary to popular belief, SWCNT nucleation may occur in the absence of a pure carbon cap.

**Corresponding Author:** Stephan Irle

TEL:+81-52-747-6397, FAX:+81-52-788-6151 E-mail: [sirle@iar.nagoya-u.a.jp](mailto:sirle@iar.nagoya-u.a.jp)

## PERIPUTOS: Purity Evaluation of SWCNTs Using Raman Spectroscopy, Effect of Surfactants

○Miki Taga<sup>1</sup>, Daisuke Nishide<sup>1,2</sup>, Shunjiro Fujii<sup>1,2</sup>, Takeshi Tanaka<sup>1</sup>, and Hiromichi Kataura<sup>1,2</sup>

<sup>1</sup> *Nanosystem Research Institute, AIST, Tsukuba 305-8562, Japan*

<sup>2</sup> *CREST, JST, Kawaguchi 330-0012, Japan*

It is really surprising that still we don't have a well-established way to evaluate the purity of single-wall carbon nanotubes (SWCNTs). From both the practical application and scientific research, reliable purity evaluation method is highly desired. Because the optical transition between one-dimensional van Hove singularities peaks is peculiar to SWCNTs, optical absorption can be a good probe for the purity evaluation. In this case, however, a background subtraction is needed and affects the obtained purity. On the other hand, we know Raman intensity is proportional to the optical absorption due to the strong resonance effect. In this case, we don't need to subtract the background because Raman intensity is automatically proportional to the net absorption of SWCNTs. Based on this idea, we recently proposed a new method, "purity evaluated by Raman intensity of pristine and ultracentrifuged topping of SWCNTs (PERIPUTOS)." [1] In this method, 100 % purity standard sample was prepared by sonication of SWCNT aqueous solution and following ultracentrifugation. Then the G-band Raman intensity was compared with that of the pristine sample.

In the previous report, we used sodium cholate (SC) as surfactant and did not try the other kinds of surfactants. In this work, we tested other surfactants for PERIPUTOS, such as deoxycholate (DOC), sodium dodecyl benzene sulfonate (SDBS), and sodium dodecyl sulfate (SDS). PERIPUTOS values obtained for commercially available SWCNTs (APJ, Meijo Nano Carbon) were 22.3 % for DOC, 23.4 % for SC, 23.7 % for SDBS, and 35.3 % for SDS. Because we used well mixed uniform sample, all the values should be the same. Higher value in SDS case indicates that the purification process to get 100 % standard sample was not sufficient probably due to less dispersion ability of SDS. Detailed analysis will be shown in the presentation.

### References:

[1] D. Nishide et al., *Phys. Status Solidi B*, **246** (2009) 2728.

Corresponding Author: Hiromichi Kataura, E-mail: h-kataura@aist.go.jp

Tel +81-29-861-2551, Fax +81-29-861-2786

## SWNT growth under low pressure using Pt catalyst by Alcohol Gas Source Method in High Vacuum

○Yoshihiro Mizutani<sup>1</sup>, \*Takahiro Maruyama<sup>1</sup> Shigeya Naritsuka<sup>1</sup> and Sumio Iijima<sup>1,2</sup>

<sup>1</sup>*Department of Materials Science and Engineering, Meijo University,  
1-501 Shiogamaguchi, Tempaku, Nagoya 468-8502, Japan*

<sup>2</sup>*Research Center for Advanced Carbon Materials, AIST, Tsukuba 305-8565, Japan*

Carbon nanotubes (CNTs) have been anticipated for application in a lot of future nanodevices. To fabricate CNT devices in a conventional LSI process, it is desirable to grow CNTs under high vacuum. Recently, we reported single-walled carbon nanotube (SWNT) growth by alcohol gas source method in an ultra-high vacuum (UHV) chamber using Co catalyst [1, 2]. By this method, we could grow SWNTs under  $1 \times 10^{-1}$  Pa at 700°C. In this study, we attempted to grow SWNT under the lower pressure using Pt catalyst, which has high capability of decomposing ethanol.

Pt (thickness: 0.025 ~ 0.4 nm) was deposited on SiO<sub>2</sub>/Si substrates by either an e-beam evaporator or a pulsed arc plasma gun. Then, they were heated up to the growth temperature (typically 700°C) in a UHV chamber, and ethanol gas (ambient pressure:  $1.0 \times 10^{-4}$  ~  $1.0 \times 10^{-1}$  Pa) was supplied to grow SWNTs. For comparison, Co catalyst was also used for the SWNT growth. The grown SWNTs were characterized by scanning electron microscopy (SEM) and Raman spectroscopy.

Fig. 1 shows SEM images of SWNTs grown on Pt/SiO<sub>2</sub>/Si ((a): EB, (b): plasma) and Co/SiO<sub>2</sub>/Si substrates (c). Pt and Co thickness were both 0.1 nm, and the ethanol pressure were  $1.0 \times 10^{-4}$  Pa (Pt) and  $1.0 \times 10^{-1}$  Pa (Co), respectively, which were optimum conditions to obtain the maximum SWNT yields. In spite of the lower ethanol pressure, the SWNT yield grown with Pt catalyst was larger than that with Co. The enhancement mechanism of Pt will be discussed based on the decomposition of ethanol and diffusion of carbon atoms on catalyst surface.

This work was partially supported by the Japan Society for the Promotion of Science (JSPS), Grant-in-aid for Scientific Research (C) 21510119. We thank Prof Yakushi and Dr. Uruichi from Institute for Molecular Science for the Raman measurements.

### References

- [1] K. Tanioku et al., *Diamond Relat. Mater.* 17 (2008) 589.  
[2] T. Maruyama et al. *J. Nanosci. Nanotechnol.* 10 (2010) 4095.

**Corresponding Author:** Takahiro Maruyama

**E-mail:** takamaru@meijo-u.ac.jp, **Tel:** +81-52-838-2386, **Fax:** +81-52-832-1172

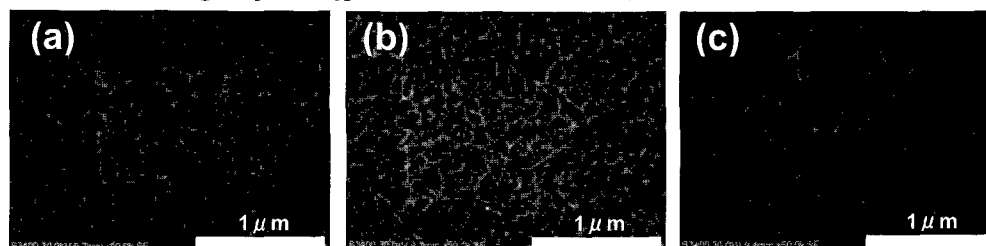


Fig.1

## Comparison of Carbon Nanotube Growth from 4H-SiC and 6H-SiC by Surface Decomposition using Raman Spectroscopy

○Yuki Ishiguro, Satoshi Sakakibara, Hiroaki Ito,  
\*Takahiro Maruyama, Shigeya Naritsuka

*Department of Materials Science and Engineering, Meijo University,  
1-501 Shiogamaguchi, Tempaku, Nagoya 468-8502, Japan*

It has been reported that well-aligned zigzag-type carbon nanotubes (CNTs) could be produced by surface decomposition of SiC(000-1) [1]. However, most of studies in this field were investigated about CNTs from 6H-SiC and few have been reported about the effect of SiC polytypes on the CNT growth. In this study, we carried out CNT growth using 6H- and 4H-SiC and the difference was discussed based on results of Raman measurements.

After HF etching for 10 min, 6H- and 4H-SiC (000-1) C-face samples were annealed at 1700°C under high vacuum ( $<10^{-4}$  Pa) for CNT growth. The annealing time was varied from 1 to 4 hours. The grown CNTs were characterized by Raman spectroscopy with an excitation wavelength of 532 nm.

Figure 1(a) shows Raman spectra of CNTs grown from 6H- and 4H-SiC after annealing for 1 hour. Although the G/D ratios were comparable between them, relative intensity of G band of CNTs grown on 4H-SiC was smaller than that on 6H-SiC. Raman spectra after annealing for 2 hours are shown in Fig. 1(b). The G/D ratio was slightly improved in both samples, but the thickness of CNT film on 4H-SiC surface was still smaller. On the contrary, the CNT growth drastically proceeded on 4H-SiC after annealing for 4 hours (Fig. 1(c)). The difference in the CNT growth rate will be discussed based on surface decomposition, taking into account formation of surface oxide layers during the heating.

[1] M. Kusunoki et al., Chem. Phys. Lett. **366**, 458 (2002).

Corresponding Author: Takahiro Maruyama  
TEL: +81-52-838-2386, FAX: +81-52-832-1172,  
E-mail: [takamaru@meijo-u.ac.jp](mailto:takamaru@meijo-u.ac.jp)

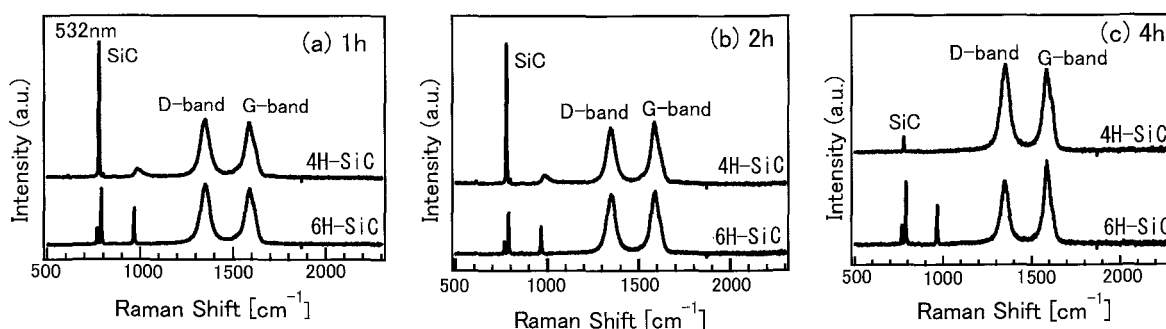


Fig.1

Novel atomization and dispersion method of CNT  
using wet-type super atomizer “Nanovater”

○Tadashi Takashima<sup>1</sup>, Yumi Murai<sup>1</sup>, Kunio Miyashiro<sup>1</sup>, Katsuyuki Utaka<sup>2</sup>, Shin-ichiro Kato<sup>2</sup>  
and Yusuke Miyazaki<sup>2</sup>

<sup>1</sup>*Yoshida Kikai Co.,Ltd Nano-tech Division, 284-5 Tadocho-katori, Kuwana, Mie 511-0102*

<sup>2</sup>*Faculty of Science and Engineering, Waseda University, 3-4-1 Okubo, Shinjuku-ku,  
Tokyo 169-8555*

**Abstract:** Carbon nanotubes(CNTs) are usually in aggregated forms because of their higher intermolecular force caused by its rod-like structure. They are difficult to disperse into water or other solvents. Beads mill or ultrasonic are used to disperse CNTs, but these methods tend to cause defects in CNT’s structure. And the method using media, such as bead mill, is liable to introduce contamination.

Authors are showing a new dispersion method of CNTs, wet type super atomizer by “Nonovater”. It does not use any media, and is a very simple principle that uses collision of water. It can attain ultra-high pressure (max. 200MPa) in the solvents. Pressure and the number of pass-through are adjustable parameters. It means that we can change the collision energy to CNTs to control the atomization.

Fig.1(a) shows the transmittance of the SW-CNT solution before the treatment. After the 3,000 pass, the transmittance contrast increased, as shown in Fig.1(b). In other words, it can say that CNTs became well dispersed. So it is very important to atomize and disperse CNT to make their own properties such as absorption spectrum be prominent.

By this high-pressure treatment the length of the CNT became as short as 70nm in average, and D/G ratio increased a little, indicating the introduction of some damages to CNT. But it is much smaller than those by other methods such as beads-mill. Moreover, all liquid can pass the narrow (100um) nozzle, we can get highly uniform solution of CNTs.

CNT solution obtained by “Nonovater” can apply for various fields. We are studying for the application to optical device using CNTs.

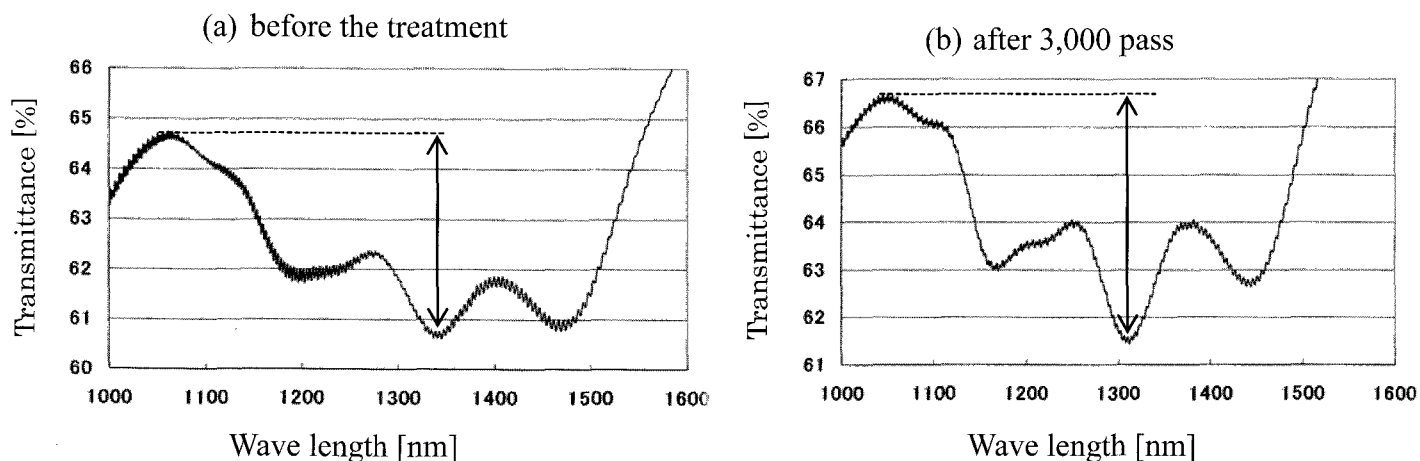


**Fig.1 Transmittance of the solution of CNTs before(a) and after(b) the pressure treatment.**

Corresponding Author : Tadashi Takashima  
E-mail : takashima@yoshidakikai.co.jp  
Tel & Fax +81-594-49-2255 / +81-594-49-2277



## Molecular-assembled synthesis of single-wall carbon nanotubes

○Yasumitsu Miyata<sup>1</sup>, Marie Suzuki<sup>1</sup>, Jinying Zhang<sup>1</sup>, Miho Fujihara<sup>1</sup>,  
Ryo Kitaura<sup>1</sup>, Hiromichi Kataura<sup>2,3</sup>, and Hisanori Shinohara<sup>1</sup>

<sup>1</sup>*Department of Chemistry, Nagoya University & Institute for Advanced Study, Nagoya  
464-8602, Japan,*

<sup>2</sup>*Nanosystem Research Institute, AIST, Tsukuba, 464-8602, Japan,* <sup>3</sup>*JST-CREST*

The inner space of carbon nanotubes (CNTs) offers a fascinating platform to perform bottom-up synthesis of one-dimensional nanomaterials. One of the representative examples is the conversion of organic molecules such as fullerenes to single-wall CNTs (SWCNTs) through thermal annealing [1,2]. This reaction includes the fusion of individual molecules and can be regarded as a molecular-assembled fabrication of SWCNTs. It is very interesting to investigate the relation of precursor molecules to the chirality distribution of SWCNTs. However, the presence of outer CNTs precludes from obtaining signals of inner materials in optical evaluation such as optical absorption and photoluminescence spectra. Recently, we have developed an efficient method to separate inner materials from outer CNTs in solution phase [3]. This method allows us to investigate the detail chirality distribution and physical properties of SWCNTs constructed from molecular assembly.

In this study, we have investigated precursor-dependent growth of SWCNTs in CNTs. Various organic molecules as shown in Fig.1 were used as the precursors. These molecules were fused inside CNTs through thermal annealing to produce SWCNTs. The inner SWCNTs were extracted from outer CNTs by the method reported previously [3]. Optical absorption spectra reveal that the chirality of SWCNTs strongly depends on the precursor molecules even with the use of same outer CNTs. Our findings provide an important insight into the bottom-up synthesis of SWCNTs with desired structure and dopant.

[1] S. Bandow et al. Chem. Phys. Lett. 337, 48 (2001).

[2] Y. Fujita et al. Chem. Phys. Lett. 413, 410 (2005).

[3] Y. Miyata et al. ACS Nano 4, 5807 (2010)

**Corresponding Author: Hisanori Shinohara**

**E-mail: noris@nagoya-u.jp**

**Tel&Fax: 052-789-2482 & 052-747-6442**

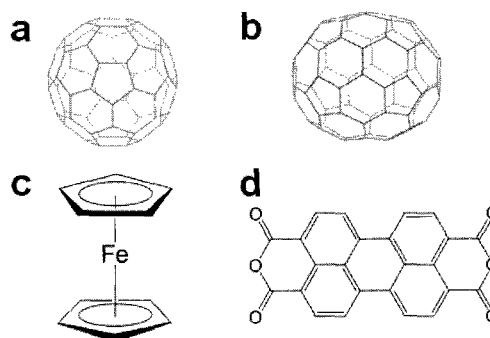


**Figure 1.** Molecular structures used in this study. (a) C60 fullerene, (b) C70 fullerene, (c) ferrocene, and (d) 3,4,9,10- perylene-tetracarboxylic dianhydride (PTCDA).

## Effect of Sn catalyst concentration on purity synthesis of carbon nanocoil by substrate CVD with catalytic vapor supply

○Y. Ishii<sup>1</sup>, K. Takimoto<sup>1</sup>, Y. Suda<sup>1</sup>, H. Tanoue<sup>1</sup>, H. Takikawa<sup>1</sup>  
H. Ue<sup>2</sup>, K. Shimizu<sup>3</sup>, Y. Umeda<sup>4</sup>

<sup>1</sup> *Department of Electrical and Electronic Information Engineering,  
Toyohashi University of Technology*

<sup>2</sup> *Fuji Research Laboratory, Tokai Carbon Co., Ltd.*

<sup>3</sup> *Shonan Plastic Mfg. Co., Ltd.*

<sup>4</sup> *Fundamental Research Department, Toho Gas Co., Ltd.*

Carbon nanocoil (CNC) is a helical carbon nanofiber and is synthesized by chemical vapor deposition (CVD) with Sn/Fe catalyst. In our previous study, Sn catalyst was formed by dropping SnO<sub>2</sub> solution or vacuum evaporation on substrate [1]. On the other hand, we developed a continuous supply system of Sn in liquid into CVD reactor for improve the purity of CNC [2]. In this study, we report the effect of concentration of Sn catalyst solution. Si is used as a substrate and solution of Fe<sub>2</sub>O<sub>3</sub> catalyst was dropped on Si substrate. Fe-coated substrate was heated in the air for 5 min at 400°C. The experimental conditions were as follows: N<sub>2</sub> gas flow rate, 1000 ml/min; C<sub>2</sub>H<sub>2</sub> gas flow rate, 50 ml/min; solution of Sn catalyst flow rate, 0.144 ml/min; reaction temperature, 700°C; reaction time, 10 min. Sn(CH<sub>3</sub>)<sub>4</sub> used as a Sn catalyst and was mixed with ethanol. At this time, the concentration of Sn(CH<sub>3</sub>)<sub>4</sub> in ethanol was changed from 0.1 to 2%. Fig. 1 shows scanning electron microscopy (SEM) micrographs of carbon products at each concentration. The number of CNC was very few at concentration of 0.1%, and a lot of amorphous carbon impurity was synthesized at the same time. CNC was synthesized very much at concentration of 0.2%. At concentration of 2%, CNC was synthesized but purity was lower than concentration of 0.2%.

This work has been partly supported by the Outstanding Research Project of the Venture Business Laboratory from Toyohashi University of Technology (TUT); Global COE Program "Frontiers of Intelligent Sensing" from the Ministry of Education, Culture, Sports, Science and Technology (MEXT); Core University Programs (JSPS-CAS program in the field of "Plasma and Nuclear Fusion") from the Japan Society for the Promotion of Science (JSPS), Grant-in-Aid for Scientific Research from the MEXT, Toukai Foundation for Technology, Research Foundation for Materials Science, and Chubu Science and Technology Center.

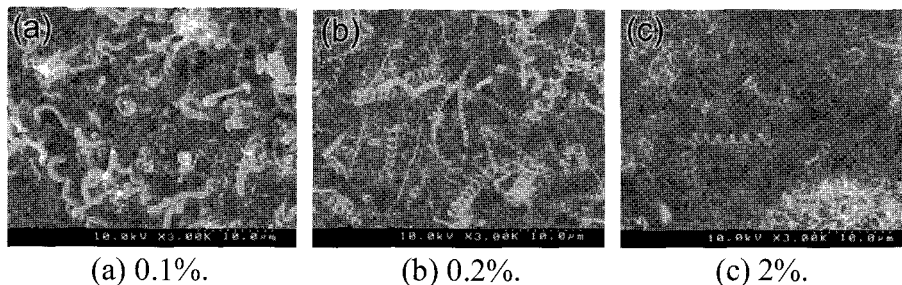


Fig. 1 SEM micrographs of carbon products.

[1] Takimoto, et al., The 37<sup>th</sup> Fullerene-Nanotubes General Symposium (2009) 3P-30

[2] Ishii, et al., The 39<sup>th</sup> Fullerene-Nanotubes General Symposium (2010) 3P-19

Corresponding Author: Yoshiyuki Suda

E-mail: suda@ee.tut.ac.jp, Tel: +81-532-44-6726

## Length Sorting of Single-Wall Carbon Nanotubes using Size Exclusion Gel Chromatography

○Satoshi Asano<sup>1</sup>, Takeshi Tanaka<sup>1,2</sup> and Hiromichi Kataura<sup>1,2</sup>

<sup>1</sup>*Technology Research Association for Single Wall Carbon Nanotubes (TASC), Tsukuba, Ibaraki, 305-8562, Japan*

<sup>2</sup>*Nanosystem Research Institute, National Institute of Advanced Industrial Science and Technology (AIST), Tsukuba, Ibaraki 305-8562, Japan*

Single-wall carbon nanotubes (SWCNTs) are promising material for various applications such as high-speed electronic devices. However, it is very difficult to control their electronic properties, precise diameter, and lengths in the growth process. SWCNTs have to be separated after the synthesis. So far we have developed effective separation methods of metallic and semiconducting SWCNTs using agarose gel<sup>1,2</sup>. Now we are focusing on the length sorting. The electronic devices comprised from long SWCNTs are expected to show higher performance<sup>3</sup>. In this presentation, we report a method for length sorting of SWCNTs by a size-exclusion chromatography and a simple length evaluation method.

Aqueous solution of SWCNTs was prepared by sonication and ultracentrifugation, and then the solution was concentrated by a long-time ultracentrifugation. Under the optimal conditions of the second ultracentrifugation, very short SWCNTs and impurities were successfully removed. The SWCNT solution was then applied to size exclusion chromatography using Sephacryl S-1000 gel (gel-filtration). Separated samples were roughly fractionated into three parts: above, within, and below the range of fractionation capability of the gel. The length distribution of SWCNTs of the each fraction was measured by atomic force microscope (AFM), and the length sorting was confirmed. Dynamic light scattering (DLS) was also measured for each fraction. Interestingly, clear peaks originating from length sorted SWCNTs were observed in DLS spectra although such peaks were hardly observed for the SWCNT solution before length sorting.

### References:

- [1] T. Tanaka et al., *Appl. Phys. Express* 2009, **24**, 125002
- [2] T. Tanaka et al., *Nano Lett.* 2009, **9**, 1497
- [3] D. Hecht et al., *Appl. Phys. Lett.* 2006, **89** 133112

Corresponding Author: Takeshi Tanaka

Tel: +81-29-861-2903, Fax: +81-29-861-2786, E-mail: tanaka-t@aist.go.jp

## Control on the Electrochemical Process at Carbon Nanotube Synthesis at Room Temperature

Ahmed Shawky, Masahiro Tanabe, Satoshi Yasuda and Kei Murakoshi

*Department of Chemistry, Faculty of Science, Hokkaido University,  
Sapporo 060-0810, Japan*

Development of well-defined Carbon nanotubes (CNTs) synthesis technique has been attractive challenge for future electrical, optical and catalytic materials.[1] In general, conventional synthesis techniques of CNTs such as arc discharge, laser ablation, chemical vapor deposition, etc., are based on the processes at high voltages, high laser power and high temperature. These high energy synthesis processes during CNT growth are expected to cause undesired defect formation due to high thermal fluctuation and less controllability of growth velocity and chemical reaction for well-defined structural control. Recently, we have employed an electrochemical technique, which is based on electrochemical reaction at room temperature in liquid phase and undergoes reaction at high speed, and succeeded in synthesizing single-walled carbon nanotube.[2] In this work, we investigated catalytic metal dependence for controlling carbon nanostructures by electrochemical process. The electrochemical system setup was a three electrode cell using an Au working electrode, a Pt counter electrode and an Ag/AgCl reference electrode (Fig. 1(a)). At first, Electrodeposition of Ni nanoparticles (NP's) as a catalyst on Au surface was carried out to prepare the surface for nanotube synthesis (Fig. 1(b)). From STM analysis of Ni NPs (Fig. 1(c)), we found that the Ni NP structure and size can be controlled by changing the deposition time. Fe and Co NPs formation was also confirmed by similar method and can be controlled the size by deposition time. Next, carbon deposition was performed using aqueous electrolyte solution containing 1 % acetic acid. Under the applied potential at -1.0 V, acetic acid molecules were reduced showing relatively large cathodic current. Raman spectra measurement showed the formation of graphitic carbon structure on each metal NPs on Au surface, however, we found that catalytic metal dependence was clearly observed for carbon structure. These results indicate the possibility of control of carbon structure by catalytic metal species.

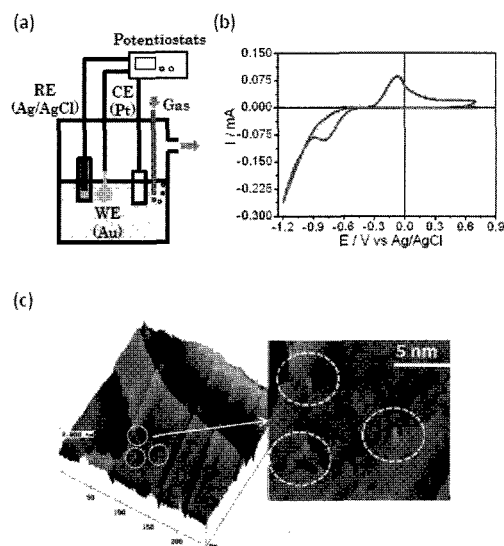


Fig. 1. (a) Schematics of electrochemical synthesis system with three electrode cell. (b) Cyclic voltammogram of Ni deposition on Au surface. (c) STM images of Ni nanoparticles formation on Au surface.

[1] S. Yasuda, T. Hiraoka, D. N. Futaba, M. Yumura, K. Hata, *Nano Lett.* **9**, 769-773 (2009).

[2] A. Shawky, S. Yasuda, K. Murakoshi to be submitted.

Corresponding Author: Satoshi Yasuda

TEL & FAX: +81-(0)11-706-4811, E-mail: [satoshi-yasuda@sci.hokudai.ac.jp](mailto:satoshi-yasuda@sci.hokudai.ac.jp)

## Selective synthesis of (6, 5) carbon nanotubes from C<sub>60</sub> precursor

○Jinying Zhang, Yasumitsu Miyata, Ryo Kitaura, and Hisanori Shinohara\*

*Department of Chemistry and Institute for Advanced Research, Nagoya University, Nagoya, 464-8602, Japan*

Selective synthesis of single-wall carbon nanotubes (SWCNTs) with single chirality has highly promising applications since the electronic and optical properties strongly depend on their diameter and chiralities. Up to date, controllable synthesis<sup>1</sup> and post-synthesis separation<sup>2</sup> are two main strategies for obtaining chirality-pure SWCNTs. Selective synthesis of (6, 5) SWCNTs with purity of more than 60% were demonstrated in this work.

Briefly, C<sub>60</sub> fullerenes were firstly encapsulated into SWCNTs ( $d \cong 1.5$  nm) and then annealed at 1200 °C for 24 h under a vacuum of 10<sup>-6</sup> Torr to produce double-wall carbon nanotubes (DWCNTs). The inner tubes were extracted from the DWCNTs using the ultrasonication and ultracentrifugation processes which we reported recently.<sup>3</sup> The extracted inner tubes were characterized by UV-Vis absorption, Raman scattering, photoluminescence (PL), and TEM observations. UV-Vis spectrum of the extracted tubes shows sharp absorption at 968 nm and 568 nm (Fig. 1a), corresponding to S<sub>11</sub> and S<sub>22</sub> bands of (6, 5) SWCNTs. Diameter of the extracted tubes was observed by TEM to be 0.76 ± 0.05 nm. The PL map shows a further evidence for the selective synthesis of high pure (6, 5) SWCNTs (Fig. 1b).

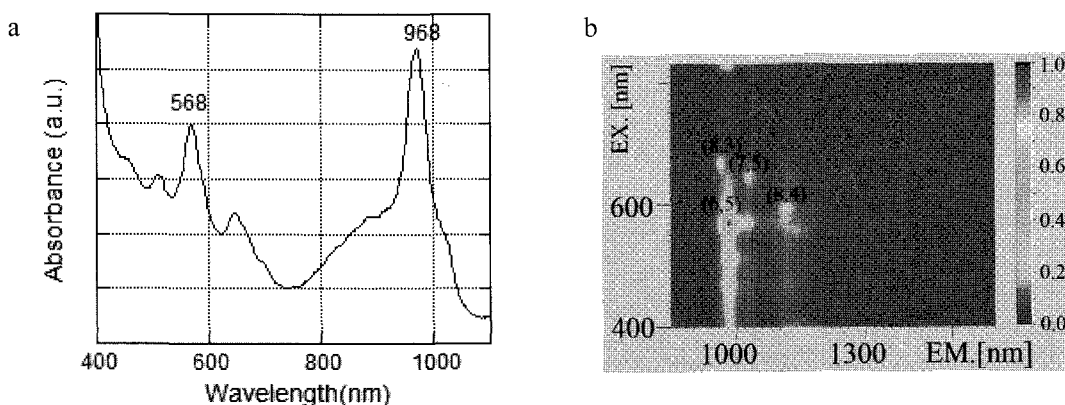


Fig. 1 (a) UV-Vis absorption spectrum and (b) 2D PL contour map of the extracted inner SWCNTs.

### References:

1. Z. Ghorannevis, *et al.*, *R. J Am. Chem. Soc.* **2010**, 132:9570.
2. M.S. Arnold, *et al.*, *Nature Nanotech.* **2006**, 1:60.
3. Y. Miyata, *et al.*, *ACS Nano* **2010**, 4: 5807.

**Corresponding Author:** Hisanori Shinohara

**E-mail:** [noris@nagoya-u.ac.jp](mailto:noris@nagoya-u.ac.jp); **Tel&Fax:** 052-789-2482& 052-747-6442

## Synthesis of Multi-Walled Carbon Nanocoils over Sn/Fe/MgO Catalyst by Catalytic CVD

○Lim Siew Ling<sup>1</sup>, Kotaro Takimoto<sup>1</sup>, Yoshiyuki Suda<sup>1</sup>, Hideto Tanoue<sup>1</sup>,  
Hirofumi Takikawa<sup>1</sup>, Hitoshi Ue<sup>2</sup>, Kazuki Shimizu<sup>3</sup>, Yoshida Umeda<sup>4</sup>

<sup>1</sup> *Department of Electrical and Electronic Information Engineering,  
Toyohashi University of Technology*

<sup>2</sup> *Fuji Research Laboratory, Tokai Carbon Co., Ltd.*

<sup>3</sup> *Shonan Plastic Mfg. Co., Ltd.*

<sup>4</sup> *Fundamental Research Department, Toho Gas Co., Ltd.*

Multi-walled carbon nanocoils (MWCNCs) have been successfully grown using codeposited Sn/Fe catalysts supported on zeolite by chemical vapor deposition (CVD) [1]. MWCNCs with their unique helical structures have attracted considerable attention in applications such as field emission device, electromagnetic wave absorber and nanospring. Large scale production of MWCNCs is very important for the applications mentioned above. In this study, MgO was used as a catalyst support material instead of zeolite. First, NACEM-Fe (NIHON KAGAKU SANGYO CO., LTD,  $\text{Fe}(\text{C}_5\text{H}_7\text{O}_2)_3$ ) and NACEM-Sn (NIHON KAGAKU SANGYO CO., LTD,  $\text{Sn}(\text{C}_4\text{H}_9)_2(\text{C}_5\text{H}_7\text{O}_2)_2$ ) were mixed in deionized water. MgO was then added into the mixed solution and calcined at 100°C either with stirring for 21 h or without stirring for 20 h. MWCNCs were synthesized by catalytic CVD using acetylene. SEM micrographs of MWCNCs with Sn/Fe/MgO are shown in Fig. 1. MWCNCs could be synthesized in both the conditions and the tube diameter of MWCNCs grown was in a range of 20-30 nm.

This work has been partly supported by the Outstanding Research Project of the Venture Business Laboratory from Toyohashi University of Technology (TUT); Global COE Program "Frontiers of Intelligent Sensing" from the Ministry of Education, Culture, Sports, Science and Technology (MEXT); Core University Programs (JSPS-CAS program in the field of "Plasma and Nuclear Fusion") from the Japan Society for the Promotion of Science (JSPS), Grant-in-Aid for Scientific Research from the MEXT, Toukai Foundation for Technology, Research Foundation for Materials Science, and Chubu Science and Technology Center.

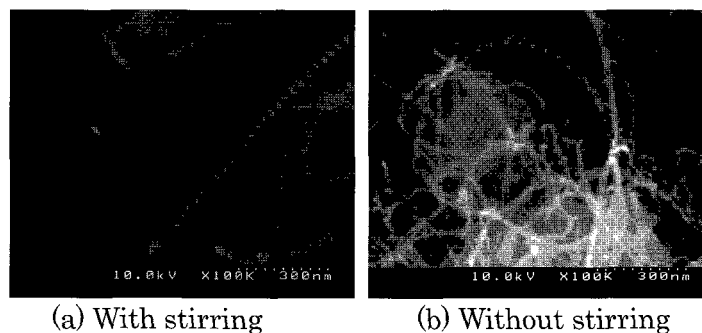


Fig. 1 SEM micrographs of MWCNCs synthesized with Sn/Fe supported on MgO

References: (1) M. Yokota, et al.: J. Nanosci. Nanotechnol, in press.

Corresponding Author: Yoshiyuki Suda

Tel & Fax: +81-532-44-6726, E-mail: suda@ee.tut.ac.jp

## Carbon nanotube growth from C<sub>60</sub>-fullerene nuclei with various source gases

D. Takagi<sup>1</sup>, F. Maeda<sup>1</sup>, R. Negishi<sup>2</sup>, S. Agata<sup>2</sup>, Y. Kobayashi<sup>2</sup>, Y. Homma<sup>3</sup>

<sup>1</sup>NTT Basic Research Laboratories, NTT Corporation, Atsugi, Kanagawa 243-0198, Japan

<sup>2</sup>Department of Applied Physics, Osaka University, Suita 565-0871, Japan

<sup>3</sup>Department of Physics, Tokyo University of Science, Shinjuku, Tokyo 162-8601, Japan

Chirality control of carbon nanotubes (CNTs) using chemical vapor deposition (CVD) remains a crucial issue for practical applications. It is well-known that the size and chirality of CNTs is decided by initial carbon cap structures during a nucleation stage as growth begins. Therefore, the cap formation process is a key to controlling the size and chirality of CNTs. Recently, it has been reported that fullerene-related molecules (fullerendione) can act as CNT growth nuclei in CVD process with ethanol, via forming hemispherical caps by thermal oxidation and initiating CNT growth at their open ends [1]. Although they found that the temperature for thermal oxidation strongly affects the cap structures and the diameter distribution of the as-grown CNTs, it has not been achieved a precise control of their size and chirality. In this study, in order to understand the growth mechanism, we investigate CNT growth from C<sub>60</sub> fullerene nuclei under various conditions.

We used sublimed C<sub>60</sub> fullerenes (MTR Ltd.) as CNT growth nuclei. C<sub>60</sub> fullerenes dispersed in ethanol were spread on substrates such as Si, quartz, and silica-gels (not containing cobalt chloride). In the CNT synthesis using C<sub>60</sub> fullerenes, it is important to prevent sublimation of the C<sub>60</sub> fullerenes at the CVD temperature. For this purpose, we annealed the substrate in air ambience at 500-550 °C. This annealing process induced defects in the C<sub>60</sub> fullerenes. A defective C<sub>60</sub> fullerene molecule has a strong interaction with other C<sub>60</sub> fullerenes and the substrate surface, resulting in prevention of the C<sub>60</sub> sublimation. After the annealing in air, CNTs were synthesized in a furnace with two temperature zones, where the temperatures can be controlled independently for the separation of source gas (ethanol vapor and/or acetylene) cracking at 850 °C and CVD growth at 700-770 °C.

Figure 1 compares SEM images of the CNTs grown from C<sub>60</sub> fullerenes and the conventional Co catalysis using CVD with (a)(d) ethanol, (b)(e) acetylene and (c)(f) mixture of ethanol and acetylene (volume ratio = 1:1). Observed growth yield of the CNTs significantly depends on growth nuclei as well as composition of the growth gases under the growth conditions optimized for the C<sub>60</sub> fullerene nuclei. In the case of Co catalysts, the CNT yield is much higher for CVD with acetylene or mixture of acetylene+ethanol than that with pure ethanol. On the other hand, C<sub>60</sub> fullerene nuclei give rise to higher yield for CVD with ethanol, contrary to Co catalysts. The reverse tendency between Co and C<sub>60</sub> fullerenes for source gases should reflect nucleation and growth mechanism of the CNTs. The active growth species including OH group decompose disordered and unstable graphitic materials formed at the initial stage of CNT growth on Co catalysts. The C<sub>60</sub> fullerenes with open ends, unlike Co catalysts provide the CNT cap structures in advance. The OH species have a function to remove disordered carbon materials and to prevent to terminate the growth process. Therefore, addition of a compound with OH group(s) such as H<sub>2</sub>O in CVD process would be very effective to enhance the CNT growth from C<sub>60</sub> fullerene nuclei, in agreement with the previous report [1].

[1] X. Yu, et al, ACS Nano Lett. **10** (2010) 3343.

E-mail: Negishi@ap.eng.osaka-u.ac.jp, TEL: 06-6879-4684, FAX: 06-6879-7863

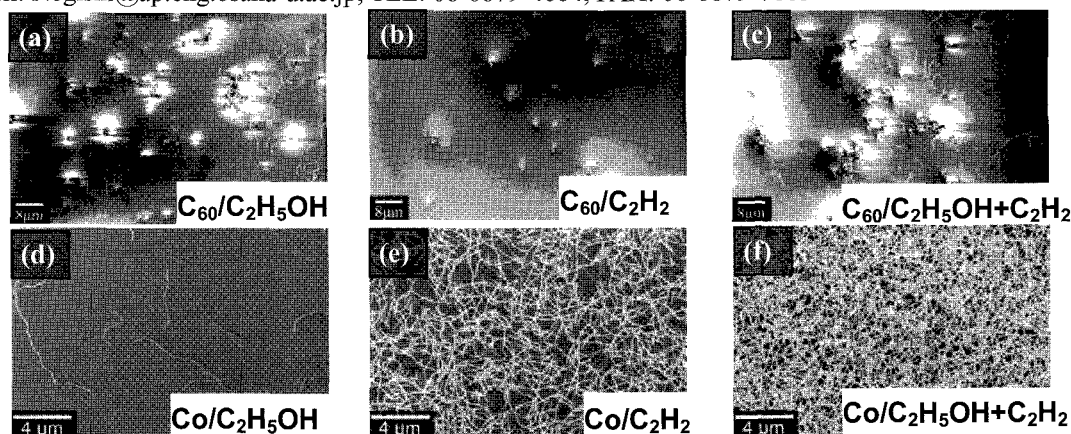


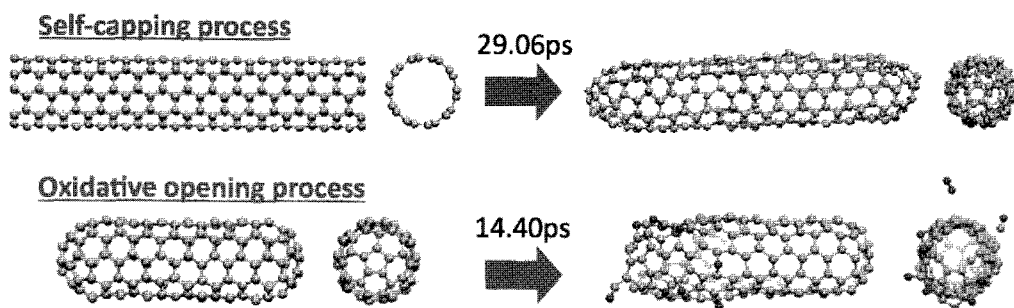
Fig. 1 SEM images of CNTs grown on SiO<sub>2</sub>/Si from C<sub>60</sub> fullerenes and Co particles by CVD with (a)(d) ethanol, (b)(e) acetylene and (c)(f) 1:1 mixture of ethanol + acetylene.

**Single-walled carbon nanotubes closing and opening:  
a density-functional tight-binding molecular dynamics study**

○Hironori Hara, Stephan Irle

*Institute for Advanced Research and Department of Chemistry, Nagoya University,  
Nagoya 464-8602, Japan*

CNTs can be opened [1,2] and closed [2] experimentally, by heating under air or using aqueous chemical oxidation, and vacuum annealing, respectively. Here we report the simulations of SWCNT transformations, closing and opening process. Using canonical (constant temperature, NVT) molecular dynamics (MD) simulations based on the density-functional tight-binding (DFTB) quantum chemical method, we studied self-capping process of open-ended SWCNTs in vapor and oxidative opening process of capped SWCNTs, under high temperature respectively. For edge non-functionalized open-ended carbon only SWCNT model, with the exception of the (3,3) SWCNT the all-carbon ends of the open-ended (n,n) [n=3~10] armchair SWCNTs are able to self-cap during simulation times on the order of 100 ps. Edge-functionalized with oxygen containing group, more realistic open-ended ones can also close their ends after releasing their functionalities. There is dependency of self-capping time on SWCNTs diameter. Length dependency, however, has not been detected. Using “oxygen atom shooting”, feeding atomic oxygen to capped SWCNTs, we reproduced oxidation process of SWCNTs. The oxidation process, making a hole on the surface of SWCNTs with releasing carbon oxides has been observed. We also found that caps are opened in shorter simulation times compared to sidewalls.



### References

- [1]C. Li *et al.* *Powder technology* (2004) **142** 175-179  
 [2]H.Z. Geng *et al.* *Chem. Phys. Lett.* (2004) **399** 109-113

**Corresponding Author:** Stephan Irle

**Tel & Fax:** +81-52-747-6397/+81-52-788-6151, **E-mail:** sirle@iar.nagoya-u.ac.jp



## Transition from [*n*]Cycloparaphenylenes to SWCNTs: SCC-DFTB Studies of Diels Alder Reactions and Raman Spectra

○Ryota Umeda, Yoshifumi Nishimura, Stephan Irle

<sup>1</sup>*Institute for Advanced Research and Department of Chemistry, Nagoya University,  
Nagoya 464-8602, Japan*

[*n*]Cycloparaphenylenes (CPP) represent formally the shortest sidewall segment of armchair (*n,n*) single-walled carbon nanotubes (SWCNTs), therefore these beautiful macrocyclic ring structures have been considered as synthetic building blocks for the organic bottom-up SWCNT synthesis [1,2]. As proposed by the group of Scott [2], a synthetic route might be realized in a step-wise Diels-Alder (DA) and hydrogen elimination reaction of CPP and subsequent reaction products with acetylene. We present self-consistent-charge density-functional tight-binding (SCC-DFTB) and density functional theory (DFT) calculations of [4+2] and [2+4] DA reactions on bay area and ring C-C bonds of [5]CPPs and longer (5,5) SWCNT belt structures with acetylene and *s-cis* [1.3]-butadiene, respectively. We show that the observed energetics of ever longer ring segments can be explained in terms of the Clar, semi-Clar, and Kekule structures characteristic for finite-length SWCNT fragments [3]. In addition, we compute Raman spectra based on SCC-DFTB for series of Clar, semi-Clar, and Kekule structures with increasing tube length and discuss the evolution of their features towards the Raman spectra of SWCNTs.

### References

- [1] H. Omachi, S. Matsuura, Y. Segawa, K. Itami, *Angew. Chem. Int. Ed.* **2011** in press
- [2] E. H. Fort, L. T. Scott, *submitted, and private communication.*
- [3] Y. Matsuo, K. Tahara, E. Nakamura, *Org. Lett.* **2003**, *5*, 3181.

**Corresponding Author:** Stephan Irle

**TEL:** +81-52-747-6397, **FAX:** +81-52-788-6151, **E-mail:** [sirle@iar.nagoya-u.a.jp](mailto:sirle@iar.nagoya-u.a.jp)

## Extraction of high purity and micrometer-long semiconducting single-wall carbon nanotubes

○Kazunari Shiozawa, Yasumitsu Miyata, Ryo Kitaura and Hisanori Shinohara

*Department of Chemistry & Institute for Advanced Research,  
Nagoya University, Nagoya 464-8602, Japan*

Single-wall carbon nanotubes (SWCNTs) are a promising material for thin film electronics because of their high carrier mobility, flexibility, and solution processability. Realizing these fascinating properties of SWCNTs in realistic electronics requires a scalable chemical process to prepare pure semiconducting SWCNTs with high-crystallinity. However, the conventional processes always produce the low-quality (i.e., short length) nanotubes that degrade their intrinsic mobility. Furthermore there are still remaining impurity m-SWCNTs in separated semiconducting fractions.

In this study, we have developed a simple method to extract micrometer-long semiconducting SWCNTs with a purity of more than 99%. Our method is based on the gel filtration [1,2]. We have found that a recycling process of the gel filtration effectively separates micrometer-long semiconducting SWCNTs from shorter ones. Figure 1 shows optical absorption spectra of before and after recycling gel filtration. The peaks of m-SWCNT (around 700 nm) were disappeared after recycling, indicating that the s-SWCNTs separated have a purity of more than 99%. In addition to the high-purity semiconductor separation, this method can be applied to length separation of semiconducting SWCNTs through the second recycling filtration. Figure 2 shows the length distribution of adsorbed and non-adsorbed s-SWCNTs. Micrometer-long s-SWCNTs are found to be included in non-adsorbed dispersion during the recycling gel filtration. The detail separation processes will be discussed in the presentation.

### Reference

- [1] K. Moshhammer et al., *Nano Res.*, **2**, 599 (2009)  
[2] Tanaka et al., *Appl. Phys. Express*, **2**, 125002 (2009)

**Corresponding Author: Hisanori Shinohara**

**E-mail: noris@nagoya-u.jp**

**Tel&Fax: 052-789-2482 & 052-747-6442**

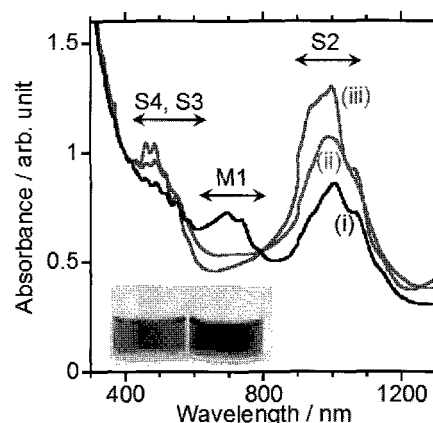


**Figure 1** Optical absorption spectra of (i) the pristine sample and the separated sample by (ii) 1 time and (iii) 15 times recycling gel filtration.

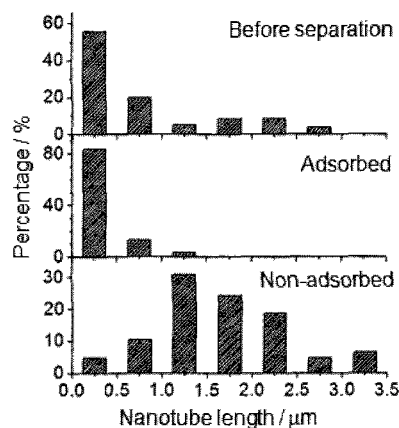


**Figure 2** Length distributions of the purified semiconducting SWCNTs before the separation, in the adsorbed fraction, and in the non-adsorbed fraction.

## Electrode Properties of Nanocarbon-Polymer Composites

○T. Sakashita, K. Okamura, S. Kawasaki

*Nagoya Institute of Technology,  
Gokiso, Showa, Nagoya 466-8555, Japan*

Li ion secondary battery (LIB) has now come to be an indispensable energy device for portable electronic devices such as mobile phones and laptop computers. Recently, it is also expected to use LIB for larger electronic devices including electric vehicles. For such various demands for LIB, tremendous amount of investigation has been done to improve LIB. Various kinds of materials have been investigated as a new component which constitute the next generation LIB. For example, Si, Sn, CuO and LiFePO<sub>4</sub> have been proposed as new anode and cathode materials. We have to develop not only such electrode active materials but also another battery component such as current collectors, separators, electrolytes and so on. Here, we report the electrode properties of several kinds of nanocarbon-polymer composites. Polymer electrodes have the benefits of firm attachment of electrode active materials, flexibility, light weight.

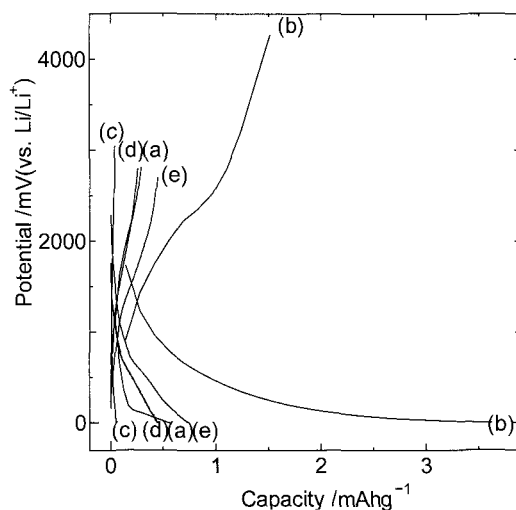


Fig.1 Charge-discharge curves of polymer electrodes including (a) Ni, (b) carbon black, (c) MWCNT, (d) nanohorn, (e) exfoliated graphite.

### Acknowledgement

This work was supported by Gunze limited.

Corresponding Author: [kawasaki.shinji@nitech.ac.jp](mailto:kawasaki.shinji@nitech.ac.jp)

Phone & Fax: +81-52-735-5221

## Electrical and Mechanical Properties of Carbon Nanotube/Polyisoprene Composites with Low Percolation Threshold and High Conductivity

○Tomoya Nagaoka, Ayumu Sakai, Katsumi Uchida, Koji Tsuchiya, Masayosi Ito,  
Takeo Furukawa, Hirofumi Yajima\*

*Department of Applied Chemistry, Faculty of Science, Tokyo University of Science  
1-3 Kagurazaka, Shinjuku-ku, Tokyo 162-8601, Japan*

Polymer composite materials containing inorganic fine particles as fillers are widely used for various industrial fields as the structural and functional materials [1]. When the filler ratio is exceeded at a certain threshold value, various phase transitions occur, for example, from the viscous material to the elastic one or from the insulator to the conductor [2]. Various carbon materials have been used as fillers in a polymer for their functionalization and improvement in the electrical conductivity, mechanical strength and electromagnetic shielding property. In practical use for polymer- carbon composite materials, a high functionality and a low percolation threshold have been required from the viewpoints of physical properties, processing, and cost. In particular, carbon nanotubes (CNTs) among carbon materials have attracted a great deal of attention for extended nanotechnological applications because of their peculiar structure, multifunctionalities, high-specific surface area, and high aspect ratio.

The objective of this paper is to develop a practical conductive elastomer-material comprising of polyisoprene rubber (IR) with CNTs with the combinational techniques of ultrasonication (US) and rotation/revolution mixing without mechanical shear. For comparison, the composite materials were prepared by a conventional method with twin-screw (Banbury) mixer or extruder. Then, the relationships between the electrical properties of the composites and the structural characteristics of the CNTs (aspect ratio, disordered graphite degree, etc) were investigated as a function of the contents of the CNTs. Moreover, the performance of the composites such as tensile strength and stability was evaluated.

As a result, CNTs/IR composites exhibited a high conductivity and a low percolation threshold without decreasing their tensile strength, compared to the composites prepared with a Banbury mixer, which was inferred to give rise to the collapse of CNTs, followed by a high percolation threshold and a low conductivity. ESR measurements suggested that the addition of CNTs to IR inhibited degradation of the rubber because of CNT's radical scavenging capacity. The present results led us to the conclusion that the rotation/revolution mixing technique was expected to be a promising procedure for the preparation of various polymer composites containing CNTs.

[1] K. Kueseng, K. I. Jacob, *European Polym. J.* 42 (2006) 220-227

[2] A. Das, K. W. Stöckelhuber, R. Jurk, M. Saphiannikova, J. Fritzsche, H. Lorenz, M. Klüppel, G. Heinrich, *Polymer* 49(2008) 5276-5283

**\*Corresponding Author:** Hirofumi Yajima

TEL: +81-3-3260-4272(ext.5760), FAX: +81-3-5261-4631, E-mail: [yajima@rs.kagu.tus.ac.jp](mailto:yajima@rs.kagu.tus.ac.jp)

## Cell aggregation to a carbon nanotube scaffold with dielectrophoresis

○Makoto Matsuoka<sup>1,2</sup>, Tsukasa Akasaka<sup>3</sup>, Takeshi Hashimoto<sup>4</sup>,  
Yasunori Totsuka<sup>1</sup>, Fumio Watari<sup>3</sup>

<sup>1</sup>*Department of Oral and Maxillofacial Surgery, Graduate School of Dental Medicine,  
Hokkaido University, Kita 13 Nishi 7, Kita-ku, Sapporo 060-8586, Japan*

<sup>2</sup>*Research Fellow of the Japan Society for the Promotion of Science, Japan*

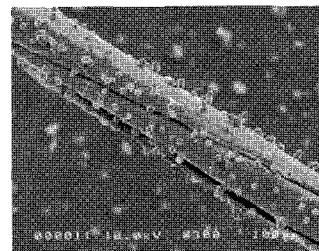
<sup>3</sup>*Department of Dental Materials and Engineering, Graduate School of Dental Medicine,  
Hokkaido University, Kita 13 Nishi 7, Kita-ku, Sapporo 060-8586, Japan*

<sup>4</sup>*Meijo Nano Carbon Co., Ltd., Otsubashi bldg. 4F, 3-4-10 Marunouchi, Nakaku,  
Nagoya 460-0002, Japan*

In regenerative medicine, it is important to grow a large number of cells on appropriate scaffolds. For that purpose, many types of cell scaffolds have been developed. Carbon nanotubes (CNTs) have attracted increasing attention owing to their mechanical, electrical, and structural properties. Because of these unique properties, increasing numbers of reports have focused on the use of CNTs as scaffolds in regenerative medicine. One of the most attractive properties of CNTs is their excellent conductivity, and they can thus provide electro-conductivity to a scaffold. Recently, many reports of cell positioning and patterning using electrical fields have been published. The dielectrophoretic approach is one of the most useful methods because of its ability to move cells in a non-uniform electric field. With this method, the scaffold with electro-conductivity would be able to attract cells efficiently. In this study, a threadlike CNT-scaffold was prepared and dielectrophoresis was performed to attract PC12 cells to the scaffold.

Single-walled CNTs (Meijo Nano Carbon Co., Ltd., Japan) were formed into a thread about 100 $\mu$ m in diameter. The CNT scaffold was connected to the electrode and soaked into PC12 cell dispersion. AC voltage was applied and PC12 cell were attracted to the scaffold within a few minutes. After 5 min, the ac voltage supply was stopped and cells were then incubated for 25 min at room temperature. The scaffold was fixed and cell numbers were counted using a scanning electron microscope (SEM). The cell number on the CNT scaffold incubated for 30 min without dielectrophoresis was also counted as control. The cell numbers with dielectrophoresis were approximately ten times higher than control. In order to evaluate the effect of dielectrophoresis to the cells, PC12 cell proliferation and differentiation after the dielectrophoresis was observed. Cells attracted to the scaffold were cultured for 8d and observed using a SEM. Cells showed good proliferation and covered the surface of the scaffold. PC12 cells attracted to the CNT scaffold were cultured with NGF for 8d and observed using a SEM and a fluorescence microscope. PC 12 cells were differentiated and neurite extension was observed.

This report shows that the PC12 cells were attracted to the thread-like CNT scaffold with dielectrophoresis and showed good proliferation and differentiation. These findings indicated that dielectrophoresis is the effective way to attract cells to the scaffold of the form that cells are hard to adhere.



Corresponding Author: Makoto Matsuoka

TEL: +81-11-706-4283, FAX: +81-11-706-4283, E-mail: matsuoka@den.hokudai.ac.jp

## **Influence of Device Processing on Electrical Properties of Carbon Nanotube Field Effect Transistors**

○Mikito Tanaka<sup>1</sup>, Yoichi Ito<sup>1</sup>, Bongyong Jang<sup>1</sup>, Yasuhiko Hayashi<sup>1</sup>, Naoki Kishi<sup>1</sup>,  
Tetsuo Soga<sup>1\*</sup>, Takashi Jimbo<sup>2</sup>

<sup>1</sup>*Department of Frontier Materials, Nagoya Institute of Technology,  
Nagoya 466-8555, Japan*

<sup>2</sup>*Research Center for Nano-Device and System, Nagoya Institute of Technology,  
Nagoya 466-8555, Japan*

Carbon nanotube field effect transistors (CNT-FETs) have attracted much attention because of their novel electrical properties based on quasi one dimensional structure. CNT growth using chemical vapor deposition (CVD) with patterned metal catalyst is one of the promising techniques to achieve position controlled fabrication of CNT-FETs[1]. In that fabrication process, CNT channels are contaminated by photoresist and solvents because photolithography and lift-off processes are performed to form pad electrodes after synthesis of the nanotube channels. Therefore development of fabrication process without contamination to the CNT channels is desired to bring out intrinsic properties of CNT-FETs. Clarification of influence of contamination on electrical properties of CNT-FETs is also required.

In this study we report the fabrication process of CNT-FETs having contamination-free nanotube channels. The influence of contamination by photoresist on the electrical properties of CNT-FETs was also investigated. We found that contamination by photoresist affects especially to on-current of CNT-FETs. The details will be discussed in our presentation.

[1] H.T.Soh et al., Appl. Phys. Lett., 75, 627 (1999).

**Corresponding Author: Tetsuo Soga**

**TEL/FAX: +81-52-735-5532**

**E-mail: [soga@nitech.ac.jp](mailto:soga@nitech.ac.jp)**

## Transparent Conductive Thin Films of Single-Wall Carbon Nanotubes Encapsulating Organic Molecules

○Naoki Kishi<sup>1\*</sup>, Ikuma Miwa<sup>1</sup>, Toshiya Okazaki<sup>2,3</sup>, Takeshi Saito<sup>2</sup>, Toshihisa Mizutani<sup>1</sup>, Hiroaki Tsuchiya<sup>1</sup>, Tetsuo Soga<sup>1</sup>, Takashi Jimbo<sup>4</sup>

<sup>1</sup>*Department of Frontier Materials, Nagoya Institute of Technology,  
Nagoya 466-8555, Japan*

<sup>2</sup>*Nanotube Research Center, National Institute of Advanced Industrial Science and  
Technology (AIST), Tsukuba 305-8565, Japan*

<sup>3</sup>*PRESTO, Japan Science and Technology Agency, Kawaguchi 332-0012, Japan*

<sup>4</sup>*Research Center for Nano-Device and System, Nagoya Institute of Technology,  
Nagoya 466-8555, Japan*

Single-wall carbon nanotube (SWCNT) thin films have attracted much attention in recent years as transparent conductive electrodes for plastic electronic devices. A lot of efforts have been dedicated on improvement of their resistivity. Chemical doping is one of the promising techniques to increase conductivity of SWCNT films. H.Z.Geng et al. reported that conductivity of transparent conductive films using SWCNTs can be improved by doping using dopants attached on the surface of nanotubes[1]. In addition to conductivity enhancement, improvement of stability is also required to employ doped SWCNT films as transparent conductive electrodes for commercial devices.

In this study we report properties of transparent conductive films using SWCNTs doped with organic molecules encapsulated inside nanotubes. Doping by molecular encapsulation provides stable conductivity enhancement because the dopant molecules are protected by nanotubes. The details will be discussed in our presentation.

[1] H.Z.Geng et al., J. Am. Chem. Soc., 129, 7758 (2007).

**Corresponding Author: Naoki Kishi**

**TEL/FAX: +81-52-735-5147**

**E-mail: kishi.naoki@nitech.ac.jp**

## Thin-film transistors using aligned semiconducting single-wall carbon nanotubes separated by agarose gel chromatography

○Shunjiro Fujii<sup>1,2</sup>, Takeshi Tanaka<sup>1</sup>, Hiromichi Kataura<sup>1,2</sup>

<sup>1</sup>*Nanosystem Research Institute, National Institute of Advanced Industrial Science and Technology (AIST), Tsukuba, Ibaraki 305-8562, Japan*

<sup>2</sup>*JST, CREST, Kawaguchi 330-0012, Japan*

Thin-film transistors (TFTs) using single-wall carbon nanotubes (SWCNTs) have attracted a great deal of attention for their possible use in transparent, flexible, high-speed, and high-current electronics. Recently, we found that TFT using a slightly aligned semiconductor enriched SWCNT (s-SWCNT) thin film shows drastically improved transfer characteristics [1]. To obtain higher on-currents and mobility, high density SWCNT thin film is required as well as high semiconductor purity. In this work, we fabricated TFTs using different densities of aligned s-SWCNT network.

In this study, s-SWCNTs separated by gel chromatography method [2] were used. The purity of semiconducting SWCNTs (in the s-SWCNTs) was ~90%. s-SWCNT solution was dropped onto a SiO<sub>2</sub>/Si substrate covered with self-assembled monolayer of 3-aminopropyltriethoxysilane. The aligned thin film was prepared by N<sub>2</sub> blow in the drying process. The SWCNT density was controlled by changing waiting times before N<sub>2</sub> blow. Au/Ti electrodes were deposited as source and drain, resulting in back-gated TFTs with top-contact structure.

Figure 1 shows typical AFM images of low and high-density s-SWCNT films. It can be seen that s-SWCNTs were aligned in the vertical direction of the figure, although they are still forming random network. Typically, TFTs using low-density film showed a mobility of 5 cm<sup>2</sup>/Vs and an on-off ratio of 10<sup>4</sup>, while those using high-density film showed the mobility of 70 cm<sup>2</sup>/Vs and the on-off ratio of 10<sup>2</sup>. Detailed device characteristics of aligned s-SWCNT films will be discussed.

[1] S. Fujii et al., The 39<sup>th</sup> F-NT General symposium 2010, 2p-39

[2] T. Tanaka et al., Appl. Phys. Express **2** (2009) 125002

**Corresponding Author:** Hiromichi Kataura

**E-mail:** h-kataura@aist.go.jp, **Tel:** +81-29-861-2551, **Fax:** +81-29-861-2786

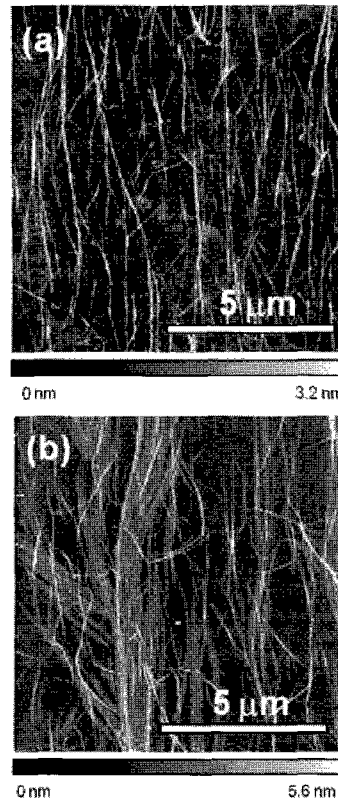


Fig.1 AFM images of (a) low and (b) high-density s-SWCNT thin films.



## The simple method for analyzing the interaction between carbon nanotube and molecules

○JongTae Yoo<sup>1</sup>, Tsuyohiko Fujigaya<sup>1</sup>, and Naotoshi Nakashima<sup>1,2</sup>

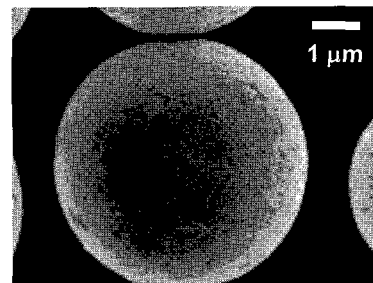
<sup>1</sup>Department of Applied Chemistry, Graduate School of Engineering, Kyushu University, 744 Motoooka, Fukuoka 819-0395, Japan

<sup>2</sup>Japan Science and Technology Agency, CREST, 5 Sanbancho, Chiyoda-ku, Tokyo, 102-0075, Japan

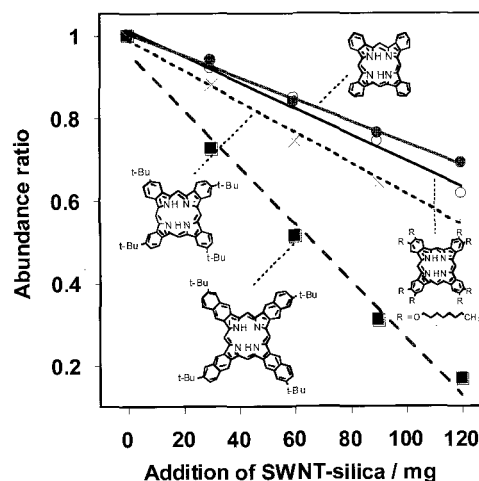
Carbon nanotubes (CNTs) have unique  $\pi$ -rich, hydrophobic and curvature surfaces. In there, interfacial interactions of CNTs with molecules have been the focus of interests for the sake of solubilization of CNTs through physisorption [1] as well as many applications of CNTs. We have reported affinity chromatography technique using CNT-coated silica gel as a stationary phase to rank the interactions. However the analysis of the molecules having extremely strong interaction was quite difficult. Here we developed the simple method to evaluate the interaction for these molecules.

Figure 1 shows silica gel microparticles coated with single-walled carbon nanotubes (SWNTs) monolayer (denote as SWNT-silica) prepared by the simple mixing of pristine SWNTs dispersed in the 1-methyl-2-pyrrolidinone (NMP) with the amino-functionalized silica gel [2]. We prepared phthalocyanines (Ph-A ~ D) solutions in THF, and then shaken after the addition of SWNT-silica. These solutions were standed a few hours and the absorption spectra of the supernatants were measured (Figure 2). The absorbance of the solutions decreased by increasing the addition of the SWNT-silica. It was revealed that Ph-C interact strongly to SWNT compared to the other phthalocyanines. We attribute that large  $\pi$ -conjugation of Ph-C gives a strong affinity onto the SWNT surface.

We believe that this simple method provides the promising opportunity for the systematic studies using wide range of molecules to achieve the understanding of the degree of interaction between CNTs and molecules.



**Fig. 1** SEM image of the SWNT-silica.



**Fig. 2** Plots of abundance ratio of phthalocyanines to addition of SWNT-silica.

[1] (a) N. Nakashima, T. Fujigaya, *Chem. Lett.*, **36**, 692. (2007).

(b) T. Fujigaya, N. Nakashima, *Polymer J.*, **40**, 577. (2008).

[2] T. Fujigaya, J. Yoo, N. Nakashima *Carbon*, **49**, 468. (2011).

Corresponding Author: Naotoshi Nakashima

E-mail: nakashima-tcm@mail.cstm.kyushu-u.ac.jp

Tel & Fax: +81-92-802-2842

## Controllable Dispersivity of Carbon Nanotubes

○Naoyuki Uchiyama,<sup>1,2</sup> Naotoshi Nakashima<sup>1,3</sup>

<sup>1</sup>Department of Applied Chemistry Graduate School of Engineering, Kyushu University,  
Fukuoka 819-0395, Japan

<sup>2</sup>Fukuoka Industrial Technical Center, 3-2-1 Kamikoga Chikushino Fukuoka 818-8540, Japan

<sup>3</sup>Japan Science and Technology Agency (JST), Core Research of Evolutional Science &  
Technology (CREST), 5 Sanbancho, Chiyoda-ku, Tokyo 102-0075, Japan

In order to utilize carbon nanotubes (CNTs) effectively for many applications, dispersion of CNTs in various media is important. Although many different kinds of dispersants for CNTs have been reported, it is still important to develop novel unique CNT dispersant. Here we report a new CNT dispersant (**1**, Fig. 1) carrying a pyrene and long-chain-hemiacetal moieties. The synthesized dispersant gave a stable dispersion of the CNTs in an organic solvent. We found that the addition of an acid to the solution produced a precipitate (Fig. 2). This would be due to the elimination of the long-chain-hemiacetal moiety from the dispersant.

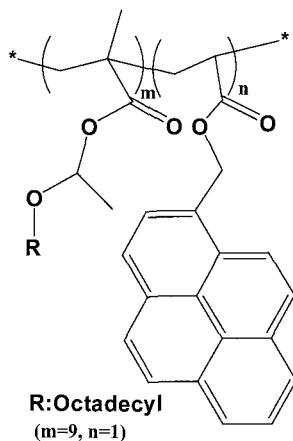


Fig. 1. Chemical structure of **1**.

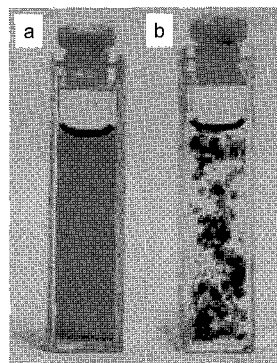


Fig. 2. A photo of CNTs dispersed by the aid of **1** in THF. before (a) and after (b) the adding an acid.

Corresponding Author : Naoyuki Uchiyama

E-mail : n-uchiya@fitc.pref.fukuoka.jp

Tel & Fax: +81-92-925-7723, +81-92-925-7724

## Highly Conductive Vein-Like SWNT Network

○Kazufumi Kobashi, Seisuke Ata, Takeo Yamada, Don N. Futaba, Motoo Yumura and Kenji Hata

*Nanotube Research Center, National Institute of Advanced Industrial Science and Technology (AIST), Technology Research Association for Single Wall Carbon Nanotubes (TASC), 1-1-1 Higashi, Tsukuba, Ibaraki 305-8565, Japan*

Carbon nanotubes (CNT) have been studied as fillers in diverse multifunctional composites due to a wide range of the excellent properties. Dispersion technology of CNTs is challenging to realize commercial products such as coatings, heat sink, and structural members. Much efforts have been focused on dispersing CNTs individually into matrix, however, deterioration in CNT quality by damaging the surface and shortening was an inevitable problem [1].

Here we present the vein-like SWNT network comprised of long (hundreds of micron), flexible nanotubes which can reach the electrical, thermal conductivity and mechanical strength throughout matrices like polymers and metals. The SWNT network was made by dispersing an as-grown SWNT forest in solvent through a shear from wet-jet mill. Different shear was applied at 20-120 MPa of the jet pressure. First, the SWNT forest suspended in solvent showing the configuration like trunks of a tree. By the shear-induced dispersion, the trunks were transformed into fine meshes (Figure 1). The SWNT meshes were discretely laid on a flat substrate to observe the structure. An SEM observation of the SWNT meshes revealed that the nanotubes spread continuously across the whole system, which differs from a network through contacts of individually-dispersed nanotubes. The trunks from the starting SWNT forest were unraveled widely with an increase of the jet pressure, resulting in more meshes as well as a reduction in the mesh size. Bucky papers made from these SWNT meshes showed a high electrical conductivity.

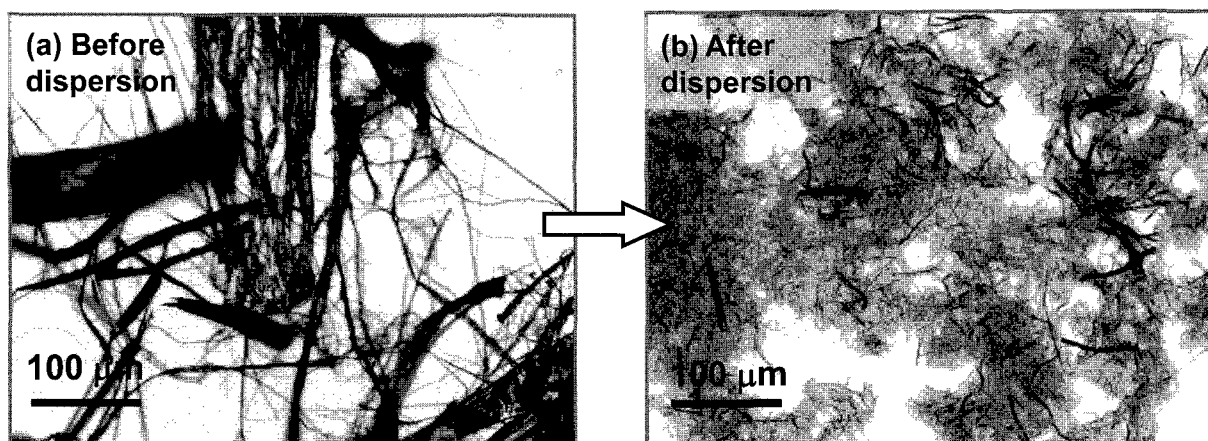


Figure 1 Optical microscope images of SWNTs (a) before and (b) after dispersion by wet-jet mill. These samples were spin-coated on flat substrates from SWNT/MIBK solution.

[1] P. M. Ajayan and J. M. Tour, *Nature*, **447**, 1066 (2007).

Corresponding Author: Kenji Hata

TEL: +81-29-861-4654, FAX: +81-29-861-4851, E-mail: kenji-hata@aist.go.jp

## Ion-Gel Gating of Single-Walled Carbon Nanotube Films

○Di Wen<sup>1</sup>, Yohei Yomogida<sup>2</sup>, Hidekazu Shimotani<sup>3</sup>, Kazuhiro Yanagi<sup>4</sup>, Yoshihiro Iwasa<sup>3</sup>,  
and Taishi Takenobu<sup>1</sup>

<sup>1</sup>*Department of Applied Physics, Waseda University, Shinjuku 169-8555, Japan*

<sup>2</sup>*Department of Physics, Tohoku University, Sendai 980-8578, Japan*

<sup>3</sup>*QPEC, The University of Tokyo/JST-CREST, Hongo 113-8656, Japan*

<sup>4</sup>*Department of Physics, Tokyo Metropolitan University, Hachioji 192-0397, Japan*

Recently, single-walled carbon nanotube (SWNT) is very attracting materials for flexible and printed electronics [1]. One of the difficult problems for SWNT film electronics is the transport control through density tuning. Generally, thick film shows metallic behavior, and semiconducting films are only obtained in very thin film. It is inevitable for SWNT transistors to fabricate moderate density films, and it makes the reproducibility of device fabrication drastically poor. Here, to break this limitation, we use one of the solid electrolytes, ion-gel, as the gate insulator for effective gating of thick SWNT film.

In this study, we selected thick SWCNT paper ( $> 200 \mu\text{m}$ ), which is just metallic film for conventional transistor structure. We fabricated the electric double layer transistor using this SWCNT paper and one of the solid electrolytes, ion gel, which consists from poly(styrene-*block*-methyl methacrylate-*block*-styrene) (PS-PMMA-PS) triblock copolymer and *N*-Methyl-*N*-propylpyrrolidinium bis(trifluoromethanesulfonyl imide) (P13-TFSI, Fig. 1) ionic liquid. We have laminated the SWCNT paper on SiO<sub>2</sub>/Si substrate and evaporated Au source/drain electrodes. Next, the PS-PMMA-PS/P12-TFSI solution in ethyl acetate was drop-casted onto the substrate. Finally, we put the Au plate on the substrate as gate electrode. All the measurement was done in the glove box with nitrogen atmosphere.

Fig.2 shows the transfer characteristic of ion-gel SWNT transistor. Importantly, 4 digits on/off ratio was obtained although the SWNT paper is very thick. It strongly suggests that the effective gating of whole SWNT film via ion-gel since it surrounds individual SWNTs and SWNT bundles completely. Moreover, operation voltage is quite low.

In summary, we successfully gated the SWNT thick film using ion-gel. This technique might improve the reproducibility of SWNT film transistor drastically.

This study was supported by Industrial Technology Research Grant Program from New Energy and Industrial Technology Development Organization (NEDO) of Japan.

[1] H. Okimoto et al., *Adv. Mater.*, **22**, 3981 (2010).

Corresponding Author: Taishi Takenobu

TEL: +03-5286-2981, FAX: +03-5286-2981, E-mail: takenobu@waseda.jp



Fig. 1 P13-TFSI

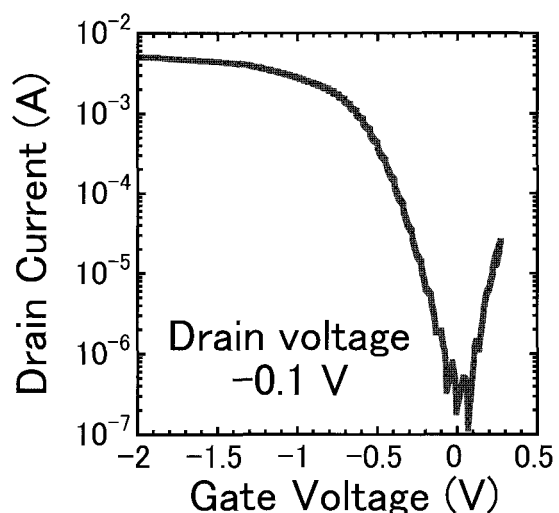


Fig. 2 Transfer characteristics

## Hybridization of DNA/carbon nanotube hybrid with biocompatible polycation.

○Tsuyohiko Fujigaya<sup>1</sup>, Yuki Yamamoto<sup>1</sup>, Arihiro Kano<sup>1</sup>, Atsushi Maruyama<sup>1</sup>, Naotoshi Nakashima<sup>1,2</sup>

<sup>1</sup>Department of Applied Chemistry, Graduate School of Engineering, Kyushu University,  
744 Motoooka, Fukuoka 819-0395, Japan

<sup>2</sup>JST-CREST, 5 Sanbancho, Chiyoda-ku, Tokyo, 102-0075, Japan

Single-walled carbon nanotubes (SWNTs) have the strong optical absorption and photoluminescence (PL) in near infrared region. Introducing of SWNTs to biological systems leads various applications such as imaging, photo thermal therapy, drug delivery system and so on. We reported that DNA solubilizes SWNTs in water [1] and the hybrids are highly stable even in the absence of unbound DNA [2][3]. DNA/SWNT hybrid has negative charge on the surface and allows interacting with cationic compounds. We studied a hybridization of DNA/SWNT with polycation by means of absorption spectra, dynamic light scattering, atomic force microscopy and so on.

Poly(L-lysine)-*graft*-polyethyleneglycol (PLL-g-PEG) having a high dispersibility, biocompatibility and strong interaction with DNA because of its cationic PLL main chain [4] was used as a polycation. From the titration, composition ration of the hybrid was determined as an approximately PLL-g-PEG : DNA/SWNT = 1 : 1. The ternary hybrid thus obtained (PLL-g-PEG/DNA/SWNT) possess remarkable stability in aqueous media, probably due to the grafted PEG chain. Cell uptaking efficiency was studied using HeLa cell, which was evaluated by Raman mapping of the cells after incubation with the both composites. Interestingly, we found that the dramatic improvement of the efficiency after the hybridization with PLL-g-PEG as shown in **Figure 1**.

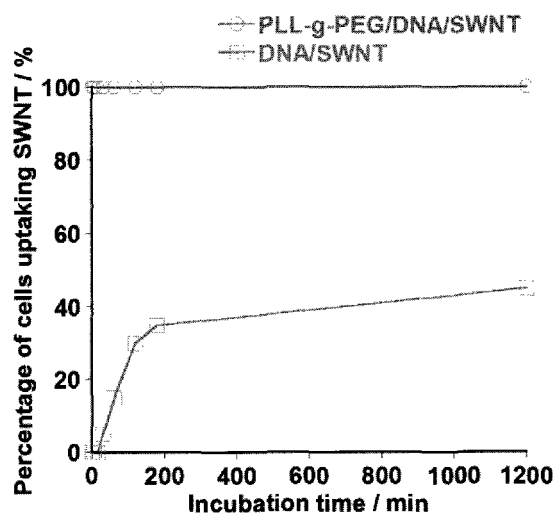


Figure 1. Polts of uptaking efficiency of DNA/SWNT hybrid with (circle) and without (square) biocompatible cationic polymer, PLL-g-PEG, by HeLa cells

[1] N. Nakashima, S. Okuzono, H. Murakami, T. Nakai, K. Yoshikawa, *Chem. Lett.* **2003**, 32, 456.

[2] Y. Noguchi, T. Fujigaya, Y. Niidome, N. Nakashima, *Chem. Phys. Lett.* **2008**, 455, 249.

[3] Y. Yamamoto, T. Fujigaya, Y. Nidome, N. Nakashima, *Nanoscale*, **2010**, 2, 1767.

[4] A. Sato, S. W. Choi, M. Hirai, A. Yamayoshi, R. Moriyama, T. Yamano, M. Takagi, A. Kano, A. Shimamoto, A. Maruyama, *J. Control. Release* **2007**, 122, 209.

Corresponding Author: Naotoshi Nakashima

E-mail: [nakashima-tcm@mail.cstm.kyushu-u.ac.jp](mailto:nakashima-tcm@mail.cstm.kyushu-u.ac.jp); Tel&Fax: +81-92-802-2840

## Inkjet carrier doping to single-walled carbon nanotube film

○Satoki Matsuzaki<sup>1</sup>, Kazuhiro Yanagi<sup>2</sup>, Taishi Takenobu<sup>1</sup>

<sup>1</sup>*Department of Applied Physics, Waseda University, Shinjuku 169-8555, Japan*

<sup>2</sup>*Department of physics, Tokyo Metropolitan University, Hachioji 192-0397, Japan*

Single-walled carbon nanotubes (SWNTs) are promising materials for building electronic devices, in particular thin film transistors (TFTs). SWNT-TFTs fabrication using an ink-jet technique has attracted especially strong interest due to wide range applications such as flexible electronics and printing electronics. [1] However realistic circuits and devices require solutions to significant challenges associated with precisely controlling the electronic properties of the SWNT films. Here we report an ink-jet carrier doping to SWNTs thin film and fabrication of complementary circuits.

Figure 1 shows a schematic illustration of ink-jet carrier doping procedure. SWNTs thin film was printed sequentially using ink-jet technique on SiO<sub>2</sub>/Si substrate. Furthermore, the PEI solution in methanol was printed position-selectively using ink-jet technique on SWNTs thin film since SWNTs can be functionalized by polyethyleneimine (PEI) to switch their operation from p-type to n-type. This procedure converted the originally p-type SWNTs-TFT into the n-type one, and both p-type and n-type TFTs allows for design of complementary circuits. Indeed, we observed inverter characteristics (Fig. 2).

In summary, we have demonstrated ink-jet carrier doping to SWNTs-TFT and fabricated the logic circuit. In the future, these results promise to push the performance limit of SWNTs-based flexible and/or printed electronics.

This study was supported by Industrial Technology Research Grant Program from New Energy and Industrial Technology Development Organization (NEDO) of Japan.

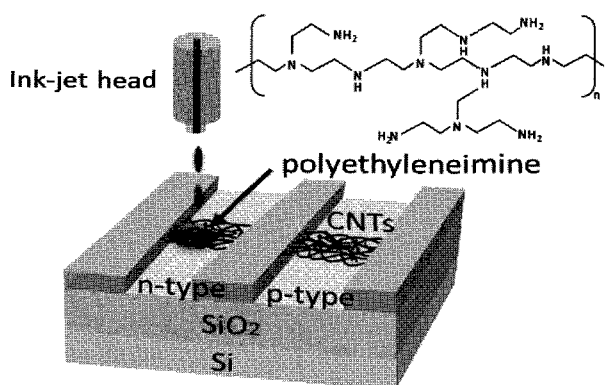


Fig.1 ink-jet carrier doping to SWNT thin film

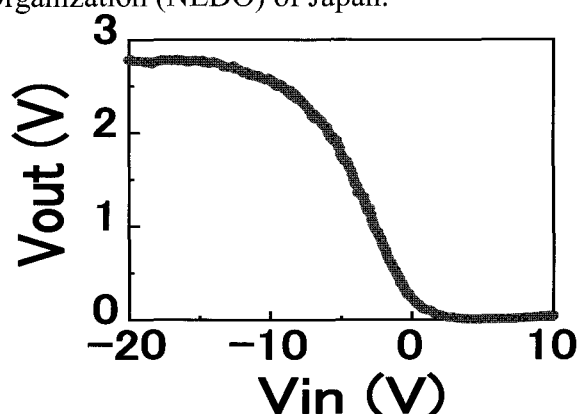


Fig.2 inverter characteristic

[1] H.Okimoto, T.Takenobu et al., *Advanced Materials* 2, 3981 (2010).

Corresponding: Taishi Takenobu E-mail: takenobu@waseda.jp Tel & Fax: +81-3-5286-2981

## Chirality dependence of coherent phonon amplitudes in single wall carbon nanotubes

○ Ahmad R.T. Nugraha, Kentaro Sato, and Riichiro Saito\*  
*Department of Physics, Tohoku University, Sendai 980-8578, Japan*

In this presentation, we review coherent phonon (CP) spectroscopy of single wall carbon nanotubes (SWNTs). In a pump-probe experiment, when a very short laser pulse ( $\sim 10$  fs) is pumped to a SWNT sample, photo excited carriers as excitons appear at the same time in the excited states of SWNTs. Before recombination of the electron-hole pair, the lattice starts to vibrate coherently by exciton-phonon interaction in the same phase, which can be observed as an oscillation of transmittance in the probe pulse. After making Fourier transform of the transmittance with respect to time, we obtain the spectrum as a function of phonon frequencies. The phenomena observed in CP spectroscopy are similar to those in Raman spectroscopy in a sense that the exciton-phonon interaction is essential for making phonon. Theoretical characterizations of CP spectra is thus needed to explain the experimental results.

We calculate the dynamics of coherent phonons in SWNTs with different chiralities by following a microscopic theory developed by Sanders et al. and Stanton [1,2]. We improve the theory by including geometry optimization and curvature effects in the calculation [3], which is necessary for considering small diameter nanotubes. In particular, we examine coherent radial breathing mode amplitudes in semiconducting SWNTs by changing excitation energies within 0.5-4.0 eV. We find that the CP amplitudes are very sensitive to the change in excitation energies and that the phase of CP oscillations for each SWNT is strongly chirality dependent. From this simulation, we can also predict how the SWNT diameter changes in response to femtosecond laser excitation, especially to understand whether the diameter of a given SWNT will initially increase or decrease.

\*This work is a collaboration between the authors with Gary Sanders and Prof. Stanton of the University of Florida, USA.

[1] G. D. Sanders, C. J. Stanton, J.-H. Kim, K.-J. Yee, Y.-S. Lim, E. H. Haroz, L. G. Booshehri, J. Kono, and R. Saito, *Phys. Rev. B* 79, 205434 (2009).

[2] A. V. Kuznetsov and C. J. Stanton, *Phys. Rev. Lett.* 73, 3243 (1994).

[3] Ge. G. Samsonidze, R. Saito, N. Kobayashi, A. Gruneis, J. Jiang, A. Jorio, S. G. Chou, G. Dresselhaus, and M. S. Dresselhaus, *Appl. Phys. Lett.* 85, 5703 (2004).

Corresponding Author: A. R. T. Nugraha

TEL: +81-22-795-7754, FAX: +81-22-795-6447, E-mail: nugraha@flex.phys.tohoku.ac.jp

## Density Functional Theory Calculations of the Cleavage of CC Bonds of Nanotubes by Diketone Formation

○Takashi Yumura and Toshiyuki Kanemitsu

*Department of Chemistry and Materials Technology, Kyoto Institute of Technology,  
Matsugasaki, Sakyo-ku, Kyoto, 606-8585, Japan*

**Abstract:** Kosynkin et al. reported longitudinal unzipping of carbon nanotubes by potassium permanganate ( $\text{KMnO}_4$ ) to form graphene ribbons at 55–70 °C [1], and proposed that diketone formation is responsible for the cleavage of CC bonds of nanotubes. To our best knowledge there are a few theoretical reports on the diketone formation on nanotube surfaces up to now. The previous studies used too short (5,5) tube whose length of  $\sim 11$  Å [2], and thus the results should be affected artificially by the edges terminated by H atoms as well as discrete energy levels of the short tube [3]. Accordingly, the structures of tubes whose CC bonds are cleaved by the diketone formation remained relatively unexplored. In the present study we employed density functional theory calculations to discuss the diketone formation on the (5,5) tube surface by using infinite-length model on the periodic boundary condition as well as the finite-length model whose length of  $\sim 27$  Å.

Figure 1 shows optimized structures for (5,5) tubes whose CC bonds are cleaved by the formation of (a) two or (b) seven diketone. As shown in Figure 1, oxygen atoms are lined up along the tube axis, which cannot be seen in the previous studies. Then the cleavage of CC bonds in the seven-diketone-attached tube is more pronounced than that in the two-diketone-attached tube. As a result of the significant CC cleavage, the seven-diketone-attached tube has larger number of six-membered rings posing planarity rather than the two-diketone-attached tube case. Because of the attached oxygen atoms lined up along the axis as well as the CC bond cleavage, orbitals that mainly consist of  $p$  orbitals of oxygen atoms appears at frontier orbital regions.

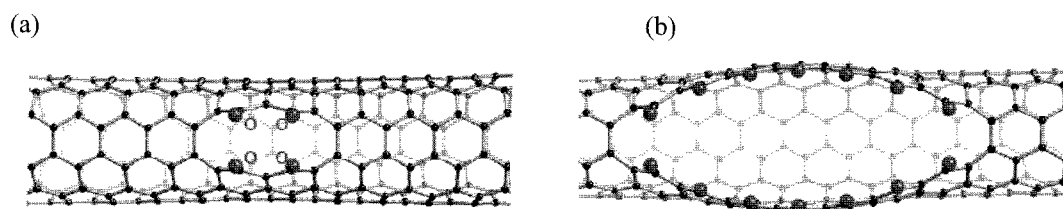


**Figure 1** Optimized structures for (5,5) tubes whose CC bonds are cleaved by the formation of (a) two or (b) seven diketones.

**References:** [1] Kosynkin, D. V. et al. *Science* **2009**, 458, 872.

[2] (a) Rangel, N. L. et al. *J. Chem. Phys.* **2009**, 131, 031105. (b) Zhang, H. et al. *Phys. Chem. Chem. Phys.* **2010**, 12, 13674.

[3] Yumura, T.; Bandow, S.; Yoshizawa, K.; Iijima, S. *J. Phys. Chem. B*, **2004**, 108, 11426.

**Corresponding Author** Takashi Yumura

**E-mail** yumura@chem.kit.ac.jp

**Tel&Fax** +81-75-724-7571



**$G^+/G^-$  behavior of SWCNTs under the dispersion process**

○Satoko Nishiyama<sup>1</sup>, Takeshi Tanaka<sup>1,2</sup>, Hiromichi Kataura<sup>1,2</sup>

<sup>1</sup>Technology Research Association for Single Wall Carbon Nanotubes (TASC), Tsukuba  
Central 5, 1-1-1 Higashi, Tsukuba 305-8565, Japan

<sup>2</sup>Nanosystem Research Institute, AIST, C4, 1-1-1 Higashi, Tsukuba 305-8562, Japan

It is well known that single wall carbon nanotubes (SWCNTs) show intense Raman peaks, “G-band”, around  $1593\text{ cm}^{-1}$ . The G-band consists of doublet,  $G^+$  (higher frequency) and  $G^-$  (lower frequency).  $G^+$  and  $G^-$  of semiconducting (s-) SWCNTs are assigned to longitudinal optical phonon mode (LO) and transverse optical phonon mode (TO), respectively, while those of metallic (m-) SWCNTs are assigned to TO and LO, respectively, due to the softening of LO in m-SWCNTs [1]. We measured G-band Raman spectra of the SWCNTs under the dispersion process in water using tip type ultrasonic homogenizer (Branson Sonifier) and  $G^+/G^-$  value was analyzed. Figure 1 shows  $G^+/G^-$  of SWCNTs produced by electric arc discharge method. Upper figure shows results of s-SWCNTs using 488 nm excitation and lower figure shows those of m-SWCNTs using 633 nm excitation. Interestingly,  $G^+/G^-$  of s-SWCNTs increased with the sonication, while that of m-SWCNTs decreased. This opposite behavior of  $G^+/G^-$  value is probably due to the opposite assignment of each peak and thus the intensity ratio LO/TO shows the similar behavior for both s- and m-SWCNTs. Present result suggests that LO/TO ratio can be used as an index of isolation status of SWCNTs in the solution. Detailed analysis will be shown.

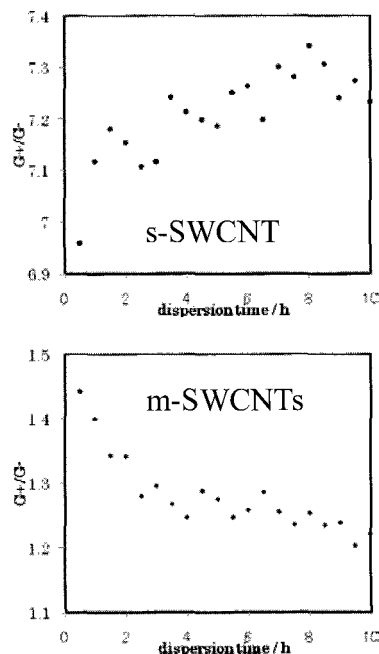


**Figure 1.**  $G^+/G^-$  of s-SWCNTs (upper) and m-SWCNTs (lower), against the dispersion time

[1] K. Ishikawa and T. Ando, *J. Phys. Soc. Jpn.*, **75**, 084713 (2006).

Corresponding Author: Hiromichi Kataura

Tel: +81-29-861-2551, Fax: +81-29-861-2786, E-mail: h-kataura@aist.go.jp

## Raman spectroscopy of SWNTs grown from boron- and nitrogen-containing feedstocks

NTT Basic Research Laboratories, NTT Corp., °Satoru Suzuki, Hiroki Hibino

E-mail: ssuzuki@will.brl.ntt.co.jp

The thermal chemical vapor deposition (CVD) technique has great potential for highly controlled doped SWNT growth. However, there have been only a limited number of studies of the direct CVD growth of doped SWNTs. Another important issue for doped SWNTs is their characterization. Evaluating the carrier concentration has not often been clarified. In this study, we grew SWNTs by the thermal CVD method using B- and (or) N- containing feedstocks. Spectral shifts, which are indicative of carrier doping, were observed in the G band in Raman spectra.

Triisopropylborate and benzylamine were used as a B- and N-containing feedstock, respectively. Thermal CVD growth of relatively thin CNTs including SWNTs from either these two chemicals has been reported [1,2]. In this study, we also succeeded to grow SWNTs by supplying both two chemicals simultaneously, as shown in Fig. 1. The diameter of the SWNTs was evaluated to be 1-2 nm by Raman (RBM) and TEM measurements. In Raman spectra, hardenings of the G+ and G- bands were systematically observed for these SWNTs, regardless of the feedstock, as shown in Fig. 2. We think that the G band shifts are caused by electron-phonon interaction changes induced by the Fermi level shift. From the amount of the spectral shifts, the carrier concentration in these SWNTs was estimated to be ~0.4 %.

### References

- [1] P. Ayala et al., *J. Mater. Chem.* **18** (2008) 5676.  
 [2] P. Ayala, et al., *J. Phys. Chem. C* **111** (2007) 2879.

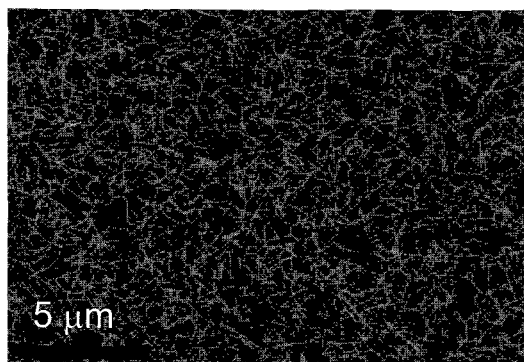


Fig. 1. SEM image of SWNTs grown from both triisopropylborate and benzylamine.

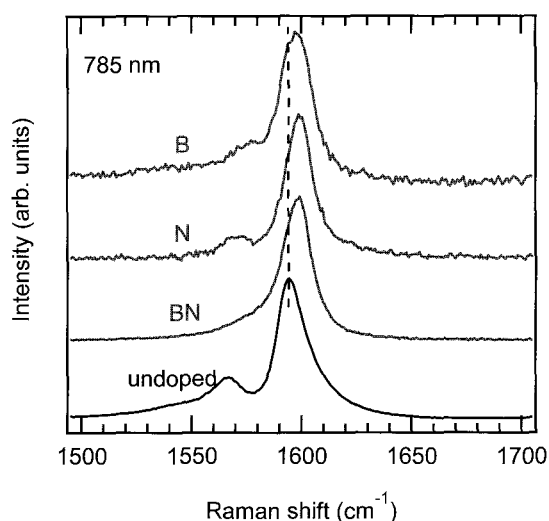


Fig. 2. Raman spectra of SWNTs grown from triisopropylborate (B), benzylamine (N), and both the two (BN). The undoped SWNTs were grown from ethanol.

## Dependence of Raman intensity and shift on different layer stacking of graphene

○Kentaro Sato<sup>1</sup>, Jin Sung Park<sup>2</sup>, and Riichiro Saito<sup>1</sup>

<sup>1</sup>*Department of Physics, Tohoku University, Sendai, 980-8578, Japan*

<sup>2</sup>*Faculty of Engineering, Shinshu University, Nagano, 380-8553, Japan*

Here we show that the calculated Raman intensity and shift of different layer stacking of graphene. It is known that the resonance condition for Raman scattering process and the properties of lattice vibration depend on the layer stacking of graphene. Thus the graphene sample can be characterized by using the Raman spectroscopy [1]. For example, the experiment and theory demonstrated that the Raman intensity and shift of the G' band, which is the overtone of the iTO phonon, are changed with increasing the number of graphene layers [2]. Moreover the Raman spectra from twisted bi-layer graphene have been reported [3]. To evaluate the origin and property of the Raman peaks of different stacking of graphene, we calculate the Raman intensity and shift of different stacking of graphene and the possible combination of phonon modes. Here the Raman spectra are calculated by using the extended tight binding (ETB) method and the force constant model [4]. The structure of the Raman spectra can be recognized by calculating the electron-phonon and -photon matrix elements, and the lattice vibration symmetry. From our calculated results we discuss the dependence of Raman intensity and shift on the structure of graphene [5]. The calculated results are compared with the experiment.

### References:

- [1] L. M. Malard *et al.*, Phys. Rep. 473, 51 (2009).
- [2] J. S. Park *et al.*, Carbon 47, 1303 (2010).
- [3] Z. Ni *et al.*, Phys. Rev. B 80, 125404 (2009).
- [4] J. Jiang *et al.*, Phys. Rev. B 72, 235408 (2005).
- [5] K. Sato *et al.*, unpublished.

Corresponding Author: Kentaro Sato

E-mail: kentaro@flex.phys.tohoku.ac.jp

Tel: +81-22-795-6442, Fax: +81-22-795-6447

## Polarization dependence of x-ray absorption spectra of Graphene

Md. Tareque Chowdhury<sup>1</sup>, Riichiro Saito<sup>1</sup>

<sup>1</sup>Department of Physics, Tohoku University, Aoba, Sendai 980-8578, Japan

Graphene, a single atomic layer of graphite has attracted much attention because of its unusual electronic properties. Recently, x-ray absorption spectroscopy (XAS) is used to determine the electronic properties of graphene [1]. It has also been shown in the experiment that the intensity of x-ray absorption spectra is strongly depends on the polarization direction of incident light [2]. We have also received some unpublished data by the courtesy of Professor Manabu Kiguchi of Tokyo Institute of Technology (TIT). Here, we calculated the x-ray absorption spectra for  $1s-\pi^*$  and  $1s-\sigma^*$  transition of graphene and compare with experimental result. Simple tight binding model is used to calculate the electronic band structure. X-ray absorption intensity is calculated within dipole approximation [3]. In case of x-ray absorption, the dipole vector for  $1s-\pi^*$  transition is directed along the perpendicular direction of graphene plane. The dipole vector for  $1s-\sigma^*$  transition lies along the graphene plane. So the intensity of  $1s-\pi^*$  and  $1s-\sigma^*$  transition change as a function of angle  $\alpha$ , which is the angle between the pointing vector and the surface normal. It is found that intensity for  $1s-\pi^*$  transition is proportional to  $\sin^2\alpha$  and intensity of  $1s-\sigma^*$  transition is proportional to  $\cos^2\alpha$ . Such an angular dependence can be used to select the final state symmetry. We also present a preliminary calculation of angle resolved photo emission spectra (ARPES) of graphene.

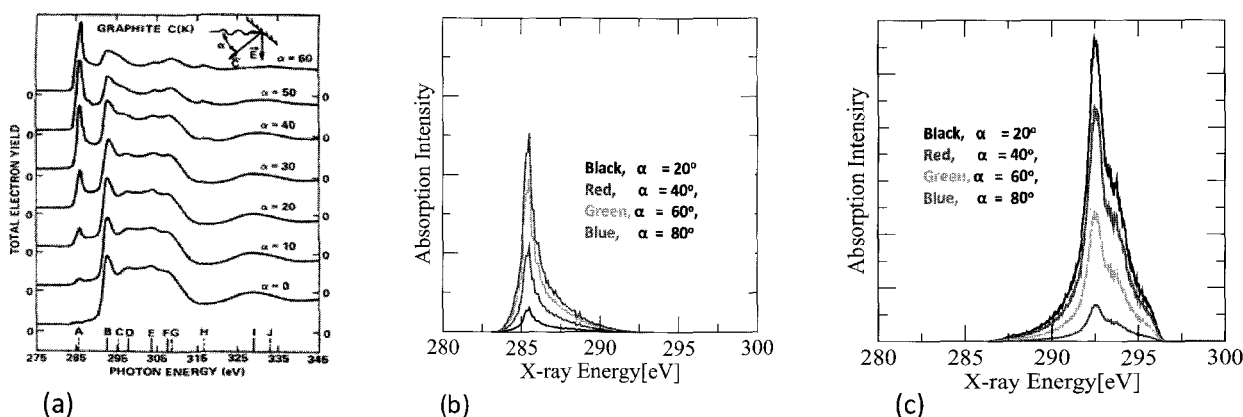


Figure: (a) Experiments: Carbon K edge photo absorption spectra of single crystal graphite at various angle of incidence  $\alpha$ , between the crystal c axis and the electric field unit vector  $\epsilon$  of the light (figure 1 of ref 2). (b) theoretical calculation of  $1s-\pi^*$  transition and (c)  $1s-\sigma^*$  transition at various angle of incidence  $\alpha$

[1] S. Y. Zhou, C. O. Girit, A. Scholl, C. J. Jozwiak, D. A. Siegel, P. Yu, J. T. Robinson, F. Wang, A. Zettl and A. Lanzara, *Phys. Rev. B*, **80**, 121409(R) (2009).

[2] R. A. Rosenberg, P. J. Love and V. Rehn, *Phys. Rev. B*, **33**, 4034 (1986).

[3] A. Gruneis, R. Saito, Ge. G Samsonidge, T. Kihura, M. A Pimenta, A. Jorio, A. G Souza Filho, G. Dresselhaus and M. S Dresselhaus, *Phys. Rev. B*, **67**, 165402(2003).

Corresponding Author: Md. Tareque Chowdhury

TEL: +81-22-795-7754 FAX: +81-22-795-6447, E-mail: [chowdhury@flex.phys.tohoku.ac.jp](mailto:chowdhury@flex.phys.tohoku.ac.jp)

## Synthesis and Spectroscopical Characterization of Peripentacene

○Yosuke Ishii<sup>1</sup>, Tomohiro Sakashita<sup>1</sup>, Hidenori Kato<sup>2</sup>, Masashige Takatori<sup>2</sup>,  
and Shinji Kawasaki<sup>1</sup>

<sup>1</sup> *Department of Materials Science and Engineering, Nagoya Institute of Technology,  
Nagoya 466-8555, Japan*

<sup>2</sup> *Kuroganekasei Co. Ltd., Chiryu 472-0016, Japan*

Graphene has attracted a great deal of attention in recent years. It is known that high-purity and high-quality graphene, but in the limited size, can be obtained by mechanical exfoliation of graphite using a scotch tape. However, it is very difficult to obtain a large amount of graphenes enough for usual physical and chemical experiments. A chemical synthesis route by enlarging the number of benzene rings in polycyclic aromatic hydrocarbons (PAH) is one of the expected large scale synthesis methods.

To synthesize large-size PAH that will be treated as model graphene material, we tried to fuse pentacenes (1) at high temperatures under vacuum. By using this method, peripentacene (2) and trisperipentacene (3) can be synthesized through a dehydrogenation condensation reaction as shown in Fig. 1.

The obtained product was characterized by elemental analysis (C, H, and N), mass spectra, Raman spectra, Fourier transform infrared spectra (FT-IR), X-ray photoelectron spectra (XPS), and X-ray emission spectra (XES). In addition, we compared the observed electronic spectroscopic data and the partial electron density of states of peripentacene derived from the first principle calculations. The observed spectra were well reproduced by the calculations.

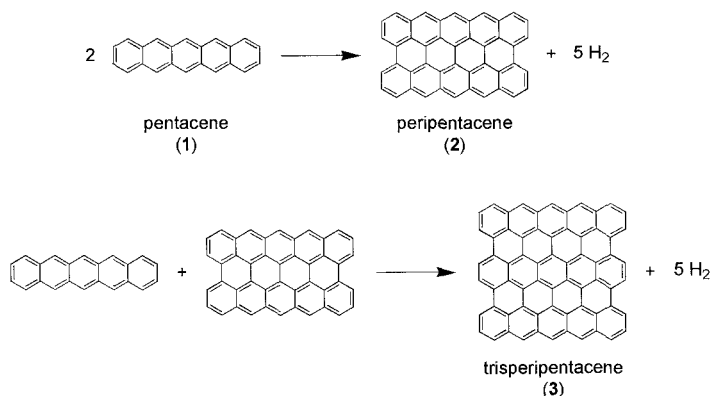


**Fig.1** Dehydrogenation condensation reaction of pentacene.

Corresponding Author: Shinji Kawasaki

TEL/FAX: +81-52-735-5221, E-mail: [kawasaki.shinji@nitech.ac.jp](mailto:kawasaki.shinji@nitech.ac.jp)

## Chemical and Electrical Characterization of Graphene Formed by Gallium Flux Liquid Phase Epitaxy

○Michael V. Lee<sup>1,2</sup>, Hidefumi Hiura<sup>1,3</sup>, Anastasia Tyurnina<sup>1</sup>, and Kazuhito Tsukagoshi<sup>1,2</sup>

<sup>1</sup> *International Center for Materials Nanoarchitectonics (MANA),  
National Institute for Materials Science (NIMS), 1-1 Namiki, Tsukuba 305-0044, Japan*

<sup>2</sup> *CREST, Japan Science and Technology Agency, Kawaguchi 332-0012, Japan*

<sup>3</sup> *Green Innovation Research Laboratories, NEC Corporation, 34 Miyukigaoka,  
Tsukuba 305-8501, Japan*

Gradually nanocarbon materials are gaining momentum as prime candidates for enabling a technology jump to overcome the limits that are looming for traditional semiconductor devices. Since 2004, the high mobility of graphene places it in position to replace natural bandgap semiconductors if a scalable method of production can be developed. Some methods have been demonstrated for producing graphene and testing devices, notably exfoliation of graphite, [1] thermal decomposition of silicon carbide, [2] [3] and CVD growth on metal substrates. [4] [5] Each of these methods faces challenges to producing wafer size graphene of nanoelectronics quality.

The main difficulties are preparing films on insulating substrates, and also producing uniform and defect-free films. Exfoliation fragments the graphene, causes defects, and aids oxidation. CVD is able to provide large-area graphene films, but it has only been successful on conductive substrates like nickel. Transfer to other substrates is possible, but such a process suffers from similar problems to those encountered during exfoliation of graphite. Decomposition of silicon carbide, especially on the silicon face, is able to produce single layer graphene films, however it requires high temperatures of >1200°C.

Recently we introduced a new scalable process for forming graphene layers directly on an insulating substrate at temperatures of only 1000°C. This new process combines characteristics of other processes.[2][6] Gallium acts as a flux for carbon and catalyzes the formation of graphene. Graphene forms only where gallium contacts the substrate. In this paper, we present chemical and electrical characterization of uniform graphene films produced by this method.

- [1] K. S. Novoselov, A. K. Geim, S. V. Morozov, D. Jiang, Y. Zhang, S. V. Dubonos, I. V. Grigorieva, and A. A. Firsov, *Science* **306**, 666-669 (2004).
- [2] A. Van Bommel, J. Crombeen, and A. Van Tooren, *Surface Science* **48**, 463-472 (1975).
- [3] C. Berger, Z. Song, X. Li, X. Wu, N. Brown, C. Naud, D. Mayou, T. Li, J. Hass, A. N. Marchenkov, E. H. Conrad, P. N. First, and W. A. de Heer, *Science* **312**, 1191-1196 (2006).
- [4] Q. Yu, J. Lian, S. Siriponglert, H. Li, Y. P. Chen, and S. Pei, *Appl. Phys. Lett.* **93**, 113103-113103-3 (2008).
- [5] X. Li, W. Cai, J. An, S. Kim, J. Nah, D. Yang, R. Piner, A. Velamakanni, I. Jung, E. Tutuc, S. K. Banerjee, L. Colombo, and R. S. Ruoff, *Science* **324**, 1312-1314 (2009).
- [6] J. Fujita, R. Ueki, Y. Miyazawa, and T. Ichihashi, *J. Vac. Sci. Technol. B* **27**, 3063 (2009).

Corresponding Author: Michael V. Lee

TEL: +81-29-851-3354 ext. 8902, FAX: +81-29-850-6139, E-mail: LEE.Michael@nims.go.jp

## Synthesis of Single-Layer Graphenes by Atmospheric Alcohol-Chemical Vapor Deposition

○Akiji Fukaya<sup>1</sup>, Naoki Kishi<sup>1\*</sup>, Ryo Sugita<sup>1</sup>, Tetsuo Soga<sup>1</sup>, Takashi Jimbo<sup>2</sup>

<sup>1</sup>*Department of Frontier Materials, Nagoya Institute of Technology,  
Nagoya 466-8555, Japan*

<sup>2</sup>*Research Center for Nano-Device and System, Nagoya Institute of Technology,  
Nagoya 466-8555, Japan*

Graphenes have attracted a great interest in recent years because of their novel electronic properties. Chemical vapor deposition (CVD) is expected as a simple and low-cost synthesis method of graphenes for industrial production. However, vacuum and explosive gases such as methane and hydrogen are generally required to synthesize single-layer graphenes in the CVD methods reported previously. Recently, Miyata et al. reported that CVD with flash cooling process can produce single-layer graphenes without using vacuum and explosive gases[1]. However, further study is required for development of simple CVD techniques toward large scale production of single-layer graphenes.

Here, we report a simple synthesis method of high quality single-layer graphenes from alcohol without using rapid cooling process. The graphenes were synthesized on Cu foils by thermal CVD under nitrogen atmosphere at ambient pressure.

Fig.1 shows a Raman spectra of graphenes synthesized on Cu. 2D band with a narrow full width of half maximum of  $35\text{ cm}^{-1}$  is observed as shown in fig. 1. The details will be discussed in our presentation.

[1]Y.Miyata et al., Appl. Phys. Lett., 96 263105 (2010)

**Corresponding Author: Naoki Kishi**

**TEL/FAX: +81-52-735-5147**

**E-mail: kishi.naoki@nitech.ac.jp**

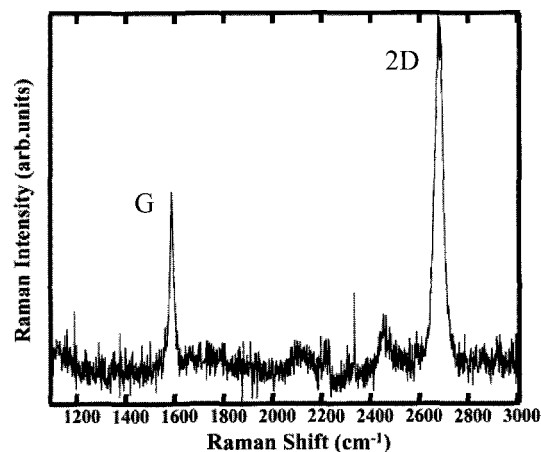


Fig.1 Typical Raman spectra of graphenes synthesized on Cu.

## Quantum capacitance of mono- bi- and tri-layer graphene with different stacking orders

○Takahiro Eguchi, Kentaro Sato and Riichiro Saito

*Department of Physics, Tohoku University, Sendai, 980-8578, Japan*

Graphene has been investigated as a semiconductor device due to its stability and high mobility at the room temperature [1]. It is expected that the graphene field effect transistor (GFET) will be a THz device. In order to get an energy gap of GFET, bi- or tri- layer graphene are widely investigated. However, it is known that the stacking order of graphene is not always AB Bernal stacking. Further, such devices generates heat by storing and emitting the electrostatic energy in a each switching process. Here we discuss the properties of the quantum capacitance (QC) of GFET for understanding electrostatic energy. In GFET, the capacitance is expressed by a serial connection of conventional geometrical capacitance and QC, as a function of gate voltage. QC is important because the electron effective mass of graphene is small and the effect of QC to the total capacitance is significant around K point of graphene [2].

In this paper we show that the calculated QC of mono-, bi-, and tri-layer graphene with different stacking orders within the tight binding method [3]. We discuss the dependence of the QC on the gate voltage and density of carrier of different stacking for graphene. The calculated results are compared with the experiment [4].

### References:

- [1] K. S. Novoselov *et al.*, *Science*. 306, 666 (2004).
- [2] J. S. Park *et al.*, *Carbon* 47, 1303 (2010).
- [3] P. Gava *et al.*, *Phys. Rev. B* 79, 165431 (2009); D. L. John *et al.*, *J. Appl. Phys.* 96, 5180 (2009); A. Gruneis *et al.*, *Phys. Rev. B* 78, 205425 (2008).
- [4] J. T. Ye *et al.*, arXiv:1010.4679v1 (2010); J. Xia *et al.*, *Nature. Nanotech.* 4, 505-509 (2009); Z. Chen *et al.*, *Electron Devices Meeting, 2008. IEEE International* (2008).

Corresponding Author: Takahiro Eguchi

E-mail: eguchi@flex.phys.tohoku.ac.jp

Tel: +81-22-795-6442, Fax: +81-22-795-6447



## Structural Changes of Carbon Nanowalls by Heat Treatment in Vacuum

○Seiya Suzuki and Masamichi Yoshimura

*Graduate School of Engineering, Toyota Technological Institute  
2-12-1 Hisakata, Tempaku, Nagoya 468-8511, Japan*

Carbon nanowall (CNW) is a two-dimensional carbon structure that stands perpendicular to the substrate like a wall. Since CNWs intrinsically consist of graphene sheets, they are expected to have high mobility. However, it has been revealed that amorphous carbon (a-C) layer exists in the surface of CNWs and/or at the interface between CNWs and substrates [1]. The removal of a-C is necessary for practical use of CNWs. In this study, we studied how the a-C was removed by heat treatment in vacuum.

Three specimens of CNWs were prepared by microwave plasma-enhanced chemical vapor deposition with different  $H_2/CH_4$  flow rate ratios of 0/20, 20/20 and 40/20 sccm on  $SiO_2$  (500 nm)/Si substrate [2]. The heat treatment was conducted by using an electrical furnace setup. Structural changes of CNWs were observed by scanning electron microscope (SEM) and Raman spectroscopy.

Fig. 1 shows SEM images of CNWs prepared with  $H_2/CH_4$  of 0/20 after (a) growth and heat treatment at (b) 1100 °C. It was observed that the size of cone-like structures (shown by arrows) on CNWs was decreased through heat treatment at 1100 °C. In addition, the vertically aligned structure of CNWs was remained upon heat treatment even at 1200 °C in vacuum, although CNWs fell down on substrate through heat treatment at 640 °C in air [3]. This is because reaction rate of a-C with oxygen was suppressed by reduced oxygen in vacuum. Fig. 2 shows  $I_G/I_D$  dependence of CNWs on heat treatment temperature in vacuum. The  $I_G/I_D$  peak intensity ratios were obtained by peak fitting of each Raman spectrum. Increase in  $I_G/I_D$ , indicating the removal of amorphous carbon, was observed. On the other hand, full width at half maximum of D peak increased from  $\sim 40$  to  $\sim 50$   $cm^{-1}$  after heat treatment at 1000 °C. This may be because defect was induced in the graphitic network of CNWs by heat treatment at high temperature.

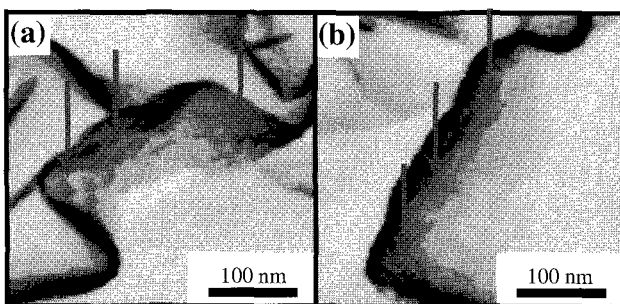


Fig. 1. SEM images of CNWs after (a) growth and (b) heat treatment at 1100 °C.

**References:**

- [1] S. Kondo, et al., *J. Appl. Phys.* **106**, 094302 (2009).  
 [2] S. Suzuki et al., *Jpn. J. Appl. Phys.* in press (2011).  
 [3] S. Suzuki et al., *The 39th Fullerene-Nanotubes General Symposium* (2010) 3P-28.

**Corresponding Author:** Masamichi Yoshimura

**E-mail:** [yoshi@toyota-ti.ac.jp](mailto:yoshi@toyota-ti.ac.jp), **Tel&Fax:** +81-52-809-1851

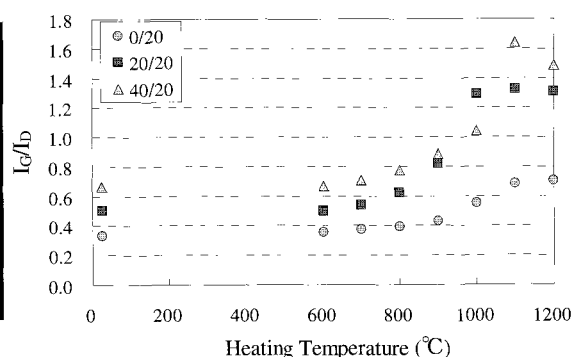


Fig. 2.  $I_G/I_D$  of CNWs prepared with  $H_2/CH_4$  flow rate ratio of 0/20, 20/20 and 40/20 as a function of heat treatment temperature.

## Electronic-structure control of thin film of graphite: Interlayer spacing and thickness dependency

○Nguyen Thanh Cuong<sup>1,3</sup>, Minoru Otani<sup>1,3</sup>, Susumu Okada<sup>2,3</sup>

<sup>1</sup>*Nanosystem Research Institute, National Institute of Advanced Industrial Science and Technology (AIST), Tsukuba 305-8568, Japan*

<sup>2</sup>*Graduate school of Pure and Applied Sciences, University of Tsukuba, Tsukuba 305-8571, Japan*

<sup>3</sup>*Japan Science and Technology Agency, CREST, 5 Sanbancho, Chiyoda-ku, Tokyo 102-0075, Japan*

Magnetic properties of carbon materials are received much attention because of their potential for application in electronic devices. Recently, a rhombohedral (ABC-stacking) graphite thin film exhibits ferrimagnetic spin ordering on its (0001) surface. Calculated a mount of magnetic moment is found to be  $0.036 \mu_B/\text{nm}^2$  [1]. The polarized electron spins on the top-most and bottom-most layers are coupled in antiparallel so that the net spin on the film vanished. Furthermore, by applying an electric field normal to the film, we demonstrated that surface magnetic state undergoes magnetic phase transition from ferromagnetic to ferromagnetic states [2]. These facts indicate that the magnetic properties of graphite thin films sensitively depend on the external conditions.

In this work, based on first-principles total-energy calculations, we systematically explore how the electronic and magnetic properties of graphite thin film depend on the interlayer spacing and number of layers. Our calculations show that there is a threshold interlayer spacing on the spin coupling between top-most and bottom-most layers. Under the interlayer spacing less that 0.3 nm (10% compress), the polarized spins on both surfaces are coupled in parallel instead of antiparallel in its equidistance. On the other hand, for the number of graphene layers less than seven, we cannot observe the spin polarization on both surfaces.

[1] M. Otani, M. Koshino, Y. Takagi, and S. Okada, *Phys. Rev. B* 81, 161403(R) (2010).

[2] M. Otani, Y. Takagi, M. Koshino, and S. Okada, *Appl. Phys. Lett.* 96, 242504 (2010).

Corresponding Author: Nguyen Thanh Cuong

E-mail: cuong-nguyen@aist.go.jp

Tel: +81-29-861-5349, Fax:+81-29-861-3171

QM/MD Simulation of Graphene Hole Repair by C<sub>2</sub> molecules

○Yoshitaka Okita, Hironori Hara, Lili Liu and Stephan Irle

*Institute for Advanced Research and Department of Chemistry, Nagoya University, Nagoya*

*464-8602, Japan*

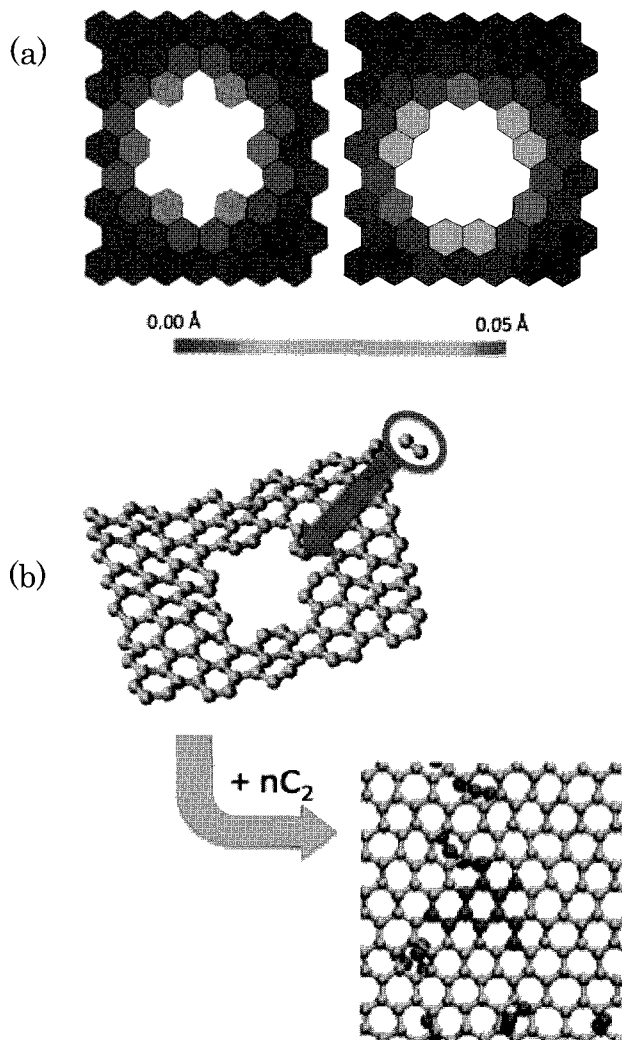


**Figure 1.** (a) Ring Bond Dispersion (RBD) plots of armchair (left side) and zigzag (right side) hole. RBD is defined according to ref. [1]. Smaller RBD value indicates that the bond lengths in the hexagon have more uniform bond lengths (as in bulk). Edge hexagons are more distorted. (b) Armchair hole in graphene was gradually healed and repaired perfectly. Carbon atoms of vapor C<sub>2</sub> molecules are shown by red atoms. in bottom figure.

Hole repair in graphene due to exposure to C<sub>2</sub> molecules was investigated by using high-T QM/MD (quantum chemical molecular dynamics) simulations. We designed two holes with dominant armchair and zigzag edges, and performed ten trajectories respectively. Because hexagons at the edge of the holes were more distorted and reactive than hexagons in the bulk (see Figure 1 (a)), they were less stable and C-C bonds located on the edge of holes were easy to break. Some floating C<sub>2</sub> molecules, which approached carbon atoms on the edge, could combine with them, while others interacted with carbons far from rim part and left after some time. Due to the C<sub>2</sub> molecules sticking at the hole edges, the holes gradually became smaller. Finally, pentagon- and heptagon-containing networks appeared in the holes, and in some trajectories, these defects were healed perfectly. In these situations, all carbons were bonded in a hexagonal lattice (see Figure 1 (b)), but in other trajectories, 5, 7 or 8-membered rings persisted during the simulation time. The simulations did not differ much between armchair and zigzag holes.

#### References

- [1] F. J. Martín-Martínez et al, *Org. Lett.* 10 (2008) 1991

**Corresponding Author:** Stephan Irle

**TEL:** +81-52-747-6397, **FAX:** +81-52-788-6151,

**E-mail:** [sirle@iar.nagoya-u.a.jp](mailto:sirle@iar.nagoya-u.a.jp)

## Field Emitter Using Upright Carbon Nanotwists with sputtered Pt coat

○Yuki Sugioka<sup>1</sup>, Yoshiyuki Suda<sup>1</sup>, Hideto Tanoue<sup>1</sup>, Hirofumi Takikawa<sup>1</sup>,  
Hitoshi Ue<sup>2</sup>, Kazuki Shimizu<sup>3</sup>, Yoshito Umeda<sup>4</sup>

<sup>1</sup> *Department of Electrical and Electronic Information Engineering,  
Toyohashi University of Technology*

<sup>2</sup> *Fuji Research Laboratory, Tokai Carbon Co., Ltd.*

<sup>3</sup> *Development Department, Shonan Plastic Mfg. Co., Ltd.*

<sup>4</sup> *Fundamental Research Department, Toho Gas Co., Ltd.*

In our previous study, carbon nanotwists (CNTw) on substrate were made to stand up by filament discharge (FD) treatment [1]. CNTw is one of fibrilliform carbon nanomaterials with a helical shape and has been shown as a good field emission material. The diameter of CNTw is larger than that of carbon nanotube (CNT). Therefore, CNTw is supposed to have less damage than CNT does by ion bombardment. In this study, CNTw emitter was coated with Pt by ion sputtering. Fabrication method of the CNTw emitter was the same as in Ref. 2. The thickness of Pt-coated film was 10 nm. Figure 1 shows SEM micrograph of Pt-coated CNTw emitter. Its upright condition was almost the same as non-coated emitter. Figure 2 shows  $J$ - $E$  characteristics of the non- and Pt-coated CNTw emitters. Turn-on field of Pt-coated was a little higher than that of non-coated. Current density at 9 V/ $\mu$ m of Pt-coated was as low as one-third of that for non-coated. In the analysis of Fowler-Nordheim (F-N) plot of  $\ln(I/V^2)$  against  $(I/V)$ , the slope of non-coated CNTw emitter was -10708.6 and that of Pt-coated was -3162.9, respectively, as shown in the inset of Fig. 2. The slope is thought to depend on the work function of CNTw emitter. The F-N plot shows that the work function was decreased by Pt-coating.

This work has been partly supported by the Outstanding Research Project of the Venture Business Laboratory from Toyohashi University of Technology (TUT); Global COE Program "Frontiers of Intelligent Sensing" from the Ministry of Education, Culture, Sports, Science and Technology (MEXT); Core University Programs (JSPS-CAS program in the field of "Plasma and Nuclear Fusion") from the Japan Society for the Promotion of Science (JSPS), Grant-in-Aid for Scientific Research from the MEXT, Toukai Foundation for Technology, Research Foundation for Materials Science, and Chubu Science and Technology Center.

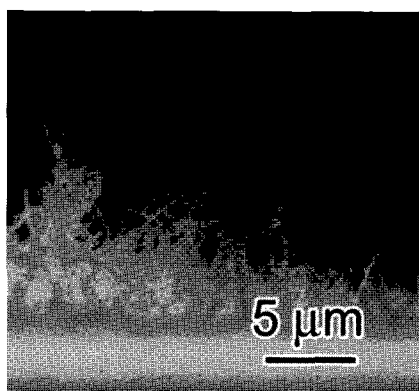


Fig. 1 SEM micrograph of Pt-coated CNTw emitter.

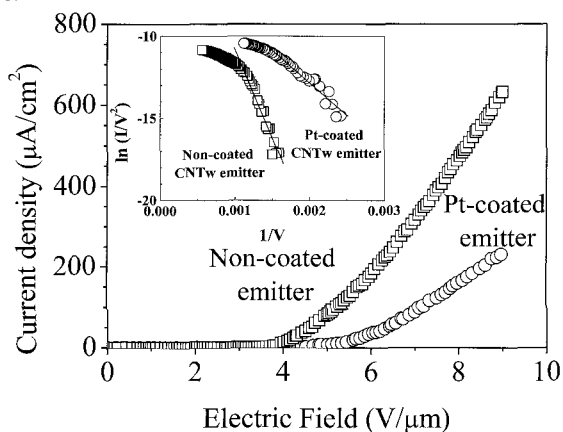


Fig. 2  $J$ - $E$  characteristics of CNTw emitters.

[1] Y. Hosokawa, et al: J. Phys. D: Appl. Phys., **41** 205418 (2008)

[2] Y. Sugioka, et al: Proceedings of 2nd International Symposium on Advanced Plasma Science and its Applications for Nitrides and Nanomaterials, PA075C, 2010

Corresponding Author: Yoshiyuki Suda

TEL: +81-532-44-6726, E-mail: suda@ee.tut.ac.jp

## Evaluation of Dispersant Effectiveness of Lipid-PEG For Nano-Carbons Using Carbon Nanohorns

Mei Yang<sup>1,2</sup>, Momoyo Wada<sup>2</sup>, Minfang Zhang<sup>2</sup>, Kostas Kostarelos<sup>3</sup>, Sumio Iijima<sup>1,2</sup>, Mitsutoshi Masuda<sup>2\*</sup>, Masako Yudasaka<sup>2\*</sup>

<sup>1</sup>*Department of Material Science and Engineering, Meijo University, 1-501 Shiogamaguchi, Tenpaku, Nagoya 468-8502, Japan*

<sup>2</sup>*Nanotube Research Center, National Institute of Advanced Industrial Science and Technology, 5-2, 1-1-1 Higashi, Tsukuba, 305-8565, Japan*

<sup>3</sup>*Nanomedicine laboratory, Center for Drug Delivery Research, The School of Pharmacy, University of London. 29-39, Brunswick Square, London WC1N 1AX, United Kingdom.*

Nanometer-sized graphene materials (NGMs) have presented versatile applications in various areas including nanobiology and medicine. Amphiphilic lipid-poly(ethylene glycol) (LPEG) materials are widely used as noncovalent functionalization agents for dispersing NGMs in aqueous solutions for biological studies. However, not much is known about the interaction between LPEG and NGMs, and how to select the optimum LPEGs is the critical issue. Taking advantage of the large available quantity of single-walled carbon nanohorns (SWNHs), a type of NGMs, we evaluated dispersant effectiveness of various LPEGs for NGMs by using SWNHs.

We compared the dispersion abilities of eight LPEGs: Two types (Ceramide-PEG and DSPE-PEG), which are frequently used for NGMs, were purchased, and the other six types were newly synthesized in this study. Each LPEG was composed of three domains: alkyl chains, PEG chains, and a liker group. LPEGs having the following structure achieve well dispersed SWNHs in water and PBS. The long alkyl and PEG chains were, indeed, favorable. The non-ionic linker group was more favorable than the ionic ones as we reported previously [1]. Interestingly, the single alkyl chains were as effective as double alkyl chains in terms of adsorption onto the SWNH surface. The surface coverage of excellent LPEG dispersants on SWNHs was high, and they were almost non-detached even when proteins were co-dispersed in PBS. Here, the quantities of attached or detached PEGs were determined by subtracting the PEG quantities in the filtrate from the starting PEG quantities. The PEG quantity in the filtrate was quantified by the Dragendorff method. Macrophage cellular uptakes of SWNHs coated with these excellent LPEG dispersants was extremely low, which is an advantage for drug delivery applications of SWNHs in order to avoid rapid capture by macrophages and to be excreted *in vivo*.

Acknowledgements: M.Y. and S.I. acknowledge Balzan Foundation for the financial support.

[1] J. Xu, S. Iijima, M. Yudasaka, *Appl. Phys. A* **99**, 15-21 (2010).

Corresponding Author: M. Masuda, M. Yudasaka

E-mail: m-masuda@aist.go.jp TEL 029-861-4545, m-yudasaka@aist.go.jp, Tel 029-861-4814

## Long-term Structural Observation of Charged Particles by Ion Trap Mobility System

○Yoshihiko Sawanishi, Masashi Shinozaki, and Toshiki Sugai

*Department of Chemistry, Toho University, Miyama 2-2-1 Funabashi, 274-8510, Japan*

Ion mobility measurements have been utilized to analyze structures of nanocarbon materials[1]. This measurements provide lots of advantages to clarify the new structures but have not been applied to observe "long-term changes". Here we present the observation of structural changes of charged particles for two hours by a new ion trap mobility system.

The charged particles were produced from NaCl water solution with concentration from 5 to 27 wt. % (saturated solution) by an atomizer where 10 kV was applied. The particles were trapped by an RF electric field (600 Vpp, 20 kHz) and were analyzed by mobility measurements with up-down movements induced by LF field (9 Vpp, 2.5 Hz). The trapped particles were irradiated by a laser and were monitored by a digital camera.

Figure 1 shows traces of the charged particles produced from 27 % NaCl (saturated) solution moving in the trap. The amplitude gradually increased as the time elapsed from 0 to 12 min., and then decreased. The data show that the particle has the most compact structure at 12 min. since the amplitude is inversely proportional to the diameter. Figure 2 shows the dependence of the time profiles on the concentration, where each amplitude is normalized by the initial one. The overall trend in the lower concentration (5~15 %) is that the amplitudes decrease with time showing the size growth of particles by humidity absorption from air[2]. In the higher concentration conditions (20 and 27 %), on the other hand, the amplitudes increase in the early stage (0 to around 10 min.). The dependence on the concentration could be explained by crystallization of NaCl on the surface of the particle and melting. This long-term monitoring could be applied to the structural changes of nanomaterials.

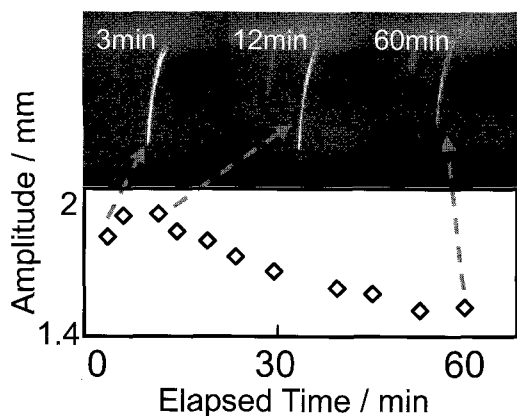


Fig.1 Traces of charged particles

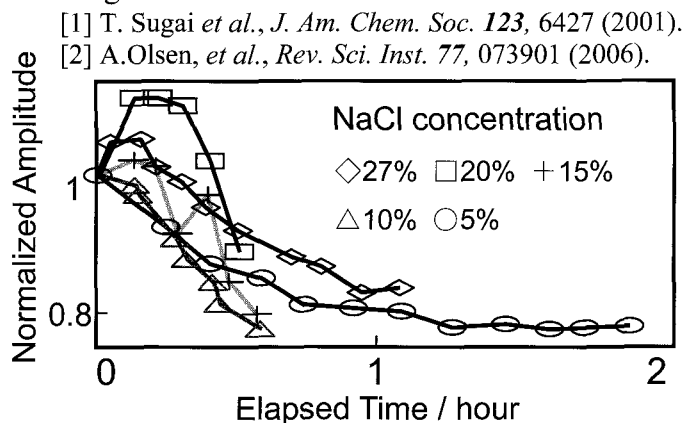


Fig.2 Concentration dependence of amplitudes

TEL: +81-47-472-4406, FAX: +81-47-472-4406, E-mail: sugai@chem.sci.toho-u.ac.jp

## Preparation of supercapacitor using RuO<sub>x</sub>-supported-Arc-Black and its specific capacitance

○Toshiyuki Sato<sup>1</sup>, Takashi Ikeda<sup>1</sup>, Yoshiyuki Suda<sup>1</sup>, Hideto Tanoue<sup>1</sup>,  
Hirofumi Takikawa<sup>1</sup>, Shinichiro Oke<sup>2</sup>, Hitoshi Hue<sup>3</sup>,  
Takashi Okawa<sup>4</sup>, Nobuyoshi Aoyagi<sup>4</sup>, Kazuki Shimizu<sup>5</sup>

<sup>1</sup> *Department of Electrical and Electronic Information Engineering,  
Toyohashi University of Technology*

<sup>2</sup> *Tsuyama National College of Technology*

<sup>3</sup> *Tokai Carbon Co., Ltd.*

<sup>4</sup> *Daiken Chemical Co., Ltd.*

<sup>5</sup> *Shonan Plastic Mfg. Co., Ltd.*

We have studied the preparation of supercapacitor using ruthenium oxide (RuO<sub>x</sub>) supported on Arc-Black (AcB) that is made by an arc discharge in N<sub>2</sub> gas [1]. In this presentation, we report the correlation between the RuO<sub>x</sub> amount on AcB and its specific capacitance.

RuO<sub>x</sub> were synthesized by dropping a NH<sub>4</sub>HCO<sub>3</sub> aqueous solution into RuCl<sub>3</sub> aqueous solution and were supported on AcB with ultrasonication. After filtration and drying, RuO<sub>x</sub>-supported-AcB (RuO<sub>x</sub>/AcB) electrodes were prepared. The amounts of RuO<sub>x</sub> were in the range of 20-47 wt.% by the measurement of Thermo Gravimetry Analyzer (TGA).

Fig. 1 shows cyclic voltammograms of the RuO<sub>x</sub>/AcB supercapacitor electrodes. The specific capacitance increased with the RuO<sub>x</sub> amount up to 41 wt.%. The maximum specific capacitance was obtained to be 224 F/g at the RuO<sub>x</sub> amount of 41 wt.%. However, the electrode at the RuO<sub>x</sub> amount of 47 wt.% showed a poor capacitance of 157 F/g.

This work has been partly supported by the Outstanding Research Project of the Venture Business Laboratory from Toyohashi University of Technology (TUT); Global COE Program "Frontiers of Intelligent Sensing" from the Ministry of Education, Culture, Sports, Science and Technology (MEXT); Core University Programs (JSPS-CAS program in the field of "Plasma and Nuclear Fusion") from the Japan Society for the Promotion of Science (JSPS), Grant-in-Aid for Scientific Research from the MEXT, Toukai Foundation for Technology, Research Foundation for Materials Science, and Chubu Science and Technology Center.

[1] H. Uruno, et al: IEEJ Transactions on Fundamentals and Materials, 130-A (3), 293-294 (2010)

Corresponding Author: Yoshiyuki Suda

Tel: +81-532-44-6726, E-mail: suda@ee.tut.ac.jp

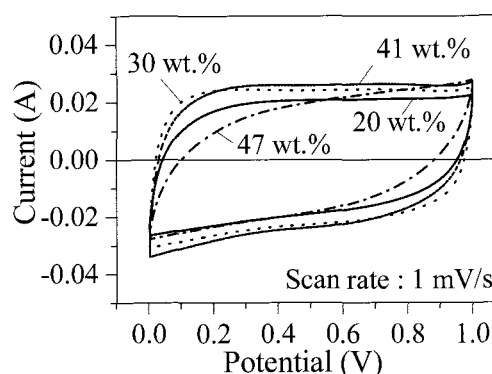


Fig.1. Cyclic voltammograms of RuO<sub>x</sub>/AcB electrodes at different RuO<sub>x</sub> amounts.

## Electron-accepting properties of fullerenes at the liquid/liquid interface

○Tsugumi Hayashi<sup>1</sup>, Tomohiko Okugaki<sup>2</sup>, Hideyuki Takahashi<sup>1</sup>,  
Kohji Maeda<sup>3</sup> and Kazuyuki Tohji<sup>1</sup>

<sup>1</sup>Graduate School of Environmental Studies, Tohoku University, Sendai 980-8579, Japan

<sup>2</sup>Graduate School of Engineering, Kyoto University, Kyoto 615-8530, Japan

<sup>3</sup>Department of Chemistry, Kyoto Institute of Technology, Kyoto 606-8585, Japan

Electrochemical studies of fullerenes have much attention because of its specific behavior. There are several reports concerning on the calculation of molecular orbital and also the electrochemical detection of C<sub>60</sub> and C<sub>70</sub> by cyclic voltammetry method (CV). These researches demonstrated that C<sub>60</sub> could be able to accept at least six electrons to form C<sub>60</sub><sup>6-</sup>. Additionally, we reported that poly sulfide ion in aqueous solution was successfully collected by stirring treatment with fullerene/toluene solution. In this reaction, it was considered that C<sub>60</sub> acted as electron acceptor at the liquid/liquid interface [1]. In this study, the electron-accepting properties of fullerene at the interface were analyzed by Voltammetry for the Charge Transfer at the Interface of Two Immiscible Electrolyte Solution (VCTIES). This technique is powerful method to understanding the dynamic feature of the charge transfer, since it can measure simultaneously transfer potential and also the amount of transferred charges [2, 3].

At first, CV with K<sub>2</sub>S and C<sub>60</sub> were analyzed to calculate potential of electron transfer at water/o-dichlorobenzene (DCB) interface. After that, ion transfer was analyzed by VCTIES method. From CV analysis, it was showed that standard redox potential of S<sup>2-</sup> ion was -0.45V vs. SSE and 1<sup>st</sup> redox potential of C<sub>60</sub> was -1.01V vs. TPenAE. From these results, it can be considered that standard potential of electron transfer of S<sup>2-</sup> ion and C<sub>60</sub> was -0.86V vs. TPhE [4]. On the other hand, clearly peak shifts mean ion transfer were not observed in VCTIES. Then, it can be considered that electron transfer is more predominant than ion transfer in this reaction.

### References:

- [1] T. Hayashi, H. Takahashi and K. Tohji, *Fullerenes, Nanotubes and Carbon Nanostructures*, in press (2011)
- [2] K. Maeda, *Bunseki*, 7, 382 (2002) (Japanese)
- [3] T. Osakai and H. Katano, *BUNSEKI KAGAKU*, 54, 4, 251-266 (2005) (Japanese)
- [4] S. Kihara and M. Matsui, *Hyomen*, 30, 367 (1992) (Japanese)

**Corresponding Author: Tsugumi Hayashi**

**E-mail: [tsugumi@bucky1.kankyo.tohoku.ac.jp](mailto:tsugumi@bucky1.kankyo.tohoku.ac.jp), Tel&Fax: +81-22-795-7412**



## Facile and efficient synthesis of high-crystallinity double-wall carbon nanotubes

○Toshiya Nakamura, Yasumitsu Miyata, Hong En Lim, Ryo Kitaura, Hisanori Shinohara

*Department of Chemistry, Nagoya University & Institute for Advanced Study,  
Nagoya 464-8602, Japan*

Carbon nanotubes (CNTs) have attracted great interest in many industrial applications including electronics because of their unique and novel electronic properties. Realizing their full potential in actual electronic device applications requires the CNT samples with high crystallization and desired conducting properties. For this purpose, double-wall CNTs (DWCNTs) are attractive since they have metallic or semiconducting properties like single-wall CNTs as well as robust mechanical and chemical stability like multi-wall CNTs. Although there are many reports on the DWCNT synthesis<sup>1-3)</sup>, high-yield synthesis of high-quality DWCNTs is still an unsolved challenge for actual industrial applications.

In this study, we have investigated effects of catalysts and reaction conditions on the DWCNT synthesis by using alcohol chemical vapor deposition (CVD) with Fe/MgO catalysts. Ethanol was used as carbon source because of its safety and user-friendliness. In an improved condition, DWCNTs with a purity of 60% were synthesized as evaluated

by transmission electron microscope (TEM) observations (Fig. 1a). For a purified sample, average outer and inner diameters were 1.4 and 0.7 nm, respectively (Fig. 1b), which is consistent with the optical absorption spectrum (Fig. 1c). Raman spectra of purified sample show high G/D ratio of around 130, suggesting the successful synthesis of high quality DWCNTs (Fig. 1d).

1) T. Hiraoka *et al. Chem.Phys.Lett.* **382**, 679 (2003).

2) T. Sugai *et al. Nano Letters*, **3**, 769 (2003).

3) P. Ramesh *et al. J.Phys.Chem.B*, **109**, 1141 (2005).

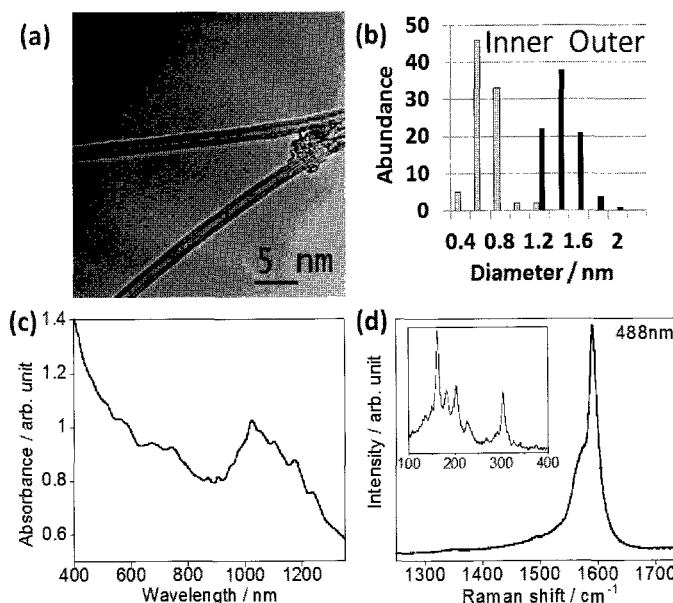


**Fig. 1.** (a) TEM image, (b) diameter distribution, (c) optical absorption and (d) Raman spectra of the purified sample.

Corresponding Author: Hisanori Shinohara

TEL: +81-52-789-2482, FAX: +81-52-747-6442, E-mail: [noris@nagoya-u.ac.jp](mailto:noris@nagoya-u.ac.jp)

## Sorting of double-wall carbon nanotubes by electronic structure

○Miho Fujihara, Yasumitsu Miyata, Marie Suzuki, Ryo Kitaura, and Hisanori Shinohara

*Department of Chemistry & Institute for Advanced Research, Nagoya University,  
Nagoya 464-8602, Japan*

Double-wall carbon nanotubes (DWCNTs) have attracted much attention for thin film electronics because of their superior conducting properties, high thermal and chemical stabilities. To put them into practical use, it is necessary to separate DWCNTs with single electronic type. Although there has been a report on the sorting of DWCNTs by electronic structure so far [2], it is still unclear whether or not the separation has been mainly conducted for impurity single-wall carbon nanotubes (SWCNT) or DWCNTs. The presence of impurity SWCNTs is a critical issue because the dispersion process with ultrasonication induces the inner/outer shell separation that generates SWCNTs with wide-range diameters [3]. To solve this problem, the careful characterization of DWCNT purity and the precise separation by layer number are required.

In this study, we demonstrate the sorting of highly-pure DWCNTs by electronic type using multistep density-gradient ultracentrifugation (DGU). The DWCNT-rich samples supplied from Toray Industries Inc. were used as a starting material. This material was dispersed with sonication in water containing sodium deoxycholate (DOC). Firstly, isolated DWCNTs were enriched by using non-linear DGU as reported by Ghosh et al.[4] (Fig.1a). The isolated DWCNTs were then separated again by using DGU with mixed surfactants of sodium cholate (SC) and sodium dodecyl sulfate (SDS) as shown in Fig.1b.

High-resolution transmission electron microscope observations reveal that the fractions indicated by arrows in Fig.1a and b contain DWCNTs with a purity of more than 80%. Optical absorption spectra show that the  $M_{11}$  absorption intensity of metallic outer shells (600~800 nm) decreases after the second DGU process (Fig.1c). This result indicates that DWCNTs can be sorted by electronic type of the outer shells. In the presentation, the optical properties of separated DWCNTs will also be discussed.

[1] K. Liu et al., *J. Am. Chem. Soc.*, 131, 62 (2008).

[2] J. Y. Huh et al., *J. Phys. Chem. C*, 114, 11343 (2010).

[3] Y. Miyata et al., *ACS Nano*, 4, 5807, (2010).

[4] S. Ghosh et al., *Nat. Nanotechnol.*, 5, 443 (2010).

Corresponding Author:

Hisanori Shinohara

TEL:+81-52-789-2482,

FAX:+81-52-789-1169,

E-mail: [noris@cc.nagoya-u.a.jp](mailto:noris@cc.nagoya-u.a.jp)

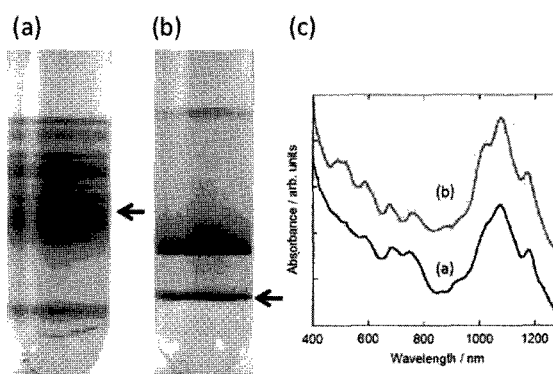


Fig.1 Photographs of centrifugal tubes after (a) the first and (b) the second DGU processes. (c) Optical absorption spectra of the fractions indicated by the arrows.

## Electronic Spectra of Polyynes-Iodine Complexes in Hexane

○Yoriko Wada and Tomonari Wakabayashi

*Department of Chemistry, Kinki University, Higashi-Osaka 577-8502, Japan*

Polyynes,  $\text{H}(\text{C}\equiv\text{C})_n\text{H}$  ( $n \geq 2$ ), are sp-hybridized carbon chain molecules with two hydrogen atoms at both ends. These molecules have cylindrically symmetric  $\pi$ -electron systems. These molecules exhibit absorption bands for the allowed transition in the UV and those for a forbidden transition in the near UV. The former is attributable to the electric-dipole-allowed transition from the ground state,  $^1\Sigma_g^+$ , to the excited state,  $^1\Sigma_u^+$ , while the latter is attributable to the symmetry-forbidden transition from the ground state,  $^1\Sigma_g^+$ , to the excited state,  $^1\Delta_u$  [1]. We have reported that the allowed transition disappears and the forbidden transition increases in intensity upon addition of iodine molecules into the solution of polyyne molecules [2].

Figure 1 shows electronic spectra for polyyne-iodine complexes (solid line) and those for polyynes (dotted line) in hexane. The forbidden transitions intensified in the spectra for polyyne-iodine complexes shifts to longer wavelength as the carbon chain become longer. This observation suggests that the product formed from polyyne and iodine molecules retains the polyynic skeleton as intact. Figure 2 shows the intensity ratio of the band of the forbidden transition to a new band in the spectra of polyyne-iodine complexes. The figure shows that the ratio decreases as the number of carbon atoms increases.

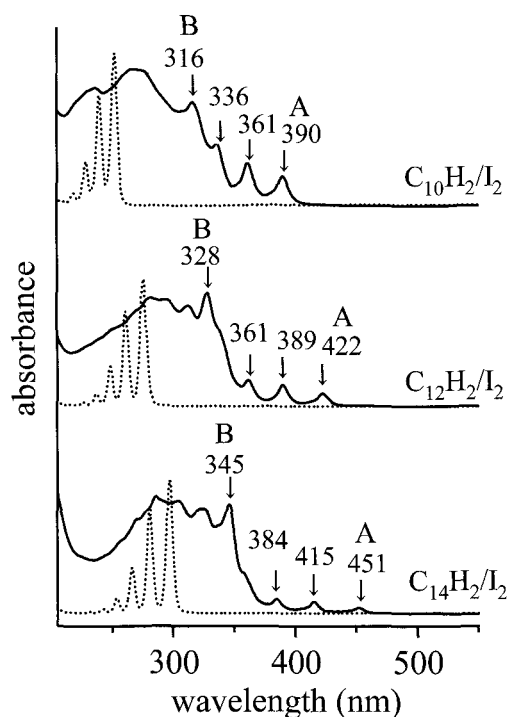


**Figure 1.** Electronic spectra of the polyyne-iodine complexes (solid line) and polyynes (dotted line).

transition to a new band in the spectra of polyyne-iodine complexes. The figure shows that the ratio decreases as the number of carbon atoms increases.

**Reference** [1] T. Wakabayashi et. al., *Chemical Physics Letters*, 446 (2007) 65.

[2] Y. Wada et. al., *Annual Meeting of Japan Society for Molecular Science*, 2008.

**Corresponding Author:** Tomonari Wakabayashi,  
E-mail: wakaba@chem.kindai.ac.jp  
Tel: 06-6730-5880 (ex4101), Fax: 06-6723-2721

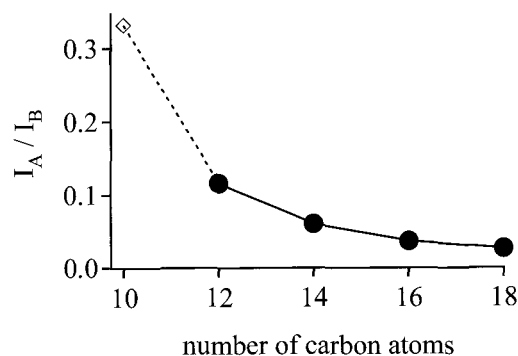


**Figure 2.** The intensity ratio of an intensified forbidden transition/new band.

## Significance of zigzag edges in electron transport properties of graphene sheets with periodic nanoholes

○Hideyuki Jippo, Mari Ohfuchi, and Chioko Kaneta

*Fujitsu Laboratories Ltd., 10-1 Morinosato-wakamiya, Atsugi, Kanagawa 243-0197, Japan*

For electronic applications of graphene, it is necessary to control its band gap because graphene itself is a semi-metal. A graphene nanomesh (GNM), which can be considered to be a highly interconnected network of graphene nanoribbons (GNRs), has recently been fabricated and shown to have a band gap [1, 2]. We have reported [3] the electronic structures of graphene having 2-dimensional (2D) periodic nanoholes with high-symmetry atomic configurations. In this article, we expand our research into 1-dimensional (1D) periodic nanoholes and irregularly shaped holes as more realistic models. We show their electron transport properties and discuss the significance of zigzag edges in determining the conduction gaps  $E_g$ .

Figure 1 shows the geometries and the current densities for graphene having 1D periodic nanoholes. We use the non-equilibrium Green's function method based on first principles. The semi-infinite graphene leads are speculated to result in a tiny  $E_g$ , removing the quantum confinement in the transport direction. Geometry (a) shows  $E_g$  of less than 0.1 eV as expected. Geometry (b), however, shows a quite wide  $E_g$  of about 0.5 eV and has two sequential zigzag edges. We have found even two sequential zigzags produce many edge states around the Fermi level  $E_F$  for the infinite geometry. These edge states do not contribute to the current, forming a wide  $E_g$ . Next, we show the correlation between  $E_g$  and the neck width  $w$  for graphene having irregularly shaped holes with large 2D periodicities in Fig. 2. The tight-binding approximation method is used to obtain the energy band structures. The  $E_g$  is defined as the energy gap between the bands with a certain dispersion based on the results for the 1D periodic nanoholes. The value of  $E_g$  is generally inversely proportional to  $w$  as well as experimentally [2]. The longer sequence of zigzag edges produces several flat bands around  $E_F$ . This results in a significantly wide conduction gap. On the other hand, the shorter sequence of zigzag edges gives dispersive bands near  $E_F$ , not completely localized to the edges. The consequent wide distribution of  $E_g$  may correspond to multiplateaus in the  $I$ - $V$  curves observed experimentally [2]. We can conclude that zigzag edges play a critical role in determining the conduction gaps for graphene with both 1D and 2D periodic nanoholes. This suggests that control of the edge structures of the holes is significant for GNM device applications.

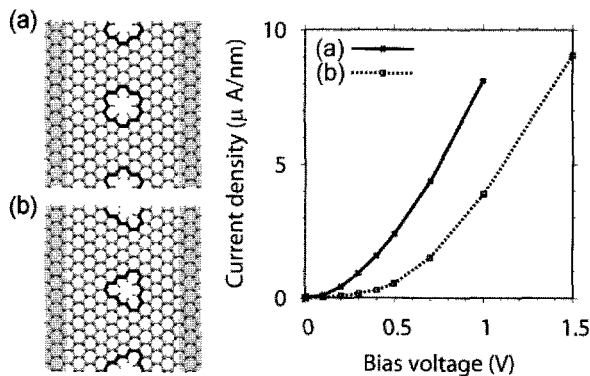


Fig. 1: Geometries and transport properties of graphene sheets with 1D periodic nanoholes (a) without and (b) with zigzag edges. The left and right sides of the models consist of semi-infinite graphene leads. All edge carbon atoms of the holes are terminated by hydrogen atoms.

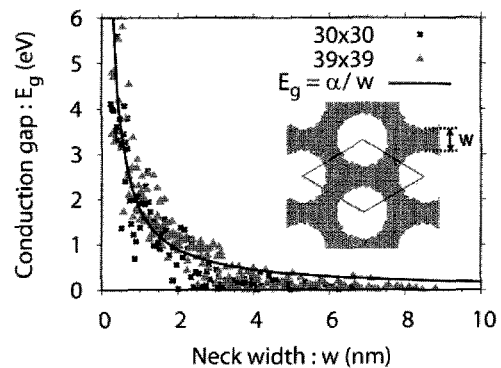


Fig. 2: Neck width ( $w$ ) dependency of the conduction gap ( $E_g$ ) for graphene with irregularly shaped holes. The solid curve is the fit of the data using  $E_g = \alpha/w$  with  $\alpha = 1.79$  nm eV (cf. Experimental  $\alpha = 0.95$  nm eV [2]). The inset is an example geometry.

- [1] J. Bai et al., *Nature Nanotech.* 5, 190 (2010). [2] X. Liang et al., *Nano Lett.* 10, 2454 (2010).  
 [3] H. Jippo et al., *The 39<sup>th</sup> Fullerenes-Nanotubes General Symposium*, 1-8 (2010).

Corresponding Author: Hideyuki Jippo

TEL: +81-46-250-8843, FAX: +81-46-250-8844, E-mail: [jippo.hideyuki@jp.fujitsu.com](mailto:jippo.hideyuki@jp.fujitsu.com)

## Spin-Related Novel Optical Phenomena in Single-Walled Carbon Nanotubes

○Satoru Konabe<sup>1,2</sup> and Susumu Okada<sup>1,2</sup>

<sup>1</sup>*Graduate School of Pure and Applied Sciences, University of Tsukuba, Tsukuba, Ibaraki 305-8571, Japan*

<sup>2</sup>*Japan Science and Technology Agency, CREST, 5 Sanbancho, Chiyoda, Tokyo 102-0075, Japan*

The interplay between conduction electrons and localized spins is one of fundamental and important problems in modern condensed matter physics giving us unexpected phenomena: It is well known that they induce resistivity minimum phenomena, known as the Kondo effect. Besides the conducting electrons, the fundamental question arises whether the interplay between photo-excited electrons and localized spins leads novel phenomena.

In this regard, semiconducting single-walled carbon nanotubes (CNTs) provide us an interesting research field of spin-related optical phenomena. Because of their quasi-one-dimensional structure, photo-excited electrons and holes in CNTs are strongly correlated and form a bound electron-hole pair, called an exciton, which has large binding energy, leading to remarkable stability up to room temperatures. Therefore, when there are localized spins in CNTs, optical phenomena are expected to exhibit wide variety.

In this paper, we demonstrate two interesting examples of novel optical properties of CNTs that are induced by localized spins based on the theoretical investigations:

(1) Recent experiments have shown the evidence in which the excitons correlate with localized spin induced by the defects in CNTs those are essential in the bipartite lattice of CNTs. However, unfortunately, the fundamental theory for this problem have not been addressed yet. We thus propose a theory that expresses the interaction between excitons and localized spins in CNT system[1]. Our theory solves one of the most important issue regarding the optically activated triplet dark excitons and first successfully provides a unified explanation for all the experimental conditions [2,3,4].

(2) It has been pointed out that ultrathin magnetic nanowires encapsulated in carbon nanotubes are potential candidates for constituent elements in the next-generation spintronics and electronics devices with nanometer scale[5]. For the device application, the evaluation methods for detecting the magnetic state of the nano-wires are essential and important. For such methods, we theoretically propose a non-contacted optical probing method based on the optical response from such magnetic nanomaterials encapsulated in carbon nanotubes. Due to the exchange interaction between excitons and polarized spins in ferromagnets, triplet excitons acquire a finite oscillator strength and can thus be excited by light[6]. This mechanism certainly detects magnetic ordering of nano-materials encapsulated in carbon nanotubes.

### References:

- [1] S. Konabe and S. Okada, submitted to PRL.
- [2] H. Harutyunyan *et al.* Nano Lett. **9** 2010 (2009).
- [3] R. Matsunaga *et al.* Phys. Rev. B. **81**, 033401 (2010).
- [4] K. Nagatsu, S. Chiashi, S. Konabe, Y. Homma, Phys. Rev. Lett. **105** 157403 (2010).
- [5] R. Kitaura *et al.* Angew. Chem. Int. Ed. **48**, 8298 (2009).
- [6] S. Konabe and S. Okada, submitted to APL.

Corresponding Author: Satoru Konabe

E-mail: [konabe@comas.frsc.tsukuba.ac.jp](mailto:konabe@comas.frsc.tsukuba.ac.jp)

Tel: +81-2-9853-5600 ext.8233

## Synthesis and characterization of AgI nanowires encapsulated in carbon nanotubes

○Shin-ichi Ito<sup>1</sup>, Ryo Kitaura<sup>1</sup>, Teppei Yamada<sup>2</sup>, Hiroshi Kitagawa<sup>2</sup>, Dong Yong Kim<sup>3</sup>, Suguru Noda<sup>3</sup>, Hirofumi Yoshikawa<sup>1</sup>, Kunio Awaga<sup>1</sup>, Hisanori Shinohara<sup>1</sup>

<sup>1</sup>*Department of Chemistry & Institute for Advanced Research, Nagoya University, Nagoya 464-8602, Japan*

<sup>2</sup>*Department of Chemistry, Faculty of Science, Kyoto University, Sakyo-ku, Kyoto 606-8502, Japan,*

<sup>3</sup>*Department of Chemical System Engineering, School of Engineering, The University of Tokyo, 7-3-1 Hongo, Bunkyo-ku, Tokyo 113-8656, Japan*

$\alpha$ -phase silver iodide ( $\alpha$ -AgI) has been well-known as a solid state ionic conductor due to its superionic conductivity and is one of the promising candidates for solid-state electrolytes for various electrochemical devices. However, below 420 K,  $\alpha$ -AgI undergoes a phase transition into the poorly conducting  $\beta$ - and  $\gamma$ -polymorphs, thereby limiting their applications. However, recently, we have found that AgI nanowires with a diameter of 10 nm can retain  $\alpha$ -phase even at 313 K where size and morphology of AgI presumably plays a great role in this  $\alpha$ -AgI stabilization.<sup>[1]</sup> To investigate the effect further, we have focused on low dimensional nanostructure of AgI, namely, AgI nanowire with a diameter of 5 - 10 nm. For this purpose, one-dimensional (1D) nanospace of carbon nanotubes (CNTs) has been employed. CNTs have unique 1D nanospace ranging in diameter from 0.4 to 50 nm, which can stabilize otherwise unstable nanomaterials. Here, we present a high yield synthesis and structural characterization of AgI nanowires that are formed in nanospace of thin-layer multi-wall carbon nanotubes (MWCNTs)

We have synthesized AgI@MWCNTs by the sublimation method already reported.<sup>[2]</sup> First, MWCNTs were oxidized in air at 823 K for 20 min to open end-caps. The cap-opened MWCNTs were then vacuum sealed together with AgI in a quartz tube under  $10^{-4}$  Pa, which was followed by thermal heating at 823 K for 2 days.

Figure 1 shows high resolution transmission electron microscope (HR-TEM) images of AgI@MWCNTs. As clearly shown in Figure 1, dark contrasts can be seen in MWCNTs, and an estimated filling ratio of AgI is as high as ca. 70 ~ 80 %.

In the presentation, we will discuss detailed characterization of structure and properties based on electron beam diffraction and HR-TEM.

[1]R. Makiura et al., *Nature. Mater.* **8**,476(2009).

[2]R. Kitaura, et al., *Angew.Chem.Int.Ed.* **48**,(2009).

**Corresponding Author:** Shin-ichi Ito

**E-mail:** noris@nagoya-u.jp

**Tel:** (+81)52-789-2482 / **Fax:** (+81)52-747-6442



**Figure 1.** HR-TEM images of AgI@MWCNTs

## Control of graphene etching by atomic structure of solid surfaces

Takahiro Tsukamoto and Toshio Ogino

*Department of Electrical and Computer Engineering, Yokohama National University,  
Yokohama 240-8501, Japan*

Graphene is one of the most notable materials in the recent progress of nanomaterial science and technology. In its device applications, control of the size, morphology, edge state, and shape is required because the electronic properties of graphene depend on those parameters. Crystallographic etching using catalytic metal nanoparticles can be applied to self-patterning of graphene, where carbon atoms of graphene are removed through a reaction between graphene and hydrogen catalyzed by metal nanoparticles during annealing in a hydrogen. Previously, we reported that etching of few layer graphene was guided by morphology of the sapphire substrates[1]. In this paper, we propose a new etching technique of single layer graphene that is controlled by atomic structures of well-defined solid surfaces.

Graphene flakes were deposited on sapphire (r-face) substrates by mechanical exfoliation of graphite[2]. A solution of  $\text{Fe}(\text{NO}_3)_3 \cdot 9\text{H}_2\text{O}$  in isopropyl alcohol was spin-coated to form metal catalysts. The samples were then annealed at  $900^\circ\text{C}$  in a hydrogen - argon mixed gas for 10 min. Surface morphology was observed by AFM and layer number of the graphene flake was estimated by Raman spectroscopy.

Graphene attached on a sapphire r-surface was etched in a particular direction, resulting in the formation of graphene nanoribbons. We investigated the relationship between the atomic arrangement of sapphire surfaces and the graphene etching. We found that graphene was etched in a  $[1-10-1]$  direction, and morphology of the sapphire surface did not affect the graphene etching. This indicates that atomic structure of the sapphire surface can be used to control graphene etching. When sapphire c-surface is used for the substrate of graphene, the graphene etching proceeds in random directions. This is the first report on control of graphene etching using atomic structure of the substrate surface.

[1] T. Tsukamoto and T. Ogino, *J. Phys. D* **43**, 374014 (2010).

[2] T. Tsukamoto and T. Ogino, *Appl. Phys. Express* **2**, 075502 (2009).

Corresponding Author: Takahiro Tsukamoto

TEL: +81-45-339-4147, FAX: +81-45-338-1157, E-mail: [tsukamoto@pc5.oginolab.dnj.ynu.ac.jp](mailto:tsukamoto@pc5.oginolab.dnj.ynu.ac.jp)

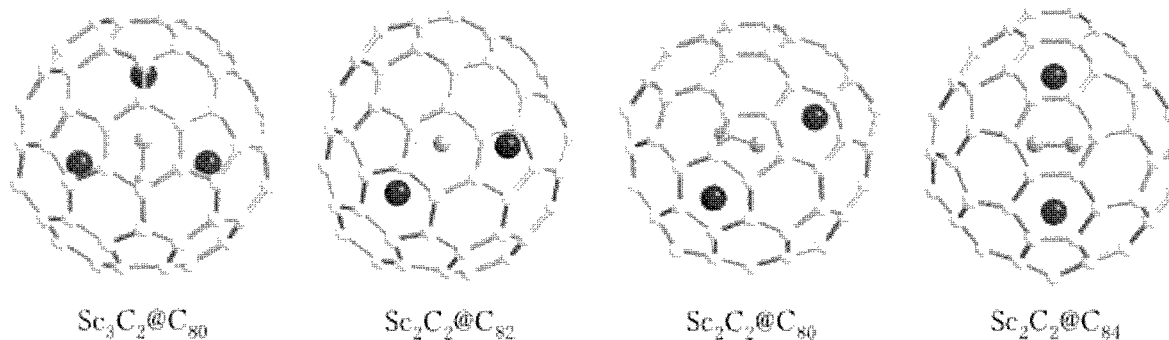
## Structures and Electronic Properties of Scandium Carbide Endohedral Metallofullerenes

○Naomi Mizorogi<sup>1</sup>, Takeshi Akasaka<sup>1</sup> and Shigeru Nagase<sup>2</sup>

<sup>1</sup>*Life Science Center of Tsukuba Advanced Research Alliance, University of Tsukuba,  
Tsukuba, Ibaraki 305-8577, Japan*

<sup>2</sup>*Department of Theoretical and Computational Molecular Science,  
Institute for Molecular Science, Okazaki Aichi 444-8585, Japan*

Endohedral metallofullerenes are known to have several unique properties. To apply these to new materials, it is important to clarify the endohedral structures and electronic properties. Scandium endohedral metallofullerenes have been extensively investigated both theoretically and experimentally. Among these, scandium carbide endohedral metallofullerenes are the most interesting because of the encapsulation of the C<sub>2</sub> unit together with several metal atoms, which is very important to the chemistry of scandium carbide endohedral metallofullerenes. However, so far there is no systematic theoretical investigation of scandium carbide endohedral metallofullerenes. We herein report density functional calculations of the endohedral structures, electronic properties, and bond information of C<sub>2</sub> unit of Sc<sub>3</sub>C<sub>2</sub>@C<sub>80</sub>, Sc<sub>2</sub>C<sub>2</sub>@C<sub>82</sub>, Sc<sub>2</sub>C<sub>2</sub>@C<sub>80</sub> and Sc<sub>2</sub>C<sub>2</sub>@C<sub>84</sub>, respectively.



### References

- [1] Y. Iiduka, T. Wakahara, T. Nakahodo, T. Tsuchiya, A. Sakuraba, Y. Maeda, T. Akasaka, K. Yoza, E. Horn, T. Kato, M. T. H. Lu, N. Mizorogi, K. Kobayashi, S. Nagase, *J. Am. Chem. Soc.* **2005**, *127*, 12500.
- [2] Y. Iiduka, K. Nakajima, T. Wakahara, T. Tsuchita, M. O. Ishitsuka, Y. Maeda, T. Akasaka, M. Waelchli, N. Mizorogi, S. Nagase, *Angew. Chem. Int. Ed.* **2008**, *47*, 7905.

Corresponding Author: Takeshi Akasaka

TEL&FAX: +81-29-853-6409, E-mail: akasaka@tara.tsukuba.ac.jp



## Synthesis and Applications of Carbon Nanotube Sponge Macrostructures

Xuchun Gui, Tianzhun Wu, Rong Xiang, Zikang Tang

*HKUST-SYSU Joint Laboratory of Nano Materials and Technology,  
State Key Laboratory of Optoelectronic Materials and Technologies, School of Physics and  
Engineering, Sun Yat-Sen University, Guangzhou 510275, China*

Carbon nanotubes (CNTs) are novel nanostructures with excellent properties and promising applications in various fields. Preparation of macroscopic structures based on assembled CNTs represents an important step towards practical applications. The engineered porous structures based on CNTs will offer a combined feature of high porosity and high performance. Here, an original macroscopic structure based on three dimensional, highly porous CNT network (CNT sponge) was synthesized in a direct and controllable way. The properties of the CNT sponges were studied for paving the way to develop high performance materials and explore new applications, including adsorption of organic solvents and spilled oil, mechanical energy absorption, nanocomposites, etc.

CNT sponges are directly synthesized by chemical vapor deposition (CVD), using dichlorobenzene and ferrocene as carbon source and catalyst precursor, respectively. The CNT sponges consist of randomly overlapped multi-walled CNTs (MWNTs), which self-assembled into a porous, highly interconnected, three-dimensional framework. On the microscale, each CNT can be considered as a high aspect-ratio skeleton to construct the porous structure. Freestanding CNT sponges have uniform structure, high flexibility and stability, with apparent densities of 5-25 mg/cm<sup>3</sup>, porosity of larger than 99 %.<sup>1-3</sup>

### References:

1. Gui X C, et al., Recyclable carbon nanotube sponges for oil absorption and recover. *Journal of Materials Chemistry*, 2010, in press.
2. Gui X C, et al., Carbon nanotube sponges. *Advanced materials*, 2010, 22, 617-621.
3. Gui X C, et al., Highly conductive nanotube sponges and composites with controlled compressibility. *ACS Nano*, 2010, 4: 2310-2326.

Correspondence may be addressed to:

Rong Xiang

[xiangr2@mail.sysu.edu.cn](mailto:xiangr2@mail.sysu.edu.cn)

+86-20-8411-0528

## Cell proliferation on Carbon Nanotubes Coated Dishes in Different Cell Lines

○Tsukasa Akasaka<sup>1</sup>, Makoto Matsuoka<sup>1</sup>, Atsuro Yokoyama<sup>1</sup>, Takeshi Hashimoto<sup>2</sup>,  
and Fumio Watari<sup>1</sup>

<sup>1</sup> Graduate School of Dental Medicine, Hokkaido University, Sapporo 060-8586, Japan

<sup>2</sup> Meijo Nano Carbon Co., Ltd., Nagoya 460-0002, Japan

In recent investigation, carbon nanotubes (CNTs) have been utilized as scaffolds for cell cultures. Despite many researchers reported cell behavior on CNTs scaffolds, the effects of CNT scaffolds on cell proliferation are highly variety (diffuse or not clear). Therefore, systematic investigations using common conditions by one researcher are required for establishment of general trends in cell proliferation on CNTs. In the present study, we prepared culture dishes with homogeneous thin or thick films of non-modified CNTs and examined the effect of different cell lines on cell proliferation in these culture dishes.

We demonstrated that the ratio of cell proliferation was strongly affected by kind of cells and substrates. Interestingly, single-walled carbon nanotubes (SWCNT) thin films were found to be the most effective substrate for the proliferation of half of the cells used in this study (ex. Saos-2, HeLa, HEK293, NIH-3T3, and MDCK). Further, thin SWCNT films indicate high transparency and electro-conductivity. Therefore, thin SWCNT films may be used as a hybrid-biomaterial such as a biosensor or an electro-stimulator for cell controls.

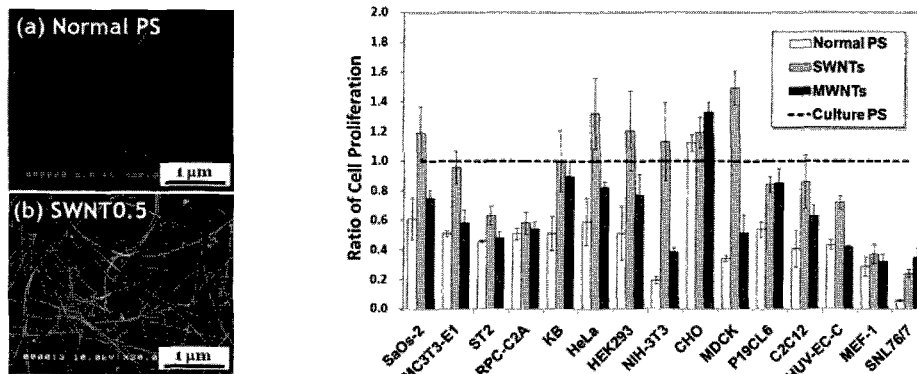


Fig. SEM images of CNT-coated dishes and cell proliferation of different cell lines on CNT-coated dishes.

[1] T. Akasaka, A. Yokoyama, M. Matsuoka, T. Hashimoto and F. Watari, *Mater. Sci. Eng. C*, **30**, 391 (2010).

Corresponding Author: Tsukasa Akasaka

TEL: +81-11-706-4251, FAX: +81-11-706-4251, E-mail: akasaka@den.hokudai.ac.jp

## 2P-3

### Synthesis and characterization of highly conducting Carbon nanotube-Copper composite

○Chandramouli Subramaniam<sup>1</sup>, Takeo Yamada<sup>2</sup>, Don N. Futaba<sup>2</sup> and Kenji Hata<sup>1,2</sup>

<sup>1</sup>*Technology Research Association for Single Wall Carbon Nanotubes, Central 5, 1-1-1 Higashi, Tsukuba, Ibaraki 305-8565*

<sup>2</sup>*Nanotube Research Centre, National Institute of Advanced Industrial Science and Technology, Central 5, 1-1-1 Higashi, Tsukuba, Ibaraki 305-8565*

The ability of water-assisted CVD<sup>1</sup> to produce aligned close-packed single wall carbon nanotubes(CNT) with superior thermal and mechanical properties make them ideal materials for use in microelectronics<sup>2</sup>. However, their poor electrical conductivity has been a major obstacle in realizing this. To overcome this, we report the synthesis of conducting CNT-copper composite (conductivity  $\sigma=10^5 \text{Scm}^{-1}$ ) through a novel organic phase electrodeposition. The composite has been thoroughly characterized using a number of spectroscopic and microscopic techniques. SEM-EDAX reveals a uniform distribution of copper in the CNT matrix. Powder X-ray diffraction and Micro-Raman analysis substantiate the observation that the high conductivity of the composite is due to a uniformly intertwined network of pure Copper and CNT. The development of this composite material augurs well for applications in microelectronics.

#### References:

1. K. Hata, D. N. Futaba, K. Mizuno, T. Namai, M. Yumura and S. Iijima, *Science*, **306**, 1362 (2004)
- 2 Y. Hayamizu, T. Yamada, K. Mizuno, R. C. Davis, D. N. Futaba, M. Yumura and K. Hata, *Nature Nanotechnology*, **3**, 289 (2008)

Corresponding Author : Kenji Hata

E-mail : kenji-hata@aist.go.jp

Tel & Fax : 0298-61-4654

## Formation of *trans*-polyacetylene from CoMoCAT carbon nanotubes by laser irradiation

Mari Hakamatsuka, ◦Fumiaki Watanabe, Masaru Tachibana

*International Graduate School of Arts and Sciences, Yokohama City University,  
22-2 Seto Kanazawa-ku, Yokohama 236-0027, Japan*

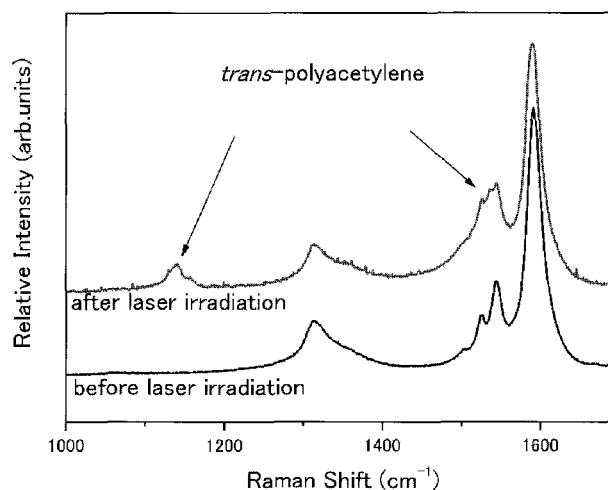
Laser irradiation has been extensively used for the synthesis of single walled carbon nanotubes (SWCNTs). It can be also used for the introduction of defects in SWCNTs [1]. Thus, the laser irradiation is interest for the tailoring of structures and properties of SWCNTs. In this paper, we report the formation of *trans*-polyacetylene from CoMoCAT SWCNTs by laser irradiation.

As-received CoMoCAT SWCNTs were used in this work. A suspension of nanotubes in ethanol was prepared by ultrasonication. The suspension was dropped on a clean quartz substrate and allowed to be air-dried at room temperature. The samples prepared in this procedure were used for laser irradiation experiments. The samples, which were exposed to air for less than one hour before laser irradiation, are called “short air-exposure” ones. Some of samples were kept in air at room temperature for more than six months before laser irradiation. They are called “long air-exposure” ones. The laser irradiation was carried out using a 532 nm from YAG laser. The power on the sample was  $17.8 \text{ mW}/\mu\text{m}^2$ .

Fig. 1 shows Raman spectra of “long-air-exposure” sample before and after laser irradiation. As seen in Fig.1, Raman spectrum of the irradiated “long air-exposure” sample exhibit the appearance of new peaks at  $1138 \text{ cm}^{-1}$  and  $1514 \text{ cm}^{-1}$ , compared with non-irradiated one [2]. These peaks are quite similar to main ones of *trans*-polyacetylene [3]. This means that the *trans*-polyacetylene can be formed in the irradiated sample.

On the other hands, no significant change in Raman spectrum of “short air-exposure” sample was observed even after irradiation.

In this presentation, the formation condition and mechanism of *trans*-polyacetylene from CoMoCAT SWCNTs are discussed in the light of the catalytic hydrogenation for the cutting of graphene and CNTs reported recently [4].



[1] D. Kang *et al.*, *Diamond Relat Mater.* **19**, 578-580 (2010)

[2] M. Hakamatsuka *et al.*, *Carbon*. (in press)

[3] H. Takeuchi *et al.*, *J. Mol. Struct.* **158**, 179-193 (1987)

[4] A. L. Elías *et al.*, *NanoLett.* **10**, 366-372 (2010)

Corresponding Author: Masaru Tachibana

TEL/FAX: 045-787-2307, E-mail: tachiban@yokohama-cu.ac.jp

## Spinning multiwalled carbon nanotube fibers and sheets

○Yoku Inoue<sup>1</sup>, Yoshinobu Shimamura<sup>2</sup>, Morihiko Okada<sup>3</sup>, Hidenori Mimura<sup>3</sup>  
and Kimiyoshi Naito<sup>4</sup>

<sup>1</sup>Dept. of Electrical and Electronic Eng, Shizuoka University, Hamamatsu 432-8651, Japan

<sup>2</sup>Department of Mechanical Engineering, Shizuoka University, Hamamatsu 432-8651, Japan

<sup>3</sup>Research Institute of Electronics, Shizuoka University, Hamamatsu 432-8651, Japan

<sup>4</sup>National Institute for Materials Science, Tsukuba 305-0047, Japan

Because of high tensile strength of carbon nanotubes (CNTs) [1], the light weight and high strength composite materials using CNTs as fillers have been intensively studied. Recently, we established growth method of ultra-long MWNT array using iron chloride [2]. Good things of the method are that millimeter scale long arrays are grown in short time and it has high drawability of MWNT web. The MWNT web is a two-dimensional MWNT network. Using the webs, we fabricated MWNT fibers and sheets. Since MWNTs are highly aligned in the drawn direction, the large scale MWNT structures fabricated from the webs are expected to show high mechanical and electrical properties in the aligned direction, and to show high anisotropic features. Such good material features would provide the advanced functions for many applications including the CNT composites.

MWNT arrays were synthesized using a conventional low pressure thermal chemical vapor deposition system. A smooth quartz substrate was placed in a horizontal quartz tube furnace with FeCl<sub>2</sub> powder, and MWNTs were grown at 830 °C. Densely grown MWNTs are vertically aligned on a quartz substrate. The height of the array reached 2.5 mm in 25 min with the growth rate over 100 μm/min. This growth rate is remarkably high. Our MWNT array samples have a high drawable feature. The MWNT webs are easily drawn using tweezers by pulling out the edge of the array, and can be drawn over 60 m just by drawing MWNTs with no twisting. During drawing, MWNTs are drawn with taking neighbors one after another with the aid of van der Waals force. The spun MWNT fibers were fabricated by twisting the MWNT web. The unidirectionally aligned MWNT sheets were fabricated by stacking the MWNT webs and shrinking with ethanol. The tensile strength of a spun fiber, spun with 2 mm-long MWNTs, was 560 MPa. Electrical resistivity of the MWNT sheet with thickness of 0.8 μm was  $2.5 \times 10^{-3} \Omega \cdot \text{cm}$  in parallel direction, and anisotropy ratio was 7. Thermal conductivity in parallel direction was 70 W/m•K and anisotropy ratio was 8.

[1] B. G. Demczyk *et al.* *Mater. Sci. Eng.* A334, 173 (2002).

[2] Y. Inoue *et al.*, *Appl. Phys. Lett.* 92, 213113 (2008)

Corresponding Author: Yoku Inoue

TEL: +81-53-478-1356, FAX: +81-53-478-1356,

E-mail: tyinoue@ipc.shizuoka.ac.jp

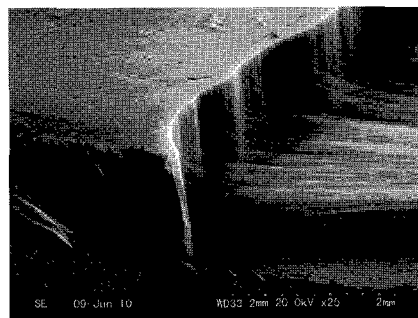


Fig. 1 Spinning MWNT web from a MWNT array

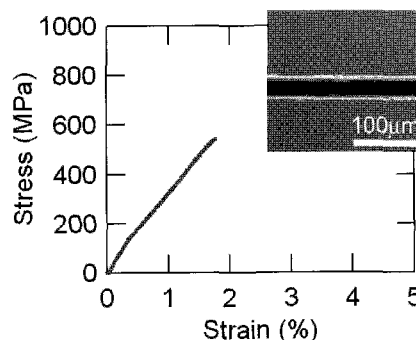


Fig. 2 Stress-strain curve of a spun MWNT fiber. Inset shows a typical spun fiber.

## 2P-6

### **Fabrication of Free-Standing Ultrathin Single-Walled Carbon Nanotube Films with Highly Conductivity and transparency**

Qingfeng Liu, Tsuyohiko Fujigaya, Naotoshi Nakashima

*Department of Applied Chemistry, Graduate School of Engineering, Kyushu University,*

*Fukuoka 812-8581, Japan*

E-mail: [qfliu@mail.cstm.kyushu-u.ac.jp](mailto:qfliu@mail.cstm.kyushu-u.ac.jp)

It is well known that single-walled carbon nanotube (SWNT) thin films have shown great promise for foreseeable applications especially in thin film devices and solution-based deposition methods such as spray coating are the most reliable ways to fabricate thin SWNT films on different substrates. Solution-based deposition methods, including dip coating, spin coating, spray coating, solution casting, Languir-Blodgett deposition, and vacuum filtration, are the most reliable and cost-effective ways to fabricate large-area thin films of single-walled carbon nanotubes (SWNTs). However, the solution-based techniques depend on the wettability of the substrates, thus limits the substrates for such applications. Therefore, certain techniques, such as dry transfer, to relocate the films from the SWNT-deposited substrates to the target substrates of interest have been established, but the force involved in the transfer process easily destroys the original network structure of the nanotubes.

We now describe a simple approach for free-standing highly-conductive transparent SWNT films with 20-150 nm thickness by spray-coating from surfactant-dispersed aqueous solutions of improved floating-catalyst grown SWNTs.<sup>1</sup> After a HNO<sub>3</sub> treatment, dipping the SWNT films supported on glass substrates, resulted in a quick and nondestructive self-release to form free-standing ultrathin SWNT films on the water surface. The obtained films have a sufficiently high transmittance (i.e., 95 %), a very low sheet resistance (i.e., ~120 Ω/sq), and a small average surface roughness (i.e., ~3.5 nm for a displayed 10×10 μm area). Such floating SWNT films on the water surface were easily transferred to any substrates of interest, without any intense mechanical and chemical treatments, to preserve the original size and network structure of the SWNT films, which is a significant advantage over conventional indium-tin oxide (ITO) and therefore strongly promise to be “post ITO” for many applications.

#### **References**

1. Liu QF, et al. *J. Am. Chem. Soc.* **2010**, *132*, 16581.

## Development of Carbon Nanotube/Polybenzoxazole Composite Films

○Takahiro Fukumaru<sup>1</sup>, Tsuyohiko Fujigaya<sup>1</sup> and Naotoshi Nakashima<sup>1,2</sup>

<sup>1</sup>Department of Applied Chemistry, Graduate School of Engineering, Kyushu University,  
744 Motoooka, Fukuoka 819-0395, Japan

<sup>2</sup>Japan Science and Technology Agency, CREST, 5 Sanbancho, Chiyoda-ku, Tokyo,  
102-0075, Japan

Carbon nanotubes (CNTs) possess remarkable mechanical and thermal properties. The superior properties make CNTs excellent candidate to substitute for the conventional fillers in the fabrication of polymer nanocomposites [1]. On the other hand, polybenzoxazoles (PBO) are known to have excellent mechanical strength and thermal stability. CNT/PBO nanocomposites expect to have excellent properties applicable for practical applications such as super high mechanical strength nanofibers and high thermal conductive films. However, the poor solubility of PBO and CNTs hinders the fabrication of CNT/PBO nanocomposites.

Recently, we successfully synthesized soluble PBO precursor (**t-Boc prePBO**: **Figure 1**) which acts as a solubilizer of single-walled carbon nanotubes (SWNTs) in dimethylacetamide (DMAc) [2].

In this presentation, we report the fabrication of CNT/PBO films without using strong acid. CNT/**t-Boc prePBO** in DMAc was cast onto a glass substrate, and dried at 60 °C for 1 h, then at 80 °C for 1 h. The film was peeled off from the glass substrate by immersing the film in water and then dried at 80 °C for 4h in a vacuum. The obtained film was then heated in a stepwise fashion at 200, 250, 300 and 350 °C under vacuum for 1 h each. The FT-IR spectrum (**Figure 2 (bottom)**) of the obtained film shows the disappearance of the characteristic vibrations of the amide and t-Boc carbonyl groups at 1640 and 1740 cm<sup>-1</sup>, respectively (**Figure 2 (top)**); while, the typical vibration mode for C=N in the oxazole ring appeared at 1620 cm<sup>-1</sup>, manifesting the successful t-Boc decomposition and transformation to the PBO upon heating in the presence of CNTs.

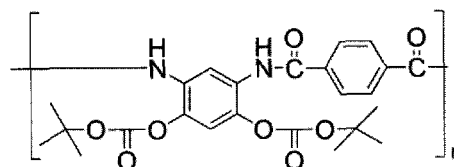


**Figure 1.** Chemical structure of **t-Boc prePBO**.

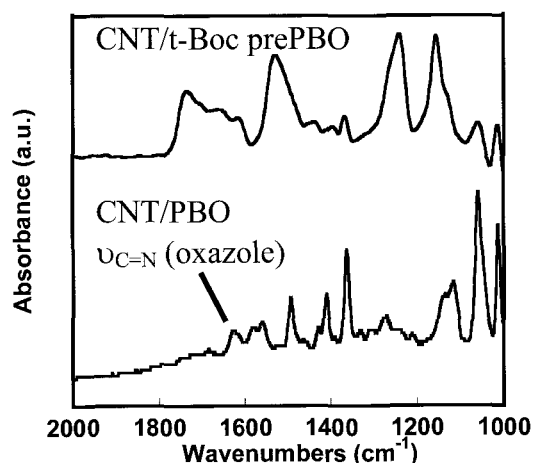


**Figure 2.** IR spectra of SWNT/**t-Boc prePBO** (upper) film and CNT/PBO (bottom) film.

[1] (a) T. Fujigaya, S. Haraguchi, T. Fukumaru, N. Nakashima, *Adv. Mater.* 20, 2151 (2008).

(b) T. Fujigaya, T. Fukumaru, N. Nakashima, *Synthetic Met.* 159, 827 (2009).

[2] T. Fukumaru, T. Fujigaya, N. Nakashima, *The 38<sup>th</sup> Fullerenes-Nanotubes General Symposium* 1P-35 (2010).

Corresponding Author: Naotoshi Nakashima

E-mail: nakashima-tcm@mail.cstm.kyushu-u.ac.jp

Tel&Fax: +81-92-802-284

## Preparation and evaluation of polymer gel capsules containing SWNTs

○Yusuke Tsutsumi<sup>1</sup>, Tsuyohiko Fujigaya<sup>1</sup>, Naotoshi Nakashima<sup>1,2</sup>

<sup>1</sup>Department of Applied Chemistry, Graduate School of Engineering, Kyushu University, 744 Motoooka, Fukuoka 819-0395, Japan

<sup>2</sup>JST-CREST, 5 Sanbancho, Chiyoda-ku, Tokyo, 102-0075, Japan

Single-walled carbon nanotubes (SWNTs) are nanomaterials that possess unique  $\pi$ -rich and hydrophobic surface and effective photothermal property. We have reported these properties were quite useful to keep a drug molecules and release them upon photo irradiation [1]. For the development of a novel drug delivery system using the findings, in this report, we develop the preparation of poly (*N*-isopropylacrylamide) (PNIPAM) gel capsules containing SWNTs inside (SWNT/PNIPAM gel capsules).

SWNT/PNIPAM gel capsules were prepared by emulsion polymerization using sodium dodecyl sulfate (SDS) as surfactant. Fig. 1 shows the schematic illustration of the formation mechanism of SWNT/PNIPAM gel capsule. Fig. 2 is the merged image of the photograph and Raman mapping (mapped by G-band) of the SWNT/PNIPAM gel capsules on silicon substrate. It was revealed that all the capsules contain SWNT. The holding and releasing of the drug molecule in the capsule will be discussed.

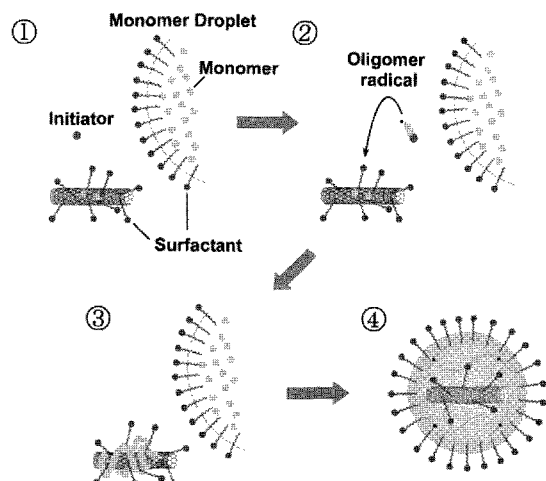


**Fig.1** Schematic illustration of the formation mechanism of SWNT/PNIPAM gel capsule.

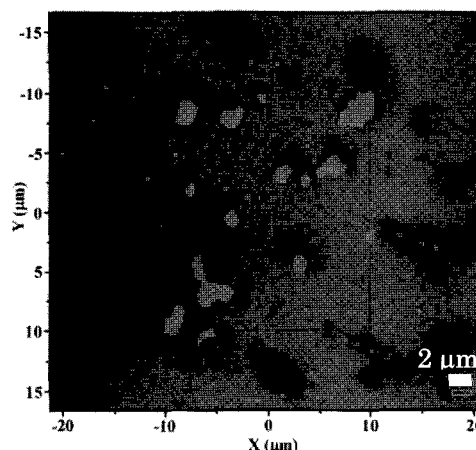


**Fig.2** Merged image of the photograph and Raman mapping (mapped by G-band) of the SWNT/PNIPAM gel capsules.

[1]T. Morimoto, T. Fujigaya, and N. Nakashima, *Soft Matter*, in press.

Corresponding Author: Naotoshi Nakashima

E-mail: [nakashima-tcm@mail.estm.kyushu-u.ac.jp](mailto:nakashima-tcm@mail.estm.kyushu-u.ac.jp)

Tel&Fax: +81-92-802-2840



## Fine patterning of single-walled carbon nanotube thin-film by surface modification

○Yuki Nobusa<sup>1</sup>, Yohei Yomogida<sup>2</sup>, Kazuhiro Yanagi<sup>3</sup>, Taishi Takenobu<sup>1</sup>

<sup>1</sup>*Department of Applied Physics, Waseda University, Shinjuku 169-8555, Japan*

<sup>2</sup>*Department of Physics, Tohoku University, Sendai 980-8578, Japan*

<sup>3</sup>*Department of Physics, Tokyo Metropolitan University, Hachioji 192-0397, Japan*

Recently, the flexible and printable electronics based on single-walled carbon nanotube (SWNT) thin-films is noteworthy. In particular, inkjet printing technology has the potential to reduce waste materials drastically, and it is expected to become the key technology for green manufacturing. We have already succeeded in the inkjet printing of high-performance SWNT thin-film transistor (TFT) [1], but further miniaturization is inevitable for application. Generally, the size limitation of inkjet microfabrication is restricted by the droplet diameter (several hundred  $\mu\text{m}$ ). Here, we pattern the SWNT film, which is smaller than the droplet size, using the functionalization of the Si surface with self-assembled monolayers (SAMs).

Si substrate was modified with 1,1,1,3,3,3-hexamethyldisilazane (HMDS) SAMs to make a surface hydrophobic. We converted the specific area to hydrophilic surface using deep ultraviolet (wavelength of 184.9-253.7 nm) irradiation through a metal mask, which selectively removes the HMDS layer [2]. A size of patterned region was  $200\mu\text{m}\times 1\text{mm}$ . We dropped SWNT dispersion in *N,N*-dimethylformamide (DMF) on the hydrophilic region by the inkjet technology, and dried them up at room temperature. The schematic diagram of fabrication procedures is illustrated in **Fig. 1**. The size of obtained thin-film was approximately identical to that of metal mask, indicating that the fine patterning less than droplet size is successfully achieved (**Fig. 2**). Importantly, the resulting  $200\mu\text{m}$  is not the minimum size for this technology and, in principle, we can reduce the size to  $< 50\ \mu\text{m}$  via metal mask and  $< 1\ \mu\text{m}$  via optical lithography. This technique will also lead to an intentional liquid flow on the patterned substrate and, then, a novel method for SWNT alignment.

This study was supported by Industrial Technology Research Grant Program from New Energy and Industrial Technology Development Organization (NEDO) of Japan.

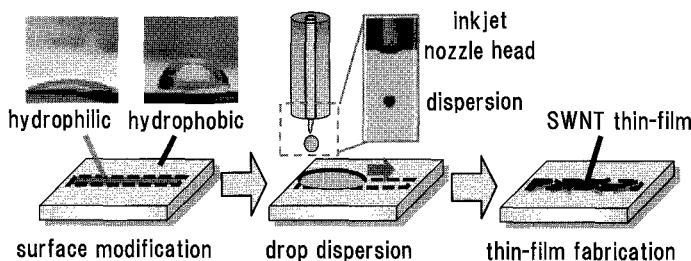


**Fig.1** The schematic of fabrication process

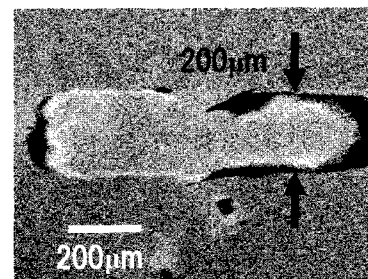


**Fig.2** Scanning Electron Microscope (SEM) image of fabricated thin-film

[1] H. Okimoto et al., *Adv. Mater.*, **22**, 3981 (2010). [2] T. Minari, et al., *Appl. Phys. Lett.*, **92**, 173301 (2008).

Corresponding Author: Taishi Takenobu

TEL/FAX: +81-3-5286-2981, E-mail: takenobu@waseda.jp

## Further development of Aligned Carbon Nanotube Wafer based Strain Sensors

○ Takeo Yamada<sup>1</sup>, Yuki Yamamoto<sup>1</sup>, Yuhei Hayamizu<sup>1</sup>, Yoshiki Yomogida<sup>1</sup>, Ali Izadi-Najafabadi<sup>1</sup>, Don N. Futaba<sup>1</sup>, Motoo Yumura<sup>1</sup>, and Kenji Hata<sup>1,2</sup>

<sup>1</sup> *Nanotube Research Center, National Institute of Advanced Industrial Science and Technology (AIST), Tsukuba 305-8565, Japan*

<sup>2</sup> *CREST, Japan Science and Technology Agency (JST), Kawaguchi 332-0012, Japan*

SWNT thin films, or “CNT-wafers,” have shown a new direction for multi-dimensional micro-electromechanical (MEMS) devices through their assembly and processing ability [1]. Interestingly, the ductile and brittle properties of the CNT-wafer open up opportunities beyond conventional MEMS devices.

We have developed a new class of wearable and “fully” stretchable devices (i.e. all device components are stretchable) that could deform as part of the human body as a form of ubiquitous motion monitoring. The sensing component of the gauge was a CNT-wafer, which, upon strain, did not break. Instead, the CNT-wafer fractured into numerous islands separated by gaps, and connected by suspended bundles bridging the gaps. This unique mechanism allowed for reversible strain measurement up to 280%, ~50 times more than conventional metal strain gauges, long cyclic lifetime (over 10,000 cycles), and millisecond-order response.

Here, we present detailed analysis of the signal response time and modeling of the sensor mechanism. Furthermore, we investigated the effects of environment and other directional motion on the sensor performance. As a demonstration of reducing environmental effects, we packaged the strain sensor. The packaged strain sensor exhibited strain property up to 150% with good linearity.

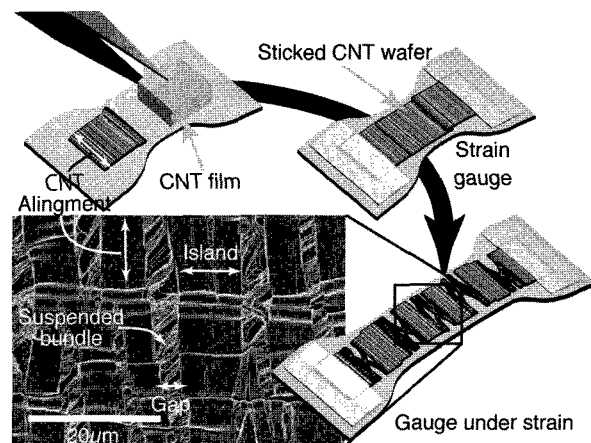


Fig. CNT strain gauge fabrication and surface structure of CNT wafer.

### References:

- [1] Y. Hayamizu, T. Yamada, K. Mizuno, R.B. Davis, D.N. Futaba, M. Yumura, and K. Hata, *Nature Nanotech.* **3**, 289 (2008)
- [2] K. Hata, D.N. Futaba, K. Mizuno, T. Namai, M. Yumura, and S. Iijima, *Science* **306**, 1362 (2004).
- [3] T. Yamada, Y. Yamamoto, Y. Hayamizu, D.N. Futaba, Y. Yomogida, A. Sekiguti, M. Yumura, and K. Hata, submitted.

**Corresponding Author: Takeo Yamada**

**E-mail: takeo-yamada@aist.go.jp**

**Tel: +81-29-861-4654, Fax: +81-29-861-4851**

## A simulation of an atomic-scale metal/nanotube/metal junction

Koichi Kusakabe<sup>1</sup>, Hokuto Saito<sup>1</sup>

<sup>1</sup>Graduate School of Engineering Science, Osaka University

In study of nanotube electronic devices, electron transport through a nanotube-metal interface have been a central topic to be explored. At a metal contact on a wall of a tube, we have an in-commensurate interface. Local chemical reaction may happen, where the charge transfer may create or modify an effective potential barrier, which determines the electron transport properties through the junction. Usage of an accurate approximation method, like the generalized gradient approximation, allows us to evaluate these effects. However, a restriction from the boundary condition applied in some fast simulation schemes might prohibit us to perform simulations of a realistic model. We need to consider a tube without defects or edges to derive transport properties of a tube device as realization of a metal/one-dimensional electron gas (1DEG)/metal junction.

We consider an atomic scale configuration of a metal-tube-metal junction. (Fig. 1) An advantage of this configuration allows us to consider,

- 1) Metal/1DEG/Metal junction,
  - 1.1) A junction with a TL liquid with multi-components,
  - 1.2) A magnetic tunnel junction with CNT,
- 2) An analogue of double-tip STM measurement.

We tested this geometry using a simulation tool, atomistix tool kit (ATK). The electron-correlation effect may be considered after obtaining reliable material structures and single-particle description as a basis for the consideration. But, the transmission spectrum (Fig. 1: (b)) contains effects from scattering at electrode. Removal of this effect is also discussed.

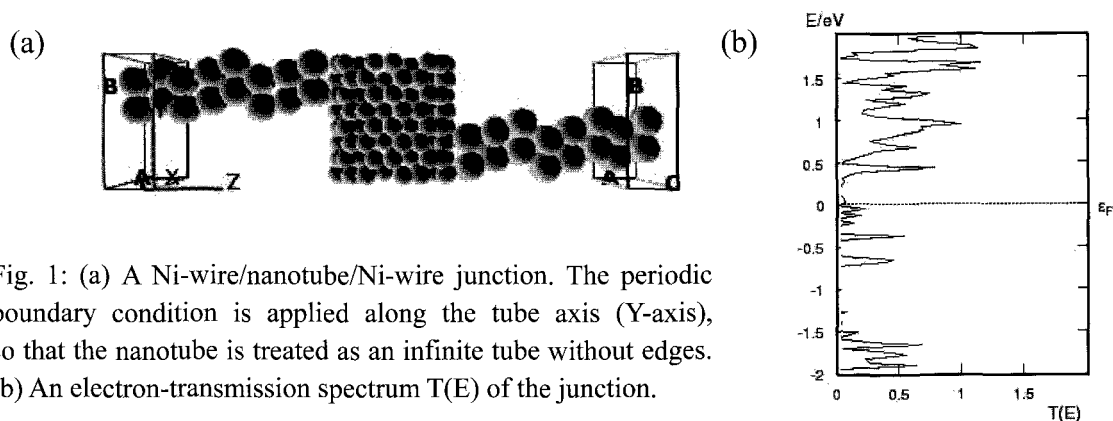


Fig. 1: (a) A Ni-wire/nanotube/Ni-wire junction. The periodic boundary condition is applied along the tube axis (Y-axis), so that the nanotube is treated as an infinite tube without edges. (b) An electron-transmission spectrum  $T(E)$  of the junction.

## Growth Termination of Millimeter-Tall Single-Walled Carbon Nanotubes

Kei Hasegawa<sup>1</sup> and Suguru Noda<sup>1,2</sup>

<sup>1</sup>Dept. of Chemical System Engineering, The University of Tokyo, Tokyo 113-8656, Japan

<sup>2</sup>PREST, JST, 4-1-8 Honcho, Kawaguchi, Saitama 332-0012 Japan

Rapid growth of millimeter-tall single-walled carbon nanotubes (SWCNTs) in 10 min was realized by adding small amount of water to C<sub>2</sub>H<sub>4</sub>/H<sub>2</sub>/He during chemical vapor deposition (CVD) [1]. By using our real-time monitoring [2] coupled by combinatorial catalyst library [3], we found a window for millimeter-tall SWCNTs growing in several minutes using only C<sub>2</sub>H<sub>2</sub>/Ar without water addition [4]. This time, we investigated what is necessary for millimeter-tall SWCNT growth. Our method by simple gas components, combinatorial catalyst and real-time monitoring makes the discussion clearer.

A gradient thickness profile of Fe was prepared on Al-Si-O layer on a substrate and CVD was carried out on it. The sample was set in a tubular CVD reactor, heated to and kept at 700-850 °C for 5 min in 5 vol% H<sub>2</sub>/ 50 ppmv H<sub>2</sub>O/ Ar, and then CVD was carried out by switching the gas to 0.05-0.60 vol% C<sub>2</sub>H<sub>2</sub>/ 50 ppmv H<sub>2</sub>O/ Ar under ambient pressure. Samples were monitored in real-time by a digital camera and CVD was continued until growth stopped.

Figure 1 shows photographs of SWCNTs grown at various temperatures and C<sub>2</sub>H<sub>2</sub> pressures on combinatorial catalyst libraries. Optimum C<sub>2</sub>H<sub>2</sub> pressure changed when the growth temperature was different. Maximum final height was 4.5 mm in 4.5 hours when CVD was carried out at 700 °C with 0.05 vol% C<sub>2</sub>H<sub>2</sub>. The effect of temperature and C<sub>2</sub>H<sub>2</sub> pressure on growth rate and growth lifetime was investigated. Careful AFM analysis provided us an evidence for Ostwald ripening causing the size change of the catalysts. We propose the two mechanisms of growth termination: one is the growth termination by excess carbon feed and another is the size change of catalysts. The dominant mechanism changes with the catalyst and CVD conditions. Suppressing the two growth termination mechanisms and prolonging the rapid growth from small catalysts are the key for millimeter-tall growth of SWCNTs.

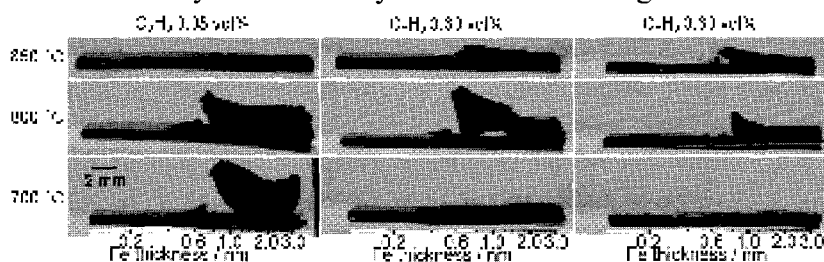


Fig. 1 Side-view photograph of SWCNTs grown on combinatorial catalysts at various CVD conditions.

[1] K. Hata, et al., *Science* **306**, 1362 (2004). [2] K. Hasegawa and S. Noda, *Jpn. J. Appl. Phys.* **49**, 085104 (2010) [3] S. Noda, et al., *Appl. Phys. Lett.* **86**, 173106 (2005). [4] K. Hasegawa and S. Noda, *ACS Nano*, in press.

Corresponding Author: Suguru Noda, TEL/FAX: +81-3-5841-7330/7332, E-mail: noda@chemsys.t.u-tokyo.ac.jp

## Synthesis of Highly Aligned Carbon Nanotubes on Stainless Steel Substrates by a Thermal CVD Method with Camphor

○Hisashi Seta, Kiyofumi Yamagiwa, Kohei Koizumi, Yusuke Ayato and Jun Kuwano

*Graduate School of Chemical Sciences and Technology, Tokyo University of Science,  
12-1 Ichigayafunagawara-machi, Shinjuku-ku, Tokyo 162-0826, Japan*

Highly aligned carbon nanotube arrays (HACNTA) have been expected to be employed in a wide range of applications, including electronic devices such as field emission display, supports of electrocatalysts for fuel cells, etc. The natural plant product, camphor  $C_{10}H_{16}O$ , were reported to be a suitable carbon source for thermal CVD process of high quality HACNTA with quartz substrates [1,2]. In this study, we used cut pieces of commercially available stainless steel (JISSUS304) plates as substrates and synthesized HACNTA with length of “submillimeter” on the substrates.

An Al buffer layer was deposited on the SUS304 substrates by direct current sputtering. A mixture of camphor and ferrocene (catalyst precursor) was inserted into the first furnace (300°C) and the vaporized mixture was sent with an Ar gas flow (100 ml/min) to the second furnace (850°C), where the SUS304 substrate was placed.

Fig. 1(a) shows SEM images of the carbonaceous products on the SUS304 substrate without the Al buffer layer. A small amount of non-aligned CNTs were grown. In contrast, on the substrate with the Al buffer layer, HACNTAs with thickness of 10-900  $\mu\text{m}$  were grown, as typically shown in Fig. 1(b). We presumed that the Al buffer layer reduced the passivation oxide layer of the substrate surface and formed fine  $\text{Al}_2\text{O}_3$  particles on the substrate. The finely concavo-convex substrate surface of the  $\text{Al}_2\text{O}_3$  nanoparticles effectively inhibited aggregation of the catalyst nanoparticles and brought formation a large amount of catalyst nanoparticles with an optimum size for HACNT growths.

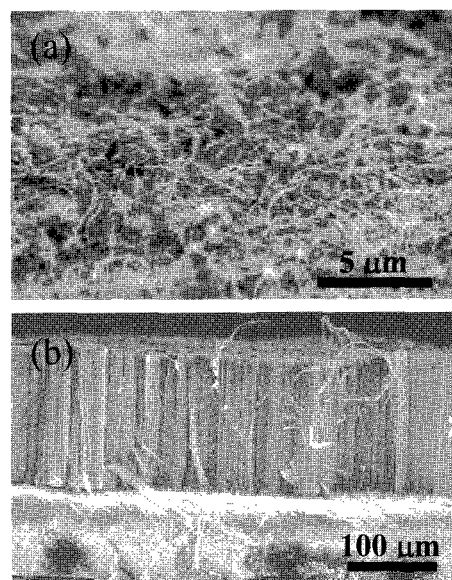


**Fig. 1.** SEM images of (a) CNTs grown on the SUS304 substrate and (b) HACNTs grown on the Al-sputtered SUS304 substrate.

[1] Kumar et al., *Chem. Phys. Lett.*, **374**, 521 (2003). [2] Yamada et al., *Key Eng. Mater.*, **320**, 163 (2006).

Corresponding Author: Jun Kuwano

TEL/FAX: +81-3-5228-8314 E-mail: kuwano@ci.kagu.tus.ac.jp

## The enhancement of zigzag and near zigzag tubes in the production of single wall carbon nanotube by alcohol CVD

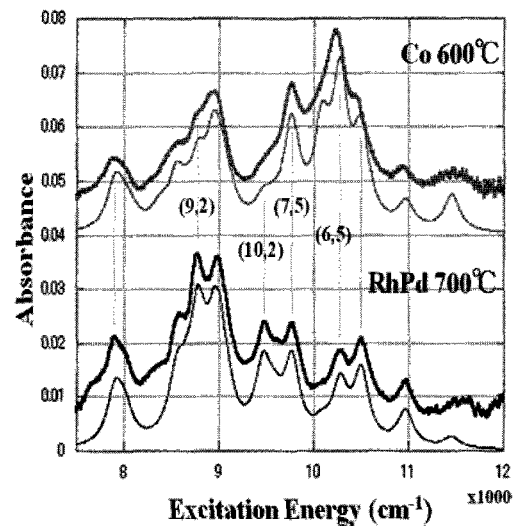
○ Yasumichi Kayo<sup>1)</sup>, Yohji Achiba<sup>1)</sup> and Toshiya Okazaki<sup>2)</sup>

1) Department of Chemistry, Tokyo Metropolitan University, Minami Osawa 1-1, Hachioji, Tokyo 192-0367, Japan

2) Advanced Industrial Science and Technology, Tsukuba, 305-8565, Ibaragi, Japan

Controlling size and chirality distributions in the production of single wall carbon nanotubes (SWNTs) is undoubtedly one of the most important issues in the potential applications of the SWNTs to nano-material technology such as a nano-electronics, a nano-photonics as well as a nano-bioelectronics. So far, many experimental attempts have been carried out on the selective production or the enrichment of specific (n,m) tubes by various kinds of the SWNT production methods. Among these attempts, so called “CoMoCAT” and “Co-MCM-41” are typical successful examples in which the (6,5) tube formation has been demonstrated to be of fairly prominence. In these experiments, the selection of the (6,5) tube seems to be realized by combination of CO disproportionation reaction and Co metal catalyst. Laser vaporization method combined with RhPd catalyst is another successful example in which the selective formation of near armchair tubes such as (6,5) and (7,6) species has clearly been shown. However, the experimental reports on the enrichment in a zigzag or a near zigzag tube production is very few, although the reason has not been clarified.

In the present paper, the effect of metal catalyst to the alcohol CVD on the synthesis of SWNTs by Rh and Rh/Pd mixed catalyst is characterized, and we demonstrate that the population of zigzag and near zigzag (n,m) species is extremely higher in comparison with those obtained by the Co-based system. Typical two absorption spectra in SDBS/H<sub>2</sub>O solution are shown in the figure to compare how the (n,m) distributions change from Co- to RhPd-catalyst system.



Corresponding Author Yohji Achiba

E-mail [achiba-yohji@tmu.ac.jp](mailto:achiba-yohji@tmu.ac.jp) Tel&Fax: +81-52-789-2482, +81-52-789-1169

## Synthesis of CNTs by Antenna-edge Microwave Plasma CVD from Carbon dioxide and Methane Gas

T. Ochiai<sup>1</sup>, K. Oohara<sup>1</sup>, M. Iizuka<sup>1</sup>, H. Kawarada<sup>1</sup>

<sup>1</sup> Waseda Univ., School of Electronic and Photonic Systems  
3-4-1, Ohkubo, Shinjyuku-ku, Tokyo 169-8555, Japan

### 1. Introduction

Using carbon monoxide(CO) as reaction gas high quality carbon nanotubes(CNTs) are formed by arc discharge or laser ablation . Also in CVD, CO has a great advantage in CNT quality compared with other carbon containing gas [1]. Unfortunately, CO should be treated as toxic gas, which limit the popular usage like acetylene. The presence of oxygen has a vital role in forming CNT with high quality. The C:O= 1:1 might be a magic ratio as previously shown in diamond deposition [2]. To reproduce the same effect by keeping the same C:O ratio, the mixture of carbon dioxide(CO<sub>2</sub>) and methane (CH<sub>4</sub>) are proposed. The chemical reaction formula is  $CO_2 + CH_4 \rightarrow 2C + 2H_2O$ , which indicates that two major green house gases forms high quality Single-Walled Carbon nanotubes (SWNTs) and the byproduct is only water

### 2. Experiment

We have synthesized SWNTs by remote plasma CVD[3]. Si substrate coated with a sandwich-like structure Al<sub>2</sub>O<sub>3</sub> / Fe / Al<sub>2</sub>O<sub>3</sub> was used as catalyst for synthesis of CNTs. H<sub>2</sub> and the mixture gas of CO<sub>2</sub> and CH<sub>4</sub> (the ratio is fifty-fifty) were used as reactive gas in Remote Plasma CVD(RPCVD). And, microwave power and pressure in chamber are 60W and 20 Torr respectively. The CNTs is analyzed by Raman spectrometry(633nm).

### 3. Results & Conclusion

Figure 1 shows the relation between the concentration of G/D and the mixed gas of CO<sub>2</sub> and CH<sub>4</sub> when the concentration is changed. It is understood that G/D has improved with the concentration of the carbon source gas. Especially, G/D becomes the maximum at 80%. Figure 2 shows the high-quality vertical aligned CNTs obtained at 80%. High quality CNTs is synthesized when ratio of C and O is 1:1. In the case of CO<sub>2</sub> and CH<sub>4</sub>, O in CO<sub>2</sub> and H in CH<sub>4</sub> interact with each other to moderate the effect of oxygen. Vertical aligned CNTs were synthesized from 80% carbon source gas as result. High quality CNTs synthesized from CO<sub>2</sub> and CH<sub>4</sub> expect might be an effective way to immobilize green house gases.

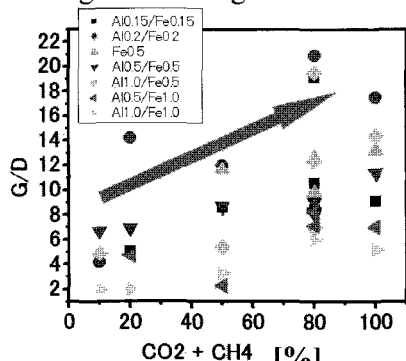


Figure 1. the relation between the concentration of the mixture gas from CH<sub>4</sub>

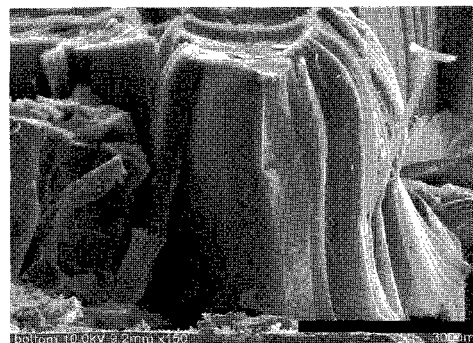


Figure 2. the SEM image of CNT when concentration of CH<sub>4</sub> and CO<sub>2</sub> is 80%

[1] T. Nishii et al. Proceedings of the 6<sup>th</sup> World Conference on Experimental Heat Transfer , Fluid Mechanics and Thermodynamics, 17(2008)

[2] P.K.Bachmann, et al. Diamond Relat. Mater. 12, 1(1991) [3] T. Iwasaki et al. Nano Lett. 8, 886 (2008)

Corresponding Author : H. Kawarada E-mail : [kawarada@waseda.jp](mailto:kawarada@waseda.jp) Tel : 03-5286-3391

## Molecular Dynamics Simulations of Metal Nanowire Formation within a SWNT and the SWNT Growth Process by Catalytic CVD

Teppe Matsuo, Takuya Noguchi, Shohei Chiashi, Junichiro Shiomi and Shigeo Maruyama  
*Department of Mechanical Engineering, The University of Tokyo, Tokyo 113-8656, Japan*

We reconstructed the Tersoff potential for use with metal-carbon structures, and applied it to cobalt, iron, nickel, and platinum systems. Potential parameters were acquired by fitting lattice constants and energies of various crystal structures. We confirmed this potential correctly reproduces many crystal structures.

In this study, we performed two simulations using our reconstructed potentials and the Brenner potential [1]. First, we simulated metal nanowire formation within a single-walled carbon nanotube (SWNT). Then, by adopting the simulation procedure of a previous report [2], we calculated the SWNT growth process by the catalytic CVD method. Classical molecular dynamics was used for both simulations.

Figures 1 and 2 show the cobalt and platinum nanowires formed inside a (5,5) SWNT. The morphology of the nanowire within the SWNT is dependent on the kind of metal. Other results for various SWNT chiralities and other metal species will be presented.

Figure 3 shows the growth process of a SWNT by the catalytic CVD method using cobalt catalyst. Carbon atoms are released from the cobalt cluster's surface, forming a tubular structure.

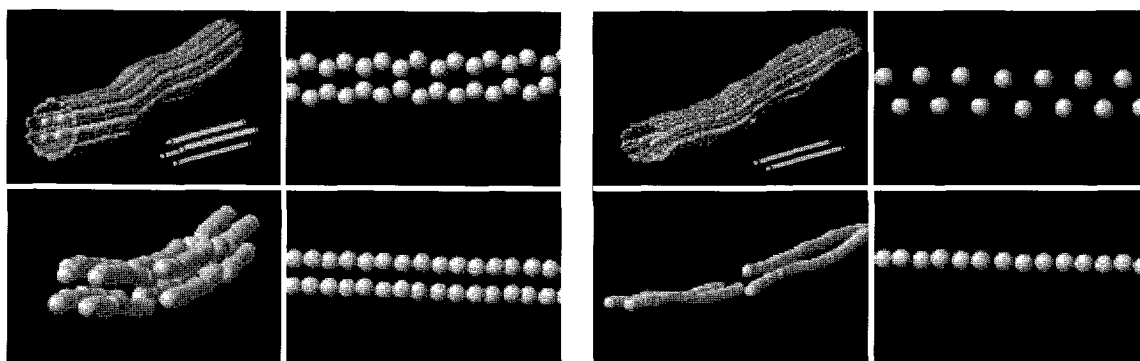


Fig. 1: Co nanowire inside a (5,5) SWNT

Fig. 2: Pt nanowire inside a (5,5) SWNT

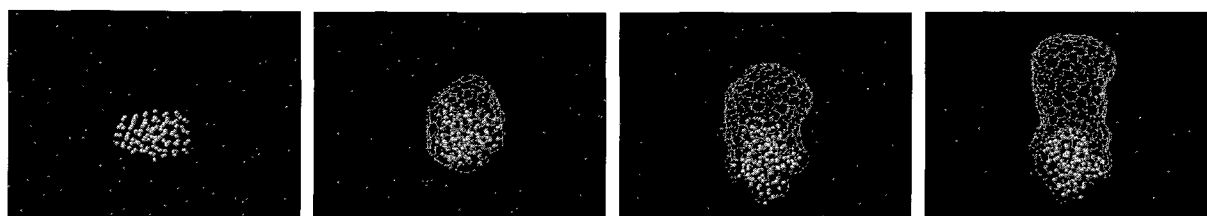


Fig. 3: Growth process of SWNT by Catalytic CVD method of cobalt catalyst (Left to right 0 ns, 10 ns, 20 ns, and 30 ns).

[1] D. W. Brenner, Phys. Rev. B, **42** (1990) 9458. [2] Y. Shibuta and S. Maruyama, Chem. Phys. Lett., **382** (2003) 381.

Corresponding Author: Shigeo Maruyama

E-mail: maruyama@photon.t.u-tokyo.ac.jp

TEL: +81-3-5841-6421, FAX: +81-3-5800-6983



## Selective growth of SWNTs on Ir catalyst combined with a laser vaporization method

○ Takuya Kodama<sup>1)</sup>, Akihito Inoue<sup>1)</sup>, Takeshi Kodama<sup>1)</sup>, Kenrou Hashimoto<sup>1)</sup>,  
Yohji Achiba<sup>1)</sup> and Toshiya Okazaki<sup>2)</sup>

1) Department of Chemistry, Tokyo Metropolitan University, Minami Osawa 1-1, Hachioji,  
Tokyo 192-0367, Japan and

2) Advanced Industrial Science and technology (AIST), Tsukuba, 305-8565 Japan

Controlling size and chirality of single-wall carbon nanotubes (SWNTs) is definitely of particular importance for the potential applications of SWNTs to the industrial field such as nano electronic devices, because the performance of SWNTs-based materials depends greatly on the diameter and chirality of the nanotubes. The ultimate goal in carbon nanotube production is to find a method and/or a catalytic system that would allow the growth of SWNTs of a single chirality. The laser vaporization method combined with RhPd catalyst has been shown to be one of the versatile methods in which the abundance of the SWNTs with a particular chiral index was found to be over 90% among other remaining SWNTs in the raw soot material.

In the present paper, we will demonstrate the experimental results on the chirality distributions of the SWNTs prepared by a laser vaporization method combined with Ir metal catalyst. Typical example of the SWNTs prepared by Ir catalyst is shown in Figs. 1 and 2, in which the 2D fluorescence and absorption spectra of the sample by Ir in SDBS/H<sub>2</sub>O solution are drawn to compare with those by RhPd under the same condition. Comparing these two spectra, it is clearly shown that the maximum of the size distribution for the SWNTs grown on the Ir catalyst shifts to the larger diameter size, resulting in the formation of (7,6) and (8,7) enriched SWNTs.

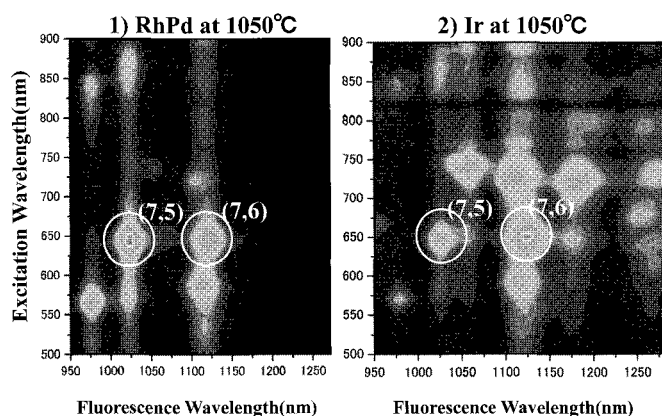


Fig.1: Fluorescence 2D mappings for the SWNTs prepared by laser vaporization with 1) RhPd and 2) Ir catalysts.

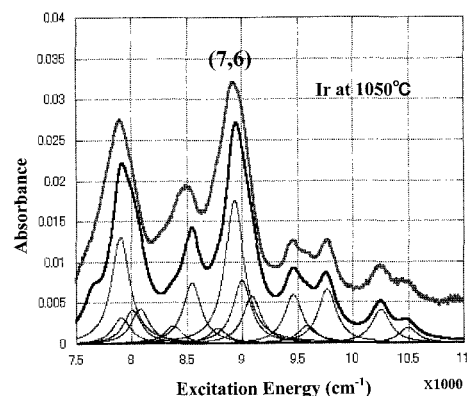


Fig. 2: Experimental and deconvoluted absorption spectra of SWNTs in SDBS/H<sub>2</sub>O solution. The deconvolution was carried out based on the fluorescence intensity for each (n,m) species.

Corresponding Author: Yohji Achiba

TEL: +81-42-677-2534, FAX: +81-42-677-2525, E-mail: achiba-yohji@tmu.ac.jp

## Epitaxial growth of faceted Co nanoparticles and their application to carbon nanotube growth

○Yui Ogawa,<sup>a</sup> Hiroki Ago,<sup>\*, b, c</sup> and Masaharu Tsuji<sup>b</sup>

<sup>a</sup>Graduate School of Integrated Frontier Sciences, Kyushu University, Fukuoka 816-8580

<sup>b</sup>Institute for Materials Chemistry and Engineering, Kyushu University, Fukuoka 816-8580

<sup>c</sup>PRESTO-JST

Metallic nanoparticles play an essential role in the catalytic growth of single-walled carbon nanotubes (SWNTs). It was reported that a graphene film epitaxially grows on single crystal fcc Ni(111) surface and that the orientation of the graphene matches with the underneath metal film [1]. This suggests that the crystallinity of the metal catalyst strongly influences the graphitization. Therefore, it is interesting to apply highly crystalline metal nanoparticles to SWNT growth in terms of possibility of controlling the SWNT structure including chirality. Here, we report preparation of crystalline Co nanoparticles on sapphire surfaces by high temperature-sputtering and successive annealing processes.

The Co film with 10 nm thickness was sputtered onto a sapphire substrate at room temperature and 500 °C. Then, the substrate was annealed at 900 °C in a H<sub>2</sub> flow, which converts the Co film to Co nanoparticles. We found that as-grown crystalline Co nanoparticles have unique faceted structure [2]. The structure of the Co nanoparticles was dependent on the sputtering temperature as well as the crystalline plane of sapphire. As seen in Fig. 1, the high temperature (500 °C) sputtering stimulated the epitaxial growth of faceted Co nanoparticles, while the room temperature-sputtered film gave a disordered film-like morphology together with irregular nanoparticles. The corresponding x-ray diffraction results indicate that the Co nanoparticles have a fcc structure. Thus, the as-grown nanoparticles are proposed to have half-octahedron with truncated {100} and {111} planes that can be explained by Wulff's theorem. The horizontally-aligned SWNT growth over these faceted Co nanoparticles is also presented.

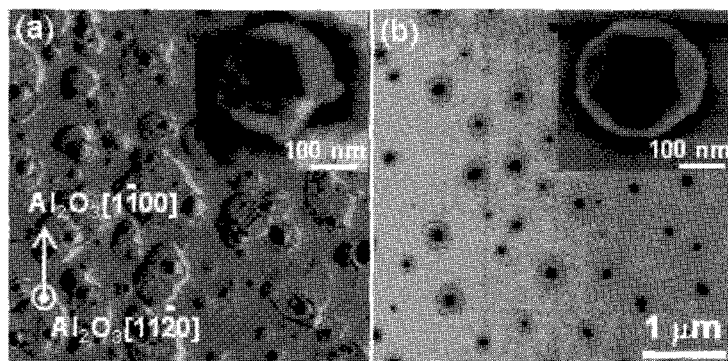


**Figure 1.** SEM images of Co/a-plane sapphire surface taken after H<sub>2</sub> annealing at 900 °C. The sputtering temperature is (a) RT and (b) 500 °C. Insets show the magnified images of typical Co nanoparticles.

**References:** [1] Y. Gomi *et al.*, *Surf. Sci.* **374** (1997) 61. [2] Y. Ogawa *et al.*, *Chem. Lett.* **39** (2010) 964.

**Corresponding Author:** Hiroki Ago (Tel&Fax: +81-92-583-7817, E-mail: ago@cm.kyushu-u.ac.jp)

## New approach for chirality recognition of single-walled carbon nanotubes using fluorene-based copolymers

○Kojiro Akazaki<sup>1</sup>, Hiroaki Ozawa<sup>1</sup>, Tsuyohiko Fujigaya<sup>1</sup>, Naotoshi Nakashima<sup>1,2</sup>

<sup>1</sup>*Department of Applied Chemistry, Graduate School of Engineering, Kyushu University, Fukuoka 819-0395, Japan*

<sup>2</sup>*JST-CREST, 5 Sanbancho, Chiyoda-ku, Tokyo 102-0075, Japan*

Much attention has been paid to single-walled carbon nanotubes (SWNTs) because of their unique physical properties [1,2]. However, the coexistence of tubes with various chiralities SWNTs has interfered with fundamental research and fabrication of devices. Separation of the mixture of SWNTs into certain chirality components has attracted considerable attention, recently [3].

Here we report a method toward selective recognition and separation of specified SWNTs having selected chiralities. Our approach is to use a family of polyfluorene (PFO)-based copolymers, composed of fluorene and alkoxy benzene (OB and EHB) having normal or branched side chains (PFO-OB and PFO-EHB, Fig. 1). Fig. 2 shows the photoluminescence (PL) maps of the SWNTs dissolved in toluene solutions of copolymers, in which we observed a strong SWNT chirality dependence. In the case of PFO-OB, the strong PL intensity from (8,6)SWNTs appeared in the homopolymer ( $x:y = 100:0$ ) became weak with increasing the contents of the OB unit ( $y$ ) (Fig. 2, upper). Similar trend was observed also for PFO-EHB (Fig. 2, lower). Absorption spectra also supported the above selectivity tendency and we will discuss the detail of the selectivity of the SWNTs depending on polymer composition.

### References

- [1] J. Bernholc, et al, *Annu. Rev. Mater. Res.* **32**, 347 (2002).
- [2] H. J. Dai, et al, *Acc. Chem. Res.* **35**, 1035 (2002).
- [3] C. H. Liu, et al, *Nanoscale* **2**, 1901 (2010).

**Corresponding Author: Naotoshi Nakashima**

**E-mail: nakashima-tcm@mail.cstm.kyushu-u.ac.jp**

**Tel&Fax: +81-92-802-2840**

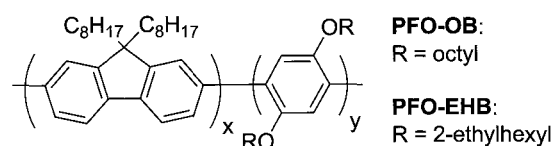


Fig. 1. Chemical structure of fluorene based copolymers.

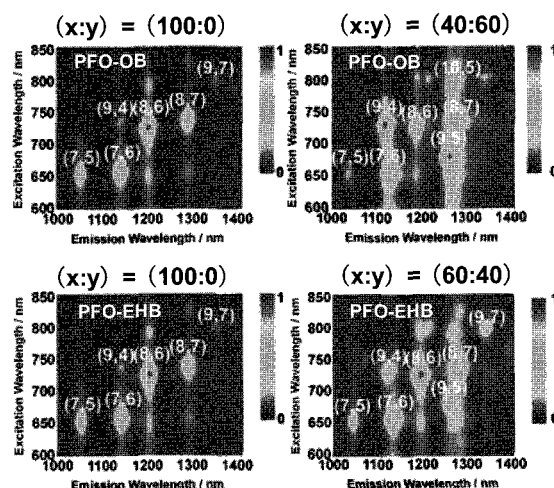


Fig. 2. PL maps of SWNTs with PFO-OB (upper left;  $x:y = 100:0$ , upper right; 40:60) and PFO-EHB (upper left;  $x:y = 100:0$ , upper right; 60:40).

## Separation of Single-Wall Carbon Nanotubes using Four Kinds of Gel Column Chromatography

○Yang Huang<sup>1,2</sup>, Huaping Liu<sup>1,2</sup>, Ye Feng<sup>1,2,3</sup>, Takeshi Tanaka<sup>1</sup>, Shunjiro Fujii<sup>1,2</sup>, and Hiromichi Kataura<sup>1,2</sup>

<sup>1</sup>*Nanosystem Research Institute, National Institute of Advanced Industrial Science and Technology (AIST), Tsukuba, Ibaraki 305-8562, Japan*

<sup>2</sup>*CREST, JST, Kawaguchi, Saitama 330-0012, Japan*

<sup>3</sup>*Institute of Materials Science, University of Tsukuba, Ibaraki 305-8573, Japan*

The electronic and optical properties of single-wall carbon nanotubes (SWNTs) strongly correlate with their structures. Various growth methods such as CoMoCAT® process have been developed to control their chiralities and diameters, but the structure control of SWCNTs is still unsatisfied. Because co-existent of metallic (m-) and semiconducting (s-) SWCNTs in as-produced soot precludes their widespread electronic applications, additional post-synthetic separation is necessary.

Recently, agarose gel column chromatography (GCC) was developed for the metal/semiconductor separation of SWCNTs [1,2]. In this method, selective adsorption of s-SWCNTs on the agarose gel beads leads to high-purity separation. Almost the same but slightly different effect is also reported for commercially available Sephacryl gel [3]. In this presentation, we report our effort on the M/S separation of SWCNTs by GCC using 4 kinds of commercially available gels: Sephacryl S-200, S-300, Sepharose 2B, and 4 Fast Flow. SWCNTs (SWeNT® SG76) were dispersed in sodium dodecyl sulfate (SDS) water solution by tip sonication and applied to the top of the gel columns after the ultracentrifugation. The m-SWCNTs were eluted with SDS solution, and the s-SWCNTs that remained in the gel columns were collected with sodium deoxycholate water solution. Analysis based on the optical measurements showed that S-200 gel showed the highest purity in M/S separation. To see the detailed separation process, a long column was applied. In the case of S-200, the semiconductor was separated into two fractions, while only one fraction was observed in the Sepharose. This additional separation process in S-200 could be attributed to the filtration of bundle size due to the size exclusion effect and leads to higher semiconductor purity. Detailed analysis will be discussed.

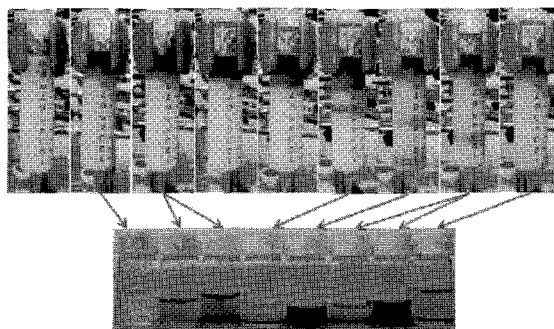


Figure 1. Separation of SWeNT® SG76 SWCNTs by Sephacryl S-200.

### References

- [1] T. Tanaka et al., *Nano Lett.* **9**, 1497 (2009). [2] T. Tanaka et al., *Appl. Phys. Express* **2**, 125002 (2009).  
[3] K. Moshhammer, F. Hennrich, and M. M. Kappes, *Nano Res.* **2**, 599 (2009).

Corresponding Author: Hiromichi Kataura

Tel: 029-861-2551, Fax: 029-861-2786, E-mail: [h-kataura@aist.go.jp](mailto:h-kataura@aist.go.jp)

## Effects of carbon source and growth temperature on diameter of horizontally-aligned single-walled carbon nanotubes on sapphire

○Takafumi Ayagaki,<sup>1,2</sup> Hiroki Ago,<sup>\*,1,2,3</sup> and Masaharu Tsuji<sup>1,2</sup>

<sup>1</sup>Graduate School of Engineering Sciences, Kyushu University, Fukuoka 816-8580

<sup>2</sup>Institute for Materials Chemistry and Engineering, Kyushu University, Fukuoka 816-8580

<sup>3</sup>PRESTO-JST

Single-walled carbon nanotube (SWNT) is a promising material for nanoelectronic devices. It has been demonstrated that single crystal substrates can assist horizontal SWNT growth [1,2], but mixed growth of metallic and semiconducting SWNTs remains a bottleneck for the future applications. This problem is caused by the fact that the as-grown SWNTs have some diameter distribution and, consequently, contain different chiralities. Thus, it is important to synthesize small-diameter SWNTs with a narrow diameter distribution while maintaining the horizontal alignment. Here, we study effects of carbon feedstock and growth temperature on the diameter of SWNTs grown on sapphire substrates.

Sapphire r-plane substrates were dipped into the Co-Mo salt solution to deposit the catalyst. SWNTs were grown by chemical vapor deposition (CVD) using either CH<sub>4</sub> or EtOH feedstock at 750 - 900 °C. As shown in Fig. 1, highly aligned SWNTs were obtained by CH<sub>4</sub> CVD as reported [2], but the nanotube density decreased significantly when the CVD temperature was lowered to 750 °C. On the other hand, the EtOH CVD gave high SWNT density even at 750 °C due to high reactivity of EtOH feedstock. However, the SWNT alignment was lost in the EtOH CVD. Raman spectra were measured at different points as shown in Fig. 2. While the diameter distributions in the methane CVD were almost independent on the reaction temperature, the ethanol CVD shifted to smaller diameter at lower reaction temperatures. We also present improvement of the SWNT alignment by addition of water vapor.

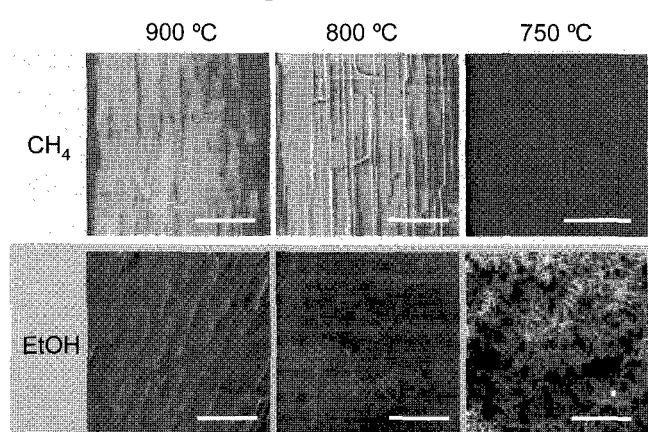


**Fig. 1.** SEM images of as-grown SWNTs from methane and ethanol at different CVD temperatures. Scale bars are 10 μm.

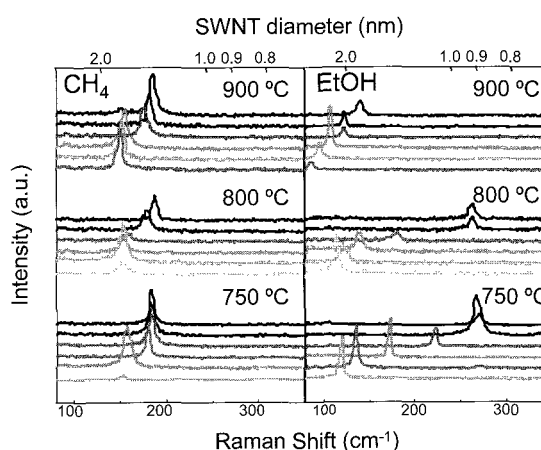


**Fig. 2.** Representative Raman spectra of the SWNTs grown from methane and ethanol measured with 514.5 nm excitation.

**References:** [1] H. Ago *et al.*, *Chem. Phys. Lett.* **408** (2005) 433. [2] N. Ishigami *et al.*, *J. Am. Chem. Soc.* **130** (2008) 30.

**Corresponding Author:** Hiroki Ago (Tel&Fax: +81-92-583-7817, E-mail: ago@cm.kyushu-u.ac.jp)

## Chemical vapor deposition growth of carbon nanotubes using cluster templates

○Takuya Nakayama<sup>1</sup>, Ryo Kitaura<sup>1</sup>, Hironori Tsunoyama<sup>2</sup>, Yasumitsu Miyata<sup>1</sup>, Sun Yun<sup>1</sup>,  
Tatsuya Tsukuda<sup>2,3</sup>, Hisanori Shinohara<sup>1</sup>

<sup>1</sup> Department of Chemistry & Institute for Advanced Research, Nagoya University, Nagoya 464-8602

<sup>2</sup> Catalysis Research Center, Hokkaido University, Nishi 10, Kita 21, Sapporo 001-0021, Japan

<sup>3</sup> CREST, Japan Science and Technology Agency, Kawaguchi, Saitama 332-0012, Japan

Carbon nanotubes (CNTs) are known to possess superior mechanical and electronic properties that initiated a broad research activity in multiple fields of nanoscience. The electronic structure of CNTs strongly depends on their geometrical structure such as the helicity.<sup>1)</sup> However, up to now, it is not possible to selectively grow CNTs with desired structure. Therefore, development of a precise control of the structure of CNTs is indispensable for the application of CNTs to nanoelectronics. To overcome this difficulty, we focused on clusters, which have uniform diameter and structure, as templates for chemical vapor deposition (CVD) growth of CNTs. Among various molecular and metal cluster templates, we have focused on gold clusters, fullerenes and Manganese clusters for CVD growth of CNTs. Especially, gold clusters are useful for CVD growth of CNTs due to the following reasons: (1) gold clusters have catalytic activity for CVD growth of CNTs<sup>2)</sup> and (2) a preparation technique of gold clusters with a uniform and desired diameter has been well-established recently.

In this study, we used gold clusters<sup>3)</sup> with average diameter of 1.3 nm (standard deviation was 0.3nm) as template for CCVD growth of CNT. The gold clusters were dispersed in ethanol (0.01 wt %) and spin-coated onto a quartz and silicon substrate. Prior to CVD growth, samples were heated in air at 500 degree for 30 min to remove poly (*N*-vinyl-2- pyrrolidone) wrapping the surface of Au clusters. After the heat treatment, CNTs were grown at 850 degree by CVD using ethanol as a carbon source.

Figure 1 shows Raman spectrum of the products that shows characteristic Raman bands to CNTs. Diameter of CNTs estimated from position of RBM Raman bands ranges from 1.0 to 1.6 nm, which is compatible with the diameter of Au clusters used in CVD growth. Figure 2 shows distribution of diameter of CNTs estimated by TEM image. This result corresponds to the result of raman spectra and gold cluster size.

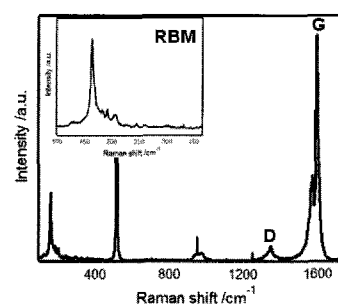


Figure 1, Raman spectra of grown CNTs from Au cluster

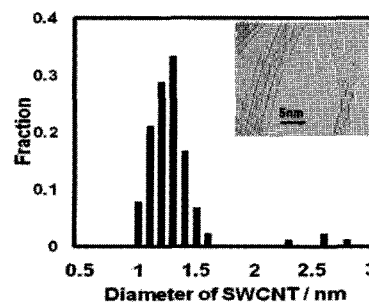


Figure 2, Distribution of the diameter of CNTs and TEM image

**Reference** 1) R. Saito *et al.*, *Phys. Rev. B.*, **46**, 1804 (1992)

2) D. Takagi *et al.*, *Nano. Let.*, **12**, 2642 (2006)

3) H. Tsunoyama *et al.*, *Langmuir.*, **20**, 11293 (2004).

**Corresponding Author:** Shinohara Hisanori

**Tel&Fax:** +81-52-789-2482/+82-52-747-6442

**E-mail:** noris@nagoya-u.jp

## Interaction-dependent Chirality Separation of Single-Wall Carbon Nanotubes by Multicolumn Gel Chromatography

○Huaping Liu<sup>1,2</sup>, Daisuke Nishide<sup>1,2</sup>, Takeshi Tanaka<sup>1</sup>, Hiromichi Kataura<sup>1,2</sup>

<sup>1</sup>*Nanosystem Research Institute, National Institute of Advanced Industrial Science and Technology (AIST), Tsukuba, Ibaraki 305-8562, Japan*

<sup>2</sup>*Japan Science and Technology Agency, CREST, Kawaguchi, Saitama 330-0012, Japan*

Small variations in diameter and chirality will bring striking changes in the electronic and optical properties of single-wall carbon nanotubes (SWCNTs). Therefore, mono-structured SWCNTs are essential for both the scientific research and practical applications such as electronic and optical devices. Recently, we developed simple methods for continuous separation of metallic (M)- and semiconducting (S)-SWCNTs using agarose gel [1-3]. Moreover, successively increasing sodium deoxycholate solution concentration during collection of S-SWCNTs permitted low-resolution diameter separation [2, 3], but further chirality separation is not possible.

In this presentation, we report a simple and effective method for large-scale chirality separation of SWCNTs using single-surfactant multicolumn gel chromatography (SS-MUGEC) that uses only one surfactant (sodium dodecyl sulfate) and a series of gel columns (commercial Sephacryl gel) [4]. We succeeded in isolating 13 kinds of single-chirality species from HiPco-SWCNTs (diameter,  $1.0\pm 0.3$  nm) just by injecting an excess of nanotube dispersion into the gel column series. This simple method is based on the structure-dependent interaction of SWCNTs with the gel. The nanotubes with the highest interaction with the gel are preferentially adsorbed in the top column whereas the nanotubes with the lower interaction with the gel are adsorbed in the following gel columns. In this manner, chirality-separation of SWCNTs was achieved. Metallic SWCNTs were finally collected as unbound nanotubes because of their lowest interaction with the gel. Because this method is simple, quick, high-efficiency, continuous and inexpensive, separation in an industrial scale is expected. We believe that this brand-new powerful method for chirality-separation will open a new research field and accelerate the practical applications of SWCNTs.

### References:

- [1] T. Tanaka et al. *Appl. Phys. Express* **2** (2009) 125002.
- [2] H. Liu et al., *J. Phys. Chem. C* **114** (2010) 9270.
- [3] H. Liu et al., *Phys. Status Solidi B* **247** (2010) 2649.
- [4] H. Liu et al. submitted.

Corresponding Author: Hiromichi Kataura

TEL: +81-29-861-2551, FAX: +81-29-861-2786, E-mail: [h-kataura@aist.go.jp](mailto:h-kataura@aist.go.jp)

## Effects of Laser Wavelength and Power on the Selective Separation for Metal Single-walled Carbon Nanotubes with OPO Laser Irradiation

Akira Kumazawa, Isamu Tajima, Katsumi Uchida, Koji Tsuchiya, Tadahiro Ishii, and Hirofumi Yajima

*Department of Applied Chemistry, Faculty of Science, Tokyo University of Science  
1-3 Kagurazaka, Shinjuku-ku, Tokyo 162-0826, Japan*

As-synthesized single-walled carbon nanotubes (SWNTs) comprise of various chiral structures responsible for metallic (m) and semiconducting (s) SWNTs. Selective separations of m- and s-SWNTs have been requested for practical and advanced applications. Thereof, we have developed a new selective separation technique for m-SWNTs with nanosecond pulsed optical parametric oscillator (OPO) laser operated with wavelength tunability.<sup>[1]</sup> This paper is concerned with the effects of the laser wavelength and power on the selective separations of m-SWNTs from individually dispersed SWNTs with the dispersants such as carboxymethylcellulose (CMC) and dodecylbenzenesulfonic acid sodium salt (NaDDBS) in aqueous solutions. Individually dispersed SWNTs exhibited the UV-vis-NIR absorption spectra with the characteristic peaks composed of three band regions (400-1600 nm) of M11, S11 and S22 corresponding to m-SWNTs first transitions, and s-SWNTs first and second transition bands, respectively. In the laser irradiation performance, the OPO laser was operated under the condition of 10 Hz with laser fluences in the range of 1.3 – 22.9 MW/cm<sup>2</sup> per one pulse at 2.16 x 10<sup>5</sup> pulse number. The characterization of SWNTs in the solutions before and after laser irradiation was carried out with UV-vis-NIR absorption/photoluminescence (PL) and resonance Raman spectral measurements, and dynamic light scattering (DLS). As a result, the OPO laser with a wavelength in the S11 or S22 region brought merely about the destruction of the dispersed s-SWNTs through photo-thermal conversion process, the m-SWNTs remaining unchanged. In the CMC dispersion system, the maximum collection efficiencies for m-SWNTs were achieved under the condition of a laser fluence of 6.4 MW/cm<sup>2</sup> at 778 nm (S<sub>22</sub>) and 19.1 MW/cm<sup>2</sup> at 989 nm (S<sub>11</sub>). Consequently, the OPO irradiation technique was suggested to be a promising method to efficiently gain m-SWNTs.

[1] Isamu Tajima et al. The 36<sup>th</sup> Fullerenes-Nanotubes General General Symposium Abstract 3P-5

\*Corresponding Author: Hirofumi Yajima

TEL: +81-3-3260-4272(ext.5760), FAX: +81-3-5261-4631, E-mail: [yajima@rs.kagu.tus.ac.jp](mailto:yajima@rs.kagu.tus.ac.jp)



## Super-growth: Combining High Yield with High Crystallinity

○ Hiroe Kimura<sup>1</sup>, Don N. Futaba<sup>1</sup>, Motoo Yumura<sup>1</sup>, and Kenji Hata<sup>1</sup>

<sup>1</sup>*Nanotube Research Center, National Institute of Advanced Industrial Science and Technology (AIST), Tsukuba, 305-8565, Japan.*

A number of obstacles face the carbon nanotube field, such as low cost, high yield, and high purity. Super-growth chemical vapor deposition (CVD) method, through the demonstration of high efficiency, vertically aligned single-walled carbon nanotube (SWNT) synthesis, has shown the potential to simultaneously overcome these three obstacles [1]. However, one aspect in the CNT field which remains a difficulty is the high yield, high purity synthesis with high crystallinity.

Here, we report the synthesis of high crystallinity, SWCNT forests based on super-growth CVD. Using an iron thin film catalyst and the sequential optimization of the temperature, the carbon level, and the water level, we succeeded in synthesizing SWNT forests with a 10-fold increase graphitic-to-disorder band ratio (G/D) from the typical  $\sim 7$  to up to 70 while maintaining SWNT selectivity. Characterization of the forest structure through transmission electron microscopy and scanning electron microscopy showed exceptionally straight SWNTs. Furthermore, characterization of the forest properties, such as thermal diffusivity and dispersion, showed significant improvement compared to the standard super-growth SWNT forests.

### References:

[1] K. Hata *et al*, *Science*, **306**, 1241 (2004)

Corresponding Author: Kenji Hata

TEL: (029) 861-44402, FAX: (029) 861-4851, E-mail: kenji-hata@aist.go.jp

## Purification and Characterization of Graphitic Polyhedra Grown by Laser Vaporization of Graphite Containing Silicon or Boron

○Eriko Noguchi, Iori Nozaki, Hajime Chigusa, Homare Tanogami, Akira Koshio,  
and Fumio Kokai

*Division of Chemistry for Materials, Graduate School of Engineering, Mie University  
1577 Kurimamachiya, Tsu, Mie 514-8507, Japan*

Graphitic carbon nanostructures are of great interest in fundamental research and application in various fields. We fabricated polyhedral graphite particles with diameters of 100–1000 nm by CO<sub>2</sub> laser vaporization of graphite at room temperature [1]. To form the particles with a 90% yield, a high-pressure (>0.8 MPa) Ar gas atmosphere was required to confine laser-vaporized carbon species and maintain their high temperatures. Transmission electron microscopy (TEM) images of the central parts of the particles showed closed shells (~5 nm in diameter) and concentric frameworks of graphene layers [2, 3]. The particles exhibited interesting behavior under high-pressure compression, probably due to a topological difference from bulk graphite [3]. However, for further investigation of other properties and applications of the particles, such as tribology [4] and battery electrodes, development of a larger-scale production and purification method is favorable. Here we report the coexistence of a small amount of silicon or boron promotes the growth of graphitic polyhedral (GP) particles and also report purification and characterization of the GP particles.

Laser vaporization of graphite containing Si or B (1 and 2 at.%) was carried out in the presence of Ar gas in the same way as reported in previous studies [1, 2]. A powder of Si or B<sub>4</sub>C was mixed with a graphite powder and was pressed into pellets. The laser beam from a continuous wave Nd:YAG laser was focused on the pellet targets through a quartz window installed in a stainless-steel chamber filled with Ar gas (0.2 and 0.3 MPa) at room temperature. The laser size and the power density on the target were adjusted to 2 mm and about 18 kW/cm<sup>2</sup>, respectively, and the laser irradiation time was set to 2 s. To purify the deposits containing GP particles, the deposits (10 mg), produced using 30–40 laser shots, were treated at 200–700 °C in a pure oxygen atmosphere for 1 h using an electric furnace.

The growth of GP particles was promoted even at low pressures of 0.1 and 0.2 MPa. After heat treatment in an oxygen atmosphere, the changes in the weights of deposits containing GP particles with incorporation of Si were measured and analyzed as a function of treatment temperature. The relative weights of the deposits gradually decreased up to 400 °C and rapidly decreased at 400–700 °C. TEM examination revealed that the removal of non-GP particles such as amorphous carbon and single-wall carbon nanohorn particles corresponded to the weight decrease. TEM examination also indicated the deposits became almost completely composed of GP particles at 550 °C. A similar behavior was also observed for GP particles containing B atoms. The removal of non-GP particles was confirmed by Raman spectra measurements. The XPS spectra of GP particles containing Si indicated the Si concentration is unusually high (Si/C = ~0.18).

[1] F. Kokai *et al.*, *Appl. Phys. A* **77**, 69 (2003).

[2] F. Kokai *et al.*, *Carbon* **42**, 2515 (2004).

[3] A. Nakayama *et al.*, *Appl. Phys. Lett.* **84**, 5112 (2004).

[4] M. Ishihara *et al.*, *Carbon* **45**, 880 (2007).

**Corresponding Author:** Fumio Kokai, **E-mail:** kokai@chem.mie-u.ac.jp, **Tel:** +81-59-231-9424.

# The molecular structure and vibrational spectroscopy of hydroxylated nanodiamonds

Kousuke Usui 1, Yoshio Nishimoto 1, Alister J. Page 2, Henryk A. Witek 3, Stephan Irle 1  
 1 Nagoya University, 2 Kyoto University, 3 National Chiao Tung University, Taiwan

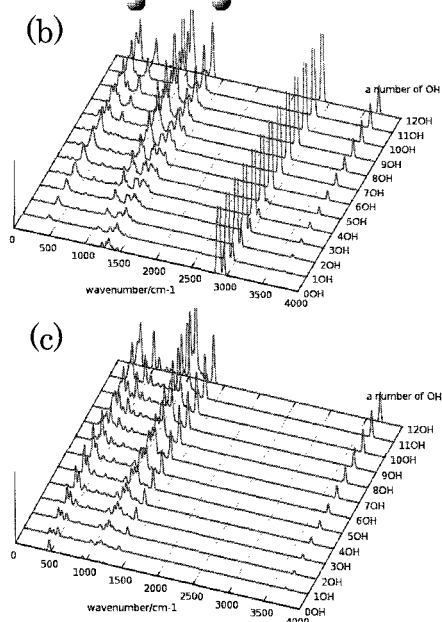
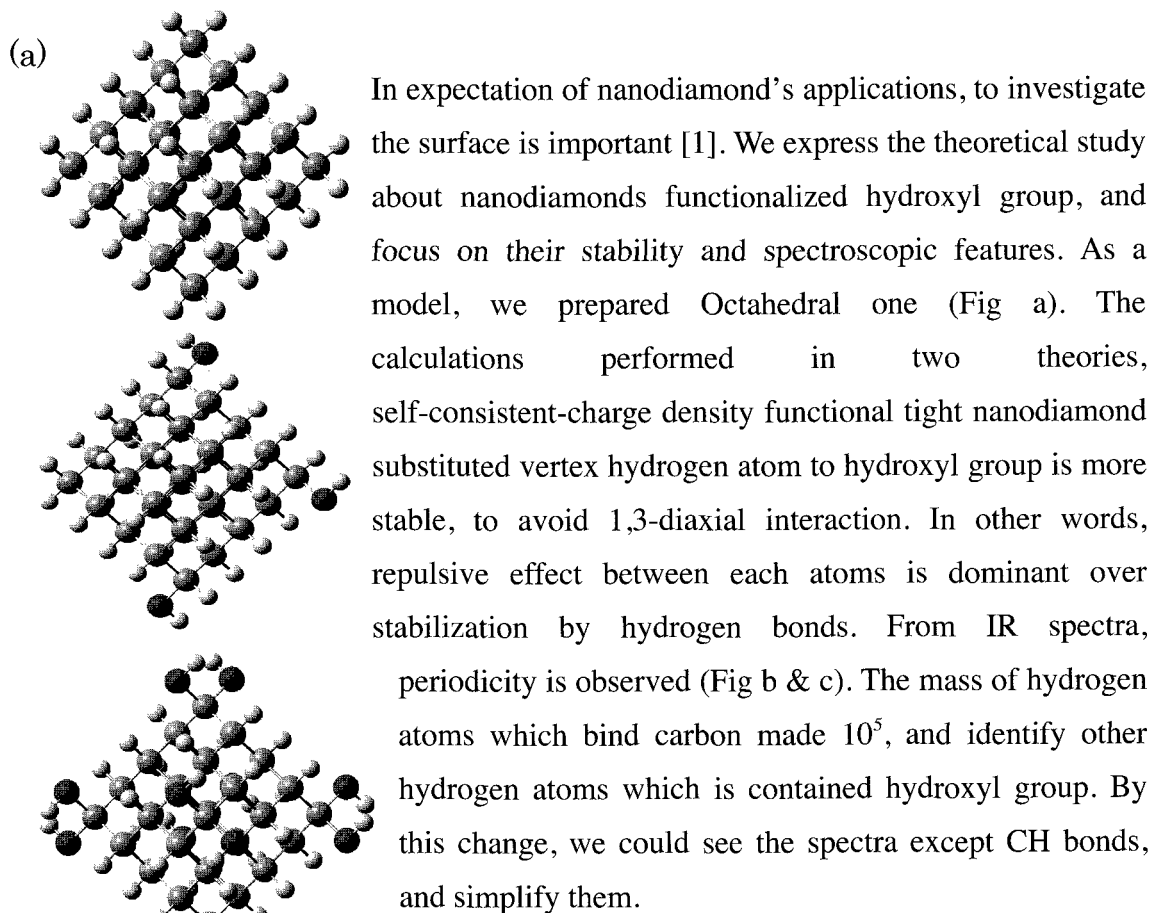


Figure 1

(a) Octahedral model. ( $C_{35}H_{36}$ ,  $C_{35}H_{36}O_3$ ,  $C_{35}H_{36}O_{12}$ )

(b) Spectra.

(c) Spectra using heavy hydrogen atom.

## References

[1] W. Li et al. ACS Nano 2010, 8, 4475-4486.

Corresponding Authors: Kousuke Usui, Stephan Irle.

E-mail: usui.kosuke@f.mbox.nagoya-u.ac.jp

## Observation of void in DMFC electrode composed with carbon nanocoil

○S. Kaida<sup>1</sup>, Y. Suda<sup>1</sup>, H. Tanoue<sup>1</sup>, H. Takikawa<sup>1</sup>, S. Oke<sup>2</sup>,  
H. Ue<sup>3</sup>, T. Okawa<sup>4</sup>, N. Aoyagi<sup>4</sup>, K. Shimizu<sup>5</sup>

<sup>1</sup>*Department of Electrical and Electronic Information Engineering,  
Toyohashi University of Technology,*

<sup>2</sup>*Tsuyama National College of Technology,*

<sup>3</sup>*Tokai Carbon Co., Ltd.,*

<sup>4</sup>*Daiken Chemical Co., Ltd.,*

<sup>5</sup>*Shonan Plastic Mfg. Co., Ltd.*

The void density in direct methanol fuel cell (DMFC) electrode has to be properly controlled for increase in performance. We have used arc-black (AcB), an amorphous carbon nanoparticle synthesized by arc discharge, as a catalyst support material in DMFC electrodes [1]. Recently, we showed that, when carbon nanocoil (CNC) was used in the DMFC cathode, the output became higher than that using AcB. Owing to its spiral shape, CNC can produce a lot of voids in the electrode. In this study, we made the DMFC cathodes using catalyst-supported AcB, CNC and crushed CNC and observed the voids in the electrodes by scanning electron microscopy (SEM). Fig. 1 shows SEM micrographs of the electrodes. (b) CNC electrode seems to have the biggest void and (a) AcB electrode the smallest.

This work has been partly supported by the Outstanding Research Project of the Venture Business Laboratory from Toyohashi University of Technology (TUT); Global COE Program "Frontiers of Intelligent Sensing" from the Ministry of Education, Culture, Sports, Science and Technology (MEXT); Core University Programs (JSPS-CAS program in the field of "Plasma and Nuclear Fusion") from the Japan Society for the Promotion of Science (JSPS), Grant-in-Aid for Scientific Research from the MEXT, Toukai Foundation for Technology, Research Foundation for Materials Science, and Chubu Science and Technology Center.



Fig.1. SEM micrographs of electrodes. (a) AcB, (b) CNC, (c) crushed CNC

[1] Oke, et al., Chemical Engineering Journal, Vol. 143 (2008) pp. 225-229.

Corresponding Author: Yoshiyuki Suda

E-mail: suda@ee.tut.ac.jp, Tel: 0532-44-6726

## Vibrational and NMR properties of Polyynes and Microscopic studies of Polyynes@SWNT

○ Md. Mahbubul Haque<sup>1</sup>, Lichang Yin<sup>2</sup>, Ahmad R. T. Nugraha<sup>3</sup>, Riichiro Saito<sup>3</sup>, Tomonari Wakabayashi<sup>4</sup>, Yohei Sato<sup>1</sup>, Masami Terauchi<sup>1</sup>

<sup>1</sup>*Institute of Multidisciplinary Research for Advanced Materials  
Tohoku University, Sendai, 980-8577, Japan*

<sup>2</sup>*Shenyang National Laboratory for Materials Science, Institute of Metal Research,  
Chinese Academy of Science, 72 Wenhua Road, Shenyang, 110016, China*

<sup>3</sup>*Department of Physics, Tohoku University, Sendai, 980-8578, Japan*

<sup>4</sup>*Department of Chemistry, School of Science and Engineering, Kinki University  
Kowakae 3-4-1, Higashi Osaka 577-8502, Japan*

Polyynes are finite-sized, one-dimensional linear molecules of carbon atoms with alternate single and triple C–C bonds and hydrogen termination at the both ends. They are commonly expressed by  $C_{2n}H_2$ , where  $n$  is an integer. The bond-stretching phonon modes of such linear polyynes are calculated as a function of chain length within the density functional theory. There are two intense Raman bands so called  $\alpha$  and  $\beta$  bands in the higher frequency region around 2000 – 2200  $cm^{-1}$ . The frequency of  $\alpha$  mode monotonically decreases with the increase of polyyne chain length while that of the  $\beta$  mode shows oscillating behavior, which are consistent with previous Raman measurements [1]. The nature of  $\alpha$  phonon mode is such that it is the bond-stretching mode with fixed hydrogen atoms while the  $\beta$  mode is the bond-stretching mode with changing the length of the molecule. The relative Raman intensities of the two phonon modes are evaluated by optimized geometries for ground states and excited states. The vibration induced by the photo-excited carriers mainly consists of  $\alpha$  mode, which explains the stronger relative Raman intensity for  $\alpha$  mode than that for the  $\beta$  mode for all  $C_{2n}H_2$  molecules. We also present a nuclear magnetic resonance (NMR) calculation for spin-spin coupling constants as a function of distance between  $^1H$  and  $^{13}C$  nuclei and, within  $^{13}C$  nuclei, up to the polyyne center of symmetry. We compare the calculated results with recent NMR experiments [2]. In the case of spin-spin coupling among  $^{13}C$  nuclei, since  $J_{CC}$  does not much depend on the atomic position but much on the relative distance between the two atoms, we expect a detailed analysis of fine structure of NMR shifts.

We recently obtained HRTEM image of polyynes@SWNT (polyyne inside single-wall carbon nanotube). We will report our microscopic study e.g. electron energy loss spectroscopy (EELS) for polyynes in the near future.

[1] Tabata H, Fujii M, Hayashi S, Doi T, Wakabayashi T, *Carbon*, **44**, 3168 (2006)

[2] Wakabayashi T, Tabata H, Doi T, Nagayama H, Okuda K, Umeda R, *Chem Phys Lett*, **433**, 296 (2007)

Corresponding Author: Md. Mahbubul Haque

TEL: + 81-(0)22-217-5374, FAX: +81-(0)22-217-5373, E-mail: [mmhaque@mail.tagen.tohoku.ac.jp](mailto:mmhaque@mail.tagen.tohoku.ac.jp)

## Chromatographic Separation of Highly Soluble Nanodiamond Prepared by Polyglycerol Grafting

○Naoki Komatsu<sup>1</sup>, Li Zhao<sup>1</sup>, Tatsuya Takimoto<sup>1</sup>, Masaaki Ito<sup>2</sup>, Naoko Kitagawa<sup>1</sup>,  
Takahide Kimura<sup>1</sup>

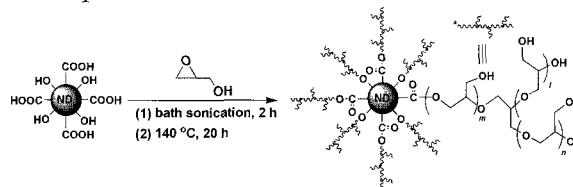
<sup>1</sup> Department of Chemistry, Shiga University of Medical Science, Seta, Otsu, 520-2192, Japan

<sup>2</sup> Organic Chemical Company, Daicel Chemical Industries, Ltd., 2-1-4 Higashisakae, Ohtake, Hiroshima 739-0605, Japan

Biomedical applications of nanodiamond (ND) have been investigated extensively due to its low toxicity, non-bleaching fluorescence and high extensibility of the surface functionality through covalent organic functionalization. For the purpose, ND should first form a stable hydrosol under a physiological environment. In

order to increase the solubility, we change the surface functionality of ND from conventional linear polyethers (PEG) [1] to hyperbranched polyglycerols (PG) (Scheme 1). We choose the PG functionality for the following reasons: high hydrophilic property, biocompatibility, hyperbranched structure and easy functionalization. As a result, the PG grafted ND (ND-PG) exhibited extremely high solubility (16 mg/mL) in phosphate buffer saline (PBS) [2].

The solubilized ND-PG passed through silica-based columns in the size exclusion chromatography (SEC) under a flow of a pH 7.0 buffer as a mobile phase [2]. The scanning transmission electron microscopy (STEM) and dynamic light scattering (DLS) measurements of the fractions reveal that ND-PG is successfully separated according to their sizes (Figure 1). Size-sorting of ND-PG by SEC is believed to make a great progress in view of cancer imaging utilizing enhanced permeability and retention (EPR) effect in solid tumors.



**Scheme 1.** Synthesis of ND functionalized by hyperbranched polyglycerol through ring-opening polymerization of glycidol

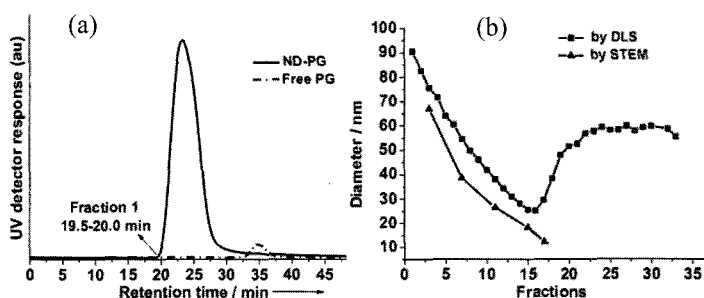


**Figure 1.** (a) Chromatograms in the elutions of ND-PG and free PG; (b) Median and average diameters (nm) of the eluted particles determined by DLS and STEM, respectively.

**Reference:** [1] T. Takimoto, N. Komatsu, et al., *Chem. Mater.*, **22**, 3462 (2010), [2] L. Zhao, T. Takimoto, N. Komatsu, et al., *Angew. Chem. Int. Ed.*, in press (10.1002/anie.201006310)

**Corresponding Author:** Naoki Komatsu, **E-mail:** nkomatsu@belle.shiga-med.ac.jp

**Tel:** +81-77-548-2102, **Fax:** +81-77-548-2405

## 1 MeV electron irradiation-induced structural changes of nanometer-sized diamond particles

○Koji Asaka<sup>1</sup>, Tomohiro Terada<sup>1</sup>, Shigeo Arai<sup>2</sup>, Nobuo Tanaka<sup>2</sup>, Eiji Ōsawa<sup>3</sup>, Yahachi Saito<sup>1</sup>

<sup>1</sup> Department of Quantum Engineering, Nagoya University, Nagoya 464-8603, Japan

<sup>2</sup> High Voltage Electron Microscope Laboratory, Nagoya University Ecotopia Science Institute, Nagoya 464-8603, Japan

<sup>3</sup> NanoCarbon Research Institute, AREC, Shinshu University, Ueda 386-8567, Japan

Electron irradiation-induced structural changes of nanometer-sized diamond particles (NDPs) were *in situ* studied by transmission electron microscopy (TEM) and electron energy loss spectroscopy (EELS).

The NDPs with an average diameter of  $4.8 \pm 0.5$  nm were supplied by NanoCarbon Research Institute, which were produced by detonation techniques. The specimens for TEM observation were prepared by dispersing the NDPs into isopropyl alcohol and dropping the alcohol solution on a molybdenum microgrid coated with a lacy carbon film. The specimen was mounted on a specimen holder with a heating stage and irradiated at room temperature and 973 K in a high-voltage transmission electron microscope (JEM-1000KRS) equipped with a post-column imaging filter. The microscope was operated at an acceleration voltage of 1 MV. The structural changes of the NDPs during irradiation were observed by a CCD camera. The EELS measurements were carried out by using the imaging filter in the imaging mode.

During the electron irradiation at room temperature, the NDPs disintegrated into disordered carbon materials such as amorphous carbon. The disordered materials sublimated and finally disappeared. On the other hand, the irradiation at 973 K caused to the transformation of the NDPs into carbon onions. Figures 1(a) and 1(b) show TEM images of the NDPs at 973 K after a few minutes of irradiation and after 20 min, respectively. The graphitic layers began to be formed at the surface of the NDPs, and proceeded to the center of the NDPs. Figure 2 shows the core-loss spectra in the carbon K-edge region for the NDPs and the transformed carbon onions. A peak appearing at  $> 290$  eV corresponds to the  $1s \rightarrow \sigma^*$  transition. For the carbon onions, in addition to the  $\sigma^*$  peak, a peak at 285 eV corresponding to the  $1s \rightarrow \pi^*$  transition appears significantly. The spectra show that the changes in the chemical bonding in the NDPs, i.e., transition of  $sp^3$  to  $sp^2$  type bonding, occurred by the electron irradiation at 973 K. In this experiment, the transformation of the carbon onion to diamond during irradiation was not observed, though this reverse transformation has been reported for the onions with more than 10 nm in diameter at a temperature above 850 K[1].

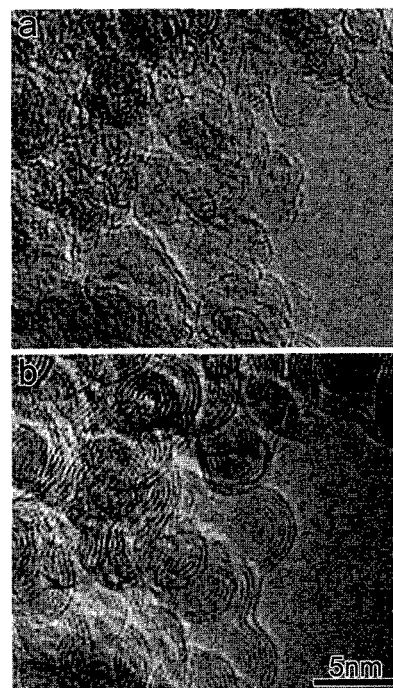


Fig. 1 TEM image of NDPs at a specimen temperature of 973 K after a few minutes of irradiation (a) and after 20 min (b).

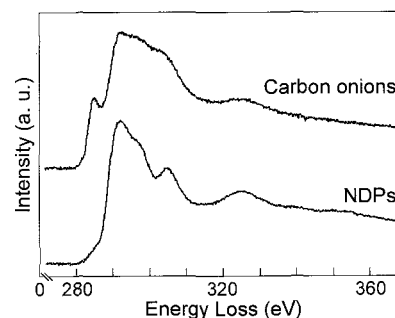


Fig. 2 EELS spectra of NDPs and carbon onions.

[1] F. Banhart, *J. Appl. Phys.* **81**, 3440 (1997).

Corresponding Author: Koji Asaka

TEL: +81-52-789-3714, FAX: +81-52-789-3703, E-mail: asaka@nuqe.nagoya-u.ac.jp

## Superparamagnetic behavior of carbon nanofoam produced from iron free carbon powder

○Makoto Jinno, Hirohito Asano, Takahiro Mizuno,  
Sumio Iijima, Shunji Bandow

*Department of Materials Science and Engineering, Meijo University,  
1-501 Shiogamaguchi, Tenpaku, Nagoya 468-8502, Japan*

Several previous studies [1,2] reported ferromagnetic behavior based on the localized zigzag edge states of graphene [3,4]. Such zigzag edge is generally unstable in air and subsequently reacts with some chemical species. This kind of reaction normally quenches the ferromagnetism. On the other hand, mono-hydrogenated zigzag edges make the system somewhat stable and the ferromagnetic spin arrangement remains along the zigzag edge [3]. Mono-hydrogenated and di-hydrogenated zigzag edges are convenient for stabilizing the edge states without quenching the strong magnetism [5].

Although the carbon ferromagnetism includes quite interesting subjects for both the fundamental science and application technology, it is very difficult to exclude the magnetic impurity effect. In the previous study, about 100-300 ppm of iron was detected in both magnetic attractive (prod. in H<sub>2</sub>) and in-attractive (prod. in Ar) carbon nanofoam (CNF). However, even detecting such quantities of iron, observed  $M_s$  (saturation magnetization) cannot be explained. In the present study, we carefully removed such ferromagnetic impurity from the starting materials by the following acid treatment and checked reproducibility of strong magnetism.

500 mg of carbon powder (Kojyundo Kagaku 99.7 %, 5  $\mu\text{m}$ ) was treated in 20 ml of concentrated HCl for 1 day. After this treatment, liquid was slightly colorized in brownish yellow, indicating the existence of Fe<sup>3+</sup> ion. Then the liquid was decanted. Carbon powder thus purified was rinsed twice by using ethanol. Then the powder was heated at 120 °C in vacuum and used for making the target for laser vaporization. CNF sample was produced by the laser vaporization in the flux (100 sccm) of 3 % H<sub>2</sub> containing Ar balance gas at 1000 °C. XRD profile of the product is in Fig. 1, which is the same as the previous CNF. MH curves at various temperatures are in Fig. 2, which clearly show easy saturatable feature at 400 K. Interesting fact is that no hysteresis was observed at 4.2 K, which indicates that the superparamagnetism is applicable down to 4.2 K.

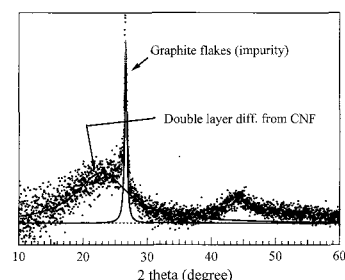


Fig. 1. XRD pattern of the product

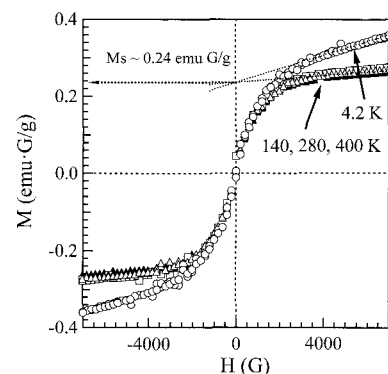


Fig. 2. MH curves at 4.2, 140, 280 and 400 K

- [1] A.V. Rode et al., *Phys. Rev.* **B70**, 054407 (2004)      [2] J. Červenka et al., *Nature Phys.* **5**, 840 (2009)  
[3] M. Fujita et al., *J. Phys. Soc. Jpn.* **65**, 1920 (1996)      [4] K. Nakada et al., *Phys. Rev.* **B54**, 17954 (1996)  
[5] K. Kusakabe, M. Maruyama, *Phys. Rev.* **B67**, 092406 (2003)

**Corresponding Author:** Shunji Bandow, **E-mail:** bandow@meijo-u.ac.jp, **Tel&Fax:** +81-52-834-4001



## Synthesis of Carbon Nanowalls by a Submarine-style Substrate Heating Method

○Hiroyuki Yokoi, Fumihiro Ishihara, Tatsunori Isoda, Kentaro Takesue

*Department of Materials Science and Engineering, Kumamoto University, Kumamoto  
860-8555, Japan*

We have developed a new method for the synthesis of carbon nanotubes (CNTs) named submarine-style substrate heating method [1]. The method is based on the liquid-phase deposition method [2], in which a catalyst-coated silicon substrate is electrically heated to high temperatures around 1000 K in liquid hydrocarbon. The liquid-phase deposition method has realized a simple and rapid growth of CNTs. However, catalysts employed in the method need to be tough enough to bear the boiling in liquid hydrocarbon, which limits the catalysts applicable to the method. In the submarine-style substrate heating method, we applied a zeolite-supported metal nanoparticle catalyst, which used to be washed away during the synthesis in the liquid-phase deposition method, and succeeded in synthesizing single-walled CNTs and double-walled CNTs [1]. In this study, we have applied the method to synthesize carbon nanowalls (CNWs). CNWs are two dimensional carbon nanostructures consisting of plane graphene layers mounted vertically on a substrate, and are attracting attentions as materials for electron field emitters, nanoparticle supporters and so on. In the previous studies, CNWs were grown by microwave plasma enhanced chemical vapor deposition [3].

In the experiments, iron-cobalt composite catalyst supported on ultra-stable Y-type zeolite was employed. Catalyst-dispersed ethanol was dropped on a silicon substrate and dried to form a catalyst coating. The substrate was inserted into ethanol liquid (99.5% in purity) with the reaction space being filled with argon gas. The substrate was electrically heated to 1173 K for 10 min. Deposits on the substrate were analyzed with scanning electron microscopy and found to consist of wall-like structures with the unit of 10-100 nm in length, which is a typical feature of CNWs. The submarine-style substrate heating method will provide much simpler approach to the growth of CNWs.

[1] H. Yokoi et al., The 38<sup>th</sup> Fullerenes Nanotubes General Symposium, 3P-21 (2010)

[2] M. Nishitani-Gamo et al., *Jpn. J. Appl. Phys.* **46**, 6329 (2007).

[3] Y. Wu et al., *Adv. Mater.* **14**, 64 (2002).

Corresponding Author: Hiroyuki Yokoi

TEL: +81-96-342-3727, FAX: +81-96-342-3710, E-mail: yokoihr@kumamoto-u.ac.jp

## Evolution of the DTA-TG curves as a function of sample mass containing LaC<sub>2</sub> nano-crystallites engaged in multi-shell carbon nanocapsules

○Kazunori Yamamoto<sup>a</sup>, Takeshi Akasaka<sup>b</sup>

<sup>a</sup>Quantum Beam Materials Synthesis Research Group, Quantum Beam Science Directorate,  
Japan Atomic Energy Agency, Tokai-mura, Naka-gun, Ibaraki 319-1195, Japan

<sup>b</sup>Center for Tsukuba Advanced Research Alliance, University of Tsukuba, Ibaraki 305-8577, Japan

### Abstract:

There has been great interest in the incorporation of metal elements into fullerenes, nanotubes, and fullerene-like multi-shell cage structures such as polyhedral multi-shell nanocapsules.

Polyhedral multi-shell nanocapsules containing La element were found for the first time in carbonaceous cathode deposits formed on the cathode surface in the conventional DC arc experiment for La fullerene formation [1, 2]. Electron diffraction (ED) revealed that the capsules were filled with LaC<sub>2</sub> single crystals, not La metals [2]. Transmission electron microscopy (TEM) characterization showed that the endohedral multi-shell nanocapsules were observed mostly in the cathode deposit, not in the fullerene soot on wall of the apparatus. Recently we reported that the endohedral multi-shell nanocapsules were obtained easily by vacuum heat treatment (1000 – 2200 °C) of La fullerene soot, which was prepared at special He pressure of 30-50 Torr [3].

It is well known that lanthanum carbide (LaC<sub>2</sub>) is a water reactive and flammable solid. However, LaC<sub>2</sub> crystallites in carbon nanocapsules cannot react with water at room temperature, because water molecules cannot penetrate graphitic wall of nanocapsules. The presence of graphitic walls lowers reactivity of the engaged LaC<sub>2</sub> and shifts the combustion reaction of LaC<sub>2</sub> toward high temperatures [3]. Thus the combustion temperature of LaC<sub>2</sub> in carbon nanocapsules should be a good measure for estimating the toughness of the individual graphitic cages.

The toughness tests of carbon nanocapsules towards the combustion of LaC<sub>2</sub> are studied by simultaneous gravimetric and differential thermal analysis (TG-DTA) with a SEIKO TGDTA6300 apparatus. 0.4-1.6 mg of the sample is loaded in an alumina crucible and heated from room temperature to 930 °C (10 deg/min) in airflow (200 mL/min). We have revealed that the sample mass can significantly influence the results of TG-DTA data. The form of the signals in TG-DTA chart varies with the sample masses. For the sample masses above than 0.6 mg, one steep and sharp exothermic peak is observed on DTA curve, which is assigned as a runaway peak.

### References:

1. R. S. Ruoff, et al., *Science*, **259**, 336(1993).
2. M. Tomita, et al., *Jpn. J. Appl. Phys.*, **32**, L280(1993).
3. K. Yamamoto, et. al., The 34th Fullerene Nanotube General Symposium Abstract 2-14.

**Corresponding Author:** Kazunori Yamamoto

**E-mail:** yamamoto.kazunori@jaea.go.jp

**Tel&Fax:** +81-29-282-6474&+81-29-284-3813.

## Chemical vapor deposition of BN-doped graphite thin films

Satoru Suzuki and Hiroki Hibino

NTT Basic Research Laboratories, NTT Corporation  
3-1 Morinosato- Wakamiya, Atsugi, Kanagawa 243-0198, Japan  
e-mail: ssuzuki@will.brl.ntt.co.jp

Graphene is one of the most promising materials as a constituent of future nanoelectronics because of the excellent electronic properties and chemical stability. Formation and tuning of a bandgap is crucial for electric applications of graphene. Doping of boron nitride, which has a large band gap, into graphene may be useful for the band gap tuning. CVD growth of BCN graphene films using a BN-containing feedstock has recently been reported [1]. Here, we report CVD growth of BN-doped graphene, using separated B- and N-containing feedstocks.

Doped graphene and graphite thin films were grown on a Ni film using the thermal CVD technique. Triisopropyl borate and benzylamine were the boron and nitrogen feedstocks, respectively. Both materials also served as a carbon feedstock, and we did not use any other carbon feedstock. In Raman spectra, the G, D, and G' bands were clearly observed, meaning that the films mainly consist of graphene. TEM observation also showed that graphene layers are formed on the Ni surface. Core-level x-ray photoelectron spectroscopy (XPS) measurements revealed that the film compositions are roughly expressed as  $B_xC_yN_x$  ( $0 \leq x \leq 0.15$ ). That is, B and N contents are close. The B, N, C 1s XP spectra of two films [samples 1 ( $B_{0.12}C_{0.74}N_{0.14}$ ) and 2 ( $B_{0.13}C_{0.72}N_{0.15}$ )] are shown in Fig. 1. The results indicate that boron (nitrogen) atoms are predominantly bonded to nitrogen (boron). Despite the use of the separated B- and N-containing feedstocks, the films seem to mainly consist of graphene and boron nitride domains which are separated from each other.

### References

- [1] Ci et al., Nat. Mater. **9**, 430 (2010).

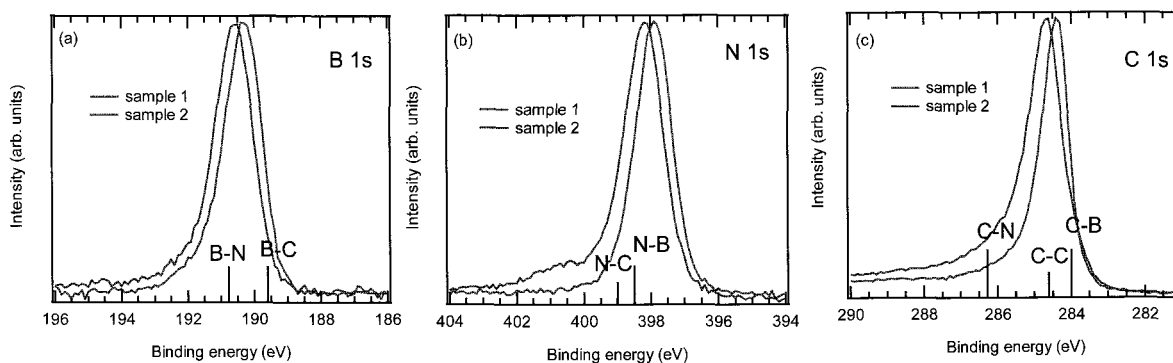


Fig. 1. (a) B, (b) N, and (c) C 1s XP spectra of two samples. Typical binding energy positions of are denoted in the figures.

## Theoretical Study of Aromaticity by Nucleus-Independent Chemical Shifts in Nanographenes

○Yoshihiro Tsumura, Hiroyuki Fueno, and Kazuyoshi Tanaka

*Department of Molecular Engineering, Graduate School of Engineering,  
Kyoto University, Kyoto, 610-8510 Japan*

The electronic structure of nanographene being fraction of a graphene sheet is of interest with respect to its aromaticity. In this work, a nanographene structure has theoretically been examined based on the DFT calculation (B3LYP/6-31G\*\*). In particular, the NICS (nucleus-independent chemical shifts) values are employed for check of the aromaticity depending on the position of benzene-like ring.

A typical result is shown in Figs.1 and 2, where the markers are common in these figures. In Fig. 2 are shown the NICS values for the fictitious atom as the probe moving from the nanographene plane to 5 Å above in each position. Since the negative NICS value represents larger aromaticity, the center and the edge areas of this nanographene are more aromatic compared with others, signifying difference of the  $\pi$ -electron delocalization features.

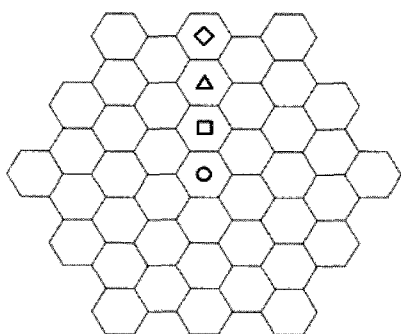


Figure 1. A nanographene structure with the armchair edge.

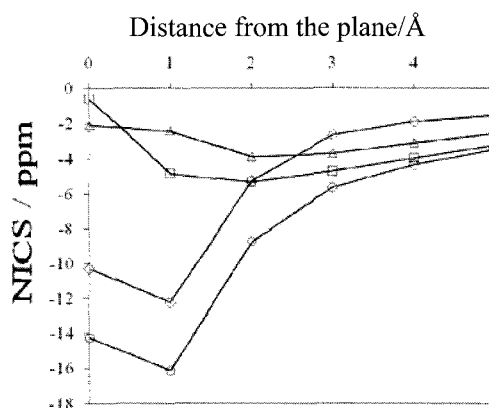


Figure 2. NICS results of the nanographene in Figure 1.

Corresponding Author: Kazuyoshi Tanaka

TEL: 075-383-2549, Fax: 075-383-2555, E-mail: [ktanaka@moleng.kyoto-u.ac.jp](mailto:ktanaka@moleng.kyoto-u.ac.jp)

## Comparison study on CVD synthesis of graphene using ethanol and dimethyl ether

○Bo Hou, Xiao Chen, Erik Einarsson, Shohei Chiashi, and Shigeo Maruyama  
Department of Mechanical Engineering, The University of Tokyo, 7-3-1 Hongo,  
Bunkyo-ku, Tokyo, 113-8656, Japan

Graphene, a monolayer of carbon atoms arranged into a hexagonal lattice, has attracted great interest because of its unique structure and promising properties. [1] Chemical vapor deposition (CVD) is a powerful tool for large-scale and low-cost synthesis of nano-carbon materials. [2,3] However, comparable simple and controllable CVD growth of graphene remains a challenge. Herein, we demonstrate a facile and stable CVD method to synthesize graphene on a Ni film and compare the results obtained when using two different carbon sources: ethanol and dimethyl ether (DME).

Monolayer graphene was synthesized on Ni film by ethanol and DME without annealing gas or special cooling steps during CVD. To investigate the carbon source decomposition conditions in the CVD synthesis of graphene, gas-phase thermal decomposition of ethanol and dimethyl ether (DME) at low pressure and various temperatures was simulated using the chemical kinetic model. Temperature of CVD synthesis of monolayer graphene from DME is lower than that from ethanol, which is in agreement with predicted simulation results. Raman spectroscopy and scanning electron microscopy were used to characterize the synthesized and transferred monolayer graphene.

[1] A. K. Geim, K. S. Novoselov: *Nat. mater.* **6** (2007) 183.

[2] S. Maruyama, E. Einarsson, Y. Murakami, T. Edamura: *Chem. Phys. Lett.* **403** (2005) 320.

[3] X. S. Li, W. W. Cai, J. H. An, S. Kim, J. Nah, D. X. Yang, R. D. Piner, A. Velamakanni, I. Jung, E. Tutuc, S. K. Banerjee, L. Colombo, R. S. Ruoff: *Science* **324** (2009) 1312.

Corresponding Author: Shigeo Maruyama

E-mail: maruyama@photon.t.u-tokyo.ac.jp

TEL: +81-03-5841-6421 FAX: +81-3-5800-6983

## Direct Fabrication of Metal-Free Multilayer Graphene on Substrates

○Soichiro Takano<sup>1</sup> and Suguru Noda<sup>1,2</sup>

<sup>1</sup>*Dept. of Chemical System Engineering, The University of Tokyo, Tokyo 113-8656, Japan*

<sup>2</sup>*PRESTO, Japan Science and Technology Agency, Saitama 332-0012, Japan*

Graphene attracts much attention for its significant electronic properties [1]. For its practical use, its fabrication is a crucial issue. Chemical vapor deposition (CVD) using metal films as catalysts is recently developed significantly [2,3]. When Ni [2] or Fe [3] are used as catalysts, carbon is dissolved in the catalyst by CVD at an elevated temperature and then graphene is precipitated from the catalyst by rapid cooling. However, CVD graphene has formed on much thicker metals and the control of its layer numbers is indirect. In CVD, the key process for graphene formation is the precipitation of graphene from carbon-metal solid solution. Based on this concept, we recently developed a novel method converting sputtered carbon into graphene by annealing and cooling of metal/carbon layers [4]. This method will realize more direct control over the layer numbers of graphene, but such graphene still has thick metals under it.

In this work, we developed a novel method yielding metal-free graphene directly on substrates. Graphene is precipitated from carbon-metal solid solution not by cooling [4] but by etching of metals at an elevated temperature. Briefly, C/Fe or Fe/C layers were sequentially deposited on SiO<sub>2</sub>/Si substrates by sputtering, set in a tubular quartz glass reactor, and reacted with 0.01 vol% Cl<sub>2</sub>/Ar at 5 Torr, 800 °C. Figure 1 shows typical scanning electron microscope (SEM) images with Raman spectra (inset) of the samples after annealing-cooling and after etching. Annealing-cooling process (a) converted sputtered carbon to graphene, in agreement with our previous report [4]. But annealing-etching process (b) yielded graphene with smaller D-band, which is possibly due to the graphene growth at a fixed temperature of 800 °C without decreasing temperature. Fe and C thicknesses were determined by XRF to be 0 and 19 nm, respectively, for the (b) annealing-etching sample which clearly shows metal free graphene. This method will provide a route for the direct formation of metal-free graphene patterns, simply by patterning the Fe/C layers.

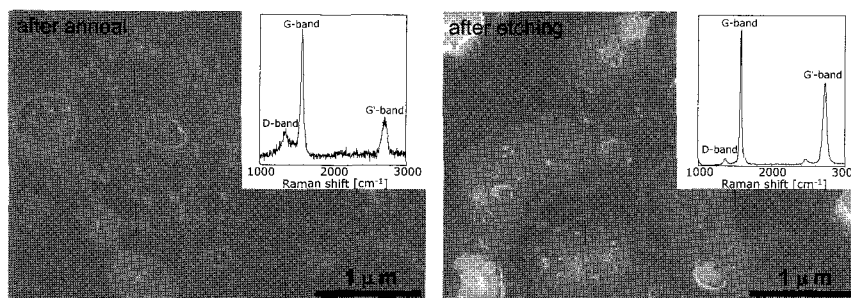


Fig. 1. SEM images of the surface at Fe/C = 2.07, inset is the representative Raman spectrum.

[1] K. S. Novoselov, et al., *Science* **306**, 666 (2004). [2] K. S. Kim, et al., *Nature* **457**, 706 (2009). [3] D. Kondo, et al., *Appl. Phys. Express* **3**, 025102 (2010). [4] H. Kang and S. Noda, *39th FNRS*, 3P-43 (2010).

Corresponding Author: Suguru Noda, TEL/FAX: +81-3-5841-7330/7332, E-mail: noda@chemsys.t.u-tokyo.ac.jp

# 2P-39

## Energetics and Electronic Structure of Corrugated Graphene

Susumu Okada

*Graduate School of Pure and Applied Sciences, University of Tsukuba, Tsukuba, Ibaraki 305-8571,  
Japan  
Japan Science and Technology Agency, CREST, 5 Sanbancho, Chiyoda, Tokyo 102-0075, Japan*

Graphene is now keeping in premier position in a constituent for the electronic devices in the post silicon era due to its perfectly planner structure and remarkable carrier mobility. Although, the technological advancing of graphene is rapidly, a little is known for the fundamental properties in its hybrid structures, such as structural undulation and interfaces with insulators/electrodes, those are essential in the device structures. Here, we investigate that the energetics and electronic structure of grapheme with structural corrugation with a period of about nano-meter scale based on the first-principles total-energy calculations within the framework of density functional theory (DFT). Our DFT calculation indicates that the energy cost for corrugation is found to be about a few tens meV per C atom indicating the possibility of structural undulation of graphene in ambient conditions. Under the corrugated structure, we find that the graphenes form tiny energy gap at the Fermi level. Furthermore, we also find that the conical structures of the conduction and valence bands are slightly distorted along parallel and normal to the corrugation.

Corresponding Author: Susumu Okada  
E-mail: [sokada@comas.frsc.tsukuba.ac.jp](mailto:sokada@comas.frsc.tsukuba.ac.jp)  
Tel: +81-29-853-59210

## Spatial Modulation of Electronic Structure of Graphene on Metal Surfaces

Yoshiteru Takagi<sup>1,2</sup> and Susumu Okada<sup>1,2</sup>

<sup>1</sup>*Center for Computational Sciences and Graduate School of Pure and Applied Science,  
University of Tsukuba, Tsukuba 305-8577, Japan*

<sup>2</sup>*CREST, Japan Science and Technology Agency, CREST, 5 Sanbancho, Chiyoda-ku, Tokyo  
102-0075, Japan*

Interaction between metal electrodes and graphene is one of fundamental factors to design the physical properties of graphene based nanoscale electronic devices. In particular, it is important to investigate how the metal electrode modulates the electronic structure of graphene as a function of a distance from an edge of the electrode. However, as far as our knowledge[1], fundamentals of electronic structure of graphene on metal electrodes are not addressed yet. Thus, we here investigate how the metal surfaces affect on electronic states of graphene by first principle total energy calculations. In particular, we investigate the spatial modulation on the electronic structure of graphene as a function of a distance from an edge of electrode (Au, Ag, Pd, and Pt). To give a theoretical insight, we consider a structural model shown in Figure. Above the metal electrode, local density of states (LDOS) for graphene is the same as that of graphene on metal surface.

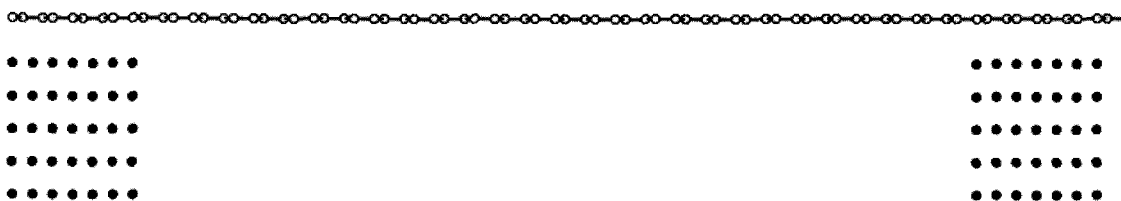


Fig. A structural model for graphene on metal surface. The gray circles and the black circles represent carbon atoms and metal atoms, respectively.

[1] Q.Ran, et al, Appl. Phys. Lett. **94**, 103511 (2009)

E-mail: [ytakagi@comas.frsc.tsukuba.ac.jp](mailto:ytakagi@comas.frsc.tsukuba.ac.jp), TEL: +81-29-853-5600(8233), FAX:+81-29-853-5924



## Raman Spectroscopic Study in a Bilayer Graphene Synthesized by Alcohol Chemical Vapor Deposition Method

Makoto Okano<sup>1</sup>, Ryusuke Matsunaga<sup>1</sup>, ○Kazunari Matsuda<sup>2</sup>, Satoshi Masubuchi<sup>3</sup>, Tomoki Machida<sup>3</sup>, and Yoshihiko Kanemitsu<sup>1</sup>

<sup>1</sup>*Institute for Chemical Research, Kyoto University, Uji, Kyoto 611-0011, Japan*

<sup>2</sup>*Institute of Advanced Energy, Kyoto University, Uji, Kyoto 611-0011, Japan*

<sup>3</sup>*Institute of Industrial Science, University of Tokyo, Meguro-ku, Tokyo 153-8505, Japan*

Graphenes have attracted wide interests from both fundamental physics and potential applications. The electronic band structure of a single-layer graphene has a characteristic linear and gapless dispersion at  $K$  point, which makes the electron to a massless Dirac fermion. The band structure of a bilayer graphene is strongly modified from a single-layer graphene because of the interaction between the layers depending on the stacking of the graphenes.

We investigated electronic band structure and interlayer interaction in graphenes synthesized by alcohol chemical vapor deposition (a-CVD) method [1] on the basis of microscopic Raman spectroscopy and comparison with a tight-binding (TB) theory. It was found that the number of layers in a-CVD graphenes was clearly identified by intensity ratio of G to 2D phonon peak and the linewidth of 2D phonon peak as well as exfoliated graphenes in the Raman spectra. The increasing of the intensity ratio with increasing number of layers indicates the interaction between each layer. We found that the strength of interlayer interaction of an a-CVD bilayer graphene is no more than one third the magnitudes of that of an exfoliated bilayer graphene from the detailed line shape analysis of 2D band of a bilayer a-CVD graphenes and TB theory.

### References:

[1] Y. Miyata, K. Kamon, K. Ohashi, R. Kitaura, M. Yoshimura, and H. Shinohara, *Appl. Phys. Lett.* 96, 263105 (2010).

Corresponding Author: Kazunari Matsuda

Tel: +81-774-38-3460, Fax +81-774-38-3460, E-mail: matsuda@scl.kyoto-u.ac.jp

## All-carbon ferromagnetism derived from edge states in antidot-lattice graphenes

○R. Miyazaki<sup>1</sup>, K. Tada<sup>1</sup>, S. Kamikawa<sup>1</sup>, J. Haruyama<sup>1</sup>, T. Matsui<sup>2</sup>, H. Fukuyama<sup>2</sup>

<sup>1</sup>*Faculty of Science and Engineering, Aoyama Gakuin University, 5-10-1 Fuchinobe, Sagami-hara, Kanagawa 252-5258, JAPAN*

<sup>2</sup>*Department of Physics, The University of Tokyo, 7-3-1 Hongo, Bunkyo-ku, Tokyo 113-8656, JAPAN*

**Abstract:** Ferromagnetism in carbon-based materials is controversial in contrast to traditional ferromagnets based on  $3d$  or  $4f$  electrons, because only  $s$  and  $p$  orbital electrons are present. The magnetic signals are also very small and the Curie temperature exceeds room temperature. In so many reports, appearance of ferromagnetism has been theoretically predicted in nano-graphite systems from viewpoints of edge-localized electrons and those spin polarization [1-3]. However, few independent observations have been reported to confirm the existence of ferromagnetic order in impurity-free carbon materials with high reproducibility, particularly in graphite [4, 5].

Here, we have studied electronic and magnetic behaviors of graphene nanoribbons (GNRs) in two material systems; (1) Low-defect GNRs fabricated by unzipping of CNTs with 3-stepped annealing [6] and (2) Antidot-lattice graphene (ADLG) with edges at hexagonal-shaped antidots [7]. In the poster, we present fabrication of monolayer ADLGs with hydrogen-terminated antidot edges by a non-lithographic method (i.e., using a nanoporous alumina template as etching masks). This allows exploration of the correlation of the edge electronic states with magnetism. We find appearance of room-temperature ferromagnetism derived from edge states of the antidots. The ferromagnetism changed to antimagnetic feature in ADLGs with oxygen terminated edges and disappears in bulk graphene without ADL. These prove presence of zigzag edge structure at the antidot edges and indicate importance of edge termination by foreign atoms. This finding must open a new door to all-carbon ferromagnetism and also (quantum) spin hall effect for novel spintronics devices.

### References:

1. Kusakabe, K., Maruyama, M., Magnetic nanographite. *Phys. Rev. B* **67**, 092406 (2003).
2. Fujita, M. et al. Peculiar localized state at zigzag graphite edge. *J.Phys.Soc.,Jpn* **65**, 1920-1923 (1996)
3. Shima, N., Aoki, H., Electronic structure of superhoneycomb systems. *Phys.Rev.Lett.* **71**, 4389 – 4392 (1993)
4. L Enoki, T. et al. The edge state of nanographene and the magnetism of the edge-state spins. *Sol. Stat. Comm.* **149**, 1144-1150 (2009).
5. Cervenka, J. et al. Room-temperature ferromagnetism in graphite driven by two-dimensional networks of point defects. *Nature Phys.* **5**, 840-844 (2009).
6. Shimizu, T., Haruyama, J. et al., Large intrinsic energy bandgaps in annealed nanotube-derived graphene nanoribbons. *Nature Nanotech.* Advance online publication (19th December 2010).
7. Shimizu, T., Haruyama, J. et al., Edge-state derived anomalous magnetoresistance oscillations in antidot-lattice graphenes. To be published on *Phys. Rev. Lett.*

**Corresponding Author Junji Haruyama**

**E-mail J-haru@ee.aoyama.ac.jp**

**Tel&Fax 042-759-6256 & 6524**

## Selective Edge Functionalization of Graphene by Room-Temperature Mild Plasma Treatment

○Toshiaki Kato<sup>1,2</sup>, Liying Jiao<sup>2</sup>, Xinran Wang<sup>2</sup>, Hailiang Wang<sup>2</sup>, Xiaolin Li<sup>2</sup>, Li Zhang<sup>2</sup>, Rikizo Hatakeyama<sup>1</sup>, and Hongjie Dai<sup>2</sup>

<sup>1</sup>*Department of Electronic Engineering, Tohoku University, Sendai 980-8579, Japan*

<sup>2</sup>*Department of Chemistry and Laboratory for Advanced Materials, Stanford University, Stanford, CA 94305, USA*

Graphene has recently received a great deal of attention because it possesses unique properties such as a linear energy dispersion relation and high carrier mobility. Graphene nano ribbons (GNRs), strips of graphene, are the counterparts of carbon nanotubes (CNTs) in terms of their all-semiconducting nature, and they could potentially solve the problem of the chirality dependence of the metal or semiconductor nature of CNTs in future nanoelectronics. The graphene edge structure is one of the most unique geometrical features of 2D graphene sheets; this is not seen in 1D CNTs. It has been theoretically predicted that, because of the narrow width of GNRs, their electronic state is strongly influenced by their edge structure. Thus, in order to obtain desirable properties for devices using GNRs, it is essential to be able to precisely control the edge structure and chemical terminations of GNRs.

In this study, we have developed a new type of functionalization and carrier doping method for graphene using a room-temperature NH<sub>3</sub> plasma gas phase reaction [1]. Evidence of the edge reaction and carrier doping was obtained by the detailed Raman mapping analysis and electrical measurement. The edge-functionalized graphene shows a pronounced D-peak only near the edge. The Dirac point position of the GNR device shifts to a negative gate-bias voltage direction after NH<sub>3</sub> plasma treatment. This is the first time that electrical data showing carrier doping and changes in edge Raman signatures have been observed in a correlate manner, suggesting that controlled room-temperature plasma reactions could be an important approach to doping without drastically perturbing the in-plane properties of graphene.

[1] Toshiaki Kato, Liying Jiao, Xinran Wang, Hailiang Wang, Xiaolin Li, Li Zhang, Rikizo Hatakeyama, and Hongjie Dai, *Small*, accepted.

Corresponding Author T. Kato

E-mail: kato12@ecei.tohoku.ac.jp

Tel&Fax: +81-22-795-7046 / +81-22-263-9225

## Electronic structure and band gap control of graphene with holes

○Masahiro Sakurai and Susumu Saito

*Department of Physics, Tokyo Institute of Technology  
2-12-1 Oh-okayama, Meguro-ku, Tokyo 152-8551, Japan*

Graphene is a good candidate material in future micro- and nanoelectronics because of the high electron mobility and its high stability. There are, however, some problems with using graphene widely to electronics. One of the fundamental problems is its lack of a band gap. In our previous studies [1,2], we have shown that periodic modification to graphene sheet introduces a band gap. Actually, some groups have demonstrated that a band gap is created in their graphene nanostructures with hexagonally packed holes (large atomic vacancies) [3,4]. With the development of fabrication technique, it would be possible to produce graphene with regularly spaced and size-controlled holes. In this work, we study the electronic structure as well as the total energy of graphene with regularly spaced holes (fig. 1) using the density-functional theory (DFT). Circular or hexagonal holes are periodically arranged in graphene sheet while the material keeps the symmetry of original graphene,  $D_{6h}$ . Carbon atoms at the edges of a hole are terminated by hydrogen atoms. Atomic configurations at the edges of a hole are found to be crucial to determine their energetics and substantial lattice relaxation takes place at armchair-edge regions. The material studied is predicted to be a direct-gap semiconductor. Band gap increases as a function of decreasing the neck width (edge-to-edge distance between two neighboring holes), which agrees qualitatively with the previous reports [4,5]. In this presentation, we will also discuss a scaling rule for the band gap values with a hole size itself and “hole density.”

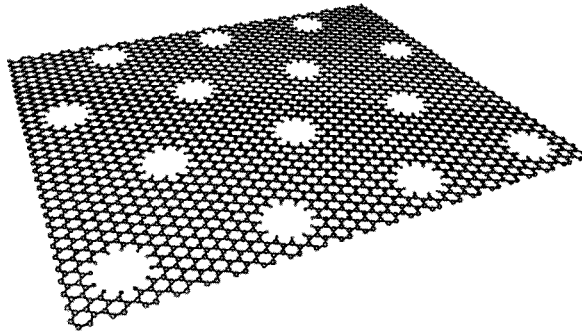


**Figure 1:** Overview of graphene with holes.

### References:

- [1] T. Matsumoto and S. Saito, *J. Phys. Soc. Jpn.* **71** (2002) 2765.
- [2] M. Sakurai and S. Saito, to be published.
- [3] J. Bai *et al.*, *Nature Nanotech.* **5** (2010) 190.
- [4] X. Liang *et al.*, *Nano Lett.* **10** (2010) 2454.
- [5] H. Jippo *et al.*, presented at the 39th Fullerenes-Nanotubes General Symposium, 2010.

**Corresponding Author:** Masahiro Sakurai, **E-mail:** sakurai@stat.phys.titech.ac.jp

## Density-Functional Tight-Binding Studies of Hexagonal Graphene Flakes

○Lili Liu<sup>1</sup>, Francisco J. Martín-Martínez<sup>2</sup>, Santiago Melchor<sup>2</sup>, Jose A. Dobado<sup>2</sup>, Thomas Heine,<sup>3</sup> Stephan Irle<sup>1\*</sup>

<sup>1</sup>*Institute for Advanced Research and Department of Chemistry, Nagoya University*

<sup>2</sup>*Grupo de Modelización y Diseño Molecular, Departamento de Química Orgánica, Facultad de Ciencias, Universidad de Granada, Spain*

<sup>3</sup>*Department of Physics, Jacobs University, Bremen, Germany*

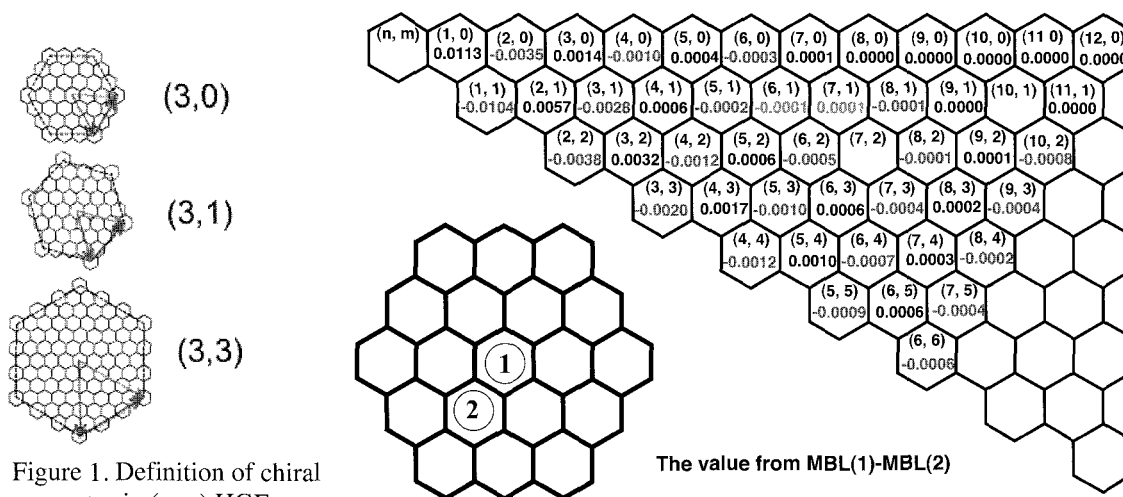


Figure 1. Definition of chiral vector in  $(n,m)$  HGFs.

Figure 1: The MBL differences between the center ring and the second layer. (When the value is a positive number, the center pattern is Kekulé structure, when the value is a negative number, the center pattern is Clar structure.)

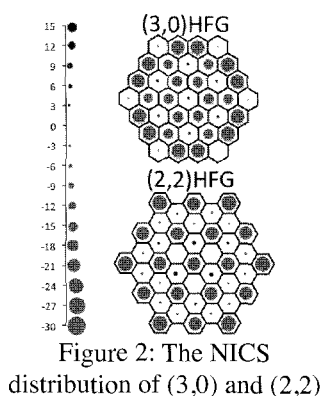


Figure 2: The NICS distribution of  $(3,0)$  and  $(2,2)$

We theoretically studied bond length alternation (BLA) patterns in  $D_{6h}$ -hexagonal graphene flakes (HGFs), based on ring bond dispersion (RBD)<sup>1</sup> and mean bond lengths (MBL)<sup>1</sup>. We find structural Clar and Kekulé<sup>1</sup> patterns, breaking the bond equivalency of infinite graphene. MBL(1)-MBL(2) values predict that BLAs in zigzag-type  $(n,0)$  HGFs converge faster to graphite than armchair-type  $(n,n)$  HGFs (see Figure 1). Nucleus-Independent Chemical Shift (NICS) analysis confirms the existence of Clar or Kekulé patterns (see Figure 2). For the general  $(n,m)$  HGFs, we find the rule that when  $n+m$  is even, the Clar configuration dominates the electronic structures, and when  $n+m$  is odd, Kekulé dominates.

**References:**[1] F. J. Martín-Martínez et al, Org. Lett. 10 (2008) 1991

**Corresponding Authors:** Stephan Irle

**TEL:**+81-52-747-6397 **FAX:**+81-52-788-6151

**E-mail:** [sirle@iar.nagoya-u.a.jp](mailto:sirle@iar.nagoya-u.a.jp),

## Morphology- and Position-Selective Growth of CNT Emitters on Glasses by Subsecond Heating Pulses

○Kotaro Sekiguchi<sup>1</sup>, Yosuke Shiratori<sup>1</sup>, and Suguru Noda<sup>1,2</sup>

<sup>1</sup>Dept. of Chemical System Engineering, The University of Tokyo, Tokyo 113-8656, Japan

<sup>2</sup>PREST, JST, 4-1-8 Honcho, Kawaguchi, Saitama 332-0012 Japan

To use carbon nanotubes (CNTs) in electronic devices such as field emitters, implementation of CNTs at specific position with controlled morphology is essential. Chemical vapor deposition (CVD) enables direct growth of such CNTs but has a main drawback in its high reaction temperature over a glass strain point  $\sim 500$  °C. Extensive efforts have been made in lowering CVD temperature, however lower temperature results in exponentially smaller growth rate and longer growth time under Arrhenius' law. Here we propose an opposite approach: high temperature CVD in a short heating time tolerable for glasses. At the elevated temperatures  $\sim 800$  °C, CNTs can grow to millimeter in height rapidly at several  $\mu\text{m/s}$ . This growth rate enables the implementation of CNT emitters in only 1 second or less. We previously demonstrated 1-second implementation of CNT emitters on glasses by a single current pulse [2].

This time, we improved the controllability of the emitter fabrication by using multiple current pulses and neck-patterned cathode lines. The cathode lines (Cr or Nb) with 0.1-0.3  $\mu\text{m}$  thickness, 1-30  $\mu\text{m}$  width and 10-200  $\mu\text{m}$  pitch were formed on glass substrates by conventional electron beam lithography and sputtering processes. An  $\text{Al}_2\text{O}_3$  buffer layer (20 nm) and a Fe catalytic layer (0.1-3.1 nm thickness) were subsequently sputtered on the cathode lines. The substrates were set in a tubular quartz glass reactor, and pulsed voltages (0.5-1.0 s) were applied to the lines under a gas atmosphere of 26 vol%  $\text{H}_2$  / Ar for catalyst pre-annealing, and then under 0.5-1.0 vol%  $\text{C}_2\text{H}_2$  / Ar at ambient pressure for CNT growth [1]. The combinatorial catalyst library [3] realized a variety of emitter morphologies and corresponding FE properties as shown in Fig. 1. A high current density ( $J$ ) of 9  $\text{mA/cm}^2$  was recorded at an applied electric field ( $E$ ) of 2.5  $\text{V}/\mu\text{m}$  for the protruding VA-SWCNTs. The neck-patterned cathodes realized the position-selective heating and thus growth of CNT emitters owing to the higher resistivity of the neck than the other parts (Fig. 2).

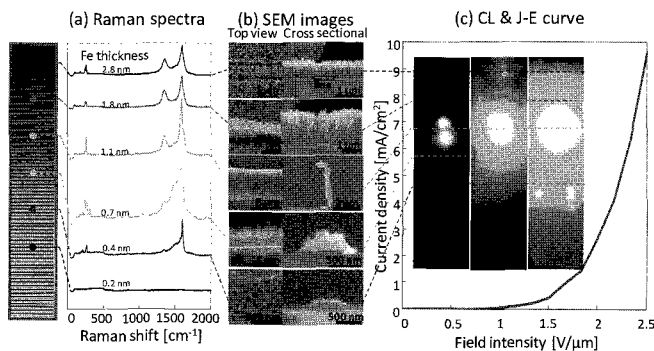


Fig. 1. A result of combinatorial FE measurement : (a) Raman spectra and (b) SEM micrographs recorded at specific positions, and (c) photographs of cathode luminescence and the obtained  $J$ - $E$  curve.

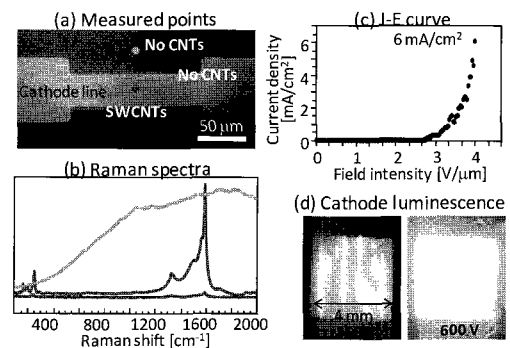


Fig. 2. (a) A SEM image of a necked cathode line, (b) Raman spectra recorded at three points indicated by different colors, (c) the  $J$ - $E$  curve, and (d) images of cathode luminescence

[1] K. Hasegawa and S. Noda, *ACS Nano*, in press (2011). [2] K. Sekiguchi, et al., 38th FNRS, 2P-39, Nagoya, Mar. 2010. [3] S. Noda et al., *Carbon* **44** (2006) 1414.

Corresponding Author: Suguru Noda TEL/FAX: +81-3-5841-7330/7332, E-mail: noda@chemsys.t.u-tokyo.ac.jp

## Highly-Efficient Synthesis of Nitrogen Atom Endohedral Fullerene by Controlling Fullerene and Plasma Ion Behaviors

○S. C. Cho, T. Kaneko, and R. Hatakeyama

*Department of Electronic Engineering, Tohoku University, Sendai 980-8579, Japan*

The nitrogen atom endohedral fullerene ( $N@C_{60}$ ) is a spin active molecule with a long electronic spin coherence time, which makes it a promising candidate for a quantum computer [1]. Although  $N@C_{60}$  has been studied over the last decade, its purity has been as low as  $10^{-3}$  to  $10^{-2}$  %. Therefore, the purpose of this research is to investigate the optimum condition for the high purity  $N@C_{60}$  synthesis using a nitrogen radio-frequency (RF) discharge plasma under the external control of direct-current (DC) bias voltages applied to functional electrodes [2]. For this end, we examine the effects of substrate bias voltage ( $V_{\text{sub}}$ ) and fullerene oven temperature ( $T_{\text{ov}}$ ) on the  $N@C_{60}$  synthesis, where  $V_{\text{sub}}$  can control the nitrogen ion ( $N_2^+$ ) irradiation energy ( $E_i$ ) to the fullerene.

Figure 1(a) shows dependences of the purity on  $V_{\text{sub}}$  with gas pressure ( $P_{N_2}$ ) as a parameter for RF power  $P_{\text{RF}}=500$  W and  $T_{\text{ov}}=850$  °C. It is found that the purity has the maximum value at the optimum  $V_{\text{sub}}$  depending on  $P_{N_2}$ . In addition, this optimum  $V_{\text{sub}}$  shifts to the negative direction with an increase in  $P_{N_2}$ , which is considered to be caused by the collision of  $N_2^+$  to neutral  $N_2$  in order to keep the  $E_i$  of  $N_2^+$  to  $C_{60}$  on the substrate. Based on these results, it is concluded that the suitable ion irradiation energy to  $C_{60}$  contributes to the highly-efficient synthesis of  $N@C_{60}$ . Furthermore, since the amount of the plasma ions irradiated to  $C_{60}$  increases with increasing  $P_{N_2}$ , the reaction rate becomes high, and as a result, the purity increases.

Figure 1(b) presents dependences of the purity and  $C_{60}$  sublimation rate ( $R_{\text{subli}}$ ) on  $T_{\text{ov}}$ . This result demonstrates the purity increases with an increase in  $T_{\text{ov}}$ , which implies that the nitrogen presumably does not enter into the  $C_{60}$  until 700 °C, although the evaporation of  $C_{60}$  and the ion irradiation energy are enough to synthesize  $N@C_{60}$ . This is because the  $C_{60}$  sublimates in an aggregation form and  $C_{60}$  thermal expansion is low. Therefore, high  $T_{\text{ov}}$  is an important factor for the synthesis of  $N@C_{60}$  in high purity.

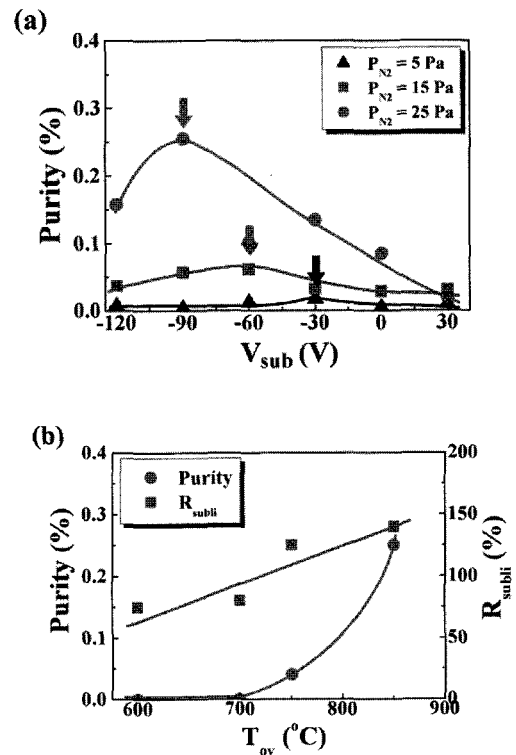


Fig. 1. (a) Purity as a function of  $V_{\text{sub}}$  and (b) purity and sublimation rate  $R_{\text{subli}}$  of  $C_{60}$  as a function of  $T_{\text{ov}}$  for  $V_{\text{sub}}=-90$  V and  $P_{\text{RF}}=500$  W.

[1] W. Harnett: Phys. Rev. A **65** (2002) 032322.

[2] S. Miyanaga, T. Kaneko, H. Ishida, and R. Hatakeyama: Thin Solid Films **518** (2010) 3509.

**Corresponding Author: Soon Cheon Cho**

**Tel: +81-22-795-7046, Fax: +81-22-263-9225, E-mail: cho@plasma.ecei.tohoku.ac.jp**

## Synthesis of Nickel Atom Endohedral Fullerene Using Plasma Ion Irradiation Method with Electron Beam Gun

○T. Umakoshi, H. Ishida, T. Kaneko, and R. Hatakeyama

*Department of Electronic Engineering, Tohoku University, Sendai 980-8579, Japan*

Although many kinds of endohedral fullerenes have been reported, a nickel atom endohedral fullerene ( $\text{Ni}@C_{60}$ ) which is expected to make a single molecular magnetic device focusing on its magnetic moment [1] has never been synthesized until now. Using a plasma ion irradiation method, we have succeeded in synthesizing the  $\text{Ni}@C_{60}$ , where plasma ions generated by an electron cyclotron resonance discharge are irradiated to the fullerene which is previously formed [2]. This time, in order to efficiently synthesize the  $\text{Ni}@C_{60}$ , we adopt the plasma irradiation method with an electron beam gun.

An experimental apparatus is shown in Fig. 1. In this experiment, nickel atoms are evaporated and ionized using the electron beam gun.  $C_{60}$  molecules from an oven are sublimated to a substrate terminating the plasma, and the nickel ions are irradiated to the  $C_{60}$  molecules.

An ion current flowing into the substrate as a function of electron beam current ( $I_{EB}$ ) is presented in Fig. 2, where a voltage of the substrate is constant ( $= -50$  V). The ion current dramatically increases with increasing  $I_{EB}$ . Figure 3(a) shows a mass spectrum of the sample deposited on the substrate. A calculated isotope distribution of the  $\text{Ni}@C_{60}$  is presented in Fig. 3(b), and coincides with the distribution of the mass spectrum of the sample on the substrate. Therefore, we can conclude that the sample indicates the existence of the  $\text{Ni}@C_{60}$ .

- [1] J. L. Li *et al.*, Appl. Phys. Lett. **96**, 233103 (2010)  
 [2] T. Umakoshi, *et al.*, Abstracts of the 38th Fullerelens-Nanotubes General Symposium, 90 (2010).

Corresponding Author: Tatsuya Umakoshi  
 TEL: +81-22-795-7046, FAX: +81-22-263-9225,  
 E-mail: [umakoshi@plasma.ecei.tohoku.ac.jp](mailto:umakoshi@plasma.ecei.tohoku.ac.jp)

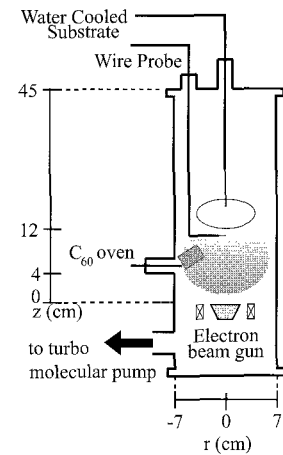


Fig 1: Experimental apparatus.

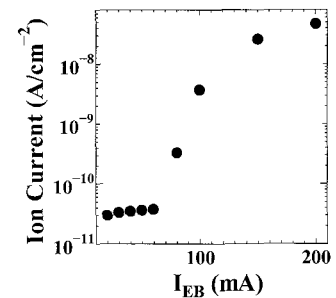


Fig 2 : An ion current into the substrate as a function of  $I_{EB}$ .

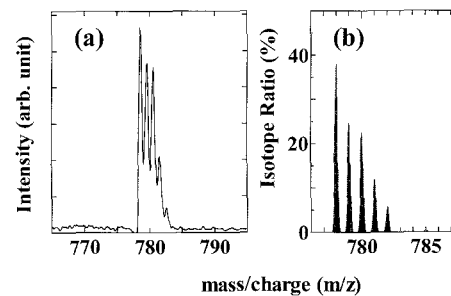


Fig 3 : (a) A mass spectrum of the sample deposited on the substrate. (b) An expected isotope distribution ratio of the  $\text{Ni}@C_{60}$ .



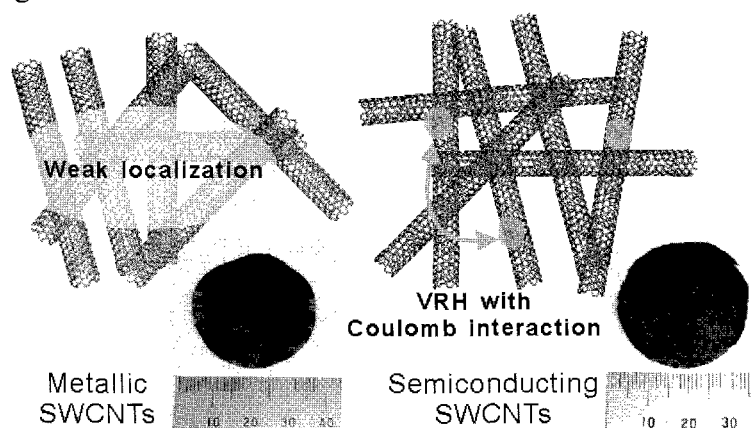
## Transport Mechanisms in Single-Wall Carbon Nanotube Networks formed by Controlled Content-ratio of Metallic and Semiconducting Types

○H. Udoguchi<sup>1</sup>, K. Yanagi<sup>1\*</sup>, Y. Oshima<sup>2</sup>, T. Takenobu<sup>3</sup>, H. Kataura<sup>4,5</sup>, T. Ishida<sup>4</sup>,  
K. Matsuda<sup>1</sup>, Y. Maniwa<sup>1,5</sup>

1. Tokyo Metropolitan University, 2. Riken, 3. Waseda University, 4. AIST, 5. JST-CREST

**Abstract:** A fundamental understanding of the conduction mechanisms in single-wall carbon nanotube (SWCNT) networks is crucial for their use in thin-film transistors and conducting films. However, the uncontrollable mixture state of metallic and semiconducting SWCNTs has always been an obstacle in this regard. We revealed that the conduction mechanisms in nanotube networks formed by high-purity metallic and semiconducting SWCNTs are completely different.<sup>1</sup> Quantum transport was observed in macroscopic networks of pure metallic SWCNTs. However, for semiconducting SWCNTs networks, Coulomb-gap-type conduction was observed, due to Coulomb interactions between localized electrons. Crossovers among a weakly localized state and strongly localized states with and without Coulomb interactions were observed for transport electrons by varying the relative content of metallic and semiconducting SWCNTs. Moreover, the dimensions of the hopping conduction become low as the content of metallic SWCNTs in the networks is decreased. We discuss here the detailed mechanisms of these conduction changes. It was found that hopping barriers, which always exist in normal SWCNT networks and are serious obstacles to achieving high conductivity, were not present in pure metallic SWCNTs networks.

This work was partially supported by a Grant-in-Aid for Scientific Research on Innovative Areas (No.21108523, " $\pi$ -Space") from MEXT, and by Industrial Technology Research Grant Program in 2007 from NEDO.



References: [1] Yanagi, Udoguchi, *et al.*, ACS Nano 7 4027-4032 (2010)

Corresponding Author: Kazuhiro Yanagi

E-mail : yanagi-kazuhiro@tmu.ac.jp

Tel & Fax : +81-42-677-2494 & 2483

# 2P-50

## The shortest nano-peapods: Complexation of fullerenes with cycloparaphenylenes

○ Yusuke Nakanishi, Yasumitsu Miyata, Haruka Omachi, Sanae Matsuura, Yasutomo Segawa,  
Kenichiro Itami, Ryo Kitaura and Hisanori Shinohara\*

*Department of Chemistry & Institute for Advanced Research, Nagoya University, Nagoya,  
Japan*

Host-guest chemistry for fullerenes has attracted much interest because of the great promising applications such as selective extraction and chemical functionalization. Recently, the group of Itami has reported the modular and size-selective synthesis of  $[n]$ cycloparaphenylene ( $[n]$ CPP) (**Figure 1**), the shortest single-wall carbon nanotubes with chiral index of  $(n,n)$ .<sup>[1]</sup> The successful synthesis of these intriguing molecules has motivated us to produce a new complex of CPPs with fullerenes, which can be regarded as “the shortest nano-peapod”.

Here we demonstrate the complexation of fullerenes with CPPs. The complexation was confirmed by using  $^1\text{H}$  NMR (**Figure 2**). For example, the  $^1\text{H}$  NMR spectrum of  $[12]$ CPP in  $\text{CDCl}_3$  exhibits a sharp peak at 7.58 ppm for the aromatic protons. On the other hand, the spectrum of a solution of  $[12]$ CPP and fullerene mixtures shows a broad peak at 7.65 ppm. This peak shift suggests the formation of a host-guest complex of  $[12]$ CPP with fullerenes. Furthermore, the mass spectra imply the enrichment and partial separation of metallofullerenes after the complexation. We believe that the CPP-fullerene complexation should provide a method for selective extraction of metallofullerenes. In the presentation, we will discuss the fullerene-cage and encapsulated-metal dependent interactions between CPPs and fullerenes.

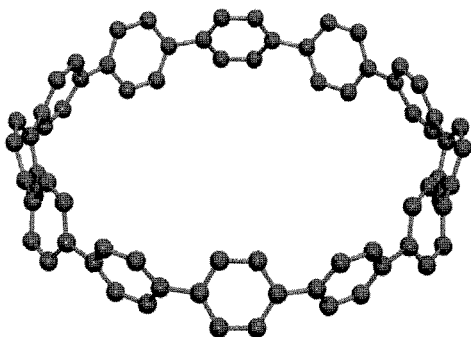


**Figure1.** Image of  $[12]$ CPP, the shortest (12,12) single-wall carbon nanotube.

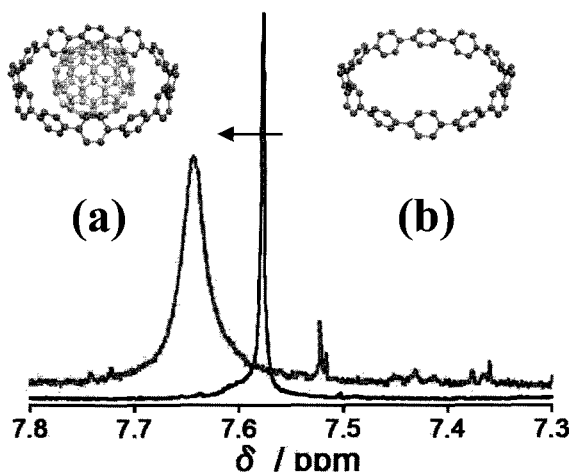


**Figure2.**  $^1\text{H}$  NMR spectra of CPP (a) with and (b) without fullerene mixtures.

**Reference:** [1]. H. Takaba *et al.*, *Angew. Chem. Int. Ed.* 48, 6112 (2009). H. Omachi *et al.*, *Angew. Chem. Int. Ed.* 49, 10202 (2010). Y. Segawa *et al.*, *Angew. Chem. Int. Ed.* 50, in press (2011).

**Corresponding Author:** Hisanori Shinohara

**E-mail:** [noris@nagoya-u.jp](mailto:noris@nagoya-u.jp),

**Tel&Fax:** 052-789-2482 & 052-747-6442

## Femtosecond Coherent Phonon Spectroscopy of Single-walled Carbon Nanotubes in Different Environments

○Kotaro Makino<sup>1</sup>, Hiroki Tadokoro<sup>1</sup>, Atsushi Hirano<sup>1</sup>, Kentaro Shiraki<sup>1</sup>,  
Yutaka Maeda<sup>2</sup>, and Muneaki Hase<sup>1</sup>

<sup>1</sup>*Institute of Applied Physics, University of Tsukuba, Tsukuba 305-8573, Japan*

<sup>2</sup>*Department of Chemistry, Tokyo Gakugei University, Tokyo 184-8501, Japan*

The interactions between single walled carbon nanotubes (SWNTs) and proteins, charge transfer between them in particular, have not yet unveiled, although they are important physical process to realize medical applications, such as drug delivery [1] and biosensors [2]. In this study, a femtosecond pump-probe impulsive Raman measurement was employed to elucidate the charge transfer by observing ultrafast dynamics of radial breathing mode (RBM) of SWNTs. The samples were sodium dodecyl sulfate (SDS)-suspended SWNTs at pH = 3-7 and protein (lysozyme, hemoglobin, and pepsin)-suspended SWNTs in aqueous solutions.

The coherent RBM spectra for SDS-SWNTs at pH = 3-7 are shown in Figure 1. Mainly two peaks at 6.4 THz from (13, 2) tubes and at 7.2 THz from (12, 1) tubes are observed. As the value of pH increases, the ratio of the intensity of the lower mode to the higher mode increases. This enhancement is attributed to the change in electron-phonon interaction [3] as well as the modification of condition of Raman scattering, both of them are caused by charge transfer between SWNTs and protons [4]. Figure 2 shows the coherent RBM spectra for proteins-SWNTs conjugates, in which the dependence of the spectra on the proteins is clearly observed. We attributed the origin of this dependence to not only charge transfer, but also difference in the conformation of proteins.

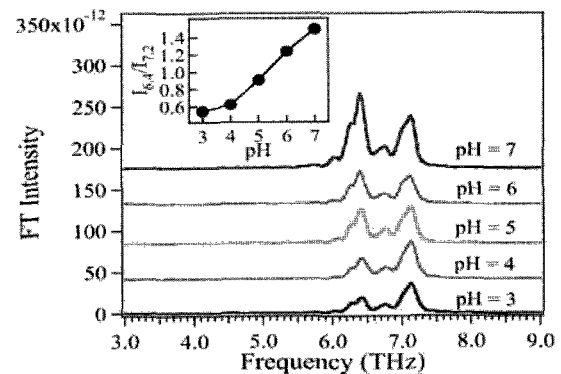


Fig. 1. The coherent RBM spectra of SDS-SWNTs at pH = 3-7. The inset shows the ratio of the intensities of main two peaks.

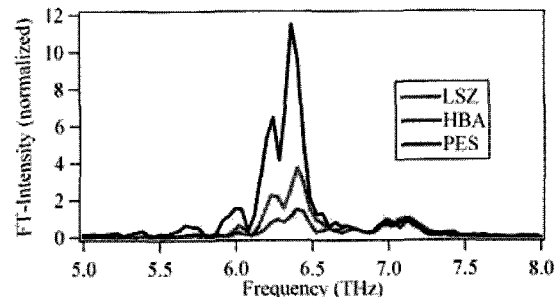


Fig. 2. The coherent RBM spectra of proteins-SWNTs conjugates.

[1] M. Zhang, T. Murakami, K. Ajima, K. Tsuchida, A. S. D. Sandanayaka, O. Ito, S. Iijima, and M. Yudasaka, *PNAS* **105**, 14773 (2008)

[2] A. Star, J. P. Gabriel, K. Bradley, and G. Gruner, *Nano Lett.* **3**, 459 (2003)

[3] K. Makino, A. Hirano, K. Shiraki, Y. Maeda, and M. Hase, *Phys. Rev. B*, **80**, 245428 (2009)

Corresponding Author: Muneaki Hase

E-mail: mhase@bk.tsukuba.ac.jp, Tel & Fax : +81-298-53-5305

## Crystallographic features of graphene on SiC (0001)

○ Wataru Norimatsu, and Michiko Kusunoki

*EcoTopia Science Institute, Nagoya University, Nagoya 464-8603, Japan*

*Japan Fine Ceramics Center, Nagoya 456-8587, Japan*

Graphene is a one-atom-thick carbon material, having a hexagonal honeycomb lattice. Graphene has an extremely high electronic mobility, in addition to anomalous electronic properties as a two-dimensional material, which raises hopes for its use in next-generation semiconducting devices. Although graphene is a promising material, some of the problems are left now. One of them is that the development of the mass production method of large-area and homogeneous graphene is required. The other is that graphene has no bandgap. In order to solve these problems, graphene produced by thermal decomposition of SiC attracts attention. By annealing SiC single-crystal in a vacuum or in an Ar atmosphere, Si atoms are removed from the surface, and then remaining C atoms form graphene spontaneously. In this study, we investigated the crystallographic features of graphene layers on SiC (0001) using high-resolution transmission electron microscopy (HRTEM).

Graphene-on-SiC samples were prepared by annealing on-axis and 4° off-axis SiC (0001) substrates at 1350~1450 °C. Thin specimens for observation were obtained by Ar-ion thinning method. Observations were carried out using JEM-2010-, JEM-2010F-, and EM-002B-type transmission electron microscopes (TEM) at an accelerating voltage of 200 kV.

First, we investigated the formation mechanism of graphene on SiC to find a clue toward the mass production method. Our TEM study suggests the following mechanism [1]. Initially, nucleation of graphene occurs at SiC steps, covering them with a few layers. These curved graphene layers subsequently grow over the terrace region. And the growth is occasionally pinned by lattice defects of the SiC substrate.

Next, an investigation using HRTEM showed that the stacking sequence of several layers of graphene exhibited an ABC-type stacking [2]. It did not depend on the stacking sequence of the SiC substrate. Although the stacking became disordered around the step of SiC, ABC-stacking was always observed on the terrace. Based on the previous theoretical reports, ABC-stacked graphene layers give rise to the electric-field-induced bandgap opening [3]. Thus, our present studies would be a key to overcome difficulties for graphene application.

[1] W. Norimatsu and M. Kusunoki, *Physica E*, **42**, 691 (2010).

[2] W. Norimatsu and M. Kusunoki, *Phys. Rev. B*, **81**, 161410 (2010).

[3] M. Aoki, et al., *Sol. Stat. Comm.*, **142**, 123 (2007).

**Corresponding Author :** Wataru Norimatsu

**E-mail :** w\_norimatsu@esi.nagoya-u.ac.jp, **Tel & Fax :** +81-52-789-5859

## Substituent Effects on the Reductive Functionalization of SWNTs

○Yuriko Chiba<sup>1</sup>, Takaaki Kato<sup>1</sup>, Yumi Okui<sup>1</sup>, Norihisa Akamatsu<sup>1</sup>, Michio Yamada<sup>1</sup>,  
Yutaka Maeda<sup>1</sup>, Tadashi Hasegawa<sup>1</sup>, Takeshi Akasaka<sup>2</sup>, Shigeru Nagase<sup>3</sup>

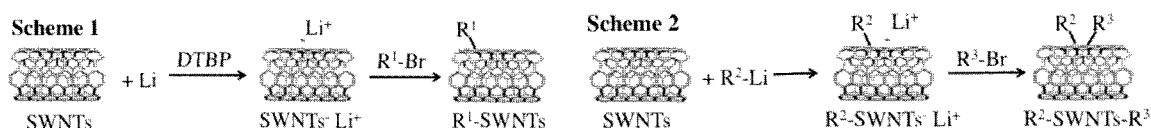
<sup>1</sup>Department of Chemistry, Tokyo Gakugei University, Koganei 184-8501, Japan

<sup>2</sup>Center for Tsukuba Advanced Research Alliance, University of Tsukuba, Tsukuba,  
Ibaraki 305-8577, Japan

<sup>3</sup>Department of Theoretical and Computational Molecular Science, Institute for  
Molecular Science, Okazaki, Aichi 444-8585, Japan

Single-walled carbon nanotubes (SWNTs) would have potential use in applications because of their excellent mechanical and electrical properties. The functionalization of SWNTs, strongly affects their solubility and electrochemical properties, is a current subject of intense researches. Billups *et al.* reported that reductive alkylation of SWNTs using lithium and alkyl halides occurred in liquid ammonia to give alkylated SWNTs via an electron-transfer process. We reported two-step alkylation of SWNTs using alkyllithiums and alkyl halides. It is important to control the functionalization of SWNTs because the degree of the functionalization affects electric properties of SWNTs. Herein we present the substituent effects on reductive alkylation of SWNTs by which the degree of the alkylation can be controlled.

Reactions of SWNTs with lithium and alkyl halides ( $R^1Br$ ) in the presence of 4,4'-di-*tert*-butylbiphenyl (DTBP) under argon gave alkylated SWNTs ( $R^1$ -SWNTs) (Scheme 1). Two-step alkylation ( $R^2$ -SWNTs- $R^3$ ) was conducted by addition of alkyllithium ( $R^2Li$ ) and alkyl bromide ( $R^3Br$ ) under argon (Scheme 2). The functionalized SWNTs obtained were characterized on the basis of their *vis*-NIR / Raman spectra and SEM and thermogravimetric analyses. The result showed the degree of functionalization of SWNTs was controlled by substituents. This might be explained by the steric repulsion between an initially introduced group on SWNTs and an alkyl group to be introduced secondary and reactivity of the corresponding radical species.



Corresponding Author Yutaka Maeda

E-mail ymaeda@u-gakugei.ac.jp

Tel&Fax +81-42-329-7512

## Generalized Preparation Method of the Catalyst for Single-Walled Carbon Nanotube Forest Growth from Various Iron Compounds

○Shunsuke Sakurai<sup>1</sup>, Hidekazu Nishino<sup>1</sup>, Don N Futaba<sup>1</sup>, Satoshi Yasuda<sup>1</sup>, Takeo Yamada<sup>1</sup>, Alan Maigne<sup>2</sup>, Eiichi Nakamura<sup>3</sup>, Motoo Yumura<sup>1</sup>, and Kenji Hata<sup>1</sup>

<sup>1</sup>Nanotube Research Center, National Institute of Advanced Industrial Science and Technology (AIST), Tsukuba 305-8565, Japan

<sup>2</sup>Gatan Inc., 5794 West Las Positas Blvd, Pleasanton, CA 94588, USA

<sup>3</sup>Department of Chemistry, School of Science, University of Tokyo, Tokyo 113-0033, Japan

Currently, catalyst for vertically-aligned SWNT forest growth was limited to only pure metal [1]. However, from application point of view, development of novel catalyst material might be a promising approach for the development of more economical or structure-controlled SWNT forest growth method. In this study, we surveyed the possibility of various iron-containing materials such as iron nitrate, iron chloride, and bucky ferrocene for the catalyst of SWNT forest growth.

Various iron-containing materials were deposited on sputtered  $\text{Al}_2\text{O}_3$  layer by spin-coating or bar-coating, and introduced water-assisted CVD furnace. Vertically-aligned SWNT forests were successfully grown from every catalyst (Fig. 1). Unexpectedly, average diameters of all SWNT samples were in the narrow range of 2.8-3.1 nm. Suggestive evidences including XPS, AFM, and SEM-EELS observations indicated that Fe atoms contained in every deposited iron compound diffused into sputtered  $\text{Al}_2\text{O}_3$  layer under annealing in  $\text{H}_2$  ambient, resulting in the formation of Fe nanoparticle on sputtered  $\text{Al}_2\text{O}_3$  layer with high density and, thus, the growth of SWNT forest with an average diameter around 3 nm in  $\text{C}_2\text{H}_4$  ambient (Fig. 2). As a summary, present result showed the possibility that any iron-containing material can be used as the catalyst for SWNT forest growth.

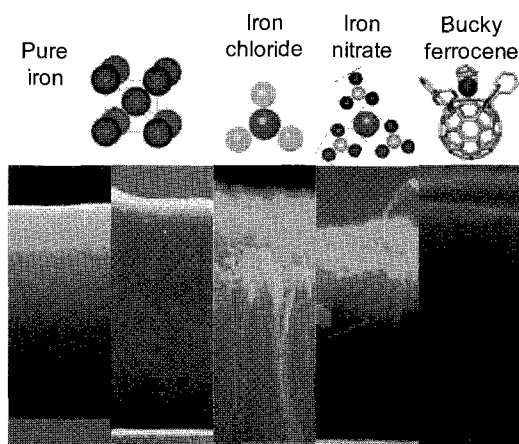


Fig. 1: SEM images of SWNT forest grown from various iron compound materials.

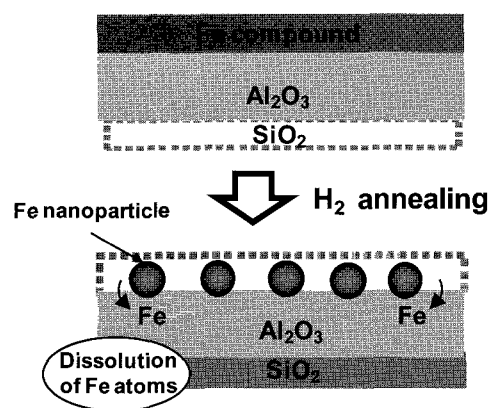


Fig. 2: Schematic representation of the Fe nanoparticle formation during annealing

[1] K. Hata, D.N. Futaba, K. Mizuno, T. Namai, M. Yumura, and S. Iijima, *Science.*, **306**, 1362 (2004).

Corresponding Author: Kenji Hata

TEL: +81-29-861-6205, FAX: +81-29-861485-1169, E-mail: kenji-hata@aist.go.jp

## Resonance Rayleigh scattering spectroscopy of CNTs grown on a tapered optical nanofiber

Takuya Nagano<sup>1</sup>, Keisuke Okada<sup>1</sup>, Hiroaki Hirai<sup>1</sup>, Shin-ichiro Mouri<sup>2</sup>,  
and Kiyofumi Muro<sup>1</sup>

<sup>1</sup> Graduate School of Science, Chiba University, 1-33 Yayoi-cho, Inage-ku, Chiba, 263-8522, Japan

<sup>2</sup> Center for Frontier Science, Chiba University, 1-33 Yayoi-cho, Inage-ku, Chiba, 263-8522, Japan

Resonance Rayleigh scattering (RRS) spectroscopy is one of the effective methods to investigate the electronic transition of single wall carbon nanotubes (CNTs) [1] [2]. However, in the previous study, observed range is limited to higher order optical transitions because of experimental difficulties.

Then, we have developed a novel technique to study RRS of CNTs in the fundamental excitonic transitions range ( $\sim$ below 1.3eV) using CNTs grown on the tapered optical nanofiber [3], whose diameter is less than the wavelength of the light, and bright broadband super continuum light source (Super-luminescent diode). The advantage of this system is the reduction of background light. Only spontaneous emission of adjacent nanotubes can be channeled into the guided mode of a tapered optical nanofiber.

We observed the RRS spectrum whose linewidth ( $\sim$ 1meV) is fairly narrower than the luminescence linewidth (Figure 1). This difference may be related with the relaxation process after excitation. The intensity of RRS spectra strongly depended on the polarization of excitation light. They were also affected by the temperatures, molecular adsorption, and applied magnetic field.

[1] M. Y. Sfeir, et al., *Science* **306**, 1540 (2004).

[2] Tony F. Heinz, *Topics Appl. Physics* **111**, 253 (2008)

[3] T. Nagano, K. Okada, S. Mouri, and K. Muro, *Proceedings of ICPS 2010*, to be published

**Corresponding Author:** Shin-ichiro Mouri

**E-mail:** [mouri@physics.s.chiba-u.ac.jp](mailto:mouri@physics.s.chiba-u.ac.jp) **Tel:**+81-43-290-2740, **Fax:**+81-43-290-2756

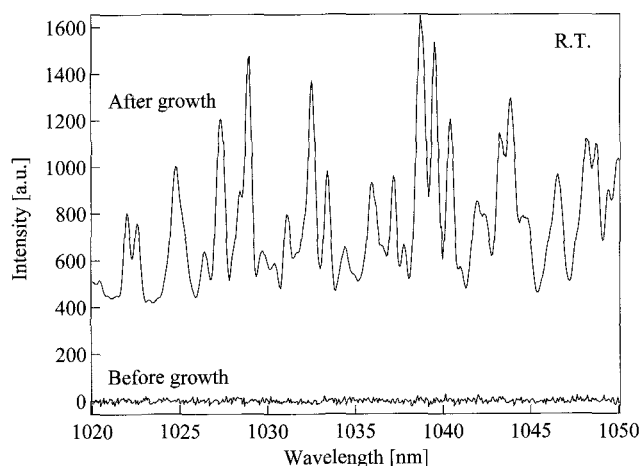


**FIGURE 1.** Resonant Rayleigh scattering spectrum of carbon nanotubes on a tapered fiber (Upper) and the reference spectrum (Lower).

## Photoemission spectroscopy of double-walled carbon nanotubes based on host metallic SWCNTs

○S. Sagitani<sup>1</sup>, K. Yonemori<sup>1</sup>, R. Kakihara<sup>1</sup>, H. Takahumi<sup>2</sup>, D. Hirayama<sup>2</sup>, H. Hayashi<sup>2</sup>, J. Jiang<sup>2</sup>,  
H. Iwasawa<sup>3</sup>, K. Shimada<sup>3</sup>, H. Namatame<sup>3</sup>, M. Taguchi<sup>3</sup>, H. Ishii<sup>1</sup>, H. Kadowaki<sup>1</sup>, K. Matsuda<sup>1,4</sup>,  
K. Yanagi<sup>1,4</sup>, Y. Maniwa<sup>1,4</sup>

1. Faculty of Science, Tokyo Metropolitan University

2. Faculty of Science, Hiroshima University

3. Hiroshima Synchrotron Radiation Center (Hisor), Hiroshima University

4. JST-CREST.

**Abstract:** Double walled carbon nanotubes (DWCNTs) are an interacting material consisting of two sub systems of inner and outer single walled carbon nanotubes (SWCNTs). Particularly, the electronic structure of DWCNTs has been expected to substantially differ from the simple superposition of those of the inner and outer SWCNTs due to the intershell interaction [1]. Photoemission spectroscopy (PES) is a powerful tool to investigate the electronic structure of valence band in solid. Therefore, PES of DWCNT bundles have been reported previously [2]. However, the DWCNT bundles studied consisted of various sets of inner and outer tubes which can be semiconducting or metallic SWCNTs. Here, we report a PES study on DWCNTs in which high-purity metallic-SWCNTs (m-SWCNTs) were used as the outer SWCNTs. The m-SWCNT-enriched DWCNTs were synthesized from m-SWCNTs by heating SWCNTs after filled with C<sub>60</sub>. In the following, this type of DWCNTs, having metallic outer tubes, is abbreviated to “m-DWCNTs”. The starting buckypaper of m-SWCNTs were prepared by using density gradient ultracentrifugation technique. High-resolution PES experiments were performed at Hisor BL1. Figure 1 shows photoemission spectra of m-DWCNTs along with that of m-SWCNTs for comparison. Spectra are normalized by the number of C atoms. M1 peaks around 1 eV originate from the 1D Van Hove singularity of SWCNTs. The spectrum of m-DWCNTs is almost similar to that of m-SWCNTs, but we found that the M1 peaks slightly shifted. The result suggests the occurrence of charge transfer from the outer tubes to the inner tubes.

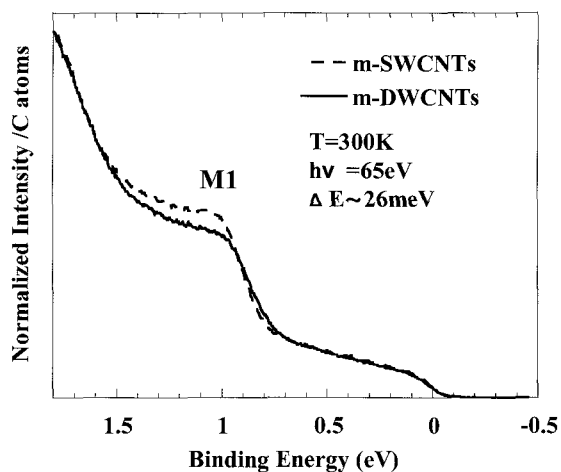


Figure.1

[1]V.Zolmy et al :Phys.Rev.B 77,245403(2008)

[2]H.Shiozawa et al :Phys.Rev.B77,153402(2008)

**Corresponding Author:** Y. Maniwa TEL:81-042-677-2490, E-mail: maniwa@phys.se.tmu.ac.jp



## Computational Chemistry Study of the Interaction between Single-walled Carbon Nanotubes and Polysaccharides

○Hiroyuki Shinomiya, Akira Itoh, Koji Tsuchiya, and Hirofumi Yajima

*Department of Applied Chemistry, Faculty of Science, Tokyo University of Science,  
1-3 Kagurazaka, Shinjuku-ku, Tokyo 162-8601, Japan*

**Abstract:** In pristine single-walled carbon nanotubes (SWNTs), there exist SWNTs with multiple chirality structures. The optical properties of SWNTs, such as UV-vis-NIR absorption/ photoluminescence (PL) and resonance Raman, are strongly correlated with the chirality, as summarized in Chirality map<sup>1)</sup> and Kataura plot<sup>2)</sup> as a function of tube diameter or chiral angle. From our selective chirality separation study for the SWNTs individually dispersed in aqueous solution with density gradient ultracentrifugation (DGU) technique using polysaccharides as dispersants, the resulting optical properties revealed that the specific interactions existed between polysaccharides and the SWNTs with peculiar chiralities.<sup>3-5)</sup> Thereof, when chitosan was used in the DGU experiments, the (9, 4) and (7, 6) chiralities SWNTs were collected. Furthermore, when carboxymethylcellulose (CMC) was used in the DGU experiments, the (8, 5), (9, 6), (8, 6), and (9, 7) chiralities SWNTs were collected.

The objective of this paper is to gain an insight into the specific interactions between the polysaccharides and the SWNTs with peculiar chiralities on the basis of the molecular dynamics (MD) simulations in water, taking the tube diameter or chiral-angle as parameters. The MD calculation was carried out using a software of *Accelrys Discovery Studio 2.1* with a molecular force field potential of *CHRAMm* under the conditions of time interval of 1 fs and periodic boundary conditions. Firstly, molecular structures were optimized, then annealing 0 K  $\rightarrow$  1000 K  $\rightarrow$  300 K was performed in 17 ps (temperature gradient is  $\pm 0.1$  K/fs.), and finally equilibration at 300 K in 1.5 ns was carried out at *NVT* ensemble.

As a result, it was found that although either chitosan or CMC intrinsically assumes an extended linear conformation in water, both the SWNTs complexes with the polysaccharides at stable energy states form the wrapping structures with the helical conformations of the polysaccharides. Essential intermolecular force between the polysaccharides and SWNTs was predicted to be originated from CH- $\pi$  interaction. The chiralities of SWNTs involved in the specific interactions with each of the polysaccharides were able to be simulated. Consequently, it was inferred that chitosan specifically interacts with the semiconductor chiral-SWNTs with a similar diameter, whereas CMC strongly interacts with the metal and/or semiconductor chiral-SWNTs with a similar chiral-angle.

### References

- [1] Z. Luo *et al.*, *Phys. Rev. B*, 70 (2004) 245429-1 - 245429-8.
  - [2] H. Kataura *et al.*, *Synth. Met.* 103 (1999) 2555-2558.
  - [3] C. Yamamoto *et al.*, *Polym. Prep., Jpn.*, 55 (2006) 5089.
  - [4] H. Shinomiya *et al.*, *Fullerene-Nanotubes General Symo.*, 37 (2009) 168.
  - [5] Y. Kaminosono *et al.*, *Polym. Prep., Jpn.*, 58 (2009) 4597.
- Corresponding Author: Hirofumi Yajima  
E-mail:yajima@rs.kagu.tus.ac.jp, Tel:+81-3-3260-4272(ext.5770), Fax: +81-3-5261-4631.

## Macroscopic Wall Number Analysis of Single-walled, Double-walled, and few-walled Carbon Nanotubes by X-ray Diffraction

○ Don N. Futaba\*<sup>1</sup>, Takeo Yamada<sup>1</sup>, Kazufumi Kobashi<sup>1</sup>, Motoo Yumura<sup>1</sup>, Kenji Hata<sup>1,2</sup>

<sup>1</sup>*Nanotube Research Center, National Institute of Advanced Industrial Science and Technology (AIST), Tsukuba, 305-8565, Japan.*

<sup>2</sup>*Japan Science and Technology Agency (JST), Kawaguchi, 332-0012, Japan*

For nanocarbon materials, as represented by carbon nanotubes (CNTs) and graphene, the number of layers (graphene shells or layers) is a fundamental structural parameter and many physical and chemical properties depend on the number of layers. This is particularly true for nanocarbon materials composed of few (~5) layers because this region is far from the 3-D bulk limit (i.e. nanofibers or bulk graphite). Within this region the properties can greatly change as exemplified by the semiconducting behavior of single-walled carbon nanotubes and the metallic behavior of multiwalled carbon nanotubes. Therefore, identifying the wall number of CNTs is paramount in understanding their properties and applying them toward the appropriate applications. Currently, only transmission electron microscopy has been the standard method for wall number analysis for CNTs.

Here, we have focused on the (002) peak of the XRD pattern to develop a simple macroscopic method to determine the average wall number of CNTs in the range of SWNTs to few-walled MWCNTs. The key was the finding that the (002) peak could be decomposed into two basic components: the intertube structure (outerwall contacts) and the intratube structure (concentric shells). Wall number estimation became possible because the contribution of the intertube structure to the (002) peak increased linearly with wall number while the contribution of the intratube structure did not.

Corresponding Author: Don Futaba

TEL: (029) 861-44402, FAX: (029) 861-4851, E-mail: d-futaba@aist.go.jp

## Dielectric Environment Effect on the Electronic States of (*n,m*) Single-Walled Carbon Nanotubes

○Yasuhiko Hirana<sup>1</sup>, Yasuhiko Tanaka<sup>1</sup>, Yasuro Niidome<sup>1</sup> and Naotoshi Nakashima<sup>1,2</sup>

<sup>1</sup>*Department of Applied Chemistry, Graduate School of Engineering,  
Kyushu University, Fukuoka 819-0395, Japan.*

<sup>2</sup>*CREST, Japan Science and Technology Agency, 5 Sanbancho, Chiyoda-ku,  
Tokyo 102-0075, Japan*

The redox properties (i.e. electronic densities, the Fermi levels, redox potentials) of single-walled carbon nanotubes (SWNTs) are related to the structures of SWNTs that have a specified diameter and chiral angle uniquely related to a pair of integers (*n,m*); the so-called chiral index. Electronic structure, one of the most fundamental features of SWNTs, also strongly depends on their diameter and chirality.

Here we report the finding that the electrochemical band gaps ( $E_g^{electr}$ ) of (*n,m*)SWNTs are strongly affected by the change in dielectric environments around the isolated SWNTs. In situ photoluminescence (PL) spectroelectrochemistry<sup>1</sup> of the films containing isolated SWNTs cast on ITO electrodes was completed in several organic solvents and then the oxidation and reduction potentials,  $E_g^{electr}$  and Fermi levels of the individual (*n,m*)SWNTs in the solvents were determined. We discovered that the  $E_g^{electr}$  of the (*n,m*)SWNTs become greater as the solvent dielectric constants decreased, which is in sharp contrast to the optical band gaps that show virtually no solvent dependence.<sup>2</sup> Moreover, the states of the  $\pi$ -electrons in the SWNTs were evaluated from the dependence of the band gaps on the diameter of the SWNTs. The present study provides useful information for a deep understanding of the fundamental electronic properties of isolated (*n,m*)SWNTs in solvents.

### References:

- [1] Y. Tanaka, Y. Hirana, Y. Niidome, K. Kato, S. Saito, N. Nakashima, *Angew. Chem. Int. Ed.* **2009**, *48*, 7655.  
[2] Y. Hirana, Y. Tanaka, Y. Niidome, N. Nakashima, *J. Am. Chem. Soc.* **2010**, *132*, 13072.

**Corresponding Author:** Naotoshi Nakashima

**E-mail:** nakashima-tcm@mail.cstm.kyushu-u.ac.jp

**Tel&Fax:** +81-92-802-2842

## Systematic First-Principles Study of Single-Walled Carbon Nanotubes with Helical-Symmetry Operation

○Koichiro Kato, Takashi Koretsune and Susumu Saito

*Department of Physics, Tokyo Institute of Technology,  
2-12-1 Oh-okayama, Meguro-ku, Tokyo 152-8551, Japan*

Many experimental and theoretical works of carbon nanotubes (CNTs) discussing the fundamental physics aspects and/or their possible applications have been reported so far. According to the study using the tight-binding approximation, their electronic structures depend on their diameter and chirality [1]. In addition, it has been pointed out from the first-principle electronic-structure calculations with structural relaxation that their electronic structures also depend sensitively on their geometrical parameters such as bond lengths and bond angles [2,3]. On the other hand, the synthesizing technique with the precise diameter and chirality control of CNT has not been established yet. Hence, the accurate measurements of not only the electronic properties but also the geometrical parameters of CNTs have been reported scarcely so far. Because it is very important to know the accurate electronic properties of CNTs for any possible electronic application, the first-principles calculations with the structural relaxation for CNTs should be of high importance. Recently, however, some interesting studies were reported and it has been revealed that near-armchair CNTs are relatively abundant in yield CNT samples [4,5]. In addition, the energetics of very thin nanotubes implies that the near-armchair nanotubes are energetically more favorable than armchair and zigzag nanotubes [3]. Therefore, the experimental measurement of the geometrical parameters and the electronic properties of near-armchair nanotubes may be achieved in the near future.

In the present work, we systematically study the geometries, electronic properties and energetics of isolated single-walled carbon nanotubes in the framework of the density functional theory (DFT). The diameters of the studied CNTs are in the range from 0.68 nm to 1.0 nm. The studied CNTs include (6,5) and (7,5) which are known to be the most abundant CNTs in some samples. Because of the huge number of atoms in the translational unit cell, the systematic first-principles studies have not been reported for these nanotubes. We adopt the real-space DFT computational code with helical-symmetry and the rotational symmetry. By using this method, we can handle all of the nanotubes in the same computational cost in principle. We discuss the influences of the structural relaxations on the geometrical parameters and the electronic properties. Moreover, we compare the total energy of the various optimized CNTs and examine the energetical favorability of the near-armchair nanotubes.

[1] N. Hamada, S. Sawada and A. Oshiyama, *Phys. Rev. Lett.*, **68**, 1579 (1992).

[2] K. Kanamitsu and S. Saito, *J. Phys. Soc. Jpn.*, **71**, 483 (2002)

[3] K. Kato and S. Saito, *Physica E*, **43**, 669 (2011)

[4] S. M. Bachilo, L. Balzano, J. E. Herrera, F. Pompeo, D. E. Resasco and R. B. Weisman, *J. Am. Chem. Soc.* **125** 11186 (2003)

[5] Y. Miyauchi, S. Chiashi, Y. Murakami, Y. Hayashida and S. Maruyama, *Chem. Phys. Lett.* **387** 198 (2004)

E-mail : kato@stat.phys.titech.ac.jp (K. Kato)

## Structural Stability and Electronic Manipulation of Nitrogen-doped Carbon Nanotube

○Yoshitaka Fujimoto and Susumu Saito

*Department of Physics, Tokyo Institute of Technology, Tokyo 152-8551, Japan*

Carbon nanotube (CNT) has been received much attention since it shows unique electronic properties such high carrier mobility, suggesting the possibility of realization of novel electron-device applications in carbon-based nano-electronics. For developments of CNT-based devices, a strict control of the electronic properties such as carrier type and carrier density is vital. Nitrogen doping is one of the most accessible means to tailor electronic properties of CNT. Nitrogen-doped CNTs have been synthesized experimentally and the existence of pyridine-type defects in N-doped CNTs has been reported [1]. Theoretical calculations has revealed that the electronic properties of pyridine-type defect in N-doped (10,0) CNT shows *p*-type semiconducting property [2]. Actually, the experimental electrical transport properties of N-doped CNT are reported to show the *p*-type behavior although N-doping is expected to induce *n*-type carrier [4]. For construct complex electronic devices with logic operations, it is essential to realize the functionalized CNTs that provide *p*-type and *n*-type conductions.

The impurity defect is generally expected to serve as a reactive site and the adsorption of several molecules would cause the change in the electronic structure. In this work, we investigate effects of the hydrogen adsorbed on the N-doped CNT using first-principles density-functional calculations. In the presentation, we will show that the electronic structures of N-doped CNT change dramatically depending on the number of hydrogen atoms adsorbed on N-doped CNT and also discuss the energetics of the hydrogen adsorption on the N-doped CNT.

This work was partly supported by grants-in-aid from MEXT Japan through Global Center of Excellence Program of Nanoscience and Quantum Physics of Tokyo Institute of Technology.

- [1] R. Czerw, M. Terrones, J. C. Charlier, X. Blasé, B. Foley, R. Kamalakaran, N. Grobert, H. Terrones, D. Tekleab, P. M. Ajayan, W. Blau, M. Ruhle, M. Ruhler, and D. L. Carroll, *Nano. Lett.* **1**, 457 (2001).
- [2] Y. Fujimoto and S. Saito, *Physica E* **43**, 677 (2011).
- [3] Y.-S. Min, E. J. Bae, U. J. Kim, E. H. Lee, N. Park, C. S. Hwang, and W. Park, *Appl. Phys. Lett.* **93** (2008) 043113.

Corresponding Author: Yoshitaka Fujimoto

TEL: +81-3-5734-2368, FAX: +81-3-5734-2368, E-mail: [fujimoto@stat.phys.titech.ac.jp](mailto:fujimoto@stat.phys.titech.ac.jp)

## Kekulé Structures and HOMO-LUMO Gaps of Armchair Carbon Nanotubes with Finite Length

○Noriyuki Mizoguchi

*Meiji Pharmaceutical University, Noshio, Kiyose, Tokyo 2-522-1, Japan*

An interesting aspect of finite-length carbon nanotubes (CNTs) is the quantum finite-size effects of the energy gap between the highest occupied molecular orbital (HOMO) and the lowest unoccupied molecular orbital (LUMO). It has been shown that the HOMO-LUMO gaps of zigzag CNTs oscillate with an odd or even number of hexagons in the circular plane of the nanotube [1]. It is known that for the armchair CNT, the HOMO-LUMO gaps show the oscillation depending on the number of carbon layers in the tubular length axis. The number of Kekulé structures (K) is an excellent index for the stability of benzenoid hydrocarbons. However, for conjugated polycyclic non-benzenoid structures, the algebraic structure count (ASC) should be used. The ASC for a conjugated molecule G is closely related to the constant term  $a_N(G)$  in the characteristic polynomial for G:

$$\text{absolute value of } a_N(G) = \text{square of ASC}(G)$$

If the algebraic structure count (ASC) is zero, then the molecule's pi-system has non-bonding molecular orbitals.

The size of the peripheral circuits in armchair  $(n,n)_m$  CNT is  $4n$ . So ASC should be used for the study of HOMO-LUMO gap in armchair  $(n,n)_m$  CNT. Here  $m$  stands for the number of layers in CNT. For example, as shown in Fig. 1, the superposition of two Kekulé structures  $K_1$  and  $K_2$  for  $(1,1)_3$  CNT produces one 4-membered circuit and so  $K_1$  and  $K_2$  possess opposite parities. We found that in the case of  $(1,1)_m$  CNT,  $\text{ASC}=1$  for  $m=1$ ,  $\text{ASC}=1$  for  $m=2$ ,  $\text{ASC}=0$  for  $m=3$ , and in the case of  $(2,2)_m$  CNT,  $\text{ASC}=5$  for  $m=1$ ,  $\text{ASC}=13$  for  $m=2$ ,  $\text{ASC}=0$  for  $m=3$ . Thus we showed that the HOMO-LUMO gaps in  $(1,1)_m$  and  $(2,2)_m$  CNT are zero if the number of layers  $m$  is 3.

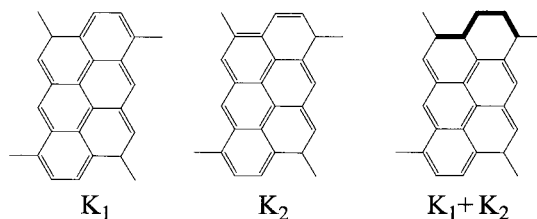


Fig. 1 Superposition of two Kekulé structures  $K_1$  and  $K_2$  for  $(1,1)_3$  CNT

[1] N. Mizoguchi, *sccj2010au.*, **2P10** (2010).

Corresponding Author: Noriyuki Mizoguchi

TEL: +81-42-495-8611, E-mail: nori@my-pharm.ac.jp

## Transport property of hydrogen adsorbed carbon nanotube : first-principles density functional study

○Tomoyo Kawasaki, Fumiyuki Ishii, Keisuke Sawada, and Mineo Saito

*Division of Mathematical and Physical Science, Graduate School of Natural Science and  
Technology, Kanazawa University, Kakuma, Kanazawa 920-1192, Japan*

Carbon nanotubes (CNTs) are expected to be suitable for nano-device applications. For an example, FETs (Field effect transistors) made of CNTs are expected to have good performance for both speed and size compared with conventional FETs. Studies of defects and impurities in CNTs are necessary since they have crucial effects on electron transport properties of CNTs [1,2]. We study electronic structure and electrical transport property of hydrogen adsorbed CNTs using first-principles non-equilibrium Green's functional method implemented in OpenMX code [3].

We have investigated electron transmission of hydrogen adsorbed (6,0) CNT (Fig.1(a)) with pure (6,0) CNT leads. Our results indicate that electron transmission is significantly affected by hydrogen adsorption (Fig. 1(b)). We will discuss the hydrogen coverage dependence and current-voltage characteristics of hydrogen adsorbed CNTs.

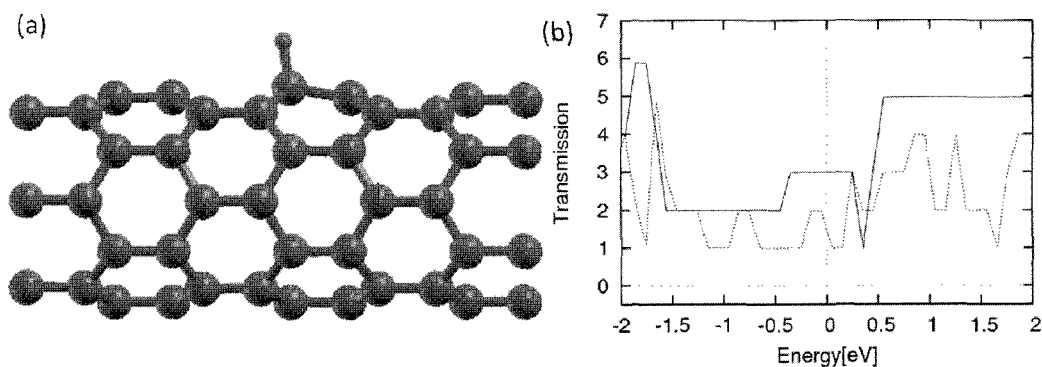


Fig 1. (a) Scattering region  $C_{72}H$  of hydrogen adsorbed (6,0) CNT and (b) energy dependence of electron transmission for pure (6,0) CNT (solid line) and hydrogen adsorbed CNT (dotted line). Fermi energy is taken at the origin of the energy.

[1] O. Gulseren, T. Yildirim, and S. Ciraci, *Phys. Rev. B* **66**, 121401 (2002).

[2] G. Zheng, Q. Li, K. Jiang, X. Zhang, J. Chen, Z. Ren, and S. Fan, *Nano Lett.*, **7**, 1622 (2007).

[3] T. Ozaki, H. Kino, J. Yu, M. J. Han, N. Kobayashi, M. Ohfuti, F. Ishii, T. Ohwaki, H. Weng, M. Toyoda and K. Terakura, <http://www.openmx-square.org/>

**Corresponding Author** : Fumiyuki Ishii

**TEL**: +81-76-264-6075, **FAX**: +81-76-264-6075, **E-mail** : ishii@cphys.s.kanazawa-u.ac.jp

## Optical response of single-walled carbon nanotubes in far-infrared region

○Soon-Kil Joung<sup>1</sup> and Toshiya Okazaki<sup>2,1</sup>

<sup>1</sup>*Technology Research Association for Single Wall Carbon Nanotubes (TASC), c/o Nanotube Research Center, AIST, Tsukuba 305-8565, Japan*

<sup>2</sup>*Nanotube Research Center, AIST, Tsukuba 305-8565, Japan*

A carbon nanotube (CNT) is one-dimensional and hollow cylindrical structure formed by wrapping a graphene sheet, and becomes either metallic or semiconducting depending on its geometry. Usually, single-walled carbon nanotubes (SWCNTs) have the order of a few nanometers in diameter and the order of several micrometers in length. Optical spectroscopy such as Raman scattering and photoluminescence is well-known to be effective technique to characterize their properties for electronic and optoelectronic applications. In addition, using infrared (IR) spectroscopy and terahertz time domain spectroscopy (THz-TDS), there has been reported the small band-gap and antenna effects of metallic SWCNTs [1-4]. The former has so far been reported theoretically and experimentally[1-3,5]. The small gaps in a few tens of meV at Fermi level were induced by the curvature effect and intertube interactions[5]. The latter, antenna effects by plasmon resonance have been predicted theoretically that frequency in far-IR spectroscopy and THz-TDS is proportional to the inverse tube length that has been one of the on-going themes in CNTs[4]. We here report optical response of SWCNTs by using FT-IR spectroscopy in mid- and far-IR range.

Several types of SWCNTs were used and prepared for thin films on silicon wafer and polyethylene IR card. For IR spectra obtained from arc discharge tubes, the signals exhibit a broad band around 100  $\text{cm}^{-1}$  and a sharp peak near 5580  $\text{cm}^{-1}$ . The latter is thought to be S1 interband transition of semiconducting SWCNTs. The former is considered to be a small gap and antenna effects-induced signal of metallic SWCNTs. To clarify the origin of this signal, we have investigated the doping dependence and  $\text{F}_4\text{TCNQ}$  was used as a dopant. Upon doping, the absorption intensity was enhanced in low-frequency region along with the strong reduction of the peak of S1 interband transitions. The possible mechanism for the experimental observations will be discussed.

- [1] M. E. Itkis, S. Niyogi, M. E. Meng, M. A. Hamon, H. Hu, and R. C. Haddon, *Nano Lett.*, **2**, 155 (2002).
- [2] H. Nishimura, N. Minami, and R. Shimano, *Appl. Phys. Lett.*, **91**, 011108 (2007).
- [3] N. Akima, Y. Iwasa, S. Brown, A. M. Barbour, J. Cao, J. L. Musfeldt, H. Matsui, N. Toyota, M. Shiraishi, H. Shimoda and O. Zhou, *Adv. Mater.* **18**, 1166 (2006).
- [4] T. Nakanishi, T. Ando, *J. Phys. Soc. Jpn.*, **78**, 114708 (2009). 18, 1166.
- [5] M. Ouyang, J.-L. Huang, C. L. Cheung and C. M. Lieber, *Science*, **292**, 702 (2001).

**Corresponding Author:** Toshiya Okazaki, **E-mail:** toshi.okazaki@aist.go.jp, **Tel:** 029-861-4173, **Fax:** 029-861-6241



## Transport properties of individual boron-doped carbon nanotube under pressure

○Tohru Watanabe<sup>1,2</sup>, Fumiaki Tomioka<sup>1</sup>, Satoshi Ishii<sup>1</sup>, Shunsuke Tsuda<sup>1</sup>,  
Takahide Yamaguchi<sup>1</sup>, Yoshihiko Takano<sup>1,2</sup>

<sup>1</sup>*National Institute for Materials Science, 1-2-1, Sengen, Tsukuba, Ibaraki, 305-0047, Japan*

<sup>2</sup>*Tsukuba University, 1-1-1, Tennodai, Tsukuba, Ibaraki, 305-8577, Japan*

Carbon nanotube (CNT), which has low resistivity, is expected to be applied to various devices, for example, transparent electrodes, nanowiring for LSIs, probes for scanning microscopes and so on. However, CNT shows semiconducting and metallic behavior depending on the chiral vector, and there have been no report on successful CNT growth with chirality control. In semiconductor, carrier doping reduce resistivity. This technique can be used for CNT and we reported boron-doped CNT has lower resistivity than it of pure CNT [1]. Another way to control resistivity is applying pressure. However, the transport properties of individual CNT under pressure have not been reported.

We investigated the effect of high pressure on the transport properties of individual boron-doped multi-walled carbon nanotube (MWNT). Boron-doped MWNT was synthesized by hot filament method [2]. Carbon nanotube was dispersed on substrate and four terminals were fabricated. Electrical resistance of individual MWNT was measured under high pressure up to 1.73 GPa. The resistance dramatically decreased with increasing pressure. I will present the detail of CNT growth, measurement method and results.

**References:** [1] APL 92 202116 (2008) S. Ishii et al.

[2] Physica C 469 1002 (2009) S. Ishii et al.

**Corresponding Author :** Tohru Watanabe

**E-mail :** WATANABE.Tohru@nims.go.jp

**Tel :** 029-859-6321, **Fax :** 029-859-2601

## Redispersing Semiconducting Single Wall Carbon Nanotubes by DNA and Their Size Exclusion Chromatography

○Yuki Asada<sup>1</sup>, Kazuki Ihara<sup>2,3</sup>, Shigekazu Ohmori<sup>1</sup>,  
Fumiyuki Nihey<sup>2,3</sup> and Takeshi Saito<sup>1,3</sup>

<sup>1</sup>*Nanotube Research Center, National Institute of Advanced Industrial Science and Technology (AIST), Tsukuba 305-8565, Japan*

<sup>2</sup>*Green Innovation Research Laboratories, NEC Corporation, Tsukuba 305-8501, Japan*

<sup>3</sup>*Technology Research Association for Single Wall Carbon Nanotubes (TASC), Tsukuba 305-8565, Japan*

Due to its absolutely isolated state in water and length sortability by using size exclusion chromatography (SEC), single wall carbon nanotubes wrapped by DNA (DNA-SWCNTs) have attracted much attention as a semiconducting material in the channel of printed thin film transistor (TFTs) [1,2]. Although various separation methods of metallic and semiconducting SWCNTs have been reported, the separation in structural properties such as their length would be also required for achieving high performance TFTs, because such structural properties should affect the dispersing characteristic and the way of forming SWCNT networks, which are expected to dominate their device performances. In this respect, the method of controlling both electronic and structural properties of SWCNTs is eagerly anticipated.

Here, for the purpose of length sorting of semiconducting SWCNTs (s-SWCNTs) and preparing uniform s-SWCNTs networks, we have tried to replace the dispersing agent (Brij 700) of s-SWCNTs obtained by Electric-field inducing Layer Formation (ELF) [3] with several kinds of DNA in order to sort obtained s-SWCNTs wrapped by DNA (DNA-s-SWCNTs) in length using SEC. Details of the redispersion and SEC results will be presented.

[1] Y. Asada, Y. Miyata, Y. Ohno, R. Kitaura, T. Sugai, T. Mizutani and H. Shinohara, *Adv. Mater.*, **22**, 2698 (2010).

[2] Y. Asada, Y. Miyata, K. Shiozawa, Y. Ohno, R. Kitaura, T. Mizutani and H. Shinohara, *J. Phys. Chem. C*, **115**, 270 (2010).

[3] K. Ihara, H. Endo, T. Saito and F. Nihey, *NT10: 11<sup>th</sup> International Conference on the Science and Application of Nanotubes 2010*, Montreal, Canada, pp 54.

Corresponding Author: Takeshi Saito

TEL: +81-29-861-4863, FAX: +81-29-861-4413, E-mail: [takeshi-saito@aist.go.jp](mailto:takeshi-saito@aist.go.jp)

### Growth control of carbon nanotubes on a metal tip apex

○ Hisanori Kanayama, Kota Shimanaka, Hideki Sato

*Graduate School of Engineering, Mie University,*

*1577 Kurima-machiya-cho, Tsu, Mie, 514-8507, Japan*

Studies for application of carbon nanotubes (CNTs) to field emitters, SPM probes, and micro discharging electrodes have been actively carried out by many researchers. It has been considered that a method that enables growth of CNTs directly onto a metal tip apex by chemical vapor deposition (CVD) is a promising method for those applications. However, this method requires appropriate method to control the growth density and the growth direction of CNTs. In this study, we have examined the growth characteristics of CNTs on the metal tips for the purpose to improve the alignment of the growth direction of the CNT.

Tungsten (W) tips with apex curvature radii of approximately  $1\mu\text{m}$  were fabricated by electrochemically etching a W-wire of 0.15 mm in diameter. Al underlayer (20 nm) and Ni catalyst layer (10 nm) were sequentially formed on the W-tip apex by a vacuum evaporation method. After that, CNTs were grown on the W-tip apex by a thermal CVD method. The CVD process was carried out for 10 min under the following conditions. The gas flow rates of Ar,  $\text{H}_2$ , and  $\text{C}_2\text{H}_2$  were 50, 12.5, and 2.1 sccm, respectively. The pressure was 1 atm, and the temperature was  $650^\circ\text{C}$ . To apply a DC voltage during the CVD, a counter electrode plate to the W-tip was placed in the CVD reactor, and the voltage was applied between the W-tip and the counter electrode. The distance between the W-tip and the counter electrode plate was 1 mm. The applied voltage was varied between 0 and -350 V.

Fig. 1(a) and (b) show SEM images of CNTs grown on the W-tip without applying the voltage (0 V), and with applying the voltage to -350 V, respectively. Randomly oriented CNT growth is observed in Fig. 1(a). On the other hand, alignment of the CNT is observed in Fig. 1(b). The CNTs grow toward the outside of the tip. The growth direction is parallel to the electric field induced on the tip surface. It was confirmed that the alignment depended on the applying voltage and also on the other conditions such as catalyst species.

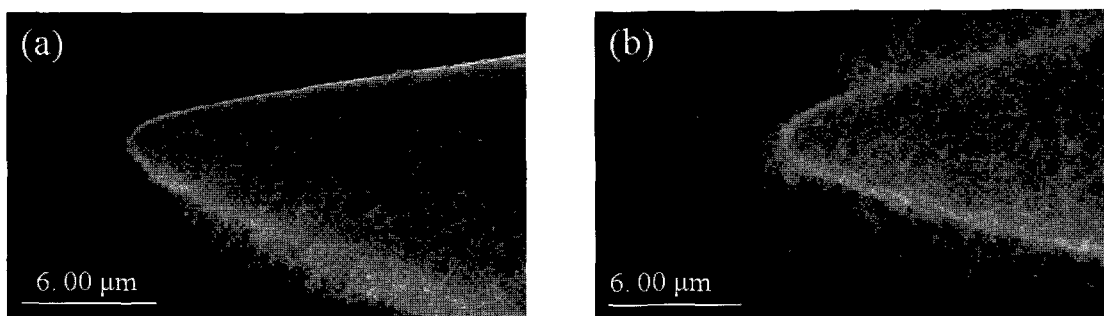


Fig. 1 SEM images of CNTs grown by CVD under application of DC voltages of (a) 0 V and (b) -350 V.

**Corresponding Author: Hisanori Kanayama**

**E-mail: hisanori.kanayama@eds.elec.mie-u.ac.jp, TEL&FAX:059-231-9404**

## Effect of Al<sub>2</sub>O<sub>3</sub> Film Thickness on Growth of MWCNT Forest with Graphite Roof

○H. Atsumi<sup>1</sup>, K. Takimoto<sup>1</sup>, Y. Suda<sup>1</sup>, H. Tanoue<sup>1</sup>, H. Takikawa<sup>1</sup>  
H. Ue<sup>2</sup>, K. Shimizu<sup>3</sup>, Y. Umeda<sup>4</sup>

<sup>1</sup> *Department of Electrical and Electronic Information Engineering,  
Toyohashi University of Technology*

<sup>2</sup> *Fuji Research Laboratory, Tokai Carbon Co., Ltd.*

<sup>3</sup> *Shonan Plastic Mfg. Co., Ltd.*

<sup>4</sup> *Fundamental Research Department, Toho Gas Co., Ltd.*

In this study, the structure that is composed of multi-walled carbon nanotubes (MWCNTs) and graphite layer were synthesized from a bi-layer catalyst of iron (Fe) and aluminum oxide (Al<sub>2</sub>O<sub>3</sub>) by chemical vapor deposition (CVD). Firstly, Al<sub>2</sub>O<sub>3</sub> film was deposited on silicon (Si) substrate with a silicon dioxide layer by vacuum evaporation. Then, Fe film was formed on the substrate by spin coating and calcination in the air at 780 °C. The CVD equipment used was developed in our laboratory. The acetylene (C<sub>2</sub>H<sub>2</sub>) and nitrogen (N<sub>2</sub>) gases were used as source and dilution gases, respectively.

Fig. 1 shows the scanning electron microscopy (SEM) of the structure. Aligned carbon nanotubes are covered with graphite roof [1]. Fig. 2 shows the effect of Al<sub>2</sub>O<sub>3</sub> film thickness on the growth rate of the structure. As the Al<sub>2</sub>O<sub>3</sub> film became thicker, the growth rate was decreased. The tallest structure with a height of approx. 60 μm was obtained, in which the thickness of graphite layers was approx. 0.5 μm.

This work has been partly supported by the Outstanding Research Project of the Venture Business Laboratory from Toyohashi University of Technology (TUT); Global COE Program "Frontiers of Intelligent Sensing" from the Ministry of Education, Culture, Sports, Science and Technology (MEXT); Core University Programs (JSPS-CAS program in the field of "Plasma and Nuclear Fusion") from the Japan Society for the Promotion of Science (JSPS), Grant-in-Aid for Scientific Research from the MEXT, Toukai Foundation for Technology, Research Foundation for Materials Science, and Chubu Science and Technology Center.

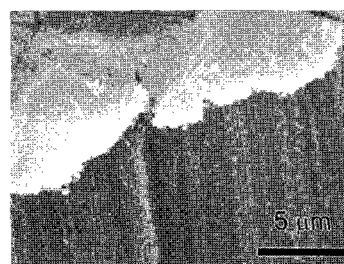


Fig. 1 SEM micrograph of the structure: aligned MWCNTs covered with graphite roof

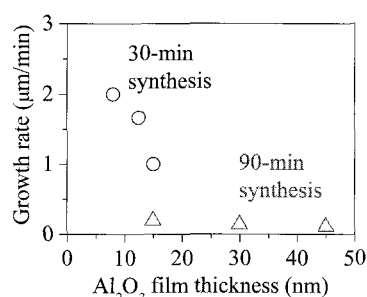


Fig. 2 Effect of Al<sub>2</sub>O<sub>3</sub> film thickness on growth rate of MWCNT with graphite roof

[1] D. Kondo, et al., Appl. Phys. Exp., 1 (2008) 074003

Corresponding Author: Yoshiyuki Suda

E-mail: suda@ee.tut.ac.jp, Tel: +81-532-44-6726

## Effect of pH and NaCl Concentration on Metal/Semiconductor Separation of Carbon Nanotubes using Gel

○Yasuko Urabe<sup>1,2</sup>, Takeshi Tanaka<sup>1</sup> and Hiromichi Kataura<sup>1,2</sup>

<sup>1</sup>Nanosystem Research Institute, National Institute of Advanced Industrial Science and Technology (AIST), Tsukuba, Ibaraki 305-8562, Japan

<sup>2</sup>JST, CREST, Kawaguchi, Saitama, 332-0012, Japan

There are two electric types of single wall carbon nanotubes (SWCNTs), metallic (M) ones and semiconducting (S) ones. For their electrical application, it is required that these two types of SWCNTs are separated into the respective type. We have developed effective M/S separation methods using agarose gel<sup>1-4</sup>. In this presentation, we report the effects of pH and NaCl concentration on the M/S separation using gel.

M/S separation was conducted using batch separation method<sup>4</sup>. HiPco-SWCNT/sodium dodecyl sulfate (SDS) dispersion was prepared by sonication and ultracentrifugation. The dispersion and agarose gel beads (Sepharose 2B) were mixed, and then a solution (unbound) fraction containing M-enriched SWCNTs and a gel (bound) fraction containing S-enriched SWCNTs eluted from the gel were collected. When pH of the mixture was changed from 10.4 to 3.2, the amount of SWCNTs of bound fraction was decreased (Fig. 1A). Similarly by increasing NaCl concentration of the mixture (from 0 to 250 mM), the amount of gel-bound SWCNTs was decreased (Fig. 1B). In the case of 500 mM NaCl, all SWCNTs aggregated, and no M/S separation was detected. In both the cases (changes of pH and NaCl concentration), decrease of the amount of the bound or unbound SWCNTs accompanied with improvement of semiconducting or metallic SWCNT purity. Detailed methods and results will be discussed.

### References:

- [1] T. Tanaka et al., *Appl. Phys. Express* 2008, **1**, 114001.
- [2] T. Tanaka et al., *Nano Lett.* 2009, **9**, 1497.
- [3] T. Tanaka et al., *Appl. Phys. Express* 2009, **2**, 125002.
- [4] T. Tanaka et al., *Phys. Status Solidi B* 2010, **247**, 2867.

Corresponding Author: Takeshi Tanaka

Tel: +81-29-861-2903, Fax: +81-29-861-2786

E-mail: tanaka-t@aist.go.jp

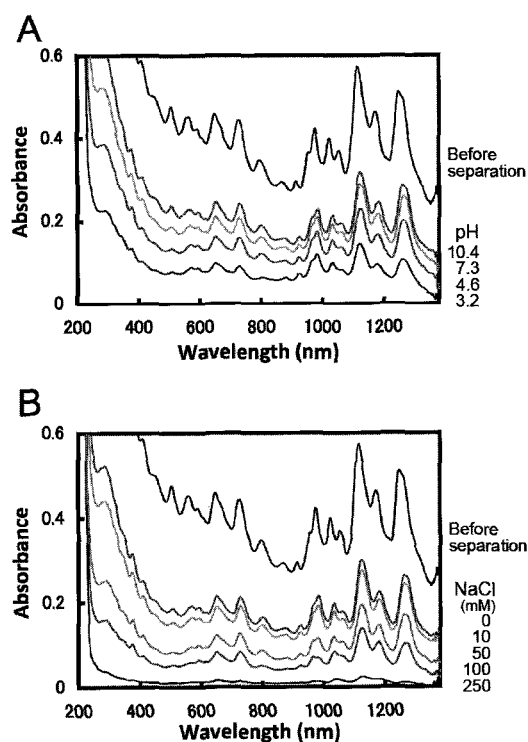


Fig. 1 Optical absorbance spectra of bound fractions after separation at different pHs (A) and NaCl concentrations (B).

## Development of large scale vertically aligned high-temperature pulsed-arc discharge

○Yuuichi Abe and Toshiki Sugai

Department of Chemistry, Toho University, Miyama 2-2-1 Funabashi, 274-8510, Japan

A high-temperature pulsed-arc discharge (HTPAD) is a production system of nanocarbon materials. The system utilizes width controlled pulsed arc discharge around ms for the vaporization of carbonaceous electrode in temperature controlled ambient rare gas around 1000 °C for the growth of the materials. With this width and temperature control, novel materials have been produced by the system such as high-quality double wall carbon nanotubes[1]. However, the production rate of the system is about 20 mg/hour because of low duty factor of the discharge (~3 %). Furthermore the horizontally aligned narrow tube reactor ( $\phi 26$  mm) of the system prevents the vaporized carbonaceous materials from growth in free space and from being collected effectively in the trap since the vapor is transferred by the convection to be stacked on the surface of the tube and the electrodes. Here we present the development of a large scale vertically aligned HTPAD to improve these points.

Figure 1 shows the schematics of the system. The vertically aligned thick ( $\phi 100$  mm) alumina tube reactor with independently controlled three heaters realizes free growth space without the wall perturbation. Ar gas flow from top to bottom also contributes to cancel the effect of the convection. Not only for the free growth, the large reactor tube enables us to install four parallel discharge electrodes pairs for the enhancement of the productivity.

With this system, the production rate is increased up to 1000 mg/hour, 50 times larger than the previous one. In addition to the productivity enhancement, the produced nanocarbon materials are also different: the large part of the products consist of SWNT with large diameters (2 to 3 nm) with little DWNTs even if the optimum condition for DWNTs is applied. The result show that the wall and flow have significant effect for the growth of nanocarbon materials. We are now optimizing conditions for novel materials.

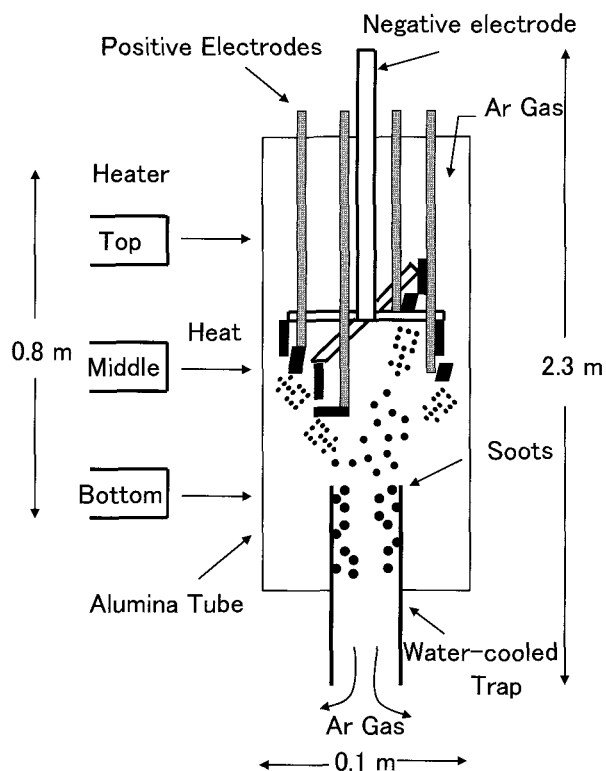


Fig.1 Schematic of large scale vertically aligned high-temperature pulsed arc discharge

[1] T. Sugai *et al.*, *Nano Lett.* **3**, 769 (2003).

TEL: +81-47-472-4406, FAX: +81-47-472-4406, E-mail: sugai@chem.sci.toho-u.ac.jp

## Diameter Selection Techniques for Single-Wall Carbon Nanotubes With Around 1.4 nm Diameters

○T. Suzuki,<sup>1</sup> K. Yanagi,<sup>1\*</sup> H. Ozaki,<sup>1</sup> H. Kataura,<sup>2,3</sup> Y. Maniwa<sup>1,3</sup>

*1. Tokyo Metropolitan University, 2. AIST, 3. JST-CREST*

**Abstract:** Single-wall carbon nanotubes (SWCNTs) with diameters around 1.4 nm, can encapsulate various kinds of organic molecules. The SWCNTs encapsulating molecules (peapods) can exhibit unique electronic and optical properties, and encapsulation of molecules is one of approaches to tune the properties of SWCNTs. Previously, we have prepared peapods with metallic or semiconducting types of SWCNTs,<sup>1</sup> but it is necessary to prepare samples with a single chirality in order to experimentally reveal the detailed interactions between encapsulated molecules and nanotubes. Thus, development of techniques to obtain a single chiral sample in this diameter region is important. Various techniques are reported to obtain a selected chirality for SWCNTs with diameters less than around 1.0 nm, but not for SWCNTs with diameters of around 1.4 nm. Metal-semiconductor (MS) separations can be easily achieved in 1.4 nm diameter SWCNTs. Therefore, it would be possible to prepare almost a single-chiral sample if we could apply MS-separations and diameter separations successively. Therefore, we investigated a diameter-sorting method which has high diameter selectivity on SWCNTs with around 1.4 nm diameters. First we examined density-gradient ultracentrifugation (DGU) methods. DGU using iodixanol, which is firstly developed by Arnold et al.,<sup>2</sup> causes both diameter and electronic selections.<sup>2</sup> However, the reported diameter selectivity by iodixanol-DGU is not so good for the nanotubes with 1.4 nm. Therefore, we investigate other gradient materials, such as sucrose<sup>3</sup> and cesium chloride, to check the selectivity with diameter of this region. As shown in Fig. 1, we found that relatively good diameter selection can be achieved by DGU using cesium chloride.

**References:** [1] Yanagi et al., *J. Phys. Chem. C* **114**, 2524 (2010), [2] Arnold et al, *Nature Nanotech.* **1**, 60 (2006). [3] Yanagi et al., *J. Phys. Chem. C* **112**, 18889 (2008)

**Corresponding Author:** Kazuhiro Yanagi

**E-mail:** yanagi-kazuhiro@tmu.ac.jp

**Tel & Fax:** 042-677-2494 (& 2483)

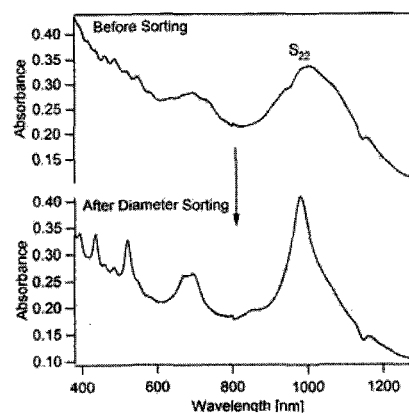


Fig. 1: Diameter sorting by using cesium chloride for gradient material on SWCNTs with diameters around 1.4 nm.

## X-ray Structure of a Divalent Metallofullerene Yb@C<sub>80</sub>

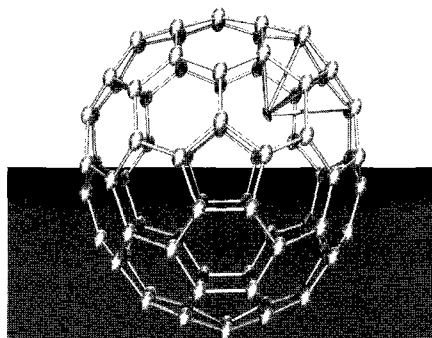
\*Xing Lu,<sup>1</sup> Naomi Mizorogi,<sup>1</sup> Zdenek Slanina,<sup>1</sup> Takeshi Akasaka,<sup>1</sup> Shigeru, Nagase<sup>2</sup>

<sup>1</sup>Center for Tsukuba Advanced Research Alliance, University of Tsukuba, Ibaraki 305-8577,  
Japan

<sup>2</sup>Department of Theoretical and Computational Molecular Science, Institute for Molecule  
Science, Okazaki, Aichi, 444-8585, Japan

Structural elucidation of endohedral metallofullerenes (EMFs) has been of fundamental importance because successful results are valuable for understanding their properties and broadening their applications.<sup>[1]</sup> Recently, we have systematically determined the cage structures of Yb@C<sub>2n</sub> (2n = 80, 82, 84) with <sup>13</sup>C NMR spectroscopy. The results revealed that the single Yb atom plays an important role in determining the cage structures of the resulting molecules.<sup>[2]</sup> However, as NMR technique is invalid to characterize the motional behaviors of the internal metal, single crystallography is always the final solution for EMF structures.

Here, we report the first X-ray results of pristine Yb@C<sub>2v(3)</sub>-C<sub>80</sub>, cocrystallized with Ni(OEP). It is disclosed that the Yb atom takes an off-center position apart from the C<sub>2</sub> axis, and it coordinates strongly with the adjacent cage carbons with Yb-C distances ranging from 2.45 Å to 2.70 Å (see picture). This is the first observation of the off-axis location of metal in mono-EMFs which is expected to be effective to induce unusual chemical behaviors of the cage carbons. Theoretical calculations disclose that this configuration is at least 6.19 kcal/mol more stable than any other possible conformer.



- [1]. (a) T. Akasaka, F. Wudl and S. Nagase, *Chemistry of Nanocarbons*, Wiley-Blackwell, London, **2010**. (b) T. Akasaka and S. Nagase, *Endofullerenes: A New Family of Carbon Clusters*, Kluwer, Dordrecht, **2002**. (c) X. Lu, T. Akasaka, and S. Nagase, *Rare Earth Metals Trapped inside Fullerenes – Endohedral Metallofullerenes*, in *Rare Earth Coordination Chemistry: Fundamentals and Applications*, C. H. Huang, Ed. John Wiley & Sons: Singapore, **2010**, pp 273-307.
- [2]. X. Lu, Z. Slanina, T. Akasaka, T. Tsuchiya, N. Mizorogi, S. Nagase, *J. Am. Chem. Soc.* **2010**, *132*, 5896-5905.

**Corresponding Author:** Xing Lu

**E-mail:** lux@tara.tsukuba.ac.jp

**Tel & Fax:** +81-29-853-7289



## Electronic Properties of $M_2(C_2)@C_{82}$ (M=Sc, Ti, Fe) Endohedral Metallofullerenes

○Yoshio Nishimoto, Stephan Irle,

*Institute for Advanced Research and Department of Chemistry, Nagoya University,  
Nagoya 464-8602, Japan*

The electronic structure of di-scandium, di-titanium and di-iron endohedral metallofullerenes (EMFs),  $M_2C_2@C_{82}$  (M = Sc, Ti, Fe) (see Fig. 1), were investigated using density functional theory (DFT) and the self-consistent-charge density-functional tight-binding (SCC-DFTB, in the following abbreviated as “DFTB” [1]) method. The latter is computationally far more economical than first principles DFT, yet allows to capture the essential features of the electronic structure and to compute molecular structure and other properties with accuracy comparable to traditional DFT methods.

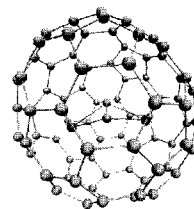


**Figure 1.** Optimized geometry of isomer 4 of  $Sc_2C_2@C_{3v}-C_{82}$  (8) at BP86/TZP

In order to validate the use of the DFTB method, we first computed orbital energies of empty cage isomers of  $C_{82}$ . We found that the DFTB method correctly reproduces the large (LUMO+2) – (LUMO+1) gap (more than 1 eV) of  $C_{3v}-C_{82}$  (IPR isomer #8), in good agreement with traditional DFT at the BP86/TZP level of theory [2].

For di-scandium and di-titanium (carbide) EMFs, we performed geometry optimizations using the DFTB and B3LYP/def-SVP methods starting from the six  $M_2C_2@C_{3v}-C_{82}$  isomers (different arrangement of metal atoms inside the cage) optimized at the BP86/TZP level of theory as reported by Valencia *et al.* [2]. We found that DFTB isomer energies well reproduce the trends obtained from the DFT methods. The agreement is not perfect, as DFTB sometimes fails to predict the most stable isomer by a few kcal/mol. We then analyzed the molecular orbital diagrams of isomer 4 and DFTB orbital occupation numbers correspond to the same formal charges predicted by DFT calculations.

Finally we investigated di-iron EMFs, which have not been synthesized yet. We considered all possible spin states, from singlet to undecet including symmetry-broken wavefunctions with anti-parallel spin alignments. In general, binding energies of iron inside the EMFs are much smaller compared to the more electropositive Sc and Ti metals, suggesting that synthesis of these species is unlikely because iron tends to form larger clusters before individual atoms can be encapsulated in fullerene cages.

### References

- [1] M. Elstner, D. Porezag, G. Jungnickel, J. Elsner, M. Haugk, T. Frauenheim, S. Suhai, G. Seifert, *Phys. Rev. B* **1998**, 58, 7260.  
[2] R. Valencia, A. Rodriguez-Forteza, J. M. Poblet, *J. Phys. Chem. A* **2008**, 112, 4550.

**Corresponding Author:** Stephan Irle

**TEL:** +81-52-747-6397, **FAX:** +81-52-788-6151, **E-mail:** [sirle@iar.nagoya-u.a.jp](mailto:sirle@iar.nagoya-u.a.jp)

## Electronic property of Li@C<sub>60</sub>

○N. Ogasawara<sup>1</sup>, H. Yagi<sup>1</sup>, M. Zenki<sup>1</sup>, T. Zaima<sup>1</sup>,  
T. Miyazaki<sup>1</sup>, M. Saida<sup>2</sup>, H. Yamashita<sup>2</sup>, S. Hino<sup>1</sup>

<sup>1</sup>Graduate school of Science and Engineering, Ehime University,  
Matsuyama 790-8577, Japan

<sup>2</sup>ideal star Inc., ICR Bldg, 6-6-3 Minami Yoshinari, Aoba-ku,  
Sendai 989-3204, Japan

Recently, Li@C<sub>60</sub> can be produced in a macroscopic quantity so that the prospect for the investigation of its physical properties opens up. Isolation of Li@C<sub>60</sub> is difficult because of its instability. Thus isolated Li@C<sub>60</sub> is either in the state of a mixture with C<sub>60</sub> or in the state of [Li@C<sub>60</sub>] cation salts. In this presentation, we give ultraviolet photoelectron spectra (UPS) and X-ray photoelectron spectra (XPS) of Li@C<sub>60</sub>.

Figure 1 shows the UPS of a [Li@C<sub>60</sub>](PF<sub>6</sub>) thin film prepared by vacuum sublimation. The UPS of C<sub>60</sub> is also shown for comparison. Spectral onset energy of Li@C<sub>60</sub> is 0.7eV below the Fermi level, which is much smaller than that of C<sub>60</sub> (1.8 eV). In the spectra of [Li@C<sub>60</sub>](PF<sub>6</sub>), a peak S which is not present in C<sub>60</sub> appears at binding energy of 1.5eV. This peak is considered due to be the result of electron transfer from Li atom to the LUMO of C<sub>60</sub>. Except for the appearance of the peak S, the spectral shape of the UPS of Li@C<sub>60</sub> and C<sub>60</sub> is almost identical, but the peak positions of corresponding structures shift slightly; particularly shift of upper valence peaks located between 1 - 7 is drastic. Figure 2 shows the UPS of the [Li@C<sub>60</sub>](PF<sub>6</sub>) deposited at various crucible temperature (550-800°C). The new peak S is observed at the film prepared at 550°C, but its intensity reduces gradually as the evaporation temperature becomes higher and finally it vanishes at the film prepared at 800°C; the spectra of [Li@C<sub>60</sub>](PF<sub>6</sub>) deposited at 800°C becomes almost identical to that of C<sub>60</sub>. It seems that encapsulated Li atom escapes from C<sub>60</sub> cage when Li@C<sub>60</sub> is heated at high temperature.

Figure 3 shows the result of curve fitting of the UPS with using Gaussian functions. The full width at half maximum (FWHM) of Li@C<sub>60</sub> is wider than that of C<sub>60</sub>. This could be due to dissolution of the orbital degeneracy of the HOMO and the HOMO-1 of C<sub>60</sub> cage. It should be noted that the area of relative peak intensity is A : B : S = 18 : 9.6 : 1.5, which is an indication of one electron transfer from Li atom to the cage.

Corresponding Author: Shojun Hino

E-mail: hino@eng.ehime-u.ac.jp, phone: 089-927-9924

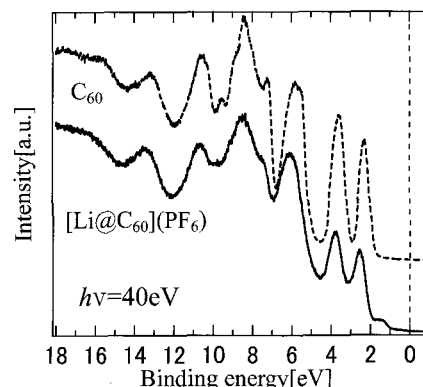


Fig1. The UPS of [Li@C<sub>60</sub>](PF<sub>6</sub>) and C<sub>60</sub>

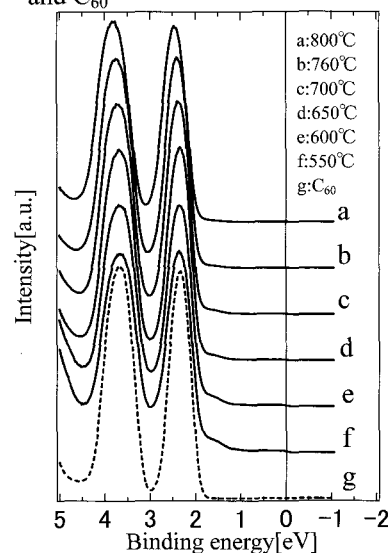


Fig2. UPS of [Li@C<sub>60</sub>](PF<sub>6</sub>) with changing evaporation temperature

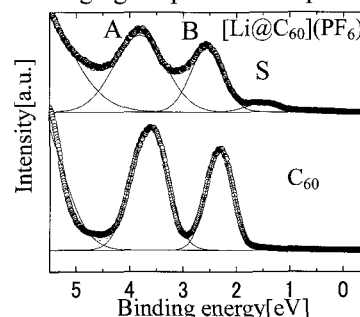


Fig3. UPS of [Li@C<sub>60</sub>](PF<sub>6</sub>) and C<sub>60</sub> with their Gaussian fitting

## Most stable structure and electronic structure of endohedral fullerenes $\text{Sc}_3\text{C}_2@\text{C}_{80}$ by density functional theory calculations

○Sosuke Okita<sup>1</sup>, Takeyuki Zaima<sup>1</sup>, Hajime Yagi<sup>1</sup>, Takafumi Miyazaki<sup>1</sup>, Haruya Okimoto<sup>2</sup>,  
Noriko Izumi<sup>2</sup>, Yusuke Nakanishi<sup>2</sup>, Hisanori Shinohara<sup>2</sup>, Shojun Hino<sup>1</sup>

<sup>1</sup>Graduate School of Science & Engineering, Ehime University

<sup>2</sup>Graduate School of Science, Nagoya University

Density functional theory calculations using Gaussian 03 program have been performed to elucidate the stable structure and the electronic structure of  $\text{Sc}_3\text{C}_2$  entrapped in the  $\text{C}_{80}$  ( $I_h$ ) fullerene cage. The structure of endohedral fullerene was optimized at the hybrid functional B3LYP level using the CEP-31G basis sets. The electronic structure was obtained by B3LYP level using 6-31G(d) basis sets for carbon, and TZVP basis sets for scandium.

Two geometries have been proposed for the entrapped  $\text{Sc}_3\text{C}_2$  cluster; trifoliate type and planar type.[1] (Fig.1)

Figure 2 shows the ultraviolet photoelectron spectra (UPS) of  $\text{Sc}_3\text{C}_2@\text{C}_{80}$  and simulation spectra obtained from two geometries. The simulation spectrum obtained from the trifoliate  $\text{Sc}_3\text{C}_2$  geometry reproduces UPS very well both in the relative intensity of corresponding peaks and their intervals, whereas that from the planar  $\text{Sc}_3\text{C}_2$  geometry shows fair correspondence. Thus, the  $\text{Sc}_3\text{C}_2$  cluster might take trifoliate geometry in  $I_h$ - $\text{C}_{80}$  cage.

Figure 3 shows the trifoliate type  $\text{Sc}_3\text{C}_2@\text{C}_{80}$  obtained from the geometry optimization.

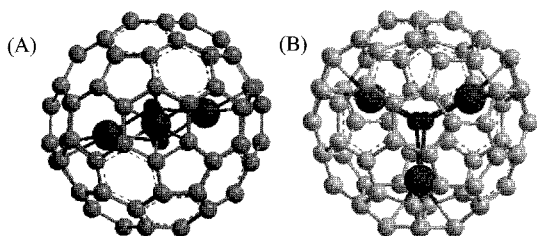


Fig.3 Trifoliate geometry of  $\text{Sc}_3\text{C}_2@\text{C}_{80}$

A : side view

B : top view

[1] K.Tan et al., J Phys. Chem. A 2006, 110, 1171-1176

Corresponding Author: S.Hino,

E-mail : hino@eng.ehime-u.ac.jp; Phone : 089-927-9924

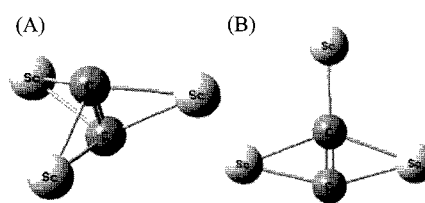


Fig.1 A : trifoliate type

B : planar type

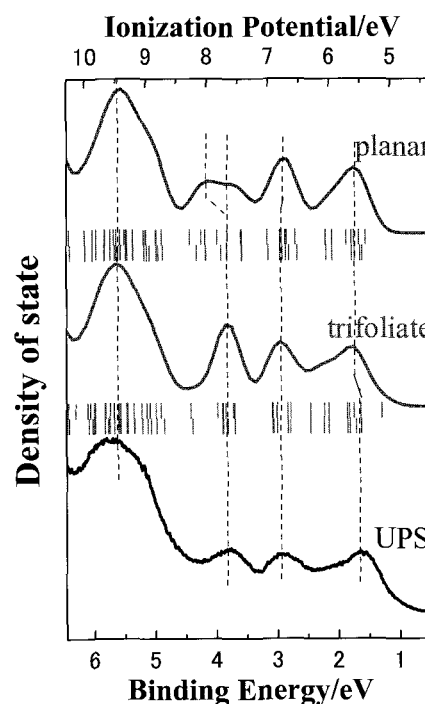


Fig.2 UPS and simulation spectra of  $\text{Sc}_3\text{C}_2@\text{C}_{80}$

## ESR measurement of N@C<sub>60</sub> encapsulated by $\gamma$ -cyclodextrin

○Tatsuhisa Kato<sup>1\*</sup>, Hiroki Shibata<sup>2</sup>, Tomonari Wakabayashi<sup>3</sup>

<sup>1</sup>*Institute for the Promotion of Excellence in Higher Education, Kyoto University, Kyoto, 606-8501 Japan*

<sup>2</sup>*Department of Chemistry, Josai University, Sakado, Saitama 350-0295, Japan*

<sup>3</sup>*Department of Chemistry, Kinki University, Higashi-Osaka 577-8502, Japan*

N@C<sub>60</sub> can be a good magnetic probe which gives the information of position as well as of chemical environment. For the biological application the probe should be soluble in water. The encapsulation of N@C<sub>60</sub> with  $\gamma$ -cyclodextrin was attained by a mechanochemical high-speed vibration technique<sup>1)</sup>, and the aqueous solution of N@C<sub>60</sub> was obtained. The ESR spectrum exhibited the broad triplet at 120K in frozen solution, as shown in Figure 1.

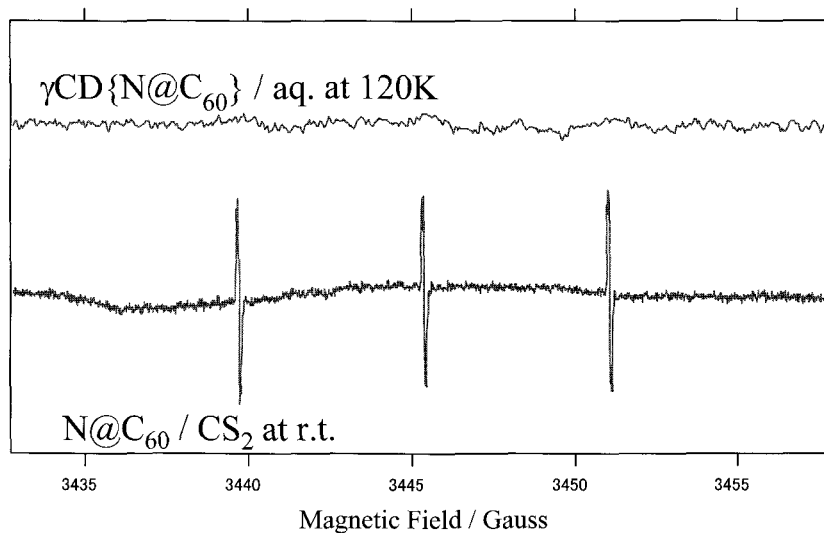


Figure 1. X-band ESR spectrum of N@C<sub>60</sub> in  $\gamma$ -cyclodextrin at 120K.

### References:

1. K.Komatsu, K. Fujiwara, Y. Murata, and T. Braun, *J. Chem. Soc., Perkin Trans 1*, 2962-2966(1999).

**Corresponding Author: Tatsuhisa Kato**

**E-mail: kato.tatsuhisa.6e@kyoto-u.ac.jp**

**Tel. & Fax : 075-753-6695**

## Implantation of Atoms into Fullerenes using High-Frequency Sputtering Apparatus

T. Wakabayashi, K. Sato, N. Kinomura, and N. Kumamoto

*Department of Chemistry, Kinki University, Higashi-Osaka 577-8502, Japan*

Ion implantation is one of the methods for encapsulation of atomic species inside the fullerene cage. Unlike the popular method of arc discharge by which metallofullerenes are obtained for higher fullerenes as hosting cages, i.e.,  $M@C_n$ ,  $n=80, 82, \text{ and } 84$ , there is in principle no limitation for the fullerene size as well as for the element to be implanted. The endofullerenes reported so far by ion implantation, or ion bombardment, are  $Li@C_{60}$ ,  $N@C_{60}$ ,  $N@C_{70}$ ,  $P@C_{60}$ ,  $Ar@C_{60}$ , and so on.

We have developed machinery for ion bombardment to produce  $N@C_{60}$  at relatively high yield. There are several points to be improved for increasing the production efficiency. To increase the ion current reaching to the surface of the electrode where the fullerene molecules are bombarded with the ions is primarily of importance. The apparatus can provide a current of positive ions on the order of  $\sim 10$  mA at 80 V. In addition, to keep the deposition rate being constant is also crucial, because the penetration depth of the ions into the sediment of fullerene molecules is not very large. For this, we have developed a PC-controlled programmable system of a crucible from which the fullerene molecules are sublimed to be deposited on the electrode. Combining the ESR detection and the HPLC separation, we can concentrate the target endofullerenes such as  $N@C_{60}$  in solutions. Eventually,  $N@C_{60}$  is detected by optical absorption in the chromatogram.

The apparatus was originally planed for sputtering solid materials of metals and semiconductors. A rod of solid elements can be set inside the plasma produced by high-frequency discharge of gases. When a positive high voltage is applied to the rod, electrons in the plasma are accelerated to sputter the surface of the rod. Then, atoms of the element of the rod are emanated into vacuum and ionized in the plasma. The ions are accelerated in the opposite direction to that of the electrons and collected onto the surface of an electrode to which fullerene molecules are deposited. In this way, the atomic species of a desired element of a solid form can be implanted into fullerene molecules. The detailed schemes and operation of the machinery will be presented.

**Correspondence to Tomonari Wakabayashi**

**E-mail: wakaba@chem.kindai.ac.jp**

**Tel. 06-6730-5880 (ex. 4101)**

Structures and Relative Stability of  $\text{Gd}_2@C_{98}$ 

W. Y. Gao and X. Zhao\*

*Institute for Chemical Physics and Department of Chemistry,  
Xi'an Jiaotong University, Xi'an 710049, P. R. China*

Endohedral metallofullerene  $\text{Gd}_2@C_{98}$  detected by chromatographic separation<sup>[1]</sup> was first reported by Balch *et al.* in 2008. However, the structural characterization of  $\text{Gd}_2@C_{98}$  has not been achieved. The extensive DFT calculations<sup>[2]</sup> on the hex-anions of all  $C_{68}$ - $C_{88}$  isomers (beyond IPR and non-IPR species) and IPR isomers of  $C_{90}$ - $C_{98}$  for endohedral fullerenes where lanthanide atoms engaged in carbon cages were performed by Popov *et al.* Clearly, it is insufficient if  $C_{98}$  IPR isomers are considered only.

We herein report a systematical investigation on the endohedral metallofullerene  $\text{Gd}_2@C_{98}$ . According to the stability criterion, we propose that the non-IPR fullerene isomers with three or more fused pentagons cannot be efficiently stabilized by the engaged metal atoms and are still encountered with energetic penalty. Therefore, IPR isomers and the non-IPR species with one and two adjacent pentagon pairs were considered in our computations. Since the ionic model of  $\text{Gd}_2@C_{98}$  were uncertain, so the total 17941  $C_{98}$  isomers beyond IPR and non-IPR species ( $PA=0\sim 2$ ) are screened on the tetra-anion and hex-anion states by AM1 calculations. Furthermore, the best structures of  $C_{98}^{6-}$  and  $C_{98}^{4-}$  as well as their corresponding metallofullerenes  $\text{Gd}_2@C_{98}$  were fully optimized at the B3LYP/6-31G(d) level of theory, respectively<sup>[3]</sup>. Vibration analyses on the best optimized geometries were carried out at the same DFT level of theory.

The results show that the lowest energy structure of  $\text{Gd}_2@C_{98}$  is still an IPR isomer but three non-IPR structures are found to be also very stable. It is revealed that HOMO-LUMO gap of the lowest energy IPR structure labeled 230924: $C_2$  is 1.35eV. Energy ranking from 2 to 4 was structure which has one pairs of adjacent pentagons, the forth one labeled 168764: $C_1$  is energy different of 0.74kcal/mol to 230924: $C_2$  and has the biggest HOMO-LUMO gap (1.85eV).

To obtain further insight into the thermodynamic stability of  $\text{Gd}_2@C_{98}$ , we will investigate the entropy effects and evaluate the relative concentrations through the Gibbs free energy terms. The most thermodynamically stability of this system over a wide range of temperatures is reported and discussed.

## Reference:

- [1] H. Yang, C. Lu, Z. Liu, H. Jin, Y. Che, M. M. Olmstead, A. L. Balch, *J. Am. Chem. Soc.* **2008**, *130*, 17296–17300
- [2] Alexey A. Popov, and Lothar Dunsch *J. Am. Chem. Soc.* **2007**, *129*, 11835–11849.
- [3] S. Yang, L. Dunsch, *Angew. Chem. Int. Ed.* **2006**, *45*, 1299–1302.

\*Corresponding Author: [x86zhao@yahoo.co.jp](mailto:x86zhao@yahoo.co.jp)

## A large-scale consecutive synthesis of metallofullerenes using the hybrid plasma method

\*Hisashi Komaki<sup>1</sup>, Yusuke Nakanishi<sup>2</sup> and Hisanori Shinohara<sup>2</sup>

<sup>1</sup>JEOL Ltd., Akishima, Tokyo 196-8558, Japan, <sup>2</sup>Department of Chemistry & Institute for Advanced Research, Nagoya University, Nagoya 464-8602, Japan

Endohedral metallofullerenes [1] can be synthesized typically in two ways similar to the synthesis of empty fullerenes, which involves the generation of a carbon-rich vapor or plasma in He or Ar gas atmosphere. The two methods have been routinely used to date for preparing macroscopic amounts of metallofullerenes: the high-temperature laser vaporization or 'laser-furnace' method [2] and the standard DC arc discharge method [3]. Both methods simultaneously generate a mixture of hollow fullerenes together with metallofullerenes.

The production of metallofullerenes can be followed by procedures to extract from soot and to separate/purify the metallofullerenes from the hollow fullerenes [1].

Metal-oxide/graphite composite rods, e.g. La<sub>2</sub>O<sub>3</sub> to prepare La@C<sub>82</sub>, are normally used as positive electrodes (anodes) after a high-temperature (above ca 1600 °C) heat treatment where the composite rods are cured and carbonized. At such high temperatures, various metal carbides in the phase of MC<sub>2</sub> are formed in the composite rods [1], which actually is crucial to an efficient production of endohedral metallofullerenes.

However, these synthesis methods are not suited for a gram and larger scale production of pure metallofullerenes, where consecutive syntheses have not been possible because the supply of the graphite in the form of rods or discs is limited in scale. This precludes metallofullerenes from such large-scale synthesis during the past 20 years. Here, we have developed a high-yield consecutive synthesis of metallofullerenes using the so-called hybrid plasma method [4] together with specially manufactured composite metal-doped graphite powder (see Fig.1). The overall production capability is 5-10 times as large as the conventional arc-discharge method. This opens a new era for the synthesis of endohedral metallofullerenes in large quantity.

**Acknowledgment:** The authors thank to Dr. Takashi Inoue and Mr. Yuji Takimoto (Toyo Tanso Co.Ltd.) for supplying a newly developed metal-doped graphite fine powder.

- [1] H. Shinohara, Rep. Prog. Phys. **63**, 843 (2000).  
 [2] R.E. Haufler et al. Cluster Assembled Materials, Vol. **206**, 627 (1991).  
 [3] W. Kraetschmer et al. Nature, **347**, 354 (1990).

Corresponding Author: Hisashi Komaki  
 TEL: +81-42-542-2324, FAX: +81-42-546-5823,  
 E-mail: [komaki@jeol.co.jp](mailto:komaki@jeol.co.jp)

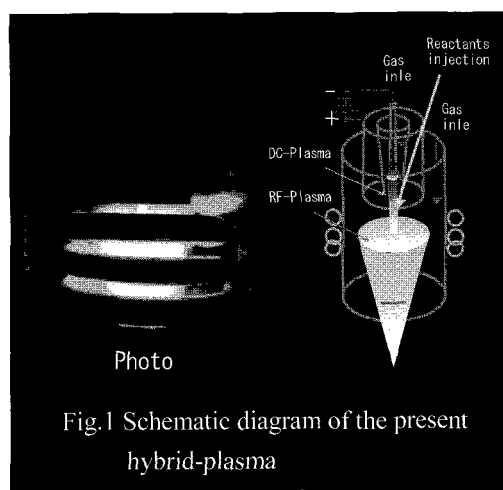


Fig.1 Schematic diagram of the present hybrid-plasma

## An Appearance of the New Electronic State in Fullerene Nano-Whisker due to UV Polymerization

○Tatsuya Doi, Kyouhei Koyama, Nobuyuki Aoki, and Yuichi Ochiai

Graduate School of Advanced Integration Science,  
Chiba University, 264-0022 Chiba, Japan

This study is aimed at clarifying the effect of UV polymerization into fullerene nano-whisker (FNW) without presence of oxygen.

Fullerenes electronics have been prevented by its instability and inability of performance in ambient atmosphere. It is important to archive air tolerability of the fullerene devices for applying broad applications such as solar cells, electron luminescence devices, field effect transistors, and gas sensors.

We have been making a study on polymerization of fullerene due to UV irradiation, especially on the FNW. FNW is a fine single crystal of  $C_{60}$  and prepared by liquid-liquid precipitation method [1]. Upon the system of *m*-xylene and isopropyl alcohol, FNW has several hundred nm of diameter and more than 10  $\mu\text{m}$  of length. It is thought that the unique structure can be used to improve performances of the electronic devices. However, detail of the electronic structure is not elucidated about both FNW and UV polymerized FNW.

To elucidate more detail of electron behavior and polymerization effect, we applied the ESR measurement. The ESR magnetic susceptibility of FNW indicates that temperature independent behavior in vacuum which illustrate that electronic structure of FNW is almost metallic. The metallic behavior of pristine FNW is suddenly vanished when air is absorbed into FNW. New ESR spectrum is appeared when UV light is irradiated into FNW placed in ESR cavity. At the beginning, the new spectrum appeared and disappeared subserviently with UV irradiation, however stable signal is remained for 8 hour irradiation (Fig. 1). The saturation of intensity  $\Delta y'_m$  is observed after irradiation for 12 h (Fig. 2). The remained spectrum has broad and weak temperature dependent peak width, and can be considered to be from electronic structure of polymeric phase. Furthermore, air exposure effect against UV polymerized FNW will be discussed to obtain air stable FNW as an *n*-type organic semiconductor.

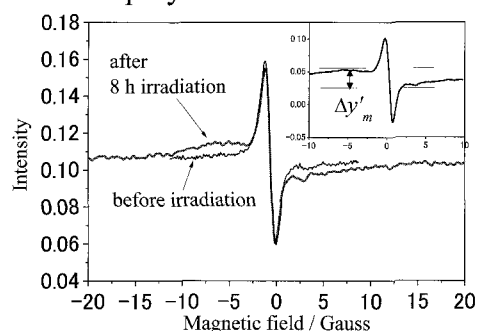


Fig. 1. ESR spectrum before irradiation (black line) and after irradiation (red line).

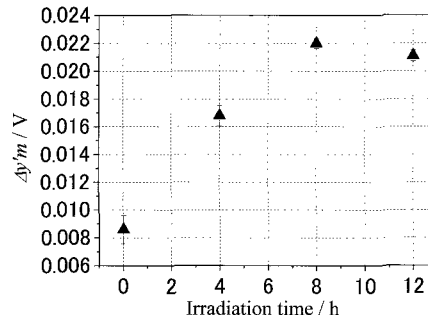


Fig. 2. Intensity of the new spectrum as a function of irradiation time.

[1] K. Miyazawa, *et al*: *J. Mater. Res.*, 20, 688 (2005).

**Corresponding Author: Tatsuya Doi**  
**E-mail: [doitatuya@graduate.chiba-u.jp](mailto:doitatuya@graduate.chiba-u.jp),**  
**Tel: +81-43-290-3430, FAX: +81-43-290-3427,**



## Optical, Electric and Magnetic Properties of Thin Polymerized Fullerene C<sub>60</sub> Films Deposited via Electron-Beam Dispersion

○ Ihar Razanau<sup>1,2</sup>, Tetsu Mieno<sup>1</sup>, Viktor Kazachenko<sup>2,3</sup>

<sup>1</sup>Department of Physics, Faculty of Science, Shizuoka University, Shizuoka 422-8529, Japan

<sup>2</sup>Francisk Skorina Gomel State University, Gomel 246019, Belarus

<sup>3</sup>Belarusian State University of Transport, Gomel 246653, Belarus

Fullerenes C<sub>60</sub> can be polymerized using high-pressure high-temperature treatment (HPHT), UV-Vis light irradiation in the absence of oxygen, electron irradiation, alkali metal doping, *etc.* We have used a novel method of electron-beam dispersion of pristine fullerite in vacuum with coating deposition onto the substrates in additional electrostatic field to form thin films of polymerized C<sub>60</sub> [1]. The characteristic feature of the method is that the coating is deposited under the irradiation of electrons from the active gas phase containing excited fullerene molecules and positive fullerene ions. Under the potential of -300 V on the substrates and thus, under bombardment of accelerated fullerene ions, highly cross-linked 3D polymer of C<sub>60</sub> has been obtained.

The estimation based on the optical spectra of the films, deposited onto the synthetic fused silica substrates, showed that the band gap of the polymerized fullerene films decreases with increase of the coating cross-linking approximately from 2.30 eV to 2.14 eV. *In-situ* measurement of the *I-V* curves of the layers deposited onto the quartz substrates with a system of 2 interdigital thin-film Ni electrodes showed that the highly cross-linked polymerized C<sub>60</sub> film exhibits Schottky barrier to Ni electrodes. The estimated *in-situ* resistivity of the film is about 50 Ω·cm which is several orders of magnitude lower than that for the nonpolymerized C<sub>60</sub> films. The films were also studied using magnetic force microscopy (MFM) and scanning spreading resistance microscopy (SSRM). Highly cross-linked C<sub>60</sub> films exhibit stable magnetic contrast in MFM (Fig. 1). Magnetic domains correlate with the topography of the film. Similar magnetic domain maps were observed by Han *et al.* [2] at some areas of the bulk samples of C<sub>60</sub> polymers synthesized using HPHT method. Electric and magnetic properties of the highly cross-linked C<sub>60</sub> polymer films are discussed.

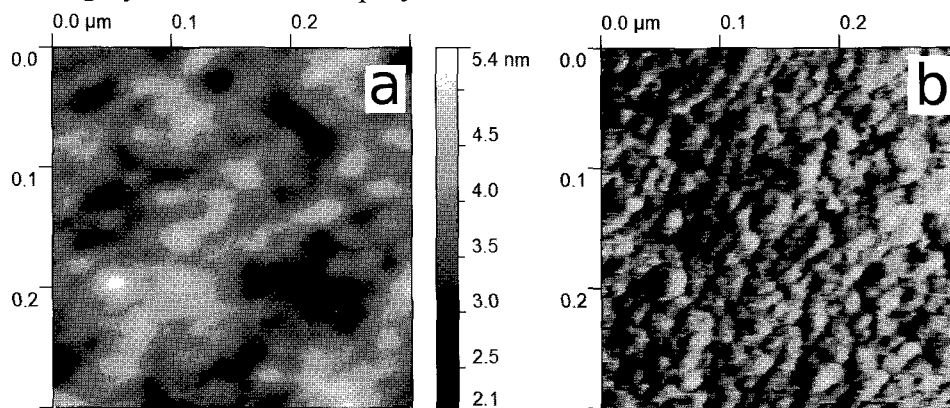


Fig.1. Topography (a) and magnetic contrast (b) AFM images of the highly cross-linked polymerized C<sub>60</sub> film

[1] I. Razanau, T. Mieno, V. Kazachenko, *Thin Solid Films*, **519**, 1285 (2010).

[2] K.-H. Han, A. Talyzin, A. Dzwilewski, T. L. Makarova, R. Hühne, P. Esquinazi, D. Spemann and L. S. Dubrovinsky, *Phys. Rev. B*, **72**, 224424 (2005).

Corresponding author: Ihar Razanau.

TEL: +81-80-6927-1152, E-mail: ir23.by@gmail.com

## Fabrication and Characterization of $C_{60}(OH)_x$ Nanocrystals by a Reprecipitation Method

Keisuke Baba<sup>1</sup>, Hironori Ogata<sup>1,2</sup>

<sup>1</sup>Department of Chemical Science and technology, Hosei University, Koganei 184-8584, Japan

<sup>2</sup> Research Center for Micro-Nano Technology, Hosei University, Koganei 184-0003, japan

Recently, various kinds of fullerene nanocrystals were reported to be easily grown by the precipitation methods[1-3]. Much interests are concentrated on these methods as the useful techniques for applications of fullerene materials. Polyhydroxylated fullerenes ( $C_{60}(OH)_x$ :fullerenol) are promising materials for use in the field of life science and so on because of their water-solubility. In this study, we report the fabrication of  $C_{60}(OH)_x$  nanocrystals by a reprecipitation method. The structural and morphological characterization of these crystals was performed by SEM and TEM.

Figure 1 shows the SEM image of  $C_{60}(OH)_{20}$  (average composition) nanocrystals by using pyridine (good solvent) and *m*-xylene(poor solvent). In this presentation, the detailed relation between morphology of the crystals and solvating media will be presented.

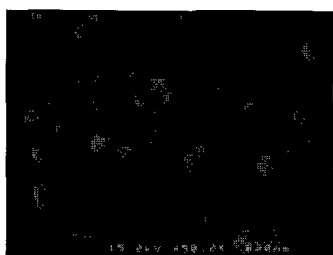


Figure 1. SEM image of  $C_{60}(OH)_{20}$  nanocrystals by the reprecipitation method using pyridine (good solvent) and *m*-xylene(poor solvent).

- [1]H. Kasai, et al., *Jpn. J. Appl. Phys.* **31** (1992) L1132.
- [2]K. Miyazawa, et al., *Journal of Materials Research*, **17**(2002) 83-88.
- [3]Akito M. et al., *Jpn. J. Appl. Phys.* **48** (2009) 050206.
- [4]L. Y. Chiang et al., *J. Org. Chem.* **59** (1994) 3960-3968.
- [5]K. Kokubo et al. *ACS Nano.*, **2** (2008) 327-333.

Corresponding Author: Hironori Ogata

TEL: +81-42-387-6229, FAX: +81-42-387-6229, E-mail: hogata@hosei.ac.jp

## Structural characterization of fullerene-nanowhiskers by powder x-ray diffraction

○Hironori Ogata<sup>1,2</sup>, Hideyuki Ohnami<sup>2</sup>

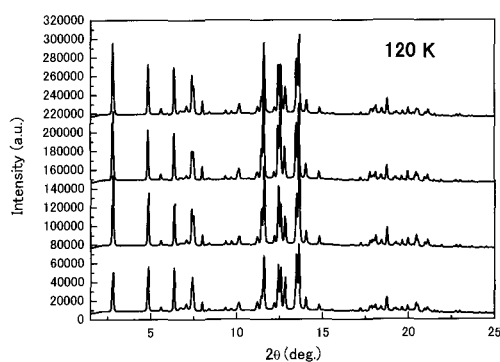
<sup>1</sup>*Department of Chemical Science and technology, Hosei University, Koganei 184-8584, Japan*

<sup>2</sup>*Research Center for Micro-Nano Technology, Hosei University, Koganei 184-0003, Japan*

New types of needle-like fullerene crystals called fullerene nanowhiskers were reported to be easily grown by the liquid-liquid interfacial precipitation method[1]. Much interests are concentrated on fullerene nanowhiskers as one of the useful nanomaterials. Solvated structure of C<sub>60</sub> nanowhiskers are reported by Minato et al[2]. However, the detailed structure of intrinsic C<sub>60</sub> nanowhiskers and the difference from the bulk crystals are not fully understood yet. In this study, we report the structural characterization of C<sub>60</sub>-nanowhiskers by powder x-ray diffraction at 120 K. The x-ray diffraction patterns of the crystals were measured with synchrotron radiation of  $\lambda=1.000 \text{ \AA}$  at BL-8B of KEK-PF.

Figure 1 shows the sample position dependence of the powder x-ray diffraction patterns of C<sub>60</sub> nanowhiskers prepared by using *m*-xylene (good solvent) and 2-propanol (poor solvent) at 120 K. All diffraction patterns can be indexed with a hexagonal lattice. However, the ratio of peak intensity of each patterns is different according to the sample position. This suggests the existence of inhomogeneity by lattice defects in the crystal. In this presentation, the detailed crystal structure with lattice defects of C<sub>60</sub>-nanowhiskers will be presented.

Figure 1. Sample position dependence of the powder x-ray diffraction patterns of C<sub>60</sub> nanowhiskers at 120 K.



[1]K. Miyazawa, et al., *Journal of Materials Research*, **17**(2002) 83-88.

[2] J.Minato and K.Miyazawa, *Carbon***43** (2005)2837.

Corresponding Author: Hironori Ogata

TEL: +81-42-387-6229, FAX: +81-42-387-6229, E-mail: hogata@hosei.ac.jp

## QM/MD Simulations of Dynamic Fullerene Self-Assembly in Carbon Vapor With Inert Carrier Gas

Hu-Jun Qian<sup>1</sup>○, Ying Wang<sup>1</sup>, Keiji Morokuma<sup>2</sup>, Stephan Irle<sup>1</sup>

<sup>1</sup>*Institute for Advanced Research, Nagoya University*

<sup>2</sup>*Fukui Institute for Fundamental Chemistry, Kyoto University*

16 Small Fullerene Cages with cage size:(50 ~74)

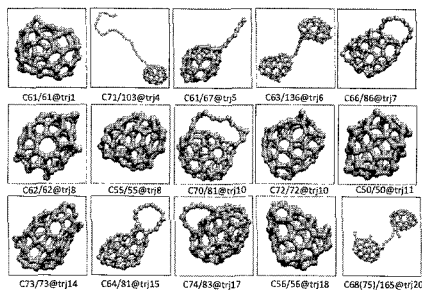


**Figure 1.** Small Fullerene cages with cage size very close to  $C_{60}$  and  $C_{70}$

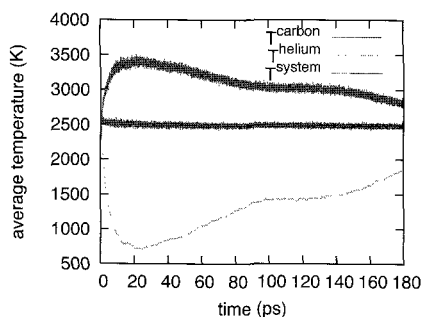


**Figure 2.** The temperatures defined by the nuclear kinetic energy of carbon clusters, He inert gases and the whole system averaged from 20 trajectories under the conditions where small cages were found.

**Abstract:** The dynamic fullerene self-assembly process in carbon vapor was studied using extensive quantum chemical molecular dynamics (QM/MD) simulations based on the density-functional tight-binding (DFTB) potential in conjunction with a finite electronic temperature. Model systems with different carbon densities and different number of helium atoms were employed in NVT simulations up to 200 ps. Similar to our previous NVT QM/MD simulations [1], only the formation of giant fullerene cages ( $> C_{80}$ ) was found in pure carbon systems with relatively high carbon density. Interestingly, in the model systems closer to experimental carbon density,  $\sim 4.7 \times 10^{20} \text{ cc}^{-1}$ , and with an optimum C/He ratio in the system [2], smaller fullerene cages with cage size close to  $C_{60}$  and  $C_{70}$  were observed (see Figure 1). The addition of inert helium gas atoms was found to influence the temperature and diffusion of carbon species. In particular the local heating of carbon clusters plays an important role in the formation of small fullerene cages. This temperature evolution is closer to the experimental setup, where the hot carbon vapor is only slowly cooled down by the buffer gas [2]. In

addition, it was found that the diffusion of carbon species was slowed down by thermal collisions between inert He gas and carbon species. Slower diffusion ensures longer growth/healing time for small polycyclic carbon clusters before they coalesce, eventually leading to the formation of smaller fullerene cages as opposed to NVT/high C density/no He simulations. We conclude that the initial cage size distribution of dynamically self-assembled fullerenes strongly depends on the carbon density, buffer gas pressure, and local temperature gradients. Our simulations demonstrate for the first time the abundant formation of small fullerene cages with cage size close to  $C_{60}$  and  $C_{70}$ .

### References:

- [1] S. Irle, et.al., Nano Lett 3, 1657, 2003; G. Zheng, et.al., J. Chem. Phys. 122, 014708, 2005.
- [2] H. W. Kroto, et.al., Nature, 318, 162-163, 1985.

**Corresponding Author:** Stephan Irle, E-mail: sirle@iar.nagoya-u.ac.jp; Tel: +81 (052) 747-6397; Fax: +81 (052) 788-6151

## Synthesis of non-IPR fullerenes from C<sub>70</sub> in Liquid Phase by Irradiation of Intense Femtosecond Laser Pulses

○Takeshi Kodama<sup>1</sup>, Yuki Sato<sup>1</sup>, Haruo Shiromaru<sup>1</sup>, Joseph H. Sanderson<sup>2</sup>, Tatsuya Fujino<sup>1</sup>, Yoriko Wada<sup>3</sup>, Tomonari Wakabayashi<sup>3</sup>, Yohji Achiba<sup>1</sup>

<sup>1</sup>Department of Chemistry, Tokyo Metropolitan University, Hachioji, 192-0397, Japan

<sup>2</sup>Department of Physics and Astronomy, University of Waterloo, Waterloo, N2L 3G1, Canada

<sup>3</sup>Department of Chemistry, Kinki University, Higashi-Osaka, 577-8502, Japan

Ultrashort pulsed lasers have traditionally been used to probe the time-domain aspects of molecular dynamics, but quite recently, they have also started to be used for the study of a new type of chemical reaction that would be taken place only under extremely high intensity laser field [1]. Furthermore, under such extreme conditions, the most of the investigations so far have been carried out for the aims of reactions in gas phase, and a few of them in liquid phase [2]. In 2008, Hu et al. demonstrated that intense femtosecond laser irradiation to organic solvents directly initiates the synthesis of polyynes without additional introduction of any carbon particles [3], and we also confirmed the production of polyynes with various chain lengths from n-hexane by intense femtosecond laser radiation [4].

Fullerenes are usually synthesized by arc discharge, laser ablation, and combustion of hydrocarbon methods. In these methods, fullerenes are formed in gas phase. All of stable fullerenes extracted from the raw soot by organic solvents are known to satisfy so called "Isolated Pentagon Rule (IPR)".

In this study, we try to synthesize a new type of fullerenes from C<sub>70</sub> in liquid phase using the intense femtosecond laser pulses, which would lead to successive C<sub>2</sub> losses from C<sub>70</sub> and the resultant C<sub>68</sub>, C<sub>66</sub>, ... would necessarily have non-IPR cage structures. The laser used for the experiment was a Ti: Sapphire ( $\lambda$ : 800 nm, pulse width: 100 fs, repetition rate: 1 kHz) with a regenerative amplifier. C<sub>70</sub> was isolated by high performance liquid chromatography and the mass spectrum of the purified C<sub>70</sub> shows no peaks from other fullerenes than C<sub>70</sub>.

When the femtosecond laser pulses were irradiated to the saturated C<sub>70</sub> toluene solution, black powder-like materials were found to appear immediately and, after 2 hours irradiation, the red color due to C<sub>70</sub> disappeared and the transparent light brown solution and the black powders were remained. Figure 1 shows the mass spectra of the black powders and the solution. The peak of C<sub>68</sub> was distinct in both samples, but in black powders, the signal intensity of C<sub>68</sub> as well as other smaller-size fragments is much larger than those in solution. All these results suggest the presence of successive C<sub>2</sub> losses and the resultant unstable species (C<sub>68</sub>, C<sub>66</sub>, C<sub>64</sub>) would be easily aggregated.

[1] K. Yamanouchi, *Science* **295**, 1659 (2002).

[2] D. Nishida, et al. *Chem. Phys. Lett.* **465**, 238 (2008).

[3] A. Hu, et al. *Carbon* **46**, 1823 (2008).

[4] Y. Sato, et al. *Carbon* **48**, 1673 (2010).

Corresponding Author: Takeshi Kodama

E-mail: kodama-takeshi@tmu.ac.jp

Tel:+81-42-677-2530, Fax:+81-42-677-2525

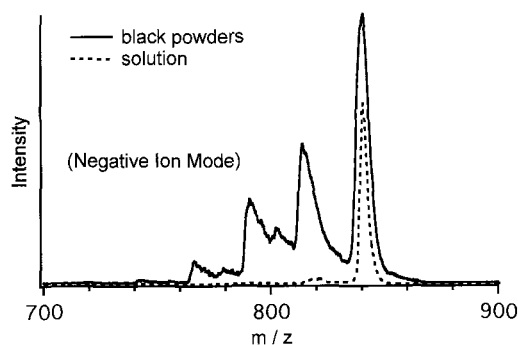


**Figure 1.** Mass spectra of the black powders and the solution.

## Supramolecular Elementary Units in Porphyrin-Fullerene Composites Revealed by Solid-State NMR

○Hironobu Hayashi<sup>1</sup>, Tomokazu Umeyama<sup>1</sup>, Yoshihiro Matano<sup>1</sup>, Hironori Kaji<sup>2</sup>, Hiroshi Imahori<sup>1,3</sup>

<sup>1</sup>Department of Molecular Engineering, Graduate School of Engineering, Kyoto University, Nishikyo-ku, Kyoto 615-8510, Japan

<sup>2</sup>Institute of Chemical Research, Kyoto University, Uji, Kyoto 611-0011, Japan

<sup>3</sup>Institute for Integrated Cell-Material Science (iCeMS), Kyoto University, Sakyo-ku, Kyoto 606-8501, Japan

Characterization of the molecular-level donor-acceptor structure is crucial to design high-performance ‘amorphous’ organic solar cells (OSCs). However, the details have been limited experimentally for such ‘amorphous’ systems, due to the absence of periodic structure. Solid-state NMR is a powerful tool for elucidating the structure of amorphous systems.<sup>1</sup> Here, we report the first solid-state NMR experiments for a supramolecular OSC system composed of tetraphenylporphyrin derivatives (TPP) and C<sub>60</sub> (Figure 1). This study focuses the existence of several different supramolecular elementary units possessing local stoichiometry between TPP and C<sub>60</sub>. The TPP and C<sub>60</sub>, dissolved in toluene, were rapidly injected into acetonitrile. This resulted in the formation of supramolecular composite clusters TPP/C<sub>60</sub>. The gently centrifuged and dried clusters were employed for the solid-state <sup>13</sup>C NMR experiments. Fully-relaxed direct polarization / magic angle spinning <sup>13</sup>C NMR experiments without <sup>1</sup>H dipolar decoupling (DP/MAS/noDD), distinguished the C<sub>60</sub>s in different states with quantitative molar ratios. In this experiment, C<sub>60</sub> carbons can be selectively detected, because the resonance lines of TPP are effectively suppressed by not applying DD. In Figure 1, a <sup>13</sup>C NMR spectrum of TPP/C<sub>60</sub> clusters in the amorphous states is presented (the resonance lines are denoted as A to F). Compared with the spectrum of pristine C<sub>60</sub>, the TPP/C<sub>60</sub> clusters display several upfield-shifted resonance lines, B – F, which indicate the occurrence of molecular-level complexation between TPP and C<sub>60</sub>.

From various considerations, the peaks A, C, E, and F are assigned to free C<sub>60</sub>, the C<sub>60</sub> in C<sub>60</sub>/TPP/C<sub>60</sub> unit, the C<sub>60</sub> in TPP/C<sub>60</sub>/TPP unit, and C<sub>60</sub> surrounded by three TPP molecules, respectively. The peak D appears between the peak C and D, suggesting the composition of C<sub>60</sub>/TPP. The peak B is considered to be C<sub>60</sub>s in defects, which are farther from the second neighbors of TPP. The origin of the upfield shifts is charge-transfer (CT) from TPP to C<sub>60</sub>. Therefore, the peaks C to F result from four distinctly different degrees of CTs in this system, which would greatly affect the cell performance of the present solar cell.<sup>2</sup>

[1] A. Heeger et al, *J. Am. Chem. Soc.*, **92**, 435 (1992). [2] H. Imahori et al, *Chem. -Eur. J.*, **13**, 10182 (2007).

Corresponding Author: Hironobu Hayashi, TEL: +81-75-383-2568, FAX: +81-75-383-2571, E-mail: [hayashihironobu@t03.mbox.media.kyoto-u.ac.jp](mailto:hayashihironobu@t03.mbox.media.kyoto-u.ac.jp)

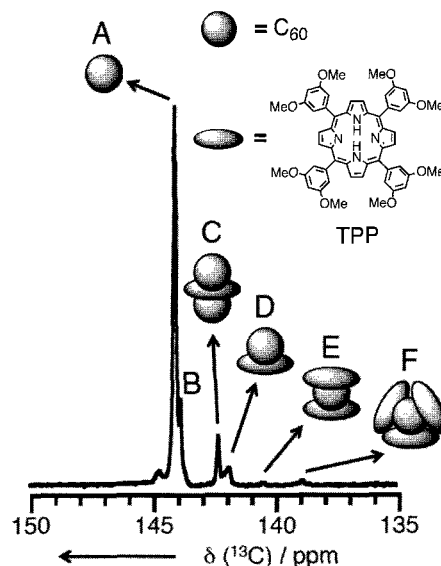


Figure 1. Fully-relaxed DP/MAS/noDD <sup>13</sup>C NMR spectra of TPP/C<sub>60</sub> composites.

## The thermal [2+2] cycloaddition of morpholinocycloalkenes with fullerene

○ Tsubasa Mikie, Haruyasu Asahara, Kazuaki Nagao, Naohiko Ikuma, Ken Kokubo, and Takumi Oshima

*Division of Applied Chemistry, Graduate School of Engineering,  
Osaka University, Suita 565-0871, Japan*

Chemical functionalization of fullerenes has attracted significant attention in view of the biological and electronic applications. Fullerene undergoes various nucleophilic additions, organometallic reactions and cycloadditions such as Bingel, Prato, Diels-Alder reaction, or addition of 1,3-dipoles. Although a variety of cycloaddition reactions have been developed, only a few [2+2] cycloadditions to fullerene have been reported. The reasons include the difficulty of the control of addition number and the absence of regioselectivity due to photoreaction. Here, we focused on thermal [2+2] cycloaddition [1] of the [60]fullerene with electron-rich double bond of enamines.

The reactions of excess morpholinocycloalkenes with  $C_{60}$ , run at reflux in dry toluene for 24 h, afforded the cyclobutane-fused fullerene derivatives **1a-c** (Scheme 1). And were conducted in dark under Ar atmosphere to avoid some photoinduced reactions, since there have already been a number of examples of photoinduced radical reactions of [60]fullerene with tertiary amines [2]. As noted in Table 1, the reactivity slightly decreases with extending carbocyclic ring. This result suggested that cycloheptene should undergo steric effect rather than cyclopentene.

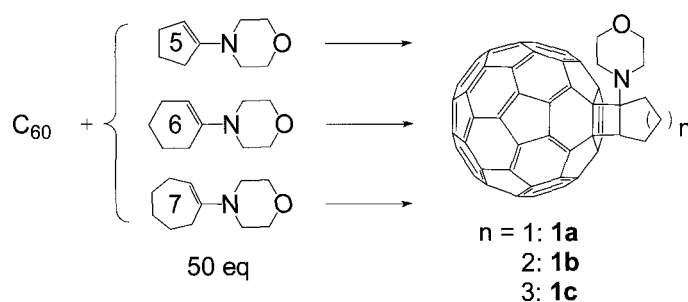


Table 1. HPLC area ratio after 24h

<b>1</b>	solvent	$C_{60}$ (%)	product (%)
<b>1a</b>	toluene	6	77 (70) <sup>a</sup>
<b>1b</b>	toluene	36	62 (54) <sup>a</sup>
<b>1c</b>	<i>o</i> -DCB	3	47

a: isolated yield

Scheme 1. Synthesis of cyclobutane-fused fullerenes

The Hydrolysis of cyclobutane-fused fullerene **1a** with an acid gave cyclopentano-fullerene. The structure was determined by  $^1\text{H-NMR}$ ,  $^{13}\text{C-NMR}$ , HSQC, HMBC,  $^1\text{H-}^1\text{H}$  COSY. Unexpectedly, it was the same product as previously reported [3]  $\beta$ -substituted cyclopentanone adduct rather than  $\alpha$ -substituted compound obtained from usual hydrolysis of enamines.

[1] S.Drioli *et al.*, *J. Chem.Soc.Perkin Trans. 1*, 2000, 2839.

[2] G.Schick, K.-D. Kampe, and A. Hirsch, *Chem. Commun.*, 2023 (1995).

[3] Xiang Gao *et al.*, *Chem. Lett.*, 671 (1999).

Corresponding Author : Takumi Oshima

E-mail: [oshima@chem.eng.osaka-u.ac.jp](mailto:oshima@chem.eng.osaka-u.ac.jp) Tel: +81-6-6879-4591 Fax: +81-6-6879-4593

## Growth Control of C<sub>60</sub> Fullerene Nanowhiskers

○Yumeno Akasaka and Kun'ichi Miyazawa

*Fullerene Engineering Group, Exploratory Nanotechnology Research Laboratory,  
National Institute for Materials Science (NIMS), Tsukuba 305-0044, Japan*

C<sub>60</sub> fullerene nanowhiskers (C<sub>60</sub>NWs) can be synthesized by liquid-liquid interfacial precipitation method (LLIP method) [1], using good solvent solutions of C<sub>60</sub> and poor solvents of C<sub>60</sub>. It has been reported that the factors of light, temperature, growth periods, water and the kind and composition of solvents influence the growth of C<sub>60</sub>NWs when the LLIP method was applied to the synthesis of C<sub>60</sub>NWs [2, 3, 4]. These studies have been performed in various conditions to get thin and long C<sub>60</sub>NWs. In addition, the growth control of C<sub>60</sub>NWs is necessary to apply them to various fields. Although much attention has been paid to the growth mechanism of long C<sub>60</sub>NWs (Fig. 1), there are little investigation about the synthesis of short C<sub>60</sub>NWs. In this study, we have successfully synthesized the short C<sub>60</sub>NWs as shown in Fig. 2 by LLIP method using various ratios of C<sub>60</sub>-saturated solution and isopropyl alcohol (IPA).

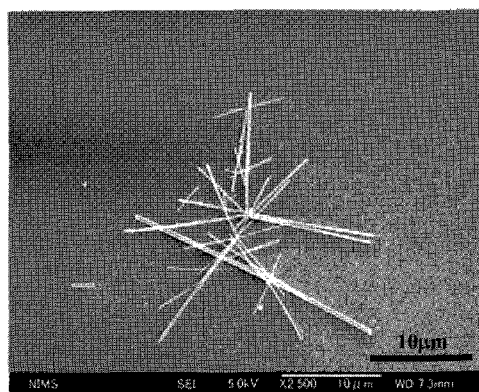


Fig. 1 SEM image of long C<sub>60</sub>NWs prepared by LLIP method.

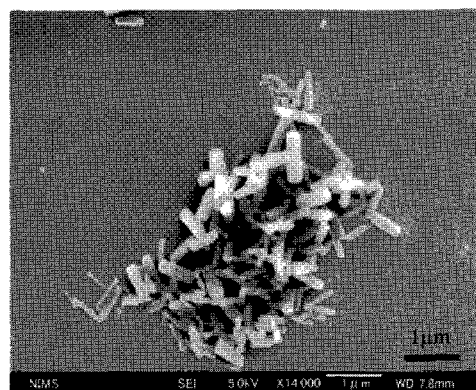


Fig. 2 SEM image of short C<sub>60</sub>NWs prepared by LLIP method.

### References

- [1] K. Miyazawa, Y. Kuwasaki, A. Obayashi and M. Kuwabara, *J. Mater. Res.*, **17**, 83-88 (2002)
- [2] M. Tachibana, K. Kobayashi, T. Uchida, K. Kojima, T. Tanimura and K. Miyazawa, *Chem. Phys. Lett.*, **374**, 279-285 (2003)
- [3] K. Hotta and K. Miyazawa, *NANO*, **3**, 355-359 (2008)
- [4] K. Miyazawa and K. Hotta, *J. Cryst. Growth*, **312**, 2764-2770 (2010)

Corresponding Author: Kun'ichi Miyazawa

E-mail: MIYAZAWA.Kunichi@nims.go.jp, Tel&Fax: +81-29-860-4667



## Effect of addition of Pt on Magnetic properties of iron-filled carbon nanotubes

○Yusuke Matsui, Tetsuya Kaneko, Atsushi Nagata, Hideki Sato, Yuji Fujiwara, Koichi Hata

*Graduate School of Engineering, Mie University,  
1577 Kurima-machiya-cho, Tsu, Mie, 514-8507, Japan*

Carbon nanotubes (CNTs) filled with ferromagnetic metal show shape anisotropy originating from the high-aspect ratio of magnetic particles[1] and anticorrosivity due to having a graphite layer acting as a protective layer of the encapsulated metal, so that are expected to apply for magnetic recording media[2] and for biomedical applications[3]. It is desirable to be able to control the magnetic properties appropriately for these applications. It is important to clarify the influence of shape and the crystallographic structure of the metal filled in CNTs in the magnetic properties for those purposes. We have investigated magnetic properties of Fe filled CNTs synthesized by a thermal CVD (TCVD) method and an effect of Pt addition to the Fe was examined to enhance the coercivity.

Fe-filled CNTs were synthesized on  $\text{SiO}_x / \text{Si}$  substrates covered with 2 nm Fe on which 0.6~1.4 nm Pt layer was deposited. Ferrocene was used as a source gas and the TCVD was carried out under the conditions of 785°C and 1 atm. The TCVD gives vertically oriented CNTs almost entirely filled with Fe [Fig. 1(a)]. It was confirmed that almost all of the encapsulated metal in the CNTs were the single crystal by selected area diffraction patterns (SAED). The SAED pattern that was identified as that of FePt was also obtained at the root of CNT grown on Pt(1.4 nm) / Fe(2.0 nm) /  $\text{SiO}_x / \text{Si}$  substrate [Fig.1(b)]. The coercivity of the CNTs perpendicular to the substrate was 1.1 kOe for Fe film. It increased up to 2.2 kOe by adding Pt layer on the Fe film [Fig.2]. On the other hand, the coercivity decreased by annealing of the CNTs in an Ar atmosphere that was carried out under an intention to enhances the coercivity. This indicates that the crystal structure of the FePt alloy was distracted by the annealing. Detailed investigation to enhance the coercivity is in progress.

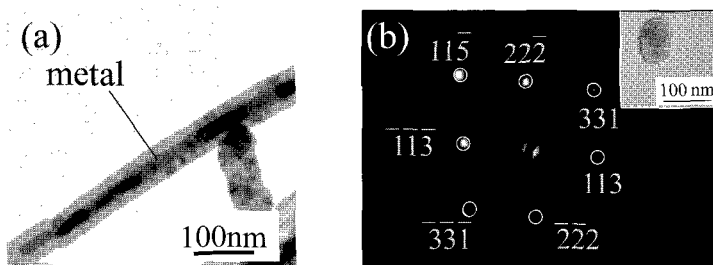


Fig.1 (a)TEM image and (b)SAED image of Fe-filled CNTs grown by TCVD method.

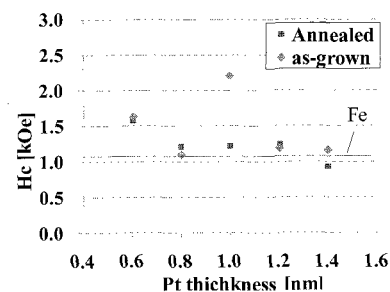


Fig.2 Dependence of Coercivity of Fe-filled CNTs on Pt thickness.

**Acknowledgment:** This study has been partly supported by JSPS KAKENHI and Mie University VBL.

**References:** [1] Y. Fujiwara et al., J. Appl. Phys. 95, 7118(2004).

[2] C. P. Luo, a) S. H. Liou, and D. J. Sellmyer, J. Appl. Phys, 87, 6941 (2000)

[3] Ian Baker, a Qi Zeng, Weidong Li, and Charles R. Sullivan, J. Appl. Phys, 08H106 (2006)

**Corresponding Author: Hideki Sato**

**E-mail: sato@elec.mie-u.ac.jp, TEL&FAX:059-231-9404**

## Water Structure inside Finite Length Single-Walled Carbon Nanotubes : SWCNT-Edge Effect

○Haruka KYAKUNO<sup>1</sup>, Kazuyuki MATSUDA<sup>1</sup>, Hitomi YAHIRO<sup>1</sup>, Yu INAMI<sup>1</sup>, Tomoko FUKUOKA<sup>1</sup>, Yasumitsu MIYATA<sup>2</sup>, Kazuhiro YANAGI<sup>1</sup>, Yutaka MANIWA<sup>1,4,\*</sup>, Kazuyuki TAKAI<sup>3</sup>, Toshiaki ENOKI<sup>3</sup>, Hiromichi KATAURA<sup>5,4</sup>, Takeshi SAITO<sup>6</sup>, Motoo YUMURA<sup>6</sup>, and Sumio IJIMA<sup>6</sup>

<sup>1</sup>*Department of Physics, Faculty of Science, Tokyo Metropolitan University, 1-1 Minami-Osawa, Hachioji, Tokyo 192-0397, Japan.*

<sup>2</sup>*Department of Chemistry & Institute for Advanced Research, Nagoya University, Nagoya, 464-8602, Japan*

<sup>3</sup>*Department of Chemistry, Tokyo Institute of Technology, Tokyo 152-8551, JAPAN*

<sup>4</sup>*JST, CREST, Kawaguchi 332-0012, Japan.*

<sup>5</sup>*Nanotechnology Research Institute, National Institute of Advanced Industrial Science and Technology (AIST), Central 4, Higashi 1-1-1, Tsukuba, Ibaraki 305-8562, Japan.*

<sup>6</sup>*Nanotube Research Center, National Institute of Advanced Industrial Science and Technology (AIST), Tsukuba 305-8565, Japan.*

Water confined in nano space exhibits unusual behavior that cannot be observed in the bulk. In a previous work, we experimentally clarified that the phase behaviors of water confined in Single-Walled Carbon Nanotubes (SWCNTs) with diameters below and above  $\sim 1.5$  nm are quite different from each other. That is, water confined in SWCNTs with diameters between 1.17 to 1.44 nm undergoes a liquid-to-solid like transition with decreasing temperature and forms ordered tubular ice structures, so-called ice nanotubes (ice-NTs), while water exhibits a wet-dry transition in a diameter range between 1.6 and 2.4 nm and is ejected from the inside of the SWCNTs at lower temperatures.

Around the intermediate diameter range, previous studies employing molecular dynamics (MD) calculations have predicted the existence of more complex nano-ice structures inside SWCNTs, such as multi-layer ice structures and ice-NTs containing one-dimensional water chain. These calculations were done on infinite length SWCNTs. In the present study, we focused on finite length SWCNTs with diameters  $\sim 1.4$  nm to examine the effect of open ends of SWCNTs on water structure. It was found that the ice structure formed at low temperatures were strongly affected by pore diameters and the number of water molecules in the system. Corresponding powder X-ray diffraction (XRD) experiments on SWCNTs with a mean diameter of 1.46 nm strongly suggested the presence of such filled structure.

Besides, the effect of heat and hydrogen treatments for SWCNTs on the wet-dry transition is also examined for SWCNTs with mean diameters 1.68 and 2.40 nm by XRD experiments.

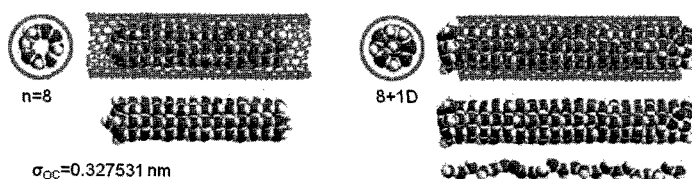


**Figure** Snapshot structures of water inside the SWCNTs. Water molecules are stuck on the inner wall of the SWCNT at first, and then fill the hollow space with increase in their number.

Corresponding Author: Yutaka MANIWA TEL: +81-42-677-2490, E-mail: maniwa@phys.se.tmu.ac.jp

## Dynamics of water confined in zeolite templated carbon

○Kazuyuki Matsuda<sup>1</sup>, Tomoko Fukuoka<sup>1</sup>, Yasufumi Sato<sup>1</sup>, Haruka Kyakuno<sup>1</sup>, Kazuhiro Yanagi<sup>1,3</sup>, Yutaka Maniwa<sup>1,3</sup>, Hiroto Nishihara<sup>2</sup>, and Takashi Kyotani<sup>2</sup>

<sup>1</sup> Faculty of Science, Tokyo Metropolitan University, 1-1 Minami-osawa, Hachioji, Tokyo 192-0397, Japan

<sup>2</sup> Institute of Multidisciplinary Research for Advanced Materials, Tohoku University, Aoba-ku, Sendai, Miyagi 980-8577, Japan

<sup>3</sup> JST, CREST, Kawaguchi, 332-0012, Japan

Zeolite templated carbon (ZTC) is an ordered microporous carbon with interconnected nanometer scale cavities forming a three-dimensional diamond like structure. We report here on studies of water adsorption and its properties in ZTC framework by means of thermo gravimetric analysis (TGA), X-ray diffraction (XRD), differential scanning calorimetry (DSC), and NMR measurements. It was found that the amount of water adsorbed inside the ZTC reaches  $\sim 140$  wt% at room temperature (RT) with a small lattice expansion. This corresponds to a mean water density of  $0.61 \text{ g/cm}^3$  and the total density of water-ZTC system of  $1.0 \text{ g/cm}^3$ . Contrary to the bulk water, XRD measurements revealed that the water-containing ZTC exhibits a gradual lattice contraction by 3 % with lowering temperature from RT to 200 K. DSC measurements suggested that specific heat of the confined water decreases from  $4.2 \text{ J g}^{-1}\text{K}^{-1}$  at 310 K to  $2.9 \text{ J g}^{-1}\text{K}^{-1}$  at 206 K without any evidence for the first order phase transition in a temperature range between 160 K and 310 K. <sup>2</sup>H- and <sup>1</sup>H-NMR of heavy and light water adsorbed to ZTC clearly indicated that the water are highly mobile above  $\sim 200$  K in ZTC: The rotational correlation time was estimated to be  $\tau_{\text{rot}} = \tau_{0,\text{rot}} \exp(T_{0,\text{rot}}/T)$  with  $\tau_{0,\text{rot}} = 1.0 \times 10^{-19} \text{ s}$  and  $T_{0,\text{rot}} = 5021 \text{ K}$ , and the translational correlation time shorter than  $1.0 \mu\text{s}$  above 200 K. The ZTC serves as a model system for fundamental studies of water with a three dimensional hydrogen network system in confined environments.

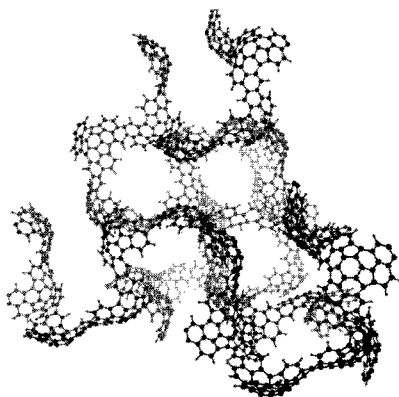


Fig. 1. Possible structural model proposed for ZTC solid.

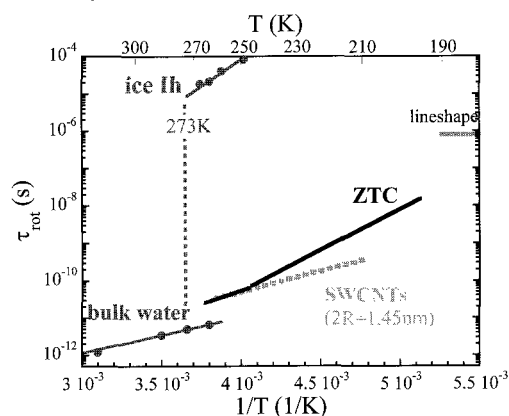


Fig. 2. Temperature dependence of rotational correlation time of water molecules in ZTC.

[1] H. Nishihara *et al.*, Carbon **47** (2009) 1220.

Corresponding Author: Kazuyuki Matsuda

E-mail: matsuda@phys.metro-u.ac.jp, TEL: +81-426-77-2498, FAX +81-426-77-2483

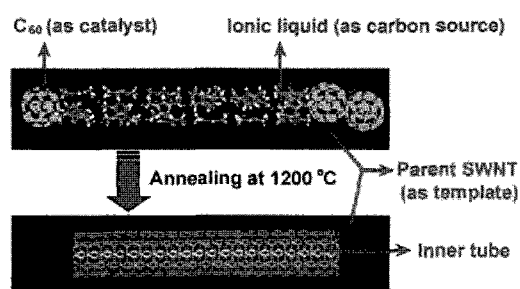
## Growth of Inner Nanotubes from Confined Ionic Liquid inside a Tip-closed SWNT

Shimou Chen<sup>1</sup>, Hong En Lim<sup>1</sup>, Yasumitsu Miyata<sup>1</sup>, Ryo Kitaura<sup>1</sup>, Takeshi Saito<sup>2</sup>, and Hisanori Shinohara<sup>1</sup>

<sup>1</sup>*Department of Chemistry and Institute for Advanced Research, Nagoya University, Nagoya, 464-8602, Japan;*

<sup>2</sup>*Nanotube Research Center, National Institute of Advanced Industrial Science and Technology, Tsukuba 305-8565, Japan and PRESTO, Japan Science and Technology Agency, 4-1-8 Honcho Kawaguchi, Saitama, Japan.*

The interior space of the single-walled carbon nanotubes (SWNT) can be utilized for the encapsulation of molecules. It provides an ideal model for the study of the so-called confined nano-reaction.<sup>1-2</sup> Herein, we report the synthesis of carbon nanotubes from an ionic liquid encapsulated inside SWNT via a nanotemplate reaction (Scheme 1). Both single-walled and multi-walled carbon nanotubes can be generated in the channel of the parent SWNT using ionic liquid as the carbon source. In comparison to the reported catalytic and noncatalytic growths of the inner-tube from filled SWNT, a new types of growth mechanism, which involves C<sub>60</sub> as the catalyst (or seed) in the first stage and finally fusing into the inner-tube network, is supposed and discussed. More importantly, we have developed a two-step filling process for the encapsulation of the ionic liquid in the tip-closed SWNT, where the fullerenes inserted at the end of the host SWNT act as a plug to prevent the leakage of the confined ionic liquid during heat treatment. This opens a new prospective path for the advancement of the tube chemistry of other liquids or low-thermal stability materials.



**Scheme 1.** Schematic diagram for the growth nanotube from confined ionic liquid in a SWNT template.

### References:

- [1] Koshino, M.; et al. *Nat. Chem.* **2010**, *2*, 117.  
 [2] Hu, J.; Bando, Y.; Zhan, J.; Zhi, C.; Golberg, D. *Nano Lett.* **2006**, *6*, 1126.

Corresponding Author: Hisanori Shinohara

TEL: +81-52-789-2482, FAX: +81-52-789-1169, E-mail: [noris@cc.nagoya-u.a.jp](mailto:noris@cc.nagoya-u.a.jp)

## Growth of Carbon Nanotubes Filled with Metal Compounds and “Tee-like” Carbon Nanotubes by Alcohol CVD

○Yusuke Furuyama, Takayuki Yamasaki, Akira Koshio, and Fumio Kokai

*Division of Chemistry for Materials, Graduate School of Engineering, Mie University, 1577 Kurimamachiya-cho, Tsu, Mie 514-8507, Japan*

Many researches on various metal/metal compound-filled carbon nanotubes (CNTs) have been reported to date. However, it is difficult to achieve long one-dimensional growth via one-step synthesis. We have succeeded in the one-step syntheses of copper and copper sulfide-filled CNTs (Cu@CNTs and CuS@CNTs) by modified arc discharge methods. Moreover, we have succeeded in vertical growth of nickel sulfide-filled CNTs (NiS@CNTs) by alcohol chemical vapor deposition (CVD). In this study, we investigated effective formation conditions of nickel and copper compound-filled CNTs grown by alcohol CVD. In addition, we found CNTs having a “tee-like” structure during the investigation of copper-filled CNTs.

Metal (Ni or Cu) compound-filled CNTs were formed by alcohol CVD method. Ethanol solutions of NiCl<sub>2</sub> or CuCl<sub>2</sub> were sprayed on a Si plate maintained at 400°C followed by heating at 640°C for 30 min. in an Ar atmosphere. Furthermore, we used copper powder in the case of the CVD growth using copper. The CVD growth was carried out at 700-1100°C for 30 min. at a vapor pressure of ethanol containing CS<sub>2</sub> in a vacuum.

The filling rate of NiS@CNTs was about 80%, and had diameters of about 100 nm and lengths of about 3 μm. The NiS@CNTs grew vertically on the substrate. On the contrary, little copper-filled CNTs were formed by alcohol CVD using the sprayed substrate (Fig. 1(a)). Only very thick copper-filled CNTs having a diameter of about 500 nm grew at the highest growth temperature (1100°C) (Fig. 1(b)). In the case of the CVD using copper powder, CNTs shown in Fig. 2(a) were formed effectively at the growth temperature of 1000°C. Diameters of the CNTs gradually became thin at the root (Fig. 2(b)), and a polyhedral copper particle was deposited at the tip (Fig. 2(c)). The structure is just like a “tee” that you stick in the ground to support a golf ball before you hit it. The root was open-end structure shown in Fig. 2(d). We will present the detail of growth conditions, mechanism and structures of the NiS@CNTs and the “tee-like” CNTs in the presentation.

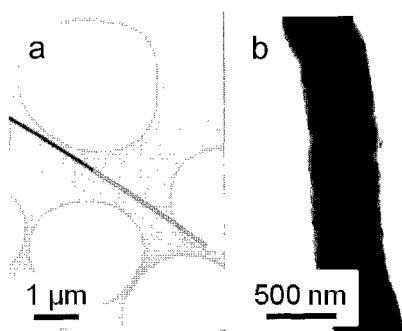


Fig. 1 TEM images of copper-filled CNTs formed by alcohol CVD using a CuCl<sub>2</sub> aq.-sprayed substrate. (a) A typical thin copper-filled CNTs and (b) a thick copper-filled CNT grown at 1100°C.

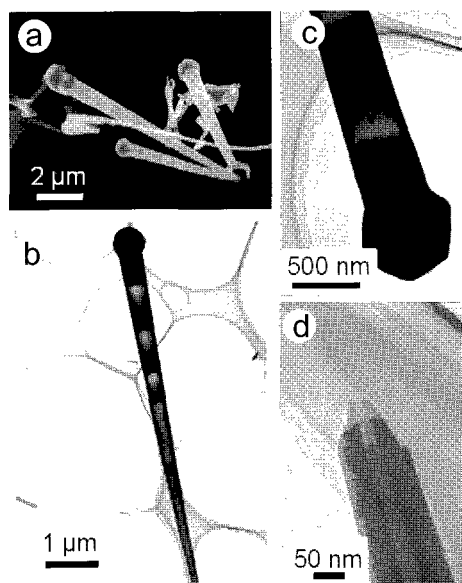


Fig. 2 “Tee-like” CNTs formed by alcohol CVD using copper powder. (a) SEM image, (b) a typical TEM image, (c) a polyhedral copper particle at the tip and (d) the open-end structure at the root.

**Corresponding Author:** Akira Koshio, E-mail: koshio@chem.mie-u.ac.jp, Tel & Fax: +81-59-231-5370

## Optical excited state induced by the interaction between rigid polymers and single-wall carbon nanotubes with large diameters

○Masayoshi Tange<sup>1</sup>, Toshiya Okazaki<sup>1,2</sup>, and Sumio Iijima<sup>1</sup>  
<sup>1</sup>Nanotube Research Center, AIST, Tsukuba, 305-8565, Japan  
<sup>2</sup>PRESTO, JST, Kawaguchi 332-0012, Japan

Techniques to extract single-wall carbon nanotubes (SWCNTs) with specific structures (i.e., chiral indices) from the carbon compounds with various structures is important for the synthesis of functional nanocomposites as well as the investigation of fundamental properties. In the techniques of extraction, the polymer wrapping with polyfluorene is a powerful method which disperses selectively semiconducting SWCNTs with specific chiral indices<sup>[1]</sup>. However, the dispersed SWCNTs are restricted to small tube diameters ( $< 1.2$  nm). In this work, we report that a fluorene-based copolymer is also effective in selecting the structures of SWCNTs with large tube diameters. Moreover, spectroscopic analysis suggests that the exciplex formation between SWCNTs and the polymers plays a key role in the effective extractions.

We find that poly(9,9-dioctylfluorene-alt-benzothiadiazole) (F8BT) can disperse selectively semiconducting SWCNTs with several large diameters ( $> 1.3$  nm) in toluene. The excitation spectrum of F8BT in toluene is significantly different in spectral pattern from the absorption spectrum as shown in Fig. 1. In the excitation spectrum, two peaks are observed at the tail of the absorption band. The discrepancy between absorption and excitation spectra indicates excimer formation due to the rigidity of the polymer. On the other hand, as shown in Fig. 2, the SWCNTs wrapped by F8BT exhibit intense near-infrared emissions at an excitation wavelength of 515 nm. The excitation energy is a little lower than the absorption energy of F8BT excimer in Fig. 1. The result suggests that the emissions of the polymer-wrapped SWCNTs are not due to energy transfer<sup>[2]</sup> from the polymer to the SWCNTs, but are associated with exciplex formation between the SWCNTs with specific structures and the polymer.

[1] A. Nish *et al.*, Nat. Nanotechnol. 2 (2007) 640.

[2] A. Nish *et al.*, Nanotechnology 19 (2008) 095603.

**Corresponding Author:** T. Okazaki and M. Tange

**E-mail:** toshi.okazaki@aist.go.jp and masa-tange@aist.go.jp

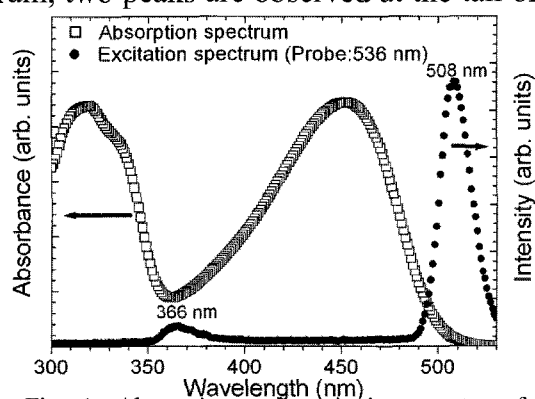


Fig. 1. Absorption and excitation spectra of F8BT in toluene (0.62 g/L).

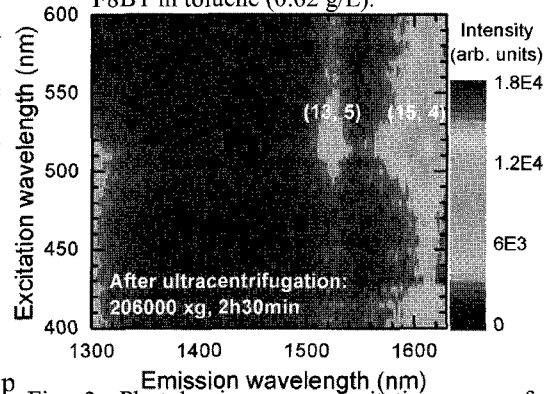


Fig. 2. Photoluminescence excitation map of SWCNTs wrapped by F8BT in toluene.

## Polyynes and Cyanopolyynes Included in $\alpha$ -Cyclodextrin Crystals

M. Saikawa and T. Wakabayashi

*Department of Chemistry, Kinki University, Higashi-Osaka 577-8502, Japan*

Inclusion compounds are known for their ability of trapping molecules to isolate desired molecular species into solutions or crystalline forms. Cyclodextrins (CDs) are cyclic oligomers of glucose having a cavity of nanometer scales inside the cup structure. They are  $\alpha$ -,  $\beta$ -, and  $\gamma$ -CDs depending on the number of glucose units forming a ring structure, i.e., 6-mer, 7-mer, and 8-mer, respectively. Fullerene  $C_{60}$  can be trapped with two  $\gamma$ -CDs and the inclusion compound is soluble in water. Polyynes  $C_{2n}H_2$  ( $n=4-8$ ) and cyanopolyynes  $HC_{2n+1}N$  ( $n=3-6$ ) are the molecules of *sp*-hybridized carbon chains with alternating single- and triple-bonds. Solubility of these molecules is excellent for organic solvents but poor for water. Under the presence of CDs and water, polyyne molecules are trapped inside the cavity of CDs and solved into water. When the concentration of CDs in water is relatively high, CDs containing hydrophobic molecules eventually precipitate to form crystalline materials. We here present our recent progress on crystallization of  $\alpha$ -CD containing size-selected polyynes or cyanopolyynes together with organic solvents such as hexane or acetonitrile.

The upper curve in Fig. 1 shows optical absorption spectrum of a solid film of  $\alpha$ -CD containing a small amount of cyanopolyyne molecules of  $HC_7N$ . On a smooth back ground due to the scattering of light, two absorption bands are discernible in 220-270 nm and in 280-360 nm. The former is associated with the allowed transition of the  $HC_7N$  molecule, which appears in 190-240 nm in a solution of acetonitrile as in the lower curve in Fig. 1. The latter band in longer wavelengths is newly appeared or intensified by inclusion processes. We discuss on the mechanism for intensification of an intrinsically forbidden transition [1], which can become allowed by symmetry lowering in the crystal field.

[1] T. Wakabayashi, H. Nagayama, K. Daigoku, Y. Kiyooka, and K. Hashimoto, *Chem. Phys. Lett.* **446**, 65 (2007)

Correspondence to Tomonari Wakabayashi  
E-mail: wakaba@chem.kindai.ac.jp  
Tel. 06-6730-5880 (ex. 4101)

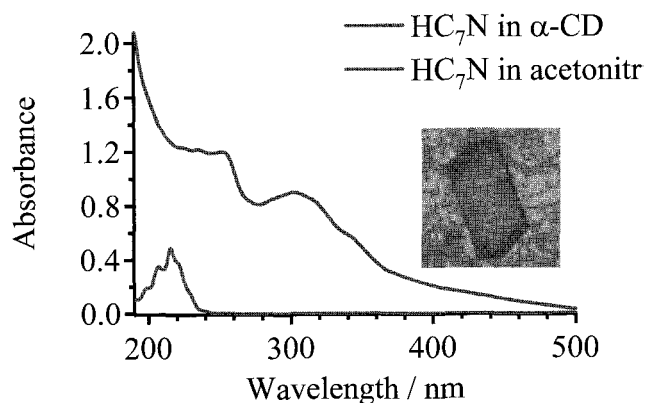


Fig. 1. Absorption spectra of crystalline  $\alpha$ -CD with  $HC_7N$  and acetonitrile (upper trace).

## Optical Absorption Spectra of Single Wall Carbon Nanotubes Containing Hydrogen-End-Capped Polyynes Inside

M. Teshiba, Y. Wada, Y. Yoshida, and T. Wakabayashi

*Department of Chemistry, Kinki University, Higashi-Osaka 577-8502, Japan*

Single wall carbon nanotubes (SWNTs) can accommodate various molecules inside. Nishide et al. reported that hydrogen-end-capped polyynes,  $C_{10}H_2$ , can be trapped inside SWNTs and was stable well above  $300^\circ C$  as revealed by Raman spectroscopic studies [1]. Raman spectra of  $C_{10}H_2@SWNTs$  and  $C_{12}H_2@SWNTs$  with the excitation at 514.5 nm (2.41 eV) exhibited combination and overtone bands, indicating the resonance effect [2]. Malard et al. observed Raman excitation profile to find resonance at  $2.1 \pm 0.15$  eV for  $C_{10}H_2@SWNTs$  [3] and attributed it to the resonance absorption of the molecule [4]. However, the resonance energy  $\sim 2.1$  eV is substantially lower, by  $>1.1$  eV, than the energy for the absorption band of  $C_{10}H_2$  in solutions [5]. Moreover, the resonance energy in SWNTs does not depend very much upon the size of polyynes, while the absorption band of polyynes in solutions systematically shifts to longer wavelength with increasing the molecular size.

For the study on the electronic states in  $C_{2n}H_2@SWNTs$ , we examined optical absorption spectra. The SWNTs formed by laser ablation were sintered in the solution of *n*-hexane containing size-selected polyynes, then sonicated and centrifuged with cholic acid in  $D_2O$ . The UV/VIS/NIR absorption spectra were recorded for  $C_{10}H_2@SWNTs$  and compared with those for SWNTs. The spectra do not differ very much between those for SWNTs with and without  $C_{10}H_2$ . The resonance curve for  $C_{10}H_2@SWNTs$  at  $\sim 2.1$  eV may rather fit to one of the absorption bands of SWNTs.

- [1] D. Nishide et al. Chem. Phys. Lett. 428, 356 (2006)  
 [2] D. Nishide et al. J. Phys. Chem. C 111, 5178 (2007)  
 [3] L. M. Malard et al. Phys. Rev. B 76, 233412 (2007)  
 [4] L. G. Moura et al. Phys Rev. B 80, 161401 (2009)  
 [5] T. Wakabayashi et al. Chem. Phys. Lett. 446, 65 (2007)

Correspondence to Tomonari Wakabayashi  
 E-mail: wakaba@chem.kindai.ac.jp  
 Tel. 06-6730-5880 (ex. 4101)

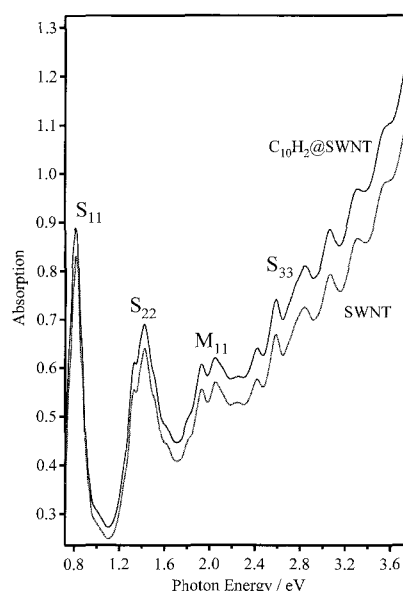


Fig. 1. Absorption Spectra for  $C_{10}H_2@SWNTs$  and SWNTs.



## Synthesis of One-Dimensional Coordination Polymer of Size-Selected Polyynes and Silver Ions

M. Tomioka, T. Wakabayashi and Y. Suenaga

*Department of Chemistry, Kinki University, Higashi-Osaka 577-8502, Japan*

Coordination compounds are known for their variety of chemistry spanning from molecular structures to applications. Ions or clusters of noble metal elements are located at the center of some coordination bonds towards the molecules. The electrons are donated to or drawn from the metallic center for stability. Polyynes with  $\pi$ -electron systems can be also candidates for creating novel coordination compounds. Lucotti et al. reported surface-enhanced Raman scattering (SERS) of polyyne mixtures deposited on silver nanoparticles and observed indication for aggregation of those molecules [1]. Tabata et al. performed SERS experiments for size-selected polyynes  $C_{2n}H_2$  ( $n=4-8$ ) adsorbed on Ag island films to find systematic shifts in vibrational frequencies for the mode in  $1800-2200\text{ cm}^{-1}$  according to the molecular size [2]. Compagnini et al. extended the SERS studies using other noble metal elements such as gold [3]. We here report on the synthesis of coordination polymer including size-selected polyynes stabilized with silver ions. Having a strand of coordination polymer of well defined structure, the interaction between the metal and the polyyne molecule is to be clarified through the detection of optical absorption and Raman scattering processes.

- [1] A. Lucotti, C.S. Casari, M. Tommasini, A. Li Bassi, D. Fazzi, V. Russo, M. Del Zoppo, C. Castiglioni, F. Cataldo, C. E. Bottani, and G. Zerbi, *Chem. Phys. Lett.* **478**, 45 (2009)
- [2] H. Tabata, M. Fujii, S. Hayashi, T. Doi, and T. Wakabayashi, *Carbon* **44**, 3168 (2006).
- [3] G. Compagnini, G. Patenè, L. D'Urso, O. Puglisi, R. S. Cataliotti, and B. Pignataro, *J. Phys. Chem. C* **112**, 20301 (2008).

**Correspondence to Tomonari Wakabayashi**

**E-mail: wakaba@chem.kindai.ac.jp**

**Tel. 06-6730-5880 (ex. 4101)**

## Weak Pre-Oxidation of Graphene-Based Nanomaterials for Enhanced Structure Distinction by Thermogravimetric Analysis

Maki Nakamura<sup>1</sup>, Ryota Yuge<sup>2</sup>, Sumio Iijima<sup>1,2,3</sup>, Masako Yudasaka<sup>1</sup>

<sup>1</sup>*AIST, 1-1-1 Higashi, Tsukuba 305-8565, Japan*

<sup>2</sup>*Green Innovation Research Laboratories, NEC, 34 Miyukigaoka, Tsukuba 305-8501, Japan*

<sup>3</sup>*Meijo University, Shiogamaguchi, Nagoya, 468-8502, Japan*

Thermogravimetric analysis (TGA) is a powerful tool for analyzing graphenous nanomaterials. We previously reported that single-walled carbon nanohorns (SWNHs) and thin graphene sheets (TGS) having close combustion temperatures can be distinguished and even quantified by employing high resolution thermogravimetric analysis (HR-TGA) which can control the specimen temperature responding to the specimen weight-loss rate [1]. However, further discrimination of the graphenous structures in the SWNHs is not easy even by using HR-TGA. We show in this report that the structure analysis of the graphenous materials by HR-TGA can be empowered by weak pre-oxidation, the immersion in H<sub>2</sub>O<sub>2</sub> solutions at room temperature.

As-grown product contained nanohorn aggregates composed of SWNHs (combustion temperature: 560°C) and TGSs (590°C), micrometer-sized graphitic balls (740°C), and small amount of non-graphitic materials (450°C) as estimated from the derivative curves of the weight-temperature curves of HR-TGA. As-grown products were immersed in H<sub>2</sub>O<sub>2</sub> solution for 1 h, 1 day, or longer at room temperature. The combustion temperature of SWNH and TGS decreased rapidly by the H<sub>2</sub>O<sub>2</sub> treatment for 1 h to 1 day, but not so much by the longer period immersions. At the same time, the number of oxygenated groups increased greatly as confirmed by TG-MS measurements. Apparently, the combustion temperature decreases were due to the number increase of oxygenated groups [2]. The combustion temperature decrease of TGS by the H<sub>2</sub>O<sub>2</sub> treatment was larger than that of SWNHs, which is reasonable because TGSs have chemically weak at the edges.

Since the oxidation effect of H<sub>2</sub>O<sub>2</sub> did not last for a long period, the second immersion in fresh H<sub>2</sub>O<sub>2</sub> was performed. As a result, the combustion temperatures of SWNH and TGS further decreased, and even appeared a “new component” (500°C, 18%). To clarify the structure of the “new component”, we stopped TGA at 500°C and took out the residue. TGA of the residue indicated that the “new component” was a part of SWNHs or has a structure similar to SWNHs. Although the exact structure assignment of the “new component” is difficult, it is certain that they are basically constructed of graphenes but had the defect sites which easily become full of oxygenated groups by the H<sub>2</sub>O<sub>2</sub> treatment.

[1] M. Irie, M. Nakamura, M. Zhang, R. Yuge, S. Iijima, M. Yudasaka, *Chem. Phys. Lett.* **500**, 96-99 (2010).

[2] J. Miyawaki, M. Yudasaka, S. Iijima, *J. Phys. Chem. B*, **108**, 10732-10735 (2004).

Corresponding Author: M. Nakamura, M. Yudasaka

E-mail: ma-ki-nakamura@aist.go.jp, m-yudasaka@aist.go.jp, Tel&Fax: 029-861-6290

## Interaction Between Carbon Nanohorns and Amino Acids

X. Zhou<sup>1</sup>, M. Zhang<sup>1</sup>, S. Iijima<sup>1,2</sup>, M. Yudasaka<sup>1</sup>

<sup>1</sup>AIST, Tsukuba, <sup>2</sup>Meijo University

Biomedical applications, including drug delivery and photo-hyperthermia agents for cancer therapy, of single wall carbon nanohorns (SWNHs) have been investigated [1-2]. SWNHs certainly interact with proteins, carbohydrates, fats, etc in a living body. Especially, the interaction with protein may strongly influence on the toxicological assay of SWNHs or therapeutic efficacy of SWNH-based drug delivery. However, it is difficult to study how SWNHs interact with the proteins because the proteins have the complex structure and there are more than tens of millions of proteins exist in living body. Here, we clarify the interaction between SWNHs and amino acid, the elementary unit of protein, to get some information about the interaction of proteins and SWNHs.

We chose five types of amino acids (lysine, phenylalanine, histidine, tryptophan, and methionine). Each amino acid was dissolved in water (Concentrations: 0.05 to 0.5 g/L), in which as-grown SWNHs were added, mixed, and stirred for overnight. Then we filtered the aqueous dispersion of SWNHs and amino acids, and estimated the quantity of amino acid attached on SWNHs through measurement of the concentration of amino acid in filtrate by optical absorption spectroscopy. The results showed that all of these amino acids were adsorbed on SWNHs but the adsorbed quantities were different. Lysine with a C4 alkyl chain had a largest quantity adsorbed on SWNHs, followed by Tryptophan and Phenylalanine, each having a benzene ring. Quantities of histidine and methionine attached on SWNHs were smaller in quantities, probably because they did not have those hydrophobic groups. The detail about the adsorption state will be discussed in conference.

Acknowledgement: X.Z. and S.I. express their appreciation to the financial support from Balzan Foundation.

[1] K. Ajima, M. Yudasaka, et al. ACS Nano, 2008( 2), 2057–2064.

[2] M. Zhang, M. Yudasaka, et al. PNAS, 2008 (105),14773–14778.

**Corresponding Author: M. Zhang, M. Yudasaka**

**E-mail:** m-zhang@aist.go.jp; m-yudasaka@aist.go.jp

## ***In-situ* Raman Spectroelectrochemical Investigation of Potential Depended Electronic Structure of Single-Walled Carbon Nanotubes**

OShingo Sakamoto and Masato Tominaga\*

*Graduate School of Science and Technology, Kumamoto University,  
Kumamoto 860-8555, Japan*

The electronic properties of single-walled carbon nanotubes (SWCNTs) strongly depend on their diameters and chiralities ((n,m): chiral indices). To develop the applications of SWCNTs such as double layered capacitors and electrochemical sensors, it is important to understand electronic structures of SWCNTs in a liquid. *In-situ* Raman spectroelectrochemistry is strong tool for investigating the properties of SWCNTs at potential applying condition [1, 2]. In this study, SWCNTs were synthesized onto an Au electrode (SWCNTs/Au) by CVD method. The relationship between the applied potential to SWCNTs and the electronic structure in an aqueous solution was investigated using *in-situ* Raman spectroelectrochemical measurements.

The intensity/potential profiles of the radial breathing mode (RBM) bands were plotted to evaluate the chirality dependence of the electronic structure (Fig. 1). In the case of semiconducting SWCNTs, plateau region of the peak intensity was observed. These results indicate that the potential range at the plateau region would correspond to the band gap of the semiconducting SWCNTs. The band gap energy increased with decreasing the diameter of semiconducting SWCNTs. This tendency was similar to the results expected by the theoretical simulation [3].

### **References:**

- [1] M. Kalbac *et al.*, *ACS Nano*, **3**, 2320 (2009).
- [2] J. S. Park *et al.*, *Phys. Rev. B* **80**, 081402 (2009).
- [3] H. Yorikawa *et al.*, *Phys. Rev. B* **52**, 2723 (1995).

**Corresponding Author:** Masato Tominaga

**TEL & FAX:** +81-96-342-3656, **E-mail:** masato@gpo.kumamoto-u.ac.jp

### **Semiconducting SWCNTs**

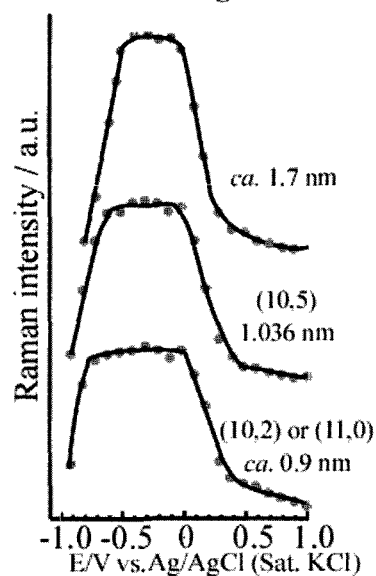


Fig. 1 The Raman peak intensity excited by 1.58 and 2.41 eV laser radiations at semiconducting SWCNTs as a function of electrode potential.

## Synthesis of metal-nanowire@SWNTs and their physical properties

○Daeheon Choi, Ryo Kitaura, Ryo Nakanishi, Yasumitsu Miyata, and Hisanori Shinohara\*

*Department of Chemistry, Nagoya University, Furo-cho, Chikusa-ku, Nagoya 464-8620, Japan*

Carbon nanotubes (CNTs) have attracted extensive interests for the application of nanoelectronic devices because of their unique structure and electrical properties. In any of such CNTs applications, control of electronic structure of CNTs is crucial, and chemical doping is one of the most important techniques to modulate the electronic structure of CNTs; encapsulating various atoms and molecules into CNTs inner-space is a stable chemical doping. In particular, recently reported metal-nanowire encapsulating CNTs[1] are expected to show a heavy electron doping due to a massive electron transfer from metal atoms to CNTs. In this study, in addition to electric properties, we have focused on investigation of doping-modulated electronic structure of the nanowire encapsulating CNTs using optical absorption spectroscopy. Single-walled carbon nanotubes (SWNTs) were synthesized by the arc-discharge method (SO-HT, Meijo Nano Carbon Inc.) and Europium metal were used to synthesize metal-nanowires inside inner-space of SWCNTs.

CNTs film, fabricated by vacuum filtration method [2], was used for characterizing optical and electrical properties of Eu-nanowire@SWNTs. In optical absorption spectra of SWNTs films, not only  $S_1$  but also  $S_2$  and  $M_1$  peaks almost completely disappeared after Eu (donor) doping as shown in Fig 1. It indicates that CNTs have been heavily electron doped up to  $M_1$  band by encapsulated Eu atoms. Raman and four probe resistance measurements of Eu-nanowire@SWCNTs films also show significant alternation that is caused by heavy electron doping. In this poster presentation, we will discuss doping effects of the Eu-nanowire @SWNTs in detail.

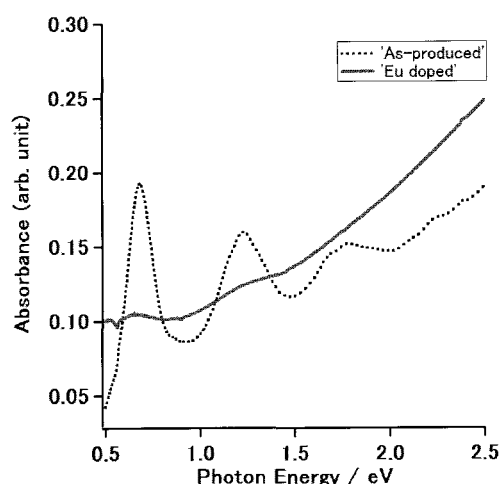


Fig1. Optical absorption spectra of SWNTs film before and after Europium doping

### References:

- [1] R. Kitaura et al., *Angew. Chem.*, **48** (2009)
- [2] Wu Z et al., *Science*, **305** 1273-6 (2004)

\*E-mail address: [noris@nagoya-u.jp](mailto:noris@nagoya-u.jp)

## Fabrication and Electrical Transport Properties of Atom Encapsulated Single-Walled Carbon Nanotubes Thin Film Transistors

○Y. Osanai, T. Kato and R. Hatakeyama

*Department of Electronic Engineering, Tohoku University, Sendai 980-8579, Japan*

Carbon nanotubes (CNTs) with nanometer-order diameter and millimeter-order length attract a great deal of attentions due to their novel applications such as next-generation nanoelectronic devices. Accommodation of various dopant atoms, molecules, and compounds makes it possible to modify the intrinsic electronic and optical properties of single-walled carbon nanotubes (SWNTs). According to our previous researches for the transport property of individual SWNT, alkali-metal-, alkali-earth metal- and halogen-encapsulated SWNTs are found to exhibit n-type and p-type semiconducting behaviors under the field-effect transistor (FETs) configuration, respectively. This indicates that alkali-metal, alkali-earth metal- and halogen atoms operate as an electron donor and an electron acceptor for SWNT, respectively [1, 2]. Based on this background, we utilize the atom-encapsulated SWNTs for the fabrication of high performance n-type thin film transistors (TFTs). In order to reveal the detailed effects of atom encapsulation on the transport property of SWNTs-TFTs, the direct comparison of electrical characteristics of SWNTs-TFTs are also carried out before and after the atom encapsulation with the same SWNTs-TFTs device.

Atom encapsulation is carried out by a plasma ion irradiation method. In this study, a Cs atom is used for the encapsulated atom. It is found that the transport properties of SWNTs-TFTs are clearly changed from p-type to n-type semiconducting characteristics by increasing the energy of ions during the encapsulation process. The highest encapsulation yield is realized under the 60 eV irradiation energy of Cs<sup>+</sup>. Higher than this value, SWNTs are damaged by ion bombardment and transport properties are significantly lowered. The Cs encapsulated SWNTs-TFTs show very high stability under the various environments, such as air, water, and high temperature conditions. It should be noted that the n-type characteristics are observed even after the 400 °C annealing. This indicates that it is possible to fabricate very stable n-type TFTs by using the Cs encapsulated SWNTs thin films.

[1] T. Izumida, R. Hatakeyama, Y. Neo, H. Miura, K. Omote, and Y. Kasama, *Appl. Phys. Lett.* **89**, 093121 (2006).

[2] J. Shishido, T. Kato, W. Oohara, R. Hatakeyama, and K. Tohji, *Jpn. J. Appl. Phys.* **47**, 2044 (2008).

Corresponding Author Y. Osanai

E-mail: osanai@plasma.ecei.tohoku.ac.jp

Tel&Fax: +81-22-795-7046 / +81-22-263-9225

## Separation of SWCNTs by gel chromatography using gradient of surfactant concentration

○Ryuji Inori, Takako Okada, Takayuki Arie, and Seiji Akita

*Department of Physics and Electronics, Osaka Prefecture University, 1-1 Gakuen-cho,  
Naka-Ku, Sakai, Osaka 599-8531, Japan*

Single walled carbon nanotubes (SWCNT) show metallic and semiconducting properties depending on their chiralities. Separations of metallic and semiconducting ones (MS separation) using gel chromatography have been reported.[1, 2] In this study, we investigate the diameter-selective MS separation of SWCNT by gel chromatography using the gradient of the surfactant concentration.

SWCNTs (HiPCO, diameter;  $1.0 \pm 0.3$  nm) were dispersed into 2 wt% sodium dodecyl sulfate (SDS) for 12h by using an ultrasonication. The SWCNT dispersion was centrifuged at  $23,470 \times g$  for 60 min to remove bundles and insoluble materials. A column (length: 20~30 cm) was filled with sephacryl gel (particle size: 25~75  $\mu\text{m}$ ) in 20% ethanol. The medium for the gel was then exchanged by 1 wt% SDS. The SWCNT suspension was applied to the top of the column, and 1 wt% SDS was applied to perform chromatography. The difference in the SDS concentration results in the gradient of the concentration at the interface between media. In this case,

we observed the gradient-induced separation of SWCNTs depending on the SDS concentration in the column, where the lower and upper parts of the column were red and green, respectively. Figure 1 shows a series of absorption spectra which were measured from the SWCNTs sequentially collected in the eluants as indexed by “a” to “j” shown in Fig. 1. This indicates that SWCNTs with the larger diameter were eluted first, possibly due to the gradient of the SDS concentration. Thus, the gradient of the SDS concentration is effective for the diameter-selective MS separation of SWCNTs using gel chromatography.

### Acknowledgement

This study is supported by Grant-in-Aid for Scientific Research on Priority Area of the Ministry of Education, Culture, Sports, Science and Technology of Japan (MEXT)

### References

- [1] T. Tanaka et al, *Appl. Phys. Express* 2 (2009) 125002.
- [2] K. Moshhammer, F. Hennrich, and M. M. Kappes, *Nano Res.* 2, 599 (2009).

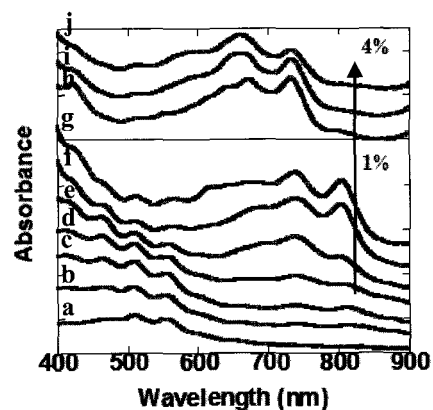


Fig. 1. A series of absorption spectra of collected SWCNTs.

## Electrochromic Carbon Electrodes: Controllable Visible Color Changes in Metallic Single-Wall Carbon Nanotubes

○Rieko Moriya<sup>1</sup>, Kazuhiro Yanagi<sup>1</sup>, Taishi Takenobu<sup>2</sup>, Yasuhisa Naitoh<sup>3</sup>, Takao Ishida,<sup>3</sup> Hiromichi Kataura<sup>3,4</sup>, Yutaka Maniwa<sup>1,4</sup>

<sup>1</sup> Tokyo Metropolitan Univ., <sup>2</sup> Waseda Univ., <sup>3</sup> AIST, <sup>4</sup> JST-CREST

Electrochromism is the phenomenon of the optical reversible changes in a material during electrochemical redox processes. Various types of materials exhibit electrochromism, and there is sustained interest in this subject because of its fundamental and practical importance. Indium-tin-oxide (ITO) transparent conductive glasses are usually used for the electrodes to apply potentials on the electrochromic materials to change their colors, however, a system without using ITO is desirable due to increasing demands on rare metal resources. In addition, for practical purposes, the development of electrochromic materials that are electrochemically stable is of great importance for durable electrochromic devices. In this study, we solved these problems by using metallic single-wall carbon nanotubes (SWCNTs) as both electrodes and electrochromic components. We prepared metallic single-wall carbon nanotubes (SWCNTs) with diameters of 0.85nm, 1.0nm, and 1.4nm, exhibiting yellow, magenta, and blue-green colors, respectively, and controlled the colors electrochemically (Fig. 1).<sup>1</sup> It has been considered that SWCNTs would be un-stable at high-electro chemical potential, but we overcame this issue by preparing high-purity samples and using ionic liquids for electrolytes. Clear changes of the optical absorption spectra of the metallic SWCNTs with diameters of 1.4, 1.0, and 0.85 nm were observed. The changes are reversible and repetitive (more than 1000 times), and a relatively good coloration efficiency  $(1.9 \pm 0.2) \times 10^2 \text{ cm}^2 \text{ C}^{-1}$ , which is sufficient for practical purposes, is achieved. Moreover, we present here a basic model of "All-Carbon Nanotube Electrochromic devices". The electrochromic color changes were achieved without using ITO layers or any electrochromic polymers; the metallic SWCNTs functioned as both the electrochromic components and electrodes, thus they can be termed "electrochromic carbon electrodes". Such electrochromic carbon electrodes are possible due to the following unique characteristics of metallic SWCNTs: (1) The stable color changes originate from electrochemically stable carbon characteristics; (2) the colors are caused by quantized conditions due to the nanotube structures; and (3) metallic nanotubes have a high conductivity. Metallic SWCNTs are thus unique and highly promising electrochromic carbon electrodes to develop durable electrochromic devices without rare metals.

This work was partially supported by a Grant-in-Aid for Scientific Research on Innovative Areas (No.21108523, "π-Space") from MEXT, and by Industrial Technology Research Grant Program in 2007 from NEDO.

**Reference:** [1] Yanagi, Moriya, et al., submitted in 2010.

**Corresponding Author: Kazuhiro Yanagi**

**E-mail:** yanagi-kazuhiro@tmu.ac.jp

**Tel&Fax:** 042-677-2494 (& 2483)

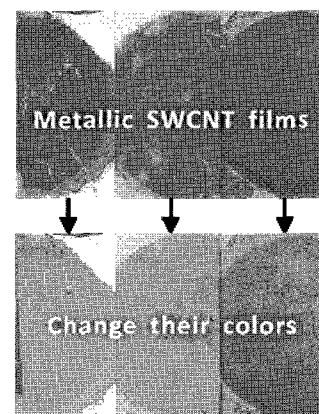


Fig. 1: Electrochromic color changes on thin films of metallic SWCNT with diameters of 1.4, 1.0, and 0.8 nm (from left to right).



## **Biocompatibility of Chitosan/Carbon Materials Composite Membranes for Tissue Engineering**

○Katsumune Takahashi<sup>1</sup>, Koji Tsuchiya<sup>1,2</sup> and Hirofumi Yajima<sup>1,2</sup>

*1. Center for Colloid and Interface, Tokyo University of Science, 2641 Yamazaki, Noda, Chiba, 278-8510, Japan*

*2. Department of Applied Chemistry, Faculty of Science, Tokyo University of Science, 1-3 Kagurazaka, Shinjuku-ku, Tokyo 162-8601, Japan*

Carbon material such as single-walled carbon nanotube (SWNTs), multi-walled carbon nanotubes (MWNTs), and graphite have paid much attention as fillers of biomaterials for controlling biocompatibility. In our previous study, chitosan-based composite membranes containing SWNTs, MWNTs and graphite were found to exhibit an inhibitory effect on fibrinogen adsorption and platelets adhesion, compared to chitosan film. On the other hands, only chitosan/SWNTs composite membrane displayed the enhancement of cell attachment and proliferation. Thus, the carbon structures and morphologies were inferred to be strongly involved in biocompatibility control.

In this study, we have focused on a unique carbon material with micro-coiled filament-like structure, named carbon micro coil (CMC). CMC has been known to assume 3D helical/spiral structure, in which the diameters and lengths of CMC are in the range from 1 to 10  $\mu\text{m}$ , and from 100  $\mu\text{m}$  to 3 mm. The objective of this study is to investigate the effect of CMC on the biocompatibility of CS/CMC composite membranes, in comparison with the effects of the other carbon materials with different geometric structures from CMC.

CS/CMC composite membranes were prepared with various contents of CMC (3, 5, 10 wt%). Raman spectral measurements implied that CMC was mainly comprised of disordered graphite and amorphous carbons, whose abundance on the membrane surface was increased with the CMC content. CS/CMC membranes exhibited a strong inhibition effect against the adsorption of plasma FN at a CMC content of more than 5 wt%, in contrast to an intrinsic CS membrane without CMC. This result suggested that the surface characteristics involving the functions of specific carbon structure and bioactivity of CMC and the membrane morphology prevent blood platelets from adhering and acting on the membrane.

**Corresponding Author:** Hirofumi Yajima

**E-mail:** yajima@rs.kagu.tus.ac.jp, **Tel:** +81-3-3260-4272 (ext. 5770), **Fax:** +81-3-5261-4631

## Evaluation of Thermal Conductivity of Single Carbon Nanotube Using Fluorescent Gel Temperature Sensor in Liquid

○Kyohei Tomita<sup>1</sup>, Hisataka Maruyama<sup>2</sup>, Fumihito Arai<sup>3, 4</sup>

<sup>1</sup>*Department of Mechanical Engineering, Nagoya University, Nagoya 464-8603, Japan*

<sup>2</sup>*Department of Mechanical Science and Engineering, Nagoya University, Nagoya 464-8603, Japan*

<sup>3</sup>*Department of Micro-Nano Systems Engineering, Nagoya University, Nagoya 464-0861, Japan*

<sup>4</sup>*Seoul National University, Seoul 151-742, Korea*

Carbon nanotube (CNT) has potential applications in various fields such as nanosensors. Although electrical and mechanical properties are investigated at single nanotube, measurement of thermal property of single CNT is difficult. Some groups measured the thermal properties of CNT by four-probe method in vacuumed condition. However, measurement by this method has problem of heat transfer from the CNT to the sensing electrodes being connected with the CNT.

Here, we propose a novel method how to measure the thermal conductivity of single CNT in liquid with polymer temperature sensor [1] as shown in Fig. 1. Single CNT was fixed to the silicon cantilever with nanomanipulation and EBID in SEM. The sensor is fixed to the end of the CNT by optical tweezers in liquid. Roles of the sensor are temperature sensing and heat input to the CNT. Here, IR laser was used to heat the sensor. Temperature sensitive quantum dots are impregnated in this sensor. Temperature is measured by detection of the color difference of the red ( $Cr$ ) in the sensor signal. The error of  $Cr$  is less than  $\pm 3\%$ . Sensitivity is  $-1\%/K$ . Resolution and accuracy of the temperature are 0.019 K and 0.14 K,

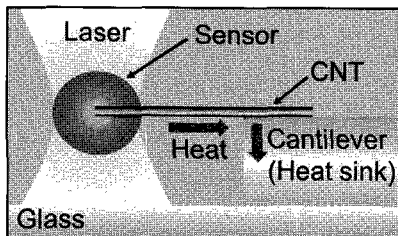


Fig. 1 Thermal conductivity measurement of CNT with temperature sensor in

respectively. The error of the heat input is less than 4%. Thermal conductivity can be calculated based on the theoretical analysis of one dimensional heat conduction. The estimated error of the thermal conductivity is less than 10%.

Acknowledgements: This work was supported by KAKENHI (20246044) and CREST, JST.

[1] H. Maruyama, F. Arai, T. Fukuda, Lab on a Chip, 8-2, (2008), 346 - 351

Corresponding Author: Kyohei Tomita

Tel: +81-52-789-4493, Fax: +81-52-789-5213, E-mail: hisataka@mech.nagoya-u.ac.jp

## Structural dependence of Multi-Walled Carbon Nanotubes on fuel cell performance

○Shinya Kitamura, Takeshi Hashishin, Jun Tamaki, Kazuo Kojima

*Department of Applied Chemistry, Ritsumeikan University, Shiga 525-8577, Japan*

It is important that the control structure of multi-walled carbon nanotubes (MWNTs) was applied to electric devices such as field emission devices and batteries. In our previous study, alumina nanohole array was used as a template for the guide growth of MWNTs [1]. As one of fuel cell application, we tried to directly grown MWNTs on the surface of carbon paper (CP), which is composed of carbon fibers with 5  $\mu\text{m}$  in diameter, in order to reduce ohmic losses between an electric collector of CP and a catalytic layer of MWNTs. In our previous study, it was confirmed that the G/D ratio of as-grown MWNTs is increased with decreasing oxygen concentration by vacuum level during CVD process.

In this study, we investigated the changing amount of the G/D ratio under electrical power loading: 0.5 V for 6 h at 80 °C in air. As the results, it was tended that the performance of fuel cell for MWNTs/CP electrode, i.e., a maximum power density and open-circuit voltage (OCV), increased with increasing the G/D ratio, as shown in Fig. 1.

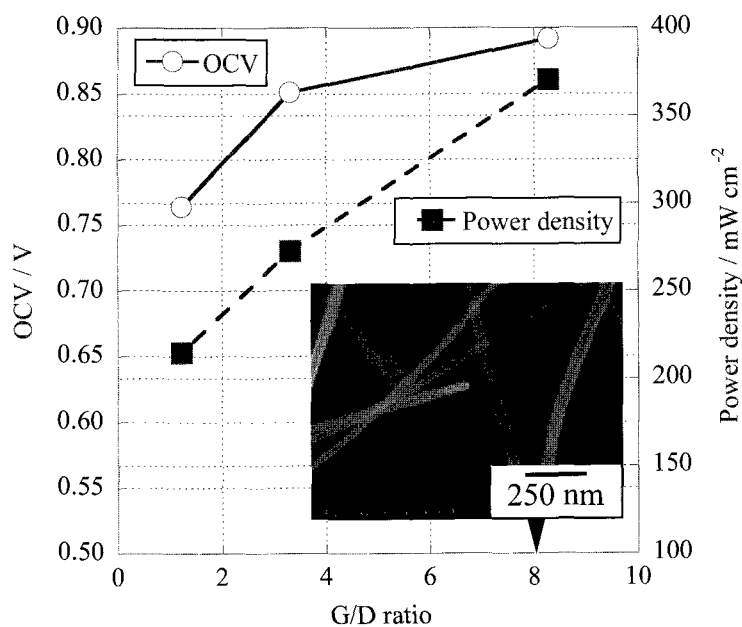


Fig. 1 Effect of G/D ratio on fuel cell performance.

[1] T. Hashishin, Y. Tono, and J. Tamaki, *Jpn. J. Appl. Phys.*, **45**, 333-337 (2006).

TEL: +81-77-561-4902, FAX: +81-77-561-2659, E-mail: hasisin@sk.ritsumei.ac.jp

発表索引  
**Author Index**

## Author Index

～A～		Chiba, Yuriko	2P-53
Abe, T.	2-8	Chigusa, Hajime	2P-26
Abe, Yuuichi	3P-16	Cho, Soon Cheon	2P-47
Achiba, Yohji	1-2, 2P-14, 2P-17, 3-10, 3P-31	Choi, Daeheon	3P-47
Agata, Shogo	1P-13	Chowdhury, Md. Tareque	1P-34
Ago, Hiroki	2P-18, 2P-21, 3-4	Cohen, Marvin L.	3-3
Aikawa, Shinya	1-7	Cong, C.	2-5
Akamatsu, Norihisa	2P-53	Cuong, Nguyen Thanh	1P-40
Akasaka, Takeshi	1P-54, 2-10, 2P-34, 2P-53, 3P-18	～D～	
Akasaka, Tsukasa	1P-19, 2P-2	Dai, Hongjie	2P-43
Akasaka, Yumeno	3P-34	Dobado, Jose A.	2P-45
Akazaki, Kojiro	2P-19	Doi, Tatsuya	2-12, 3P-26
Akita, Seiji	3P-49	Dresselhaus, M. S.	2-5
Aoki, Nobuyuki	2-8, 2-12, 3P-26	～E～	
Aoki, Yusuke	2-11	Eguchi, Takahiro	1P-38
Aoyagi, Nobuyoshi	1P-45, 2P-28	Einarsson, Erik	1-7, 2P-37
Arai, Fumihito	3P-52	Enoki, Toshiaki	3P-36
Arai, Shigeo	2P-31	～F～	
Arie, Takayuki	3P-49	Feng, Lai	2-10
Asada, Yuki	1-6, 2-3, 3P-12	Feng, Ye	2P-20
Asahara, Haruyasu	3P-33	Fueno, Hiroyuki	2P-36
Asaka, Koji	2P-31	Fujigaya, Tsuyohiko	1-9, 1-12, 1P-23, 1P-27, 2P-6, 2P-7, 2P-8, 2P-19
Asano, Hirohito	2P-32	Fujihara, Miho	1P-7, 1P-48
Asano, Satoshi	1P-9	Fujii, Shunjiro	1-1, 1P-3, 1P-22, 2P-20
Ata, Seisuke	1-10, 1P-25	Fujimoto, Yoshitaka	3P-7
Atsumi, Hiroki	3P-14	Fujino, Tatsuya	3P-31
Awaga, Kunio	1P-52	Fujiwara, Yuji	3P-35
Awazu, Masayuki	1-2	Fukaya, Akiji	1P-37
Ayagaki, Takafumi	2P-21	Fukumar, Takahiro	2P-7
Ayato, Yusuke	2P-13	Fukuoka, Tomoko	3P-36, 3P-37
～B～		Fukuyama, Hiroshi	2P-42
Baba, Keisuke	3P-28	Furukawa, Takeo	1P-18
Bandow, Shunji	2P-32	Furuyama, Yusuke	3P-39
Barnard, Amanda S.	1S-2	Futaba, Don N	2P-54, 1-10, 1-11, 1P-25, 2P-10, 2P-25, 3P-4, 2P-3
Bird, Jonathan P.	2-8, 2-12	～G～	
～C～		Gao, W. Y.	3P-24
Chen, Shimou	3P-38	Gui, Xuchun	2P-1
Chen, Xiao	2P-37	Guldi, Dirk M.	2-10
Chiashi, Shohei	1-7, 2P-16, 2P-37, 3-9		

~H~

Hakamatsuka, Mari	2P-4	Iizumi, Yoko	3-1
Haque, Md. Mahbulul	2P-29	Ikeda, Ken-ichi	3-4
Hara, Hironori	1P-14, 1P-41	Ikeda, Takashi	1P-45
Haruyama, Junji.	2P-42	Ikeda, Yasuro	1-2
Hase, Muneaki	2P-51	Ikuma, Naohiko	2-14, 3P-33
Hasegawa, Daisuke	3-9	Imahori, Hiroshi	2-9, 3P-32
Hasegawa, Kei	2P-12	Inami, Yu	3P-36
Hasegawa, Masataka	3S-6	Inori, Ryuji	3P-49
Hasegawa, Tadashi	2P-53	Inoue, Akihito	2P-17, 3-10
Hashimoto, Kenro	3-10, 2P-17	Inoue, Taiki	3-9
Hashimoto, Takeshi	1P-19, 2P-2	Inoue, Yoku	2P-5
Hashishin, Takeshi	3P-53	Iokawa, Takayasu	1P-1
Hata, Kenji	1-10, 1-11, 1P-25, 2P-3, 2P-10, 2P-25, 2P-54, 3P-4	Irle, Stephan	1P-2, 1P-14, 1P-15, 1P-41, 2-4, 2P-27, 2P-45, 3P-19, 3P-30
Hata, Koichi	3P-35	Ishida, Hiroyasu	2P-48
Hatakeyama, Rikizo	1-8, 2P-43, 2P-47, 2P-47, 2P-48, 3P-48	Ishida, Takao	2P-49
Hatano, Yuuya	1-2	Ishiguro, Yuki	1P-5
Hayamizu, Yuhei	2P-10	Ishihara, Fumihiko	2P-33
Hayashi, H.	3P-2	Ishii, Fumiyuki	3P-9
Hayashi, Hironobu	3P-32	Ishii, H.	3P-2
Hayashi, Kenjiro	3-5	Ishii, Satoshi	3P-11
Hayashi, Tsugumi	1P-46	Ishii, Tadahiro	2P-24
Hayashi, Yasuhiko	1P-20	Ishii, Yosuke	1P-35
Heine, Thomas	2P-45	Ishii, Yuichi	1P-8
Hibino, Hiroki	1P-32, 2P-35	Isoda, Tatsunori	2P-33
Hino, Shojun	2-11, 3P-20, 3P-21	Itami, Kenichiro	2P-50
Hirai, Hiromasa	3P-1	Ito, Hiroaki	1P-5
Hiramoto, Masahiro	2S-4	Ito, Masaaki	2P-30
Hirana, Yasuhiko	3P-5	Ito, Masayosi	1P-18
Hirano, Atsushi	2P-51	Ito, Shin-ichi	1P-52
Hirayama, D.	3P-2	Ito, Yoichi	1P-20
Hiura, Hidefumi	1P-36, 3-7	Ito, Yoshito	3-4
Homma, Yoshikazu	1P-13	Itoh, Akira	3P-3
Hou, Bo	2P-37	Iwasa, Yoshihiro	1-4, 1P-26
Hu, Baoshan	3-4	Iwasawa, H.	3P-2
Huang, Yang	2P-20	Izadi-Najafabadi, Ali	2P-10
Hue, Hitoshi	1P-45	Izumi, Noriko	3P-21

~J~

~I~		J. Page, Alister	2P-27
Ihara, Kazuki	2-1, 3P-12	Jang, Bongyong	1P-20
Iiduka, Masatomo	3-8	Jiang, J.	3P-2
Iijima, Sumio	1-15, 1P-4, 1P-43, 1S-1 2-3, 2P-32, 3-1, 3P-36, 3P-40, 3P-44, 3P-45	Jiao, Liying	2P-43
		Jimbo, Takashi	1P-20, 1P-21, 1P-37
		Jinno, Makoto	2P-32

Jippo,Hideyuki	1P-50	Kitaura,Ryo	1-6, 1P-7, 1P-11, 1P-16,
Joung,Soon-Kil	3P-10		1P-47, 1P-48, 1P-52, 2P-22,
			2P-50, 3P-38, 3P-47
~K~		Kobashi,Kazufumi	1P-25
K.Ferry,D.	2-8	Kobashi,Kazufumi	3P-4
Kadowaki,H.	3P-2	Kobayashi,Keita	1-16
Kaida,Shota	2P-28	Kobayashi,Yoshihiro	1P-13
Kaji,Hironori	3P-32	Kodama,Soichiro	1-8
Kakihara,R.	3P-2	Kodama,Takeshi	2P-17, 3-10, 3P-31
Kalita,Golap	2-7	Kodama,Takuya	2P-17
Kamikawa,Syota.	2P-42	Koizumi,Kohei	2P-13
Kamiya,Katsumasa	2-6	Koji,Tsuchiya	2P-24
Kanayama,Hisanori	3P-13	Kojima,Kazuo	3P-53
Kaneko,Tetsuya	3P-35	Kokai,Fumio	2P-26, 3-2, 3P-39
Kaneko,Toshiro	1-8, 2P-47, 2P-48	Kokubo,Ken	2-14, 3P-33
Kanemitsu,Toshiyuki	1P-30	Komaki,Hisashi	3P-25
Kanemitsu,Yoshihiko	2P-41	Komatsu,Naoki	2-2, 2P-30
Kaneta,Chioko	1P-50	Konabe,Satoru	1P-51
Kano,Arihiro	1P-27	Kondo,Daiyu	3-5
Kashihara,Miyato	2-14	Koretsune,Takashi	3-3, 3P-6
Kataura,Hiromichi	1-1, 1P-3, 1P-7, 1P-9, 1P-22,	Koshio,Akira	2P-26, 3-2, 3P-39
	1P-31, 2P-20, 2P-23, 2P-49,	Kostarelos,Kostas	1P-43
	3-1, 3P-15, 3P-17, 3P-36	Koyama,Kyouhei	2-12, 3P-26
Kato,Hidenori	1P-35	Koyama,Takeshi	1-3
Kato,Koichiro	3P-6	Kumamoto,Nagisa	3P-23
Kato,Shin-ichiro	1P-6	Kumazawa,Akira	2P-24
Kato,Takaaki	2P-53	Kusakabe,Koichi	2P-11
Kato,Tatsuhisa	3P-22	Kushida,Yoshihiro	3-6
Kato,Toshiaki	2P-43, 3P-48	Kusunoki,Michiko	2P-52
Kauppinen,Esko I.	1-5	Kuwano,Jn	2P-13
Kawarada,Hiroshi	2P-15, 3-8	Kyakuno,Haruka	3P-36, 3P-37
Kawasaki,Shinji	1P-35, 1P-17	Kyotani,Takashi	3P-37
Kawasaki,Tomoyo	3P-9		
Kayo,Yasumichi	2P-14	~L~	
Kazachenko,Viktor	3P-27	Lee,Michael V.	1P-36, 3-7
Kim,Dong Yong	1P-52	Lee,Young Hee	3S-5
Kimura,Hiroe	2P-25	Li,Xiaolin	2P-43
Kimura,Takahide	2-2, 2P-30	Li,Yongfeng	1-8
Kinomura,Naoya	3P-23	Lim,Hong En	1P-47, 3P-38
Kishi,Naoki	1P-20, 1P-21, 1P-37	Ling,Lim Siew	1P-12
Kishida,Hideo	1-3	Liu,Huaping	2P-20, 2P-23
Kishimoto,Shigeru	1-5	Liu,Lili	1P-41, 2P-45
Kitagawa,Hiroshi	1P-52	Liu,Qingfeng	2P-6
Kitagawa,Naoko	2P-30	Liu,Zhen	3-1
Kitamura,Shinya	3P-53	Lu,Xing	3P-18

～M～

Machida, Tomoki	2P-41	Mizorogi, Naomi	1P-54, 2-10, 3P-18
Maeda, Fumihiko	1P-13	Mizuno, Seigi	3-4
Maeda, Kohji	1P-46	Mizuno, Takahiro	2P-32
Maeda, Yutaka	2P-51, 2P-53	Mizusawa, Takashi	1-2
Mahjoub, A.	2-8	Mizuta, Noriaki	3-4
Maigne, Alan	2P-54	Mizutani, Takashi	1-5, 1-6
Makino, Kotaro	2P-51	Mizutani, Toshihisa	1P-21
Maniwa, Yutaka	2P-49, 3P-2, 3P-17, 3P-36, 3P-37, 3P-50	Mizutani, Yoshihiro	1P-4
Martín, Nazario	2-10	Moriya, Rieko	1-4, 3P-50
Martin-Martinez, Francisco J.	2P-45	Moriyama, Hiroshi	2-13
Maruyama, Atsushi	1P-27	Morokuma, Keiji	1P-2, 2-4, 3P-30
Maruyama, Hisataka	3P-52	Motooka, S.	2-8
Maruyama, Shigeo	1-7, 2P-16, 2P-37, 3-9	Mouri, Shinichiro	3P-1
Maruyama, Takahiro	1P-1, 1P-4, 1P-5	Murai, Yumi	1P-6
Masubuchi, Satoshi	2P-41	Murakoshi, Kei	1P-10
Masuda, Mitsutoshi	1P-43	Muro, Kiyofumi	3P-1
Matano, Yoshihiro	2-9, 3P-32		
Matsuda, Kazunari	2-2, 2P-41	～N～	
Matsuda, Kazuyuki	2P-49, 3P-2, 3P-36, 3P-37, 3P-50	Nagano, Takuya	3P-1
Matsui, Takashi	2P-42	Nagao, Kazuaki	3P-33
Matsui, Yusuke	3P-35	Nagaoka, Tomoya	1P-18
Matsunaga, Ryusuke	2P-41	Nagase, Shigeru	1P-54, 2-10, 2P-53, 3P-18
Matsuo, Teppei	2P-16	Nagata, Atsushi	3P-35
Matsuoka, Makoto	1P-19, 2P-2	Naito, Kimiyoshi	2P-5
Matsushima, Masahiro	2-7	Naitoh, Yasuhisa	3P-50
Matsuura, Sanae	2P-50	Nakae, Takahiro	3-6
Matsuzaki, Satoki	1P-28	Nakamura, Arai	1-3
Melchor, Santiago	2P-45	Nakamura, Eiichi	2P-54
Mieno, Tetsu	3P-27	Nakamura, Maki	3P-44
Mikie, Tsubasa	3P-33	Nakamura, Toshiya	1P-47
Mimura, Hidenori	2P-5	Nakanishi, Midori	1-2
Miwa, Ikuma	1P-21	Nakanishi, Ryo	3P-47
Miyamoto, Katsuhiko	2-12	Nakanishi, Yusuke	2P-50, 3P-21, 3P-25
Miyashiro, Kunio	1P-6	Nakashima, Naotoshi	1-9, 1-12, 1P-23, 1P-24, 1P-27, 2P-6, 2P-7, 2P-8, 2P-19, 3P-5
Miyata, Yasumitsu	1-3, 1-6, 1P-7, 1P-11, 1P-16, 1P-47, 1P-48, 2P-22, 2P-50, 3P-36, 3P-38, 3P-47	Nakayama, Takuya	2P-22
Miyazaki, Ryo	2P-42	Namatame, H.	3P-2
Miyazaki, Takafumi	2-11, 3P-20, 3P-21	Naritsuka, Shigeiya	1P-1, 1P-4, 1P-5
Miyazaki, Yusuke	1P-6	Nasibulin, Albert G.	1-5
Miyazawa, Kun'ichi	2-15, 3P-34	Negishi, Ryota	1P-13
Mizobuchi, Shingo	3-6	Nihey, Fumiyuki	2-1
Mizoguchi, Noriyuki	3P-8	Niidome, Yasuro	3P-5
		Nikawa, Hidefumi	2-10
		Nishide, Daisuke	1-1, 1P-3, 2P-23
		Nishihara, Hirotomo	3P-37



Nishikawa,Eiichi	1-7	Omatsu,Takashige	2-12
Nishimoto,Yoshio	2P-27, 3P-19	Ono,Akira	1-2
Nishimura,Yoshifumi	1P-15	Oohara,Kazuyoshi	3-8, 2P-15
Nishino,Hidekazu	2P-54	Orofeo,Carlo	3-4
Nishiyama,Satoko	1P-31	Osanai,Yosuke	3P-48
Nobusa,Yuki	2P-9	Osawa,Eiji	2P-31
Noda,Suguru	1P-52, 2P-12, 2P-38, 2P-46	Oshima,Takumi	2-14, 3P-33
Noffsinger,Jesse	3-3	Oshima,Yugo	2P-49
Noguchi,Eriko	2P-26	Otani,Minoru	1P-40
Noguchi,Takuya	2P-16	Ozaki,Hiroyuki	3P-17
Nonoguchi,Yoshiyuki	1-10	Ozawa,Hiroaki	2P-19
Norimatsu,Wataru	2P-52		
Nozaki,Iori	2P-26	~P~	
Nugraha,Ahmad R. T.	2P-29, 1P-29	Page,Alister J	2-4, 1P-2
		Park,Jin Sung	1P-33
~O~			
Ochiai,Takumi	2P-15, 3-8	~Q~	
Ochiai,Yuichi	2-8, 2-12, 3P-26	Qian,HuJun	1P-2, 3P-30
Ogasawara,Naoko	3P-20		
Ogata,Hironori	3P-28, 3P-29	~R~	
Ogawa,Yui	2P-18	Radhakrishnan,Shankara Gayathri	2-10
Ogino,Toshio	1P-53	Rahman,A. F. M. Mustafizur	2-2
Ohfuchi,Mari	1P-50	Razanau,Ihar	3P-27
Ohmori,Shigekazu	2-3, 3P-12		
Ohnami,Hideyuki	3P-29	~S~	
Ohnishi,Ryuji	3-6	Sada,Takao	1-12
Ohno,Yutaka	1-5, 1-6	Sagitani,S.	3P-2
Ohta,Y.	2-4	Saida,Morihiko	3P-20
Okada,Keisuke	3P-1	Saikawa,Mao	1-14
Okada,Morihiro	2P-5	Saito,Hokuto	2P-11
Okada,Susumu	1P-40, 1P-51, 2-6, 2P-39,	Saito,Mineo	3P-9
	2P-40, 3-1	Saito,Riichiro	1P-29, 1P-33, 1P-34, 2-5,
Okada,Takako	3P-49		2P-29, 1P-38
Okamura,Kouki	1P-17	Saito,Susumu	2P-44, 3-3, 3P-6, 3P-7
Okano,Makoto	2P-41	Saito,Takeshi	1P-21, 2-1, 2-3, 3P-12,
Okawa,Takashi	1P-45, 2P-28		3P-36, 3P-38
Okazaki,Toshiya	1-2, 1P-21, 2P-14, 2P-17,	Saito,Yahach	2P-31
	3-1, 3-10, 3P-10, 3P-40	Sakaguchi,Hiroshi	3-6
Oke,Shinichiro	1P-45, 2P-28	Sakai,Ayumu	1P-18
Okimoto,Haruya	3P-21	Sakakibara,Satoshi	1P-5
Okita,Sosuke	3P-21	Sakamoto,Shingo	3P-46
Okita,Yoshitaka	1P-41	Sakashita,Tomohiro	1P-17, 1P-35
Okubo,Shingo	3-1	Sakurai,Masahiro	2P-44
Okugaki,Tomohiko	1P-46	Sakurai,Shunsuke	2P-54
Okui,Yumi	2P-53	Sanderson,Joseph H.	3P-31
Omachi,Haruka	2P-50	Sato,Hideki	3P-13, 3P-35

Sato,Hisako	3-6	Suzuki,Takuya	3P-17
Sato,Kentaro	1P-29, 1P-33, 1P-38, 2-5		
Sato,Kosuke	3P-23	～T～	
Sato,Shintaro	3-5	Tachibana,Masaru	2P-4
Sato,Toshiyuki	1P-45	Tada,Kengo	2P-42
Sato,Yasufumi	3P-37	Tadokoro,Hiroki	2P-51
Sato,Yohei	2P-29	Taga,Miki	1P-3
Sato,Yuki	3P-31	Taguchi,M.	3P-2
Sawada,Keisuke	3P-9	Tahara,Yoshio	1-15, 3-1
Sawanishi,Yoshihiko	1-13, 1P-44	Tajima,Isamu	2P-24
Segawa,Yasutomo	2P-50	Takagi,Daisuke	1P-13
Sekiguchi,Kotaro	2P-46	Takagi,Yoshirteru	2P-40
Seta,Hisashi	2P-13	Takahashi,Hideyuki	1P-46
Shawky,Ahmed	1P-10	Takahashi,Katsumune	3P-51
Shibata,Hiroki	3P-22	Takahashi,H.	3P-2
Shimada,K.	3P-2	Takai,Kazuyuki	3P-36
Shimamura,Yoshinobu	2P-5	TAKANO,Soichiro	2P-38
Shimanaka,Kota	3P-13	Takano,Yoshihiko	3P-11
Shimizu,Kazuki	1P-8, 1P-12, 1P-42, 1P-45, 2P-28, 3P-14	Takashima,Tadashi	1P-6
Shimotani,Hidekazu	1-4, 1P-26	Takatori,Masashige	1P-35
Shinohara,Hisanori	1-3, 1-6, 1P-7, 1P-11, 1P-16, 1P-47, 1P-48, 1P-52, 2P-22, 2P-50, 3P-21, 3P-25, 3P-38, 3P-47	Takenobu,Taishi	1-4, 1P-26, 1P-28, 2P-9, 2P-49, 3P-50
Shinomiya,Hiroyuki	3P-3	Takesue,Kentaro	2P-33
Shinozaki,Masashi	1-13, 1P-44	Takikawa,Hirofumi	1P-8, 1P-12, 1P-42, 1P-45, 3P-14, 2P-28
Shiomi,Junichiro	1-7, 2P-16	Takimoto,Kotaro	1P-8, 1P-12, 3P-14
Shiozawa,Kazunari	1-6, 1P-16	Takimoto,Tatsuya	2P-30
Shiraki,Kentaro	2P-51	Tamaki,Jun	3P-53
Shiratori,Yosuke	2P-46	Tanabe,Masahiro	1P-10
Shiromaru,Haruo	3P-31	Tanaka,Katsutomo	2-14
Slanina,Zdenek	2-10, 3P-18	Tanaka,Kazuyoshi	2P-36
Soga,Tetsuo	1P-20, 1P-21, 1P-37	Tanaka,Mikito	1P-20
Subramaniam,Chandramouli	2P-3	Tanaka,Nobuo	2P-31
Suda,Yoshiyuki	1P-8, 1P-12, 1P-42, 1P-45, 2P-28, 3P-14	Tanaka,Takeshi	1-1, 1P-3, 1P-9, 1P-22, 1P-31, 2P-20, 2P-23, 3P-15
Suenaga,Kazu	1-16, 3-1	Tanaka,Yasuhiko	3P-5
Sugai,Toshiki	1-13, 1P-44, 2-13, 3P-16	Tang,Zikang	2P-1
Sugioka,Yuki	1P-42	Tange,Masayoshi	3P-40
Sugita,Ryo	1P-37	Tanogami,Homare	2P-26
Sun,Dong-Ming	1-5	Tanoue,Hidetou	1P-8, 1P-12, 1P-42, 1P-45, 2P-28, 3P-14
Suzuki,Marie	1P-7, 1P-48	Terada,Tomohiro	2P-31
Suzuki,Satoru	1P-32, 2P-35	Terauchi,Masami	2P-29
Suzuki,Seiya	1P-39	Teshiba,Masashi	1-14
Suzuki,Shinzo	1-2	Tezuka,Noriyasu	2-9
		Tian,Ying	1-5

Timmermans, Marina Y.	1-5	Wang, Xinran	2P-43
Ting, Y.	2-5	Wang, Ying	1P-2, 3P-30
Tohji, Kazuyuki	1P-46	Wang, Ying-Hui	2-15
Tominaga, Masato	3P-46	Watanabe, Fumiaki	2P-4
Tomioaka, Shirou	3P-11	Watanabe, Tohru	3P-11
Tomita, Kyohei	3P-52	Watari, Fumio	1P-19, 2P-2
Tomomi, Yano	2-14	Wei, Xiaojun	2-12
Totsuka, Yasunori	1P-19	Wen, Di	1P-26
Tsuchiya, Hiroaki	1P-21	Witek, Henryk A.	2P-27
Tsuchiya, Takahiro	2-10	Wu, Tianzhun	2P-1
Tsuda, Satoshi	1-4		
Tsuda, Shunsuke	3P-11	~X~	
Tsuji, Masaharu	2P-18, 2P-21, 3-4	Xiang, Rong	2P-1
Tsukagoshi, Kazuhito	1P-36, 3-7	Xu, Ming	1-11
Tsukamoto, Takahiro	1P-53		
Tsukuda, Tatsuya	2P-22	~Y~	
Tsumura, Yoshihiro	2P-36	Yagi, Hajime	2-11, 3P-20, 3P-21
Tsunoyama, Hironori	2P-22	Yagi, Katsunori	3-5
Tsutsui, Tomoyuki	1P-1	Yahiro, Hitomi	3P-36
Tsutsumi, Yusuke	2P-8	Yajima, Hirofumi	2P-24, 3P-3, 3P-51, 1P-18
Tyurnina, Anastasia V.	1P-36, 3-7	Yamada, Michio	2P-53
		Yamada, Takeo	1P-25, 2P-3, 2P-10, 2P-54, 3P-4
~U~			
Uchida, Katsumi	1P-18, 2P-24	Yamada, Teppei	1P-52
Uchinoumi, Takeshi	1-9	Yamagiwa, Kiyofumi	2P-13
Uchiyama, Naoyuki	1P-24	Yamaguchi, Takahide	3P-11
Udoguchi, Hiroki	2P-49	Yamamoto, Kazunor	2P-34
Ueno, Hiroshi	2-13	Yamamoto, Makoto	3-2
Umakoshi, Tatsuya	2P-48	Yamamoto, Yuki	1P-27
Umeda, Ryota	1P-15	Yamamoto, Yuki	2P-10
Umeda, Yoshito	1P-8, 1P-12, 1P-42, 3P-14	Yamane, Honami	2-4
Umeno, Masayoshi	2-7	Yamasaki, Takayuki	3-2, 3P-39
Umeyama, Tomokazu	2-9, 3P-32	Yamashita, Fuyuko	3P-20
Umezawa, Naoto	2-6	Yanagi, Kazuhiro	1-4, 1P-26, 1P-28, 2P-9, 2P-49, 3P-2, 3P-17, 3P-36, 3P-37, 3P-50
Urabe, Yasuko	3P-15		
Usui, Kousuke	2P-27	Yang, Mei	1P-43
Utaka, Katsuyuki	1P-6	Yasuda, Satoshi	1P-10, 2P-54
		Yin, Lichang	2P-29
~W~		Yokoi, Hiroyuki	2P-33
Wada, Momoyo	1P-43	Yokoyama, Atsuro	2P-2
Wada, Yoriko	1-14, 1P-49, 3P-31	Yokoyama, Naoki	3-5
Wakabayashi, Tomonari	1-14, 1P-49, 2P-29, 3P-22, 3P-23, 3P-31	Yomogida, Yohei	1-4, 1P-26, 2P-9
Wakita, Koichi	2-7	Yomogida, Yoshiki	2P-10
Wang, Feng	2-2	Yonemori, K.	3P-2
Wang, Hailiang	2P-43	Yoo, JongTae	1P-23

Yoshikawa,Hirofumi	1P-52
Yoshimura,Masamichi	1P-39
Yuan,Hongtao	1-4
Yudasaka,Masako	1-15, 1P-43, 3-1, 3P-44, 3P-45
Yuge,Ryota	2S-3, 3P-44
Yumura,Motoo	1-10, 1-11, 1P-25, 2-3, 2P-10, 2P-25, 2P-54, 3P-4, 3P-36
Yumura,Takashi	1P-30
Yun,Sun	2P-22

~Z~

Zaima,Takeyuki	3P-20, 3P-21
Zenki,Masashi	3P-20
Zhang,Jinying	1P-7, 1P-11
Zhang,Li	2P-43
Zhang,Minfang	1-15, 1P-43, 3P-45
Zhao,Li	2P-30
Zhao,X.	3P-24
Zhou,Xin	1-15, 3P-45

### 複写をご希望の方へ

フラーレン・ナノチューブ学会は、本誌掲載著作物の複写に関する権利を一般社団法人学術著作権協会に委託しております。

本誌に掲載された著作物の複写をご希望の方は、(社)学術著作権協会より許諾を受けて下さい。但し、企業等法人による社内利用目的の複写については、当該企業等法人が社団法人日本複写権センター((社)学術著作権協会が社内利用目的複写に関する権利を再委託している団体)と包括複写許諾契約を締結している場合にあつては、その必要はございません(社外頒布目的の複写については、許諾が必要です)。

権利委託先：一般社団法人学術著作権協会

〒107-0052 東京都港区赤坂 9-6-41 乃木坂ビル 3 階

電話：03-3475-5618 FAX：03-3475-5619 E-Mail：info@jaacc.jp

注意：複写以外の許諾(著作物の引用、転載・翻訳等)に関しては、(社)学術著作権協会に委託致しておりません。直接、フラーレン・ナノチューブ学会へお問い合わせください。

### Reprographic Reproduction outside Japan

Making a copy of this publication

Please obtain permission from the following Reproduction Rights Organizations (RROs) to which the copyright holder has consigned the management of the copyright regarding reprographic reproduction.

Obtaining permission to quote, reproduce; translate, etc.

Please contact the copyright holder directly.

→Users in countries and regions where there is a local RRO under bilateral contract with Japan Academic Association for Copyright Clearance(JAACC)

Users in countries and regions of which RROs are listed on the following website are requested to contact the respective RROs directly to obtain permission.

Japan Academic Association for Copyright Clearance (JAACC)

Address : 9-6-41 Akasaka, Minato-ku, Tokyo 107-0052 Japan

Website : <http://www.jaacc.jp/>

E-mail : info@jaacc.jp TEL : 81-3-3475-5618 FAX : 81-3-3475-5619

2011年3月8日発行

## 第40回記念フラーレン・ナノチューブ総合シンポジウム 講演要旨集

<フラーレン・ナノチューブ学会>

〒464-8602 愛知県名古屋市千種区不老町

名古屋大学大学院理学研究科 物質理学専攻

篠原研究室内

Tel : 052-789-5948

Fax : 052-747-6442

E-mail : fullerene@nano.chem.nagoya-u.ac.jp

URL : <http://fullerene-jp.org>

印刷 / 製本 (有) イヅミ印刷所

# ナノラプター NANORUPTOR<sup>®</sup> サンプル密閉式超音波分散装置

——— バイオの技術をナノテクへ ———

本装置はグラフェン・カーボンナノチューブや燃料電池用触媒を始めとする  
各種ナノ粒子を分散させる事を目的に開発いたしました。

実施例：グラフェン・カーボンナノチューブの分散、燃料電池用触媒評価、  
納入実績：各大学、自動車メーカー、光学機器メーカー、電子部品メーカー

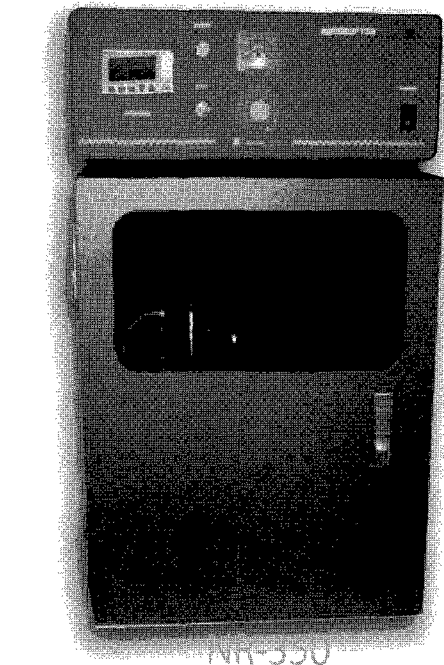
## 特 長

- **分散に最適**  
各種ナノ粒子(グラフェン、カーボンナノチューブ、フラーレン等)の分散処理に最適。
- **密閉処理**  
溶媒の蒸発・揮散やコンタミがありません。
- **多検体同時処理**  
試料チューブの選択により、複数試料を同時に処理できます。
- **再現性良好**  
回転機構の採用により均一な超音波照射が可能です。
- **低騒音**  
高性能消音箱により超音波特有の騒音を防止します。

NR-350仕様表 (予告無く変更する場合があります)

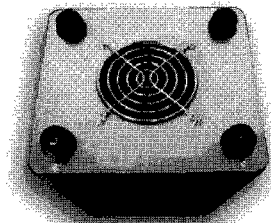
品番	NR-350
品名	密閉式超音波分散装置 Nanoruptor
超音波周波数	20 kHz
超音波出力	380,300,250,130 W (切替式)
電源	100 V、50/60 Hz、5.5 A
最低設置スペース概寸	400 (W) × 350 (D) × 680 (H) mm
発振ユニット概寸	400 (W) × 280 (D) × 160 (H) mm
処理ユニット概寸	250 (W) × 200 (D) × 300 (H) mm
消音箱概寸	400 (W) × 350 (D) × 520 (H) mm
NR-350 全体重量	36 Kg
ランタイム	599 サイクル
インターバルタイマー(ON)	0 ~ 59 秒、デジタル
インターバルタイマー(OFF)	0 ~ 59 秒、デジタル
処理本数	1 本 (50 mL チューブ) ~ 各種
付属品	消音箱、電源ケーブル、接続ケーブル、排水ポンプ、取り扱い説明書、ユーザー登録カード
備考	NR-350 は機器のみです。別途処理量に応じたアクセサリ(ギヤ・板+チップ)をお買い求め下さい。

品名	品番	包装	希望販売価格
超音波密閉式分散装置 Nanoruptor <sup>®</sup>	NR-350	1 UNIT	¥1,950,000
*アクセサリユニットは含みません			
50 mL チューブ用チップ	MM-50WS	1 SET	¥54,000
使用可能チューブ: マルエム社製 50 mL ねじ口試験管			
ギヤ板	NG350-50	1 PC	¥9,000
冷水循環器	CP80-R	1 UNIT	¥264,000
冷水循環器接続ケーブル	TU-100	1 PC	¥15,000



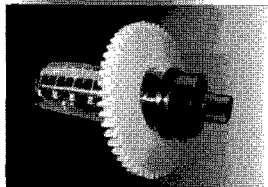
収束装置付超音波処理槽

エネルギー収束装置を新たに開発、高効率化を実現。



冷却ファン

冷却ファン及び専用回路の採用により長時間運転が可能。



・ギヤ板(品番: NG-350-50)  
・50 mL 専用共振棒 1 本入りセット(品番: MM-50WS)

販売



人と科学のステキな未来へ

コスモ・バイオ株式会社

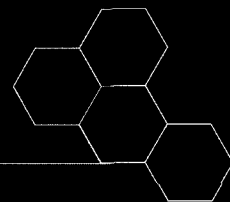
〒135-0016 東京都江東区東陽2-2-20 東陽駅前ビル  
URL: <http://www.cosmobio.co.jp>  
TEL (03) 5632-9610 FAX (03) 5632-9619  
営業部 栗原 mkurihar@cosmobio.co.jp  
開発部 笹原 ksasahar@cosmobio.co.jp

製造



東湘電機株式会社

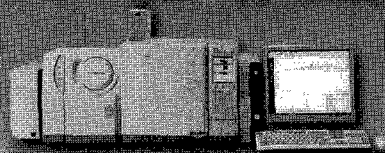
〒232-0027 神奈川県横浜市南区新川町5-29-2 新井ビル2F  
TEL (045) 261-8388 FAX (045) 252-8935  
技術部長 伊藤  
e-mail: k-ito@bioruptor.jp



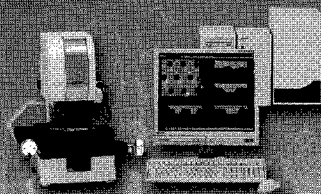
# Best for Our Customers

～すべてはお客様のために～ を合言葉にカーボン系新材料における最高のソリューションを提供します。

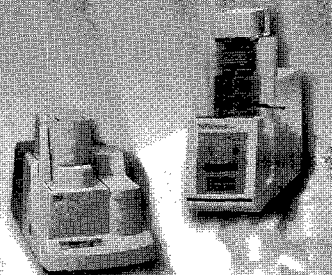
**NEW**  
熱分解生成物・発生ガスの分析  
ガスクロマトグラフ質量分析計  
GCMS-QP2010 Ultra



あらゆるナノテク材料を  
観察・測定  
アノサーチ顕微鏡  
SFT-3500



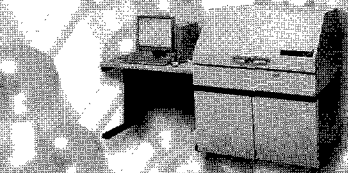
微量CNTの純度・熱特性評価  
CNTの結晶性と耐熱性の評価  
マイクロ熱量測定装置  
TGA-50  
TG/DTA同時測定装置  
DTG-60/60H



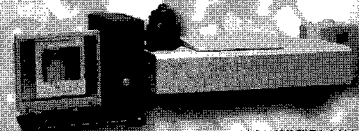
**NEW**  
直径測定  
精製前後の観察  
CNTとポリマーコンポジット  
試料の観察  
走査型プローブ顕微鏡  
SPM-9700



CNTの紫外可視近赤外  
吸収スペクトル測定  
紫外可視近赤外分光光度計  
SolidSpec-3700



SWNTの近赤外PL  
3次元分布測定  
近赤外フォトルミネッセンス測定システム  
NIR-PL System



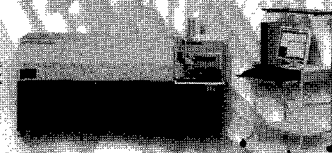
紫外可視近赤外分光光度計  
UV-3600



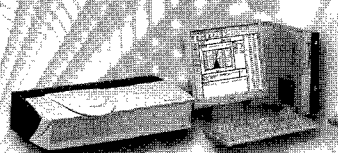
**NEW**  
分散・凝集過程評価  
高感度ナノ粒子径分布測定装置  
SALD-7100H



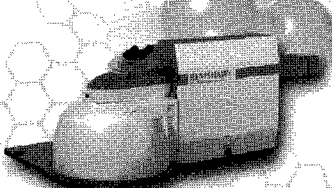
触媒元素の測定  
ツインシーケンシャル形ICP発光分析装置  
ICPS-8100



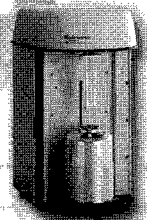
独自のIG法による  
シングルナノ領域の粒子径評価  
シングルナノ粒子径測定装置  
IG-1000



直径測定  
結晶性と耐熱性の評価  
ラマン分光光度計  
inVia シリーズ(レニショー社製)



比表面積と吸着特性  
マイクロメリテックス  
自動比表面積/細孔分布測定装置  
トライスター-II 3020シリーズ



**nanotech**  
SHIMADZU

## Total solutions for the future of nanotechnology

株式会社島津製作所

分析計測事業部 マーケティング部 プロモーションG  
〒604-8511 京都市中京区西ノ京桑原町1  
TEL075-823-1468 FAX075-841-9325 <http://www.an.shimadzu.co.jp>



溶液中の粒子のナノレベル微細化・分散に

# BRANSON 超音波ホモジナイザー

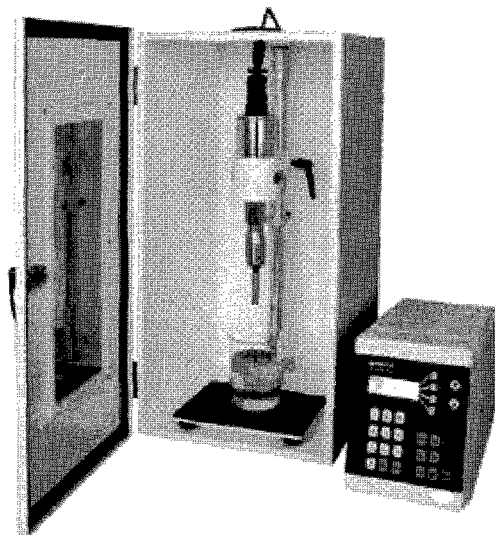
ホーン先端部の振幅の安定性を、より高めた Advance タイプ になりました。

近年のナノテクノロジーの発展及び粉体関連技術の向上により、より微細な粒子に対する乳化分散処理の要望が増えてまいりました。

超音波ホモジナイザーを使用し、均質な乳化分散処理を行い、安定させることにより製品の機能は向上します。

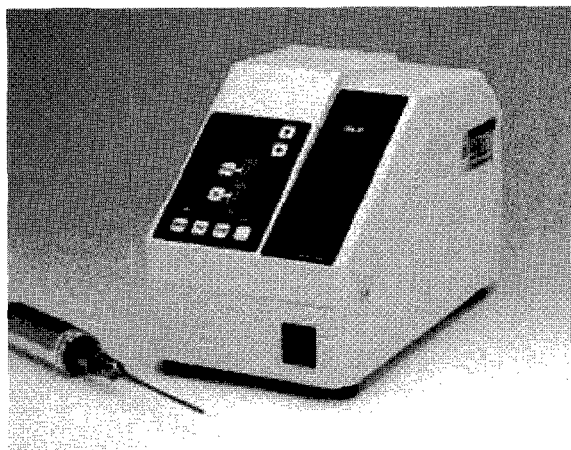
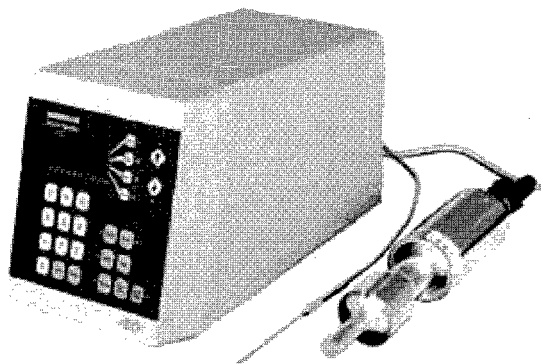
ブランソン社では 20kHz 機と、40kHz 機の 2 タイプを用意しております。

1次粒子の凝集力にも拠りますが、20kHz 機では 100nm 程度までの分散力があります。40kHz 機は、さらに細かいレベルで分散ができる可能性があります。



20KHz 超音波ホモジナイザー  
BRANSON SONIFIER シリーズ

高周波 40KHz 超音波ホモジナイザー  
BRANSON SLPe シリーズ



ブランソン社の製品は、ホーン先端部の振幅の安定性が高く、強力なキャビテーションが得られ、効率良く、再現性の高い分散処理が行えます。

## 主なアプリケーション

### 分散

カーボンナノチューブ 有機顔料 無機顔料 セラミック セメント 感光体 記録材料  
磁性粉 粉末冶金 酸化鉄 金属酸化物 シリカ アルミナ カーボンブラック  
ポリマー ラテックス 製紙 ファンデーション  
研磨剤 電池 フィラー 光触媒 触媒 ワクチン 体外診断薬 歯磨き粉 シャンプー  
半導体 電子基盤 液晶 貴金属 金属 宝石 タイヤ 発酵菌類 その他

### 乳化

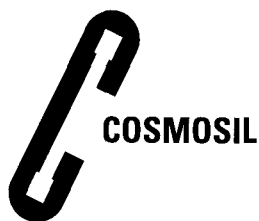
エマルジョン製剤 農薬 トナー ラテックス 界面活性剤 クリーム 乳液 クリーム 等

SCC 株式会社 **セントラル** 科学貿易

本社：111-0052 東京都台東区柳橋 1-8-1  
Tel 03-5820-1500 Fax 03-5820-1515  
URL <http://www.cscjp.co.jp/>

大阪支店：Tel 06-6325-3171 Fax 06-6325-5180  
福岡営業所：Tel 092-482-4000 Fax 092-482-3797  
札幌出張所：Tel 011-764-3611 Fax 011-764-3612





# COSMOSIL® CNT

- 可溶化カーボンナノチューブをサイズで分離!
- 親水性基(中性)コーティングタイプ!
- 3種類の細孔径(300 Å, 1000 Å, 2000 Å)!
- 高い耐久性!

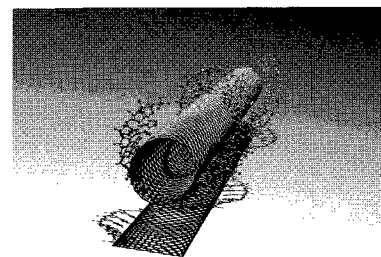
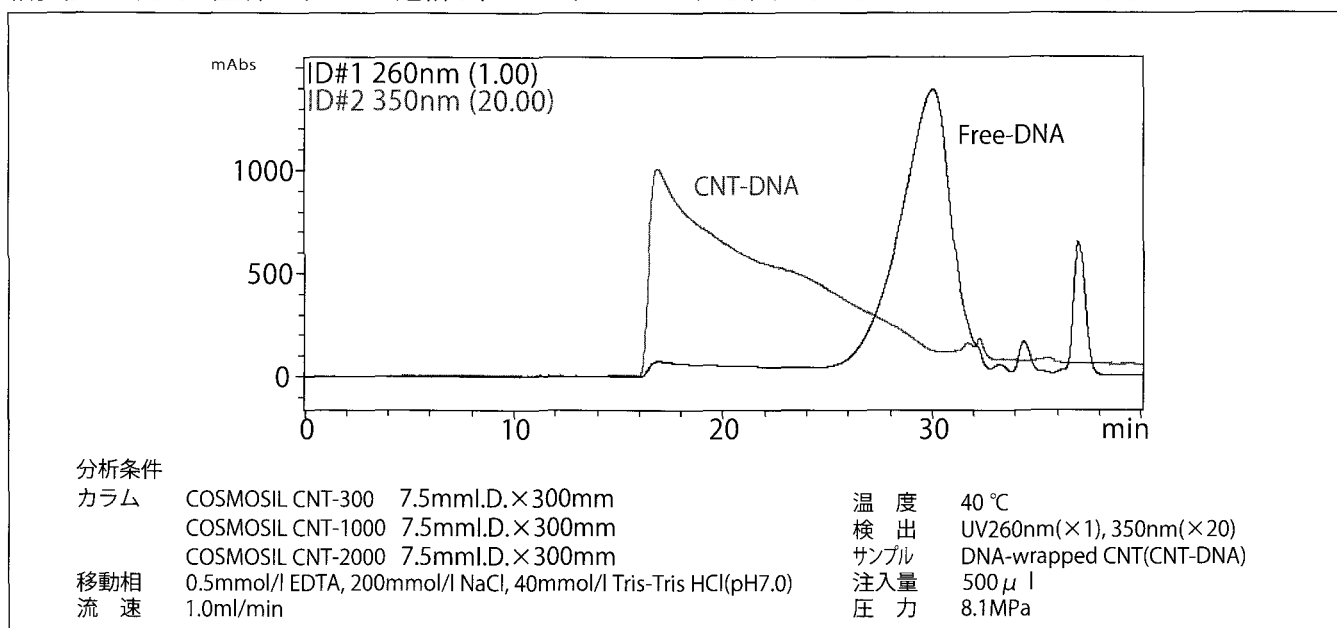


Image courtesy of Dr. Y. Ito, Univ. of Oxford

## ■分離例

### カーボンナノチューブのサイズ分離

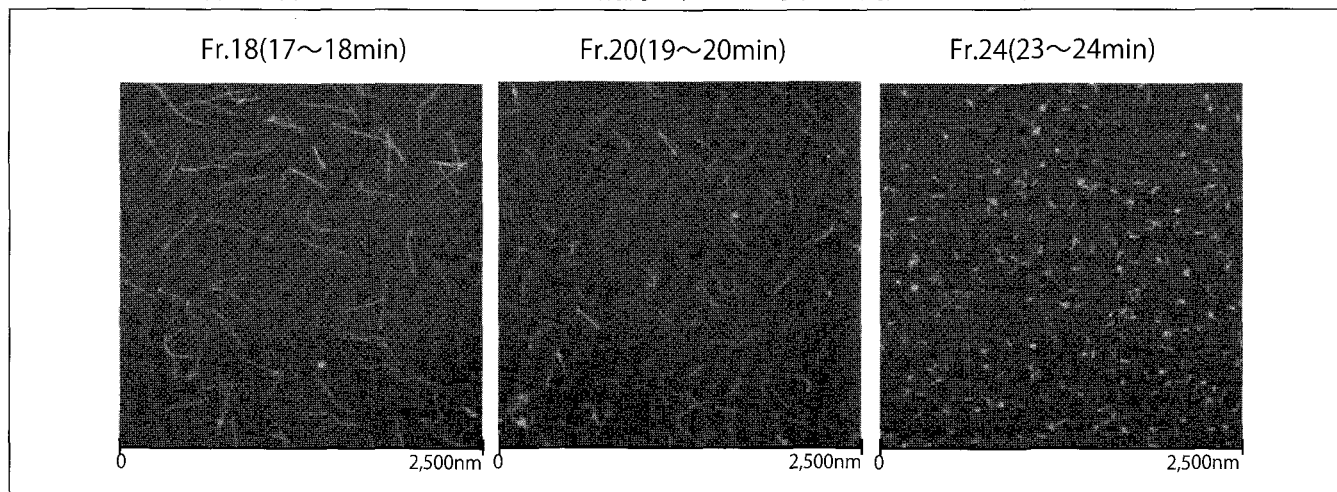
細孔径の異なる3種類のカラムを連結し、DNAでラッピングされたカーボンナノチューブを分離しました。



【サンプルのご提供 : 名古屋大学大学院理学研究科物質理学専攻 篠原研究室】

### AFM(原子間力顕微鏡)によるサイズ観察

上記分離時に分取した各フラクションをAFMにて観測し、CNTの長さを測定しました。



【撮影・データのご提供 : 名古屋大学大学院理学研究科物質理学専攻 篠原久典教授・浅田有紀様】

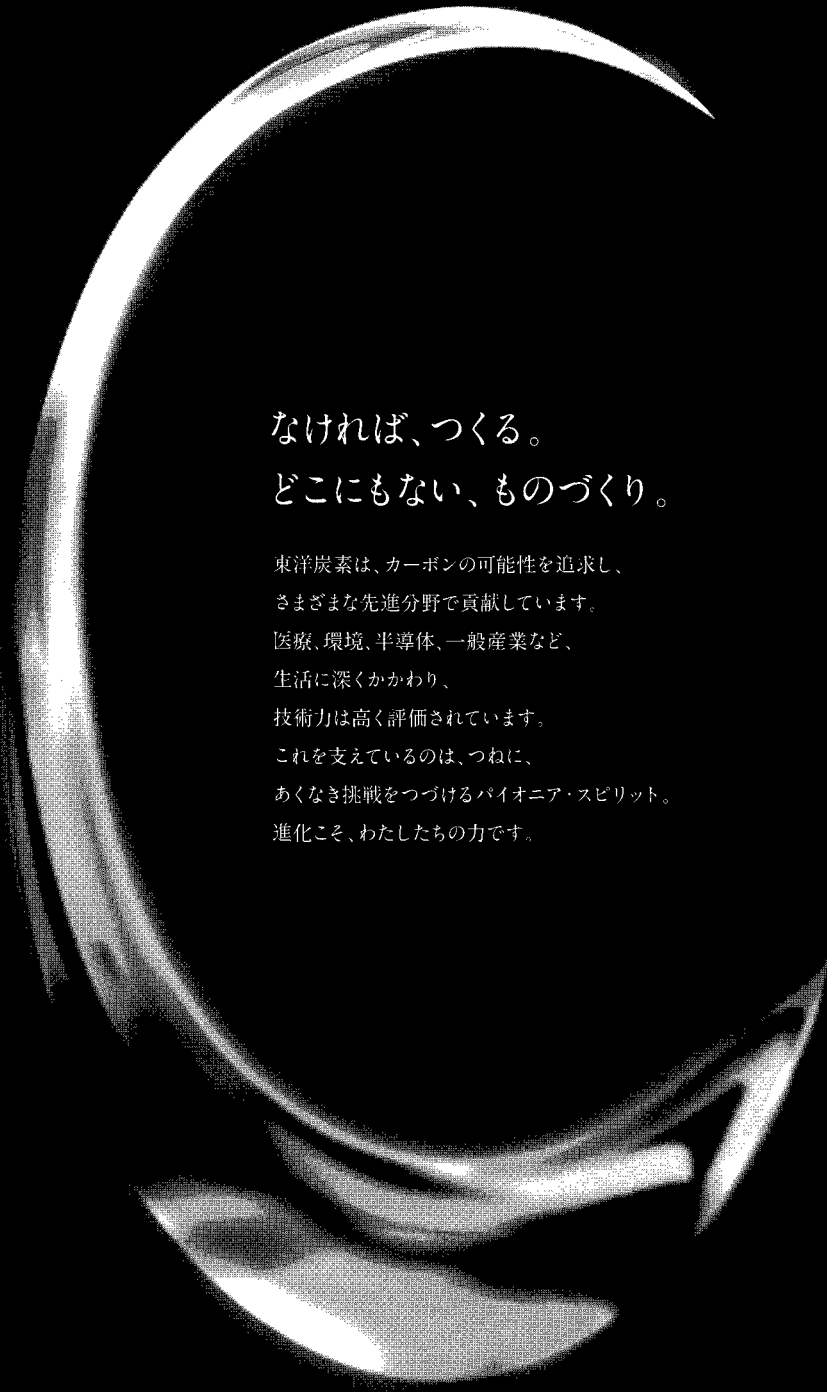
詳しい情報はWeb siteをご覧ください。

**ナカライテスク株式会社**

〒604-0855 京都市中京区二条通烏丸西入東玉屋町498

価格・納期のご照会 フリーダイヤル 0120-489-552  
 製品に関するご照会 TEL: 075-211-2746 FAX: 075-211-2710

Web site : <http://www.nacalai.co.jp>



なければ、つくる。  
どこにもない、ものづくり。

東洋炭素は、カーボンの可能性を追求し、  
さまざまな先進分野で貢献しています。  
医療、環境、半導体、一般産業など、  
生活に深くかかわり、  
技術力は高く評価されています。  
これを支えているのは、つねに、  
あくなき挑戦をつづけるバイオニア・スピリット。  
進化こそ、わたしたちの力です。



**TOYO TANSO**  
Inspiration for Innovation

東洋炭素株式会社

本社 〒530-0001 大阪市北区梅田3-3-10 梅田ダイビル10F Tel 06-6451-2114 Fax 06-6451-2186 [www.toyotanso.co.jp](http://www.toyotanso.co.jp)

# 最新の超高真空走査型プローブ顕微鏡システム・・・

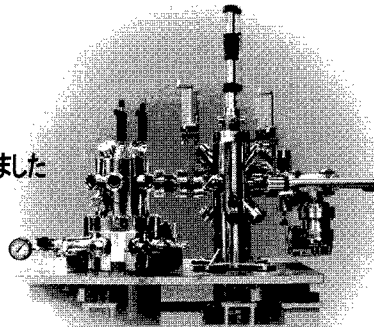
## USM1400

極低温型 (2.5K~室温)

冷却タンク構造改良モデル販売開始!!

従来より冷却温度ダウン、液体ヘリウム消費量ダウンを実現しました

- 2.5K~室温まで幅広い範囲でSTM温度可変測定が可能
- ±0.5テスラ磁場中測定に対応 (オプション)
- レンズステージ組み込みによりトンネル発光観察、近接場励起による分光測定が可能。
- AFM, MFM, EFM, KFM測定対応可能 (オプション)



STM Image of Si(111) surface

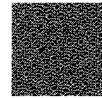


Fig. 1  
Temperature:83K  
Scan area:21.72nm × 21.72nm  
Sample bias:1.8V  
Tunnel current:0.54nA

STM Image of Si(100) surface



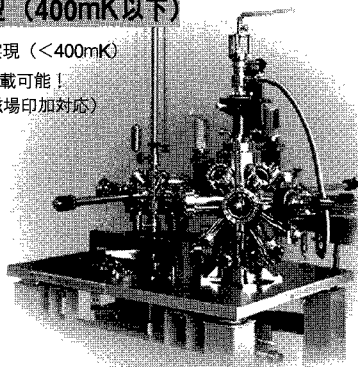
Fig. 2  
Temperature:83K  
Scan area:15.5nm × 4.3nm  
Sample bias:1.2V  
Tunnel current:1.0nA

Yuko Yamamoto Unisoku Co., Ltd.

## USM1300S 3He

超低温・強磁場対応型 (400mK以下)

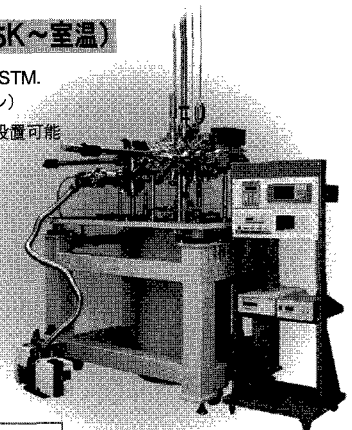
- 3He 使用で超低温測定を実現 (<400mK)
- 1テスラベクターマグネット搭載可能!  
(標準仕様は7テスラ垂直磁場印加対応)



## USM1500

極低温・強磁場対応型 (2.5K~室温)

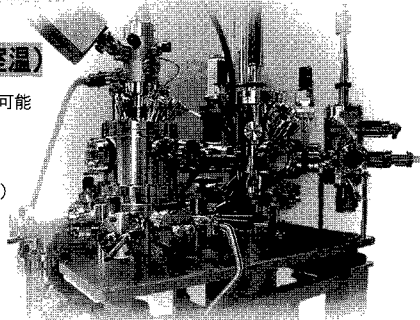
- コンパクトで低価格な極低温磁場中 STM.  
(8テスラ超伝導マグネットはオプション)
- 全高3m以内で標準的な研究室に設置可能
- 2.5K~室温まで幅広い範囲でSTM温度可変測定が可能
- AFM測定対応可能 (オプション)



## USM1400-4P

極低温・4プローブ多探針型 (2.5K~室温)

- 2.5K~室温まで幅広い範囲でSTM温度可変測定が可能
- 各プローブ独立制御可能
- FE-SEMを標準装備
- AFM, MFM, EFM, KFM測定対応可能 (オプション)



4 point measurement



4-probe stage



USM-1400 及び USM-1400-4P は

JST 科学技術振興機構

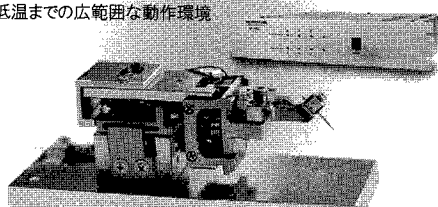
先端計測分析技術・機器開発事業において  
東京大学・大阪大学・豊田工業大学と  
共同で開発されました。

SEM, FIB, 光学顕微鏡観察下での  
ナノ/マイクロ マニピュレーション・プロービングに最適・・・

大気中、真空中、低温環境に対応

## XYZ3軸 ナノマニピュレータ/プローバ UP-100U

- 簡単操作、粗動(数百nm動作)と微動(0.5nm以下)の切り替え式で素早い位置合わせが可能
- 低価格を実現! (価格はお問い合わせください。)
- 市販のSEM/FIB/光学顕微鏡に組み合わせ可能
- 大気中~超高真空まで、室温から極低温までの広範囲な動作環境
- マルチプロービングにも対応
- マニピュレーション、  
半導体ナノデバイスのIV測定、  
抵抗測定、EBIC測定等  
幅広い用途に対応



## ナノ・マイクロ回転ステージ UP-200Rシリーズ

- 大気中、及び高真空中で微小回転動作と位置検出(オプション)のニーズに対応
- SEM, FIBへの組み込み可能
- 回転ステージのみ、及び、XYZ+回転(4軸)の選択可能



株式会社 **ユニソク**

〒573-0131 大阪府枚方市春日野2丁目4番3号  
TEL : 072-858-6456 FAX : 072-859-5655  
http://www.unisoku.co.jp E-mail: info@unisoku.co.jp

# 私たちの使命は 最新の 情報と技術を 研究者のもとへ

「生命科学」の世界は、驚くべき早さで発展しています。その欠かせない要素こそが

私たちの提案する「モノ」なのです。

世界の優れた商品や技術を研究者に提供し、研究そのものをサポートします。

また、各種機器やシステムの提案だけでなく、研究者とメーカーをつなぐ架け橋として

研究者の声をメーカーにフィードバックすることも RIKAKEN の役割と考えます。

RIKAKEN CO., LTD.

 理科研株式会社

<http://www.rikaken.co.jp>

- 本社 / 〒463-8528 名古屋市守山区元郷2-107  
TEL 052-798-6151(代) FAX 052-798-6157
- 岡崎営業所 / 〒444-0864 愛知県岡崎市明大寺町字西長峰50番  
TEL 0564-57-1751(代) FAX 0564-57-1757
- 福井営業所 / 〒910-0842 福井県福井市開発3丁目3010  
TEL 0776-52-1651(代) FAX 0776-52-1653
- 岐阜営業所 / 〒500-8225 岐阜県岐阜市岩地2-25-2  
TEL 058-240-0721(代) FAX 058-240-1082
- 津営業所 / 〒514-0036 三重県津市丸之内養正町20-14  
TEL 059-224-6661(代) FAX 059-224-6671
- 四日市営業所 / 〒512-1211 三重県四日市市桜町2129-1  
TEL 059-326-0231(代) FAX 059-326-3577
- 静岡営業所 / 〒421-0121 静岡市駿河区広野3-29-8  
TEL 054-256-3751(代) FAX 054-256-3755

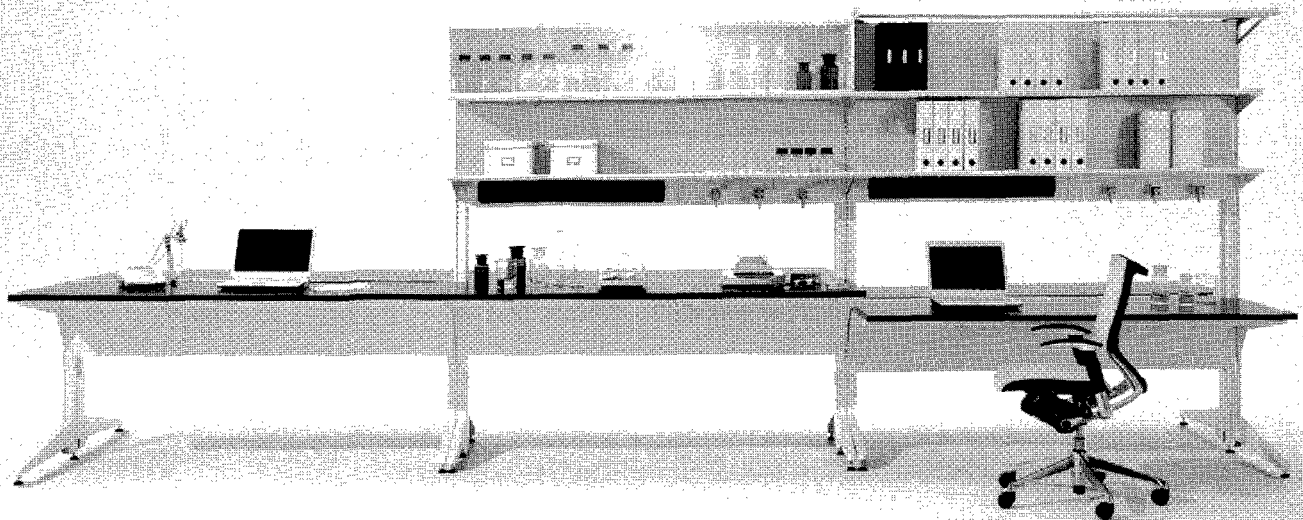
- 東京支店 / 〒113-0033 東京都文京区本郷7-2-1  
TEL 03-3815-8951(代) FAX 03-3818-0889
- つくば営業所 / 〒305-0074 茨城県つくば市高野台3-16-2  
TEL 029-839-1251(代) FAX 029-839-1255
- 柏営業所 / 〒277-0871 千葉県柏市若柴197-17  
TEL 04-7135-6651(代) FAX 04-7135-6751
- 神奈川営業所 / 〒226-0025 横浜市緑区十日市場町901-31  
TEL 045-989-6551(代) FAX 045-989-6701
- 鶴見営業所 / 〒230-0033 横浜市鶴見区朝日町1-49  
TEL 045-500-4551(代) FAX 045-500-4571
- 三島営業所 / 〒411-0943 静岡県駿東郡長泉町下土狩217-1  
TEL 055-980-1101(代) FAX 055-980-1105
- RIKAKEN USA / 4800 Hampden Lane, Suite #255 Bethesda, MD 20814  
アメリカ合衆国 メリーランド州  
TEL 240-482-3735 FAX 240-482-3759

関連会社 / 並木薬品株式会社 〒930-0834 富山県富山市問屋町3-1-33 TEL 076-451-4545(代) FAX 076-451-0085

[取扱品目] ライフサイエンス関連機器・試薬 / 分析機器・試薬 / 臨床機器・試薬 / RI 関連機器  
輸入試薬・特殊試薬・特注試薬 / 各種研究用設備 / 動物飼育関連機器・飼料 / DNA 受託合成



研究者の創造性を刺激し、あらゆる実験・研究にフレキシブルに対応。  
いま、研究施設に求められるもの——オカムラからの答えです。



# RIFORMA

## ラボ・システム[RIFORMA]

豊富なオプションパーツにより、用途や使用する機器に合わせて自由自在に組合せ・組替えが可能です。機能性と同時にスマートなデザインを追求、研究施設にこれまでにない洗練された雰囲気をつくります。

### DESIGN

研究者が快適に実験・研究に集中できるシンプルでスマートなデザイン。

### FUNCTION

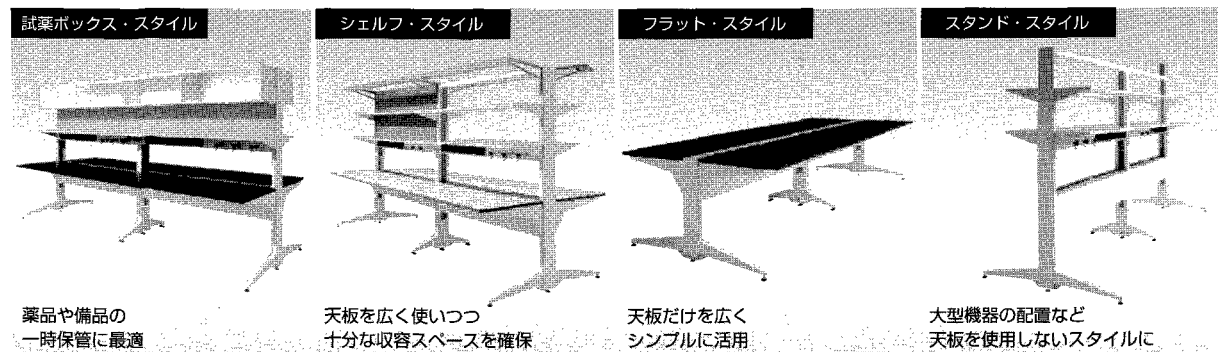
高さ調整可能な天板、支柱を用いた配線機能など、隅々にまで使いやすさを追求。

### ABILITY

安全性や耐久性に加えて、点検もスムーズに行える高いメンテナンス性を確保。

### FLEXIBILITY

オプションを用いて自由自在にカスタマイズ可能。拡張性に優れ、組替えも簡単に行えます。



薬品や備品の一時保管に最適

天板を広く使いつつ十分な収容スペースを確保

天板だけを広くシンプルに活用

大型機器の配置など天板を使用しないスタイルに

ホームページアドレス <http://www.okamura.co.jp/>

お問い合わせ・ご相談はフリーダイヤル ☎0120-81-9060 月曜～金曜(祝日を除く) 9:00～18:00

よい品は結局おトクです

**オカムラ**  
株式会社 岡村製作所



NanoCarbon Research Institute Ltd.

株式会社ナノ炭素研究所

http://nano-carbon.com

## 一桁ナノダイヤモンド分散粒子

# NanoAmando<sup>®</sup> 粉末状水性ゲル

### 特徴

ナノアマンダ粉末状水性ゲルは、特殊製法によってナノダイヤモンド重量の22~23%に当たる量の水が粒子表面に強く配向吸着されているので、超音波洗浄浴に2~3時間浸しておくだけで完全に再分散して、高純度の一桁ナノダイヤモンドコロイドを与えます。

### 仕様

添加物：なし

規格：分散時の粒度

4.8±0.7nmを示す主成分の重量分率95%以上

その他：副成分の粒度分布と分率(平均粒度約 50nm、平均重量分率 5%以下)、および含水率をラベルに記載



## 金属ナノチューブと

## Nan<sup>☀</sup>Integris

## 半導体ナノチューブを選別可能!

密度勾配超遠心分離法 (Density gradient ultra-centrifugation) により、金属SWNT (単層カーボンナノチューブ) と半導体SWNTの作り分けが可能になりました。

● 製品および規格 ●

ISONANOTUBES<sup>™</sup>: 均一な電気的特性を持つSWNT

### IsoNanotubes-S : 半導体SWNT

純度: 90%、95%、98%、99%

SWNT径: 1.2~1.6nm

納入形態: 水溶液

SWNT含有量: 1mg、10mg

### IsoNanotubes-M : 金属SWNT

純度: 70%、95%、98%

SWNT径: 1.2~1.6nm

納入形態: 水溶液

SWNT含有量: 1mg、10mg



### 販売代理店

## 株式会社 ニューメタルス エンド ケミカルス コーポレーション

URL: <http://www.newmetals.co.jp>

本社 東京都中央区京橋1-2-5 京橋TDビル Tel.03-5202-5624 Fax.03-3271-5860

担当: 電子材料営業部 伊藤 E-mail: [ito@newmetals.co.jp](mailto:ito@newmetals.co.jp)

大阪支店 大阪市中央区北浜2-5-23 小寺プラザビル Tel.06-6202-5108 Fax.06-6223-0987

担当: 電子材料営業部 栗谷 E-mail: [kuriya@newmetals.co.jp](mailto:kuriya@newmetals.co.jp)

*Beluga*<sup>®</sup>

**JEM-ARM200F**

*Atomic Resolution  
Analytical Microscope*

新たな扉を開く鍵…

お問い合わせは、電子光学機器営業本部 (EO販促グループ) TEL: (042)528-3353

**JEOL**  
Serving Advanced Technology

日本電子株式会社

本社・昭島製作所 〒196-8558 東京都昭島市武蔵野3-1-2 TEL(042)543-1111  
営業ソリューション統括本部 〒190-0012 東京都立川市曙町2-8-3新鈴春ビル3F TEL(042)528-3381  
札幌 (011) 726-9680・仙台 (022) 222-3324・筑波 (029) 856-3220・東京 (042) 528-3211・横浜 (045) 474-2181  
名古屋 (052) 581-1406・大阪 (06) 6304-3941・広島 (082) 221-2500・福岡 (092) 411-2381

<http://www.jeol.co.jp/>



CaHC

# 研究開発支援企業として、 「産・学・官・医」を支えています。

株式会社カークは、「創造と努力」「誠実と感謝」の企業理念のもと、  
試薬、分析機器、検査薬、工業薬品などの販売を通して社会に貢献しています。  
研究開発支援企業としてあらゆるニーズにお応えいたします。



株式会社 **カーク**

〒460-0002 名古屋市中区丸の内 3-8-5 TEL.052-971-6533(代)

営業第一部 TEL.052-971-6771 営業第二部 TEL.052-971-6551  
営業第三部 TEL.052-624-5821 愛知東営業所 TEL.0564-66-1580  
浜松営業所 TEL.053-431-6801 岐阜営業所 TEL.058-268-8151  
三重営業所 TEL.059-236-2531 東京営業所 TEL.03-3868-3951

<http://www.cahc.co.jp>

検索



# シーエムシー出版おすすめ書籍のご案内

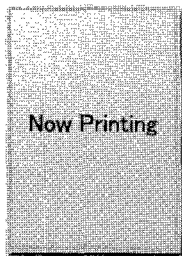
★各書籍の詳細な目次は、弊社ホームページでご確認下さい。  
★弊社へのアクセスは、下記URLもしくは「シーエムシー」でご検索下さい!!

<http://www.cmcbooks.co.jp/>

篠原久典先生監修の新刊書籍!

## ナノカーボンの応用と実用化

—フラーレン、ナノチューブ、グラフェンを中心に—

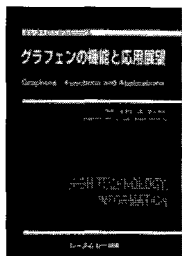


発行: 2011年6月発行予定  
 予定価格: 68,250円  
 (本体65,000円+税5%)  
 監修: 篠原久典

### 予定目次

ナノカーボン材料の応用展開と実用化に向けての展望/大量生産と応用展開/金属内包フラーレンの多量合成/C60内包フラーレン:生成と分離/有機薄膜太陽電池/フラーレンの造影剤応用/フラーレンの生体応用/フラーレンのビジネス展開/カーボンナノチューブの合成・販売/透明導電性フィルム/透明導電塗料/電子デバイス(薄膜トランジスタ)/キャパシタ/リチウムイオン2次電池/放熱・配線応用/導電繊維/大面積合成/SiC上のグラフェン成長/グラファイト系炭素の合成と物性/酸化グラフェン膜/透明導電性フィルム/電子デバイス/絶縁体上へのグラフェンの直接形成/LSI配線技術/スピンドデバイス/ナノカーボン材料の安全性/細胞培養における安全性/ 他

## グラフェンの機能と応用展望 (T0697)



発行: 2009年7月  
 価格: 68,250円  
 (本体65,000円+税5%)  
 監修: 齊木幸一郎  
 徳本洋志

### 目次

グラフェンのエッジ状態の起源/ドーブしたグラフェンの電子状態・触媒活性/酸化グラフェンとコンポジット材料の電子状態/グラフェンの物性、評価(グラフェンの作製、膜厚の評価、観察)/グラフェンの超伝導近接効果/グラフェンの光電子分光/STM/STSによるグラフェン端の電子状態解析/ニッケル単結晶基板上グラフェンのスピン偏極/シリコン基板上のグラフェン薄膜成長/グラフェンの化学的作製法と有機半導体素子電極への応用/ナノグラフェンの低温成長と物性解析/カーボンナノウォール成長と電子放出/CVD法によるナノグラフェンの成長と電子状態/超高温基板を用いた新規カーボン薄膜蒸着成長とラマン分光による評価/グラフェンの超高周波光・電子デバイス応用 他

## ナノカーボンの材料開発と応用 (B0862)



発行: 2008年12月  
 価格: 4,410円  
 (本体4,200円+税5%)  
 監修: 篠原久典

### 目次

金属内包フラーレンの量産技術の開発/パルスアーク放電法による2層ナノチューブの生成/コア/シェル型ポリマー粒子の紡糸によるカーボンナノチューブの調製/カーボンナノチューブによる燃料電池/フラーレン誘導体を用いた有機太陽電池/アモルファスカーボンナノチューブの水素吸蔵/カーボンナノチューブ単一電子トランジスタ/金属内包フラーレンによるピーボットの電子物性とデバイス応用/カーボンナノチューブの電気二重層キャパシタへの応用/走査型プローブ顕微鏡探針およびナノピンセットに向けたナノエンジニアリング/カーボンナノチューブFED 他

## カーボンナノチューブ (B0637)

—期待される材料開発—



発行: 2001年11月  
 価格: 3,675円  
 (本体3,500円+税5%)  
 編集: (株)シーエムシー出版  
 編集部

## ナノマテリアルの市場実態と展望 (Z0183)



発行: 2008年2月  
 価格: 68,250円  
 (本体65,000円+税5%)

## ナノ材料の安全性 (T0761)

—世界最前線—



発行: 2010年11月  
 価格: 68,250円  
 (本体65,000円+税5%)  
 編集: ナノファイバー学会  
 「ナノ材料の安全性」編集委員会

今すぐお申し込みはE-mail, FAXで!

● E-mail [info@cmcbooks.co.jp](mailto:info@cmcbooks.co.jp)  
 ● FAX 03 (3293) 2069

# 株式会社 マシナックス

代表取締役 佐野隆治

〒454-0856 名古屋市中川区小碓通 2-6

TEL 052-654-5021(代) FAX 052-654-5125

HP <http://www.mashinax.jp/>

メール [mashinax@sf.starcat.ne.jp](mailto:mashinax@sf.starcat.ne.jp)

## 菱田商店会社案内

### オフィス家具

メーカー(既製品) オカムラ・コクヨ・プラス等  
木製家具 好みにあわせて作ります

### 室内装飾

ブラインド 立川・日米  
カーテン・カーペット スミノエ・サンゲツ・タジマ等  
床仕上げ フリーアクセス・Pタイル・ロンリウム等  
クロス ルノン・サンゲツ等  
間仕切り 各種パーティション

### 学校関連

黒板・ホワイトボード・掲示板  
実験台・薬品棚・吊棚  
既製品から特注品まで、もちろん取り付けます。

(有)菱田 商店

名古屋市緑区浦里4-207

Tel 891-8125

Fax 891-3957

CVDのリーディングカンパニー

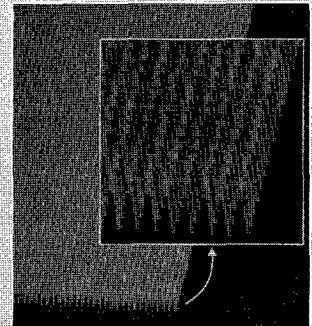
**AIXTRON**

アイクストロン社の

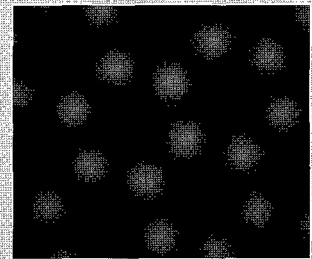
ウェハースケールCNT・グラフェン成膜装置 **Black Magic**



Dense CNT



Horizontal SWCNT



Graphene

- 装置導入後、すぐに希望のCNTやグラフェンを成長可能
- オリジナルのレシピ付き「Thermal CVDとPlasma CVDの2モードに対応」  
(シングルCNT用、ダブルCNT用、マルチCNT用、グラフェン用、横方向CNT用、低圧カプロセス用、高速成長CNT用など)
- あらゆる基板サイズに対応 (研究用: 2~6インチ、量産用: 最大12インチまで)
- プラズマによる簡単クリーニングと高メンテナンス性
- 世界中の大学・研究所・企業に導入済み

アイクストロン株式会社

<http://www.aixtron.com>

E-mail: [JAPANINFO@aixtron.com](mailto:JAPANINFO@aixtron.com)

〒140-0001 東京都品川区北品川1-8-11 Daiwa 品川 Northビル9F TEL: 03-5781-0931 FAX: 03-5781-0940

**ALWAYS ONE STEP AHEAD**

The Next Generation Nanotech

株式会社ATRは、次世代ナノテクノロジーをリードします。

フラーレン  
PCBM  
グラフェン  
ナノサイズ微粒子  
金ナノ微粒子  
カーボンナノチューブ  
超小型データロガー

WEB サイトリニューアル致しました！

<http://atr-atr.co.jp>



株式会社 **ATR**

Advanced Technology Research

〒270-0021 千葉県松戸市小金原 7-10-25  
TEL : 047-394-2112 FAX : 047-394-2100  
Mail : sales@atr-atr.co.jp



# フラーレン誘導体化合物

## Small Gap フラーレン **NEW!**

製品番号 : 707503

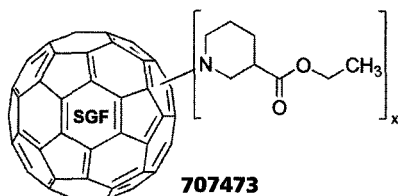
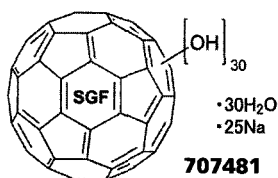
Small gap fullerenes

製品番号 : 707481

Polyhydroxy small gap fullerenes, hydrated

製品番号 : 707473

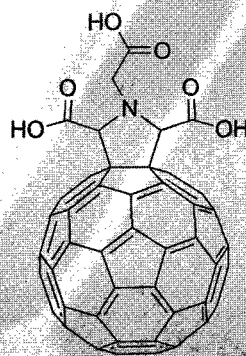
Small gap fullerene-ethyl nipecotate,  $\geq 95\%$



バンドギャップの小さな「Small Gap フラーレン」は極めて多様なかごの大きさのフラーレン類です。既存の溶媒抽出法によるフラーレンには存在しないような異性体、たとえば  $C_{74}$  などを含んでいます。

【参考文献】

- Diener, M. D.; Alford, J. M. *Nature* 1998, 393, 668.
- Raebiger J. W.; Alford J. M.; Bolskara R. D.; Diener M. D. *Carbon* 2011, 49, 37.



水溶性フラーレン誘導体

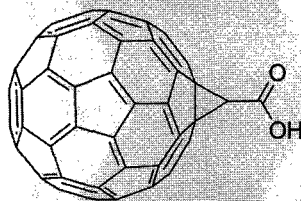
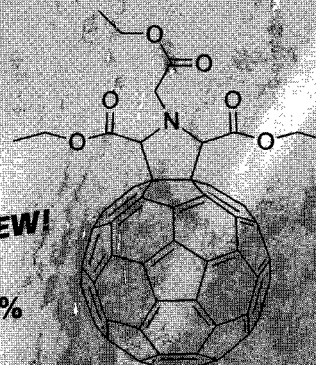
製品番号 : 709085 **NEW!**

$C_{60}$  Pyrrolidine tris-acid, 97%

有機溶媒可溶性

製品番号 : 709093 **NEW!**

$C_{60}$  Pyrrolidine tris-acid ethyl ester, 97%



機能性フラーレンのビルディングブロック

製品番号 : 658847

(1,2-Methanofullerene  $C_{60}$ )-61-carboxylic acid

[www.sigma-aldrich.com/nano-jp](http://www.sigma-aldrich.com/nano-jp)

**SIGMA-ALDRICH®**

シグマ アルドリッチ ジャパン株式会社

〒140-0002 東京都品川区東品川2-2-24  
天王洲セントラルタワー4階

■製品に関するお問い合わせは、弊社テクニカルサポートへ  
TEL : 03-5796-7330 FAX : 03-5796-7335  
E-mail : sialjpts@sial.com

■在庫照会・ご注文方法に関するお問い合わせは、弊社カスタマーサービスへ  
TEL : 03-5796-7320 FAX : 03-5796-7325  
E-mail : sialjpcs@sial.com

<http://www.sigma-aldrich.com/japan>